



BACTERIAL CELL WALL STRUCTURE AND DYNAMICS

EDITED BY: Tobias Dörr, Partick J. Moynihan and Christoph Mayer
PUBLISHED IN: Frontiers in Microbiology



frontiers

Frontiers Copyright Statement

© Copyright 2007-2019 Frontiers Media SA. All rights reserved.

All content included on this site, such as text, graphics, logos, button icons, images, video/audio clips, downloads, data compilations and software, is the property of or is licensed to Frontiers Media SA ("Frontiers") or its licensees and/or subcontractors. The copyright in the text of individual articles is the property of their respective authors, subject to a license granted to Frontiers.

The compilation of articles constituting this e-book, wherever published, as well as the compilation of all other content on this site, is the exclusive property of Frontiers. For the conditions for downloading and copying of e-books from Frontiers' website, please see the Terms for Website Use. If purchasing Frontiers e-books from other websites or sources, the conditions of the website concerned apply.

Images and graphics not forming part of user-contributed materials may not be downloaded or copied without permission.

Individual articles may be downloaded and reproduced in accordance with the principles of the CC-BY licence subject to any copyright or other notices. They may not be re-sold as an e-book.

As author or other contributor you grant a CC-BY licence to others to reproduce your articles, including any graphics and third-party materials supplied by you, in accordance with the Conditions for Website Use and subject to any copyright notices which you include in connection with your articles and materials.

All copyright, and all rights therein, are protected by national and international copyright laws.

The above represents a summary only. For the full conditions see the Conditions for Authors and the Conditions for Website Use.

ISSN 1664-8714

ISBN 978-2-88963-152-0

DOI 10.3389/978-2-88963-152-0

About Frontiers

Frontiers is more than just an open-access publisher of scholarly articles: it is a pioneering approach to the world of academia, radically improving the way scholarly research is managed. The grand vision of Frontiers is a world where all people have an equal opportunity to seek, share and generate knowledge. Frontiers provides immediate and permanent online open access to all its publications, but this alone is not enough to realize our grand goals.

Frontiers Journal Series

The Frontiers Journal Series is a multi-tier and interdisciplinary set of open-access, online journals, promising a paradigm shift from the current review, selection and dissemination processes in academic publishing. All Frontiers journals are driven by researchers for researchers; therefore, they constitute a service to the scholarly community. At the same time, the Frontiers Journal Series operates on a revolutionary invention, the tiered publishing system, initially addressing specific communities of scholars, and gradually climbing up to broader public understanding, thus serving the interests of the lay society, too.

Dedication to Quality

Each Frontiers article is a landmark of the highest quality, thanks to genuinely collaborative interactions between authors and review editors, who include some of the world's best academicians. Research must be certified by peers before entering a stream of knowledge that may eventually reach the public - and shape society; therefore, Frontiers only applies the most rigorous and unbiased reviews.

Frontiers revolutionizes research publishing by freely delivering the most outstanding research, evaluated with no bias from both the academic and social point of view. By applying the most advanced information technologies, Frontiers is catapulting scholarly publishing into a new generation.

What are Frontiers Research Topics?

Frontiers Research Topics are very popular trademarks of the Frontiers Journals Series: they are collections of at least ten articles, all centered on a particular subject. With their unique mix of varied contributions from Original Research to Review Articles, Frontiers Research Topics unify the most influential researchers, the latest key findings and historical advances in a hot research area! Find out more on how to host your own Frontiers Research Topic or contribute to one as an author by contacting the Frontiers Editorial Office: researchtopics@frontiersin.org

BACTERIAL CELL WALL STRUCTURE AND DYNAMICS

Topic Editors:

Tobias Dörr, Cornell University, United States

Partick J. Moynihan, University of Birmingham, United Kingdom

Christoph Mayer, University of Tübingen, Germany

Bacterial cells are encased in a cell wall, which is required to maintain cell shape and to confer physical strength to the cell. The cell wall allows bacteria to cope with osmotic and environmental challenges and to secure cell integrity during all stages of bacterial growth and propagation, and thus has to be sufficiently rigid. Moreover, to accommodate growth processes, the cell wall at the same time has to be a highly dynamic structure: During cell enlargement, division, and differentiation, bacteria continuously remodel, degrade, and resynthesize their cell wall, but pivotally need to assure cell integrity during these processes. Finally, the cell wall is also adjusted according to both environmental constraints and metabolic requirements. However, how exactly this is achieved is not fully understood. The major structural component of the bacterial cell wall is peptidoglycan (PG), a mesh-like polymer of glycan chains interlinked by short-chain peptides, constituting a net-like macromolecular structure that has historically also termed murein or murein sacculus. Although the basic structure of PG is conserved among bacteria, considerable variations occur regarding cross-bridging, modifications, and attachments. Moreover, different structural arrangements of the cell envelope exist within bacteria: a thin PG layer sandwiched between an inner and outer membrane is present in Gram-negative bacteria, and a thick PG layer decorated with secondary glycopolymers including teichoic acids, is present in Gram-positive bacteria. Furthermore, even more complex envelope structures exist, such as those found in mycobacteria. Crucially, all bacteria possess a multitude of often redundant lytic enzymes, termed “autolysins”, and other cell wall modifying and synthesizing enzymes, allowing to degrade and rebuild the various structures covering the cells. However, how cell wall turnover and cell wall biosynthesis are coordinated during different stages of bacterial growth is currently unclear. The mechanisms that prevent cell lysis during these processes are also unclear.

This Research Topic focuses on the dynamics of the bacterial cell wall, its modifications, and structural rearrangements during cell growth and differentiation. It pays particular attention to the turnover of PG, its breakdown and recycling, as well as the regulation of these processes. Other structures, for example, secondary polymers such as teichoic acids, which are dynamically changed during bacterial growth and differentiation, are also covered. In recent years, our view on the bacterial cell envelope has undergone a dramatic change that challenged old models of cell wall structure, biosynthesis, and turnover. This collection of articles aims to contribute to new understandings of bacterial cell wall structure and dynamics.

Citation: Dörr, T., Moynihan, P. J., Mayer, C., eds. (2019). Bacterial Cell Wall Structure and Dynamics. Lausanne: Frontiers Media. doi: 10.3389/978-2-88963-152-0

Table of Contents

05 Editorial: Bacterial Cell Wall Structure and Dynamics

Tobias Dörr, Patrick J. Moynihan and Christoph Mayer

CHAPTER 1

THE CELL WALL AS A TARGET FOR ANTIBIOTIC DISCOVERY

09 Anthranilic Acid Inhibitors of Undecaprenyl Pyrophosphate Synthase (UppS), an Essential Enzyme for Bacterial Cell Wall Biosynthesis

Marko Jukič, Kaja Rožman, Matej Sova, Hélène Barreateau and Stanislav Gobec

18 Revisiting Anti-tuberculosis Therapeutic Strategies That Target the Peptidoglycan Structure and Synthesis

Maria João Catalão, Sérgio R. Filipe and Madalena Pimentel

CHAPTER 2

CELL WALL SYNTHESIS AND ARCHITECTURE

29 Recognition of Peptidoglycan Fragments by the Transpeptidase PBP4 From *Staphylococcus aureus*

Roberto Maya-Martinez, J. Andrew N. Alexander, Christian F. Otten, Isabel Ayala, Daniela Vollmer, Joe Gray, Catherine M. Bougault, Alister Burt, Cédric Laguri, Matthieu Fonvielle, Michel Arthur, Natalie C. J. Strynadka, Waldemar Vollmer and Jean-Pierre Simorre

43 N-Acetylmuramic Acid (MurNAc) Auxotrophy of the Oral Pathogen *Tannerella forsythia*: Characterization of a MurNAc Kinase and Analysis of its Role in Cell Wall Metabolism

Isabel Hottmann, Valentina M. T. Mayer, Markus B. Tomek, Valentin Friedrich, Matthew B. Calvert, Alexander Titz, Christina Schäffer and Christoph Mayer

55 Atomic Force Microscopy of Side Wall and Septa Peptidoglycan From *Bacillus subtilis* Reveals an Architectural Remodeling During Growth

Kang Li, Xiao-Xue Yuan, He-Min Sun, Long-Sheng Zhao, Rucong Tang, Zhi-Hua Chen, Qi-Long Qin, Xiu-Lan Chen, Yu-Zhong Zhang and Hai-Nan Su

61 The Mycobacterial Cell Envelope: A Relict From the Past or the Result of Recent Evolution?

Antony T. Vincent, Sammy Nyongesa, Isabelle Morneau, Michael B. Reed, Elitza I. Tocheva and Frederic J. Veyrier

CHAPTER 3

CELL WALL TURNOVER AND MODIFICATION

70 Distinct and Specific Role of NlpC/P60 Endopeptidases LytA and LytB in Cell Elongation and Division of *Lactobacillus plantarum*

Marie-Clémence Duchêne, Thomas Rolain, Adrien Knoops, Pascal Courtin, Marie-Pierre Chapot-Chartier, Yves F. Dufrêne, Bernard F. Hallet and Pascal Hols

- 88** *Recovery of the Peptidoglycan Turnover Product Released by the Autolysin Atl in Staphylococcus aureus Involves the Phosphotransferase System Transporter MurP and the Novel 6-phospho-N-acetylmuramidase MupG*
Robert Maria Kluj, Patrick Ebner, Martina Adamek, Nadine Ziemert, Christoph Mayer and Marina Borisova
- 102** *Functional Characterization of Enzymatic Steps Involved in Pyruvylation of Bacterial Secondary Cell Wall Polymer Fragments*
Fiona F. Hager, Arturo López-Guzmán, Simon Krauter, Markus Blaukopf, Mathias Polter, Inka Brockhausen, Paul Kosma and Christina Schäffer
- 118** *Activation of the PhoPR-Mediated Response to Phosphate Limitation is Regulated by Wall Teichoic Acid Metabolism in Bacillus subtilis*
Kevin M. Devine
- 125** *Cell Wall Hydrolases in Bacteria: Insight on the Diversity of Cell Wall Amidases, Glycosidases and Peptidases Toward Peptidoglycan*
Aurore Vermassen, Sabine Leroy, Régine Talon, Christian Provot, Magdalena Popowska and Mickaël Desvaux
- 152** *Peptidoglycan Muropeptides: Release, Perception, and Functions as Signaling Molecules*
Oihane Irazoki, Sara B. Hernandez and Felipe Cava
- 169** *The Pathogenic Neisseria Use a Streamlined Set of Peptidoglycan Degradation Proteins for Peptidoglycan Remodeling, Recycling, and Toxic Fragment Release*
Ryan E. Schaub and Joseph P. Dillard
- 181** *Mechanistic Pathways for Peptidoglycan O-Acetylation and De-O-Acetylation*
David Sychantha, Ashley S. Brott, Carys S. Jones and Anthony J. Clarke



Editorial: Bacterial Cell Wall Structure and Dynamics

Tobias Dörr^{1,2†}, Patrick J. Moynihan^{3†} and Christoph Mayer^{4**}

¹ Department of Microbiology, Weill Institute for Cell and Molecular Biology, Ithaca, NY, United States, ² Cornell Institute of Host-Microbe Interactions and Disease, Cornell University, Ithaca, NY, United States, ³ School of Biosciences, Institute of Microbiology and Infection, University of Birmingham, Birmingham, United Kingdom, ⁴ Department of Biology, Interfaculty Institute of Microbiology and Infection Medicine Tübingen, University of Tübingen, Tübingen, Germany

Keywords: peptidoglycan, cell wall, autolysin, PG recycling, turnover

OPEN ACCESS

Edited by:

Kürşad Turgay,
Max-Planck-Gesellschaft, Germany

Reviewed by:

Peter Graumann,
University of Marburg, Germany
Leendert Hamoen,
University of Amsterdam, Netherlands

*Correspondence:

Christoph Mayer
christoph.mayer@uni-tuebingen.de

†ORCID:

Tobias Dörr
0000-0003-3283-9161
Patrick J. Moynihan
0000-0003-4182-6223
Christoph Mayer
0000-0003-4731-4851

Specialty section:

This article was submitted to
Microbial Physiology and Metabolism,
a section of the journal
Frontiers in Microbiology

Received: 25 July 2019

Accepted: 20 August 2019

Published: 04 September 2019

Citation:

Dörr T, Moynihan PJ and Mayer C
(2019) Editorial: Bacterial Cell Wall
Structure and Dynamics.
Front. Microbiol. 10:2051.
doi: 10.3389/fmicb.2019.02051

Editorial on the Research Topic

Bacterial Cell Wall Structure and Dynamics

The bacterial cell wall is a complex, mesh-like structure that in most bacteria is essential for maintenance of cell shape and structural integrity. Historically, the cell wall has been of intense research interest due to its necessity for most bacteria and absence from the eukaryotic realm, positioning it as an ideal target for some of our most powerful antibiotics (Schneider and Sahl, 2010). In addition, bacterial cell wall fragments can have immunostimulatory and cytotoxic properties and thus play important roles in pathogenesis and disease (Goldman et al., 1982; Fleming et al., 1986; Royet et al., 2011; Sorbara and Philpott, 2011; Jutras et al., 2019).

The cell wall consists mainly of peptidoglycan (PG), a mesh of polysaccharide strands (composed of a poly-[N-acetylglucosamine (GlcNAc)-N-acetylmuramic acid (MurNAc)] backbone) cross-linked via short peptide bridges attached to the MurNAc residues (Vollmer et al., 2008a). PG is synthesized on the external face of the cytoplasm. Synthesis steps include cytoplasmic generation of the lipid-linked disaccharide-pentapeptide precursor lipid II, translocation of lipid II to the outside of the cell by flippases (MurJ and/or Amj); and finally assembly of the cell wall by penicillin-binding proteins (PBPs) and Shape, Elongation, Division, and Sporulation (SEDS) proteins (Ruiz, 2008; Typas et al., 2011; Meeske et al., 2015, 2016; Cho et al., 2016; Taguchi et al., 2019). The assembly process can be further subdivided into polymerization of the GlcNAc-MurNAc-pentapeptide via glycosyltransferase reactions catalyzed by class A PBPs and SEDS proteins, and crosslinking of the peptide sidestems into a tight meshwork by class A and B PBPs and L,D-transpeptidases in a not (yet) fully-understood manner (Zhao et al., 2017). In addition, the PG mesh can be decorated with secondary cell wall polymers, such as wall teichoic acids (polyol-phosphate polymers) or capsule polysaccharides that are covalently attached to PG (Rajagopal and Walker, 2017). In the case of mycobacteria, layers of polysaccharides and long-chain lipids are added to the PG layer, making the cell wall structure even more complex (Jankute et al., 2015).

While the cell wall must be rigid enough to maintain high intracellular pressures and withstand environmental assaults, it also needs to be flexible enough to allow for cellular expansion. In addition to synthesis functions, the cell wall is thus also constantly broken down, turned over, and remodeled (Park and Uehara, 2008; Reith and Mayer, 2011; Mayer et al., 2019). This is accomplished by a poorly-understood, remarkable group of enzymes that collectively can cleave and/or modify a variety of PG structures. So-called “autolysins,” for example, are a functionally

diverse group of enzymes that cut PG crosslinks (endopeptidases), peptide sidestems (amidases, carboxypeptidases), or the sugar backbone (muramidases, lytic transglycosylases) (Scheurwater et al., 2008; Vollmer et al., 2008b). PG-acetyltransferases “decorate” MurNAc backbone structures with acetyl residues, imparting increased lysozyme resistance (Moynihan and Clarke, 2011). L,D-transpeptidases (Mainardi et al., 2008) orchestrate D-amino acid (DAA) exchange reactions that can replace terminal D-Ala residues with a variety of alternative DAAs (Cava et al., 2011); this can be exploited to label PG with fluorescent compounds (Kuru et al., 2012). Many of these systems fulfill important functions such as daughter cell separation, sacculus expansion during growth, insertion of macromolecular trans-envelope protein complexes, and PG recycling (Scheurwater and Burrows, 2011; Vollmer, 2012; Johnson et al., 2013).

Due to its importance for bacterial survival and the many open questions concerning mechanistic details of synthesis and turnover, the cell wall remains at the center of a large number of active research programs. The last decade in particular has seen a resurgence in interest in the bacterial cell wall—a Pubmed search with the keywords “peptidoglycan synthesis bacteria” reveals a total of 7,762 publications, of which 3,532 (45%) were published in the last 10 years. This renewed interest has been fueled by novel imaging techniques (super-resolution imaging and the development of live cell wall stains) and by new revelations of processes that had been thought to be well-understood for decades. Some recent examples include the finding that the class A “penicillin-binding proteins” (aPBPs) require outer membrane cofactors for *in vivo* function (Paradis-Bleau et al., 2010; Typas et al., 2010), and that RodA/FtsW possess glycosyltransferase activity (Taguchi et al., 2019). At the same time, the cell wall remains a highly attractive target for antibiotic development, which has in the last decade become ever more important due to the rise in antibiotic resistance development.

In this special topic issue, we explore some new developments in the realm of bacterial cell wall biology. This collection of articles touches upon several cornerstones of PG research, with contributions focusing on the cell wall as a target for novel antibiotics, and aspects of its synthesis, turnover and modification.

THE CELL WALL AS A TARGET FOR ANTIBIOTIC DISCOVERY

In a bioinformatics tour-de-force, Jukić et al. describe novel inhibitors of UppS, an isoprenyl transferase enzyme that catalyzes a critical step in the biosynthesis of the lipid carrier molecule undecaprenol pyrophosphate (UPP). UPP is essential for the translocation of the PG precursor lipid II and other extracellular polysaccharides and thus constitutes a promising target for a novel class of cell envelope antibiotics. These inhibitors were identified by virtual docking models that predicted molecule binding based on UppS crystal structures and their interaction with a known inhibitor, bisphosphonate BPH-629. This clever

approach resulted in the identification of several inhibitors, one of them with μM range inhibitory activity.

Drug-resistant *Mycobacterium tuberculosis* strains are a major global threat that is not being adequately met with current drug discovery efforts. In their review article, Catalão et al. describe the history of peptidoglycan-targeting drugs and their use in mycobacteria. The authors provide a potential path forward by discussing recent advances such as therapies using β -lactam/ β -lactamase inhibitor combinations and the use of phage endolysins for the treatment of mycobacterial infections.

CELL WALL SYNTHESIS AND ARCHITECTURE

Using X-ray crystallography and liquid state NMR, Maya-Martinez et al. investigate the structure-function relationships of PBP4 of *Staphylococcus aureus*, a class C PBP that unexpectedly has no PG hydrolase (D,D-peptidase) activity, but only transpeptidase activity. *S. aureus* is characterized by a very high degree of PG cross-linking and PBP4 apparently plays a major role in this hyper-crosslinking. The authors show transpeptidase activity of PBP4 with disaccharide peptides *in vitro*, producing dimeric, multimeric, and cyclic products. Structural studies with an active site mutant (S75C) revealed potential binding sites for the donor and acceptor stem peptides involved in the transpeptidation reaction.

Hottmann et al. report on peptidoglycan metabolism in the oral Gram-negative pathogen *Tannerella forsythia* (Phylum Bacteroidetes). *T. forsythia* depends on an exogenous supply of the cell wall sugar N-acetylmuramic acid (MurNAc), as it lacks genes generally essential for bacteria for *de novo* synthesis of the peptidoglycan precursor UDP-MurNAc. A pathway for the catabolism of MurNAc involving a MurNAc-6 kinase (MurK) and a MurNAc-6P hydrolase (MurQ etherase) was established in *T. forsythia*, which counteracts a proposed cell wall synthesis pathway that utilizes salvaged MurNAc from the medium. Accordingly, a mutant in *murK* exhibited increased tolerance to low external MurNAc concentrations, presumably since blocking MurNAc degradation enhances peptidoglycan precursor synthesis.

The exact *in vivo* architecture of PG is poorly understood. Li et al. used Atomic Force Microscopy (AFM) for a detailed study of PG architecture, particularly at the septum, in *B. subtilis*. Surprisingly, *B. subtilis* undergoes significant changes in thickness and overall cell wall architecture in different growth phases. Li et al. were also able to isolate and image septa at varying stages of completion, visualizing the PG dynamics of septal closure at high resolution.

In a thought-provoking perspective article, Vincent et al. present a hypothesis for the evolutionary origins of the unique mycobacterial cell wall through a series of horizontal gene transfers. They support their argument by observing the distribution of key cell-wall biosynthetic enzymes across the order, which suggests that the arabinogalactan components pre-date the outer membrane and virulence related lipids. In their article, the authors propose an experiment whereby the

evolutionary origins of the leaflet could be tested by attempting to reconstruct the mycobacterial cell wall in an *Actinobacterium* that currently lacks this feature.

CELL WALL TURNOVER AND MODIFICATION

Duchêne et al. describe new phenotypes for endopeptidase mutants in *Lactobacillus plantarum*. The mechanisms of regulation and physiological functions of cell wall lytic enzymes are still poorly understood, particularly in non-model organisms. *L. plantarum* is an ideal system to study PG hydrolase phenotypes due to its relatively small number of PG lytic enzymes (a “mere” twelve!). The authors carefully dissect the cell biological consequences of the loss of *L. plantarum*’s endopeptidases and assign new putative functions to these enzymes. This study thus lifts the curtain on endopeptidase function in a Gram-positive non-model organism, which is of particular importance given the high level of redundancy of PG lytic enzymes in many model bacteria, which ordinarily makes gene-phenotype association difficult.

During cell wall turnover in the Gram-positive pathogen *S. aureus*, the MurNAc-GlcNAc disaccharide is released from PG by the major autolysin Atl and its components eventually reused for PG biogenesis. Kluj et al. report on the fate of this disaccharide, which is taken up and is concomitantly phosphorylated by a phosphotransferase system (PTS) transporter. In order to facilitate PG recycling, the product MurNAc-6P-GlcNAc is split intracellularly by a novel phospho-glycosidase (MupG), constituting the first characterized representative of a novel class of phospho-muramidase enzymes distributed mainly within the *Firmicutes* bacteria.

Hager et al. report on an intriguing mode of attachment used by some bacteria (e.g., *Bacillus anthracis* and *Paenibacillus alvei*) to bind cell-surface proteins to the cell envelope: pyruvylated secondary cell wall polymers act as high-affinity ligands for binding. In this study, the enzymatic pathway leading to the synthesis of pyruvylated disaccharide repeats, [-4-beta-GlcNAc-1,3-(4,6-Pyr)-beta-ManNAc-1-], of the *P. alvei* cell wall polymer was reconstituted. The reconstitution involved recombinant CsaB enzyme, catalyzing the attachment of a pyruvate to position 4 and 6 of ManNAc in the lipid-linked precursor molecule.

Devine provides a concise mini-review about the phosphate starvation regulation in the Gram-negative *E. coli* and the Gram-positive *B. subtilis*. In both organisms, phosphate limitation is sensed by the two-component system PhoPR. However, the mechanisms controlling the Pho response differ. In *Bacillus subtilis*, phosphate-limitation response is linked with wall teichoic acid metabolism. PhoR activity is controlled by biosynthetic intermediates of WTA metabolism, which either promotes or inhibits autokinase activity. In *E. coli*, phosphate is sensed directly through substrate-responsive conformational changes in a phosphate transporter.

Vermassen et al. give a comprehensive overview of the biochemistry and *in vivo* cleavage activity of PG lytic enzymes.

This review highlights the “mix and match” approach that many cell wall lytic enzymes have undergone, combining different PG cleavage catalytic functions (e.g., lytic transglycosylase and peptidase activity) within the same enzyme.

The unique chemical nature of PG allows it to act as a potent signaling molecule. Irazoki et al. provide an overview of the process of PG release across a broad range of bacteria and PG sensing by a wide range of hosts. The authors highlight the multiplicity of systems to generate and sense bacterial PG and suggest that there is still a great deal to be learned about the sensing of these important molecules. They conclude that this field will be driven by the development and application of new analytical technologies to identify novel PG receptors.

Peptidoglycan recycling among many Gram-negative bacteria is achieved through a core pathway of degradation, recovery and recycling. In some pathogenic *Neisseria*, the recycling system is partially defective, which leads to an increase in the release of immunostimulatory PG fragments. In their review article, Schaub and Dillard discuss some of the differences between *Neisseria* PG turnover and other, more intensively studied bacteria such as *E. coli*. They conclude by proposing *Neisseria* sp. as an attractive model system for the study of cell wall growth and turnover due to their lower number of cell wall-active enzymes, variation in cell shape, and natural competence.

In addition to variations in glycan composition and stem-peptide composition, PG can also be O-acetylated at the C-6 of MurNAc, or, less frequently, GlcNAc. Sychanta et al. provide an overview of recent advances in understanding the biochemistry of O-acetyltransferase systems in Gram-positive and Gram-negative bacteria. They also discuss current efforts at understanding the impact of inhibiting these systems and address unanswered biological questions such as the source of acetate for wall modification.

Bacterial cell wall biology remains a major frontier, both in our quest to develop a profound understanding of fundamental microbiology and to discover novel compounds that may be used to treat infections caused by antibiotic resistant bacteria. We hope that this special issue further advances this frontier and inspires additional exploration—peptidoglycan is, in many ways, still as mysterious as it was 7,762 publications ago.

AUTHOR CONTRIBUTIONS

All authors listed have made a substantial, direct and intellectual contribution to the work, and approved it for publication.

FUNDING

Research in the TD lab was supported by National Institutes of Health (NIH) grants R01AI143704 and R01GM130971. PM was supported by a BBSRC David Phillips Fellowship (grant BB/S010122/1). CM acknowledges financial support by the German research foundation (DFG: grants MA2436/7, SFB766-A15, GRK1708-B2, and TRR261-A06) and the government of the state of Baden-Württemberg (MWK-Glycobiology/Glycobiotechnology).

REFERENCES

- Cava, F., de Pedro, M. A., Lam, H., Davis, B. M., and Waldor, M. K. (2011). Distinct pathways for modification of the bacterial cell wall by non-canonical D-amino acids. *EMBO J.* 30, 3442–3453. doi: 10.1038/emboj.2011.246
- Cho, H., Wivagg, C. N., Kapoor, M., Barry, Z., P., Rohs, D. A., Suh, J. A., et al. (2016). Bacterial cell wall biogenesis is mediated by SEDS and PBP polymerase families functioning semi-autonomously. *Nat. Microbiol.* 1:16172. doi: 10.1038/nmicrobiol.2016.172
- Fleming, T. J., Wallsmith, D. E., and Rosenthal, R. S. (1986). Arthropathic properties of gonococcal peptidoglycan fragments: implications for the pathogenesis of disseminated gonococcal disease. *Infect. Immun.* 52, 600–608.
- Goldman, W. E., Klapper, D. G., and Baseman, J. B. (1982). Detection, isolation, and analysis of a released Bordetella pertussis product toxic to cultured tracheal cells. *Infect. Immun.* 36, 782–794.
- Jankute, M., Cox, J. A., Harrison, J., and Besra, G. S. (2015). Assembly of the mycobacterial cell wall. *Annu. Rev. Microbiol.* 69, 405–423. doi: 10.1146/annurev-micro-091014-104121
- Johnson, J. W., Fisher, J. F., and Mobashery, S. (2013). Bacterial cell-wall recycling. *Ann. N. Y. Acad. Sci.* 1277, 54–75. doi: 10.1111/j.1749-6632.2012.06813.x
- Jutras, B. L., Lochhead, R. B., Kloos, Z. A., Biboy, J., Strle, K., Booth, C. J., et al. (2019). Borrelia burgdorferi peptidoglycan is a persistent antigen in patients with Lyme arthritis. *Proc. Natl. Acad. Sci. U.S.A.* 116, 13498–13507. doi: 10.1073/pnas.1904170116
- Kuru, E., Hughes, H. V., Brown, P. J., Hall, E., Tekkam, S., Cava, F., et al. (2012). *In situ* probing of newly synthesized peptidoglycan in live bacteria with fluorescent D-amino acids. *Angew. Chem. Int. Ed Engl.* 51, 12519–12523. doi: 10.1002/anie.201206749
- Mainardi, J. L., Villet, R., Bugg, T. D., Mayer, C., and Arthur, M. (2008). Evolution of peptidoglycan biosynthesis under the selective pressure of antibiotics in Gram-positive bacteria. *FEMS Microbiol. Rev.* 32, 386–408. doi: 10.1111/j.1574-6976.2007.00097.x
- Mayer, C., Kluj, R. M., Muhleck, M., Walter, A., Unsleber, S., Hottmann, I., et al. (2019). Bacteria's different ways to recycle their own cell wall. *Int. J. Med. Microbiol.* doi: 10.1016/j.ijmm.2019.06.006. [Epub ahead of print].
- Meeske, A. J., Riley, E. P., Robins, W. P., Uehara, T., Mekalanos, J. J., Kahne, D., et al. (2016). SEDS proteins are a widespread family of bacterial cell wall polymerases. *Nature* 537, 634–638. doi: 10.1038/nature19331
- Meeske, A. J., Sham, L. T., Kimsey, H., Koo, B. M., Gross, C. A., Bernhardt, T. G., et al. (2015). MurJ and a novel lipid II flippase are required for cell wall biogenesis in *Bacillus subtilis*. *Proc. Natl. Acad. Sci. U.S.A.* 112, 6437–6442. doi: 10.1073/pnas.1504967112
- Moynihan, P. J., and Clarke, A. J. (2011). O-Acetylated peptidoglycan: controlling the activity of bacterial autolysins and lytic enzymes of innate immune systems. *Int. J. Biochem. Cell Biol.* 43, 1655–1659. doi: 10.1016/j.biocel.2011.08.007
- Paradis-Bleau, C., Markovski, M., Uehara, T., Lupoli, T. J., Walker, S., Kahne, D. E., et al. (2010). Lipoprotein cofactors located in the outer membrane activate bacterial cell wall polymerases. *Cell* 143, 1110–1120. doi: 10.1016/j.cell.2010.11.037
- Park, J. T., and Uehara, T. (2008). How bacteria consume their own exoskeletons (turnover and recycling of cell wall peptidoglycan). *Microbiol. Mol. Biol. Rev.* 72, 211–227. doi: 10.1128/MMBR.00027-07
- Rajagopal, M., and Walker, S. (2017). Envelope structures of gram-positive bacteria. *Curr. Top. Microbiol. Immunol.* 404, 1–44. doi: 10.1007/82_2015_5021
- Reith, J., and Mayer, C. (2011). Peptidoglycan turnover and recycling in Gram-positive bacteria. *Appl. Microbiol. Biotechnol.* 92, 1–11. doi: 10.1007/s00253-011-3486-x
- Royet, J., Gupta, D., and Dziarski, R. (2011). Peptidoglycan recognition proteins: modulators of the microbiome and inflammation. *Nat. Rev. Immunol.* 11, 837–851. doi: 10.1038/nri3089
- Ruiz, N. (2008). Bioinformatics identification of MurJ (MviN) as the peptidoglycan lipid II flippase in *Escherichia coli*. *Proc. Natl. Acad. Sci. U.S.A.* 105, 15553–15557. doi: 10.1073/pnas.0808352105
- Scheurwater, E., Reid, C. W., and Clarke, A. J. (2008). Lytic transglycosylases: bacterial space-making autolysins. *Int. J. Biochem. Cell Biol.* 40, 586–591. doi: 10.1016/j.biocel.2007.03.018
- Scheurwater, E. M., and Burrows, L. L. (2011). Maintaining network security: how macromolecular structures cross the peptidoglycan layer. *FEMS Microbiol. Lett.* 318, 1–9. doi: 10.1111/j.1574-6968.2011.02228.x
- Schneider, T., and Sahl, H. G. (2010). An oldie but a goodie—cell wall biosynthesis as antibiotic target pathway. *Int. J. Med. Microbiol.* 300, 161–169. doi: 10.1016/j.ijmm.2009.10.005
- Sorbara, M. T., and Philpott, D. J. (2011). Peptidoglycan: a critical activator of the mammalian immune system during infection and homeostasis. *Immunol. Rev.* 243, 40–60. doi: 10.1111/j.1600-065X.2011.01047.x
- Taguchi, A., Welsh, M. A., Marmont, L. S., Lee, W., Sjodt, M., Kruse, A. C., et al. (2019). FtsW is a peptidoglycan polymerase that is functional only in complex with its cognate penicillin-binding protein. *Nat. Microbiol.* 4, 587–594. doi: 10.1038/s41564-018-0345-x
- Typas, A., Banzhaf, M., Gross, C. A., and Vollmer, W. (2011). From the regulation of peptidoglycan synthesis to bacterial growth and morphology. *Nat. Rev. Microbiol.* 10, 123–136. doi: 10.1038/nrmicro2677
- Typas, A., Banzhaf, M. B., van den Berg van Saparoea B., Verheul, J., Biboy, J., Nichols, R. J., et al. (2010). Regulation of peptidoglycan synthesis by outer-membrane proteins. *Cell* 143, 1097–1109. doi: 10.1016/j.cell.2010.11.038
- Vollmer, W. (2012). Bacterial growth does require peptidoglycan hydrolases. *Mol. Microbiol.* 86, 1031–1035. doi: 10.1111/mmi.12059
- Vollmer, W., Blanot, D., and de Pedro, M. A. (2008a). Peptidoglycan structure and architecture. *FEMS Microbiol. Rev.* 32, 149–167. doi: 10.1111/j.1574-6976.2007.00094.x
- Vollmer, W., Joris, B., Charlier, P., and Foster, S. (2008b). Bacterial peptidoglycan (murein) hydrolases. *FEMS Microbiol. Rev.* 32, 259–286. doi: 10.1111/j.1574-6976.2007.00099.x
- Zhao, H., Patel, V., Helmann, J. D., and Dorr, T. (2017). Don't let sleeping dogmas lie: new views of peptidoglycan synthesis and its regulation. *Mol. Microbiol.* 106, 847–860. doi: 10.1111/mmi.13853

Conflict of Interest Statement: The authors declare that the research was conducted in the absence of any commercial or financial relationships that could be construed as a potential conflict of interest.

Copyright © 2019 Dörr, Moynihan and Mayer. This is an open-access article distributed under the terms of the Creative Commons Attribution License (CC BY). The use, distribution or reproduction in other forums is permitted, provided the original author(s) and the copyright owner(s) are credited and that the original publication in this journal is cited, in accordance with accepted academic practice. No use, distribution or reproduction is permitted which does not comply with these terms.



Anthranilic Acid Inhibitors of Undecaprenyl Pyrophosphate Synthase (UppS), an Essential Enzyme for Bacterial Cell Wall Biosynthesis

Marko Jukič¹, Kaja Rožman¹, Matej Sova¹, Hélène Barreteau² and Stanislav Gobec^{1*}

¹ Faculty of Pharmacy, University of Ljubljana, Ljubljana, Slovenia, ² Bacterial Cell Envelopes and Antibiotics Group, Institute for Integrative Biology of the Cell (I2BC), CEA, CNRS, Université Paris-Sud, Université Paris-Saclay, Gif-sur-Yvette, France

OPEN ACCESS

Edited by:

Tobias Dörr,
Cornell University, United States

Reviewed by:

Evi Stegmann,
University of Tübingen, Germany
Thomas Exner,
University of Tübingen, Germany

*Correspondence:

Stanislav Gobec
stanislav.gobec@ffa.uni-lj.si

Specialty section:

This article was submitted to
Microbial Physiology and Metabolism,
a section of the journal
Frontiers in Microbiology

Received: 04 July 2018

Accepted: 20 December 2018

Published: 14 January 2019

Citation:

Jukič M, Rožman K, Sova M,
Barreteau H and Gobec S (2019)
Anthranilic Acid Inhibitors
of Undecaprenyl Pyrophosphate
Synthase (UppS), an Essential
Enzyme for Bacterial Cell Wall
Biosynthesis.
Front. Microbiol. 9:3322.
doi: 10.3389/fmicb.2018.03322

We report the successful implementation of virtual screening in the discovery of new inhibitors of undecaprenyl pyrophosphate synthase (UppS) from *Escherichia coli*. UppS is an essential enzyme in the biosynthesis of bacterial cell wall. It catalyzes the condensation of farnesyl pyrophosphate (FPP) with eight consecutive isopentenyl pyrophosphate units (IPP), in which new *cis*-double bonds are formed, to generate undecaprenyl pyrophosphate. The latter serves as a lipid carrier for peptidoglycan synthesis, thus representing an important target in the antibacterial drug design. A pharmacophore model was designed on a known bisphosphonate **BPH-629** and used to prepare an enriched compound library that was further docked into UppS conformational ensemble generated by molecular dynamics experiment. The docking resulted in three anthranilic acid derivatives with promising inhibitory activity against UppS. Compound **2** displayed high inhibitory potency (IC₅₀ = 25 μM) and good antibacterial activity against *E. coli* BW25113 Δ*tolC* strain (MIC = 0.5 μg/mL).

Keywords: UppS, inhibitors, cell-wall, pharmacophore model, antibacterial agents, undecaprenyl pyrophosphate synthase

INTRODUCTION

The alarming increase in number of resistant bacterial strains is forcing academia and pharmaceutical companies into a hasten development of new antibacterial drugs. Therefore, new design approaches leading to discovery of new compounds, mechanisms of action or even new bacterial targets are desirable (Van Geelen et al., 2018). One of the most recent and fairly underexplored targets is UppS (EC: 2.5.1.31) (Jukic et al., 2016).

Undecaprenyl pyrophosphate synthase is an essential cytoplasmic enzyme in the biosynthesis of peptidoglycan that catalyzes the formation of isoprenoid UPP (C₅₅-PP) from FPP and IPP in

Abbreviations: AUC, area under the curve; cpds, compounds; FPP, farnesyl pyrophosphate; GlcNAc-MurNAc-pentapeptide, *N*-acetylglucosamine-*N*-acetylmuramyl-pentapeptide; IPP, isopentenyl pyrophosphate; MD, molecular dynamics; PMB, polymyxin B; ROC, receiver operating characteristic curve; SAR, structure-activity relationship; UPP, undecaprenyl pyrophosphate; UppS, undecaprenyl pyrophosphate synthase.

the presence of Mg^{2+} . UPP is a constituent of lipid II, the last peptidoglycan precursor, which is responsible for the flip-flop of the GlcNAc-MurNAc-pentapeptide moiety across the cytoplasmic membrane (Liang et al., 2002; Teng and Liang, 2012b). The enzyme is specific for the bacteria and is not present in the human cell, thus representing an important target in the development of novel antibacterial agents (Apfel et al., 1999). Despite the many published crystal structures of apo enzyme (Ko et al., 2001) or enzyme co-crystallized with substrates (Chang et al., 2004) and inhibitors (Guo et al., 2007), there is still no registered drug targeting UppS (Jukic et al., 2016).

There are currently 40 crystal structures in the PDB. Historically, first two published structures came from from *Micrococcus luteus* (PDB ID: 1F75) (Fujihashi et al., 2001) and *Escherichia coli* (PDB ID: 1JP3) (Ko et al., 2001) and were published back in 2001. Nowadays, the majority of reported crystal complexes are from the *E. coli*, but all of the reported structures belong to the same sequence similarity cluster with > 40% similarity and include Gram positive and Gram negative bacteria. Analysis of available crystal structures shows that UppS is a homodimer composed of two identical subunits, each composed of approximately 250 amino acids in length, totaling to 29 kDa. The essential information about the subunits is the extensive movement of the enzyme core and most importantly the loop at the top of the active site. More specifically, while the substrate is bound to the enzyme, the active site remains closed, however, it normally opens during the product binding before it is released (Fujihashi et al., 2001; Ko et al., 2001).

The active site of UppS is particularly large due to a rather sizable final product (55 carbon atoms), which needs to be accommodated at the catalytic gorge. Thus, it is not unexpected that the active site is shaped as a long tunnel along the length of enzyme core. The complexity of this active site is a challenge for the pharmaceutical chemists, because it can accommodate a greater number of small-molecule inhibitors and also possesses several distinct binding sites. This information has to be taken into account during an *in silico* design of new UppS inhibitors (Teng and Liang, 2012a; Kim et al., 2014).

Among the most potent UppS inhibitors are bisphosphonates, traditionally indicated for bone-related diseases, namely suppressing bone resorption and bone loss. Ever since the pamidronate FDA approval in 1991, bisphosphonates have been widely prescribed, yet the precise mechanistic properties are still unclear (Allen, 2018). Surprisingly, the most recent studies suggest that bisphosphonates are promising opioid alternatives for the treatment of chronic pain, more specifically the complex regional pain syndrome type I (CRPS-I); however, this mechanism of action also needs to be clarified (Kaye et al., 2018). Ultimately, it has been shown that some bisphosphonates bind to and inhibit UppS. Their structure mimics the pyrophosphate moiety of the substrates IPP and FPP, thus indicating the possible mechanism of action, which was solidified with published co-crystal structures (Figure 1). With 40 available crystal structures, 19 report small-molecule inhibitors and amongst them, 6 are with bisphosphonate inhibitors (Guo et al., 2007). Among all of 40 reported structures, crystal complex of bisphosphonate inhibitor BPH-629 in *E. coli* UppS (PDB ID: 2E98) displays the

highest resolution of 1.9 Å and was used in our work. One of the four known binding sites of bisphosphonates coincides with the FPP binding site, shown as binding site 1 on Figure 1.

Over the years, there has been a few *in silico* studies performed on UppS in an attempt to design new UppS inhibitors (Kuo et al., 2008; Peukert et al., 2008; Kim et al., 2014; Sinko et al., 2014). They have been successful only to some extent due to the complexity of the enzyme dynamics and high flexibility of the enzyme. However, bisphosphonates remain the most visible inhibitors to this day (Jukic et al., 2016).

Another extensive study of UppS active site flexibility using a molecular dynamics simulation showed the importance of the so called expanded pocket for the computer-aided drug design (Sinko et al., 2011). This expanded pocket state occurs during the ligand binding and reaches up to a total volume of 1032 Å³, as could be seen in a co-crystal structure of bisphosphonate BPH-629 (Figure 2) with *E. coli* UppS (PDB: 2E98). Upon ligand removal the active site pocket shrinks down to a volume of 432 Å³, which is slightly larger than a final volume of an *apo*-UppS form (332 Å³, PDB: 3QAS). These types of inhibitors compared to non-bisphosphonates need a greater active site expanding due to the nature of their multiple binding. For example, the known tetramic acids and dihydropyridin-2-one-3-carboxamide inhibitors (Peukert et al., 2008), which bind to FPP binding site (Binding site 1; Figure 1), only require an active site of approximately 300 Å³ in volume. This implies that of the known UppS inhibitors, only bisphosphonates bind to an open enzyme form, while others bind to the closed form, which is similar to the non-ligand bound *apo* state (Sinko et al., 2011). The expanded pocket of the open enzyme form was thus proven to be the most suitable for molecular docking.

In this paper, we present a combination of pharmacophore design and molecular dynamics as a possible approach for discovery of new UppS inhibitors. For this purpose a known crystal structure of the enzyme with the bisphosphonate BPH-629 (PDB ID: 2E98) was taken as a starting point for the design of new UppS inhibitors.

MATERIALS AND METHODS

Cloning, Overexpression, and Purification of the *E. coli* UppS

An overnight preculture of *E. coli* C43(DE3) carrying the pET2130::uppS_{Ec} plasmid was used to inoculate 1 liter of 2YT medium supplemented with ampicillin. The culture was incubated with shaking at 37°C until the optical density at 600 nm reached 0.8. Isopropyl-β-D-thiogalactopyranoside (IPTG) was added to a final concentration of 1 mM and incubation was continued for 3 h at 37°C. The cells were then harvested at 4°C and the pellet was washed with buffer A (20 mM Hepes (pH 7.5), 150 mM NaCl). The cells were resuspended in the same buffer (10 mL) and disrupted by sonication in the cold using a Bioblock Vibracell 72412 sonicator. The resulted suspension was centrifuged at 4°C for 30 min at 100,000 × g with a Beckman

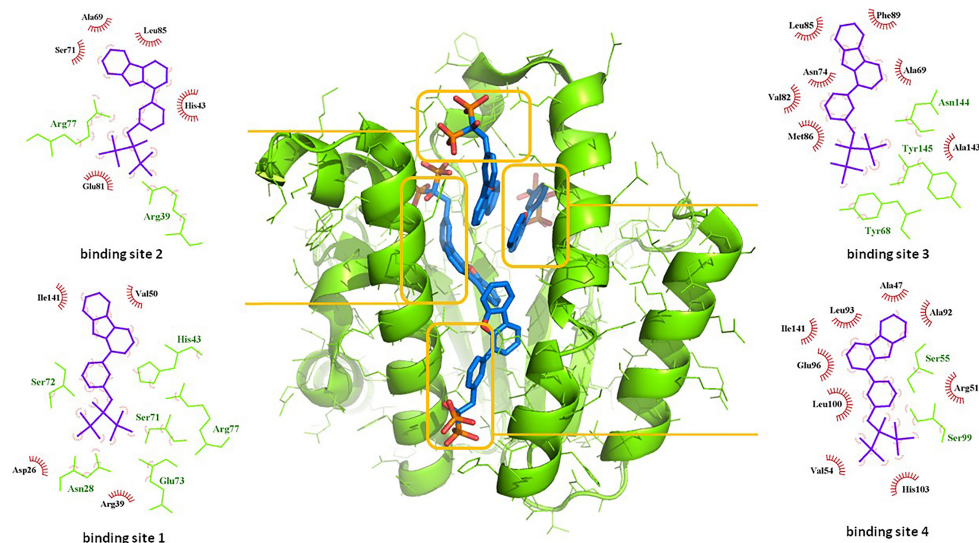


FIGURE 1 | Binding sites of co-crystallised bisphosphonate inhibitor (depicted in blue stick model; BPH-629) in *E. coli* UppS (presented as a green-colored ribbon model; PDB ID: 2E98). Four observed binding sites (emphasized) are presented with small-molecule inhibitor in blue, amino acid residues forming polar contacts in green with residues that form lipophilic interactions in red.

TL100 apparatus and the pellet was discarded. The supernatant was kept at -20°C until purification.

The N-terminal His₆-tagged UppS_{Ec} protein was purified on Ni²⁺-nitrilotriacetate (Ni²⁺-NTA) agarose according to Qiagen® recommendations. All procedures were performed at 4°C . To perform the binding experiment, the supernatant was mixed with Ni²⁺-NTA-agarose beads for 1 h that had previously been washed with buffer B (buffer A containing 10 mM imidazole). The washing and elution steps were performed with a discontinuous gradient of imidazole (10 to 250 mM) in buffer A. Eluted proteins were analyzed by sodium dodecyl sulfate-polyacrylamide gel electrophoresis (SDS-PAGE) and the relevant fractions were pooled and dialyzed into 100 V of buffer A. The protein concentration was determined by nano-volume spectrophotometry (molecular mass of Nter-His₆ UppS = 29,542 Da; $\epsilon_{\text{M}} = 38,960 \text{ M}^{-1}\cdot\text{cm}^{-1}$). For the storage of the protein at -20°C , glycerol was added to the buffer to a final concentration of 10%.

UppS Inhibition Assay

The UppS enzymatic activity was determined by using a kinetics-based assay utilizing a radiolabeled substrate. The assay revolves on the measuring of UPP formation in the reaction mixture in a final volume of 40 μL . Stock solutions of all compounds (2 mM) were prepared in DMSO and the final concentration of DMSO in the assay was 5% (v/v). The enzyme was diluted in buffer A to appropriate concentration so that the consumption of the substrate in the assay is no higher than 30%. The reaction mixture consisted of 20 μL of 100 mM HEPES, pH 7.5, 50 mM KCl, 0.5 mM MgCl₂, 1.5 μM FPP, 12 μM [¹⁴C]-IPP ([¹⁴C]-IPP; 289 Bq), 2 μL DMSO with or without the inhibitor and 18 μL of optimal enzyme solution. The reaction was initiated by adding the

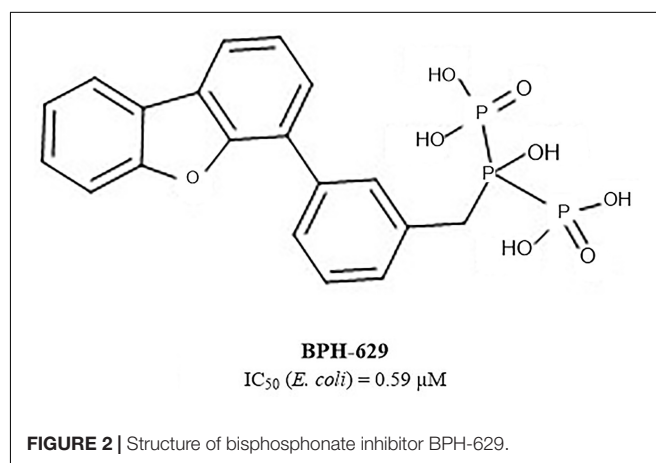


FIGURE 2 | Structure of bisphosphonate inhibitor BPH-629.

enzyme to the reaction mixture and was observed for 30 min at 25°C before being stopped by freezing with liquid nitrogen. Reaction mixture was lyophilized and resuspended in 10 μL of purified water. The radiolabeled substrate, [¹⁴C]-IPP, and the product, [¹⁴C]UPP, were separated on a Silica gel 60 TLC plate using 1-propanol / ammonium hydroxide / water in ratio of 6/3/1 (v/v/v) as a mobile phase ($R_{\text{f}}([^{14}\text{C}]\text{-IPP}) = 0.21$, $R_{\text{f}}([^{14}\text{C}]\text{-UPP}) = 0.56$), and quantified with a radioactivity scanner (Rita Star, Raytest Isotopenmessgeräte GmbH, Straubenhardt, Germany). Residual activities (RAs) were calculated with respect to a control reaction without the tested compounds and with 5% DMSO. All the experiments were run in duplicate with standard deviations within $\pm 10\%$. The IC_{50} values represented the concentrations for which the RA was 50% and were determined by measuring the RAs at seven different compound concentrations.

TABLE 1 | Antibacterial activity of the most potent three UppS inhibitors against wild-type and efflux pump-deficient *E. coli* BW25113 strains with (+PMB) or without (–PMB) polymyxin B-formed permeable membrane.

	MIC (μg/mL)							
	BW25113		BW25113 Δ acrA		BW25113 Δ acrB		BW25113 Δ tolC	
	–PMB	+PMB	–PMB	+PMB	–PMB	+PMB	–PMB	+PMB
1	>32	>32	>32	2	>32	2	>32	>32
2	>32	>32	>32	>32	>32	>32	0.5	0.5
3	>32	>32	>32	2	>32	2	>32	>32

Microbiological Evaluation

The three compounds 1, 2, and 3 were tested for their antibacterial activity against the WT and efflux pump-deficient (Δ acrA, Δ acrB and Δ tolC) *E. coli* BW25113 strain (Table 1). The strains were cultivated in liquid medium at 37°C and inoculated in a 3-mL top agar at a final concentration of 10⁸ CFU/mL on agar plates. Then, spots of 4 μL of each compound (range concentration serially diluted from 32 μg/mL to 0.5 μg/mL) were performed on each strain, in the presence or not of 0.025 μg/mL of polymyxine B to assess the impact of outer-membrane permeability on antimicrobial activity. Finally, the antibacterial activity was observed after incubating the plates ON at 37°C. All the experiments were performed according to CLSI guidelines.

RESULTS AND DISCUSSION

Pharmacophore Modeling

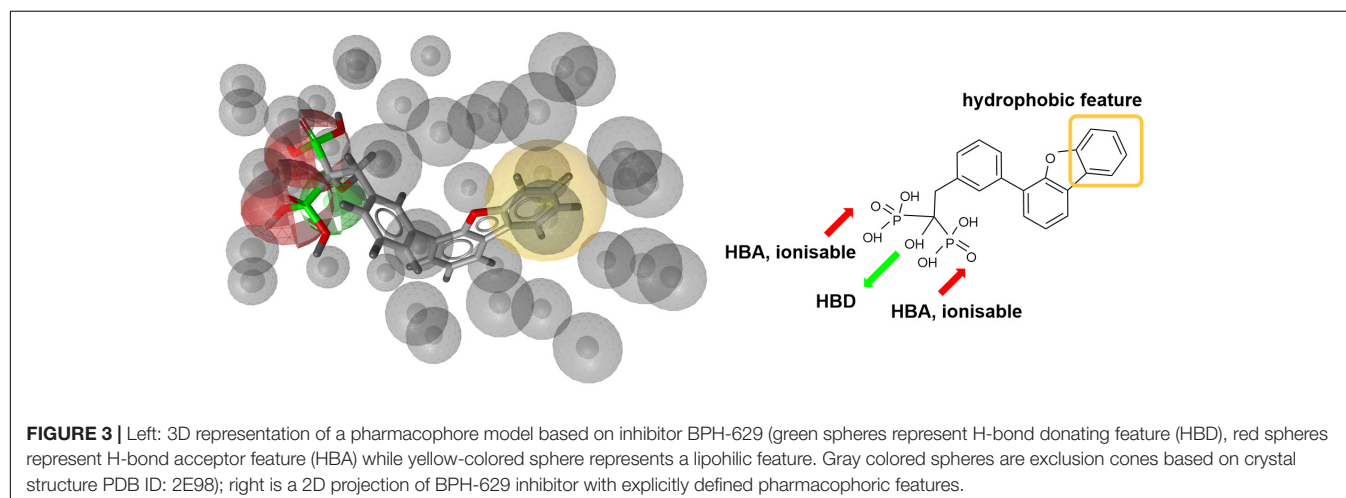
Docking of large libraries of compounds is not only complex but also time-consuming. Therefore, it is highly important to use a quality compound database for any *in silico* drug design. We used ZINC database of compounds, specifically 10.7 million Drugs Now subset of the ZINC library where compounds with immediate commercial availability are collected (Irwin and Shoichet, 2005). Prior to our docking experiment, hierarchical

filtering of the compound database was performed. Database was first processed with the FILTER software (OpenEye Scientific Software, Inc., Santa Fe, NM, United States¹) to eliminate small fragments or molecules with a greater MW than 1000 g/mol, known or predicted aggregators and the compounds with predicted poor solubility (Shoichet, 2006). Compound retention parameters used were 300 ≤ MW ≤ 1000, 0 ≤ rotational bonds ≤ 15, 4 ≤ rigid bonds ≤ 55, –4 ≤ clogP ≤ 6.85; detailed filter configuration can be found in supporting information. Finally, compound database was filtered for PAINS using RDKit² Python API software (Baele and Holloway, 2010). In this final step, every structure in the library was compared to the selection of PAINS structures defined in SMARTS format and removed from the database if found similar (Saubern et al., 2011; PAINS definitions in SMARTS format can be found in supporting info.). The initial compound library was thus reduced to a library of approximately 6.5 million compounds and 3D conformer database prepared with omega2 fast protocol within LigandScout as detailed in the supporting information.

Next step was pharmacophore modeling in a consecutive library filtering effort in order to produce an enriched library for docking experiments. Pharmacophore model (Figure 3) was designed using LigandScout program (Wolber and Langer, 2005) based on the structural data of known bisphosphonate inhibitor BPH-629 (Figure 2) binding mode in UppS binding site 1 (Figure 1; PDB ID: 2E98). Specific features of the inhibitor were used to pinpoint the previously described key interactions with the enzyme (Jukic et al., 2016). Ten similar pharmacophore models were generated and validated in a VS experiment using a library of reported bisphosphonates (Guo et al., 2007) and decoy compounds generated on the basis of each active bisphosphonate with the help of DUD-E database (Mysinger et al., 2012). The best model according to ROC AUC was used for filtering of prepared compound library (Figure 3). The model was defined by specifically negative ionisable features and/or H-bond acceptors at the BPH-629 bisphosphonic acid moiety, aliphatic hydroxyl

¹www.eyesopen.com

²http://www.rdkit.org/; access September 16, 2018



group was marked as hydrophilic H-bond donor feature and distant aromatic ring as a hydrophobic feature in order to keep the pharmacophore model feature count low and produce a useful model for future filtering (Wolber and Langer, 2005). The exclusion zones calculated by the software on the basis of crystallized **BPH-629** binding mode (PDB ID: 2E98) have been included in the final pharmacophore model. If additional lipophilic features were used in the pharmacophore model or tolerance spheres defined closely along the **BPH-629** features, constructed models proved to be over-defined and could not be used as a filter in future steps. In the final step, initial compound library was filtered where individual conformer molecular features were enumerated and a 3D superposition on the pharmacophore model was attempted where pharmacophoric elements had to be satisfied within the defined spherical bounds and one possible missing feature (LigandScout software Pharmacophore-Fit scoring function). The exclusion zones further limited the space available for the individual conformer to superpose and satisfy the pharmacophore model. Thus a final library of 13530 compounds was prepared and docked in the protein conformation ensemble obtained from MD experiment and clustering of protein conformations along the MD trajectory (see **Supplementary Data** for more details).

Molecular Dynamics

Crystal complex (PDB ID: 2E98) was prepared with Yasara software (Krieger and Vriend, 2015). Missing hydrogens were added, overlapping atoms adjusted, missing residues modeled, hydrogen bonds optimized and residue ionization assigned at pH = 7.4, consistently with previous reports (Krieger et al., 2006; Krieger et al., 2012; Jukic et al., 2016). Cubic system (10 Å around all atoms) was solvated using TIP3P water model and 0.9% of NaCl added to the solvation system. Finally, NPT (periodic boundary conditions) ensemble production run at 310 K was initiated. Simulation using AMBER14 force field produced 20 ns

trajectory with snapshot saved every 10 ps (Hornak et al., 2006). Energy parameters of the system were stable through production run as was root-mean-square deviation (RMSD) values for protein backbone. MD snapshots in 100 ps increments were collected (200 protein conformation models), clustered using ClusCo software and visually analyzed with Pymol 3 software (DeLano, 2002). ClusCo software parameters used were hierarchical clustering in a pairwise average-linkage manner with backbone rmsd score. 10 clusters were identified by ClusCo and centroid structures were selected as protein conformations that represent the movement of the *E. coli* UppS (**Figure 4**, left) (Jamroz and Kolinski, 2013).

Structure-Based Virtual Screening

Ensemble docking experiment (**Figure 4**, right) was performed using GOLD (CCDC Enterprise; 5.5 version). Ten protein structures obtained from clustered (ClusCo) MD trajectory were aligned to the first structure used in the trajectory, imported in Hermes GOLD where hydrogens were corrected/added. Positioning of Asn, Gln, and His tautomers were left intact as calculated through MD experiment. Waters and Ligands were removed and the proteins were kept rigid during docking experiment. Binding site was defined as a 7 Å region around the area occupied by BPH-629 co-crystallized ligand in the binding site 1 relative to the spacing of first structure used in the trajectory (**Figure 1**). Detect cavity setting was used and all H-bond donors/acceptors were forced to be treated as solvent accessible. All planar R-NR₁R₂ were able to flip as well as protonated carboxylic acids. Torsion angle distributions and rotatable bond postprocessing were set at default. Docking was performed with Chemscore scoring function with early termination enabled and default GOLD parameter file used. Genetic algorithm settings were set at ensemble. Parallel gold calculation was performed with concatenation of results and retention of best binding poses. No constraints were used in docking experiment. The results

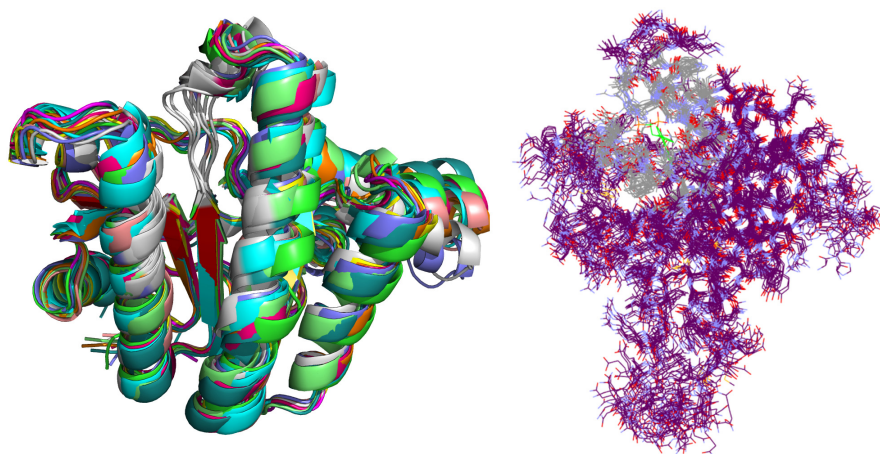


FIGURE 4 | Selected snapshots of *E. coli* UppS obtained with MD and ClusCo clustering. Individual chains are presented in ribbon model colored distinctly for every snapshot used in the ensemble docking experiment. In this manner, movement of the protein along the MD trajectory is emphasized and observed (left). Defined binding site for GOLD ensemble docking experiment in gray-colored line model representation; in green colored line representation there is the center residue of the defined binding site for docking experiment while the rest of the protein is depicted as purple colored line model (right).

were analyzed using DataWarrior software and sorted according to the GOLD ChemScore Fitness. From the entire workflow as composed in **Figure 5**, the 34 top-scoring compounds were purchased from several vendors (see **Supplementary Data** and **Supplementary Table S1**) and evaluated biochemically and microbiologically.

Biological Evaluation

The 34 purchased compounds were tested for their inhibitory potencies against *E. coli* UppS using a radioactivity-based assay. In these test conditions, the [^{14}C]-UPP formation is observed thanks to a radiolabeled substrate ([^{14}C]-IPP) and quantified with a radioactivity scanner. The results are presented as RAs of UppS in the presence of 100 μM of each compound (**Supplementary Table S1**). For the compounds with RAs below 50%, the IC_{50} values were determined. Sodium risedronate was used as a positive control to enable the comparison of the purchased compounds to a known inhibitor and to confirm the results of the UppS inhibition assay. Three compounds showed promising inhibitory potencies against *E. coli* UppS in micromolar range (1–3, **Figure 6**). All three inhibitors are anthranilic acid derivatives with a larger hydrophobic moiety attached to the amide group *via* different linkers, 2-cyanoacryloyl for compounds 1 and 2 and 2-thioacetyl for compound 3. Of those, compound 1 was the highest ranking virtual screening hit with ChemScore GOLD Fitness ChemScore of 41.82 and

an IC_{50} value of 45 μM . On the other hand, the compound 3 showed the highest *in vitro* potency with IC_{50} value of 24 μM (*in silico* ChemScore of 32.9201) and is approximately 28-fold more potent than risedronate ($\text{IC}_{50} = 660 \mu\text{M}$) (Guo et al., 2007). The inhibitory potency of compound 2 ($\text{IC}_{50} = 25 \mu\text{M}$) is considered similar as in compound 3.

Binding Site Analysis

Interestingly, the ensemble docking experiment identified anthranilic acid moiety as favorable and compounds were commonly bound to similar protein conformations and binding site volumes, specifically, superimposed protein conformations on the starting crystal complex (PDB ID: 2E98) with backbone RMSD of 1.23 Å, binding site volume 814.625 Å³ (compounds 1, 2) and 1.39 Å, binding site volume 968.975 Å³ for compound 3. Calculation is in accordance with previous observations and alike bisphosphonates, identified inhibitors bind to the open enzyme form. Similar observations were reported earlier for benzoic acid inhibitors (Figure 6; Zhu et al., 2013) where benzoic acid moiety served as a pyrophosphate mimetic and was connected to a polyaromatic scaffold as mimic of the native substrate (FPP) lipophilic tail (PDB ID: 3SGV; Figure 6). Thus, we postulate the new reported inhibitors (compounds 1–3) could bind to FPP binding site and act as competitive inhibitors. Furthermore, anthranilic acid moiety as a pyrophosphate mimetic has been reported previously, and it has also been conjugated to the

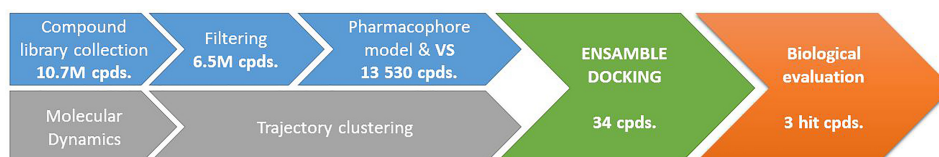


FIGURE 5 | Completed workflow used for identification of UppS inhibitors. Number of processed compounds (cpds.) is indicated under individual steps.

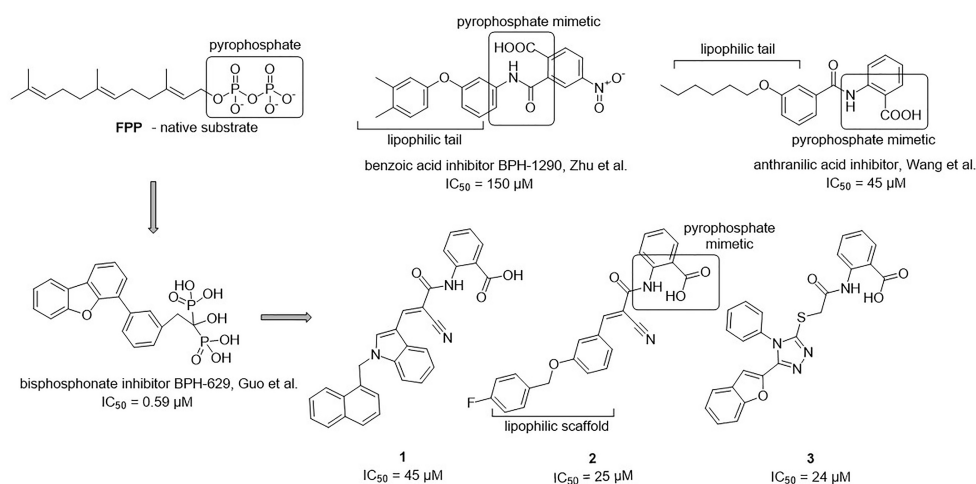


FIGURE 6 | Structural comparison of UppS native substrate farnesyl pyrophosphate (FPP), benzoic acid inhibitor (Zhu et al., 2013), anthranilic acid inhibitor (Wang et al., 2016), bisphosphonate inhibitor (Guo et al., 2007) and new inhibitors of *E. coli* UppS discovered by structure-based virtual screening.

lipophilic tail in order to mimic FPP. Wang and coworkers also commented that the electron withdrawing groups on the anthranilic acid moiety improved the potency, while phosphonic acid analogs demonstrated reduced activity (Wang et al., 2016). This reported data can be directly applied for future optimisation of reported inhibitors. Namely, compounds **1–3** possess an

unsubstituted anthranilic acid as a known pyrophosphate mimetic moiety with distinct lipophilic scaffolds to previously published inhibitors. Furthermore, the aforementioned inhibitors by Wang et al. were not evaluated on *E. coli* UppS but Gram positive *Staphylococcus aureus* bacterial strain. Accordingly, to the best of our knowledge, this is the first time this type of compounds

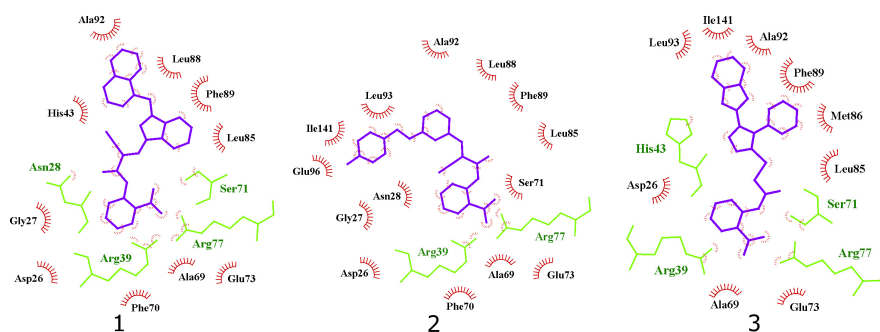


FIGURE 7 | 2D projection of calculated binding modes of reported inhibitors **1–3** in their respective UppS protein binding sites. 1. Small-molecules are colored blue, amino acid residues forming polar contacts are green. Residues that form lipophilic contacts with small-molecule are presented in black and red and are partially encircled.

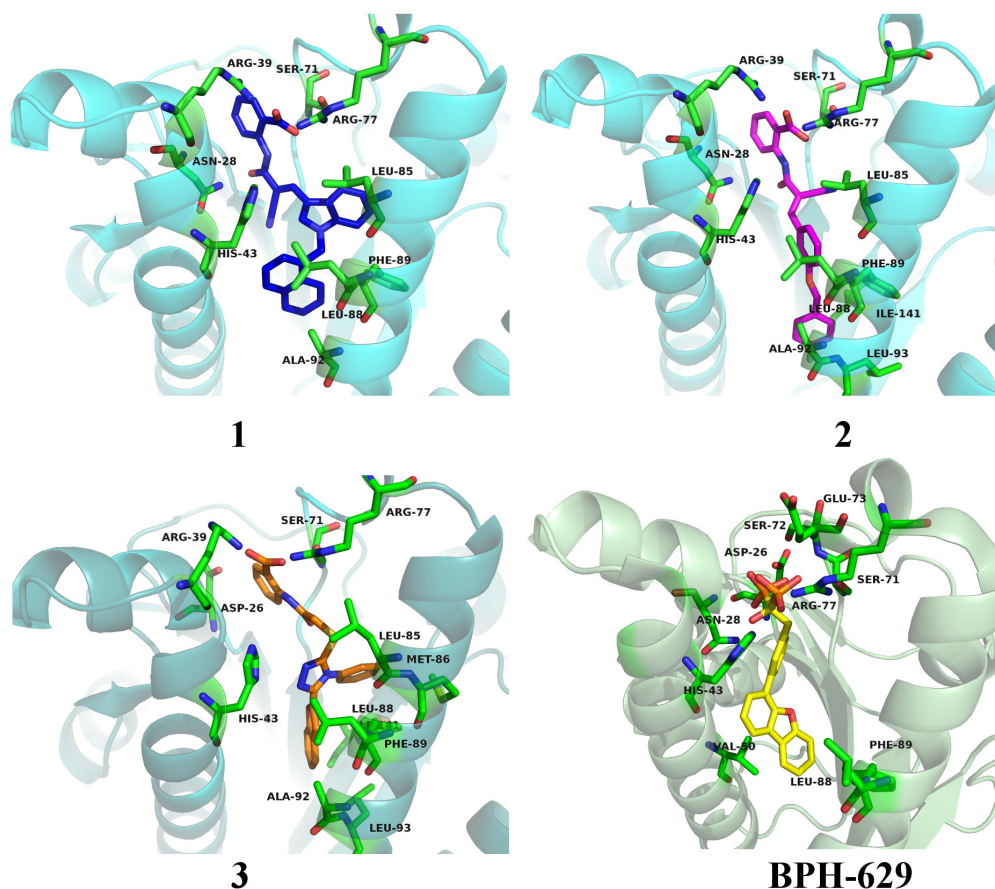


FIGURE 8 | Binding modes of compounds **1–3** (presented in blue, magenta and orange colored stick models, respectively) in UppS active site (PDB ID: 2E98). Co-crystallised ligand **BPH-629** is shown as yellow stick model. Protein is depicted as blue or green colored ribbon model with amino acid residues around ligands presented green colored stick models.

are shown to inhibit *E. coli* UppS. The predicted binding mode of inhibitors **1–3** is shown in **Figure 7** (Laskowski and Swindells, 2011).

All three compounds share a similar binding motif where anthranilic acid moiety interacts with phosphate binding pocket (**Figure 7**). Anthranilic acid carboxylate forms ionic and H-bonds with Arg39 and Arg77 residues that are further stabilized with H-bond toward Ser71. Amide bond connecting anthranilic fragment in all three molecules is positioned in a polar pocket where favorable H-bond interactions with Ala69, Phe70, Ser71 or Met25, Asp26 backbone amides are available. Compounds **1** and **2** therefore form H-bonds with Asn28 or Ser71 through amide or neighbor nitrile functional groups while compound **3** forms a H-bond with His43 via its central triazole moiety. Most potent compound **3** further descends in a voluminous UppS active site gorge where its flexible tie-ether linker enables effective π - π stacking interaction between Phe89 and phenyltriazole central moiety. Compound **3** additionally makes hydrophobic contacts with Ala47, Val50, Leu85, Met86, Leu88, Phe89, Ala92, Leu93, and Ile141 residues. Compounds **1** and **2** share a similar binding motif, reaching deeper into active site gorge via an acrylonitrile linker moiety. Compounds **1** and **2** therefore make hydrophobic contacts toward Leu85, Leu88, Phe89, and Ala92, while compound **2** additionally interacts with Leu93 and Ile141. Comparatively, co-crystallized bisphosphonate BPH-629 analogously positions its acidic moieties at the top of the gorge making an ionic interaction with Arg77 and H-bonds toward Gly29, Ser72, His43, and Asn28 (**Figure 8**). It then immediately descends to the lipophilic gorge via a 1,3-substituted benzene fragment where it forms lipophilic contacts with Met25, His43, Ala47, Val50, Ala69, and Ile141. Branched nature of compounds **1** and **3** can thus effectively account for favorable positioning in a lipophilic active site gorge with additional lipophilic contacts (Leu85, Leu88, Met86, and Phe89). Compound **2** reaches down the active site gorge due to sheer compound length where lipophilic interactions with Ala92 and Leu93 are possible (**Figure 8**). All three compounds can also be described as spanning to other binding sites (**2, 3, Figure 1**) and have space for further optimization.

Antimicrobial Evaluation

Upon *in vitro* examination, no antibacterial activity was observed for all three inhibitors (**1–3**) when evaluated with wild-type *S. aureus* and *E. coli* bacterial strains so further examination was conducted (**Table 1**). *E. coli* AcrAB-TolC is a tripartite multidrug efflux pump system that expels compounds from the cell and this represents one of the possible mechanisms of bacterial defence against xenobiotics (Kim et al., 2015). Further microbiological evaluation revealed that lack of antibacterial activity of UPPS inhibitors against *E. coli* can be attributed to their active transport from the bacterial cytoplasm by efflux pumps. Compounds **1** and **3** were inactive against all strains without a permeable membrane (MIC > 32 μ g/mL), but showed improved MIC values in efflux deficient *E. coli* BW25113 Δ acrA and Δ acrB strains in the presence of PMB (MIC = 2 μ g/mL in both). On the other hand, compound **2** inhibited bacterial growth in both *E. coli* BW25113 Δ tolC strains with or without permeable membrane

(MIC = 0.5 μ g/mL). The antibacterial activity in the efflux pump-deficient *E. coli* BW25113 Δ tolC strain is independent from the presence of polymyxine B. Therefore, it can be postulated on the basis of the evaluation of compound **2**, that transport across *E. coli* cell membrane is possible. This compound therefore represents an interesting starting point for further development, for example computational searches of similar compounds and analog synthesis.

CONCLUSION

We have demonstrated a successful implementation of virtual screening techniques in the discovery of *E. coli* UppS inhibitors. With the use of molecular modeling software, we designed a bisphosphonate-based pharmacophore model and used molecular dynamics together with ensemble docking to obtain three novel micromolar UppS inhibitors. These reported anthranilic acid derivatives mimic the structure of polar pyrophosphate and lipophilic moieties of UppS substrates FPP and IPP. Among the 34 top-scoring compounds, the most potent compound **2** displayed inhibitory potency with an IC₅₀ value of 25 μ M and good antibacterial activity against *E. coli* BW25113 Δ tolC with or without a permeable membrane (MIC = 0.5 μ g/mL). Our anthranilic acid derivatives **1–3** have distinct chemical structures compared to previously known *E. coli* UppS inhibitors, therefore representing a novel starting point for antibacterial drug design targeting UppS.

AUTHOR CONTRIBUTIONS

MJ, KR, and SG conceived and designed the experiments. MJ, KR, MS, and HB performed the experiments. MJ, KR, MS, and SG analyzed the data. All co-authors wrote the manuscript.

FUNDING

This study was supported by the Slovenian Research Agency (Grant P1-0208) and by the Centre National de la Recherche Scientifique [CNRS, Projet International de Recherche Scientifique (PICS) 7757].

ACKNOWLEDGMENTS

We thank Inte:Ligand (Software-Entwicklungs und Consulting GmbH, Maria Enzersdorf, Austria) and CCDC (The Cambridge Crystallographic Data Centre) for their support. We also thank Delphine Patin (I2BC) and Rodolphe Auger (I2BC) for technical help.

SUPPLEMENTARY MATERIAL

The Supplementary Material for this article can be found online at: <https://www.frontiersin.org/articles/10.3389/fmicb.2018.03322/full#supplementary-material>

REFERENCES

- Allen, M. R. (2018). Recent advances in understanding bisphosphonate effects on bone mechanical properties. *Curr. Osteoporos. Rep.* 16, 198–204. doi: 10.1007/s11914-018-0430-3
- Apfel, C. M., Takacs, S., Fountoulakis, M., Stieger, M., and Keck, W. (1999). Use of genomics to identify bacterial undecaprenyl pyrophosphate synthetase: cloning, expression, and characterization of the essential *uppS* gene. *J. Bacteriol.* 181, 483–492.
- Baell, J. B., and Holloway, G. A. (2010). New substructure filters for removal of pan assay interference compounds (PAINS) from screening libraries and for their exclusion in bioassays. *J. Med. Chem.* 53, 2719–2740. doi: 10.1021/jm901137j
- Chang, S. Y., Ko, T. P., Chen, A. P. C., Wang, A. H. J., and Liang, P. H. (2004). Substrate binding mode and reaction mechanism of undecaprenyl pyrophosphate synthase deduced from crystallographic studies. *Protein Sci.* 13, 971–978. doi: 10.1110/ps.03519904
- DeLano, W. L. (2002). The PyMOL Molecular Graphics System. Available at: <http://www.pymol.org>
- Fujihashi, M., Zhang, Y. W., Higuchi, Y., Li, X. Y., Koyama, T., and Miki, K. (2001). Crystal structure of cis-prenyl chain elongating enzyme, undecaprenyl diphosphate synthase. *Proc. Natl. Acad. Sci. U.S.A.* 98, 4337–4342. doi: 10.1073/pnas.071514398
- Guo, R. T., Cao, R., Liang, P. H., Ko, T. P., Chang, T. H., Hudock, M. P., et al. (2007). Bisphosphonates target multiple sites in both cis- and trans-prenyltransferases. *Proc. Natl. Acad. Sci. U.S.A.* 104, 10022–10027. doi: 10.1073/pnas.0702254104
- Hornak, V., Abel, R., Okur, A., Strockbine, B., Roitberg, A., and Simmerling, C. (2006). Comparison of multiple amber force fields and development of improved protein backbone parameters. *Proteins* 65, 712–725. doi: 10.1002/prot.21123
- Irwin, J. J., and Shoichet, B. K. (2005). ZINC - A free database of commercially available compounds for virtual screening. *J. Chem. Inf. Model.* 45, 177–182. doi: 10.1021/ci049714+
- Jamroz, M., and Kolinski, A. (2013). ClusCo: clustering and comparison of protein models. *BMC Bioinformatics* 14:62. doi: 10.1186/1471-2105-14-62
- Jukic, M., Rozman, K., and Gobec, S. (2016). Recent advances in the development of undecaprenyl pyrophosphate synthase inhibitors as potential antibacterials. *Curr. Med. Chem.* 23, 464–482. doi: 10.2174/0929867323666151231094854
- Kaye, A. D., Cornett, E. M., Hart, B., Patil, S., Pham, A., Spalitta, M., et al. (2018). Novel pharmacological nonopioid therapies in chronic pain. *Curr. Pain Headache Rep.* 22:31. doi: 10.1007/s11916-018-0674-8
- Kim, J. S., Jeong, H., Song, S., Kim, H. Y., Lee, K., Hyun, J., et al. (2015). Structure of the tripartite multidrug efflux pump AcrAB-TolC suggests an alternative assembly mode. *Mol. Cells* 38, 180–186. doi: 10.14348/molcells.2015.2277
- Kim, M. O., Feng, X. X., Feixas, F., Zhu, W., Lindert, S., Bogue, S., et al. (2014). A molecular dynamics investigation of mycobacterium tuberculosis prenyl synthases: conformational flexibility and implications for computer-aided drug discovery. *Chem. Biol. Drug Design* 85, 756–769. doi: 10.1111/cbdd.12463
- Ko, T. P., Chen, Y. K., Robinson, H., Tsai, P. S., Gao, Y. G., Chen, A. P. C., et al. (2001). Mechanism of product chain length determination and the role of a flexible loop in *Escherichia coli* undecaprenyl-pyrophosphate synthase catalysis. *J. Biol. Chem.* 276, 47474–47482. doi: 10.1074/jbc.M106747200
- Krieger, E., Dunbrack, R. L., Hooft, R. W., and Krieger, B. (2012). Assignment of protonation states in proteins and ligands: combining pKa prediction with hydrogen bonding network optimization. *Methods Mol. Biol.* 819, 405–421. doi: 10.1007/978-1-61779-465-0_25
- Krieger, E., Nielsen, J. E., Spronk, C. A., and Vriend, G. (2006). Fast empirical pKa prediction by Ewald summation. *J. Mol. Graph. Model.* 25, 481–486. doi: 10.1016/j.jmgm.2006.02.009
- Krieger, E., and Vriend, G. (2015). New ways to boost molecular dynamics simulations. *J. Comput. Chem.* 36, 996–1007. doi: 10.1002/jcc.23899
- Kuo, C. J., Guo, R. T., Lu, I. L., Liu, H. G., Wu, S. Y., Ko, T. P., et al. (2008). Structure-based inhibitors exhibit differential activities against *Helicobacter pylori* and *Escherichia coli* undecaprenyl pyrophosphate synthases. *Biomed. Res. Int.* 2008:841312. doi: 10.1155/2008/841312
- Laskowski, R. A., and Swindells, M. B. (2011). LigPlot+: multiple ligand-protein interaction diagrams for drug discovery. *J. Chem. Inf. Model.* 51, 2778–2786. doi: 10.1021/ci200227u
- Liang, P. H., Ko, T. P., and Wang, A. H. J. (2002). Structure, mechanism and function of prenyltransferases. *Eur. J. Biochem.* 269, 3339–3354. doi: 10.1046/j.1432-1033.2002.03014.x
- Mysinger, M. M., Carchia, M., Irwin, J. J., and Shoichet, B. K. (2012). Directory of useful decoys, enhanced (DUD-E): better ligands and decoys for better benchmarking. *J. Med. Chem.* 55, 6582–6594. doi: 10.1021/jm300687e
- Peukert, S., Sun, Y. C., Zhang, R., Hurley, B., Sabio, M., Shen, X., et al. (2008). Design and structure-activity relationships of potent and selective inhibitors of undecaprenyl pyrophosphate synthase (UPPS): tetramic, tetrionic acids and dihydropyridin-2-ones. *Bioorg. Med. Chem. Lett.* 18, 1840–1844. doi: 10.1016/j.bmcl.2008.02.009
- Saubern, S., Guha, R., and Baell, J. B. (2011). KNIME workflow to assess PAINS filters in SMARTS format. Comparison of RDKit and Indigo cheminformatics libraries. *Mol. Inform.* 30, 847–850. doi: 10.1002/minf.201100076
- Shoichet, B. K. (2006). Interpreting steep dose-response curves in early inhibitor discovery. *J. Med. Chem.* 49, 7274–7277. doi: 10.1021/jm061103g
- Sinko, W., de Oliveira, C., Williams, S., Van Wynsberghe, A., Durrant, J. D., Cao, R., et al. (2011). Applying molecular dynamics simulations to identify rarely sampled ligand-bound conformational states of undecaprenyl pyrophosphate synthase, an antibacterial target. *Chem. Biol. Drug Design* 77, 412–420. doi: 10.1111/j.1747-0285.2011.01101.x
- Sinko, W., Wang, Y., Zhu, W., Zhang, Y., Feixas, F., Cox, C. L., et al. (2014). Undecaprenyl diphosphate synthase inhibitors: antibacterial drug leads. *J. Med. Chem.* 57, 5693–5701. doi: 10.1021/jm5004649
- Teng, K. H., and Liang, P. H. (2012a). Structures, mechanisms and inhibitors of undecaprenyl diphosphate synthase: a cis-prenyltransferase for bacterial peptidoglycan biosynthesis. *Bioorg. Chem.* 43, 51–57. doi: 10.1016/j.bioorg.2011.09.004
- Teng, K. H., and Liang, P. H. (2012b). Undecaprenyl diphosphate synthase, a cis-prenyltransferase synthesizing lipid carrier for bacterial cell wall biosynthesis. *Mol. Membr. Biol.* 29, 267–273. doi: 10.3109/09687688.2012.674162
- Van Geelen, L., Meier, D. D., Rehberg, N., and Kalscheuer, R. (2018). Some current concepts in antibacterial drug discovery. *Appl. Microbiol. Biotechnol.* 102, 2949–2963. doi: 10.1007/s00253-018-8843-6
- Wang, Y., Desai, J., Zhang, Y., Malwal, S. R., Shin, C. J., Feng, X., et al. (2016). Bacterial cell growth inhibitors targeting undecaprenyl diphosphate synthase and undecaprenyl diphosphate phosphatase. *Chemmedchem* 11, 2311–2319. doi: 10.1002/cmdc.201600342
- Wolber, G., and Langer, T. (2005). LigandScout: 3-d pharmacophores derived from protein-bound Ligands and their use as virtual screening filters. *J. Chem. Inf. Model.* 45, 160–169. doi: 10.1021/ci049885e
- Zhu, W., Zhang, Y., Sinko, W., Hensler, M. E., Olson, J., Molohon, K. J., et al. (2013). Antibacterial drug leads targeting isoprenoid biosynthesis. *Proc. Natl. Acad. Sci. U.S.A.* 110, 123–128. doi: 10.1073/pnas.1219899110

Conflict of Interest Statement: The authors declare that the research was conducted in the absence of any commercial or financial relationships that could be construed as a potential conflict of interest.

Copyright © 2019 Jukić, Rožman, Sova, Barreteau and Gobec. This is an open-access article distributed under the terms of the Creative Commons Attribution License (CC BY). The use, distribution or reproduction in other forums is permitted, provided the original author(s) and the copyright owner(s) are credited and that the original publication in this journal is cited, in accordance with accepted academic practice. No use, distribution or reproduction is permitted which does not comply with these terms.



Revisiting Anti-tuberculosis Therapeutic Strategies That Target the Peptidoglycan Structure and Synthesis

Maria João Catalão^{1*}, Sérgio R. Filipe^{2,3} and Madalena Pimentel¹

¹Research Institute for Medicines (iMed.Ulisboa), Faculty of Pharmacy, Universidade de Lisboa, Lisbon, Portugal, ²UCIBIO-REQUIMTE, Departamento de Ciências da Vida, Faculdade de Ciências e Tecnologia, Caparica, Portugal, ³Laboratory of Bacterial Cell Surfaces and Pathogenesis, Instituto de Tecnologia Química e Biológica António Xavier, Universidade Nova de Lisboa, Oeiras, Portugal

OPEN ACCESS

Edited by:

Christoph Mayer,
University of Tübingen, Germany

Reviewed by:

Frédéric J. Veyrier,
Institut National de la Recherche
Scientifique (INRS), Canada
Patrick Joseph Moynihan,
University of Birmingham,
United Kingdom
Nicolas Gisch,
Forschungszentrum Borstel (LG),
Germany

*Correspondence:

Maria João Catalão
mjatalao@ff.ulisboa.pt

Specialty section:

This article was submitted to
Microbial Physiology and Metabolism,
a section of the journal
Frontiers in Microbiology

Received: 04 October 2018

Accepted: 23 January 2019

Published: 11 February 2019

Citation:

Catalão MJ, Filipe SR and
Pimentel M (2019)
Revisiting Anti-tuberculosis
Therapeutic Strategies That
Target the Peptidoglycan
Structure and Synthesis.
Front. Microbiol. 10:190.
doi: 10.3389/fmicb.2019.00190

Tuberculosis (TB), which is caused by *Mycobacterium tuberculosis* (*Mtb*), is one of the leading cause of death by an infectious diseases. The biosynthesis of the mycobacterial cell wall (CW) is an area of increasing research significance, as numerous antibiotics used to treat TB target biosynthesis pathways of essential CW components. The main feature of the mycobacterial cell envelope is an intricate structure, the mycolyl-arabinogalactan-peptidoglycan (mAGP) complex responsible for its innate resistance to many commonly used antibiotics and involved in virulence. A hallmark of mAGP is its unusual peptidoglycan (PG) layer, which has subtleties that play a key role in virulence by enabling pathogenic species to survive inside the host and resist antibiotic pressure. This dynamic and essential structure is not a target of currently used therapeutics as *Mtb* is considered naturally resistant to most β -lactam antibiotics due to a highly active β -lactamase (BlaC) that efficiently hydrolyses many β -lactam drugs to render them ineffective. The emergence of multidrug- and extensive drug-resistant strains to the available antibiotics has become a serious health threat, places an immense burden on health care systems, and poses particular therapeutic challenges. Therefore, it is crucial to explore additional *Mtb* vulnerabilities that can be used to combat TB. Remodeling PG enzymes that catalyze biosynthesis and recycling of the PG are essential to the viability of *Mtb* and are therefore attractive targets for novel antibiotics research. This article reviews PG as an alternative antibiotic target for TB treatment, how *Mtb* has developed resistance to currently available antibiotics directed to PG biosynthesis, and the potential of targeting this essential structure to tackle TB by attacking alternative enzymatic activities involved in *Mtb* PG modifications and metabolism.

Keywords: mycobacteria, cell wall, tuberculosis, antibiotic resistance, peptidoglycan, β -lactams, mycobacteriophage lysis enzymes

INTRODUCTION

According to the latest report available from the World Health Organization (WHO), it is estimated that in 2017, there were about 10.3 million new cases of TB worldwide and about 1.8 million people died from this infection. The emergence of multidrug-resistant (MDR) and extensive drug-resistant (XDR) strains to the available antibiotics is a worldwide public health problem of increasing importance, with a treatment success rate of only about 50%, which decreases to 23% in the case of XDR-TB (World Health Organization, 2010, 2011, 2014, 2017; Horsburgh et al., 2015). The lack of effective treatment regimens against MDR-TB and XDR-TB isolates has highlighted the potential of repurposing existing antibiotic options in alternative and innovative ways (Mainardi et al., 2011) as all drugs, except for bedaquiline and delamanid, which are currently used to treat TB, were approved several years ago, demonstrating the complexity of TB drug development (Wong et al., 2013; Keener, 2014; Diacon et al., 2016).

A hallmark of *Mtb*, the causative agent of TB, as a successful pathogen is its intricate CW (Brennan and Nikaido, 1995; Jankute et al., 2015) that has been associated with the genetic differences among human lineages of *Mtb* (Portevin et al., 2011). The core of the mycobacteria cell envelope is composed of three main structures: (1) the characteristic long-chain mycolic acids (MA); (2) a highly branched arabinogalactan (AG) polysaccharide; and (3) a very cross-linked and modified meshwork of PG. The entire complex, referred to as mycolyl-arabinogalactan-peptidoglycan (mAGP) (Brennan and Nikaido, 1995; Alderwick et al., 2015; Jankute et al., 2015), is essential for *Mtb* viability, virulence, and persistence and can modulate the innate immune response (Brennan and Nikaido, 1995; Stanley and Cox, 2013; Jankute et al., 2015). In addition, it acts as an impregnable external barrier responsible for the intrinsic resistance of *Mtb* to several drugs (Nikaido, 1994; Gygli et al., 2017; Nasiri et al., 2017). The essential nature of CW synthesis and assembly has rendered the mycobacterial CW as the most extensively exploited target of anti-TB drugs (Wong et al., 2013; Bhat et al., 2017). Ethambutol, isoniazid, and ethionamide successfully target the synthesis of the various components of mAGP (Jackson et al., 2013), and resistance to these drugs, which is mediated by the accumulation of chromosomal mutations in genes involved in CW biosynthesis pathways, can arise under selective pressure of antibiotic use (Eldholm and Balloux, 2016; Gygli et al., 2017; Nasiri et al., 2017). *Mtb* has been considered innately resistant to most β -lactam antibiotics that target PG biosynthesis due to (1) a highly active β -lactamase (BlaC) that efficiently inactivates many β -lactams (Wang et al., 2006; Hugonnet and Blanchard, 2007) and (2) the fact that a large proportion of the CW PG is cross-linked by non-classical L,D-transpeptidases, which are intrinsically impervious to these antibiotics (Lavollay et al., 2008; Cordillot et al., 2013). Widespread antibiotic resistance in *Mtb*, in combination with the lack of progress in developing new effective treatments, is threatening the ability of tackling the outcomes caused by highly resistant *Mtb* strains. This highlights the need of considering alternative therapeutic

schemes to combat the global increase in resistance to the current anti-TB regimens. This review summarizes the current knowledge about the mechanisms employed by mycobacteria to circumvent the activity of currently available antibiotics that target PG biosynthesis with an emphasis on recent advancements regarding the efficacy of carbapenems, a more recent class of extended-spectrum β -lactams against highly drug-resistant *Mtb* clinical strains, and the potential application of mycobacteriophage-encoded lysis proteins to kill mycobacteria by weakening the CW.

IMPACT OF THE ATYPICAL MYCOBACTERIAL PG STRUCTURE ON RESISTANCE TO ANTIBIOTICS THAT TARGET PG BIOSYNTHESIS

A distinctive feature of the mycobacterial CW is its unusual PG layer (Alderwick et al., 2015; Jankute et al., 2015), which is essential for survival of *Mtb* and that is linked with the exceptional immunogenic activity associated with the CW. The PG macromolecule contains a number of unique subtleties that enable *Mtb* to survive inside the host and resist different antibiotics (Gygli et al., 2017; Nasiri et al., 2017). The PG layer of *Mtb* is surrounded by other layers dominated by lipids, carbohydrates, and phosphatidyl-myo-inositol-based lipoglycans that provide a permeability barrier against hydrophilic drugs (Nikaido, 1994; Brennan and Nikaido, 1995; Hoffmann et al., 2008). PG acts as a pro-inflammatory inducer that is hypothetically masked within the mAGP complex (Brennan and Nikaido, 1995; Jankute et al., 2015), which constitutes the major structural component of the cell envelope. Access of antibiotics that target PG biosynthesis is critical for their efficacy, and it is now assumed that several pathogenic bacteria have developed different strategies to hide PG (Atilano et al., 2011, 2014), thus circumventing their antibacterial activity. Mycobacterial PG forms the basal layer of the mAGP complex, where glycan chains composed of alternating *N*-acetylglucosamine (GlcNAc) and modified *N*-acetylmuramic acid (MurNAc) residues, linked in a β (1 \rightarrow 4) configuration (Alderwick et al., 2015), are interconnected through oligopeptides. The muramic acid residues in *Mtb* are found containing a combination of *N*-acetyl and *N*-glycolyl derivatizations. In the latter case, the *N*-acetyl group present in MurNAc residues has been oxidized to an *N*-glycolyl group through the action of the enzyme *N*-acetyl muramic acid hydroxylase (NamH) to form MurNGly (Raymond et al., 2005). Although the precise function of the *N*-glycolyl modification, a structural modification that is unique to mycobacteria (and closely related genera) is yet to be elucidated, it has been hypothesized that it contributes to: (1) the stability of the mycobacterial CW, by strengthening the mesh-like structure of the PG layer providing sites for additional hydrogen bonding between different parts of the PG macromolecule (Brennan and Nikaido, 1995); (2) the increase of β -lactam resistance (Raymond et al., 2005); (3) the protection of bacteria from degradation *via* lysozyme (Raymond et al., 2005); and (4) the overall innate immune response triggered by the CW of

mycobacteria, as the glycolylated form of the muramyl dipeptide is an important contributor to the unusual immunogenicity of mycobacteria. This component of the mycobacterial PG is a strong inducer of NOD2-mediated host responses (Coulombe et al., 2009; Schenk et al., 2016), although playing a limited role in the pathogenesis of *Mtb* infection (Hansen et al., 2014). Beside the contribution of glycolylated muramic acid residues to the overall host-mycobacteria interaction, *Mtb* PG-derived muropeptides released by the action of a group of enzymes called “resuscitation-promoting factors,” encoded by the *rpf* genes have also been associated with β -lactam and vancomycin tolerance and increased outer membrane (OM) impermeability (Kana et al., 2010; Wivagg and Hung, 2012). The pentapeptide chains of the mycobacterial PG can also be modified by amidation, glycylation, or methylation (Mahapatra et al., 2005), which contributes to its resistance to endopeptidase activity of PG hydrolases (Lavollay et al., 2008). However, the functional significance of these modifications for *Mtb* drug resistance is unknown.

The mature PG architecture is also marked by a high degree of direct peptide cross-links, a characteristic that is not frequently found in other bacteria. Overall, 80% of the peptides are cross-linked in two types of linkages in order to maintain the complexity of the mycobacterial cell envelope during growth and under non-replicating conditions (Lavollay et al., 2008). Mycobacterial PG cross-linking is catalyzed by D,D-transpeptidases (penicillin-binding proteins) and typically by the combined action of non-classical L,D-transpeptidases (Ldts) and D,D-carboxypeptidases. The action of these enzymes results in PG peptides, which connect neighboring glycan chains, that are linked through 4 \rightarrow 3 (D-Ala-mDAP) and 3 \rightarrow 3 (mDAP-mDAP) linkages, respectively (Figure 1; Lavollay et al., 2008). The latter set of proteins contributes to the intrinsic resistance to β -lactams and provides protection from PG endopeptidases (Lavollay et al., 2008; Cordillot et al., 2013). Another unique feature of mycobacterial PG is that it provides the attachment site for AG (which is catalyzed by the Lcp1 phosphotransferase) (McNeil et al., 1990; Baumgart et al., 2016; Grzegorzewicz et al., 2016; Harrison et al., 2016), a highly branched molecule assembled from arabinofuranose and galactofuranose monosaccharides, which overlays the PG and that can also preclude PG synthesis from being targeted by β -lactams (Schubert et al., 2017).

MYCOBACTERIAL INTRINSIC RESISTANCE TO ANTIBIOTICS THAT TARGET PG BIOSYNTHESIS: A NEW TRICK FOR AN OLD DOGMA

PG biosynthesis (Figure 1) represents the site of action of the most widely used class of antibacterial agents for infection treatment (Vollmer et al., 2008; Bugg et al., 2011; Cho et al., 2014; Pavelka et al., 2014). However, except for D-cycloserine, an oral antimycobacterial agent that is specifically recommended by the WHO as a second-line anti-TB agent used as a last option for

the treatment of TB (Hwang et al., 2013), antibiotics that target PG synthesis such as the β -lactams are only rarely used in the treatment of TB (Wong et al., 2013; Wivagg et al., 2014). This lack of efficacy against *Mtb* has primarily been attributed to a chromosomally encoded broad spectrum class A β -lactamase enzyme BlaC (Flores et al., 2005; Wang et al., 2006; Hugonnet and Blanchard, 2007), which hydrolyses the core β -lactam ring and deactivates the antibiotic, to different drug efflux pumps, to low affinity penicillin-binding proteins (PBPs) and to the expression of PG-biosynthetic enzymes insensitive to β -lactams (non-classical transpeptidases) (Wivagg et al., 2014; Gygli et al., 2017; Nasiri et al., 2017). In addition, the PG is camouflaged by the MA-rich mycobacterial OM that limits penetration of antibiotics (Figure 2; Brennan and Nikaido, 1995; Jankute et al., 2015).

Resistance to D-Cycloserine in *Mtb*

D-cycloserine is a structural analog of D-alanine and interferes with the formation of PG biosynthesis, by acting as a competitive inhibitor of alanine racemase (Alr) and D-alanine-D-alanine ligase (Ddl) enzymes, which are involved in PG synthesis (Prosser and de Carvalho, 2013a,b,c). Ddl is the main target of D-cycloserine and is preferentially inhibited over Alr in *Mtb* (Prosser and de Carvalho, 2013a). Resistance to this antibiotic has been associated with loss-of-function mutations in metabolism-related genes of ubiquinone and menaquinone and *ald* (Rv2780), which encodes an L-alanine dehydrogenase (Hong et al., 2014; Desjardins et al., 2016). A recent study has identified novel mutations connected with D-cycloserine resistance in MDR and XDR *Mtb* strains, which demonstrate that resistance to this antibiotic is highly complex and involves diverse genes associated with different cellular processes such as lipid metabolism, methyltransferase, stress response, and transport systems (Chen et al., 2017). In another study, a genomic screening of more than 1,500 drug-resistant strains of *Mtb* revealed the presence of three main *alr* mutations (*alr_{Mtb}* M319 T, *alr_{Mtb}* Y364D, *alr_{Mtb}* R373L) that confer D-cycloserine resistance (Nakatani et al., 2017). Despite the importance of D-cycloserine as a second-line drug used to treat MDR- and XDR-TB, the mechanisms underlying D-cycloserine resistance in *Mtb* clinical strains are still undetermined.

The emergence of MDR and XDR *Mtb* strains has become a serious health threat and has initiated the search for new therapeutic strategies. Some of those strategies include revisiting the potential use of β -lactams as an alternative therapeutic approach to tackle drug-resistant TB when no acceptable alternative exists (Hugonnet et al., 2009; Keener, 2014; Diacon et al., 2016).

Resistance to β -Lactams in *Mtb*

Recent developments have led to the suggestion of using carbapenems, a modern class of extended-spectrum β -lactams, as the last line of defense against recalcitrant drug-resistant TB (Hugonnet et al., 2009; Payen et al., 2012; Gonzalo and Drobniewski, 2013; Davies Forsman et al., 2015; Jaganath et al., 2016; Payen et al., 2018). Among β -lactams, carbapenems are unique as they are not only relatively resistant to the hydrolytic

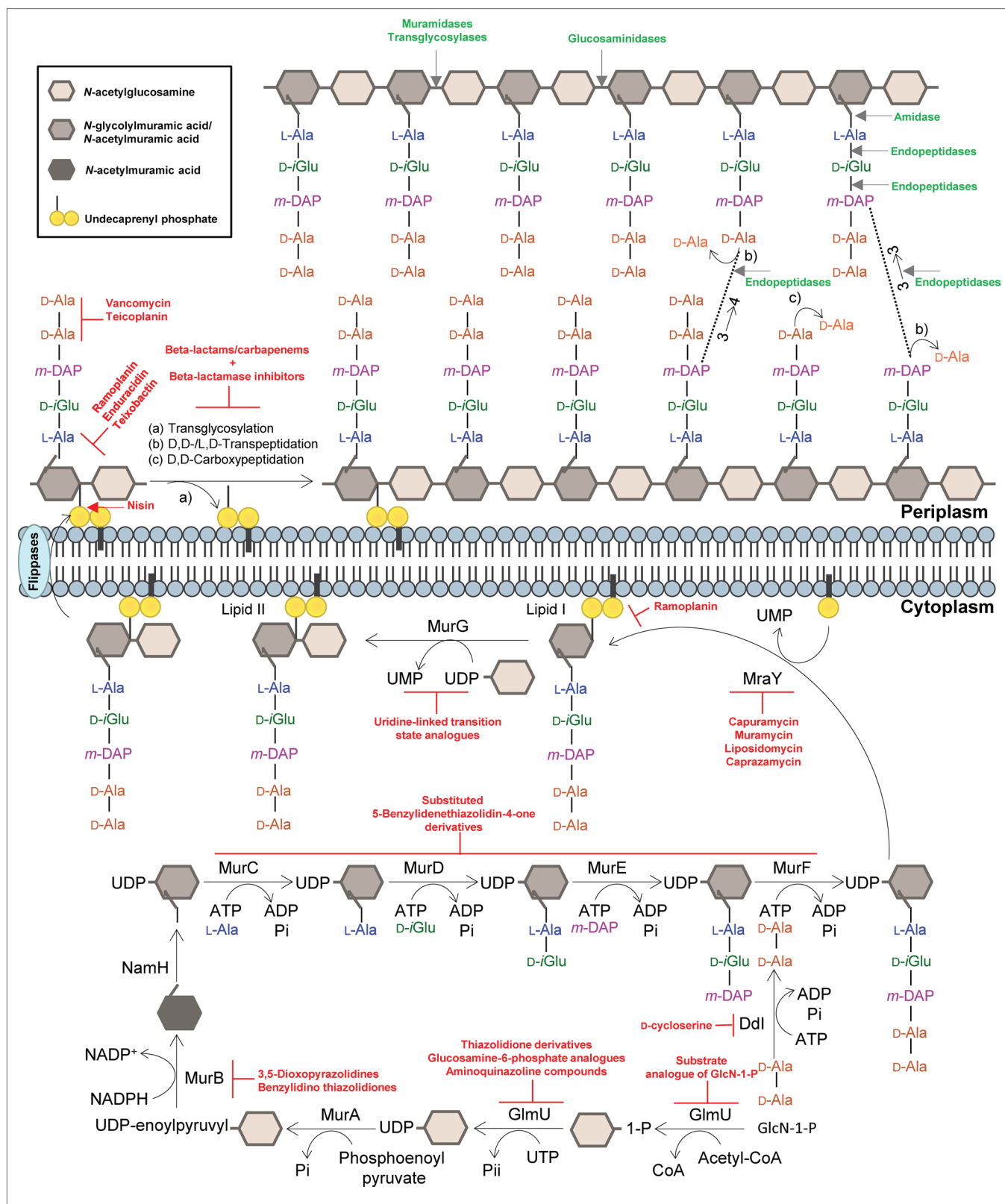


FIGURE 1 | Summary of the mycobacterial peptidoglycan biosynthesis pathway. The peptidoglycan precursors are produced in the cytoplasm, and peptidoglycan monomeric units are assembled in the inner leaflet of the cytoplasmic membrane. Polymerization and cross-linking of tetrapeptide side chains take place at the periplasm. Inhibitors of the peptidoglycan biosynthetic enzymes are colored in red, and peptidoglycan bonds that are targeted by mycobacteriophage endolysins are colored in green. Adapted from Abrahams and Besra, 2018, with permission.

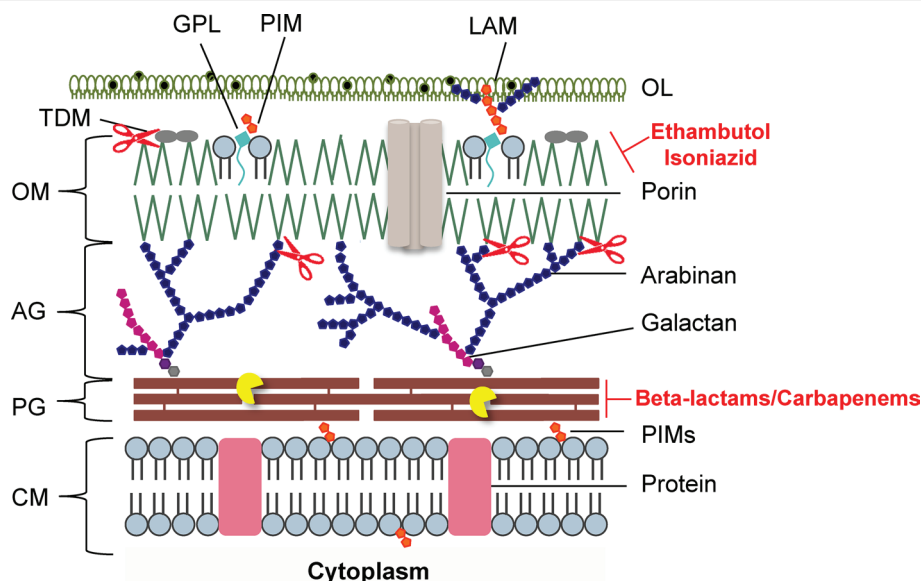


FIGURE 2 | Schematic representation of the mycobacterial cell envelope layers. Inhibitors of mycolic acids and peptidoglycan biosynthesis are indicated in red. The mycobacteriophage lysis protein targets are indicated as follows: the pacman cartoon represents digestion of the PG by the endolysins; scissors illustrate LysB detachment of the OM. AG, arabinogalactan; CM, cytoplasmic membrane; GPL, glycolipids; LAM, liparabinomannan; OL, outer layer; OM, outer membrane; PG, peptidoglycan; PIMs, phosphatidylinositol mannosides; PLs, phospholipids; TDM, trehalose dimycolate. Adapted from Catalão and Pimentel, 2018 with permission from the authors.

activity of BlaC, but also act as potent inhibitors of this enzyme (Tremblay et al., 2010). The efficacy of carbapenems in killing *Mtb* is further increased by the ability of these compounds to inhibit the different enzymes that contribute to the assembly of mycobacterial PG (Gupta et al., 2010; Dubée et al., 2012; Erdemli et al., 2012; Cordillot et al., 2013; Bianchet et al., 2017; Kumar et al., 2017a). While most β -lactams inhibit D,D-transpeptidases (PBPs), which are the enzymes that catalyze the formation of 4 \rightarrow 3 transpeptide linkages in the PG network (Zapun et al., 2008), they are unable to inhibit the L,D-transpeptidases (Ldts) that catalyze the formation of 3 \rightarrow 3 transpeptide linkages. As the PG of mycobacteria contains a high proportion (up to 80%) of 3 \rightarrow 3 cross-links (Lavollay et al., 2008; Cordillot et al., 2013), β -lactams will not fully prevent the assembly of the mycobacterial PG. Carbapenems inhibit not only D,D-transpeptidases but also L,D-transpeptidases (as well as D,D-carboxypeptidases) (Baranowski et al., 2018; García-Heredia et al., 2018).

Ldt and PBP enzymes are structurally unrelated and contain cysteine and serine residues in their active sites, respectively. *Mtb* genome encodes five L,D-transpeptidases, designated by Ldt_{Mt1} to Ldt_{Mt5} (Cordillot et al., 2013). It was shown that the presence of L,D-transpeptidases can markedly alter β -lactam susceptibility (Lavollay et al., 2008; Gupta et al., 2010; Dubée et al., 2012; Kumar et al., 2012; Cordillot et al., 2013; Kieser et al., 2015; Wivagg et al., 2016). In addition, recent studies indicate that *Mtb* strains that lack both *ldt_{Mt1}* and *ldt_{Mt2}* display enhanced susceptibility not only to amoxicillin, a β -lactam antibiotic, but also to vancomycin, a glycopeptide antibiotic (Schoonmaker et al., 2014). Furthermore, a synergistic effect

of carbapenem with rifampicin was observed against rifampicin-resistant clinical isolates of *Mtb* (Kaushik et al., 2015, 2017).

Most of the anti-TB drugs associated with CW biosynthesis inhibition lack the ability to reduce treatment duration of TB drug regimens. This is related to the fact that some bacteria can withstand the presence of the antibiotics by becoming dormant, i.e., being unable to replicate, as dormant bacteria do not actively synthesize the CW and are presumably not affected by the presence of inhibitors of the CW synthesis. Recent research has shown that a combinatorial treatment that is based on the use of the β -lactamase inhibitor clavulanate and meropenem is effective against both actively replicating and non-replicating XDR *Mtb* isolates (Solapure et al., 2013). However, its high cost and intravenous administration present challenges to its widespread use. According to the WHO anti-tuberculosis classification, the carbapenems are included in Group D3, which indicates that safety and efficacy information to support its use against TB is restricted and should not be considered as an alternative regimen designated to treat TB (WHO, 2011, 2014). The existing *in vivo* and clinical studies suggest that there are advantages in carbapenem use as they are usually well-tolerated, although the variance in the extent of the treatment, dosing, and the absence of pharmacokinetic data limit interpretation of the effectiveness of these antibiotics against TB. Information regarding carbapenem resistance is scarce; mutations in CW biosynthesis genes and in *crfA* have been associated with resistance to different carbapenem antibiotics such as imipenem, meropenem, and biapenem (Lun et al., 2014; Kumar et al., 2017b). Nevertheless, these studies have been an enormous contribution to the recent and increased effort for repurposing β -lactams as an ultimate therapeutic option

to treat life-threatening TB-infected patients and to unveil to what extent the wider *Mtb* human clinical isolates population may be susceptible to these antibiotics (Tiberi et al., 2016).

MYCOBACTERIAL PG ASSEMBLY ENZYMES AS TARGETS FOR ANTIBIOTICS

The PG layer provides shape and rigidity to an individual cell of *Mtb* (Brennan, 2003). Since it is mainly restricted to bacterial cells, the enzymes that are involved in the biosynthesis of PG offer an attractive target for the development of new antibiotics against TB. In addition, the enzymes that catalyze the PG biosynthesis pathway in mycobacteria are essential, and therefore, their inhibition is expected to result in selective destruction of the bacteria (Moraes et al., 2015; Bhat et al., 2017; Abrahams and Besra, 2018). The biosynthesis process of mycobacterial PG is similar to other bacteria (Figure 1). The first step is catalyzed by the acetyltransferase and uridylyltransferase activities of GlmU (Rv1018c), to yield UDP-GlcNAc (Zhang et al., 2009). The functional resemblance of the GlmU uridylyltransferase with human enzymes (Peneff et al., 2001) turns this enzyme into an unsuitable target (Rani and Khan, 2016). However, the lack of GlcN-1-P from mammals makes the acetyltransferase domain a promising target, and different substrate analogs of GlcN-1-P have been designed and shown to exhibit an inhibitory effect against GlmU by blocking synthesis of UDP-GlcNAc (Figure 1; Li et al., 2011; Tran et al., 2013; Rani et al., 2015). The sequential MurA-F ligase pathway involves the formation of the UDP-*N*-acetylmuramic acid (UDP-MurNAc)-pentapeptide. MurA (Rv1315), a UDP-*N*-acetylglucosamine 1-carboxyvinyltransferase, and MurB (Rv0482), a UDP-*N*-acetylenolpyruvoylglucosamine reductase, are implicated in the formation of UDP-MurNAc. NamH (Rv3808), a UDP-*N*-acetylmuramic acid hydroxylase, hydroxylates UDP-MurNAc to UDP-*N*-glycolylmuramic acid (UDP-MurNGlyc) in the cytoplasm to generate both types of UDP-muramyl substrates, although *Mtb* PG is enriched in the latter (Mahapatra et al., 2005; Raymond et al., 2005). Specific inhibitors of *Mtb* MurA and MurB have not been described to date. The broad-spectrum antibiotic, fosfomycin, which targets Gram-negative MurA, has no activity against *Mtb* since the critical cysteine (Cys₁₁₇) residue, which is required for inhibition by the drug, is replaced in *Mtb* by an aspartic acid residue, contributing to the intrinsic resistance against this antibiotic (Kim et al., 1996). A limited number of inhibitors have been reported against MurB, specifically the 3,5-dioxypyrazolidine and benzylidene thiazolidinedione derivatives which can competitively inhibit the formation of UDP-MurNAc (Figure 1; Kumar et al., 2011; Rana et al., 2014). Inhibitors of NamH have not been reported, probably due to the fact that *namH* is not essential in *Mtb* (Hansen et al., 2014). Therefore, NamH may not be a key target for anti-TB therapy. However, *Mtb* strains that lack *namH* are hypersusceptible to β -lactam antibiotics, and therefore, inhibitors of NamH could potentiate the effect of carbapenems (Raymond et al., 2005; Hansen et al., 2014). From this point, the pentapeptide chain is attached to UDP-MurNAc/

Glyc by the ATP-dependent Mur ligases (Figure 1), beginning with UDP-*N*-acetylmuramoyl-L-alanine addition by MurC (Rv2151c). This is followed by D-isoglutamate addition by MurD (Rv2155c), m-DAP addition by MurE (Rv2158c), and finally D-alanyl-D-alanine addition by MurF (Rv2157c). This generates the muramyl-pentapeptide product UDP-MurNAc/Glyc-L-Ala-D-isoGlu-m-DAP-D-Ala-D-Ala, also known as Park's nucleotide (Figure 1; Pavelka et al., 2014). Several inhibitors of the Mur ligases have been identified (Hrast et al., 2014). One example is the substituted 5-benzylidenethiazolidin-4-one derivatives that inhibit the formation of the pentapeptide chains (Tomasic et al., 2010). However, their utilization is limited against *Mtb* Mur ligases given that only MurC and MurE have been biochemically characterized (Mahapatra et al., 2000; Li et al., 2011). Ddl is the target of D-cycloserine, a structural analog of D-Ala, inhibiting the binding of either the two D-Ala substrates to Ddl (Bruning et al., 2011; Prosser and de Carvalho, 2013c). The assembled Park's nucleotide is then transferred to undecaprenyl phosphate present at the membrane by MraY (Rv2156c) generating Lipid I. Nucleoside-peptide antibiotics that inhibit MraY have been described, including muramycin, liposidomycin, caprazamycin, and capuramycin (Dini, 2005; Wiegmann et al., 2016; Tran et al., 2017). Remarkably, capuramycin has been shown to kill non-replicating *Mtb*, an uncommon characteristic of the majority of CW biosynthesis inhibitors (Koga et al., 2004; Reddy et al., 2008; Nikonenko et al., 2009; Siricilla et al., 2015). The final intracellular step of PG synthesis is catalyzed by MurG, a glycosyltransferase that is responsible for producing lipid II, the final monomeric block of PG. An *Escherichia coli* designed inhibitor of MurG was tested against *Mtb* with limited success and has become the first inhibitor identified against the *Mtb* glycosyltransferase (Trunkfield et al., 2010).

Translocation of lipid II across the plasma membrane is carried out by a flippase. This was initially thought to be an FtsW-like protein, Rv2154c (Mohammadi et al., 2011). However, recent research has shown that FtsW/RodA enzymes elongate PG chains through a transglycosylase activity (Meeske et al., 2016; Emami et al., 2017), and therefore, the best candidate for the PG precursor flippase is currently MurJ (Rv3910). Following the transport of PG precursor across the mycobacterial membrane, the bifunctional PonA1/PBP1 (Rv0050) and PonA2/PBP2 (Rv3682) enzymes, PBPs that possess both the transglycosylase and transpeptidase domains attach the GlcNAc moiety to the muramyl moiety of the nascent PG chain (Figure 1). Lipid II inhibitors, such as the depsipeptide antibiotics ramoplanin and enduracidin (Fang et al., 2006) and teixobactin (Ling et al., 2015), that prevent the transglycosylation of the translocated lipid II by binding to it have been described recently. The transpeptidase activity of PonA1 and PonA2 catalyzes the classical 4 \rightarrow 3 cross-linkages between m-DAP and D-Ala of the adjacent pentapeptide chains present in neighboring glycan chains, with the cleavage of the terminal D-Ala. Other D,D-transpeptidation and D,D-carboxypeptidation reactions are catalyzed by the monofunctional PBPs, both resulting in the cleavage of the terminal D-Ala of the peptide stem (Zapun et al., 2008). Among the mucopeptides present in the *Mtb* PG, up to 80% of the cross-links are 3 \rightarrow 3 links between m-DAP residues of two adjacent tetrapeptide

stems, with the release of the fourth position D-Ala (Lavollay et al., 2008), performed by non-classical L,D-transpeptidases, Ldt_{Mt1} (Rv0116c), Ldt_{Mt2} (Rv2518c), Ldt_{Mt3} (Rv1433), Ldt_{Mt4} (Rv0192), and Ldt_{Mt5} (Rv0483) (Lavollay et al., 2008; Cordillot et al., 2013). As mentioned before, the L,D-transpeptidase and D,D-carboxypeptidase activities are unaffected by most β -lactam antibiotics, except the carbapenems (Gupta et al., 2010; Dub  e et al., 2012; Kumar et al., 2012; Cordillot et al., 2013; Rullas et al., 2015; Bianchet et al., 2017; Kumar et al., 2017a). Moenomycin, a glycolipid that inhibits the transglycosylase activity of PBPs (van Heijenoort et al., 1987) is yet to have recognized efficacy against *Mtb*. The existence of other antibiotics that act on the availability of PG precursors: (1) the glycopeptides, vancomycin and teicoplanin, that bind to the D-Ala-D-Ala terminus of the pentapeptide stem and prevent PG polymerization (Reynolds, 1989); (2) the lantibiotic family of antibiotics, such as nisin, that interact with the pyrophosphate moiety of lipid II, with the consequent delocalization of this molecule that can form a pore in the cytoplasmic membrane and inhibit PG biosynthesis (Wiedemann et al., 2001), opens new avenues to find suitable synergistic antibiotic combination schemes for effective treatments.

PROSPECTIVE USE OF MYCOBACTERIOPHAGE ENDOLYSINS TO DEGRADE THE MYCOBACTERIAL PG

The mycobacterial PG is modified by several enzymes, which confer resistance to some widely used antibiotics (Mahapatra et al., 2005; Raymond et al., 2005). Mycobacteriophages, the viruses of mycobacteria, synthesize enzymes to eliminate each layer of the cell envelope (recently reviewed in Catal  o and Pimentel, 2018), so that phage particles can escape from the bacterial cell at the end of a replicating cycle. Mycobacteriophage-encoded PG hydrolases (endolysins) are predicted to target and degrade nearly every bond in mycobacterial PG (Figure 1; Payne and Hatfull, 2012; Catal  o et al., 2013; Pimentel, 2014). Given the essentiality of the mycobacterial cell envelope (Brennan and Nikaido, 1995; Jankute et al., 2015; Chiaradia et al., 2017), it is reasonable to consider that the enzymatic degradation of mycobacterial CW by the mycobacteriophage lytic enzymes (Gil et al., 2008, 2010; Payne et al., 2009; Catal  o et al., 2011; Gigante et al., 2017) may be a promising therapeutic approach to kill extracellular pathogenic mycobacteria (Grover et al., 2014) or after their internalization by macrophages (Lai et al., 2015). However, access of mycobacteriophage endolysins to their substrate, the PG, is hindered by the MA-rich mycobacterial OM, which restrains their use as anti-TB therapeutic agents (Figure 2). Therefore, transport of phage enzymes and/or antibiotics that target the PG metabolism through this OM remains the major constraint in the application of these compounds in therapy (Catal  o and Pimentel, 2018). As the enzymes involved in MA and AG biosynthesis and integrity play an important role in the development of drug resistance in *Mtb*, inhibition of the synthesis of these CW layers would

damage the CW as a barrier, increase its permeability, and increase the susceptibility of bacteria to various anti-mycobacterial drugs (Figure 2). Mycobacteriophage-encoded LysB proteins are specific lysis proteins that act enzymatically, not only hydrolyzing lipids on the outer leaflet of the OM, but also, importantly, detaching it from the CW by cleaving the ester linkage to the AG polymer due to a mycolyl-arabinogalactan esterase activity (Figure 2; Gil et al., 2008, 2010; Payne et al., 2009; Gigante et al., 2017). Interestingly, it has been recently reported that ethambutol, one of the first-line drugs for TB treatment, leads to the loss of the MA layer by blocking polymerization of arabinose in AG, which impairs *de novo* synthesis of the outer envelope layers (Schubert et al., 2017). As cell division seems to be unaffected by ethambutol, the authors proposed that the inhibition of MA synthesis generates a defective CW composed predominately of exposed PG. Inactivation of the Ag85 complex (*fbpA*, *fbpB*, and *fbpC*) proteins that possess mycolyltransferase activity and are involved in biogenesis of trehalose dimycolate (TDM), a glycolipid that has been proposed to be present in the outer leaflet of the mycobacterial OM, increased sensitivity both to first-line TB drugs and to erythromycin, imipenem, rifampicin, and vancomycin (Lingaraju et al., 2016). Since production of TDM by Ag85 is essential for the intrinsic antibiotic resistance of mycobacteria (Morris et al., 2005), Ag85-specific inhibitors or TDM hydrolysis by LysB (Figure 2; Gil et al., 2010) can have a positive impact on the fight to control mycobacterial drug resistance.

Understanding the mechanisms used by mycobacteriophages to deteriorate each layer of the extremely complex mycobacterial cell envelope is highly relevant for the design of new strategies against mycobacteria. Given the abundance of isolated mycobacteriophages, which constitute an enormous reservoir of CW degrading enzymes capable of hydrolyzing each specific linkage of the mycobacterial cell envelope (Hatfull, 2006; Payne and Hatfull, 2012), it is worth to consider the possibility of using these enzymes in synergistic combinations with CW targeting antibiotics, which have a limited access to their target, the PG in normally growing bacteria (Figure 2).

CONCLUDING REMARKS

Inhibition of the assembly of the bacterial CW by anti-mycobacterial agents that successfully target the synthesis of its various components has proven useful in tackling TB (Wong et al., 2013; Bhat et al., 2017). However, modification of CW targets mediated by specific enzymes or the accumulation of chromosomal mutations and degradation/modification of drugs by production of antibiotic inactivating enzymes has rendered *Mtb* resistant to most classes of antimicrobials (Eldholm and Balloux, 2016; Gygli et al., 2017; Nasiri et al., 2017). Infections due to *Mtb* are an increasing problem worldwide, and the emergence of XDR-TB suggests that *Mtb* may become refractory to any chemotherapeutic agent in the future (Horsburgh et al., 2015; World Health Organization, 2017). The limited number of new anti-mycobacterial agents approved for therapy and the wide variety of *Mtb* intrinsic and acquired drug resistance

mechanisms to the available drugs have contributed to an increased effort to repurpose the use of antibiotics that are not commonly used in anti-TB therapy and to find suitable synergistic antibiotic combinations for effective treatment of life-risk TB (Mainardi et al., 2011; Wong et al., 2013; Keener, 2014; Diacon et al., 2016). Recent studies have uncovered the possibility of targeting the mycobacterial PG biosynthesis and degradation as an alternative option for anti-TB therapy (Tomasich et al., 2010; Trunkfield et al., 2010; Li et al., 2011; Rana et al., 2014; Ling et al., 2015; Rani et al., 2015; Rullas et al., 2015; Tran et al., 2017). In addition, several observations suggest that inhibition of PG synthesis by transpeptidase inhibitors such as the carbapenems or glycopeptide antibiotics could synergize with other CW inhibitors and increase their efficacy (Figures 1 and 2; Hugonnet et al., 2009; Kumar et al., 2012; Kieser et al., 2015; Schubert et al., 2017). The recent developments toward the potential application of mycobacteriophage-dedicated enzymes targeting the complex mycobacterial CW arrangement have also renewed the interest of repurposing mycobacterial PG metabolism as an anti-TB therapy target (Gil et al., 2008, 2010; Payne and Hatfull, 2012; Catalão and Pimentel, 2018).

More research is needed in the near future that could lead to the design and development of therapeutics that increase the efficacy of currently available antibiotics and enzymes that target PG metabolism, which is not currently considered as an alternative to treat TB.

AUTHOR CONTRIBUTIONS

MC and MP conceived and designed the study and wrote the manuscript. MC, SF, and MP participated in manuscript revising and editing.

FUNDING

This work was funded by a Research Grant 2018 of the European Society of Clinical Microbiology and Infectious Diseases (ESCMID) and Fundação para a Ciência e Tecnologia (FCT), Lisbon, Portugal, through research grant PTDC/BIA-MIC/31233/2017 awarded to MC.

REFERENCES

- Abrahams, K. A., and Besra, G. S. (2018). Mycobacterial cell wall biosynthesis: a multifaceted antibiotic target. *Parasitology* 145, 116–133. doi: 10.1017/S003182016002377
- Alderwick, L. J., Harrison, J., Lloyd, G. S., and Birch, H. L. (2015). The mycobacterial cell wall-peptidoglycan and arabinogalactan. *Cold Spring Harb. Perspect. Med.* 5:a021113. doi: 10.1101/cshperspect.a021113
- Atilano, M. L., Yates, J., Glittenberg, M., Filipe, S. R., and Ligoxygakis, P. (2011). Wall teichoic acids of *Staphylococcus aureus* limit recognition by the *Drosophila* peptidoglycan recognition protein-SA to promote pathogenicity. *PLoS Pathog.* 7:e1002421. doi: 10.1371/journal.ppat.1002421
- Atilano, M. L., Pereira, P. M., Vaz, F., Catalão, M. J., Reed, P., Grilo, I. R., et al. (2014). Bacterial autolysins trim cell surface peptidoglycan to prevent detection by the *Drosophila* innate immune system. *elife* 3:e02277. doi: 10.7554/eLife.02277
- Baranowski, C., Welsh, M. A., Sham, L. T., Eskandarian, H. A., Lim, H. C., Kieser, K. J., et al. (2018). Maturing *Mycobacterium smegmatis* peptidoglycan requires non-canonical crosslinks to maintain shape. *elife* 7:e37516. doi: 10.7554/eLife.37516
- Baumgart, M., Schubert, K., Bramkamp, M., and Frunzke, J. (2016). Impact of LytR-CpsA-Psr proteins on cell wall biosynthesis in *Corynebacterium glutamicum*. *J. Bacteriol.* 198, 3045–3059. doi: 10.1128/JB.00406-16
- Bhat, Z. S., Rather, M. A., Maqbool, M., Lah, H. U., Yousuf, S. K., and Ahmad, Z. (2017). Cell wall: a versatile fountain of drug targets in *Mycobacterium tuberculosis*. *Biomed. Pharmacother.* 95, 1520–1534. doi: 10.1016/j.biopha.2017.09.036
- Bianchet, M. A., Pan, Y. H., Basta, L. A. B., Saavedra, H., Lloyd, E. P., Kumar, P., et al. (2017). Structural insight into the inactivation of *Mycobacterium tuberculosis* non-classical transpeptidase Ldt_{M2} by biapenem and tebipenem. *BMC Biochem.* 18:8. doi: 10.1186/s12858-017-0082-4
- Brennan, P. J. (2003). Structure, function, and biogenesis of the cell wall of *Mycobacterium tuberculosis*. *Tuberculosis* 83, 91–97. doi: 10.1016/S1472-9792(02)00089-6
- Brennan, P. J., and Nikaido, H. (1995). The envelope of mycobacteria. *Annu. Rev. Biochem.* 64, 29–63. doi: 10.1146/annurev.bi.64.070195.000333
- Bruning, J. B., Murillo, A. C., Chacon, O., Barletta, R. G., and Sacchettini, J. C. (2011). Structure of the *Mycobacterium tuberculosis* D-alanine:D-alanine ligase, a target of the antituberculosis drug D-cycloserine. *Antimicrob. Agents Chemother.* 55, 291–301. doi: 10.1128/AAC.00558-10
- Bugg, T. D., Braddick, D., Dowson, C. G., and Roper, D. I. (2011). Bacterial cell wall assembly: still an attractive antibacterial target. *Trends Biotechnol.* 29, 167–173. doi: 10.1016/j.tibtech.2010.12.006
- Catalão, M. J., Milho, C., Gil, F., Moniz-Pereira, J., and Pimentel, M. (2011). A second endolysin gene is fully embedded in-frame with the *lysA* gene of mycobacteriophage Ms6. *PLoS One* 6:e20515. doi: 10.1371/journal.pone.0020515
- Catalão, M. J., Gil, F., Moniz-Pereira, J., São-José, C., and Pimentel, M. (2013). Diversity in bacterial lysis systems: bacteriophages show the way. *FEMS Microbiol. Rev.* 37, 554–571. doi: 10.1111/1574-6976.12006
- Catalão, M. J., and Pimentel, M. (2018). Mycobacteriophage lysis enzymes: targeting the mycobacterial cell envelope. *Viruses* 10:E428. doi: 10.3390/v10080428
- Chen, J., Zhang, S., Cui, P., Shi, W., Zhang, W., and Zhang, Y. (2017). Identification of novel mutations associated with cycloserine resistance in *Mycobacterium tuberculosis*. *J. Antimicrob. Chemother.* 72, 3272–3276. doi: 10.1093/jac/dkx316
- Chiaradia, L., Lefebvre, C., Parra, J., Marcoux, J., Burlet-Schiltz, O., Etienne, G., et al. (2017). Dissecting the mycobacterial cell envelope and defining the composition of the native mycomembrane. *Sci. Rep.* 7:12807. doi: 10.1038/s41598-017-12718-4
- Cho, H., Uehara, T., and Bernhardt, T. G. (2014). Beta-lactam antibiotics induce a lethal malfunctioning of the bacterial cell wall synthesis machinery. *Cell* 157, 1300–1311. doi: 10.1016/j.cell.2014.11.017
- Cordillot, M., Dubé, V., Triboulet, S., Dubost, L., Marie, A., Hugonnet, J. E., et al. (2013). *In vitro* cross-linking of *Mycobacterium tuberculosis* peptidoglycan by L,D-transpeptidases and inactivation of these enzymes by carbapenems. *Antimicrob. Agents Chemother.* 57, 5940–5945. doi: 10.1128/AAC.01663-13
- Coulombe, F., Divangahi, M., Veyrier, F., de Léséleuc, L., Gleason, J. L., Yang, Y., et al. (2009). Increased NOD2-mediated recognition of N-glycolyl muramyl dipeptide. *J. Exp. Med.* 206, 1709–1716. doi: 10.1084/jem.20081779
- Davies Forsman, L., Giske, C. G., Bruchfeld, J., Schön, T., Juréen, P., and Ångeby, K. (2015). Meropenem-clavulanic acid has high in vitro activity against multidrug-resistant *Mycobacterium tuberculosis*. *Antimicrob. Agents Chemother.* 59, 3630–3632. doi: 10.1128/AAC.00171-15
- Desjardins, C. A., Cohen, K. A., Munsamy, V., Abeel, T., Maharaj, K., Walker, B. J., et al. (2016). Genomic and functional analyses of *Mycobacterium tuberculosis* strains implicate *ald* in D-cycloserine resistance. *Nat. Genet.* 48, 544–551. doi: 10.1038/ng.3548
- Diacon, A. H., van der Merwe, L., Barnard, M., von Groote-Bidlingmaier, F., Lange, C., Garcia-Basteiro, A. L., et al. (2016). β -Lactams against tuberculosis—new trick for an old dog? *N. Engl. J. Med.* 375, 393–394. doi: 10.1056/NEJMc1513236

- Dini, C. (2005). MraY inhibitors as novel antibacterial agents. *Curr. Top. Med. Chem.* 5, 1221–1236. doi: 10.2174/156802605774463042
- Dubée, V., Triboulet, S., Mainardi, J. L., Ethève-Quelejeu, M., Gutmann, L., Marie, A., et al. (2012). Inactivation of *Mycobacterium tuberculosis* L,D-transpeptidase LdtMt₁ by carbapenems and cephalosporins. *Antimicrob. Agents Chemother.* 56, 4189–4195. doi: 10.1128/AAC.00665-12
- Eldholm, V., and Balloux, F. (2016). Antimicrobial resistance in *Mycobacterium tuberculosis*: the odd one out. *Trends Microbiol.* 24, 637–648. doi: 10.1016/j.tim.2016.03.007
- Emami, K., Guyet, A., Kawai, Y., Devi, J., Wu, L. J., Allenby, N., et al. (2017). RodA as the missing glycosyltransferase in *Bacillus subtilis* and antibiotic discovery for the peptidoglycan polymerase pathway. *Nat. Microbiol.* 2:16253. doi: 10.1038/nmicrobiol.2016.253
- Erdemli, S. B., Gupta, R., Bishai, W. R., Lamichhane, G., Amzel, L. M., and Bianchet, M. A. (2012). Targeting the cell wall of *Mycobacterium tuberculosis*: structure and mechanism of L,D-transpeptidase 2. *Structure* 20, 2103–2115. doi: 10.1016/j.str.2012.09.016
- Fang, X., Tiyanont, K., Zhang, Y., Wanner, J., Boger, D., and Walker, S. (2006). The mechanism of action of ramoplanin and enduracidin. *Mol. Biosyst.* 2, 69–76. doi: 10.1039/b515328j
- Flores, A. R., Parsons, L. M., and Pavelka, M. S. Jr. (2005). Characterization of novel *Mycobacterium tuberculosis* and *Mycobacterium smegmatis* mutants hypersusceptible to beta-lactam antibiotics. *J. Bacteriol.* 187, 1892–1900. doi: 10.1128/JB.187.6.1892-1900.2005
- Gigante, A. M., Hampton, C. H., Dillard, R. S., Gil, F., Catalão, M. J., Moniz-Pereira, J., et al. (2017). The Ms6 Mycolyl-Arabinogalactan Esterase LysB is Essential for an Efficient Mycobacteriophage-Induced Lysis. *Viruses* 9:E343. doi: 10.3390/v9110343
- García-Heredia, A., Pohane, A. A., Melzer, E. S., Carr, C. R., Fiolek, T. J., Rundell, S. R., et al. (2018). Peptidoglycan precursor synthesis along the sidewall of pole-growing mycobacteria. *elife* 7:e37243. doi: 10.7554/eLife.37243
- Gil, F., Catalão, M. J., Moniz-Pereira, J., Leandro, P., McNeil, M., and Pimentel, M. (2008). The lytic cassette of mycobacteriophage Ms6 encodes an enzyme with lipolytic activity. *Microbiology* 154, 1364–1371. doi: 10.1099/mic.0.2007/014621-0
- Gil, F., Grzegorzewicz, A. E., Catalão, M. J., Vital, J., McNeil, M. R., and Pimentel, M. (2010). Mycobacteriophage Ms6 LysB specifically targets the outer membrane of *Mycobacterium smegmatis*. *Microbiology* 156, 1497–1504. doi: 10.1099/mic.0.032821-0
- Gonzalo, X., and Drobniński, F. (2013). Is there a place for β -lactams in the treatment of multidrug-resistant/extensively drug-resistant tuberculosis? Synergy between meropenem and amoxicillin/clavulanate. *J. Antimicrob. Chemother.* 68, 366–369. doi: 10.1093/jac/dks395
- Grover, N., Paskaleva, E. E., Mehta, K. K., Dordick, J. S., and Kane, R. S. (2014). Growth inhibition of *Mycobacterium smegmatis* by mycobacteriophage-derived enzymes. *Enzym. Microb. Technol.* 63, 1–6. doi: 10.1016/j.enzmictec.2014.04.018
- Grzegorzewicz, A. E., de Sousa-d'Auria, C., McNeil, M. R., Huc-Claustre, E., Jones, V., Petit, C., et al. (2016). Assembling of the *Mycobacterium tuberculosis* cell wall core. *J. Biol. Chem.* 291, 18867–18879. doi: 10.1074/jbc.M116.739227
- Gupta, R., Lavollay, M., Mainardi, J. L., Arthur, M., Bishai, W. R., and Lamichhane, G. (2010). The *Mycobacterium tuberculosis* protein Ldt_{Mt2} is a nonclassical transpeptidase required for virulence and resistance to amoxicillin. *Nat. Med.* 16, 466–469. doi: 10.1038/nm.2120
- Gygli, S. M., Borrell, S., Trauner, A., and Gagneux, S. (2017). Antimicrobial resistance in *Mycobacterium tuberculosis*: mechanistic and evolutionary perspectives. *FEMS Microbiol. Rev.* 41, 354–373. doi: 10.1093/femsre/fux011
- Hansen, J. M., Golchin, S. A., Veyrier, F. J., Domenech, P., Boneca, I. G., Azad, A. K., et al. (2014). N-glycosylated peptidoglycan contributes to the immunogenicity but not pathogenicity of *Mycobacterium tuberculosis*. *J. Infect. Dis.* 209, 1045–1054. doi: 10.1093/infdis/jit622
- Harrison, J., Lloyd, G., Joe, M., Lowary, T. L., Reynolds, E., Walters-Morgan, H., et al. (2016). Lcp1 is a phosphotransferase responsible for ligating arabinogalactan to peptidoglycan in *Mycobacterium tuberculosis*. *MBio* 7:e00972–16. doi: 10.1128/mBio.00972-16
- Hatfull, G. F., Pedulla, M. L., Jacobs-Sera, D., Cichon, P. M., Foley, A., Ford, M. E., et al. (2006). Exploring the mycobacteriophage metaproteome: phage genomics as an educational platform. *PLoS Genet.* 2:e92. doi: 10.1371/journal.pgen.0020092
- Hoffmann, C., Leis, A., Niederweis, M., Plitzko, J. M., and Engelhardt, H. (2008). Disclosure of the mycobacterial outer membrane: cryo-electron tomography and vitreous sections reveal the lipid bilayer structure. *Proc. Natl. Acad. Sci. USA* 105, 3963–3967. doi: 10.1073/pnas.0709530105
- Hong, W., Chen, L., and Xie, J. (2014). Molecular basis underlying *Mycobacterium tuberculosis* D-cycloserine resistance. Is there a role for ubiquinone and menaquinone metabolic pathways? *Expert Opin. Ther. Targets* 18, 691–701. doi: 10.1517/14728222.2014.902937
- Horsburgh, C. R. Jr., Barry, C. III., and Lange, C. (2015). Treatment of tuberculosis. *New Engl. J. Med.* 373, 2149–2160. doi: 10.1056/NEJMra1413919
- Hrast, M., Susic, I., Sink, R., and Gobec, S. (2014). Inhibitors of the peptidoglycan biosynthesis enzymes MurA-F. *Bioorg. Chem.* 55, 2–15. doi: 10.1016/j.bioorg.2014.03.008
- Hugonnet, J. E., and Blanchard, J. S. (2007). Irreversible inhibition of the *Mycobacterium tuberculosis* beta-lactamase by clavulanate. *Biochemistry* 46, 11998–12004. doi: 10.1021/bi701506h
- Hugonnet, J. E., Tremblay, L. W., Boshoff, H. I., Barry, C. E. 3rd., and Blanchard, J. S. (2009). Meropenem-clavulanate is effective against extensively drug-resistant *Mycobacterium tuberculosis*. *Science* 323, 1215–1218. doi: 10.1126/science.1167498
- Hwang, T. J., Wares, D. F., Jafarov, A., Jakubowiak, W., Nunn, P., and Keshavjee, S. (2013). Safety of cycloserine and terizidone for the treatment of drug-resistant tuberculosis: a meta-analysis. *Int. J. Tuberc. Lung Dis.* 17, 1257–1266. doi: 10.5588/ijtld.12.0863
- Jackson, M., McNeil, M. R., and Brennan, P. J. (2013). Progress in targeting cell envelope biogenesis in *Mycobacterium tuberculosis*. *Future Microbiol.* 8, 855–875. doi: 10.2217/fmb.13.52
- Jaganath, D., Lamichhane, G., and Shah, M. (2016). Carbapenems against *Mycobacterium tuberculosis*: a review of the evidence. *Int. J. Tuberc. Lung Dis.* 20, 1436–1447. doi: 10.5588/ijtld.16.0498
- Jankute, M., Cox, J. A., Harrison, J., and Besra, G. S. (2015). Assembly of the mycobacterial cell wall. *Annu. Rev. Microbiol.* 69, 405–423. doi: 10.1146/annurev-micro-091014-104121
- Kana, B. D., Mizrahi, V., and Gordhan, B. G. (2010). Depletion of resuscitation-promoting factors has limited impact on the drug susceptibility of *Mycobacterium tuberculosis*. *J. Antimicrob. Chemother.* 65, 1583–1585. doi: 10.1093/jac/dkq199
- Kaushik, A., Makkar, N., Pandey, P., Parrish, N., Singh, U., and Lamichhane, G. (2015). Carbapenems and rifampin exhibit synergy against *Mycobacterium tuberculosis* and *Mycobacterium abscessus*. *Antimicrob. Agents Chemother.* 59, 6561–6567. doi: 10.1128/AAC.01158-15
- Kaushik, A., Ammerman, N. C., Tasneen, R., Story-Roller, E., Dooley, K. E., Dorman, S. E., et al. (2017). *In vitro* and *in vivo* activity of biapenem against drug-susceptible and rifampicin-resistant *Mycobacterium tuberculosis*. *J. Antimicrob. Chemother.* 72, 2320–2325. doi: 10.1093/jac/dkx152
- Keener, A. B. (2014). Oldie but goodie: repurposing penicillin for tuberculosis. *Nat. Med.* 20, 976–978. doi: 10.1038/nm0914-976
- Kieser, K. J., Baranowski, C., Chao, M. C., Long, J. E., Sassetti, C. M., Waldor, M. K., et al. (2015). Peptidoglycan synthesis in *Mycobacterium tuberculosis* is organized into networks with varying drug susceptibility. *Proc. Natl. Acad. Sci. USA* 112, 13087–13092. doi: 10.1073/pnas.1514135112
- Kim, D. H., Lees, W. J., Kempell, K. E., Lane, W. S., Duncan, K., and Walsh, C. T. (1996). Characterization of a Cys115 to Asp substitution in the *Escherichia coli* cell wall biosynthetic enzyme UDP-GlcNAc enolpyruvyl transferase (MurA) that confers resistance to inactivation by the antibiotic fosfomycin. *Biochemistry* 35, 4923–4928. doi: 10.1021/bi952937w
- Koga, T., Fukuoka, T., Doi, N., Harasaki, T., Inoue, H., Hotoda, H., et al. (2004). Activity of capuramycin analogues against *Mycobacterium tuberculosis*, *Mycobacterium avium* and *Mycobacterium intracellulare* *in vitro* and *in vivo*. *J. Antimicrob. Chemother.* 54, 755–760. doi: 10.1093/jac/dkh417
- Kumar, V., Saravanan, P., Arvind, A., and Mohan, C. G. (2011). Identification of hotspot regions of MurB oxidoreductase enzyme using homology modeling, molecular dynamics and molecular docking techniques. *J. Mol. Model* 17, 939–953. doi: 10.1007/s00894-010-0788-3
- Kumar, P., Arora, K., Lloyd, J. R., Lee, I. Y., Nair, V., Fischer, E., et al. (2012). Meropenem inhibits D,D-carboxypeptidase activity in *Mycobacterium tuberculosis*. *Mol. Microbiol.* 86, 367–381. doi: 10.1111/j.1365-2958.2012.08199.x
- Kumar, P., Kaushik, A., Lloyd, E. P., Li, S. G., Mattoo, R., Ammerman, N. C., et al. (2017a). Non-classical transpeptidases yield insight into new antibacterials. *Nat. Chem. Biol.* 13, 54–61. doi: 10.1038/nchembio.2237

- Kumar, P., Kaushik, A., Bell, D. T., Chauhan, V., Xia, F., Stevens, R. L., et al. (2017b). Mutation in an unannotated protein confers carbapenem resistance in *Mycobacterium tuberculosis*. *Antimicrob. Agents Chemother.* 61:e02234–16. doi: 10.1128/AAC.02234-16
- Lai, M. J., Liu, C. C., Jiang, S. J., Soo, P. C., Tu, M. H., and Lee, J. J. (2015). Antimycobacterial activities of endolysins derived from a mycobacteriophage, BTCU-1. *Molecules* 20, 19277–19290. doi: 10.3390/molecules201019277
- Lavollay, M., Arthur, M., Fourgeaud, M., Dubost, L., Marie, A., Veziris, N., et al. (2008). The peptidoglycan of stationary-phase *Mycobacterium tuberculosis* predominantly contains cross-links generated by L,D-transpeptidation. *J. Bacteriol.* 190, 4360–4366. doi: 10.1128/JB.00239-08
- Li, Y., Zhou, Y., Ma, Y., and Li, X. (2011). Design and synthesis of novel cell wall inhibitors of *Mycobacterium tuberculosis* GlmM and GlmU. *Carbohydr. Res.* 346, 1714–1720. doi: 10.1016/j.carres.2011.05.024
- Ling, L. L., Schneider, T., Peoples, A. J., Spoering, A. L., Engels, I., Conlon, B. P., et al. (2015). A new antibiotic kills pathogens without detectable resistance. *Nature* 517, 455–459. doi: 10.1038/nature14098
- Lingaraju, S., Rigouts, L., Gupta, A., Lee, J., Umubyeyi, A. N., Davidow, A. L., et al. (2016). Geographic differences in the contribution of *ubiA* mutations to high-level ethambutol resistance in *Mycobacterium tuberculosis*. *Antimicrob. Agents Chemother.* 60, 4101–4105. doi: 10.1128/AAC.03002-15
- Lun, S., Miranda, D., Kubler, A., Guo, H., Maiga, M. C., Winglee, K., et al. (2014). Synthetic lethality reveals mechanisms of *Mycobacterium tuberculosis* resistance to β -lactams. *MBio* 5:e01767–14. doi: 10.1128/mBio.01767-14
- Mahapatra, S., Crick, D. C., and Brennan, P. J. (2000). Comparison of the UDP-N-acetylmuramate-L-alanine ligase enzymes from *Mycobacterium tuberculosis* and *Mycobacterium leprae*. *J. Bacteriol.* 182, 6827–6830. doi: 10.1128/JB.182.23.6827-6830.2000
- Mahapatra, S., Scherman, H., Brennan, P. J., and Crick, D. C. (2005). N-glycosylation of the nucleotide precursors of peptidoglycan biosynthesis of *Mycobacterium* spp. is altered by drug treatment. *J. Bacteriol.* 187, 2341–2347. doi: 10.1128/JB.187.7.2341-2347.2005
- Mainardi, J., Hugonnet, J., Gutmann, L., and Arthur, M. (2011). Fighting resistant tuberculosis with old compounds: the carbapenem paradigm. *Clin. Microbiol. Infect.* 17, 1755–1756. doi: 10.1111/j.1469-0691.2011.03699.x
- McNeil, M., Daffe, M., and Brennan, P. J. (1990). Evidence for the nature of the link between the arabinogalactan and peptidoglycan of mycobacterial cell walls. *J. Biol. Chem.* 265, 18200–18206.
- Meeske, A. J., Riley, E. P., Robins, W. P., Uehara, T., Mekalanos, J. J., Kahne, D., et al. (2016). SEDS proteins are a widespread family of bacterial cell wall polymerases. *Nature* 537, 634–638. doi: 10.1038/nature19331
- Mohammadi, T., van Dam, V., Sijbrandi, R., Vernet, T., Zapun, A., Bouhss, A., et al. (2011). Identification of PtsW as a transporter of lipid-linked cell wall precursors across the membrane. *EMBO J.* 30, 1425–1432. doi: 10.1038/emboj.2011.61
- Moraes, G. L., Gomes, G. C., Monteiro de Sousa, P. R., Alves, C. N., Govender, T., Kruger, H. G., et al. (2015). Structural and functional features of enzymes of *Mycobacterium tuberculosis* peptidoglycan biosynthesis as targets for drug development. *Tuberculosis* 95, 95–111. doi: 10.1016/j.tube.2015.01.006
- Morris, R. P., Nguyen, L., Gatfield, J., Visconti, K., Nguyen, K., Schnappinger, D., et al. (2005). Ancestral antibiotic resistance in *Mycobacterium tuberculosis*. *Proc. Natl. Acad. Sci. USA* 102, 12200–12205. doi: 10.1073/pnas.0505446102
- Nasiri, M. J., Haeili, M., Ghazi, M., Goudarzi, H., Pormohammad, A., Imani Fooladi, A. A., et al. (2017). New insights in to the intrinsic and acquired drug resistance mechanisms in mycobacteria. *Front. Microbiol.* 8:681. doi: 10.3389/fmicb.2017.00681
- Nakatani, Y., Opel-Reading, H. K., Merker, M., Machado, D., Andres, S., Kumar, S. S., et al. (2017). Role of alanine racemase mutations in *Mycobacterium tuberculosis* D-cycloserine resistance. *Antimicrob. Agents Chemother.* 61, e01575–e01517. doi: 10.1128/AAC.01575-17
- Nikaido, H. (1994). Prevention of drug access to bacterial targets: permeability barriers and active efflux. *Science* 264, 382–388. doi: 10.1126/science.8153625
- Nikonenko, B. V., Reddy, V. M., Protopenova, M., Bogatcheva, E., Einck, L., and Nacy, C. A. (2009). Activity of SQ641, a capuramycin analog, in a murine model of tuberculosis. *Antimicrob. Agents Chemother.* 53, 3138–3139. doi: 10.1128/AAC.00366-09
- Pavelka, M. S. Jr., Mahapatra, S., and Crick, D. C. (2014). Genetics of peptidoglycan biosynthesis. *Microbiol. Spectr.* 2:MGM2-0034-2013. doi: 10.1128/microbiolspec.MGM2-0034-2013
- Payen, M. C., De Wit, S., Martin, C., Sergysels, R., Muylle, I., Van Laethem, Y., et al. (2012). Clinical use of the meropenem-clavulanate combination for extensively drug-resistant tuberculosis. *Int. J. Tuberc. Lung Dis.* 16, 558–560. doi: 10.5588/ijtld.11.0414
- Payen, M. C., Muylle, I., Vandenberg, O., Mathys, V., Delforge, M., Van den Wijngaert, S., et al. (2018). Meropenem-clavulanate for drug-resistant tuberculosis: a follow-up of relapse-free cases. *Int. J. Tuberc. Lung Dis.* 22, 34–39. doi: 10.5588/ijtld.17.0352
- Payne, K., Sun, Q., Sacchettini, J., and Hatfull, G. F. (2009). Mycobacteriophage Lysin B is a novel mycolylarabinogalactan esterase. *Mol. Microbiol.* 73, 367–381. doi: 10.1111/j.1365-2958.2009.06775.x
- Payne, K. M., and Hatfull, G. F. (2012). Mycobacteriophage endolysins: diverse and modular enzymes with multiple catalytic activities. *PLoS One* 7:e34052. doi: 10.1371/journal.pone.0034052
- Peneff, C., Ferrari, P., Charrier, V., Taburet, Y., Monnier, C., Zamboni, V., et al. (2001). Crystal structures of two human pyrophosphorylase isoforms in complexes with UDPGlc(Gal)NAC: role of the alternatively spliced insert in the enzyme oligomeric assembly and active site architecture. *EMBO J.* 20, 6191–6202. doi: 10.1093/emboj/20.22.6191
- Pimentel, M. (2014). Genetics of phage lysis. *Microbiol. Spectr.* 2, 1–13. doi: 10.1128/microbiolspec.MGM2-0017-2013
- Portevin, D., Gagneux, S., Comas, I., and Young, D. (2011). Human macrophage responses to clinical isolates from the *Mycobacterium tuberculosis* complex discriminate between ancient and modern lineages. *PLoS Pathog.* 7:e1001307. doi: 10.1371/journal.ppat.1001307
- Prosser, G. A., and de Carvalho, L. P. (2013a). Metabolomics reveal D-alanine-D-alanine ligase as the target of D-cycloserine in *Mycobacterium tuberculosis*. *ACS Med. Chem. Lett.* 4, 1233–1237. doi: 10.1021/ml400349n
- Prosser, G. A., and de Carvalho, L. P. (2013b). Reinterpreting the mechanism of inhibition of *Mycobacterium tuberculosis* D-alanine-D-alanine ligase by D-cycloserine. *Biochemistry* 52, 7145–7149. doi: 10.1021/bi400839f
- Prosser, G. A., and de Carvalho, L. P. (2013c). Kinetic mechanism and inhibition of *Mycobacterium tuberculosis* D-alanine-D-alanine ligase by the antibiotic D-cycloserine. *FEBS J.* 280, 1150–1166. doi: 10.1111/febs.12108
- Rana, A. M., Trivedi, P., Desai, K. R., and Jauhari, S. (2014). Novel S-triazine accommodated 5-benzylidino-4-thiazolidinones: synthesis and in vitro biological evaluations. *Med. Chem. Res.* 23, 4320–4336. doi: 10.1007/s00044-014-0995-z
- Rani, C., Mehra, R., Sharma, R., Chib, R., Wazir, P., Nargotra, A., et al. (2015). High-throughput screen identifies small molecule inhibitors targeting acetyltransferase activity of *Mycobacterium tuberculosis* GlmU. *Tuberculosis* 95, 664–677. doi: 10.1016/j.tube.2015.06.003
- Rani, C., and Khan, I. A. (2016). UDP-GlcNAc pathway: potential target for inhibitor discovery against *Mycobacterium tuberculosis*. *Eur. J. Pharm. Sci.* 83, 62–70. doi: 10.1016/j.ejps.2015.12.013
- Raymond, J. B., Mahapatra, S., Crick, D. C., and Pavelka, M. S. Jr. (2005). Identification of the *namH* gene, encoding the hydroxylase responsible for the N-glycosylation of the mycobacterial peptidoglycan. *J. Biol. Chem.* 280, 326–333. doi: 10.1074/jbc.M411006200
- Reddy, V. M., Einck, L., and Nacy, C. A. (2008). In vitro antimycobacterial activities of capuramycin analogues. *Antimicrob. Agents Chemother.* 52, 719–721. doi: 10.1128/AAC.01469-07
- Reynolds, P. E. (1989). Structure, biochemistry and mechanism of action of glycopeptide antibiotics. *Eur. J. Clin. Microbiol. Infect. Dis.* 8, 943–950. doi: 10.1007/BF01967563
- Rullas, J., Dhar, N., McKinney, J. D., Garcia-Perez, A., Lelievre, J., Diacon, A. H., et al. (2015). Combinations of beta-lactam antibiotics—currently in clinical trials are efficacious in a DHP-I-deficient mouse model of tuberculosis infection. *Antimicrob. Agents Chemother.* 59, 4997–4999. doi:10.1128/AAC.01063-15
- Schenk, M., Mahapatra, S., Le, P., Kim, H. J., Choi, A. W., Brennan, P. J., et al. (2016). Human NOD2 recognizes structurally unique muramyl dipeptides from *Mycobacterium leprae*. *Infect. Immun.* 84, 2429–2438. doi: 10.1128/IAI.00334-16
- Schoonmaker, M. K., Bishai, W. R., and Lamichhane, G. (2014). Nonclassical transpeptidases of *Mycobacterium tuberculosis* alter cell size, morphology, the cytosolic matrix, protein localization, virulence, and resistance to β -lactams. *J. Bacteriol.* 196, 1394–1402. doi: 10.1128/JB.01396-13

- Schubert, K., Sieger, B., Meyer, F., Giacomelli, G., Böhm, K., Rieblinger, A., et al. (2017). The antituberculosis drug ethambutol selectively blocks apical growth in CMN group bacteria. *MBio* 8:e02213–16. doi: 10.1128/mBio.02213-16
- Siricilla, S., Mitachi, K., Wan, B., Franzblau, S. G., and Kurosu, M. (2015). Discovery of a capuramycin analog that kills non-replicating *Mycobacterium tuberculosis* and its synergistic effects with translocase I inhibitors. *J. Antibiot.* 68, 271–278. doi: 10.1038/ja.2014.133
- Solapure, S., Dinesh, N., Shandil, R., Ramachandran, V., Sharma, S., Bhattacharjee, D., et al. (2013). *In vitro* and *in vivo* efficacy of β -lactams against replicating and slowly growing/non-replicating *Mycobacterium tuberculosis*. *Antimicrob. Agents Chemother.* 57, 2506–2510. doi: 10.1128/AAC.00023-13
- Stanley, S. A., and Cox, J. S. (2013). Host-pathogen interactions during *Mycobacterium tuberculosis* infections. *Curr. Top. Microbiol. Immunol.* 374, 211–241. doi: 10.1007/82_2013_332
- Tiberi, S., Payen, M. C., Sotgiu, G., D'Ambrosio, L., Alarcon Guizado, V., Alffenaar, J. W., et al. (2016). Effectiveness and safety of meropenem/clavulanate-containing regimens in the treatment of MDR- and XDR-TB. *Eur. Respir. J.* 47, 1235–1243. doi: 10.1183/13993003.02146-2015
- Tomasic, T., Zidar, N., Kovac, A., Turk, S., Simcic, M., Blanot, D., et al. (2010). 5-Benzylidenethiazolidin-4-ones as multi-target inhibitors of bacterial Mur ligases. *Chem. Med. Chem.* 5, 286–295. doi: 10.1002/cmdc.200900449
- Tran, A. T., Wen, D., West, N. P., Baker, E. N., Britton, W. J., and Payne, R. J. (2013). Inhibition studies on *Mycobacterium tuberculosis* N-acetylglucosamine-1-phosphate uridylyltransferase (GlmU). *Org. Biomol. Chem.* 11, 8113–8126. doi: 10.1039/c3ob41896k
- Tran, A. T., Watson, E. E., Pujari, V., Conroy, T., Dowman, L. J., Giltrap, A. M., et al. (2017). Sansanmycin natural product analogues as potent and selective anti-mycobacterials that inhibit lipid I biosynthesis. *Nat. Commun.* 8:14414. doi: 10.1038/ncomms14414
- Tremblay, L. W., Fan, F., and Blanchard, J. S. (2010). Biochemical and structural characterization of *Mycobacterium tuberculosis* β -lactamase with the carbapenems ertapenem and doripenem. *Biochemistry* 49, 3766–3773. doi: 10.1021/bi100232q
- Trunkfield, A. E., Gurcha, S. S., Besra, G. S., and Bugg, T. D. (2010). Inhibition of *Escherichia coli* glycosyltransferase MurG and *Mycobacterium tuberculosis* Gal transferase by uridine-linked transition state mimics. *Bioorg. Med. Chem.* 18, 2651–2663. doi: 10.1016/j.bmc.2010.02.026
- van Heijenoort, Y., Leduc, M., Singer, H., and van Heijenoort, J. (1987). Effects of moenomycin on *Escherichia coli*. *J. Gen. Microbiol.* 133, 667–674. doi: 10.1099/00221287-133-3-667
- Vollmer, W., Blanot, D., and de Pedro, M. A. (2008). Peptidoglycan structure and architecture. *FEMS Microbiol. Rev.* 32, 149–167. doi: 10.1111/j.1574-6976.2007.00094.x
- Wang, F., Cassidy, C., and Sacchettini, J. C. (2006). Crystal structure and activity studies of the *Mycobacterium tuberculosis* beta-lactamase reveal its critical role in resistance to beta-lactam antibiotics. *Antimicrob. Agents Chemother.* 50, 2762–2771. doi: 10.1128/AAC.00320-06
- Wiedemann, I., Breukink, E., van Kraaij, C., Kuipers, O. P., Bierbaum, G., de Kruijff, B., et al. (2001). Specific binding of nisin to the peptidoglycan precursor lipid II combines pore formation and inhibition of cell wall biosynthesis for potent antibiotic activity. *J. Biol. Chem.* 276, 1772–1779. doi: 10.1074/jbc.M006770200
- Wiegmann, D., Koppermann, S., Wirth, M., Niro, G., Leyerer, K., and Ducho, C. (2016). Muramycin nucleoside peptide antibiotics: uridine derived natural products as lead structures for the development of novel antibacterial agents. *Beilstein J. Org. Chem.* 12, 769–795. doi: 10.3762/bjoc.12.77
- Wivagg, C. N., and Hung, D. T. (2012). Resuscitation-promoting factors are required for β -lactam tolerance and the permeability barrier in *Mycobacterium tuberculosis*. *Antimicrob. Agents Chemother.* 56, 1591–1594. doi: 10.1128/AAC.06027-11
- Wivagg, C. N., Bhattacharyya, R. P., and Hung, D. T. (2014). Mechanisms of β -lactam killing and resistance in the context of *Mycobacterium tuberculosis*. *J. Antibiot.* 67, 645–654. doi: 10.1038/ja.2014.94
- Wivagg, C. N., Wellington, S., Gomez, J. E., and Hung, D. T. (2016). Loss of a class A penicillin-binding protein alters β -lactam susceptibilities in *Mycobacterium tuberculosis*. *ACS Infect. Dis.* 2, 104–110. doi: 10.1021/acsinfecdis.5b00119
- World Health Organization. (2011). *Guidelines for the Programmatic Management of Drug-Resistant Tuberculosis-2011 Update*. Geneva.
- World Health Organization. (2014). *Companion Handbook to the WHO Guidelines for the Programmatic Management of Drug-Resistant Tuberculosis*. Geneva.
- World Health Organization. (2010). *Treatment for Tuberculosis. Guidelines*. Geneva.
- World Health Organization. (2017). *Global Tuberculosis Report 2017*. Geneva.
- Wong, E. B., Cohen, K. A., and Bishai, W. R. (2013). Rising to the challenge: new therapies for tuberculosis. *Trends Microbiol.* 21, 493–501. doi: 10.1016/j.tim.2013.05.002
- Zapun, A., Contreras-Martel, C., and Vernet, T. (2008). Penicillin-binding proteins and beta-lactam resistance. *FEMS Microbiol. Rev.* 32, 361–385. doi: 10.1111/j.1574-6976.2007.00095.x
- Zhang, Z., Bulloch, E. M., Bunker, R. D., Baker, E. N., and Squire, C. J. (2009). Structure and function of GlmU from *Mycobacterium tuberculosis*. *Acta Crystallogr. D Biol. Crystallogr.* 65, 275–283. doi: 10.1107/S0907444909001036

Conflict of Interest Statement: The authors declare that the research was conducted in the absence of any commercial or financial relationships that could be construed as a potential conflict of interest.

Copyright © 2019 Catalão, Filipe and Pimentel. This is an open-access article distributed under the terms of the Creative Commons Attribution License (CC BY). The use, distribution or reproduction in other forums is permitted, provided the original author(s) and the copyright owner(s) are credited and that the original publication in this journal is cited, in accordance with accepted academic practice. No use, distribution or reproduction is permitted which does not comply with these terms.



Recognition of Peptidoglycan Fragments by the Transpeptidase PBP4 From *Staphylococcus aureus*

Roberto Maya-Martinez¹, J. Andrew N. Alexander², Christian F. Otten^{3†}, Isabel Ayala¹, Daniela Vollmer³, Joe Gray⁴, Catherine M. Bougault¹, Alister Burt¹, Cédric Laguri¹, Matthieu Fonvielle⁵, Michel Arthur⁵, Natalie C. J. Strynadka², Waldemar Vollmer³ and Jean-Pierre Simorre^{1*}

OPEN ACCESS

Edited by:

Christoph Mayer,
University of Tübingen, Germany

Reviewed by:

Friedrich Götz,
University of Tübingen, Germany
Shahriar Mobashery,
University of Notre Dame,
United States
Mark Horsman,
University of Notre Dame,
United States, in collaboration
with SM

*Correspondence:

Jean-Pierre Simorre
jean-pierre.simorre@ibs.fr

†Present Address:

Christian F. Otten,
Institute for Pharmaceutical
Microbiology, University of Bonn,
Bonn, Germany

Specialty section:

This article was submitted to
Microbial Physiology and Metabolism,
a section of the journal
Frontiers in Microbiology

Received: 22 September 2018

Accepted: 11 December 2018

Published: 18 January 2019

Citation:

Maya-Martinez R, Alexander JAN,
Otten CF, Ayala I, Vollmer D, Gray J,
Bougault CM, Burt A, Laguri C,
Fonvielle M, Arthur M, Strynadka NCJ,
Vollmer W and Simorre J-P (2019)
Recognition of Peptidoglycan
Fragments by the Transpeptidase
PBP4 From *Staphylococcus aureus*.
Front. Microbiol. 9:3223.
doi: 10.3389/fmicb.2018.03223

¹ University Grenoble Alpes, CNRS, CEA, IBS, Grenoble, France, ² Department of Biochemistry and Molecular Biology and Centre for Blood Research, The University of British Columbia, Vancouver, BC, Canada, ³ Centre for Bacterial Cell Biology, Institute for Cell and Molecular Biosciences, Newcastle University, Newcastle upon Tyne, United Kingdom, ⁴ Institute for Cell and Molecular Biosciences, Newcastle University, Newcastle upon Tyne, United Kingdom, ⁵ Centre de Recherche des Cordeliers, LRMA, Equipe 12, Université Sorbonne-Paris, Paris, France

Peptidoglycan (PG) is an essential component of the cell envelope, maintaining bacterial cell shape and protecting it from bursting due to turgor pressure. The monoderm bacterium *Staphylococcus aureus* has a highly cross-linked PG, with ~90% of peptide stems participating in DD-cross-links and up to 15 peptide stems connected with each other. These cross-links are formed in transpeptidation reactions catalyzed by penicillin-binding proteins (PBPs) of classes A and B. Most *S. aureus* strains have three housekeeping PBPs with this function (PBP1, PBP2, and PBP3) but MRSA strains have acquired a third class B PBP, PBP2a, which is encoded by the *mecA* gene and required for the expression of high-level resistance to β -lactams. Another housekeeping PBP of *S. aureus* is PBP4, which belongs to the class C PBPs, and hence would be expected to have PG hydrolase (DD-carboxypeptidase or DD-endopeptidase) activity. However, previous works showed that, unexpectedly, PBP4 has transpeptidase activity that significantly contributes to both the high level of cross-linking in the PG of *S. aureus* and to the low level of β -lactam resistance in the absence of PBP2a. To gain insights into this unusual activity of PBP4, we studied by NMR spectroscopy its interaction *in vitro* with different substrates, including intact peptidoglycan, synthetic peptide stems, mucopeptides, and long glycan chains with uncross-linked peptide stems. PBP4 showed no affinity for the complex, intact peptidoglycan or the smallest isolated peptide stems. Transpeptidase activity of PBP4 was verified with the disaccharide peptide subunits (mucopeptides) *in vitro*, producing cyclic dimer and multimer products; these assays also showed a designed PBP4(S75C) nucleophile mutant to be inactive. Using this inactive but structurally highly similar variant, liquid-state NMR identified two interaction surfaces in close proximity to the central nucleophile position that can accommodate the potential donor and acceptor stems for the transpeptidation reaction. A PBP4:mucopeptide model structure was built from these experimental restraints, which provides new mechanistic insights into *mecA* independent resistance to β -lactams in *S. aureus*.

Keywords: peptidoglycan, NMR, X-ray crystallography, penicillin-binding protein 4, *Staphylococcus aureus*, cyclic mucopeptides

INTRODUCTION

Monoderm bacteria are surrounded by a cell wall containing a multi-layered peptidoglycan (PG) sacculus and secondary cell wall polymers such as teichoic acid and capsular polysaccharide (Silhavy et al., 2010). The PG is a mesh-like polymer that encases the cytoplasmic membrane to maintain the shape and rigidity of the cell. It is composed of glycan chains made of alternating β -1,4-linked *N*-acetylmuramic acid (MurNAc) and *N*-acetylglucosamine (GlcNAc) residues, which are connected by short peptides (Vollmer et al., 2008). PG precursor synthesis starts in the cytoplasm, where the UDP-MurNAc-peptide and UDP-GlcNAc precursors are assembled. The final PG precursor, lipid II, is then assembled at the inner leaflet of the cytoplasmic membrane, flipped across to the outer leaflet, and utilized by PG synthases to polymerize the glycan chains in processive glycosyltransferase (GTase) reactions and form the peptide cross-links by transpeptidation (TPase reactions) (Macheboeuf et al., 2006). The latter activity, catalyzed by penicillin-binding proteins (PBPs), is the target of β -lactam and glycopeptide antibiotics. In the context of the increasing problem of antimicrobial drug resistance and the role of PG fragments in the innate immune response, it is crucial to get more information on the interactions between proteins and cell wall components such as PG (Zapun et al., 2008; Sung et al., 2009). Some PG-interacting proteins are able to bind antibiotics or soluble PG fragments with an affinity that is amenable to structural studies using X-ray crystallography (Sobhanifar et al., 2013). For example, the structure of the TPase PBP2x from *Streptococcus pneumoniae* has been determined by crystallography. A hypothetical model of the possible complex with a large peptidoglycan fragment has been proposed based on structures of non-covalent and covalent PBP complexes with β -lactam antibiotics (Bernardo-García et al., 2018). Liquid-state NMR has also been used to determine the structure of complexes with lower affinity (Lehotzky et al., 2010). However, interaction studies involving large fragments or the entire peptidoglycan polymer are in most cases not amenable to liquid-state NMR. Furthermore, the peptidoglycan sacculus is a large (10^9 Da), dynamic, and heterogeneous structure, which hampers structural investigations by electron microscopy and X-ray crystallography. Solid-state NMR has emerged as a promising method to characterize peptidoglycan structure and dynamics (Kern et al., 2010; Romaniuk and Cegelski, 2015). Solid-state NMR can be used with any sample whose molecules re-orient on a time scale that is much slower than the ms-range time-scale of the NMR experiment. Thus, solid-state NMR can be applied to hydrated insoluble cell walls or hydrated intact cell samples, with the advantage of an improved spectral resolution resulting from the local dynamics present in the hydrated state (Gang et al., 1997; Kern et al., 2010). In this context, solid-state NMR has been used to measure structural constraints on a complex formed between the LD-transpeptidase from *Bacillus subtilis* Ldt_{Bs} and intact peptidoglycan sacculi (Schanda et al., 2014).

Infection with methicillin-resistant *Staphylococcus aureus* (MRSA) results in diverse clinical manifestations, ranging from minor skin infections to life-threatening bacteremia and pneumonia. *S. aureus* has one monofunctional GTase and

four PBPs, of which PBP2, the sole bifunctional class A PBP, is responsible for the majority of PG synthesis (Pinho and Errington, 2004; Sauvage et al., 2008). PBP2 is essential in *S. aureus* strains susceptible to methicillin, but its TPase activity can be replaced by that of an acquired and unusual class B PBP, PBP2a, when cells are grown in the presence of methicillin (Pinho et al., 2001). Of the two other class B PBPs, the essential PBP1 plays a role in cell division and separation, whereas the function of the non-essential PBP3 is still vague (Pinho et al., 2000; Pereira et al., 2007). PBP4 is the only class C PBP present in *S. aureus*. Members of this class usually exhibit DD-carboxypeptidase (DD-CPase) or endopeptidase (DD-EPase) activity. PBP4 from *S. aureus* is unique within the class C PBPs, as it was shown *in vivo* and *in vitro* to possess DD-TPase activity in addition to DD-CPase activity, leading to a highly cross-linked PG (Wyke et al., 1981; Loskill et al., 2014; Srisuknimit et al., 2017). PBP4 does not appear to work on nascent PG, but catalyzes further cross-linking reactions in polymeric PG (Atilano et al., 2010).

To perform its transpeptidase activity, PBP4 initiates a nucleophilic attack by the hydroxyl group of the catalytic Ser75 residue on the terminal D-Ala-D-Ala amide bond of the peptidoglycan stem peptide. The C-terminal D-Ala is subsequently released from the peptide and an acylenzyme intermediate forms. Enzyme deacylation follows when the terminal amino group of the glycine bridge of a second peptide stem acts as an acyl acceptor, resulting in a peptide cross-link between two adjacent peptidoglycan stems. The CPase activity follows a similar reaction scheme, except that the acceptor is a water molecule, yielding a tetrapeptide stem after enzyme deacylation. The β -lactam ring of methicillin and other antibiotics of the β -lactam family can act as mimics of the D-Ala-D-Ala extremity of the acyl-donor peptide stem. However, unlike the natural substrate, the β -lactam-PBP acylenzyme is very stable and results in long-term inactivation of the PBPs. Different β -lactam-PBP acylenzymes have been structurally characterized at atomic resolution but mucopeptide- or peptidoglycan-PBP adducts have thus far only been modeled due to the intractable nature of crystallizing these larger substrate complexes (Bernardo-García et al., 2018). Some methicillin-resistant strains of *S. aureus* carry mutations in either the promotor region or the *pbp4* gene itself, leading to an increased expression of PBP4 and/or increased PG cross-linkage but without significantly altering β -lactam binding (Chatterjee et al., 2017; Hamilton et al., 2017).

Rational modification of the β -lactam scaffold to potentially overcome PBP4-mediated resistance would therefore require additional structural information on the PG fragment-PBP4 adducts. To obtain such data, we studied here the interaction of PBP4 with different natural substrates or substrate analogs. We characterized the activity of PBP4 *in vitro* and measured the interaction between PBP4 and different PG fragments by X-ray crystallography, liquid- and solid-state NMR. From the NMR data obtained we built a structural model of a peptidoglycan fragment-PBP4 complex that may help explain the unusual DD-TPase activity of this PBP.

MATERIALS AND METHODS

Preparation of Peptidoglycan and Muropeptides

S. aureus strain SH1000 (wild type) was a generous gift of S. J. Foster (University of Sheffield). *S. aureus* cells were grown in 1.5 L of Tryptic Soy Broth (TSB) until an OD₆₀₀ of 0.8–0.9 (Bui et al., 2012; Figueiredo et al., 2012). Cells were subsequently cooled down at 4°C and harvested by centrifugation at 10,000 × g for 20 min. Bacterial cell walls were purified from the cell pellets according to a published protocol for *Streptococcus pneumoniae* (Bui et al., 2012). To remove wall teichoic acids, 10 mg of cell wall was treated with 48% hydrofluoric acid at 4°C for 48 h. PG (~5 mg) was recovered by centrifugation at 264,000 × g and 4°C for 45 min. The PG pellet was washed with water and resuspended in 1 mL of buffer containing 0.02% sodium azide for storage at 4°C. Uniformly ¹³C,¹⁵N-labeled peptidoglycan SH1000 samples were obtained by growing *S. aureus* cells in a M9 medium containing 4 g/L of ¹³C-glucose and 1 g/L of ¹⁵NH₄Cl.

To generate muropeptides, 150 µL of the *S. aureus* SH1000 stock suspension of PG was incubated overnight at 37°C with 50 µL of 320 mM sodium phosphate, pH 4.8 and 10 µL of 1 mg/mL cellosyl (Höchst AG, Frankfurt, Germany). The mixture was boiled at 100°C for 10 min to inactivate the enzyme, the sample was centrifuged at 10,000 × g for 20 min, and the supernatant containing the muropeptides was collected. The muropeptide solution was stored at 2–8°C. To generate the soluble PG glycan chains with monomeric peptides the PG was digested with recombinant lysostaphin from *Staphylococcus simulans* (Sigma-Aldrich). In a typical preparation, 20 mL of a 5 mg/mL suspension of unlabeled or ¹³C,¹⁵N-labeled PG in 5 mM sodium phosphate at pH 7.0 was incubated under stirring at 37°C for 24 h with 2 mg of lysostaphin (final concentration 100 µg/mL). Lysostaphin was inactivated and precipitated by placing the mixture at 100°C for 10 min. The mixture was centrifuged at 10,000 × g for 30 min and the supernatant containing the PG fragments was recovered and stored at –20°C.

Soluble fragments were dialyzed against water. Before aliquoting the samples or before lyophilization, the concentration of the stock solution was estimated by liquid-state NMR using the Eretic pulse sequence (Frank et al., 2014) and a reference 1 mM sucrose sample in 90%:10% H₂O:D₂O.

Synthesis of Branched Lactoyl Peptides

Fmoc-D-Glu-NHTrt and D-LacO^tBu were synthesized as previously described (see Supporting Information in Ngadjewa et al., 2018). Orthogonal Fmoc and 1-(4,4-dimethyl-2,6-dioxocyclohexylidene)-3-methylbutyl (ivDde) protecting groups were used for sequential assembly of the branched peptide stem (see Ngadjewa et al., 2018 for similar peptides containing a D-iAsn bridge). First, the main peptide stem (D-Lac-L-Ala-D-iGln-L-Lys-D-Ala_{10r2}) was elongated from the Wang-D-Ala resin by successive coupling reactions with Fmoc-protected amino-acids. Second, the ε-NH₂ group of L-Lys was deprotected by hydrazinolysis, and Fmoc-Gly and 2 Fmoc-Gly-Gly were successively introduced to build the pentaglycine-bridge in three steps (Figure 2A). Final deprotection of

acid-labile Fmoc and Trt protecting groups and cleavage from the resin was achieved under gentle stirring at room temperature with 2 mL of a TFA solution containing DCM, TIPS, and water (80:20:5:5 v:v:v:v). The solution was filtered to remove the resin, which was washed with 1 mL of the TFA solution. The TFA solutions were pooled and evaporated under reduced pressure before solvent extraction and purification by *rp*HPLC (Supplementary Information). 11 mg (14.2 µmol) and 4 mg (4.7 µmol) of pure tetrapeptide and pentapeptide, respectively, were isolated. The purity of each sample was analyzed by HPLC and their chemical structure characterized by mass spectrometry (Supplementary Figure S2) and NMR (Supplementary Figure S1 and Supplementary Table 1).

Expression and Purification of *S. aureus* PBP4 and PBP4(S75C)

Unlabeled recombinant native PBP4 (residues 21–383) was expressed as previously published (Hamilton et al., 2017). Unlabeled PBP4(S75C) was expressed, purified and treated with thrombin to remove the His-tag as previously reported for the native enzyme, except that 5 mM TCEP was included in all buffers used during purification (Alexander et al., 2018). The expression and purification protocol was adapted for the production of ¹³C,¹⁵N-labeled PBP4 and PBP4(S75C) samples for NMR studies. To maintain good protein yields, thrombin cleavage of the GSSHHHHHHSSGLVPRGSHM N-terminal His-tag was not performed. Plasmid carrying the PBP4 or PBP4(S75C) gene was transformed into *E. coli* BL21(DE3). Freshly transformed bacteria were sequentially adapted over 1 day from LB to minimal M9 medium (37 mM Na₂HPO₄, 22 mM KH₂PO₄, 8.5 mM NaCl, 1 g L^{–1} ¹⁵NH₄Cl, 2 g L^{–1} D-glucose-¹³C₆ for ¹³C,¹⁵N-labeled proteins or D-glucose for ¹⁵N-only labeled proteins, 1 mM MgSO₄, 0.1 mM CaCl₂, 0.1 mM MnCl₂, 50 µM ZnSO₄, 50 µM FeCl₃, 1 mg pyridoxine, 1 mg biotin, 1 mg hemicalcium salt of pantothenic acid, 1 mg folic acid, 1 mg choline chloride, 1 mg niacinamide, 0.1 mg riboflavin, 5 mg thiamine). M9 preculture grown overnight at 37°C with OD₆₀₀ ~2–2.5 was used to inoculate 1 L of M9 culture medium in a 1:10 ratio. The latter culture was grown at 37°C until OD₆₀₀ = 1. Expression was then induced for 3 h at 37°C with 1 mM IPTG. After harvesting the cells by centrifugation at 6,000 × g and 4°C for 20 min, the pellet was resuspended in 20 mL of lysis buffer (25 mM Tris-HCl, 500 mM NaCl, 20 mM imidazole at pH 7.5, which contained in addition 2 mM β-mercaptoethanol in the case of PBP4(S75C)). One tablet of cOmplete EDTA-free (Roche), 10 mg of lysozyme and RNase/DNase were added, and cells were disrupted by sonication. The lysate was clarified by centrifugation at 46,000 × g during 45 min at 4°C and cell debris were discarded. The supernatant was loaded onto a HisTrapTM (GE Healthcare) chromatography column. A wash was performed with 5 column-volumes of Buffer A (25 mM Tris-HCl, 1 M NaCl, 20 mM imidazole at pH 7.5). The protein was eluted with a 10–100% linear gradient of Buffer B (25 mM Tris-HCl, 500 mM NaCl, 500 mM imidazole at pH 7.5). Fractions containing the protein were pooled and concentrated and then loaded to a Superdex200 (16/60) column pre-equilibrated with

the NMR buffer (100 mM potassium phosphate, 150 mM KCl at pH 7.0). Fractions containing the pure protein were pooled and concentrated for the requirements of NMR studies. For the production of the ^{13}C , ^{15}N , ^2H -labeled PBP4 sample, two additional pre-cultures were performed before the 1L-culture for the sequential adaptation of cells to a 50% H_2O :50% D_2O M9 medium and 100% D_2O M9 medium. The 1L-culture was furthermore achieved in 100% D_2O with D-Glucose- $^{13}\text{C}_6\text{H}_7$.

Pull-Down Experiments

Stored sacculi were resuspended, washed twice with water and twice with the interaction buffer, 100 mM potassium phosphate (pH 7.0), and isolated by centrifugation for 10 min at $16,000 \times g$. The PBP4 protein sample was prepared as described previously and the buffer was exchanged on a NAPTM-5 desalting column (GE-Healthcare) pre-equilibrated with the interaction buffer, and the protein concentration was adjusted to 20 μM . After resuspension in the interaction buffer, 100 μL of sacculi solution was incubated with 100 μL of 20- μM PBP4 at 4°C overnight. The supernatant was discarded and kept for analysis by SDS-PAGE. Sacculi were washed 3 times with 100 μL of interaction buffer and finally resuspended in Laemmli buffer for SDS-PAGE analysis.

PBP4 Activity Assays With Muropeptides or With PG From *S. aureus* SH1000

Assays were carried out in a final volume of 50 μL containing 10 mM Tris/HCl at pH 7.5, 10 mM MgCl_2 , 0.1% Triton X-100, and 10 μM PBP4 or PBP4(S75C). A $\sim 5 \text{ mg mL}^{-1}$ suspension of PG or 25 μL of a $\sim 5 \text{ mg mL}^{-1}$ solution of muropeptides were added and the reaction mixture was incubated at 37°C overnight. The enzymatic reaction was stopped by boiling the samples for 10 min. Muropeptides were reduced and analyzed by HPLC as described (Boneca et al., 1997).

PBP4(S75C) Activity Assays With Imipenem and Native Mass Spectrometry

Purified PBP4(S75C) at 1.2 mg mL^{-1} was incubated at $\sim 23^\circ\text{C}$ for 30 min in buffer C (20 mM MES pH 6, 300 mM NaCl, 5 mM Tris(2-carboxyethyl)phosphine (TCEP)) with or without 1.25 mM imipenem prior to being frozen at -20°C . For mass spectrometry analysis, samples were thawed and diluted 500 times in 5% acetonitrile and 0.1% formic acid. 5 μL of each sample was injected onto a 5-mm C4 column connected to a Waters Xevo GS-2 QToF mass spectrometer via a NanoAquity UPLC system. Samples were eluted in a 2-min gradient from 5 to 100% acetonitrile at a flow rate of 20 $\mu\text{L min}^{-1}$. Mass spectra (Supplementary Figure S3) were summed and peak masses deconvoluted using Waters' MassLynx software (V4.1).

X-Ray Crystallography of PBP4(S75C)

PBP4(S75C) was crystallized using the sitting drop vapor diffusion method with streak seeding. Protein at 25–35 mg mL^{-1} was added to precipitant solution (8 mM zinc chloride, 80 mM sodium acetate pH 5, 100 mM sodium fluoride, and 16% polyethylene glycol 6000) in a 1:1 (v/v) ratio and incubated at 23°C. Immediately after mixing the protein and precipitant solution, the drops were streak-seeded with a housecat whisker

that had been swished through a drop containing PBP4(S75C) crystals. Prior to harvesting, the PBP4(S75C) crystals were soaked in 1 mM ampicillin and 8 mM HO-D-Lac-L-Ala-D-iGln-[L-Lys(Gly)₅]-D-Ala-D-Ala-COOH pentapeptide for 40–60 min before glycerol was added to 15% (v/v). Crystals were then promptly harvested and stored in liquid nitrogen.

Data collection was performed under cryogenic temperatures (100 K) at the Advanced Light Source synchrotron (U.C. Berkeley) on beamline 5.0.2. Data from one crystal that diffracted to 1.9 Å resolution were processed using Xia2 (Winter et al., 2013) and XDS (Kabsch, 2010) with a space group of C121 and merged with Aimless in the CCP4 software package (Winn et al., 2011). Phaser (McCoy et al., 2007) was employed to solve the structure by molecular replacement using PDB ID 5TXI as the starting model. The Phenix suite of programs was used for model generation and refinement (Adams et al., 2010). Briefly, AutoBuild was used with several iterative rounds of manual manipulation of the model with Coot (Emsley et al., 2010) followed by refinement with Phenix.refine with TLS being used in the later stages of refinement. **Supplementary Figure S4** was generated using PyMOL (The PyMOL Molecular Graphics System, Version 2.1.1 Schrödinger, LLC). The final structure was deposited into the PDB under the accession code 6DZ8.

NMR Resonance Assignment

Data for ^1H - and ^{13}C -NMR resonance assignment of synthetic tetra- and pentapeptide were recorded at 20°C on a 2 mg mL^{-1} solution of the peptide in 50 mM potassium phosphate buffer at pH 6.5 with 10% D_2O on a Bruker 600-MHz spectrometer equipped with an Avance IIIHD console and a cryogenically cooled triple-resonance probe. Collected experiments on both peptides included 1D ^1H , 2D-TOCSY and 2D-NOESY with excitation sculpting for water suppression and sensitivity-enhanced ^{13}C -HSQC.

Data for ^{13}C , ^{15}N -labeled peptidoglycan fragments from *S. aureus* strain SH1000 obtained by lysostaphin digestion were recorded at 20°C on a 2 mg mL^{-1} solution in 50 mM potassium phosphate buffer at pH 6.5 with 10% D_2O on a Bruker 850-MHz spectrometer equipped with an Avance IIIHD console and a cryogenically cooled triple-resonance probe. 2D ^{13}C -HSQC and ^{15}N -BEST-TROSY experiments served as starting points for assignments. 3D BEST-HNCACB, BEST-HNcoCACB, BEST-HNCO, HccoNH, hCcoNH, hNcacoNH experiments were collected for the assignment of resonances to nuclei of peptide stems ^1H , ^{13}C and ^{15}N (Favier and Brutscher, 2011). These experiments were complemented with ^{15}N - and ^{13}C -NOESY-HSQC. A 2D hCcH-TOCSY dataset was collected for the assignment of carbohydrate resonances.

Data for ^1H -, ^{13}C - and ^{15}N -NMR backbone resonance assignment of wild-type PBP4 were recorded at 25°C on an 800 μM ^{13}C , ^{15}N , ^2H -labeled PBP4 sample in 100 mM potassium phosphate buffer containing 300 mM KCl and 5% D_2O at pH 7.5 on Bruker spectrometers with ^1H Larmor frequencies ranging from 700 to 950 MHz equipped with an Avance IIIHD console and a cryogenically cooled triple-resonance probe. The superimposition of the ^{15}N -BEST-TROSY of this sample and an equivalent ^{13}C , ^{15}N -only labeled sample proved the H/D

back-exchange to be essentially complete in the conditions used to purify the protein. Collected experiments included a ^{15}N -BEST-TROSY, a BEST-HNCACB/BEST-HNcoCACB pair, a BEST-HNCA/BEST-HNcoCA pair, a BEST-HNCO/BEST-HNcaCO pair, and a ^{15}N -NOESY-HSQC. Deuteration of this 384-amino acid protein construct was instrumental for magnetization transfer through scalar couplings in 3D experiments. All NMR data were processed with Topspin 3.5 (Bruker) and analyzed with CcpNmr (Vranken et al., 2005) for resonance assignment. Assignments were 100% complete for synthetic peptides and peptidoglycan fragments. For PBP4 unambiguous resonance assignment was obtained for 65.5, 67.7, 69.0, and 67.0% of the backbone amide nuclei, carbonyl carbons, α -carbons, and β -carbons, respectively. Close to 13% of the amide resonances remained undetected at pH 7.5 and on the pH-stability range of the protein. The corresponding residues are probably in dynamic part of the protein in solution or their backbone amide is largely accessible to the solvent. Among the amide resonances, 25% were detected but remained unambiguously assigned due to coherence transfer issues in the 3D experiments and signal overlap. Assignments of resonances on wild-type PBP4 were transferred to PBP4(S75C) upon superimposition of ^{15}N -BEST-TROSY experiments recorded in the same conditions.

NMR Titration Experiments

Interaction studies with ^{15}N -labeled PBP4(S75C) and different substrates were monitored by superimposition of ^{15}N -BEST-TROSY spectra at 25°C for different substrate-to-protein ratio. Synthetic peptide stems and peptidoglycan fragments were extensively dialyzed against water using a Spectra/Por™ dialysis membrane with a 100–500 Da cutoff (Spectrum Laboratories, Inc.) and lyophilized before preparation of a few-mM stock solution in the protein buffer, with 50 mM potassium phosphate at pH 6.5. A 326- μM solution of PBP4(S75C) was titrated with 2, 8, 22, and 52 molar equivalents of tetrapeptide. A 150- μM solution of PBP4(S75C) was titrated with an estimated 2, 10, 25, 50, 100, and 180 molar equivalents of mucopeptides from *S. aureus* strain SH1000. A 150- μM solution of PBP4(S75C) was titrated with estimated 2, 10, and 16 molar equivalents of peptidoglycan fragments obtained by lysostaphin digestion. A 150- μM solution of PBP4(S75C) was incubated with 1.2 molar equivalents of imipenem and showed significant chemical shift changes for some of the resonances. Addition of another 1.2 molar equivalents of imipenem did not yield further chemical shift changes. CcpNmr was used to monitor protein chemical shift perturbations (CSP) for every assigned amide resonance by superimposition of the ^{15}N -BEST-TROSY spectra. CSPs ($\Delta\delta$) were calculated on a per-residue basis for the highest substrate-to-protein ratio as follows:

$$\Delta\delta = \sqrt{\left(\delta_{\text{PBP4(S75C):sub}}^{1\text{H}} - \delta_{\text{PBP4(S75C)}}^{1\text{H}}\right)^2 + \left[\frac{\gamma_{\text{N}}}{\gamma_{\text{H}}} \left(\delta_{\text{PBP4(S75C):sub}}^{15\text{N}} - \delta_{\text{PBP4(S75C)}}^{15\text{N}}\right)\right]^2},$$

where γ_{N} and γ_{H} are the ^1H and ^{15}N gyromagnetic ratios, respectively, and $\delta_{\text{PBP4(S75C):sub}}^{\text{X}}$ and $\delta_{\text{PBP4(S75C)}}^{\text{X}}$ are the

protein resonance chemical shift value in the presence and absence, respectively, of the substrate at the highest ratio.

NMR-Data Driven Docking

Models of PBP4 in complex with mucopeptides were built with the version HADDOCK2.2 of “The HADDOCK web server for data-driven biomolecular docking” (de Vries et al., 2010). As starting structures, we used the X-ray crystallography structure of PBP4 (PDB ID 6C39) and a GlcNAc-MurNAc-L-Ala-D-iGln-[L-Lys(Gly)₅]-D-Ala mucopeptide structure generated in-house using CNS (Schanda et al., 2014). The PBP4 and two mucopeptide structures were then docked within HADDOCK. All atoms of the mucopeptides were considered as passive Ambiguous Restraints (AIR). Residues of PBP4 that showed chemical shift perturbations above the threshold in **Supplementary Figure S6** were considered as active AIRs. Calculations were performed with 2,000 structures during the HADDOCK rigid body energy minimization, 400 structures during the refinement, and 200 structures during the refinement in explicit water. Structure scores were calculated from the weighted energy average, $\text{HADDOCK score} = E_{\text{vdW}} + 0.2 E_{\text{Electrostatics}} + 0.1 E_{\text{Air}} + E_{\text{desolvation}}$. The output model structures were sorted with the HADDOCK built-in clustering tool using the Fraction of Common Contacts (FCC) method (Rodrigues et al., 2012) with a 0.61-Å cutoff and a minimum of 4 structures per cluster. To improve the convergence during the HADDOCK run, a 2.5-Å unambiguous restraint was introduced between the oxygen of the catalytic serine S75 of PBP4 and the carbonyl carbon of D-Ala⁴ of one mucopeptide stem, as well as between the oxygen of the catalytic serine S75 of PBP4 and the amine nitrogen of the bridging Gly5 of another mucopeptide stem. After on-line FCC clustering of the solutions, the two clusters with the best HADDOCK scores and lower energy were analyzed in more detail within PyMOL.

RESULTS

PBP4 Does Not Interact With High-Molecular Weight PG

As PBP4 contributes to the high degree of cross-linking in the PG of *S. aureus*, we first considered the mature peptidoglycan of *S. aureus* as a substrate for PBP4 DD-TPase activity. We thus incubated the enzyme with PG from *S. aureus* strain SH1000, digested the resulting PG with cellosyl muramidase, and analyzed the obtained mucopeptide profile by HPLC. PBP4 did not alter the mucopeptide profile, indicating that high-molecular weight PG is not a substrate for the transpeptidase reaction (**Figure 1A**). However, it is possible that high-molecular weight PG is recognized and coordinated by the enzyme in an accessory role. To test this, we isolated PG from *S. aureus* cells and assayed for interaction with PBP4 by a pull-down experiment. PBP4 was not pulled down with PG, showing that the enzyme does not have a high affinity for PG (**Figure 1B**). This result also precluded being able to perform binding experiments by solid-state NMR spectroscopy and, therefore, we turned to liquid-state NMR spectroscopy approaches to probe for interactions between PBP4 and soluble peptidoglycan fragments.

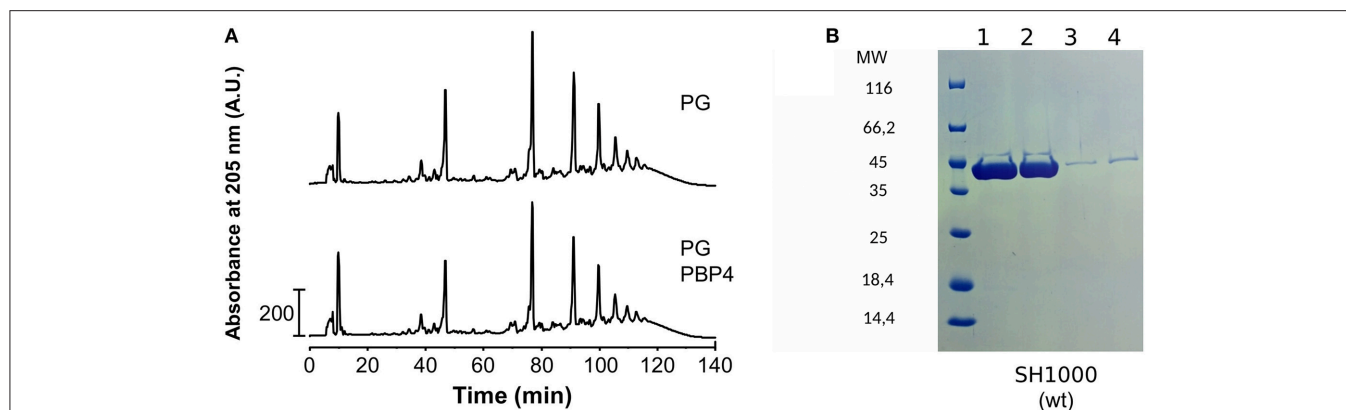


FIGURE 1 | PBP4 does not modify or interact with purified PG. **(A)** PG from *S. aureus* SH1000 was incubated with PBP4, followed by preparation and HPLC analysis of mucopeptides. The mucopeptide profile of the sample with PBP4 (bottom chromatogram) showed no significant difference to the control sample without PBP4 (top). This shows that PG is not a substrate for PBP4. **(B)** Interaction of PBP4 with peptidoglycan sacculi using pull-down experiments. Pull-down experiments were performed with purified PG from *S. aureus* strain SH1000. Samples were analyzed by SDS-PAGE stained by Coomassie Blue. PBP4 was present in the supernatant fractions (lanes 1 and 2) and largely absent in the PG fractions (lanes 3 and 4) showing that PBP4 does not interact with PG.

Preparation of Different Soluble Peptidoglycan Fragments

In order to proceed we aimed to prepare different soluble peptidoglycan fragments to analyze enzyme/substrate complexes by X-ray crystallography or liquid-state NMR spectroscopy. As potential DD-TPase, DD-CPase and DD-EPase activities of PBP4 target the peptides in PG, we first considered chemical synthesis of defined tetrapeptide and pentapeptide stems. To this end, we synthesized two branched lactoyl-peptides, HO-D-Lac-L-Ala-D-iGln-L-Lys(Gly)₅-D-Ala-COOH tetrapeptide and HO-D-Lac-L-Ala-D-iGln-[L-Lys(Gly)₅]-D-Ala-D-Ala-COOH pentapeptide, which both resemble the native peptides in the PG of *S. aureus*, by divergent Fmoc solid-phase peptide synthesis using orthogonal protecting groups (see Methods) in 24 and 8% yield, respectively (**Figure 2A**). Milligram quantities were obtained for each of the tetrapeptide and pentapeptide products, following HPLC purification, solvent exchange against water and lyophilization. We also prepared alternative possible substrates for PBP4 by digesting PG from *S. aureus* by different hydrolases (**Figure 2B**). For this, PG was prepared from *S. aureus* grown either in unlabeled growth media or in growth media for ¹³C,¹⁵N-isotopic labeling. The PG was digested overnight with the cellosyl muramidase or the lysostaphin endopeptidase. Cellosyl generates a mixture of cross-linked and un-crosslinked disaccharide peptide subunits (mucopeptides); lysostaphin generates glycan chains bearing un-crosslinked peptides. After heat inactivation of the hydrolases, the PG fragments were extensively dialyzed against water using a 500-kDa cut-off membrane, and lyophilized. In each case we recovered a few mg of a white powder of soluble peptidoglycan fragment mixture from approximately 10 mg of PG. Synthetic peptides and ¹³C,¹⁵N-labeled soluble fragments prepared from PG were analyzed by liquid-state NMR spectroscopy using different homonuclear or heteronuclear experiments. **Figure 2C** shows the resonance assignments for the ¹H,¹³C-correlation spectrum of the synthetic pentapeptide, confirming its chemical structure (see **Supplementary Figure S1A** for tetrapeptide spectra,

Supplementary Figure S2 for HPLC and MS characterization and **Supplementary Table 1** for resonance assignments on both peptides). **Figure 2D** shows the ¹H,¹⁵N-correlation spectrum of soluble PG fragments obtained by digestion with lysostaphin (see **Supplementary Figure S1B** for ¹H,¹³C-correlations). The intensities and line widths of the resonances suggested that the generated fragments behave mainly as monomers in solution. Resonance assignments through 3D heteronuclear experiments aided the characterization of fragments of different chemical structures within the mixture (**Figure 2D**). The amide resonances of terminal residues of a peptide chain could be clearly distinguished from the resonances derived from amino acids present within the peptide. This allowed us to identify the terminal D-Ala⁴ and D-Ala⁵ in the tetrapeptides and pentapeptides, respectively, and to quantify each species in the mixture. Similarly, terminal glycines with a free carboxylic acid and penultimate glycines with a free amine (resulting from the hydrolysis of a Gly-Gly peptide bond by lysostaphin) produce a ¹⁵N-chemical shift ranging from 114 to 117 ppm, while amide resonances from internal glycine residues show ¹⁵N chemical shifts ranging from 107 to 111 ppm (in pink in **Figure 2D**). Quantifying the signals from these two sets of Gly resonances revealed that lysostaphin cleaved the glycine bridge to leave mainly 2 to 3 Gly residues at the Lys, showing that lysostaphin predominantly cleaves the pentaglycine-bridge at these positions. This observation is in agreement with results obtained from lysostaphin digestion of the cell wall-anchored MalE-Cws protein, which yielded a major soluble protein fraction with the addition of three Gly from the PG pentaglycine bridge at its C-terminus as shown by mass spectrometry (Schneewind et al., 1995).

PBP4 Produces Cyclic Mucopeptides by TPase Reactions

To test the activity of *S. aureus* PBP4, we incubated the enzyme with mucopeptides from *S. aureus* SH1000 and analyzed the reaction products by HPLC and MS (**Figure 3**). PBP4

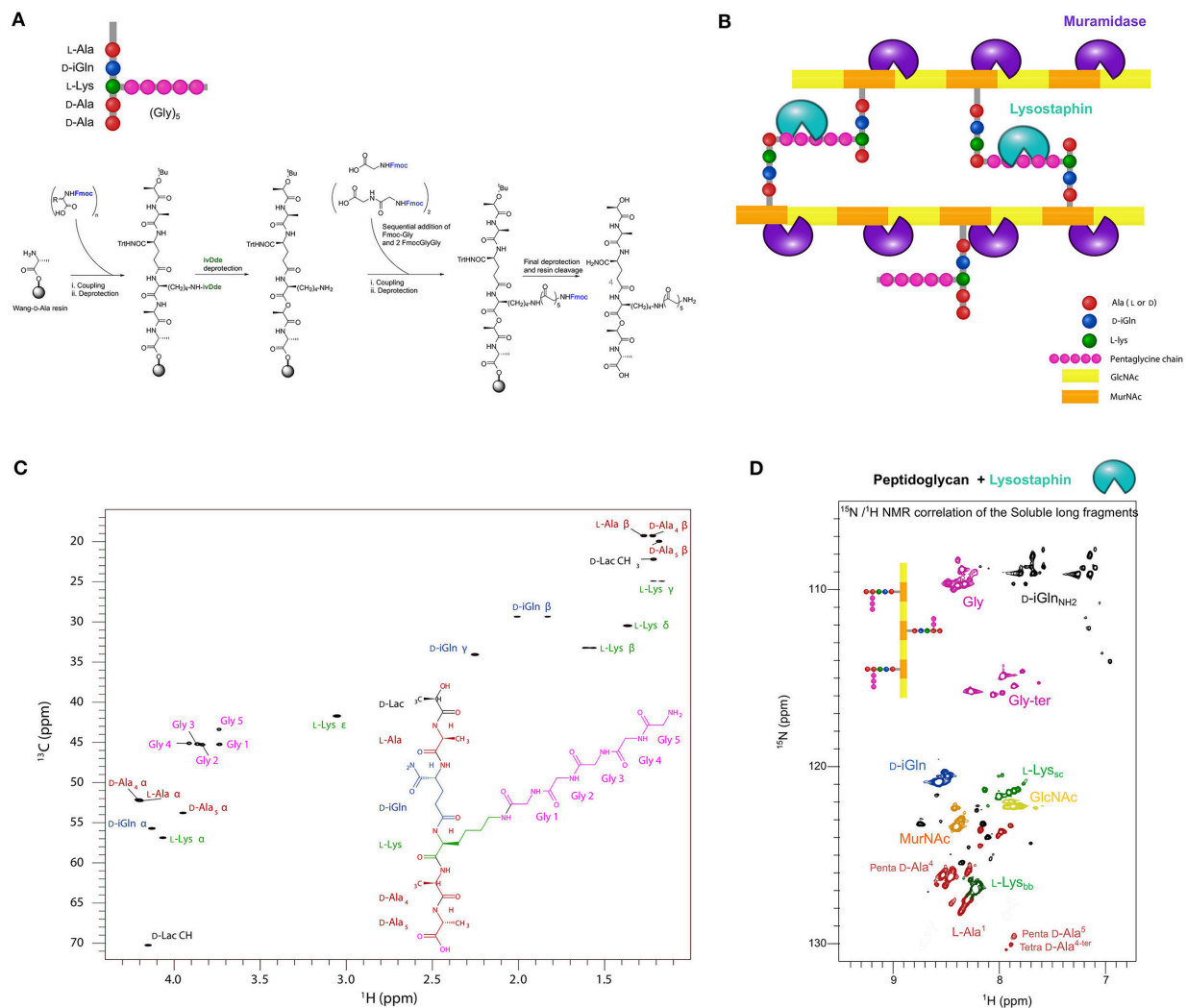


FIGURE 2 | Preparation and NMR spectroscopy of PG fragments **(A)** Scheme of the synthetic route to branched lactoyl-peptides. Wang-D-Ala resin was obtained by Fmoc deprotection of the commercially available functionalized solid-phase support for peptide synthesis. Protecting groups: Fmoc, fluorenylmethoxycarbonyl; Trt, trityl; IvDde, 1-(4,4-dimethyl-2,6-dioxocyclohexylidene)-3-methylbutyl. **(B)** Scheme of the PG structure showing the cleavage sites of the muramidase cellosyl (purple) and the endopeptidase lysostaphin (green). **(C)** ^1H , ^{13}C -correlation NMR spectrum (^{13}C -HSQC) collected at 20°C on a 2.3 mM sample of HO-D-Lac-L-Ala-D-Igln-L-Lys(Gly)₅-D-Ala-D-Ala-COOH pentapeptide in 50 mM potassium phosphate buffer, pH 6.5 containing 10% D₂O. **(D)** ^1H , ^{15}N -correlation NMR spectrum (^{15}N -HSQC) of a ~500 μM solution of PG fragments obtained by digestion with lysostaphin of PG from *S. aureus* SH1000 grown in a ^{13}C , ^{15}N -labeled medium. Resonances are color-coded with residue-type. Bb and sc indices stand for backbone and side-chain, respectively. The percentage of peptides with one, two or more Gly residues attached to the ε- amino group of Lys (after processing with lysostaphin) was ~6% of (1 Gly), ~51% of (2 Gly), and ~42% of (more than 2 Gly), suggesting a preferred cleavage of the pentaglycine bridge between the Gly residues at positions 2 and 3.

showed DD-CPase activity against the monomeric mucopeptide, disaccharide pentapeptide(Gly₅) (peak5), which was nearly quantitatively converted to disaccharide tetrapeptide(Gly₄) (peak A). Interestingly, all the oligomeric peaks (for example, the dimer 11, trimer 15, tetramer 16, or pentamer 17) were completely converted by PBP4 to products with higher retention times (peaks B, C, D, and E). MS analysis of these products identified these as cyclic products, ostensibly as a result of intramolecular TPase activity of PBP4 (Figures 3B,C). As expected, the active site mutant PBP4(S75C) was inactive in this assay (Figure 3A). Remarkably, although PBP4(S75C) lacked CPase or TPase activity with mucopeptide substrates, this version

was nevertheless sensitive to acylation by β-lactams and, more specifically, by the carbapenem class compound imipenem as shown by MS (Supplementary Figure S3).

PBP4 Does Not Interact With Synthetic Stem Peptides

X-ray structures of wild-type PBP4 alone or in complex with β-lactams have been previously deposited in the PDB (PDB IDs: 6C39, 5TW8, 5TXI, 5TY7). Here we chose to study interactions with stem peptides using the catalytic serine mutant (S75C) to prevent any possible TPase activity that might interfere with the

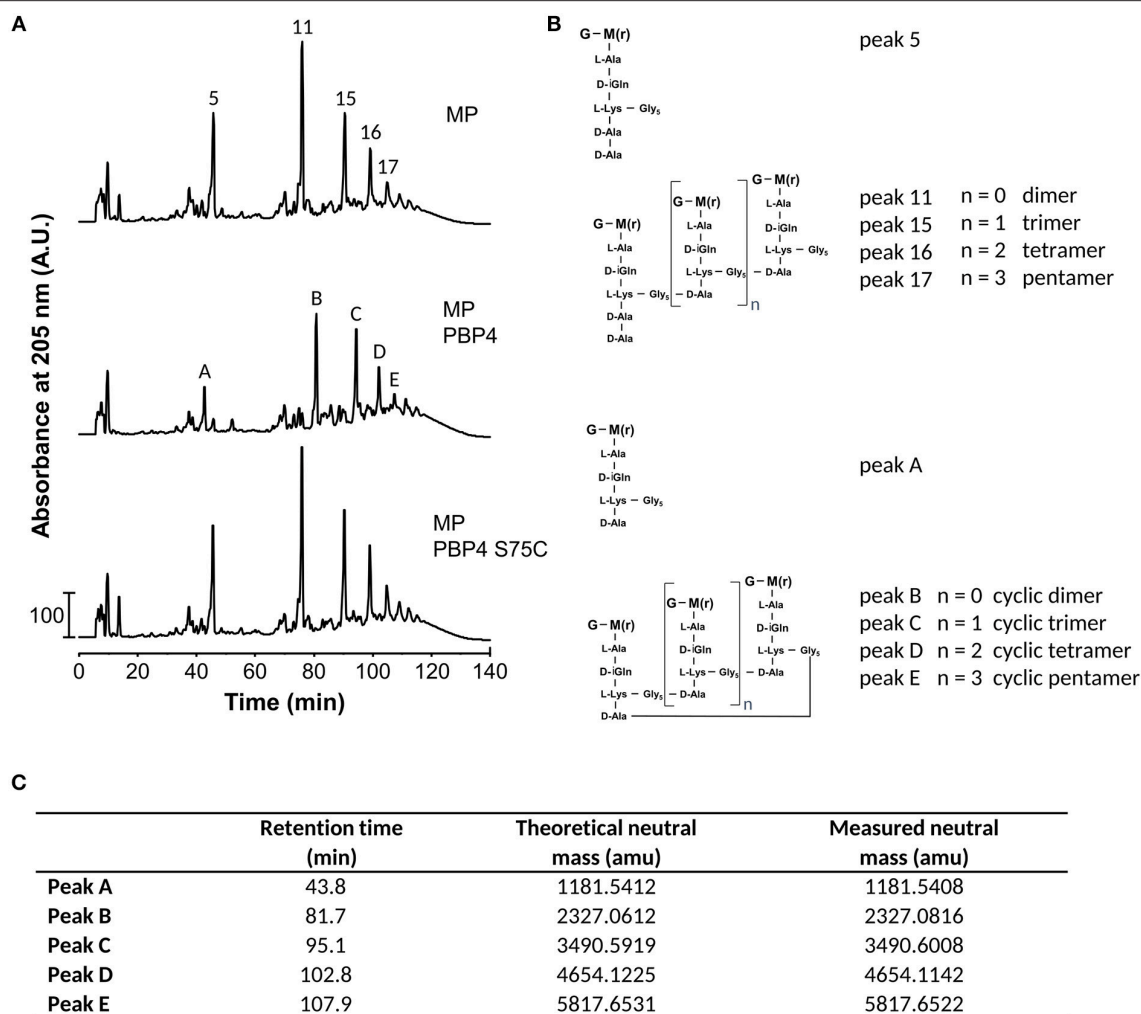


FIGURE 3 | PBP4 forms cyclic mucopeptides *in vitro*. **(A)** HPLC chromatograms of mucopeptides from *S. aureus* SH1000 incubated with PBP4 or the inactive version PBP4(S75C). **(B)** Proposed structures of mucopeptides present in the fractions in panel A and consistent with the molecular weight determined by mass spectrometry. G, N-acetylglucosamine; M(r), N-acetylmuramitol; L-Ala, L-alanine; D-Igln, D-isoglutamine; D-Ala, D-alanine; L-Lys, L-lysine; Gly, glycine. **(C)** Theoretical and measured neutral atomic mass units (amu) determined by MS of fractions collected from the PBP4 products in the middle chromatogram in **(A)**.

formation of a complex amenable for structural characterization by X-ray crystallography or NMR spectroscopy.

PBP4(S75C) was crystallized under similar conditions to those previously used for wild-type PBP4 (Alexander et al., 2018), yielding data to 1.86-Å resolution. **Supplementary Table 2** shows the details of the data collection and refinement statistics for PBP4(S75C). PBP4(S75C) crystallized with two highly similar molecules present in the asymmetric unit (C α alignment of chains A and B gives an r.m.s.d. of 0.35 Å over 359 aligned atoms). As expected, the structure of PBP4(S75C) (deposited under PDB ID 6DZ8) closely aligns with the structure of wild-type PBP4 (PDB ID 6C39), giving a C α r.m.s.d. of 0.41 Å over 359 aligned atoms (**Supplementary Figure S4**). Despite soaking ampicillin and the synthetic pentapeptide stem with PBP4(S75C) or PBP4, we were unable to identify electron density for either of these compounds in the maps generated.

In the absence of a clear extra density that could correspond to the peptide stem in the PBP4 or PBP4(S75C) crystals, we investigated this interaction by liquid-state NMR. Assignment of the sequential backbone resonances of PBP4 was first achieved by using a series of conventional 3D heteronuclear experiments recorded on a ^1H , ^{13}C , ^{15}N -labeled sample of PBP4 complemented with data on a ^2H , ^{13}C , ^{15}N -labeled sample due to the size (over 30-kDa) of the protein (**Figure 4**). Backbone resonance assignment was achieved at 70% and was mainly limited by sensitivity issues in the 3D experiments in relation to the relatively high molecular weight of the protein. Assignments were transferred to PBP4(S75C) by superimposing the 2D ^1H , ^{15}N -BEST-TROSY experiments (Favier and Brutscher, 2011) of the two proteins (**Supplementary Figure S5**). The spectra showed a very limited number of chemical shift variations, indicating that the structure is not significantly

affected by the S75C substitution. This is in agreement with the highly similar structures of the wild-type and mutated protein determined by X-ray crystallography at similarly high resolution.

A 326 μ M sample of 15 N-labeled PBP4(S75C) was then incubated with increasing amounts (2, 8, 22, and 52 molar equivalents to the protein) of the synthetic unlabeled lactoyl-tetrapeptide HO-D-Lac-L-Ala-D-iGln-L-Lys(Gly)₅-D-Ala-COOH, and 2D 1 H, 15 N-correlation spectra (15 N-BEST-TROSY) were collected for each titration point (Figure 5A). The addition of the peptide did not create any significant chemical shift perturbations for the amide resonances of PBP4(S75C), showing that any possible interaction of the stem peptide with the protein must have a dissociation constant that exceeds 110 mM. This result likely explains the failure to obtain co-crystals or loaded (soaked) crystals of PBP4(S75C) and PBP4 with synthetic peptides.

PBP4 Interacts With Larger PG Fragments

We asked whether the low affinity of PBP4 for small peptide substrates, too low for structural studies by either X-ray or NMR, could be due to the absence of the GlcNAc-MurNAc disaccharide motif or extended glycan strands. To address this question, we tested for interactions between PBP4(S75C) and PG fragments obtained by either cellosyl or lysostaphin digestion, using the same NMR approach as before (Figures 5B,C, left). In both cases, the 1 H, 15 N-correlation spectra revealed small but consistent chemical shift perturbations following the addition of increasing amounts of PG fragments, suggesting binding with a fast exchange regime and a dissociation constant in the range of hundreds of μ M to a few mM.

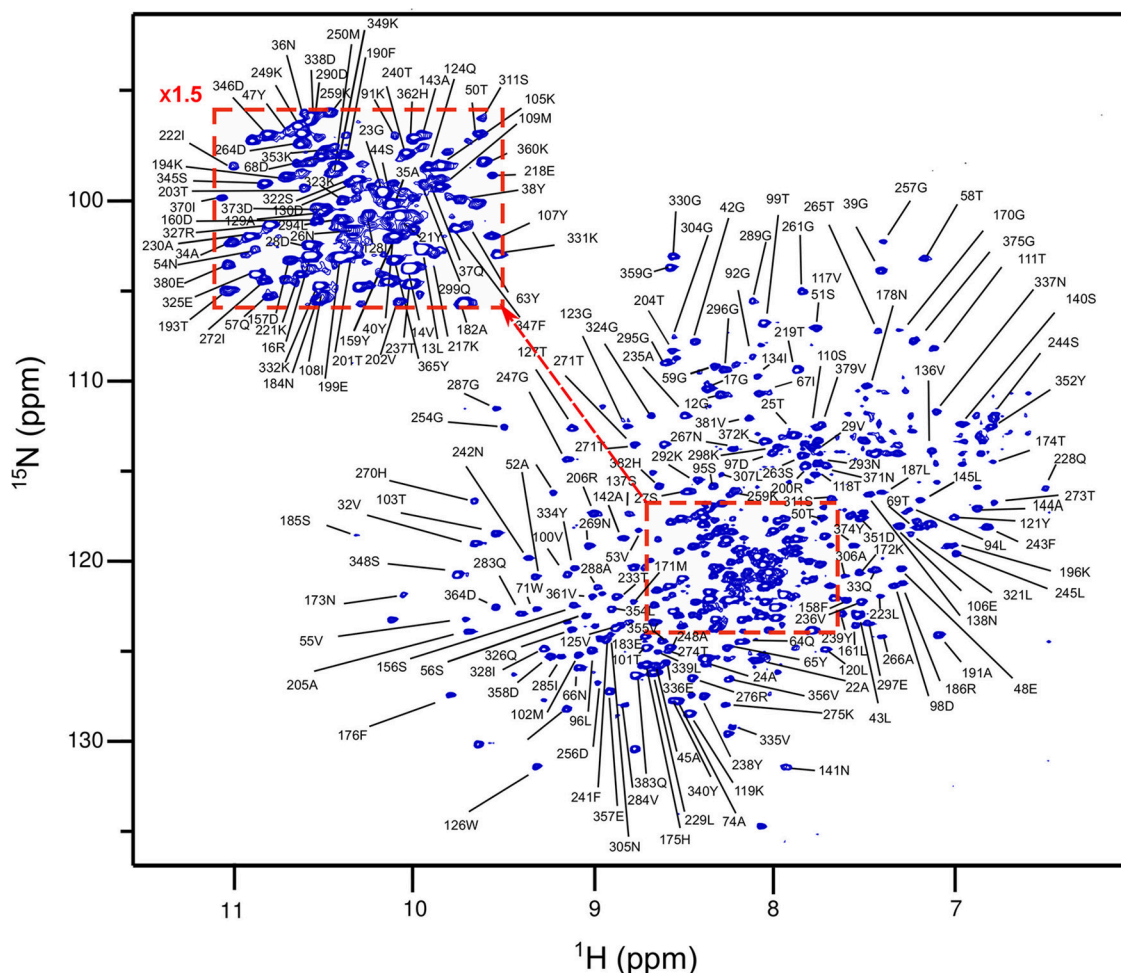
Our next goal was to determine the interaction site(s) on PBP4(S75C) for the soluble peptidoglycan fragments. Chemical shift perturbations were calculated for the highest fragment-to-protein ratio of 180 and 16 molar equivalents for the soluble fragments obtained by cellosyl and lysostaphin digestion (Supplementary Figure S6), respectively, and reported on the PBP4 structure to localize interaction interfaces on the protein (Figures 5B,C, right). These results were compared to the one obtained for the interaction of PBP4(S75C) with the previously mentioned carbapenem, imipenem (Figure 5D). We found that the natural substrates and the antibiotic bound to the same regions of PBP4 that are shared with the published binding sites of cepheids (ceftaroline) and penams (nafcillin) on wild-type PBP4. However, we observed additional residues with perturbed chemical shifts in the case of the soluble PG fragments, suggesting a more extended interface encompassing surfaces flanking both sides of the central serine nucleophile and catalytic pocket. The positioning of these two extended surfaces suggests that they indeed mimic the binding sites of the extended donor and acceptor substrates of the TPase reaction. Several residues remote from the β -lactam binding site and located in the C-terminal domain of PBP4 (I328, K331, V336, F347, V356, and V361) also experienced significant chemical shift perturbations with mucopeptides (Figure 5, Supplementary Figure S7). These shifts could be caused by a secondary mucopeptide binding site or a remote allostery.

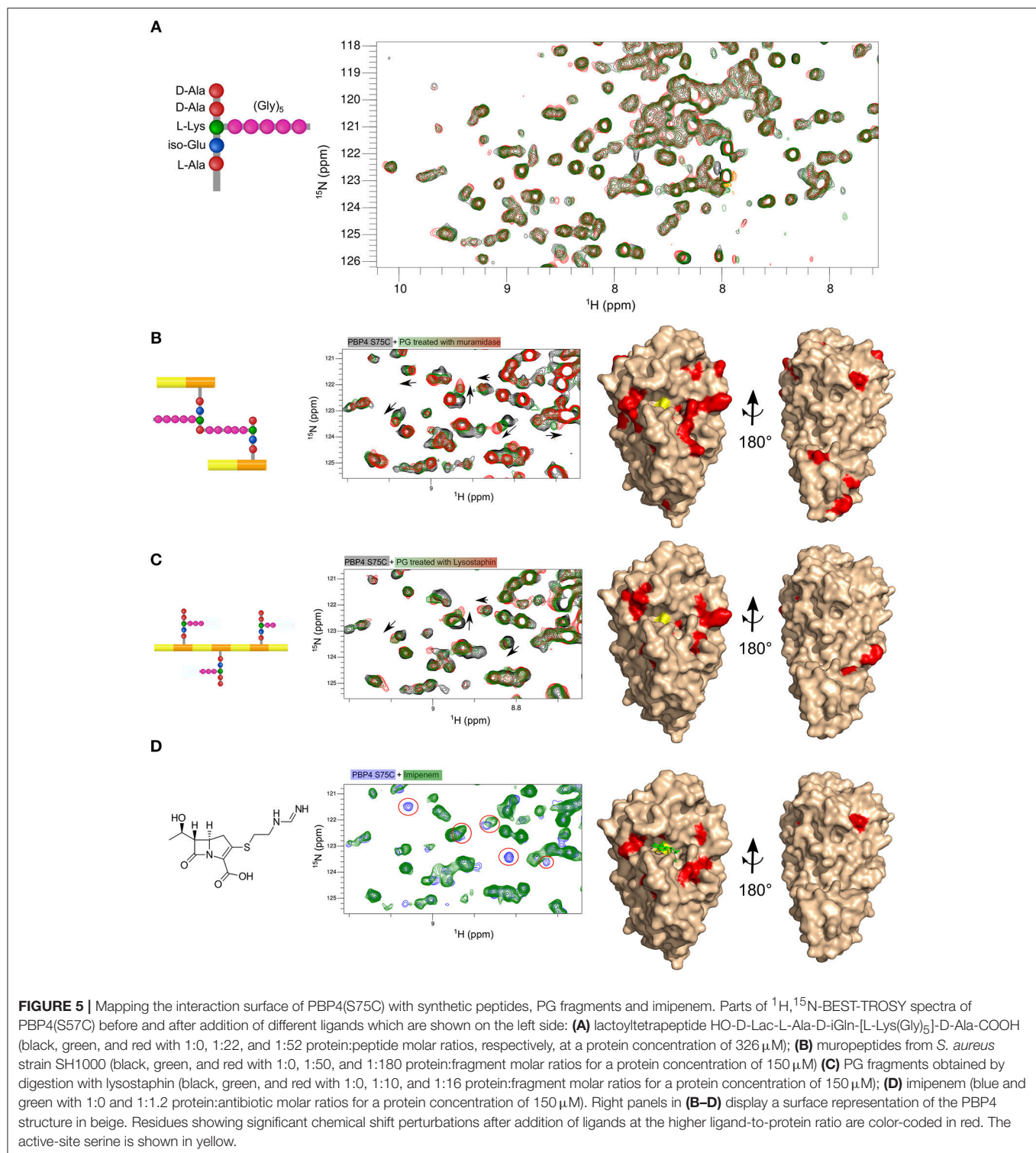
Structural Model of a PBP4:Mucopeptide Complex

We then calculated a model of the complex formed between PBP4 and the acceptor and donor mucopeptides using HADDOCK 2.2/CNS by docking two mucopeptide structures with tetrapeptide stems onto the PBP4 structure and using the measured NMR chemical shift perturbations as ambiguous distance restraints to drive the docking during the energy minimization process. Based on the evidence that S75 is required for the TPase catalysis (by analogy to the reactivity with carbapenem antibiotic), the distances from the S75 serine oxygen atom to both the carbonyl carbon of D-Ala⁴ of the donor peptide stem and the amine nitrogen atom at the N-terminus of the pentaglycine bridge of the acceptor peptide were constrained to 2.5 Å. These two restraints, justified by the necessity to bind both substrate peptides near the active site residue, improved the convergence of this multi-body docking process. The calculation was run with 4,000 structures during the rigid body energy minimization and 200 structures during the first and second energy refinements (the latter in explicit water). All residues of the protein that made intermolecular contacts within a 5-Å cutoff in the initial rigid body docking were allowed structural reorientations during the simulated annealing process. The mucopeptides were assumed fully flexible and all of their atoms were considered as ambiguous interaction sites to facilitate the sampling of different structural conformations at all steps of the simulated annealing process. The final minimization of the complexes in water revealed the presence of two clusters of similar energies (HADDOCK score: -93.5 ± 2.7 and -93.3 ± 3.7 ; electrostatic energy: -375.5 ± 70.0 and -416.2 ± 5.5 kcal mol⁻¹; desolvation energy: -10.9 ± 10.1 and -0.1 ± 4.1 kcal mol⁻¹; cluster size 120 and 35 structures, respectively) (Figures 6A,B). They show an inverse position of the donor and acceptor mucopeptides relative to the catalytic pocket (centered on the central nucleophile S75 as depicted in Figure 6C).

DISCUSSION

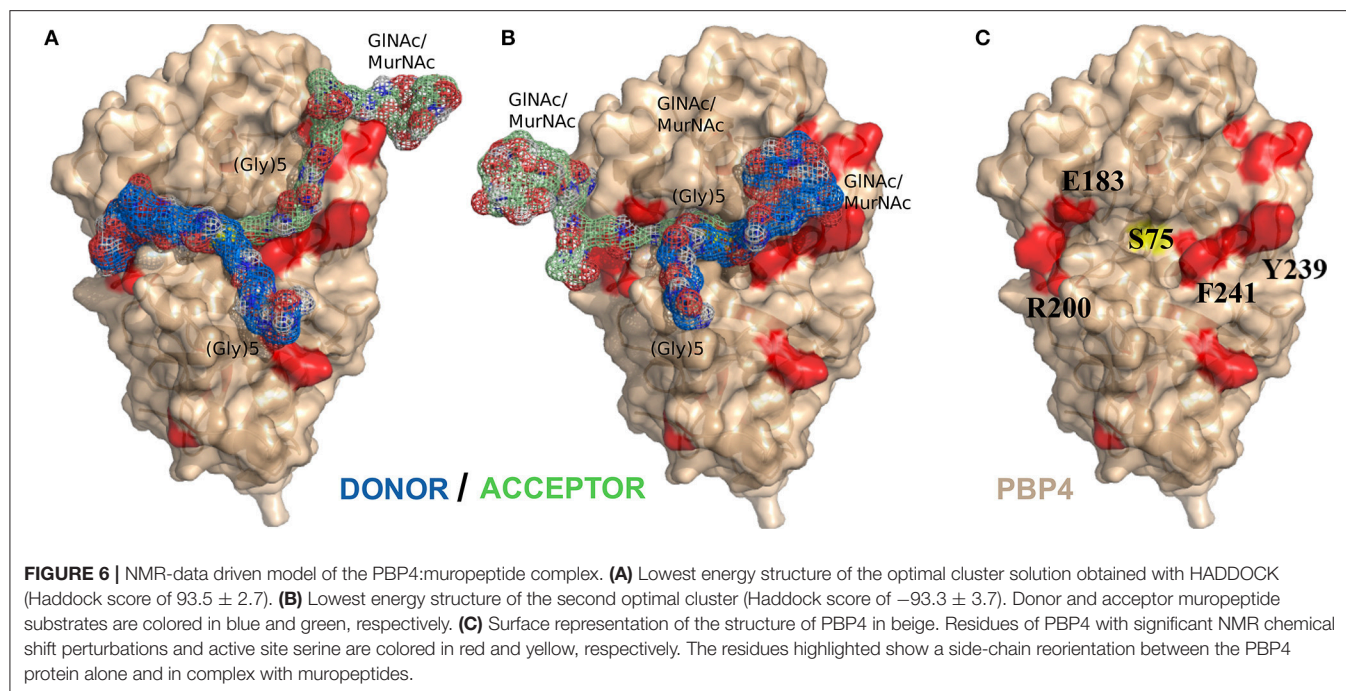
S. aureus PBP4 is an unusual class C PBP showing TPase activity *in vivo* (Loskill et al., 2014; Hamilton et al., 2017) and *in vitro* (Qiao et al., 2014; Srisuknimit et al., 2017) in addition to its expected CPase activity. PBP4 is involved in β -lactam resistance in the *S. aureus* laboratory mutant 27s, in which the deletion of PBP4 led to a decrease in cross-linking and an increase in ceftizoxime susceptibility. The authors further observed that deletion of the PBP4 gene resulted in the disappearance of a peak within the mucopeptide profile (Leski and Tomasz, 2005), which was previously identified as a cyclic mucopeptide predominantly naturally occurring in methicillin- and cefotaxime-resistant mutants of *S. aureus* (Boneca et al., 1997). However, there was no direct evidence for the hypothesis that PBP4 produces these cyclic structures. Here we show that purified PBP4 is indeed able to catalyze the formation of cyclic mucopeptides *in vitro*. The cyclisation reaction might merely be the result of a hyper-active TPase enzyme. Alternatively, cyclisation reactions might have the function to limit the





to dock the mucopeptide on PBP4, and the initial structures were energy minimized. We obtained models for the complex that satisfied the experimental observations of two different interaction regions for the disaccharide-peptide units, which could represent the donor and acceptor strands (**Figures 6A,B**).

In the two final models, the donor and acceptor peptides access the catalytic pocket from two opposite sites, thus solving the steric problem of approaching the two Lys and (Gly) $_5$ bulky chains near the catalytic serine S75. The somewhat similar energies obtained for the two clusters did not permit however to



discriminate unequivocally between the two sets of solutions. In the lowest energy model (**Figure 6A**), the donor strand follows an orientation that would place the D-Ala⁴-D-Ala⁵ scissile bond in a similar geometry to that of the opened β -lactam ring in the acylenzyme (PDB IDs 5TW8, 5TXI, 5TY7). The lysine side-chain and glycine bridge then point in the same direction as the β -lactam's adjacent ring side-chain, while the terminal nitrogen of the pentaglycine bridge of the acceptor strand lines up with the β -lactam nitrogen. This arrangement is consistent with the analogy model suggested by Tipper and Strominger in 1965 for the donor substrate and the inhibitor (Tipper and Strominger, 1965). In the second model (**Figure 6B**), the donor stem approaches the catalytic cavity on its more open side (F241, Y239) and the terminal carboxylic group of the D-Ala localizes at the same place as the β -lactam carboxylate in the structure of the acylenzyme (PDB IDs 5TW8, 5TXI, 5TY7). In this model, the longest and narrowest side of the catalytic pocket (E183, R200) is occupied by the long glycine chain of the acceptor (**Figure 6B**). This model can explain the selectivity of PBP4 during the transpeptidation reaction for acceptor peptide stands containing complete (Gly₅) chains (Srisuknimit et al., 2017). Both models suggest that side-chain reorientations must occur in particular for residues R200, E183, R186, E114, and F241 during the docking protocol in order to accommodate the substrates (**Supplementary Figure S8A**). This structural reorganization enhances accessibility of the long peptide stems to the otherwise more closed S75 catalytic cavity (**Figure 6C**).

Interestingly, a ceftobiprole-resistant *Staphylococcus aureus* strain (CRB), which displays resistance to a variety of β -lactams, has three mutations in the *pbp4* gene that result in E183A and F241R amino-acid substitutions in PBP4 (Banerjee et al., 2010). The structure of the latter protein acylated by the ceftobiprole and

ceftaroline cepheems has been solved by crystallography (PDB IDs 5TX9, 5TW4) and shows few structural differences in proximity to the antibiotic (Alexander et al., 2018). The replacement of E183 by an alanine disrupts the Van-der-Waals interaction between this residue and R200 and induces a rotation of R200, increasing significantly the accessibility of the catalytic pocket for one of the substrates, donor and acceptor peptide stems in models of **Figures 6A,B**, respectively (**Supplementary Figure S8B**). The mutation of F241 to an arginine could have a similar impact on the accessibility of the catalytic serine S75 to the second substrate, acceptor and donor stem peptide models of **Figures 6A,B**, respectively. Based on our results, we suggest that the CRB mutations, by changing the accessibility to the catalytic serine S75, facilitates the transpeptidation of the two substrates, whereas this could also facilitate the hydrolysis of the antibiotic acylenzyme. These hypotheses need to be further tested *in vitro* and *in vivo* in CRB mutants.

AUTHOR CONTRIBUTIONS

RM-M contributed to NMR sample preparation and was in charge of NMR data collection and analysis on PBP4 and PBP4(S75C). JA was in charge of all of the X-ray PBP4(S75C) sample preparation, data collection and analysis. CO was in charge of the characterization of the peptidoglycan. IA has prepared all peptidoglycan and most protein samples for NMR. DV has prepared all peptidoglycan samples for HPLC and mass spectrometry. JG was in charge of the mass spectrometry. CB has performed some NMR data collection and analysis and has contributed to MS writing. CL was in charge of the docking with HADDOCK. AB has assigned the NMR peptidoglycan fragments and participated in PBP4-fragment interaction studies. MF has

synthesized the tetra- and pentapeptide stems. MA has supervised the production of the peptide stems. NS has supervised the X-ray. WV has supervised the peptidoglycan characterization and has contributed to the MS writing. J-PS has supervised the complete study and has contributed to MS writing and supervision.

ACKNOWLEDGMENTS

This research used resources of the Advanced Light Source, which is a DOE Office of Science User Facility under contract no. DE-AC02-05CH11231. The authors thank the staff of beamline 5.0.2 for their assistance with data collection. WV was supported by

a Wellcome Trust Senior Investigator award (101824/Z/13/Z), NS by HHMI Senior International Scholar and CRC awards, JA by a Vanier scholarship, and MA, NS, WV, and J-PS by the NAPCLI project within the JPI AMR programme, funded in the UK by the Medical Research Council (MR/N501840/1) (to WV), in Canada by CIHR (to NS), and in France by the ANR (ANR-14-JAMR-0003) (to MA and J-PS).

SUPPLEMENTARY MATERIAL

The Supplementary Material for this article can be found online at: <https://www.frontiersin.org/articles/10.3389/fmicb.2018.03223/full#supplementary-material>

REFERENCES

- Adams, P. D., Afonine, P. V., Bunkóczi, G., Chen, V. B., Davis, I. W., Echols, N., et al. (2010). PHENIX: a comprehensive Python-based system for macromolecular structure solution. *Acta Crystallogr. Sect. D Biol. Crystallogr.* 66, 213–221. doi: 10.1107/S0907444909052925
- Alexander, J. A. N., Chatterjee, S. S., Hamilton, S. M., Eltis, L. D., Chambers, H. F., and Strynadka, N. C. J. (2018). Structural and kinetic analyses of penicillin-binding protein 4 (PBP4)-mediated antibiotic resistance in *Staphylococcus aureus*. *J. Biol. Chem.* 293, 19854–19865. doi: 10.1074/jbc.RA118.004952
- Atilano, M. L., Pereira, P. M., Yates, J., Reed, P., Veiga, H., Pinho, M. G., et al. (2010). Teichoic acids are temporal and spatial regulators of peptidoglycan cross-linking in *Staphylococcus aureus*. *Proc. Natl. Acad. Sci. U.S.A.* 107, 18991–18996. doi: 10.1073/pnas.1004304107
- Banerjee, R., Gretes, M., Harlem, C., Basuino, L., and Chambers, H. F. (2010). A mecA-negative strain of methicillin-resistant *Staphylococcus aureus* with high-level β -lactam resistance contains mutations in three genes. *Antimicrob. Agents Chemother.* 54, 4900–4902. doi: 10.1128/AAC.00594-10
- Bernardo-García, N., Mahasenan, K. V., Batuecas, M. T., Lee, M., Heseck, D., Petráčková, D., et al. (2018). Allosteric recognition of nascent peptidoglycan, and cross-linking of the cell wall by the essential Penicillin-Binding Protein 2x of *Streptococcus pneumoniae*. *ACS Chem. Biol.* 13, 694–702. doi: 10.1021/acschembio.7b00817
- Boneca, I. G., Xu, N., Gage, D. A., De Jonge, B. L. M., and Tomasz, A. (1997). Structural characterization of an abnormally cross-linked muropeptide dimer that is accumulated in the peptidoglycan of methicillin- and cefotaxime-resistant mutants of *Staphylococcus aureus*. *J. Biol. Chem.* 272, 29053–29059. doi: 10.1074/jbc.272.46.29053
- Bui, N. K., Eberhardt, A., Vollmer, D., Kern, T., Bougault, C., Tomasz, A., et al. (2012). Isolation and analysis of cell wall components from *Streptococcus pneumoniae*. *Anal. Biochem.* 421, 657–666. doi: 10.1016/j.ab.2011.11.026
- Carlomagno, T. (2012). NMR in natural products: understanding conformation, configuration and receptor interactions. *Nat. Prod. Rep.* 29:536. doi: 10.1039/c2np00098a
- Chatterjee, S. S., Chen, L., Gilbert, A., da Costa, T. M., Nair, V., Datta, S. K., et al. (2017). PBP4 mediates β -Lactam resistance by altered function. *Antimicrob. Agents Chemother.* 61, e00932–e00917. doi: 10.1128/AAC.00932-17
- de Vries, S. J., van Dijk, M., and Bonvin, A. M. J. J. (2010). The HADDOCK web server for data-driven biomolecular docking. *Nat. Protoc.* 5, 883–897. doi: 10.1038/nprot.2010.32
- Emsley, P., Lohkamp, B., Scott, W. G., and Cowtan, K. (2010). Features and development of Coot. *Acta Crystallogr. Sect. D Biol. Crystallogr.* 66, 486–501. doi: 10.1107/S0907444910007493
- Favier, A., and Brutscher, B. (2011). Recovering lost magnetization: polarization enhancement in biomolecular NMR. *J. Biomol. NMR* 49, 9–15. doi: 10.1007/s10858-010-9461-5
- Figueiredo, T. A., Sobral, R. G., Ludovice, A. M., de Almeida, J. M. F., Bui, N. K., Vollmer, W., et al. (2012). Identification of genetic determinants and enzymes involved with the amidation of glutamic acid residues in the peptidoglycan of *Staphylococcus aureus*. *PLoS Pathog.* 8:e1002508. doi: 10.1371/journal.ppat.1002508
- Frank, O., Kreissl, J. K., Daschner, A., and Hofmann, T. (2014). Accurate determination of reference materials and natural isolates by means of quantitative ^1H NMR spectroscopy. *J. Agric. Food Chem.* 62, 2506–2515. doi: 10.1021/jf405529b
- Gang, T., Pan, Y., Dong, H., Pryor, R. G., Edwin Wilson, and Schaefer, J. (1997). Structure and dynamics of pentaglycyl bridges in the cell walls of *Staphylococcus aureus* by ^{13}C - ^{15}N REDOR NMR. *Biochemistry* 36, 691–697. doi: 10.1021/BI970495D
- Hamilton, S. M., Alexander, J. A. N., Choo, E. J., Basuino, L., da Costa, T. M., Severin, A., et al. (2017). High-Level resistance of *Staphylococcus aureus* to β -lactam antibiotics mediated by Penicillin-Binding Protein 4 (PBP4). *Antimicrob. Agents Chemother.* 61, e02727–e02716. doi: 10.1128/AAC.02727-16
- Kabsch, W. (2010). XDS. *Acta Crystallogr. Sect. D Biol. Crystallogr.* 66, 125–132. doi: 10.1107/S0907444909047337
- Kern, T., Giffard, M., Hediger, S., Amoroso, A., Giustini, C., Bui, N. K., et al. (2010). Dynamics characterization of fully hydrated bacterial cell walls by solid-state NMR: evidence for cooperative binding of metal ions. *J. Am. Chem. Soc.* 132, 10911–10919. doi: 10.1021/ja104533w
- Lehotzky, R. E., Partch, C. L., Mukherjee, S., Cash, H. L., Goldman, W. E., Gardner, K. H., et al. (2010). Molecular basis for peptidoglycan recognition by a bactericidal lectin. *Proc. Natl. Acad. Sci. U.S.A.* 107, 7722–7727. doi: 10.1073/pnas.0909449107
- Leski, T., and Tomasz, A. (2005). Role of Penicillin-Binding Protein 2 (PBP2) in the antibiotic susceptibility and cell wall cross-linking of *Staphylococcus aureus*. *J. Bacteriol.* 187, 1815–1824. doi: 10.1128/JB.187.5.1815
- Loskill, P., Pereira, P. M., Jung, P., Bischoff, M., Herrmann, M., Pinho, M. G., et al. (2014). Reduction of the peptidoglycan crosslinking causes a decrease in stiffness of the *Staphylococcus aureus* cell envelope. *Biophys. J.* 107, 1082–1089. doi: 10.1016/j.bpj.2014.07.029
- Macheboeuf, P., Contreras-Martel, C., Job, V., Dideberg, O., and Dessen, A. (2006). Penicillin Binding Proteins: key players in bacterial cell cycle and drug resistance processes. *FEMS Microbiol. Rev.* 30, 673–691. doi: 10.1111/j.1574-6976.2006.00024.x
- McCoy, A. J., Grosse-Kunstleve, R. W., Adams, P. D., Winn, M. D., Storoni, L. C., and Read, R. J. (2007). Phaser crystallographic software. *J. Appl. Crystallogr.* 40, 658–674. doi: 10.1107/S0021889807021206
- Ngadjieu, F., Braud, E., Saidjalolov, S., Iannazzo, L., Schnappinger, D., Ehrt, S., et al. (2018). Critical impact of peptidoglycan precursor amidation on the activity of L,D-transpeptidases from *Enterococcus faecium* and *Mycobacterium tuberculosis*. *Eur. J.* 24, 5743–5747. doi: 10.1002/chem.201706082
- Pereira, S. F. F., Henriques, A. O., Pinho, M. G., de Lencastre, H., and Tomasz, A. (2007). Role of PBP1 in cell division of *Staphylococcus aureus*. *J. Bacteriol.* 189, 3525–3531. doi: 10.1128/JB.00044-07

- Pinho, M. G., de Lencastre, H., and Tomasz, A. (2000). Cloning, characterization, and inactivation of the gene *pbpC*, encoding penicillin-binding protein 3 of *Staphylococcus aureus*. *J. Bacteriol.* 182, 1074–1079. doi: 10.1128/JB.182.4.1074-1079.2000
- Pinho, M. G., and Errington, J. (2004). Recruitment of penicillin-binding protein PBP2 to the division site of *Staphylococcus aureus* is dependent on its transpeptidation substrates. *Mol. Microbiol.* 55, 799–807. doi: 10.1111/j.1365-2958.2004.04420.x
- Pinho, M. G., Filipe, S. R., de Lencastre, H., and Tomasz, A. (2001). Complementation of the essential peptidoglycan transpeptidase function of penicillin-binding protein 2 (PBP2) by the drug resistance protein PBP2A in *Staphylococcus aureus*. *J. Bacteriol.* 183, 6525–6531. doi: 10.1128/JB.183.22.6525-6531.2001
- Qiao, Y., Lebar, M. D., Schirner, K., Schaefer, K., Tsukamoto, H., Kahne, D., et al. (2014). Detection of lipid-linked peptidoglycan precursors by exploiting an unexpected transpeptidase reaction. *J. Am. Chem. Soc.* 136, 14678–14681. doi: 10.1021/ja508147s
- Rodrigues, J. P. G. L. M., Trellet, M., Schmitz, C., Kastiritis, P., Karaca, E., Melquiond, A. S. J., et al. (2012). Clustering biomolecular complexes by residue contacts similarity. *Proteins* 80, 1810–1817. doi: 10.1002/prot.24078
- Romaniuk, J. A. H., and Cegelski, L. (2015). Bacterial cell wall composition and the influence of antibiotics by cell-wall and whole-cell NMR. *Philos. Trans. R. Soc. Lond. B. Biol. Sci.* 370, 20150024. doi: 10.1098/rstb.2015.0024
- Sauvage, E., Kerff, F., Terrak, M., Ayala, J. A., and Charlier, P. (2008). The penicillin-binding proteins: structure and role in peptidoglycan biosynthesis. *FEMS Microbiol. Rev.* 32, 234–258. doi: 10.1111/j.1574-6976.2008.00105.x
- Schanda, P., Triboulet, S., Laguri, C., Bougault, C. M., Ayala, I., Callon, M., et al. (2014). Atomic model of a cell-wall cross-linking enzyme in complex with an intact bacterial peptidoglycan. *J. Am. Chem. Soc.* 136, 17852–17860. doi: 10.1021/ja5105987
- Schneewind, O., Fowler, A., and Faull, K. F. (1995). Structure of the cell wall anchor of surface proteins in *Staphylococcus aureus*. *Science* 268, 103–106.
- Silhavy, T. J., Kahne, D., and Walker, S. (2010). The bacterial cell envelope. *Cold Spring Harb. Perspect. Biol.* 2:a000414. doi: 10.1101/cshperspect.a000414
- Sobhanifar, S., King, D. T., and Strynadka, N. C. (2013). Fortifying the wall: synthesis, regulation and degradation of bacterial peptidoglycan. *Curr. Opin. Struct. Biol.* 23, 695–703. doi: 10.1016/j.SBI.2013.07.008
- Srisuknimit, V., Qiao, Y., Schaefer, K., Kahne, D., and Walker, S. (2017). Peptidoglycan cross-linking preferences of *Staphylococcus aureus* Penicillin-Binding Proteins have implications for treating MRSA Infections. *J. Am. Chem. Soc.* 139, 9791–9794. doi: 10.1021/jacs.7b04881
- Sung, M.-T., Lai, Y.-T., Huang, C.-Y., Chou, L.-Y., Shih, H.-W., Cheng, W.-C., et al. (2009). Crystal structure of the membrane-bound bifunctional transglycosylase PBP1b from *Escherichia coli*. *Proc. Natl. Acad. Sci. U.S.A.* 106, 8824–8829. doi: 10.1073/pnas.0904030106
- Tipper, D. J., and Strominger, J. L. (1965). Mechanism of action of penicillins: a proposal based on their structural similarity to acyl-D-alanyl-D-alanine. *Proc. Natl. Acad. Sci. U.S.A.* 54, 1133–1141.
- Vollmer, W., Blanot, D., and De Pedro M. A. (2008). Peptidoglycan structure and architecture. *FEMS Microbiol. Rev.* 32, 149–167. doi: 10.1111/j.1574-6976.2007.00094.x
- Vranken, W. F., Boucher, W., Stevens, T. J., Fogh, R. H., Pajon, A., Llinas, M., et al. (2005). The CCPN data model for NMR spectroscopy: development of a software pipeline. *Proteins-Structure Funct. Bioinforma* 59, 687–696. doi: 10.1002/prot.20449
- Winn, M. D., Ballard, C. C., Cowtan, K. D., Dodson, E. J., Emsley, P., Evans, P. R., et al. (2011). Overview of the CCP4 suite and current developments. *Acta Crystallogr. Sect. D Biol. Crystallogr.* 67, 235–242. doi: 10.1107/S0907444910045749
- Winter, G., Lobley, C. M. C., and Prince, S. M. (2013). Decision making in xia2. *Acta Crystallogr. D. Biol. Crystallogr.* 69, 1260–1273. doi: 10.1107/S0907444913015308
- Wyke, A. W., Ward, J. B., Hayes, M. V., and Curtis, N. A. C. (1981). A role *in vivo* for Penicillin-Binding Protein-4 of *Staphylococcus aureus*. *Eur. J. Biochem.* 119, 389–393. doi: 10.1111/j.1432-1033.1981.tb05620.x
- Zapun, A., Contreras-Martel, C., and Vernet, T. (2008). Penicillin-binding proteins and β -lactam resistance. *FEMS Microbiol. Rev.* 32, 361–385. doi: 10.1111/j.1574-6976.2007.00095.x

Conflict of Interest Statement: The authors declare that the research was conducted in the absence of any commercial or financial relationships that could be construed as a potential conflict of interest.

Copyright © 2019 Maya-Martinez, Alexander, Otten, Ayala, Vollmer, Gray, Bougault, Burt, Laguri, Fonvielle, Arthur, Strynadka, Vollmer and Simorre. This is an open-access article distributed under the terms of the Creative Commons Attribution License (CC BY). The use, distribution or reproduction in other forums is permitted, provided the original author(s) and the copyright owner(s) are credited and that the original publication in this journal is cited, in accordance with accepted academic practice. No use, distribution or reproduction is permitted which does not comply with these terms.



N-Acetylmuramic Acid (MurNAc) Auxotrophy of the Oral Pathogen *Tannerella forsythia*: Characterization of a MurNAc Kinase and Analysis of Its Role in Cell Wall Metabolism

Isabel Hottmann¹, Valentina M. T. Mayer², Markus B. Tomek², Valentin Friedrich², Matthew B. Calvert^{3,4,5}, Alexander Titz^{3,4,5}, Christina Schäffer^{2*} and Christoph Mayer^{1*}

OPEN ACCESS

Edited by:

Matthias Boll,
Albert Ludwigs University of Freiburg,
Germany

Reviewed by:

Ali Al-Ahmad,
Universitätsklinikum Freiburg,
Germany
P. V. G. K. Sarma,
Sri Venkateswara Institute of Medical
Sciences, India

*Correspondence:

Christina Schäffer
christina.schaeffer@boku.ac.at
Christoph Mayer
christoph.mayer@uni-tuebingen.de

Specialty section:

This article was submitted to
Microbial Physiology and Metabolism,
a section of the journal
Frontiers in Microbiology

Received: 17 November 2017

Accepted: 05 January 2018

Published: 26 January 2018

Citation:

Hottmann I, Mayer VMT, Tomek MB,
Friedrich V, Calvert MB, Titz A,
Schäffer C and Mayer C (2018)
N-Acetylmuramic Acid (MurNAc)
Auxotrophy of the Oral Pathogen
Tannerella forsythia: Characterization
of a MurNAc Kinase and Analysis
of Its Role in Cell Wall Metabolism.
Front. Microbiol. 9:19.
doi: 10.3389/fmicb.2018.00019

¹ Microbiology and Biotechnology, Interfaculty Institute of Microbiology and Infection Medicine Tübingen, Department of Biology, Eberhard Karls Universität Tübingen, Tübingen, Germany, ² NanoGlycobiology Unit, Department of NanoBiotechnology, Universität für Bodenkultur Wien, Vienna, Austria, ³ Chemical Biology of Carbohydrates, Helmholtz Institute for Pharmaceutical Research Saarland, Saarbrücken, Germany, ⁴ Deutsches Zentrum für Infektionsforschung, Partner Site Hannover-Braunschweig, Brunswick, Germany, ⁵ Department of Pharmacy, Saarland University, Saarbrücken, Germany

Tannerella forsythia is an anaerobic, Gram-negative oral pathogen that thrives in multispecies gingival biofilms associated with periodontitis. The bacterium is auxotrophic for the commonly essential bacterial cell wall sugar N-acetylmuramic acid (MurNAc) and, thus, strictly depends on an exogenous supply of MurNAc for growth and maintenance of cell morphology. A MurNAc transporter (Tf_MurT; Tanf_08375) and an ortholog of the *Escherichia coli* etherase MurQ (Tf_MurQ; Tanf_08385) converting MurNAc-6-phosphate to GlcNAc-6-phosphate were recently described for *T. forsythia*. In between the respective genes on the *T. forsythia* genome, a putative kinase gene is located. In this study, the putative kinase (Tf_MurK; Tanf_08380) was produced as a recombinant protein and biochemically characterized. Kinetic studies revealed Tf_MurK to be a 6-kinase with stringent substrate specificity for MurNAc exhibiting a 6×10^4 -fold higher catalytic efficiency (k_{cat}/K_m) for MurNAc than for N-acetylglucosamine (GlcNAc) with k_{cat} values of 10.5 s^{-1} and 0.1 s^{-1} and K_m values of $200 \mu\text{M}$ and 116 mM , respectively. The enzyme kinetic data suggest that Tf_MurK is subject to substrate inhibition ($K_{\text{IS}} = 4.2 \text{ mM}$). To assess the role of Tf_MurK in the cell wall metabolism of *T. forsythia*, a kinase deletion mutant ($\Delta\text{Tf_murK}::\text{erm}$) was constructed. This mutant accumulated MurNAc intracellularly in the exponential phase, indicating the capability to take up MurNAc, but inability to catabolize MurNAc. In the stationary phase, the MurNAc level was reduced in the mutant, while the level of the peptidoglycan precursor UDP-MurNAc-pentapeptide was highly elevated. Further, according to scanning electron microscopy evidence, the $\Delta\text{Tf_murK}::\text{erm}$ mutant was more tolerant toward low MurNAc concentration in the medium (below $0.5 \mu\text{g/ml}$) before transition from healthy, rod-shaped to fusiform cells occurred, while the parent strain

required $> 1 \mu\text{g/ml}$ MurNac for optimal growth. These data reveal that *T. forsythia* readily catabolizes exogenous MurNac but simultaneously channels a proportion of the sugar into peptidoglycan biosynthesis. Deletion of *Tf_murK* blocks MurNac catabolism and allows the direction of MurNac solely to peptidoglycan biosynthesis, resulting in a growth advantage in MurNac-depleted medium. This work increases our understanding of the *T. forsythia* cell wall metabolism and may pave new routes for lead finding in the treatment of periodontitis.

Keywords: oral pathogen, red complex consortium, *N*-acetylmuramic acid kinase, MurNac auxotrophy, peptidoglycan metabolism, cell wall recycling

INTRODUCTION

Tannerella forsythia is an anaerobic, Gram-negative oral pathogen affiliated to the *Bacteroidetes* phylum of bacteria (Tanner and Izard, 2006). It acts as a late colonizer within oral biofilms and is found alongside *Porphyromonas gingivalis* and *Treponema denticola*, together constituting the so called “red complex.” This bacterial consortium is associated with severe forms of periodontitis, an inflammatory oral disease of global importance that is characterized by destruction of alveolar bone and soft tissues, ultimately leading to tooth loss if untreated (Holt and Ebersole, 2005; Hajishengallis and Lamont, 2012). Anne Tanner initially described the “fusiform” (spindle-shaped) morphology of a slow-growing *Bacteroidetes* strain isolated from the human oral cavity, formerly named *Bacteroidetes forsythus* or *Tannerella forsythensis*, and finally renamed *Tannerella forsythia* (Tanner et al., 1986). It was later recognized by Wyss that the organism has a strict dependency on the amino sugar *N*-acetylmuramic acid (MurNac) and that growth defects and morphological changes, such as fusiform morphology, are consequences of impaired cell wall metabolism caused by MurNac depletion (Wyss, 1989). MurNac and *N*-acetylglucosamine (GlcNac) are essential components of the peptidoglycan (PGN) of the bacterial cell wall. Alternatingly connected, these amino sugars form the glycan strands of PGN which are crosslinked via peptides to form a net-like polymeric fabric surrounding and stabilizing the bacterial cell and conferring cell shape (Höltje, 1998; Young, 2003).

Inspection of available *T. forsythia* genome sequences revealed that this bacterium lacks genes commonly required for the *de novo* biosynthesis of PGN in bacteria (Friedrich et al., 2015). These are the *glmS* and *glmU* genes, required for UDP-GlcNac biosynthesis and the *murA* and *murB* genes, which encode enzymes involved in the formation of the PGN precursor uridine diphosphate-*N*-acetylmuramic acid (UDP-MurNac) (Mengin-Lecreux et al., 1982; Typas et al., 2012). *T. forsythia*'s inability to *de novo* synthesize MurNac implicates that the bacterium has to attain this compound from external sources for viability. *Escherichia coli* and other bacteria possess a phosphotransferase system (PTS) transporter (MurP) for the uptake and concomitant phosphorylation of MurNac yielding MurNac-6P (Dahl et al., 2004; Borisova et al., 2016), as well as a MurNac-6P etherase (MurQ) for catabolization of MurNac-6P by cleaving off the lactyl ether substituent, yielding GlcNac-6P and D-lactate (Jaeger

et al., 2005; Hadi et al., 2008; Jaeger and Mayer, 2008). According to genome analysis, in *T. forsythia*, PTS-type transporters are missing; however, recently, a PTS-independent uptake system for MurNac (Tf_MurT; Tanf_08375) was identified in the *T. forsythia* type strain ATCC 43037, which belongs to the sodium symporter superfamily (Ruscitto et al., 2016). The corresponding *Tf_murT* gene is present within an operon, together with an ortholog of the *E. coli* MurNac-6-phosphate etherase gene *murQ* (*Tf_murQ*; Tanf_08385) and a putative sugar kinase gene *Tf_murK* (Tanf_08380). We have shown in a recent study, that an *E. coli* MurNac-PTS transporter mutant ($\Delta murP$) can be rescued for growth on MurNac as sole carbon source only upon co-expression of the transporter Tf_MurT and the putative kinase Tf_MurK. This suggested that Tf_MurK would phosphorylate MurNac, yielding MurNac-6P, which would be subsequently cleaved by the etherase Tf_MurQ, yielding GlcNac-6P (Ruscitto et al., 2016).

In the present study, we biochemically characterized the *T. forsythia* kinase Tf_MurK of the *Tf_murTKQ* operon from the type strain ATCC 43037 revealing stringent specificity of the enzyme for MurNac. Further, we constructed a *Tf_murK* deletion mutant and characterized changes of this mutant in cell wall metabolism in comparison to the parental strain, providing evidence for the steady uptake of exogenous MurNac by *T. forsythia* cells as well as for the presence of a novel pathway that channels MurNac to PGN biosynthesis and is elaborated in parallel to MurNac catabolism.

MATERIALS AND METHODS

Bacterial Strains, Growth Conditions, and Growth Curves

T. forsythia type strain ATCC 43037 - in the following referred to as *T. forsythia* wild-type (WT) - was obtained from the American Type Culture Collection (Manassas, VA, United States). *T. forsythia* WT and an isogenic $\Delta Tf_murK::erm$ mutant created in the course of this study (see Supplementary Figure S1) were grown in liquid or solid-agar brain heart infusion (BHI) medium (37 g/l; Oxoid, Basingstoke, United Kingdom) at 37°C for 4–7 days under anaerobic conditions in an anaerobe jar (AnaeroJar; Oxoid). The media were supplemented with 10 g/l yeast extract (Sigma, Vienna, Austria), 1 g/l L-cysteine (Sigma), 5 $\mu\text{g/ml}$ hemine (Sigma), 2 $\mu\text{g/ml}$ menadione (Sigma),

5%(v/v) horse serum (Thermo Fisher Scientific, Vienna, Austria), and MurNAc (Carbosynth, Compton, United Kingdom) at a concentration of 20 µg/ml (Tomek et al., 2014) if not stated otherwise. Erythromycin (Erm; 5 µg/ml) and gentamycin (Gm; 50 µg/ml) were added to the media when appropriate.

To determine the influence of MurNAc depletion on the growth of *T. forsythia* WT and $\Delta Tf_murK::erm$ mutant, growth curves were recorded upon supplementation of the culture medium with 0.1, 0.5, 1.0, and 20.0 µg/ml MurNAc. Bacterial cells were inoculated to a starting optical density at 600 nm (OD₆₀₀) of 0.1 and grown until the stationary phase had been reached (75 h). Biological triplicates were measured with a cell density meter (Ultraspec 10; Amersham Biosciences, Austria), three times, each, at any given time point.

Escherichia coli BL21(DE3) was grown in lysogeny broth (LB Lennox, 10 g/l tryptone, 5 g/l yeast extract, 5 g/l NaCl) at 37°C under continuous shaking at 140 rpm; kanamycin (Km; 50 µg/ml) was added when appropriate.

Plasmid Construction, Expression, and Purification of Tf_MurK

For recombinant production of C-terminally His₆-tagged Tf_MurK in *E. coli*, the *T. forsythia murK* gene (*Tf_murK*, *Tanf_08380*) was cloned in the expression vector pET28a (Novagen, Darmstadt, Germany). Genomic DNA of *T. forsythia* ATCC 43037 was prepared, using the GenElute Bacterial Genomic DNA Kit (Sigma, Vienna, Austria) and served as a template to amplify a 852-bp DNA fragment containing *Tf_murK* by PCR, using the primer pair 1068for/1068rev (Table 1). PCR product and vector were digested with *Nco*I and *Xho*I (NEB, Frankfurt, Germany) and ligated into pET28a using T4 DNA ligase (Thermo Fisher Scientific, Waltham, MA, United States). The resulting plasmid, was named pET28_Tf_MurK and transformed into *E. coli* BL21(DE3) by electroporation.

For overexpression of Tf_MurK, 2 l of LB medium supplemented with Km were inoculated with 20 ml of an overnight culture of *E. coli* BL21(DE3) harboring pET28_Tf_MurK. The cells were grown at 37°C in a baffled 5 l-flask and vigorous shaking. At an OD₆₀₀ ~0.7, protein expression was induced by addition of isopropyl-β-D-thiogalactopyranoside (IPTG; 1 mM final concentration) and the culture was further incubated overnight at 20°C. Cells were harvested by centrifugation at 4000 g for 20 min at 4°C (F12-6 x 500 LEX rotor, Thermo Fisher Scientific, Waltham, MA, United States). The cell pellet was resuspended in 20 ml of 20 mM Na₂HPO₄ (pH 7.5) containing 500 mM NaCl and 1 mM DTT (buffer A), and cell lysis was achieved using a French cell disruptor (Sim Aminco Spectronic Instruments, Inc. Rochester, NY, United States), three times at 1'000 psi. Subsequently, the soluble extract was separated from cell debris by centrifugation at 38'000 g (Sorvall, SS-34 rotor, Beckmann, Krefeld, Germany) for 60 min at 4°C.

For purification of recombinant Tf_MurK (rTf_MurK) by Ni²⁺ affinity chromatography, the supernatant obtained before was filtered through a 0.2-µm filter (Sarstedt, Nümbrecht, Germany) and loaded on a 1-ml His-Trap column (GE

TABLE 1 | Oligonucleotide primers used for PCR amplification reactions.

Primer	Sequence (5'-3')
1068for	GCGCCATGGCGATACTGATTGCAGATAGC
1068rev	GCGCTCGAGTACGGTTTTTGCAACTGTCTGAATAG
622	ATAATCCCGGATCATGGTCGTTTCG
623	CTTTGCGCACCCGACGAGATGATG
624	TTCAGACGCCGGAAGAGATG
625	GGATTGCGAACGATTGTACC
1068upfor	ACACCGACCGACCTCGTATTTCCCTTTT
1068uprev	CGAACCGGCAATTTCTTTTTTGTCAT ATTTTGATATATATT TTTTCTTATACAAGAT
1068downfor	GTCCCTGAAAAATTCATCCTTCGTAG ATGACATTATCA AAATAACAGAACAGG
1068downrev	GGTAAGCGGTCATCATCTCTCGTCGG
524	GTAAACGAACGGGCAATTTCTTTTTTGTCAT
525	CCCTGAAAAATTCATCCTTCGTAG
460	ATGACAAAAAGAAATTGCCCGTTCGTTTTAC
461	CTACGAAGGATGAAATTTTCAGGACAAC

Nucleotides used for overlap-extension PCRs are written in bold, artificially introduced restriction enzyme sites are italicized.

Healthcare, Freiburg, Germany), pre-equilibrated with ten column volumes each of H₂O and buffer A (20 mM Na₂HPO₄, 500 mM NaCl, 1 mM DTT, pH 7.5), using a protein purification system (Äkta Purifier, GE Healthcare). Protein elution was achieved by applying a linear gradient from 0 to 500 mM imidazole in buffer A. Elution fractions were analyzed by SDS-PAGE using 12% polyacrylamide gels stained with Coomassie Brilliant Blue G250 (Laemmli, 1970) and rTf_MurK-containing fractions were pooled and applied to size-exclusion-chromatography (HiLoad 16/60 Superdex 200 column, GE Healthcare) using buffer A as eluent; fractions containing pure rTf_MurK according to SDS-PAGE were pooled. The protein concentration of the rTf_MurK pool was calculated using the extinction coefficient at 280 nm (20,775 M⁻¹ cm⁻¹, ExPASy, ProtParam tool) as measured in a 1-ml quartz cuvette (Hellma, Müllheim, Germany) using a SpectraMax M2 spectrometer (Molecular Devices, Biberach, Germany).

Activity of rTf_MurK, Mg²⁺-Dependency and Identification of the Reaction Product

Product formation upon rTf_MurK kinase activity was analyzed by electrospray ionization-time of flight mass spectrometry (ESI-TOF-MS) using a Micro-TOF II (Bruker Daltonics, Bremen Germany), operated in negative ion mode, after separation on an UltiMate 3000 RS, high-performance liquid chromatography (HPLC) system (Dionex, Thermo Scientific, Sunnyvale, USA). 1 µg of Tf_MurK was added to a 100-µl reaction mixture containing 1 mM MurNAc, 10 mM ATP, 100 mM Tris-HCl (pH 7.6) and incubated for 1 h at room temperature (RT). In a parallel approach, 10 mM MgCl₂ was added to the reaction mixture to determine the effect of Mg²⁺ on catalysis. Reaction aliquots of 10 µl, each, were separated on a ZIC-HILIC column (150 × 7.5 mm, 200 Å, 5 µm; Merck) at 37°C, applying

a 40-min elution program as described previously (Unsleber et al., 2017). Extracted ion chromatograms (EICs) for MurNac-P [(M-H)⁻¹ = 372.070 *m/z*] were obtained with the software Data Analysis (Bruker), the area under the curve (AUC) values for the EICs for MurNac-P were determined using the Prism 6 program (GraphPad Software, La Jolla, CA, United States) and the relative activity of the enzyme was calculated using these values following a published protocol (Borisova and Mayer, 2017).

The *m/z* value obtained by MS analyses does not allow to distinguish between the stereochemistry of phosphosugars. To show that the product formed by Tf_MurK is indeed MurNac-6P, it was cleaved with the etherase rTf_MurQ - available in our laboratory from a previous study (Ruscitto et al., 2016) - which specifically converts this phosphosugar into GlcNac-6P and D-lactate. For this assay, 1 µg of rTf_MurK was added to a 100-µl reaction mixture containing 5 mM MurNac, 10 mM ATP and 10 mM MgCl₂ in 100 mM Tris-HCl (pH 7.6) and incubated overnight at RT. Subsequently, 10 µg (2 µl) of rTf_MurQ were mixed with 20 µl of the reaction and incubated for 1 h at 37°C. The negative control contained 2 µl of distilled water instead of rTf_MurQ. After stopping the reaction, the product was analyzed by ESI-TOF-MS as described above except for using a Gemini C18 HPLC column (150 × 4.6 mm, 110 Å, 5 µm; Phenomenex, Aschaffenburg, Germany) (Borisova et al., 2014).

Determination of the Substrate Specificity of rTf_MurK

Substrate specificity of rTf_MurK was assayed as described previously (Reith et al., 2011). ATP, glucose (Glc), GlcNac, glucosamine (GlcN), *N*-acetyl galactosamine (GalNac) and GlcNac-6P were obtained from Sigma-Aldrich (Taufkirchen, Germany), MurNac was obtained from Bachem (Bubendorf, Switzerland). MurNac-6P was available from a previous study (Unsleber et al., 2017) and 1,6-anhydro-MurNac (anhMurNac) was synthesized according to a published protocol (Calvert et al., 2017).

For the substrate specificity assay, the different sugars - MurNac, GlcNac, GalNac or GlcN at 50 mM final concentration, each, Glc at 1 mM final concentration or anhMurNac at 10 mM final concentration - were added to a 100-µl reaction mixture containing 100 mM Tris-HCl (pH 7.6), 100 mM ATP and 10 mM MgCl₂. The reaction was started by addition of rTf_MurK (10 nM final concentration) and continued for 16 h at RT. 3-µl samples were taken from each reaction mixture at time points 0 (*t*₀) and 16 h (*t*₁₆) and spotted on a TLC plate (Silica 60 F₂₅₄ Merck, Darmstadt, Germany). The reaction mixtures were separated using a basic solvent of *n*-butyl alcohol/methanol/25% (w/v) ammonium hydroxide/water in a ratio of 5:4:2:1 (v/v/v/v). The separated compounds were visualized by carbonization, for which the TLC plate was quickly dipped in a 5% methanolic solution of sulfuric acid, followed by drying and final development of the plate by heating for 15 min at 180°C.

Determination of pH Optimum and Temperature Stability of Tf_MurK

To determine pH stability and pH optimum of rTf_MurK, buffers in the pH range of 2.0–11.0 were used, i.e., Clark and Lubs buffer (pH 2.0), sodium acetate buffer (pH 3.0–6.0), sodium phosphate buffer (pH 6.0–8.0), and sodium carbonate buffer (pH 9.0–11.0). For the pH stability test, rTf_MurK was diluted in buffer to a final concentration of 2 ng/ml and pre-incubated for 30 min at 20°C. The reaction was started by adding 5 µl of the pre-incubated enzyme (10 ng) to a 45-µl mixture containing 1 mM MurNac, 10 mM MgCl₂ and 10 mM ATP in 50 mM phosphate buffer (pH 7.0). After incubation for 30 min at 20°C, the reaction was stopped by adding 50 µl of a solution containing 1% formic acid and 0.5% ammonium formate (pH 3.2; stopping solution). For the pH optimum test, 100-µl reaction mixtures were prepared, containing 1 mM MurNac, 10 mM MgCl₂ and 10 mM ATP, in a 50 mM buffer of a particular pH in the range of 2.0 to 11.0. The reaction was started by adding 10 ng of rTf_MurK followed by incubation for 30 min at 20°C; the reaction was stopped by adding 100 µl of stopping solution. Samples were analyzed by HPLC connected to ESI-TOF-MS (MicrO-TOF II; Bruker) and quantified using the Prism 6 program (GraphPad), as described above (Borisova and Mayer, 2017; Unsleber et al., 2017).

To determine the temperature stability of rTf_MurK, the purified enzyme was pre-incubated at different temperatures (i.e., 4, 20, 37, 45, 55, and 65°C) for 30 min. Subsequently, an aliquot of that solution corresponding to 10 ng of rTf_MurK was added to a 50 µl reaction mixture (20°C). The reaction was carried out and terminated as described above. To investigate the temperature optimum of rTf_MurK, a standard 50-µl reaction containing 10 ng of rTf_MurK was carried out for 30 min at different temperatures (i.e., 4, 20; 37, 45, 55, and 65°C) and samples were subsequently analyzed and the reaction quantified as described above.

Determination of Enzyme Kinetic Parameters

Kinetic parameters of Tf_MurK-catalyzed phosphorylation of MurNac and GlcNac with ATP were determined by using a coupled enzyme assay as described previously (Reith et al., 2011), with minor modifications. In a 96-well plate (Greiner, Frickenhausen, Germany), a 100-µl reaction mixture containing additionally 1 mM phosphoenolpyruvate, 0.2 mM NADH, 10 U of pyruvate kinase, and 7 U of lactate dehydrogenase (all from Sigma-Aldrich, Taufkirchen, Germany) was incubated with the amino sugar substrates, ranging from 0.05 to 2 mM for MurNac or 0.1 to 250 mM for GlcNac. The reaction was started by the addition of freshly prepared rTf_MurK; 10 ng (3 nmol) enzyme was used for the reaction with MurNac and 1 µg (300 nmol) enzyme for the reaction with GlcNac. The change of NADH absorbance was monitored at 340 nm in a spectrophotometer (Spark 10 M; Tecan, Männedorf, Switzerland) for 45 min at 20°C. The experimental data were fitted to the Michaelis-Menten equation and, taking into account substrate inhibition, also to the equation $Y = v_{\max} \cdot [S] / (K_m + [S] \cdot (1 + [S]/K_i))$, using the program GraphPad Prism 6. The molar extinction coefficient of NADH at

340 nm ($6220 \text{ M}^{-1} \text{ cm}^{-1}$) was used to calculate v_{\max} and k_{cat} values.

Construction of a *T. forsythia* MurNac 6-Kinase Deletion Mutant

A knock-out vector was constructed to exchange the *Tf_murK* gene of *T. forsythia* ATCC 43037 (*Tanf_08380*) in frame with an erythromycin resistance (*erm*) marker (see Supplementary Figure S1). A detailed description of the cloning procedure and the transformation of the knock-out cassettes into *T. forsythia* is published elsewhere (Tomek et al., 2014, 2017). For PCR amplifications, Phusion High-Fidelity DNA polymerase (Thermo Fisher Scientific, Austria) was used according to the manufacturer's instructions. Oligonucleotides (Thermo Fisher Scientific) used in this study are listed in Table 1. Extraction of genomic DNA was conducted according to a published protocol (Cheng and Jiang, 2006). The knock-out vector contains two homology regions approximately 1-kbp up-stream and down-stream of *Tf_murK* and the *erm* marker cloned in between. Primer pairs 1068upfor/1068uprev and 1068downfor/1068downrev, respectively, were used to amplify the up- and down-stream homology regions from genomic DNA of *T. forsythia* ATCC 43037. The *erm* gene (805 bp, without the promotor region) of pJET/TF0955ko (Tomek et al., 2014) was amplified using primers 460 and 461. Subsequently, the knock-out cassette was blunt-end cloned into the cloning vector pJET1.2, creating the final knock-out vector pJET1.2/ Δ *Tanf_08380*. Transformed and viable clones on selective plates containing Erm were further tested for correct integration of the knock-out cassette by screening PCR and sequencing (Supplementary Figure S1). The deletion mutant strain, thus, carries an *erm* marker in place of the *Tf_murK* gene and, accordingly, was named Δ *Tf_murK::erm*.

Preparation of Cytosolic Fractions and Metabolite Analysis

The intracellular accumulation of cell wall metabolites in *T. forsythia* Δ *Tf_murK::erm* in comparison to *T. forsythia* WT was investigated in both the exponential and the stationary phase; these phases had been determined before by recording growth curves of the strains as described above (time points are indicated in Figure 4). For that purpose, two different volumes of liquid medium (i.e., 50 and 200 ml) supplemented with 20 $\mu\text{g/ml}$ MurNac (the MurNac concentration routinely used for optimal growth of the bacterium) and appropriate antibiotics were inoculated with *T. forsythia* WT and mutant cells at an $\text{OD}_{600} \sim 0.05$. The 200-ml cultures were harvested (5000 g) after 3 days of incubation under anaerobic conditions, corresponding to the exponential growth phase ($\text{OD}_{600} \sim 0.6$); the 50-ml cultures were harvested on day 4, corresponding to the stationary growth phase ($\text{OD}_{600} \sim 1.7$, wild-type; $\text{OD}_{600} \sim 1.2$, mutant). Metabolite extraction was performed as described with minor modifications (Gisin et al., 2013; Borisova et al., 2014). After correcting for differences in ODs and culture volumes, equal amounts of cells were washed with 20 ml of 10 mM Tris-HCl (pH 8.0), resuspended in 400 μl of Millipore water, boiled

at 100°C for 1 h and centrifuged at 21000 g for 15 min. The supernatant was then transferred into a fresh tube and treated with 1.5 ml of acetone (HPLC grade). After centrifugation at 21000 g for 15 min, the supernatant was transferred into a fresh tube and left open to evaporate under vacuum overnight at 37°C. The residual liquid was dried off in a centrifugal evaporator. Dried samples were resuspended in 50 μl of Millipore water and 5- μl aliquots were analyzed by LC-MS using a Gemini C18 column (150 \times 4.6 mm, 110 Å, 5 μm ; Phenomenex) and a UltiMate 3000 RS (Dionex) coupled to a Micro-TOF II mass spectrometer (Bruker) operated in negative ion mode (Borisova et al., 2014). EICs were used to calculate the area under the curve (AUC) using Prism6 (GraphPad). Data were presented as mean of three replicates.

Scanning Electron Microscopy (SEM)

T. forsythia WT and Δ *Tf_murK::erm* mutant were cultivated as described above, using MurNac concentrations of 0.1, 0.5, 1.0, and 20.0 $\mu\text{g/ml}$, respectively. Briefly, at an OD_{600} of ~ 0.5 (exponential growth phase) or ~ 1.5 (stationary growth phase), 1 ml of bacterial culture was harvested, each, and centrifuged at 5000 g for 7 min. Cell pellets were washed twice with phosphate-buffered saline (PBS), suspended in 500 μl of ethanol (25% in PBS), incubated for 7 min at RT and centrifuged. This step was repeated using solutions of 35, 50, 60, 70, 80, 90, and 95% ethanol in PBS and finally 100% ethanol. Finally, the samples were sputter-coated with gold (EM SDC005 apparatus; Leica, Wetzlar, Germany) and imaged with an Inspect S50 scanning electron microscope (FEI, Eindhoven, Netherlands). A detailed description of sample preparation for sputter-coating and SEM is published elsewhere (Tomek et al., 2014).

RESULTS

Tf_MurK Is a Specific MurNac-6-Kinase

To determine function and specificity of the putative kinase Tf_MurK (*Tanf_08380*), the 283-amino acid enzyme (theoretical pI, 6.54; calculated molecular mass, 31.3 kDa) was produced as a recombinant protein (rTf_MurK) in *E. coli* BL21(DE3) cells. The protein was equipped with a C-terminal His₆-tag for purification purposes. Applying Ni²⁺ affinity chromatography followed by size exclusion chromatography, rTf_MurK was purified to near homogeneity, as judged by SDS-PAGE analysis (Supplementary Figure S2), whereat rTf_MurK migrated at about the expected size. rTf_MurK was obtained at a yield of 4 mg per liter of bacterial culture.

The activity of rTf_MurK was first assayed with MurNac and ATP as substrates applying ESI-TOF-MS (Figure 1). A product at low intensity (EIC peak height of 2.6×10^5 cps) appeared with a mass in negative ion mode (M-H)⁻ of 372.072 m/z , which is in agreement with the m/z of a supposed MurNac-phosphate product. The product yield increased ~ 10 -fold (EIC peak height of 2.3×10^6 cps) upon addition of 10 mM MgCl₂ to the reaction, (Figure 1), indicating that MurK activity is dependent on Mg²⁺ ions. Thus, all subsequent reactions were supplemented with 10 mM MgCl₂. We next determined the stereochemistry of the

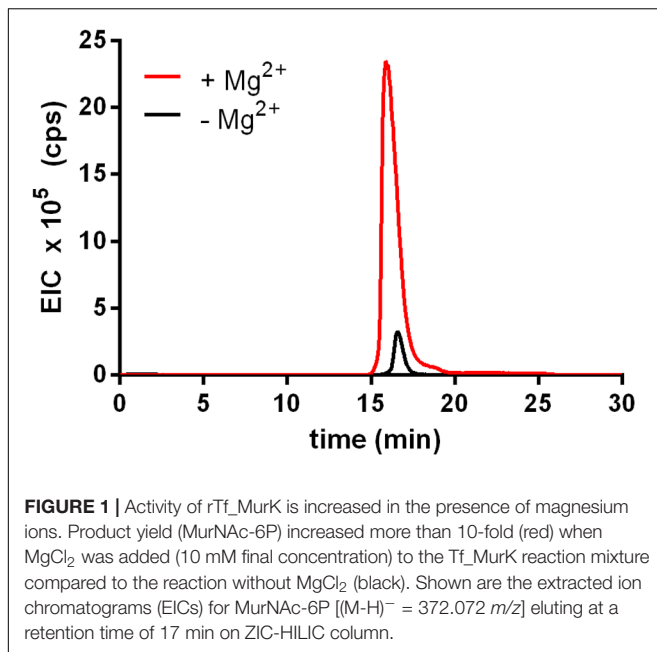


FIGURE 1 | Activity of rTf_MurK is increased in the presence of magnesium ions. Product yield (MurNAc-6P) increased more than 10-fold (red) when MgCl_2 was added (10 mM final concentration) to the Tf_MurK reaction mixture compared to the reaction without MgCl_2 (black). Shown are the extracted ion chromatograms (EICs) for MurNAc-6P [$(\text{M}-\text{H})^- = 372.072 \text{ m/z}$] eluting at a retention time of 17 min on ZIC-HILIC column.

product generated upon rTf_MurK catalysis using *T. forsythia* MurNAc-6P etherase (rTf_MurQ) (Ruscitto et al., 2016). The rTf_MurK product ($(\text{M}-\text{H})^- = 372.072 \text{ m/z}$, retention time of 22 min) was completely converted by rTf_MurQ into a product with $(\text{M}-\text{H})^- = 300.059 \text{ m/z}$ (retention time 12 min), which is in agreement with the expected mass of GlcNAc-6P (Figure 2). Hence, we identified the rTf_MurK reaction product using MurNAc and ATP as MurNAc-6P.

To determine the substrate specificity of rTf_MurK, different sugar substrates, including MurNAc, GlcNAc, anhMurNAc, Glc, GalNAc, and GlcN, were tested in a 16-h reaction followed by TLC analysis (Figure 3). Of the sugars tested, only MurNAc and GlcNAc, albeit apparently very slow, were converted by rTf_MurK to the corresponding phosphosugar; simultaneously ATP was converted into ADP, which was also detected on the TLC plate. The other tested sugars, including anhMurNAc, Glc, GalNAc, and GlcN obviously did not serve as substrates for the rTf_MurK reaction (Figure 3).

Biochemical Characterization of Tf_MurK and Determination of Kinetic Parameters

Prior to the determination of the kinetic parameters, the pH and temperature optima of rTf_MurK were determined. Product formation of the enzyme with MurNAc and ATP was followed at different pH values and temperatures by determining the EICs of MurNAc-6P ($(\text{M}-\text{H})^- = 372.070 \text{ m/z}$) and quantifying the AUC in comparison to a standard. rTf_MurK was shown to be stable over a wide pH range between 3.0 and 11.0, with maximal activity detected between pH 7.0 and 9.0 (Supplementary Figure S3). For determining enzyme kinetic parameters, 50 mM phosphate buffer (pH 7.0) was chosen, because the enzyme's activity was highest in that buffer; furthermore, the buffering capacity is

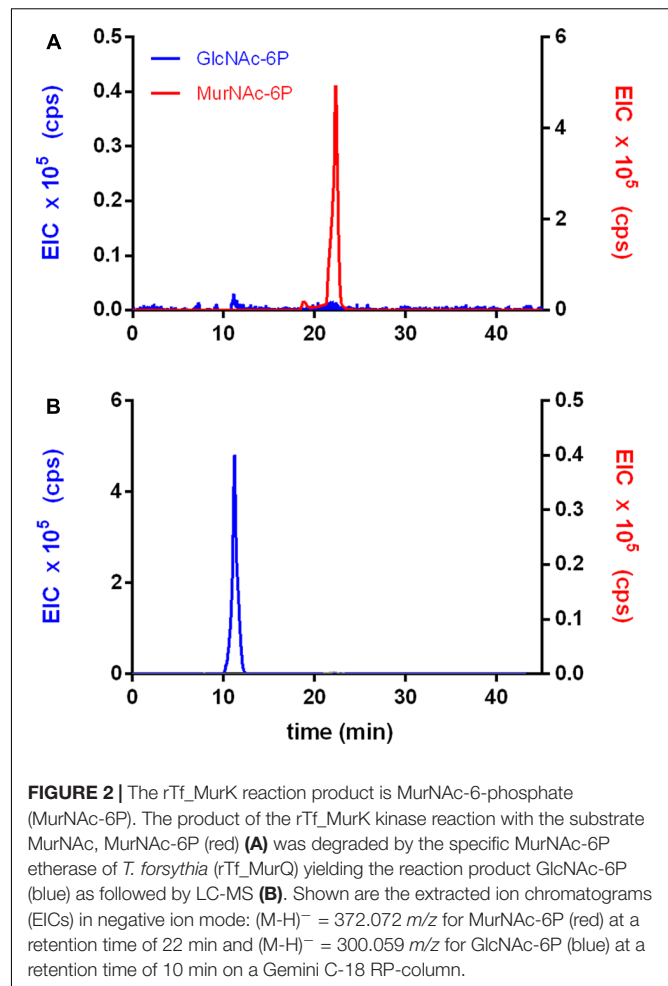


FIGURE 2 | The rTf_MurK reaction product is MurNAc-6-phosphate (MurNAc-6P). The product of the rTf_MurK kinase reaction with the substrate MurNAc, MurNAc-6P (red) (A) was degraded by the specific MurNAc-6P etherase of *T. forsythia* (rTf_MurQ) yielding the reaction product GlcNAc-6P (blue) as followed by LC-MS (B). Shown are the extracted ion chromatograms (EICs) in negative ion mode: $(\text{M}-\text{H})^- = 372.072 \text{ m/z}$ for MurNAc-6P (red) at a retention time of 22 min and $(\text{M}-\text{H})^- = 300.059 \text{ m/z}$ for GlcNAc-6P (blue) at a retention time of 10 min on a Gemini C-18 RP-column.

maximal in the optimal pH range of the enzyme. The temperature optimum for the rTf_MurK reaction was determined to be 37°C, when the reaction time was restricted to 3 min (Supplementary Figure S3). However, incubation at 37°C for 30 min almost completely inactivated the enzyme and incubation at 20°C for 30 min reduced the activity by ~50% (Supplementary Figure S3). We thus limited the reaction time to 3 min in the kinetic experiments and choose a reaction temperature of 20°C, as a compromise between sufficient activity and stability of rTf_MurK.

For the determination of rTf_MurK kinetic parameters we used a coupled enzyme assay (Reith et al., 2011) in which the formation of ADP is stoichiometrically coupled to NADH oxidation by pyruvate kinase and lactate dehydrogenase. Kinetic parameters were calculated therefrom (Table 2; see also Supplementary Figure S4). The reaction of rTf_MurK with MurNAc as substrate was much faster than that with GlcNAc as substrate (V_{max} of 39.5 versus 0.5 $\mu\text{mol/min mg}$) and a 1000-fold lower K_m was determined for MurNAc compared to GlcNAc (K_m of 113 versus 116700 μM). With the latter substrate, the maximum activity at saturation was not reached, not even with 250 mM GlcNAc added to the reaction. With MurNAc, saturation was reached; however, at concentrations higher than 1 mM the

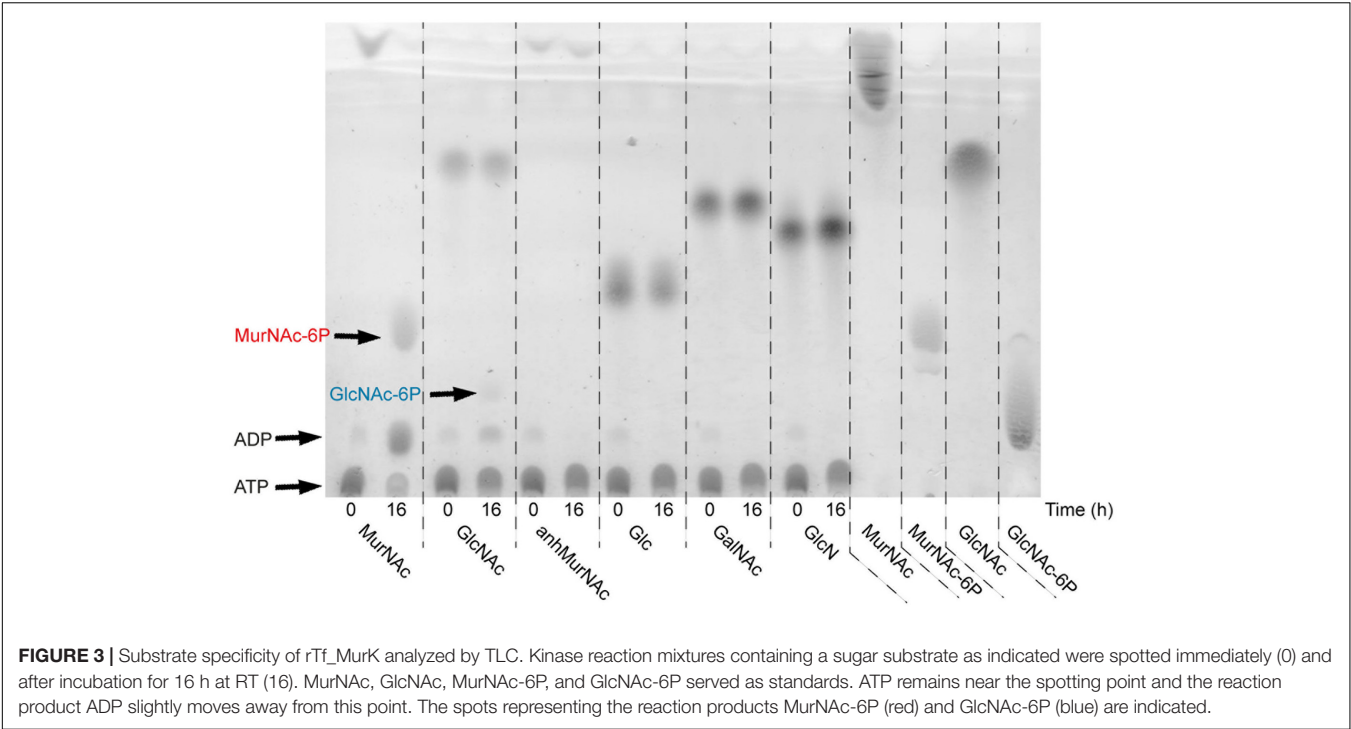


TABLE 2 | Kinetic parameters of Tf_MurK.

Substrate	K_M [μM]	V_{max} [$\mu\text{mol min}^{-1} \text{mg}^{-1}$]	k_{cat} [s^{-1}]	k_{cat}/K_M [$\text{s}^{-1} \text{M}^{-1}$]	$K_{i(S)}$ [mM]
Kinetic parameters fitted to Michaelis-Menten equation:					
MurNAc	113	39.5	7.9	69910	nd
GlcNAc	116700	0.5	0.1	0.86	nd
Kinetic parameters fitted considering substrate inhibition:					
MurNAc	200	52.6	10.5	52550	4.2

nd, not determined.

enzyme’s activity dropped slightly, indicating that the enzyme was subject to substrate inhibition. Thus, the kinetic parameters were re-fitted to an equation that considers substrate inhibition. This yielded kinetic parameters of rTf_MurK for MurNAc of K_m of 200 μM and a V_{max} of 52.6 $\mu\text{mol/min mg}$ (k_{cat} of 10.5 s^{-1}), and a MurNAc inhibitory constant ($K_{i(S)}$) of 4.2 mM was determined (Table 2).

Growth Advantage of a *Tf_murK* Mutant in MurNAc-Limited Medium

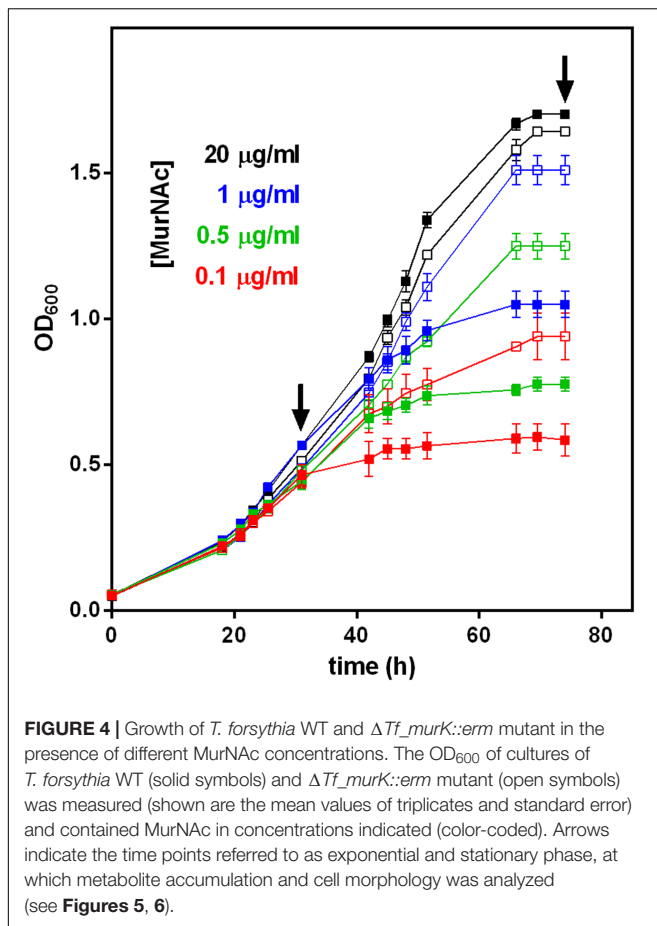
A *Tf_murK* mutant was constructed by insertional inactivation of the *Tanf_08380* gene using an *erm* marker ($\Delta Tf_murK::erm$) (Supplementary Figure S1). This strategy of mutation in *T. forsythia* has been established in our laboratory (Tomek et al., 2017). A comparison of the SDS-PAGE migration pattern of the $\Delta Tf_murK::erm$ mutant with that of *T. forsythia* WT cells did not reveal major difference in cellular proteins; especially the presence of the two S-layer proteins TfsA and TfsB characteristic of optimally growing *T. forsythia* cells was a clear indication

that no changes had occurred in the cell wall composition of the mutant (Supplementary Figure S1). In addition, when grown in complex medium supplemented with an excess of MurNAc (20 $\mu\text{g/ml}$), *T. forsythia* WT and $\Delta Tf_murK::erm$ mutant showed very similar growth curves, reaching both a maximum of OD_{600} of ~ 1.6 after 70 h (Figure 4).

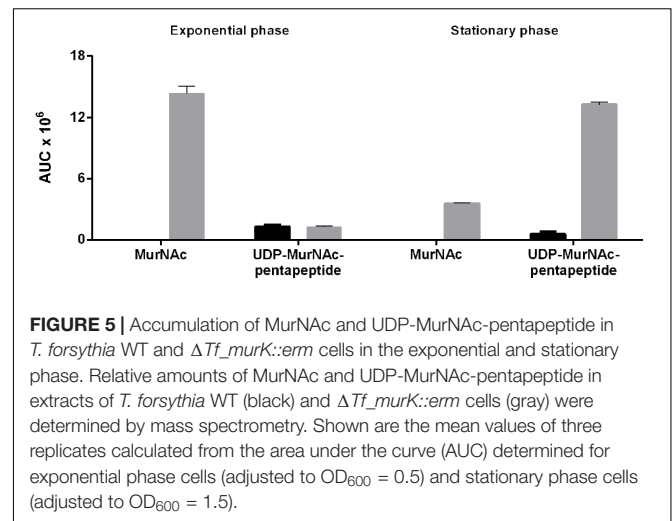
However, when the MurNAc concentration in the medium was reduced to 1.0, 0.5, or 0.1 $\mu\text{g/ml}$, growth of WT and mutant cells was different. For the initial 30 h roughly corresponding to the exponential growth phase, *T. forsythia* WT and mutant cells grew identically in complex medium supplemented with limiting amounts of MurNAc (1.0, 0.5, or 0.1 $\mu\text{g/ml}$). After this time point, however, the mutant grew to higher OD_{600} values compared to the WT, revealing a clear growth advantage during the late exponential and stationary phases (Figure 4). In MurNAc-limited medium *T. forsythia* WT cells reached final OD_{600} values of ~ 1.0 , ~ 0.8 , and ~ 0.6 , respectively (Figure 4). In contrast, mutant cells continued their growth and reached under the same conditions final OD_{600} values of 1.5 (almost matching growth upon 20 $\mu\text{g/ml}$ MurNAc supplementation), 1.2 and 0.9, respectively (Figure 4).

Growth Phase-Dependent Accumulation of MurNAc and UDP-MurNAc-Pentapeptide in a *Tf_murK* Mutant

In an attempt to understand the unexpected growth advantage of the $\Delta Tf_murK::erm$ mutant under MurNAc limitation, we examined the accumulation of MurNAc and other cell wall metabolites within the cytosolic fractions of mutant and WT cells by LC-MS, comparing the situation in the exponential growth phase at 30 h ($\text{OD}_{600} \sim 0.5$) and stationary phase at 75 h ($\text{OD}_{600} \sim 1.6$) of growth (indicated with arrows in Figure 4).



During the exponential growth phase, the $\Delta Tf_murK::erm$ mutant accumulated two major metabolites with m/z of $(M-H)^- = 292.107$ and $(M-2H)^{2-} = 595.670$, corresponding to MurNAc and UDP-MurNAc-pentapeptide, respectively (Supplementary Figure S5). The theoretical m/z values of the investigated molecules are 292.110 for MurNAc and 1192.340 for UDP-MurNAc-pentapeptide. Of the latter, the single charged ion was detected only with low intensity and mainly the doubly charged ion $(M-2H)^{2-} = 595.670$ m/z appeared. This was used to quantify the UDP-MurNAc-pentapeptide content in the extracts (Supplementary Figure S5). MurNAc appeared as a double peak, because of the separation of the α - and β -anomers (Supplementary Figure S5C). **Figure 5** summarizes the accumulation data determined by integration of the EICs that were obtained by MS measurements. Assuming that MurNAc and UDP-MurNAc-pentapeptide have roughly the same response factors in the MS experiments, we can conclude that in the exponential growth phase, the relative concentration of MurNAc in the mutant cell extract was ~10-fold higher than that of UDP-MurNAc-pentapeptide (**Figure 5**). *T. forsythia* WT cells, in contrast, showed no accumulation of MurNAc, but yielded UDP-MurNAc-pentapeptide in the exponential growth phase, in the same relative concentration as the $\Delta Tf_murK::erm$ mutant (**Figure 5** and Supplementary Figure S5). However, when $\Delta Tf_murK::erm$ cells from the



stationary phase were analyzed, a different accumulation pattern was observed in comparison to that from the exponential growth phase. Here, the intracellular concentration of MurNAc decreased almost 5-fold and that of UDP-MurNAc-pentapeptide increased roughly 10-fold (**Figure 5**), thus reversing the MurNAc:UDP-MurNAc-pentapeptide ratio from the exponential growth phase. For *T. forsythia* WT cells, a slight decrease of the UDP-MurNAc-pentapeptide level could be observed (**Figure 5**).

Thus, in *T. forsythia* WT cells, in neither growth phase, a measurable level of MurNAc was detected, indicating rapid metabolization. In $\Delta Tf_murK::erm$ cells, in contrast, MurNAc and UDP-MurNAc-pentapeptide readily accumulated – with a MurNAc:UDP-MurNAc-pentapeptide ratio of 10:1 and 1:5 in the exponential and stationary growth phase, respectively.

Morphological Defects of *T. forsythia* Cells Grown under MurNAc Limitation

Confirming the previously reported MurNAc auxotrophy of *T. forsythia* (strains OMZ 408, FDC 331, and the ATCC 43037 type strain) (Wyss, 1989), in this study, we visualized the effect of step-wise MurNAc depletion of the culture medium on *T. forsythia* ATCC 43037 cell morphology by applying SEM. In parallel experiments, we compared the situation in *T. forsythia* WT and $\Delta Tf_murK::erm$ cells, in both the exponential and stationary growth phase (**Figure 6**).

For optimal growth of *T. forsythia*, MurNAc supplementation of the medium was routinely done at a concentration of 20 $\mu\text{g/ml}$, which in our previous experiment resulted in almost identical growth characteristics for the WT and $\Delta Tf_murK::erm$ mutant, in both growth phases analyzed (**Figure 4**). Under this “optimal” condition, also no difference of either cell shape or cell aggregation was apparent from the SEM micrographs (**Figure 6**, lane 1).

However, we found that reduction of MurNAc supplementation, besides causing growth defects in *T. forsythia* cells, reflected by reduced cell densities at OD₆₀₀ (cf. **Figure 4**), caused severe morphological changes, such as cell thickening

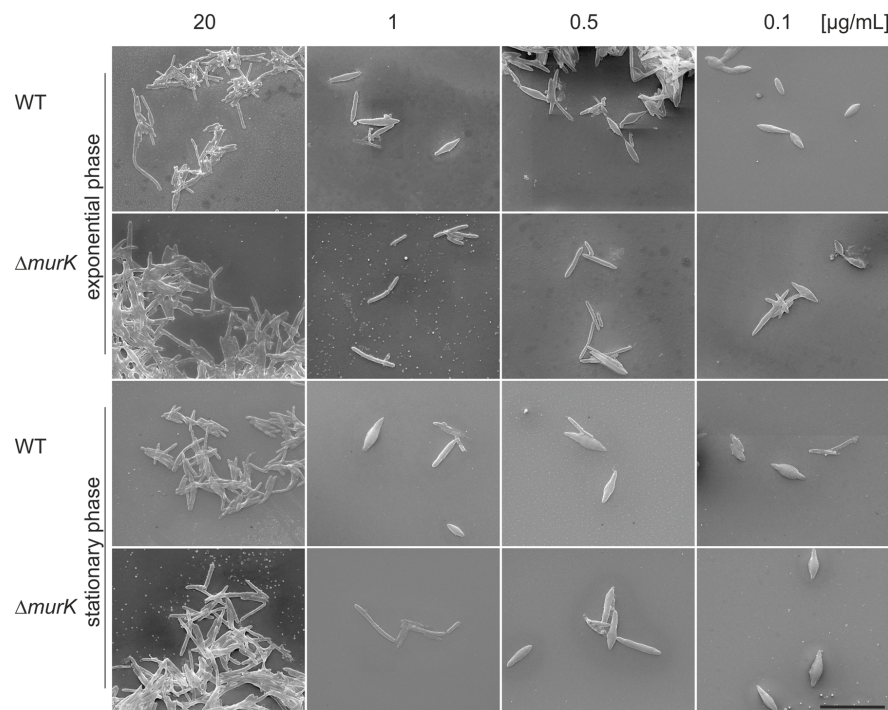


FIGURE 6 | SEM micrographs of *T. forsythia* wild-type (WT) and $\Delta Tf_murK::erm$ ($\Delta murK$) mutant cells when grown under full MurNac supplementation (first row) and under MurNac limiting conditions (rows two to four). Media were supplemented with 20 $\mu\text{g/ml}$ (full supplementation), 1 $\mu\text{g/ml}$, 0.5 $\mu\text{g/ml}$, and 0.1 $\mu\text{g/ml}$ of MurNac. The $\Delta murK$ mutant is more tolerant toward MurNac limitation as can be seen from transition from rod-shaped to fusiform cells occurring only at 0.1 $\mu\text{g/ml}$ MurNac, with this effect being more profound in the exponential growth phase. Scale bar, 10 μm .

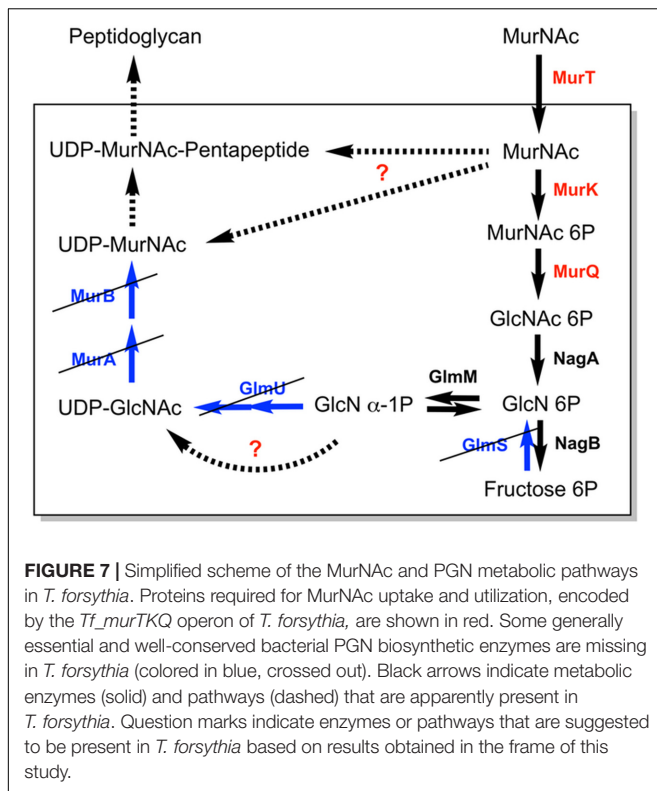
and development of fusiform cell morphology (Figure 6). These morphological changes occasionally appeared in the *T. forsythia* WT already when the MurNac concentration was reduced to 1 $\mu\text{g/ml}$ (which is the second highest MurNac concentration that was tested in the course of this study), but they became more evident when MurNac in the medium was reduced to 0.5 $\mu\text{g/ml}$, and were dominant at 0.1 $\mu\text{g/ml}$, where almost exclusively fusiform cells were present (Figure 6). Whether the evident loss of aggregation capability of fusiform *T. forsythia* cells is a direct effect of the morphological change upon MurNac depletion or rather of the concomitant decrease of overall cell density needs to be further investigated.

Intriguingly, $\Delta Tf_murK::erm$ mutant cells appeared to be more tolerant toward MurNac depletion compared to the *T. forsythia* WT implicating that they seemed to require less MurNac to maintain their rod-shaped cells in comparison to the WT. Exponential-phase mutant cells grew mostly as normal rods in medium containing 1 or 0.5 $\mu\text{g/ml}$ MurNac. Only further reduction to 0.1 $\mu\text{g/ml}$ MurNac caused the transformation to fusiform morphology. In mutant cells from the stationary phase, fusiform cells were already visible at 0.5 $\mu\text{g/ml}$ MurNac and were prominent at 0.1 $\mu\text{g/ml}$ MurNac. Thus, morphological alteration of *T. forsythia* cells due to MurNac depletion occurs in WT cells already at higher MurNac concentration than in a $\Delta Tf_murK::erm$ mutant.

DISCUSSION

In this study, a specific MurNac-kinase of *T. forsythia* ATCC 43037, Tf_MurK (Tanf_08380), was biochemically characterized. Of all tested sugars only MurNac and, albeit marginally, GlcNac were phosphorylated by the kinase. The reaction of rTf_MurK with MurNac as the sugar substrate was about 100-times faster than with the GlcNac substrate (V_{max} of 52.6 versus 0.5 $\mu\text{mol/min mg}$). Moreover, with GlcNac, rTf_MurK did not reach substrate saturation, reflected by an exceedingly high K_M of 116 mM. To clearly define substrate specificity of an enzyme acting on alternative substrates, the specificity constants (k_{cat}/K_M) have to be determined (Eisenthal et al., 2007). For Tf_MurK acting on MurNac and GlcNac, we determined k_{cat}/K_M values of 52550 and 0.86 $\text{s}^{-1} \text{M}^{-1}$, respectively, resulting in a ratio of the specificity constants of >60000, which demonstrates the enzyme's strong preference for MurNac. Moreover, the reaction product was identified as MurNac-6P through cleavage by the specific MurNac-6P etherase Tf_MurQ identified previously (Ruscitto et al., 2016). Thus, Tf_MurK can be unambiguously assigned as a specific MurNac 6-kinase. The GlcNac kinase activity of the enzymes is only marginal and likely physiologically not relevant.

This is the first report on an enzyme with a stringent substrate specificity for MurNac. In 2011, Reith et al. reported a kinase from *Clostridium acetobutylicum* (Ca_MurK) with specificity for MurNac (Reith et al., 2011). Although this enzyme was named



MurK, too, it has only limited overall amino acid sequence identity with Tf_MurK (26.7%, *E*-value of 8.9×10^{-4}) and was shown to act on both, MurNAc and GlcNAc, with a slight preference for the latter (ratio of specificity constants < 0.4 -fold, and $k_{\text{cat}}/K_M = 225000$ and $510000 \text{ s}^{-1} \text{ M}^{-1}$, for MurNAc and GlcNAc, respectively). The K_M value of Tf_MurK for MurNAc (200 μM) and K_M values of Ca_MurK for MurNAc (190 μM) and GlcNAc (127 μM) were in the same range, reflecting similar affinities of the enzymes for their substrates. Tf_MurK is slightly slower (turnover number $k_{\text{cat}} = 10.5 \text{ s}^{-1}$) compared to Ca_MurK ($k_{\text{cat}} = 42.8 \text{ s}^{-1}$ and 65 s^{-1} , for MurNAc and GlcNAc, respectively), in agreement with its stringent substrate specificity.

Evaluation of the kinetic data indicated that Tf_MurK is inhibited by its substrate MurNAc, in excess. Substrate inhibition is a widespread phenomenon among enzymes (Reed et al., 2010; Yoshino and Murakami, 2015), leading to velocity curves that rise to a maximum and then descend as the substrate concentration increases. For some enzymes, substrate inhibition is a means of allosteric feedback regulation (Reed et al., 2010). The biological significance of the inhibition of Tf_MurK by MurNAc, however, is questionable, since the effect occurs only at very high MurNAc concentration ($K_{\text{I[S]}}$ of 4.2 mM).

Based on amino acid sequence identity Tf_MurK can be classified as a member of the BcrAD/BadFG-like ATPase family (PF01869). These kinases are proposed to require Mg^{2+} ions for ATP binding and catalytic activity. Mg^{2+} -dependency of Tf_MurK was confirmed in this study. Tf_MurK was found to be rather unstable. The enzyme loses activity within minutes at temperatures $\geq 20^\circ\text{C}$, which may explain problems with

obtaining catalytically active pure enzyme in a previous study (Ruscitto et al., 2016). MurNAc 6-kinase activity of Tf_MurK, was indirectly shown in that study by rescuing growth on MurNAc of an *E. coli* mutant defective in the MurNAc-specific phosphotransferase type transporter Ec_MurP by providing a plasmid expressing both Tf_MurT and Tf_MurK, but not by expressing one of the two proteins alone (Ruscitto et al., 2016). Rapid degradation of rTf_MurK might also be the reason for the appearance of smaller bands besides the major protein band in SDS-PAGE analysis (Figure 1). A crystal structure of a Tf_MurK-like protein of *Porphyromonas gingivalis* (PG1100) deposited to the structure database by the Northeastern Structural Genomics Consortium (pdb code 1ZBS) revealed an open and flexible structure that might explain the functional instability.

Wyss (1989) reported that *T. forsythia* strains OMZ 408, FDC 331 and ATCC 43047 strictly depend on MurNAc for growth and rod-shaped cell morphology. According to that study, a *T. forsythia* cell population remained morphologically homogeneous and cell densities exceeded 10^7 cells per ml, when grown in a medium supplemented with 1 $\mu\text{g/ml}$ of MurNAc, whereas 0.1 $\mu\text{g/ml}$ MurNAc was found to be the minimal effective concentration, with a large portion of cells developing into unusual spherical or spindle-formed “fusiform” cells (Wyss, 1989). Growth experiments presented in the course of this study confirmed MurNAc auxotrophy for *T. forsythia* ATCC 43037. Moreover, we imaged morphological changes of *T. forsythia* cells in response to MurNAc limitation by SEM. We observed an evident growth defect of *T. forsythia* WT cells already with 1 $\mu\text{g/ml}$ of MurNAc in the medium (Figure 4) and, consistently, the cells grown under these conditions were shown to exhibit severe morphological alterations, starting with thickening and shortening of the cells, followed by converting to fusiform cell-shape, and finally appearance of thick “lemon-shaped” cells (Figure 6). Surprisingly, the $\Delta\text{Tf_murK::erm}$ mutant was less affected by MurNAc limitation than the *T. forsythia* WT. This was evident already from the recorded growth curves (Figure 4), and supported by less pronounced morphological changes upon growth in MurNAc-limited medium (Figure 6).

The accumulation of MurNAc in $\Delta\text{Tf_murK::erm}$ mutant cells confirms the function of Tf_MurK as a MurNAc kinase and demonstrates effective MurNAc uptake but a lack of catabolization capability of MurNAc caused by deletion of Tf_MurK. In WT cells, in contrast, MurNAc does not accumulate; it is catabolized via Tf_MurK and the downstream acting Tf_MurQ enzyme (Figure 7). Recently, a MurNAc transporter of the major facilitator superfamily (Tf_MurT) was identified in *T. forsythia* which is highly conserved within the *Bacteroidetes* phylum of bacteria (Ruscitto et al., 2016). Our data strongly suggest that the bacterium salvages MurNAc from the medium using this transporter and mainly channels it to the catabolic pathway. Besides utilizing MurNAc and presumably also muropeptides (Ruscitto et al., 2017) as nutrient source, *T. forsythia* assumedly also salvages these compounds directly for cell wall biosynthesis. Since *T. forsythia* is auxotrophic for MurNAc but a mutant defective in this kinase is still viable, an additional pathway must exist in the pathogen that shunts MurNAc to the peptidoglycan biosynthesis.

Accumulation of the PGN precursor UDP-MurNac-pentapeptide in stationary phase $\Delta Tf_murK::erm$ cells shows that part of the MurNac is indeed used for cell wall synthesis. In exponential phase cells, however, the levels of UDP-MurNac-pentapeptide are low, as this precursor is readily consumed for peptidoglycan biosynthesis during bacterial growth. In stationary phase, when PGN biosynthesis is slowed down, UDP-MurNac-pentapeptide levels increase dramatically, since the membrane-located steps of PGN biosynthesis are rate limiting (Lara et al., 2005). We have recently identified a salvage pathway for MurNac that bypasses *de novo* biosynthesis of the PGN precursor UDP-MurNac (Gisin et al., 2013; Borisova et al., 2014, 2017; Renner-Schneck et al., 2015). This pathway presumably is present in many Gram-negative bacteria, including *T. forsythia* and other members of the Bacteroidetes phylum. Interference with this pathway in *Pseudomonas* sp. leads to increased susceptibility to the antibiotic fosfomycin in pathogens harboring the target enzyme MurA (Gisin et al., 2013; Borisova et al., 2014). However, as *T. forsythia* lacks MurA, inhibition of the MurNac salvage route will likely block PGN biosynthesis in this organism. We are currently attempting to characterize the route from MurNac to the PGN biosynthesis, which represents a valuable target for the treatment of *T. forsythia*-associated periodontal diseases (Figure 7).

CONCLUSION

A new sugar kinase from the oral pathogen *T. forsythia* was characterized, showing narrow specificity for MurNac and an essential role in MurNac catabolism in this organism. Surprisingly, the kinase mutant revealed a growth benefit and less morphological perturbations under MurNac limitation conditions, indicating that a block in MurNac catabolism affects peptidoglycan biosynthesis. The detailed characterization of the MurNac kinase Tf_MurK and the $\Delta Tf_murK::erm$ mutant increases our understanding of the unique cell wall and amino sugar metabolism of the oral pathogen *T. forsythia* that may pave new routes for lead finding in the treatment of periodontitis.

REFERENCES

- Borisova, M., Gaupp, R., Duckworth, A., Schneider, A., Dalugge, D., Mühleck, M., et al. (2016). Peptidoglycan recycling in gram-positive bacteria is crucial for survival in stationary phase. *mBio* 7:e00923-16. doi: 10.1128/mBio.00923-16
- Borisova, M., Gisin, J., and Mayer, C. (2014). Blocking peptidoglycan recycling in *Pseudomonas aeruginosa* attenuates intrinsic resistance to fosfomycin. *Microb. Drug Resist.* 20, 231–237. doi: 10.1089/mdr.2014.0036
- Borisova, M., Gisin, J., and Mayer, C. (2017). The N-acetylmuramic acid 6-phosphate phosphatase MupP completes the *Pseudomonas* peptidoglycan recycling pathway leading to intrinsic fosfomycin resistance. *mBio* 8:e00092-17. doi: 10.1128/mBio.00092-17
- Borisova, M., and Mayer, C. (2017). Analysis of N-acetylmuramic acid-6-phosphate (MurNac-6P) Accumulation by HPLC-MS. *Bio Protoc.* 7:e2420. doi: 10.21769/BioProtoc.2420
- Calvert, M. B., Mayer, C., and Titz, A. (2017). An efficient synthesis of 1,6-anhydro-N-acetylmuramic acid from N-acetylglucosamine. *Beilstein J. Org. Chem.* 13, 2631–2636. doi: 10.3762/bjoc.13.261

AUTHOR CONTRIBUTIONS

IH cloned rTf_MurK, biochemically characterized the enzyme, and conducted kinetic experiments by coupled enzymatic and HPLC-MS assays. IH analyzed the accumulation of metabolites by HPLC-MS. MT constructed and confirmed the $\Delta Tf_murK::erm$ mutant. VM and VF conducted growth experiments with *T. forsythia* strains and VM conducted the SEM experiments with help of VF and prepared cells for accumulation studies. MC and AT synthesized substrates for the kinetic studies. CS and CM formulated the original problem and provided guidance throughout the study. IH and CM designed the experiments and developed methodology. IH, CS, and CM wrote the manuscript. CM resolved final approval of the version to be published.

FUNDING

This work was supported by the German Research Foundation (DFG), project MA2436/7-1 and the research training group GRK1708 (both to CM), by the Austrian Science Fund FWF, projects P24317-B22 and I2875-B22 (to CS), and the FWF Doctoral Program “Biomolecular Technology of Proteins” W1224.

ACKNOWLEDGMENTS

The authors thank Marina Borisova for technical support and help with experimental planning.

SUPPLEMENTARY MATERIAL

The Supplementary Material for this article can be found online at: <https://www.frontiersin.org/articles/10.3389/fmicb.2018.00019/full#supplementary-material>

- Cheng, H. R., and Jiang, N. (2006). Extremely rapid extraction of DNA from bacteria and yeasts. *Biotechnol. Lett.* 28, 55–59. doi: 10.1007/s10529-005-4688-z
- Dahl, U., Jaeger, T., Nguyen, B. T., Sattler, J. M., and Mayer, C. (2004). Identification of a phosphotransferase system of *Escherichia coli* required for growth on N-acetylmuramic acid. *J. Bacteriol.* 186, 2385–2392. doi: 10.1128/JB.186.8.2385-2392.2004
- Eisenthal, R., Danson, M. J., and Hough, D. W. (2007). Catalytic efficiency and k_{cat}/K_M : a useful comparator? *Trends Biotechnol.* 25, 247–249. doi: 10.1016/j.tibtech.2007.03.010
- Friedrich, V., Pabinger, S., Chen, T., Messner, P., Dewhurst, F. E., and Schäffer, C. (2015). Draft genome sequence of *Tannerella forsythia* type strain ATCC 43037. *Genome Announc.* 3:e00660-15. doi: 10.1128/genomeA.00660-15
- Gisin, J., Schneider, A., Nagele, B., Borisova, M., and Mayer, C. (2013). A cell wall recycling shortcut that bypasses peptidoglycan *de novo* biosynthesis. *Nat. Chem. Biol.* 9, 491–493. doi: 10.1038/nchembio.1289
- Hadi, T., Dahl, U., Mayer, C., and Tanner, M. E. (2008). Mechanistic studies on N-acetylmuramic acid 6-phosphate hydrolase (MurQ): an etherase involved in peptidoglycan recycling. *Biochemistry* 47, 11547–11558. doi: 10.1021/bi8014532

- Hajishengallis, G., and Lamont, R. J. (2012). Beyond the red complex and into more complexity: the polymicrobial synergy and dysbiosis (PSD) model of periodontal disease etiology. *Mol. Oral Microbiol.* 27, 409–419. doi: 10.1111/j.2041-1014.2012.00663.x
- Holt, S. C., and Ebersole, J. L. (2005). *Porphyromonas gingivalis*, *Treponema denticola*, and *Tannerella forsythia*: the "red complex", a prototype polybacterial pathogenic consortium in periodontitis. *Periodontol.* 2000 38, 72–122. doi: 10.1111/j.1600-0757.2005.00113.x
- Höltje, J. V. (1998). Growth of the stress-bearing and shape-maintaining murein sacculus of *Escherichia coli*. *Microbiol. Mol. Biol. Rev.* 62, 181–203.
- Jaeger, T., Arsic, M., and Mayer, C. (2005). Scission of the lactyl ether bond of *N*-acetylmuramic acid by *Escherichia coli* "etherase". *J. Biol. Chem.* 280, 30100–30106. doi: 10.1074/jbc.M502208200
- Jaeger, T., and Mayer, C. (2008). *N*-acetylmuramic acid 6-phosphate lyases (MurNac etherases): role in cell wall metabolism, distribution, structure, and mechanism. *Cell. Mol. Life Sci.* 65, 928–939. doi: 10.1007/s00018-007-7399-x
- Laemmli, U. K. (1970). Cleavage of structural proteins during the assembly of the head of bacteriophage T4. *Nature* 227, 680–685. doi: 10.1038/227680a0
- Lara, B., Mengin-Lecreulx, D., Ayala, J. A., and Van Heijenoort, J. (2005). Peptidoglycan precursor pools associated with MraY and FtsW deficiencies or antibiotic treatments. *FEMS Microbiol. Lett.* 250, 195–200. doi: 10.1016/j.femsle.2005.07.005
- Mengin-Lecreulx, D., Flouret, B., and Van Heijenoort, J. (1982). Cytoplasmic steps of peptidoglycan synthesis in *Escherichia coli*. *J. Bacteriol.* 151, 1109–1117.
- Reed, M. C., Lieb, A., and Nijhout, H. F. (2010). The biological significance of substrate inhibition: a mechanism with diverse functions. *Bioessays* 32, 422–429. doi: 10.1002/bies.200900167
- Reith, J., Berking, A., and Mayer, C. (2011). Characterization of an *N*-acetylmuramic acid/*N*-acetylglucosamine kinase of *Clostridium acetobutylicum*. *J. Bacteriol.* 193, 5386–5392. doi: 10.1128/JB.05514-11
- Renner-Schneck, M., Hinderberger, I., Gisin, J., Exner, T., Mayer, C., and Stehle, T. (2015). Crystal structure of the *N*-acetylmuramic acid alpha-1-phosphate (MurNac-alpha1-P) uridylyltransferase MurU, a minimal sugar nucleotidyltransferase and potential drug target enzyme in Gram-negative pathogens. *J. Biol. Chem.* 290, 10804–10813. doi: 10.1074/jbc.M114.620989
- Ruscitto, A., Honma, K., Veeramachineni, V. M., Nishikawa, K., Stafford, G. P., and Sharma, A. (2017). Regulation and molecular basis of environmental muropeptide uptake and utilization in fastidious oral anaerobe *Tannerella forsythia*. *Front. Microbiol.* 8:648. doi: 10.3389/fmicb.2017.00648
- Ruscitto, A., Hottmann, I., Stafford, G. P., Schaffer, C., Mayer, C., and Sharma, A. (2016). Identification of a novel *N*-acetylmuramic acid transporter in *Tannerella forsythia*. *J. Bacteriol.* 198, 3119–3125. doi: 10.1128/JB.00473-16
- Tanner, A. C. R., and Izard, J. (2006). *Tannerella forsythia*, a periodontal pathogen entering the genomic era. *Periodontol.* 2000 42, 88–113. doi: 10.1111/j.1600-0757.2006.00184.x
- Tanner, A. C. R., Listgarten, M. A., Ebersole, J. L., and Strezempko, M. N. (1986). *Bacteroides forsythus* sp. nov, a slow-growing, fusiform *Bacteroides* sp. from the human oral cavity. *Int. J. Syst. Bacteriol.* 36, 213–221. doi: 10.1099/00207713-36-2-213
- Tomek, M. B., Janesch, B., Maresch, D., Windwarder, M., Altmann, F., Messner, P., et al. (2017). A pseudaminic acid or a legionaminic acid derivative transferase is strain-specifically implicated in the general protein O-glycosylation system of the periodontal pathogen *Tannerella forsythia*. *Glycobiology* 27, 555–567. doi: 10.1093/glycob/cwx019
- Tomek, M. B., Neumann, L., Nimeth, I., Koerdt, A., Andesner, P., Messner, P., et al. (2014). The S-layer proteins of *Tannerella forsythia* are secreted via a type IX secretion system that is decoupled from protein O-glycosylation. *Mol. Oral Microbiol.* 29, 307–320. doi: 10.1111/omi.12062
- Typas, A., Banzhaf, M., Gross, C. A., and Vollmer, W. (2012). From the regulation of peptidoglycan synthesis to bacterial growth and morphology. *Nat. Rev. Microbiol.* 10, 123–136. doi: 10.1038/nrmicro2677
- Unsleber, S., Borisova, M., and Mayer, C. (2017). Enzymatic synthesis and semi-preparative isolation of *N*-acetylmuramic acid 6-phosphate. *Carbohydr. Res.* 445, 98–103. doi: 10.1016/j.carres.2017.04.005
- Wyss, C. (1989). Dependence of proliferation of *Bacteroides forsythus* on exogenous *N*-acetylmuramic acid. *Infect. Immun.* 57, 1757–1759.
- Yoshino, M., and Murakami, K. (2015). Analysis of the substrate inhibition of complete and partial types. *Springerplus* 4:292. doi: 10.1186/s40064-015-1082-8
- Young, K. D. (2003). Bacterial shape. *Mol. Microbiol.* 49, 571–580. doi: 10.1046/j.1365-2958.2003.03607.x

Conflict of Interest Statement: The authors declare that the research was conducted in the absence of any commercial or financial relationships that could be construed as a potential conflict of interest.

Copyright © 2018 Hottmann, Mayer, Tomek, Friedrich, Calvert, Titz, Schäffer and Mayer. This is an open-access article distributed under the terms of the Creative Commons Attribution License (CC BY). The use, distribution or reproduction in other forums is permitted, provided the original author(s) and the copyright owner are credited and that the original publication in this journal is cited, in accordance with accepted academic practice. No use, distribution or reproduction is permitted which does not comply with these terms.



Atomic Force Microscopy of Side Wall and Septa Peptidoglycan From *Bacillus subtilis* Reveals an Architectural Remodeling During Growth

Kang Li¹, Xiao-Xue Yuan¹, He-Min Sun¹, Long-Sheng Zhao¹, Ruocong Tang¹, Zhi-Hua Chen¹, Qi-Long Qin¹, Xiu-Lan Chen¹, Yu-Zhong Zhang^{1,2,3} and Hai-Nan Su^{1,3*}

¹ State Key Laboratory of Microbial Technology, Marine Biotechnology Research Center, Shandong University, Jinan, China,

² Laboratory for Marine Biology and Biotechnology, Qingdao National Laboratory for Marine Science and Technology, Qingdao, China, ³ College of Marine Life Sciences, Ocean University of China, Qingdao, China

OPEN ACCESS

Edited by:

Stephane Mesnage,
University of Sheffield,
United Kingdom

Reviewed by:

Etienne Dague,
Centre National de la Recherche
Scientifique (CNRS), France
Emma Joanne Hayhurst,
University of South Wales,
United Kingdom

*Correspondence:

Hai-Nan Su
suhn@sdu.edu.cn

Specialty section:

This article was submitted to
Microbial Physiology and Metabolism,
a section of the journal
Frontiers in Microbiology

Received: 13 December 2017

Accepted: 16 March 2018

Published: 29 March 2018

Citation:

Li K, Yuan X-X, Sun H-M, Zhao L-S,
Tang R, Chen Z-H, Qin Q-L,
Chen X-L, Zhang Y-Z and Su H-N
(2018) Atomic Force Microscopy
of Side Wall and Septa Peptidoglycan
From *Bacillus subtilis* Reveals an
Architectural Remodeling During
Growth. *Front. Microbiol.* 9:620.
doi: 10.3389/fmicb.2018.00620

Peptidoglycan is the fundamental structural constituent of the bacterial cell wall. Despite many years of research, the architecture of peptidoglycan is still largely elusive. Here, we report the high-resolution architecture of peptidoglycan from the model Gram-positive bacterium *Bacillus subtilis*. We provide high-resolution evidence of peptidoglycan architecture remodeling at different growth stages. Side wall peptidoglycan from *B. subtilis* strain AS1.398 changed from an irregular architecture in exponential growth phase to an ordered cable-like architecture in stationary phase. Thickness of side wall peptidoglycan was found to be related with growth stages, with a slight increase after transition to stationary phase. Septal disks were synthesized progressively toward the center, while the surface features were less clear than those imaged with side walls. Compared with previous studies, our results revealed slight differences in architecture of peptidoglycan from different *B. subtilis* strains, expanding our knowledge about the architectural features of *B. subtilis* peptidoglycan.

Keywords: cell wall, peptidoglycan, structure, remodeling, atomic force microscopy

INTRODUCTION

Peptidoglycan is the major constituent of bacterial cell wall, and it is essential for bacteria to maintain their specific shape and to protect the cells from rupture by the internal turgor pressure (Typas et al., 2012). Moreover, peptidoglycan is important because it is the target of many antibiotics (Bugg et al., 2011). Elucidating the structure of peptidoglycan is a basic objective for microbiological research, but despite decades of work, the architecture of peptidoglycan is still not fully understood (Vollmer and Seligman, 2010; Turner et al., 2014). Although the chemical composition of peptidoglycan is well-characterized, the peptidoglycan architecture and their dynamics during growth and division are largely elusive. Several peptidoglycan models such as layered model and scaffold model have been proposed (Dmitriev et al., 2003; Gan et al., 2008). But direct observation of peptidoglycan architecture has been poorly documented so far.

Atomic force microscopy (AFM) is a powerful technique that allows direct observation of the surface structure of biological samples with high-resolution (Dufrêne, 2008, 2014; Müller and Dufrêne, 2011), and a series of surprising discoveries about the architecture of peptidoglycan from

both isolated sacculi and living bacterial cells based on AFM works were reported during the past decade (Hayhurst et al., 2008; Andre et al., 2010; Turner et al., 2010, 2013; Wheeler et al., 2011; Dover et al., 2015). One of the breakthroughs was the first high-resolution architecture analysis of isolated sacculi from the rod-shaped bacterium *Bacillus subtilis* by direct observation with AFM in Hayhurst et al. (2008). The side wall peptidoglycan was reported to be organized into a regular structure of 50-nm wide “cables” with cross striations running across the short axis of the cells (Hayhurst et al., 2008). A coiled-coil model for peptidoglycan architecture was proposed based on AFM observations (Hayhurst et al., 2008). However, despite extensive researches, arguments about the peptidoglycan architecture remained. For example, studies with electron cryotomography suggested that glycan strands in Gram-positive cell walls run circumferentially around the cells (Beeby et al., 2013).

Peptidoglycan composition is known to change during growth. Both glycan chain length and crosslinkage are changing during the transition from exponential to stationary phase (Fordham and Gilvarg, 1974; Atrih et al., 1999; Typas et al., 2012). Bacteria can release D-amino acids into growth medium where they accumulate to millimolar concentrations in stationary phase (Lam et al., 2009). These D-amino acids can be incorporated into peptidoglycan and govern peptidoglycan remodeling in stationary phase (Lam et al., 2009). However, it remains unknown if peptidoglycan architecture changes depending on the growth phase.

Septa (or cross walls), which are formed between two bacterial daughter cells, are critical wall structures responsible for the bacterial division. A recent work showed that muropeptides with unprocessed stem peptides were accumulated in peptidoglycan at septa sites from *B. subtilis*, indicating a possible local difference in chemical composition between septa and side walls (Angeles et al., 2017). AFM studies on isolated sacculi pieces from *B. subtilis* showed that septal peptidoglycan was organized into ~135-nm-wide “cable” like structures forming a spiral appearance toward the center (Hayhurst et al., 2008). However, no information on septal architecture in exponential and stationary phase is available.

In this report, peptidoglycan from *B. subtilis* strain AS1.398 was isolated and analyzed by high-resolution AFM. The results revealed the spatial organizations of side wall peptidoglycan and septa at a nanometer scale, suggesting the structural remodeling of the peptidoglycan during growth. Compared with previous studies, our results revealed slight structural differences in spatial organizations of peptidoglycan from different *B. subtilis* strains. This work expanded our current knowledge and provided new information about peptidoglycan architecture.

MATERIALS AND METHODS

Bacterial Strain and Growth Condition

Bacterial growth was monitored by measuring the optical density at 600 nm (OD₆₀₀) with a UV/VIS-550 spectrophotometer (Jasco, Japan). *B. subtilis* strain AS1.398 from a single colony was grown Luria-Bertani (LB) broth at 25°C overnight with

shaking at 180 rpm. Then bacterial culture was diluted with fresh LB broth to a volume of 200 mL to reach a starting cell density of approximately 0.02 at OD₆₀₀. The cell suspension was then incubated at 25°C with shaking at 180 rpm. The growth of the bacteria was monitored at OD₆₀₀ at different time points, with three replicates at each time point. *B. subtilis* cells grown to mid-exponential phase (OD₆₀₀ ≈ 1.2), late exponential phase (OD₆₀₀ ≈ 1.8), and stationary phase were collected for optical microscopic imaging. Optical microscopic images were taken with an OMV optical microscope (Bruker AXS, Germany) affiliated with atomic force microscopy (Bruker AXS, Germany).

Purification of Sacculi

According to growth curves, *B. subtilis* cells grown to mid-exponential phase, late exponential phase, and stationary phase were collected. Peptidoglycan was purified as described previously (Hayhurst et al., 2008). Briefly, cells were harvested, boiled (7 min), broken by ultrasonication (200~400w) or high pressure cell disrupter (Constant Systems, Ltd., United Kingdom). When isolating intact sacculi, the breakage step was not needed. Extraction was treated by boiling in SDS (5% w/v), RNase (0.5 mg/ml), DNase (0.5 mg/ml), and pronase (2 mg/ml) treatment. Removal of accessory polymers was achieved by incubation in 48% v/v HF at 4°C for 24 h. Purified sacculi were washed at least three times with MilliQ water at room temperature. Then the samples were diluted in MilliQ water and air dried onto freshly cleaved mica before AFM imaging. At least three replicates were performed in each isolation experiment.

AFM Operation

Atomic force microscopy imaging was carried out using a Multimode VIII AFM with Nanoscope V controller (Bruker AXS, Germany) equipped with an OMV optical microscope (Bruker AXS, Germany). All AFM imaging was carried out in scanasyst mode. Silicon cantilevers (XSC11/ALBS, MikroMash, Bulgaria) with a spring constant about 2.7 n/m were used for imaging in ambient conditions. Image processing and analysis were performed with AFM off-line software NanoScope Analysis (Bruker AXS, Germany).

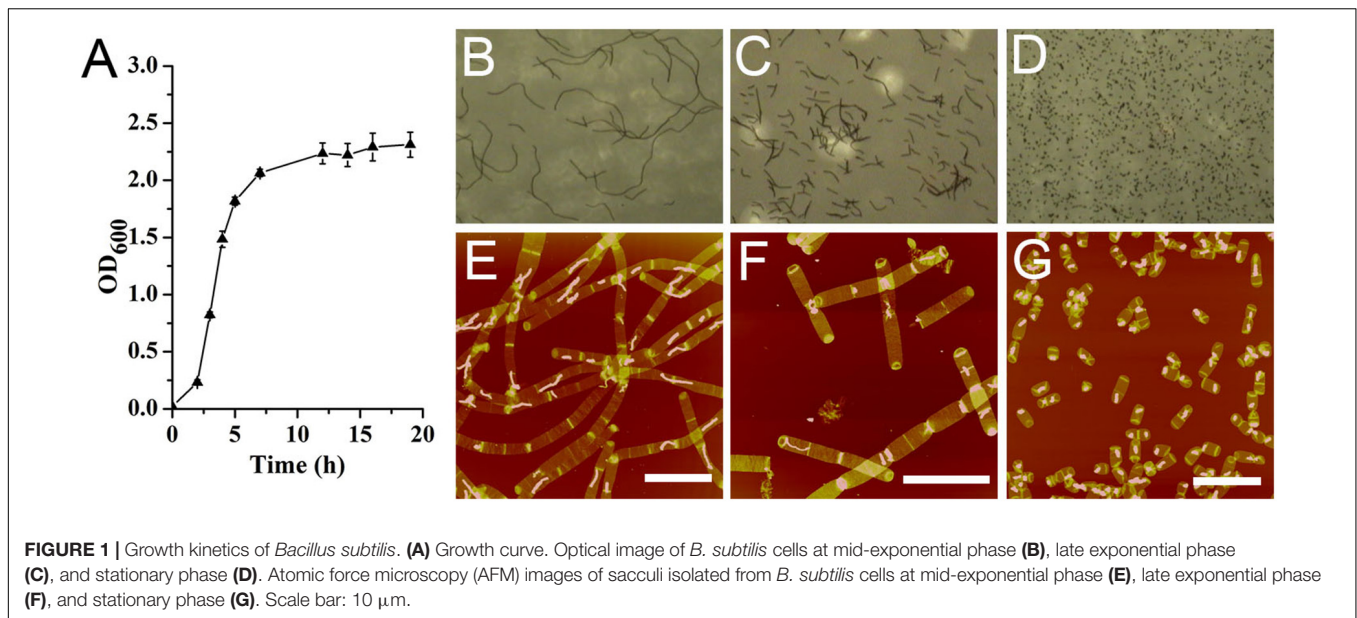
Statistical Analysis

Data are presented as the arithmetic mean ± standard deviation (SD). Statistical significance was evaluated using Student's *t*-test. *p*-Values less than 0.05 were considered statistically significant.

RESULTS

Growth Kinetics and Morphologies of Bacterial Cells

Bacillus subtilis exhibited a typical bacterial growth curve (Figure 1A). *B. subtilis* cells formed long filamentous chains which could be as long as 150 μm in mid-exponential phase observed with optical microscope (Figure 1B). In late exponential phase, the filamentous chains of *B. subtilis* cells were



much shorter than those in mid-exponential phase (Figure 1C). In stationary phase, only very short cells were observed (Figure 1D). Except for our *Bacillus* strain, some other *Bacillus* strains were known to be able to form long filamentous chains (Trick et al., 1984; Ajithkumar et al., 2002). It seemed that growth conditions could also influence the formation of filamentous chains in *Bacillus* species (Fan, 1970; Ferroni and Inniss, 1973).

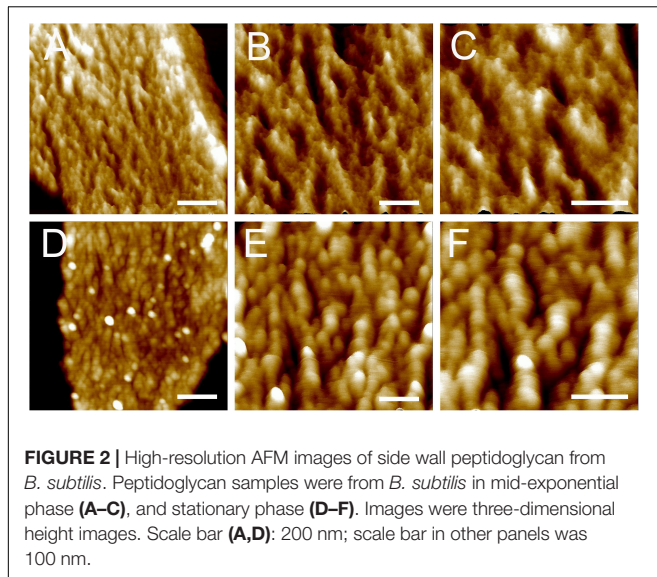
From observations of isolated intact sacculi of the bacterial cells at different growth stages, multiple septation sites could be noticed along the bacterial filamentous chains (Figures 1E,F). Therefore it seemed that the filamentous chains of *B. subtilis* were not formed by loosely associated cells, but fast growing cells with multiple septa yet to be divided. The average cell length in stationary phase was $2.72 \pm 0.63 \mu\text{m}$ (60 measurements from three replicates) (Figure 1G), while the measured average length between each adjacent septation sites was $3.78 \pm 1.28 \mu\text{m}$ in mid exponential cells (70 measurements in 15 bacterial filamentous chains from three replicates), which was longer than the average cell length in stationary phase ($p < 0.05$).

Structure of Side Wall Peptidoglycan

Thickness of isolated sacculi was measured in air by AFM. Samples from three independent replicates were used for measurements. The average thickness of single layered side wall peptidoglycan was $12.59 \pm 0.89 \text{ nm}$ ($n = 59$) in mid-exponential phase. This measured value was slightly larger than the measured thickness of side wall peptidoglycan in another *B. subtilis* strain in a previous report (Hayhurst et al., 2008), and the difference in the measured value might be due to the different strains used for experiments. The measured average thickness of single layered side wall peptidoglycan of our *B. subtilis* strain increased to $14.44 \pm 0.92 \text{ nm}$ ($n = 52$) in stationary phase, which was larger than that in mid-exponential phase ($p < 0.05$). This result indicates that the thickness of bacterial peptidoglycan might not be a fixed value, but varies during bacterial growth.

Broken sacculi from *B. subtilis* which exposed inner surface of the side wall peptidoglycan were imaged with AFM to check the surface features both the inner and outer surfaces. The inner surface of the side wall peptidoglycan exhibited a relatively rough surface feature, and the overall organization of inner-side peptidoglycan was largely parallel to the short axis of the cell (Supplementary Figure 1). However, the outer surface of sacculi was relatively featureless compared to the inner surface. It was suggested that hydrolysis of the peptidoglycan by endogenous autolysins might be one of the reasons that were responsible for such surface characteristics on outer side walls (Hayhurst et al., 2008). Our observations on the inner and outer side of the side wall peptidoglycan were in consistent with previous AFM observation (Hayhurst et al., 2008).

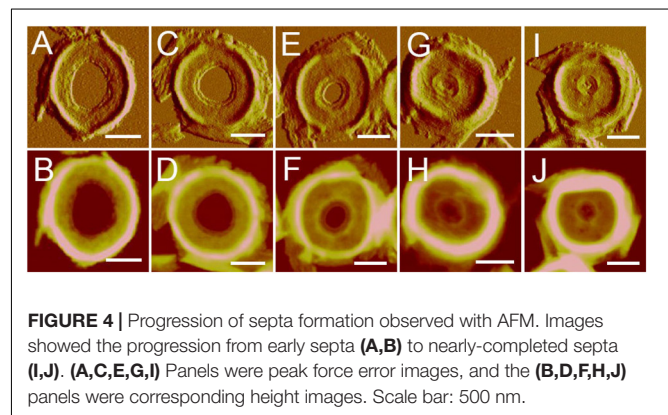
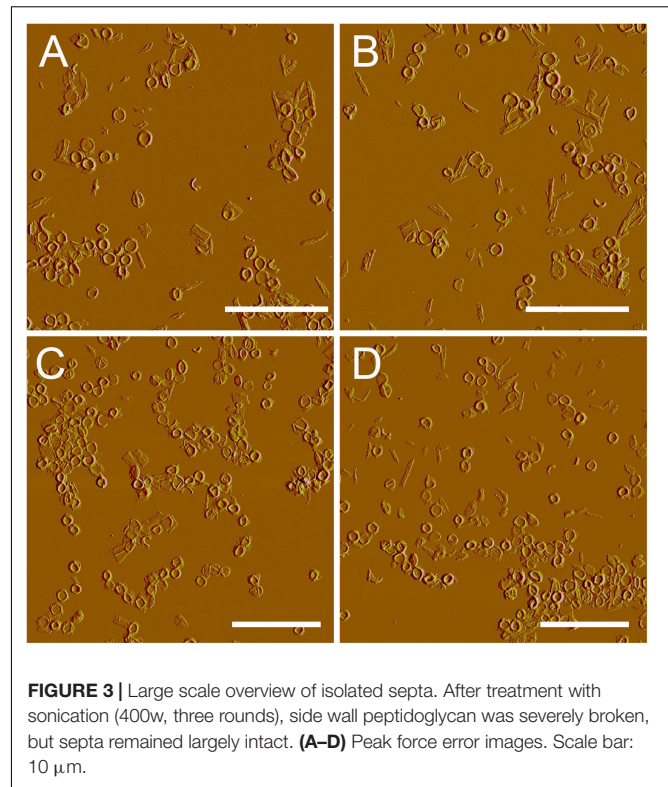
Next, the architecture of peptidoglycan on the inner surface of purified sacculi was imaged using high-resolution AFM. In stationary phase, the spatial organization of the peptidoglycan resembled the previously reported “cable-like” model (Hayhurst et al., 2008). These “cables” were densely packed together and roughly running in a parallel orientation (Figures 2D–F), and the result could be confirmed in each replicates. Small cables entangled into larger ones could sometimes be noticed. The average width of these “cables” was $29.11 \pm 5.79 \text{ nm}$ ($n = 32$), which was much smaller as compared to that in another *B. subtilis* strain in a previous report (Hayhurst et al., 2008). However, a structural difference was observed on side-wall peptidoglycans from *B. subtilis* in mid-exponential phase compared to that in stationary phase (Figures 2A–C). Peptidoglycan in mid-exponential phase seemed to be less ordered than in stationary phase, and it might be roughly characterized as a network like structure, with “ridge-and-groove” like appearances. These “ridge-and-groove” structures were largely parallel oriented. Small “ridges” were sometimes to be noticed to entangle into larger “ridges” (Figures 2A–C).



Structures of Septal Peptidoglycan

After treatment with high-power sonication, the isolated sacculi were broken into pieces. It was surprising to notice that most of the side wall peptidoglycan was broken into small pieces, while large amounts of intact septa-like structures were observed (Figure 3). A large number of peptidoglycan fragments corresponded to incomplete septa, appearing as annulus-like structures. Annulus-like structures with attached side wall peptidoglycans could usually be observed (Supplementary Figure 2), further confirming that they were incomplete septa. When more septa were checked, septa structures that represent all stages of formation through the progression from newly forming septa to complete septa could be observed (Figure 4). A thin interior leading edge could be noticed in incomplete septal disk. Except the interior leading edge, thicknesses at other parts of the septal disks were evenly distributed. A likely process was that a thin leading ring was formed at the interior edge and then thickened with the growth of the septa, until the septa were completely sealed (Figure 4). This result may provide some new hints of how septa were progressively formed.

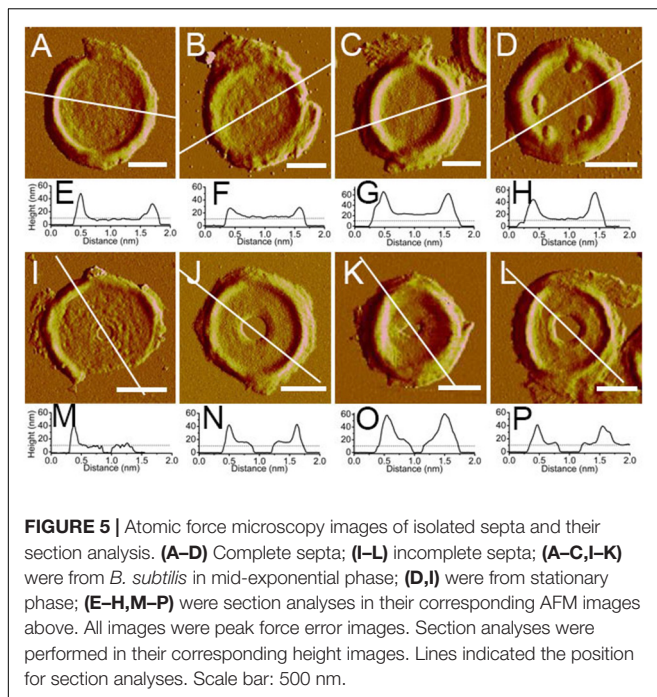
The thicknesses of complete and incomplete septa from cells at mid-exponential phase ($n = 48$) and stationary phase ($n = 45$) were measured. The thicknesses of most septa at both growth stages were between 11 and 16 nm. However, in exponential phase, small amount of septa with unusual thicknesses of less than 8 nm (5 out of 48) or as much as 20 nm (4 out of 48) could be found (Figure 5). Septa with different thicknesses could be noticed not only in complete septa but also in incomplete septa, indicating that formation of different thicknesses was determined before the septa were complete. Unlike the possible spiral cable-like structure of the septa in previous report (Hayhurst et al., 2008), the surfaces of most septal disks isolated from our *B. subtilis* strain were relatively smooth, with no obvious supramolecular structural organizations as in side walls. However, only in some case, “cables” like organizations



with ~ 35 nm ($n = 7$) width forming concentric rings toward the center were observed on septa with thin thickness (~ 8 nm) (Supplementary Figure 3). The width of the “cables” in our strain was much smaller than that in the other strain in previous report (Hayhurst et al., 2008).

DISCUSSION

Bacterial peptidoglycan plays important roles in various biological processes (de Pedro and Cava, 2015). The peptidoglycan of Gram-positive bacteria is significantly thicker and more complex than the peptidoglycan of Gram-negative bacteria, and the three dimensional architectures of Gram-positive peptidoglycan was largely unclear in the past.



Application of novel high-resolution techniques such as AFM in recent years revealed the surface architecture of bacterial peptidoglycan (Turner et al., 2014). To date, the only previous AFM work to study the architecture of isolated sacculi from model Gram-positive rod bacterium *B. subtilis* was reported by Hayhurst et al. (2008). They found that the peptidoglycan in the inner surface of the sacculi was organized into a regular structure of 50-nm wide “cables” (Hayhurst et al., 2008). We found that the inner surface of side wall peptidoglycan from *B. subtilis* in stationary phase exhibited a “cable” like structure, quite similar to the previous observation (Hayhurst et al., 2008). However, the average width of the “cables” was about 29 nm, which was much smaller than that in the other *B. subtilis* strain in previous report (Hayhurst et al., 2008). This result suggests the existence of differences in peptidoglycan architectures from different *Bacillus* strains.

A coiled-coil model was proposed based on previous AFM observations about the side wall peptidoglycan from *B. subtilis* (Hayhurst et al., 2008). However, this model was argued because the peptidoglycan from *B. subtilis* seemed to be a uniformly dense layer observed with electron cryo-tomography (Beeby et al., 2013) or electron cryo-microscopy (Matias and Beveridge, 2005). Our work confirmed that the “cable” like structure in side wall peptidoglycan from *B. subtilis* exists. Work is still needed in the future to reconcile the observations by different techniques.

Our high-resolution AFM images showed that there were slight differences in architecture of side wall peptidoglycan from different growth stages. In mid-exponential phase, the side wall peptidoglycan was organized into a “ridge-and-groove” like structure, which differed from the “cable” like structure in side wall peptidoglycan from stationary phase. Moreover, the thicknesses of side-wall peptidoglycan slightly increased

from exponential phase to stationary phase. This variation in thicknesses might be related to the architectural changes in side walls. It has been known that bacterial peptidoglycan undergoes a remodeling process during different growth stage, both in Gram-positive and Gram-negative bacteria (Typas et al., 2012). In stationary phase, the crosslinks in peptidoglycan from *B. subtilis* were found to increase (Atrih et al., 1999). The peptidoglycan remodeling in bacteria at stationary phase was known to be governed by D-amino acids (Lam et al., 2009). Our work on the architecture of peptidoglycan from *B. subtilis* at different growth stages might reflect a remodeling of spatial organization in peptidoglycan structures.

The septum is an important structure that is responsible for the division in Gram-positive bacteria (Wu and Errington, 2011). In our work, we found that when treated with high-power sonication, side wall peptidoglycan was mostly broken into small pieces, leaving large amounts of intact septa. Previous research indicated that the circumferential stress in bacterial cells was greater than the longitudinal stress (Yao et al., 1999), and therefore it is likely that the general mechanics of stress in rod shaped cells are the possible reason for the side wall splitting while the septa remains largely intact. Another possible explanation that could not be fully excluded was that there might be difference in rigidity between side walls and septa. A recent work showed that local differences in the chemical composition of peptidoglycan between septa and side walls existed in *B. subtilis* (Angeles et al., 2017). However, whether local differences in chemical composition would result in different rigidity, or whether the septa might be truly more rigid than side wall peptidoglycan is unknown and awaits further analysis.

Previous AFM work suggested that the septal disk had up to three cables across their radius forming a spiral like structure toward the center (Hayhurst et al., 2008). However, results with the *B. subtilis* strain in this report showed that the septal disk of most observed septa were relatively smooth, with no obvious surface features. Apart from the surface features of septa, there were slight differences in the thicknesses and spatial organization of side wall peptidoglycan between the *B. subtilis* strain in previous report (Hayhurst et al., 2008) and the strain we used. Therefore, we consider that the differences in the surface features of septal disks might result from different bacterial strains used.

AUTHOR CONTRIBUTIONS

H-NS, Y-ZZ, and X-LC conceived and designed the experiments. KL, X-XY, H-MS, L-SZ, RT, Z-HC, and H-NS performed the experiments. H-NS and Q-LQ analyzed the data. H-NS wrote the paper. All authors read and approved the finalized manuscript.

FUNDING

This work was supported by the National Natural Science Foundation of China (31570066, U1706207, 41376153,

31670038), the AoShan Talents Cultivation Program supported by Qingdao National Laboratory for Marine Science and Technology (2017ASTCP-OS14), the Program of Shandong for Taishan Scholars (2009TS079), and the Young Scholars Program of Shandong University (2017WLJH22, 2016WLJH36).

REFERENCES

- Ajithkumar, V. P., Ajithkumar, B., Iriye, R., and Sakai, T. (2002). *Bacillus funiculus* sp. nov., novel filamentous isolates from activated sludge. *Int. J. Syst. Evol. Microbiol.* 52, 1141–1144.
- Andre, G., Kulakauskas, S., Chapot-Chartier, M.-P., Navet, B., Deghorain, M., Bernard, E., et al. (2010). Imaging the nanoscale organization of peptidoglycan in living *Lactococcus lactis* cells. *Nat. Commun.* 1:27. doi: 10.1038/ncomms1027
- Angeles, D. M., Liu, Y., Hartman, A. M., Borisova, M., Borges, A. D. S., Kok, N. D., et al. (2017). Pentapeptide-rich peptidoglycan at the *Bacillus subtilis* cell-division site. *Mol. Microbiol.* 104, 319–333. doi: 10.1111/mmi.13629
- Atrih, A., Bacher, G., Allmaier, G., Williamson, M. P., and Foster, S. J. (1999). Analysis of peptidoglycan structure from vegetative cells of *Bacillus subtilis* 168 and role of PBP 5 in peptidoglycan maturation. *J. Bacteriol.* 181, 3956–3966.
- Beeby, M., Gumbart, J. C., Roux, B., and Jensen, G. J. (2013). Architecture and assembly of the Gram-positive cell wall. *Mol. Microbiol.* 88, 664–672. doi: 10.1111/mmi.12203
- Bugg, T. D. H., Braddick, D., Dowson, C. G., and Roper, D. I. (2011). Bacterial cell wall assembly: still an attractive antibacterial target. *Trends Biotechnol.* 29, 167–173. doi: 10.1016/j.tibtech.2010.12.006
- de Pedro, M. A., and Cava, F. (2015). Structural constraints and dynamics of bacterial cell wall architecture. *Front. Microbiol.* 6:449. doi: 10.3389/fmicb.2015.00449
- Dmitriev, B. A., Toukach, F. V., Schaper, K.-J., Holst, O., Rietschel, E. T., and Ehlers, S. (2003). Tertiary structure of bacterial murein: the scaffold model. *J. Bacteriol.* 185, 3458–3468. doi: 10.1128/JB.185.11.3458-3468.2003
- Dover, R. S., Bitler, A., Shimon, E., Trieu-Cuot, P., and Shai, Y. (2015). Multiparametric AFM reveals turgor-responsive net-like peptidoglycan architecture in live streptococci. *Nat. Commun.* 6:7193. doi: 10.1038/ncomms8193
- Dufrène, Y. F. (2008). Towards nanomicrobiology using atomic force microscopy. *Nat. Rev. Microbiol.* 6, 674–680. doi: 10.1038/nrmicro1948
- Dufrène, Y. F. (2014). Atomic force microscopy in microbiology: new structural and functional insights into the microbial cell surface. *mBio* 5:e01363-14. doi: 10.1128/mBio.01363-14
- Fan, D. P. (1970). Autolysin(s) of *Bacillus subtilis* as dechaining enzyme. *J. Bacteriol.* 103, 494–499.
- Ferroni, G. D., and Inniss, W. E. (1973). Thermally caused filament formation in the psychrophile *Bacillus insolitus*. *Can. J. Microbiol.* 19, 581–584. doi: 10.1139/m73-095
- Fordham, W. D., and Gilvarg, C. (1974). Kinetics of cross-linking of peptidoglycan in *Bacillus megaterium*. *J. Biol. Chem.* 249, 2478–2482.
- Gan, L., Chen, S., and Jensen, G. J. (2008). Molecular organization of Gram-negative peptidoglycan. *Proc. Natl. Acad. Sci. U.S.A.* 105, 18953–18957. doi: 10.1073/pnas.0808035105
- Hayhurst, E. J., Kailas, L., Hobbs, J. K., and Foster, S. J. (2008). Cell wall peptidoglycan architecture in *Bacillus subtilis*. *Proc. Natl. Acad. Sci. U.S.A.* 105, 14600–14605. doi: 10.1073/pnas.0804138105
- Lam, H., Oh, D.-C., Cava, F., Takacs, C. N., Clardy, J., Pedro, M. A. D., et al. (2009). D-amino acids govern stationary phase cell wall re-modeling in bacteria. *Science* 325, 1552–1555. doi: 10.1126/science.1178123
- Matias, V. R. F., and Beveridge, T. J. (2005). Cryo-electron microscopy reveals native polymeric cell wall structure in *Bacillus subtilis* 168 and the existence of a periplasmic space. *Mol. Microbiol.* 56, 240–251. doi: 10.1111/j.1365-2958.2005.04535.x
- Müller, D. J., and Dufrène, Y. F. (2011). Atomic force microscopy: a nanoscopic window on the cell surface. *Trends Cell Biol.* 21, 461–469. doi: 10.1016/j.tcb.2011.04.008
- Trick, I., Salcher, O., and Lingens, F. (1984). Characterization of filament forming *Bacillus* strains isolated from bulking sludge. *Appl. Microbiol. Biotechnol.* 19, 120–124. doi: 10.1007/BF00302452
- Turner, R. D., Hurd, A. F., Cadby, A., Hobbs, J. K., and Foster, S. J. (2013). Cell wall elongation mode in Gram-negative bacteria is determined by peptidoglycan architecture. *Nat. Commun.* 4:1496. doi: 10.1038/ncomms2503
- Turner, R. D., Ratcliffe, E. C., Wheeler, R., Golestanian, R., Hobbs, J. K., and Foster, S. J. (2010). Peptidoglycan architecture can specify division planes in *Staphylococcus aureus*. *Nat. Commun.* 1:26. doi: 10.1038/ncomms1025
- Turner, R. D., Vollmer, W., and Foster, S. J. (2014). Different walls for rods and balls: the diversity of peptidoglycan. *Mol. Microbiol.* 91, 862–874. doi: 10.1111/mmi.12513
- Typas, A., Banzhaf, M., Gross, C. A., and Vollmer, W. (2012). From the regulation of peptidoglycan synthesis to bacterial growth and morphology. *Nat. Rev. Microbiol.* 10, 123–136. doi: 10.1038/nrmicro2677
- Vollmer, W., and Seligman, S. J. (2010). Architecture of peptidoglycan: more data and more models. *Trends Microbiol.* 18, 59–66. doi: 10.1016/j.tim.2009.12.004
- Wheeler, R., Mesnage, S., Boneca, I. G., Hobbs, J. K., and Foster, S. J. (2011). Super-resolution microscopy reveals cell wall dynamics and peptidoglycan architecture in ovococcal bacteria. *Mol. Microbiol.* 82, 1096–1109. doi: 10.1111/j.1365-2958.2011.07871.x
- Wu, L. J., and Errington, J. (2011). Nucleoid occlusion and bacterial cell division. *Nat. Rev. Microbiol.* 10, 8–12. doi: 10.1038/nrmicro2671
- Yao, X., Jericho, M., Pink, D., and Beveridge, T. (1999). Thickness and elasticity of gram-negative murein sacculi measured by atomic force microscopy. *J. Bacteriol.* 181, 6865–6875.

SUPPLEMENTARY MATERIAL

The Supplementary Material for this article can be found online at: <https://www.frontiersin.org/articles/10.3389/fmicb.2018.00620/full#supplementary-material>

Conflict of Interest Statement: The authors declare that the research was conducted in the absence of any commercial or financial relationships that could be construed as a potential conflict of interest.

Copyright © 2018 Li, Yuan, Sun, Zhao, Tang, Chen, Qin, Chen, Zhang and Su. This is an open-access article distributed under the terms of the Creative Commons Attribution License (CC BY). The use, distribution or reproduction in other forums is permitted, provided the original author(s) and the copyright owner are credited and that the original publication in this journal is cited, in accordance with accepted academic practice. No use, distribution or reproduction is permitted which does not comply with these terms.



The Mycobacterial Cell Envelope: A Relict From the Past or the Result of Recent Evolution?

Antony T. Vincent^{1,2}, Sammy Nyongesa¹, Isabelle Morneau³, Michael B. Reed^{2,4,5},
Elitza I. Tocheva³ and Frederic J. Veyrier^{1,2*}

¹ INRS-Institut Armand-Frappier, Bacterial Symbionts Evolution, Laval, QC, Canada, ² McGill International TB Centre, Montreal, QC, Canada, ³ Faculty of Dentistry, Université de Montréal, Montreal, QC, Canada, ⁴ Department of Medicine, McGill University, Montreal, QC, Canada, ⁵ Infectious Diseases and Immunity in Global Health Program, Research Institute of the McGill University Health Centre, Montreal, QC, Canada

OPEN ACCESS

Edited by:

Christoph Mayer,
Eberhard Karls Universität Tübingen,
Germany

Reviewed by:

Andreas Burkovski,
Friedrich-Alexander-Universität
Erlangen-Nürnberg, Germany
Patrick Joseph Moynihan,
University of Birmingham,
United Kingdom
Hesper Rego,
Yale School of Medicine,
United States

*Correspondence:

Frederic J. Veyrier
frederic.veyrier@iaf.inrs.ca

Specialty section:

This article was submitted to
Microbial Physiology and Metabolism,
a section of the journal
Frontiers in Microbiology

Received: 27 June 2018

Accepted: 12 September 2018

Published: 09 October 2018

Citation:

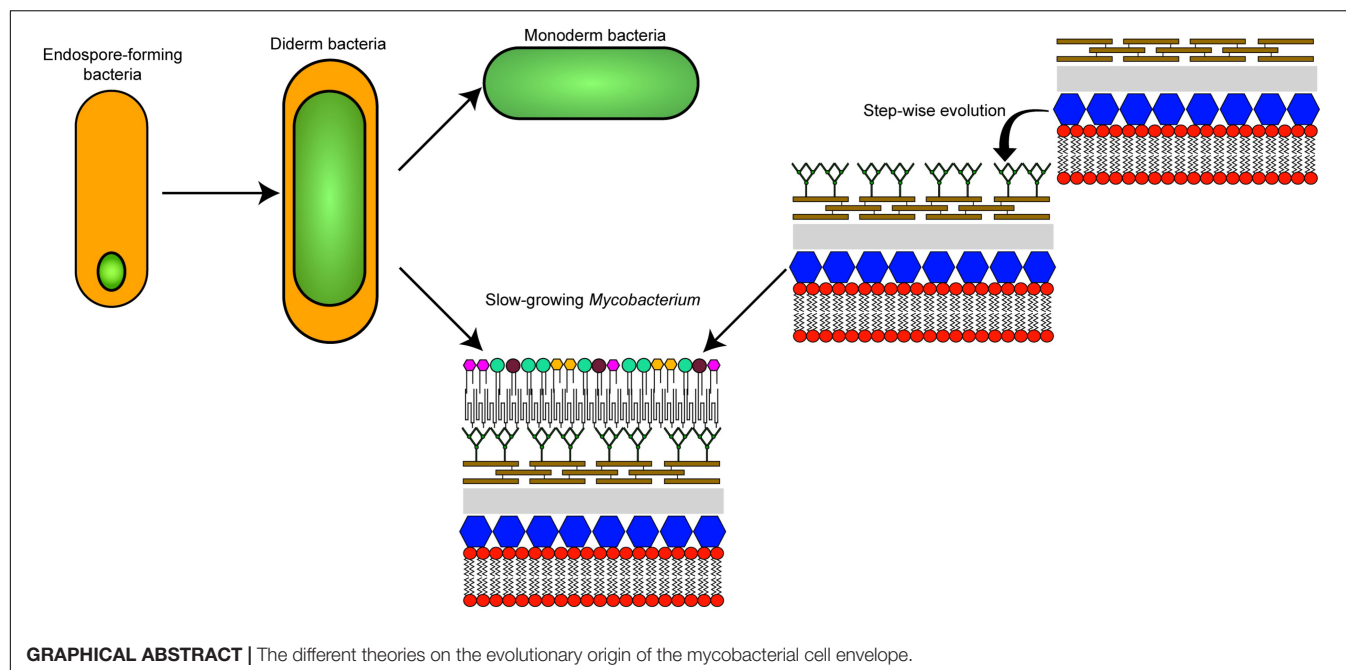
Vincent AT, Nyongesa S, Morneau I,
Reed MB, Tocheva EI and Veyrier FJ
(2018) The Mycobacterial Cell
Envelope: A Relict From the Past or
the Result of Recent Evolution?
Front. Microbiol. 9:2341.
doi: 10.3389/fmicb.2018.02341

Mycobacteria are well known for their taxonomic diversity, their impact on global health, and for their atypical cell wall and envelope. In addition to a cytoplasmic membrane and a peptidoglycan layer, the cell envelope of members of the order *Corynebacteriales*, which include *Mycobacterium tuberculosis*, also have an arabinogalactan layer connecting the peptidoglycan to an outer membrane, the so-called “mycomembrane.” This unusual cell envelope composition of mycobacteria is of prime importance for several physiological processes such as protection from external stresses and for virulence. Although there have been recent breakthroughs in the elucidation of the composition and organization of this cell envelope, its evolutionary origin remains a mystery. In this perspectives article, the characteristics of the cell envelope of mycobacteria with respect to other actinobacteria will be dissected through a molecular evolution framework in order to provide a panoramic view of the evolutionary pathways that appear to be at the origin of this unique cell envelope. In combination with a robust molecular phylogeny, we have assembled a gene matrix based on the presence or absence of key determinants of cell envelope biogenesis in the *Actinobacteria* phylum. We present several evolutionary scenarios regarding the origin of the mycomembrane. In light of the data presented here, we also propose a novel alternative hypothesis whereby the stepwise acquisition of core enzymatic functions may have allowed the sequential remodeling of the external cell membrane during the evolution of *Actinobacteria* and has led to the unique mycomembrane of slow-growing mycobacteria as we know it today.

Keywords: cell envelope, *Actinobacteria*, *Mycobacterium*, evolution, genomics

INTRODUCTION

The *Actinobacteria* phylum of Gram-positive bacteria forms an extremely diverse group that includes several species that have evolved specific symbioses (commensal or parasitic) with a wide range of hosts including numerous mammals. For example, certain species from the genera *Mycobacterium* and *Nocardia* are pathogenic while others, belonging to the genus *Bifidobacterium*, are part of the normal gut microbial flora and are known to have a beneficial and important effect on human health (Barka et al., 2016; O’Callaghan and van Sinderen, 2016). Several *Actinobacteria*

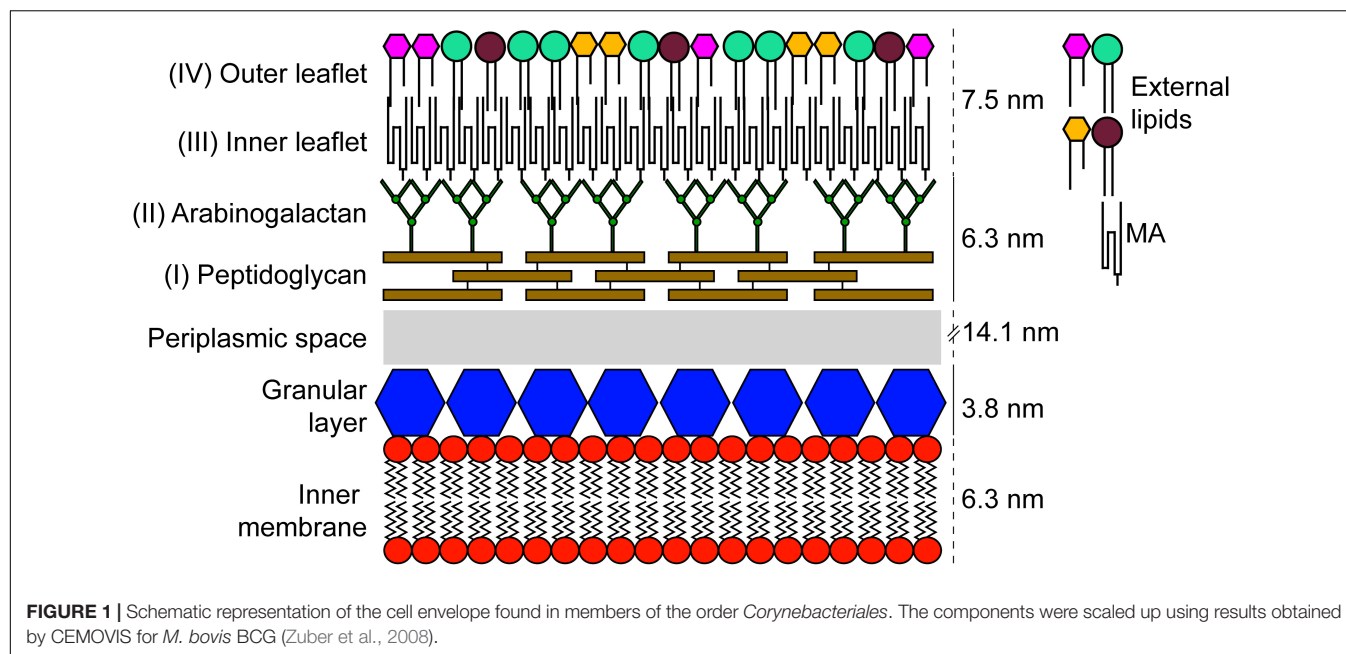


are also involved in the production of antibiotic compounds (e.g., *Streptomyces* sp.), amino acids (e.g., *Corynebacterium* sp.), biofuels, and other bioproducts (Becker and Wittmann, 2016; Lewin et al., 2016).

One of the most studied bacteria from the *Actinobacteria* phylum is *Mycobacterium tuberculosis*, the etiological agent of tuberculosis, a disease that causes significant morbidity and mortality. It is a leading cause of death worldwide making its control a top priority for the World Health Organization (Pai et al., 2016; Friedrich, 2017). Several bacteria from the *Corynebacteriales* order, that includes *M. tuberculosis*, are studied for having an atypical structural characteristic: the presence of a so-called “mycomembrane” that, in an organizational sense, is believed to resemble the outer membrane of typical Gram-negative bacteria (Zuber et al., 2008; Touchette and Seeliger, 2017; **Figure 1**). This mycomembrane is limited to members of the *Corynebacteriales* with some species-specific variation (Goodfellow and Jones, 2015; Mohammadipanah and Dehghani, 2017). Besides the components common to other Gram-positive bacteria, *Corynebacteriales* also have a layer of arabinogalactan attached to the peptidoglycan layer and to the inner leaflet of the mycolic-acid containing mycomembrane. This unusual structure, along with some phylogenetic ambiguity, have led certain authors to suggest that *M. tuberculosis* has more in common with Gram-negative bacteria than with their Gram-positive relatives (Fu and Fu-Liu, 2002). In the 1970s, two distinct cell envelope cleavage planes were recorded for freeze-etched mycobacteria (Barksdale and Kim, 1977). These findings contributed to the original proposal for a mycobacterial outer membrane. Further unequivocal evidence was provided by labeling with selective fluorescent probes (Christensen et al., 1999). In fact, the debate about the existence and composition of the mycomembrane was partially resolved

only 10 years ago when it was visualized by cryo-electron microscopy of vitreous sections (CEMOVIS) (Hoffmann et al., 2008; Zuber et al., 2008). The reasons for the evolution of this membrane are still not totally clear, although we know that it is important for several aspects of the virulence and intrinsic antibiotic resistance of pathogenic species such as *M. tuberculosis* (Forrellad et al., 2013; Becker and Sander, 2016). In addition, as this membrane (along with the rest of the cell envelope) is at the frontline of environmental interactions, it is expected that differences in the constitution of the mycomembrane are associated with adaptation to specific environments or ecological niches (Veyrier et al., 2009).

In this era of large-scale DNA sequencing (Vincent et al., 2017), we can now investigate and compare the genomic sequences of bacteria at an unprecedented rate (Land et al., 2015) and infer the key steps that have led to the development and modification of the various subcomponents of bacterial cells. In recent years, numerous actinobacterial genomes have been sequenced including a broad representation of each genus. As expected, analysis of these data revealed a great heterogeneity in terms of the many biological functions associated with these bacteria (Ventura et al., 2007; Gomez-Escribano et al., 2016). Based on this large amount of sequence information, it is now possible to carry out an evolutionary analysis of the cell envelope in order to dissect the genetic events that have led to its development. Here, we describe the different layers of the cell envelope for the *Actinobacteria* phylum with a specific emphasis on species that harbor the mycomembrane. Although a number of mysteries still remain, our goal for this article is to provide new perspectives on the evolutionary path and benefits surrounding the unique membrane features of this important group of bacteria.



ACTINOBACTERIAL CELL ENVELOPE LAYERS

Granular Layer

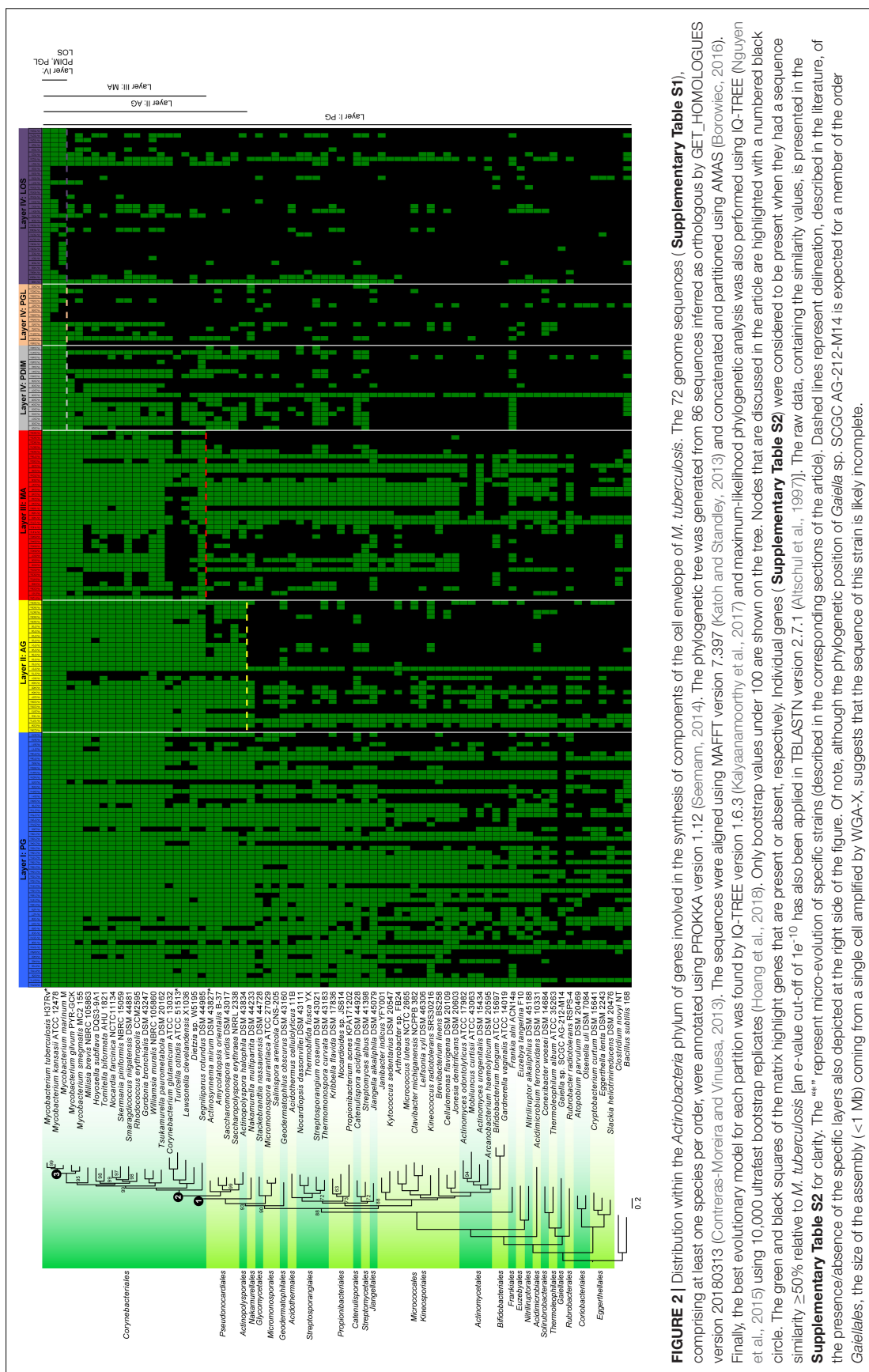
By using CEMOVIS, it is possible to visualize a “granular layer” in between the plasma membrane and the peptidoglycan layer of *Mycobacterium bovis* BCG, *Mycobacterium smegmatis*, and *Corynebacterium glutamicum* (Zuber et al., 2008). A previous study made on other Gram-positive bacteria has shown that the granular layer is possibly linked to the plasma membrane and composed of penicillin-binding proteins, lipoproteins, and lipoteichoic acids (or teichuronic acid in some species; for review see Tul'skaya et al., 2011) (Zuber et al., 2006). Although, it seems this structure is common to several Gram-positive bacteria, the function and its precise composition are poorly characterized.

Layer I: Peptidoglycan

The cell envelope of *Actinobacteria* is composed of a layer of peptidoglycan that provides essential functions such as rigidity and helps to maintain an optimal osmotic stability (Vollmer et al., 2008; Jankute et al., 2015). Although peptidoglycan is common amongst bacteria, there are many subtle differences in its composition that have been used in the past as a way to identify distinct species in the context of chemotaxonomy (Lechevalier and Lechevalier, 1970). The standard peptidoglycan consists of short peptides and glycan strands that are composed of *N*-acetylglucosamine (GlcNAc) and *N*-acetylmuramic acid (MurNAc) residues linked by β -1 \rightarrow 4 bonds. The third amino acid in the peptide stem is usually *meso*-diaminopimelic acid (*meso*-DAP) for Gram-negative and L-lysine for Gram-positive bacteria (Egan et al., 2017). In *Actinobacteria*, this amino acid is variable

with numerous species (including the *Corynebacteriales* order) that harbor *meso*-DAP. This property is potentially due to the species-specific affinity of the ligase MurE (UDP-*N*-acetylmuramoylalanyl-D-glutamate-2,6-diaminopimelate ligase) for *meso*-DAP (Hammes et al., 1977; Basavannacharya et al., 2010). Furthermore, differences in these third amino-acids were used as a marker for *Actinobacteria* cell wall types II, III, and IV (Lechevalier and Lechevalier, 1970).

In addition to having *meso*-DAP, the peptidoglycan of members of the *Corynebacteriales* order has another major distinction: a portion of MurNAc molecules is oxidized to become *N*-glycolylmuramic acid (MurNGlyc). This characteristic, in addition to playing an important role in the structure of peptidoglycan, has been suggested to increase resistance to lysozyme and β -lactam antibiotics (Raymond et al., 2005). The hydroxylase responsible for this modification is encoded by the gene *namH* (Rv3818; as per the reference *M. tuberculosis* H37Rv genome) (Raymond et al., 2005; Coulombe et al., 2009; Hansen et al., 2014). As expected, this gene is found in several members of the *Corynebacteriales* order (Figure 2). However, it appears to be absent from the genomes of genera such as *Hoyosella* and in those that are the most “basal” of the order: *Corynebacterium*, *Turicella*, *Lawsonella*, *Dietzia*, and *Segniliparus*. Interestingly, a few other genera in the *Actinobacteria* phylum, but not in the *Corynebacteriales*, also have a putative *namH* homolog (Figure 2). This is the case for *Stackebrandtia* (Glycomycetales), *Micromonospora* (Micromonosporales), and *Salinispora* (Micromonosporales) that form a discrete sub-lineage and have been described to harbor a cell wall with MurNGlyc (Parte et al., 2012). As an exception, a few scattered species (such as *Catenulispora acidiphila* and *Rubrobacter radiotolerans*) possess a homologous copy of *NamH*, although to the best of our knowledge there is no evidence for



the presence of MurNGlyc in their peptidoglycan (Parte et al., 2012).

Layer II: Arabinogalactan

In addition to its distinct composition, the peptidoglycan of *Corynebacteriales* is also the point of attachment of arabinogalactan, a highly branched heteropolysaccharide composed of galactose and arabinose in a furanoid form (Figure 1; McNeil et al., 1987). It is estimated that approximately 10% of the MurNAc residues of the peptidoglycan are covalently linked to arabinogalactan [α -L-rhamnopyranose-(1 \rightarrow 3- α -D-GlycNAc-(1 \rightarrow P))] (McNeil et al., 1990). Although this linkage is unique, it resembles the one that connects cell wall teichoic acids to peptidoglycan in other Gram-positive species. This similarity led to the discovery of a phosphotransferase of the LytR-CpsA-Psr family, named Lcp1, which is encoded by the Rv3267 gene and plays a leading role in linking arabinogalactan to peptidoglycan in *M. tuberculosis* (Baumgart et al., 2016; Grzegorzewicz et al., 2016; Harrison et al., 2016).

In terms of its distribution within the *Actinobacteria* phylum, arabinogalactan is produced exclusively by the members of the *Corynebacteriales* order and in some species from related orders such as *Pseudonocardiales* and *Actinopolysporales* (Goodfellow et al., 1984) [with the exception of *Actinosynnema mirum* (Hasegawa et al., 1978)]. These latter two orders possess a typical type IV cell wall (Lechevalier and Lechevalier, 1970), although they lack mycolic acids (Ludwig et al., 2015). The global distribution of genes implicated in the synthesis and transport of arabinogalactan is well correlated with the fact that these species produce arabinogalactan (see Figure 2). Nevertheless, a deeper investigation of these latter two orders will be required to exclude possible exceptions or misinterpretation.

Layer III: Mycolic Acids

The inner leaflet of the external mycomembrane is homogeneous and is mainly composed of mycolic acids (MAs) – long-chain fatty acids that are exclusive to the order *Corynebacteriales* (Bansal-Mutalik and Nikaido, 2014; Marrakchi et al., 2014). On one hand, MAs form a barrier to hydrophilic molecules including several antibiotics (Liu et al., 1995), while on the other hand, they are also the target of some first- and second-line anti-TB drugs including isoniazid (Jackson et al., 2013; Marrakchi et al., 2014). In an evolutionary context, MAs play a prominent role in taxonomic differentiation within the *Corynebacteriales* order. In this sense, there is a great diversity in the number of carbons and functional groups comprising the MAs, thus making it possible to use them as a chemotaxonomic marker to differentiate between genera and also at the species level (Minnikin et al., 1984; Barry et al., 1998; Song et al., 2009; Marrakchi et al., 2014).

As reviewed elsewhere (Marrakchi et al., 2014), the raw materials of MAs, fatty acids, are produced by the combination of two fatty acid synthases (FAS-I and FAS-II). The first, FAS-I, is a eukaryotic-like protein narrowly distributed in bacteria (Cabruja et al., 2017) and encoded by the *fas* gene (Rv2524c).

FAS-I produces acyl-CoAs with a bimodal distribution of C₁₆-C₁₈ and C₂₄-C₂₆. FAS-II, on the other hand, is far more common across bacterial species (Cabruja et al., 2017) and begins with the formation of β -ketoacyl-ACP by Claisen condensation of malonyl-ACP [produced from malonyl-CoA by MtFabD (Rv2243)], with acyl-CoA (the product of FAS-I), through the action of MtFabH (Rv0533). Other enzymes such as HadA (Rv0635), HadB (Rv0636), HadC (Rv0637), InhA (Rv1484), KasA (Rv2245), and KasB (Rv2246) are involved in the subsequent steps of elongation and maturation of fatty acids by FAS-II. The final MA structure is produced through several crucial steps that include, among others, activation (FadD32 and Rv3801c), condensation (Pks13 and Rv3800c) and reduction (CmrA and Rv2509).

Although the presence of MAs is well-conserved throughout the *Corynebacteriales*, there are some exceptions. For example, basal species of *Corynebacteriales* (such as *Corynebacterium*, *Dietzia*, *Lawsonella*, and *Turicella*) that form a monophyletic group, lack multiple genes confirming the well described diversity in length and composition of MA. It has already been reported that some species of *Corynebacterium* possess two FAS-I genes (such as *C. glutamicum*), while some do not have the genes encoding for the typical FAS-II machinery (Radmacher et al., 2005). Interestingly, *Corynebacterium* cannot elongate MAs (Radmacher et al., 2005; Burkovski, 2013), which is consistent with the lack of more than 50% of genes implicated in this pathway.

Turicella otitidis possesses almost none of the genes involved in MA biosynthesis (see “*” in Figure 2). This species is clearly in the order *Corynebacteriales* based on its genome sequence (Baek et al., 2018). However, a recent study suggests that the genome of *T. otitidis* has lost the key genes involved in MA synthesis (Baek et al., 2018). This result corroborates the fact that this bacterium does not produce MAs which is exceptional for a bacterium of the order *Corynebacteriales* and this microevolution has made its positioning within this order rather difficult (Funke et al., 1994). Interestingly, this species still produces arabinogalactan (Renaud et al., 1996).

Layer IV: External Lipids

While the composition of the inner leaflet of the mycomembrane is homogenous, the outer leaflet is highly heterogeneous and consists of lipids, lipoglycans, and proteins (Chiaradia et al., 2017). Due to its complexity and species-specific constitution, it remains poorly characterized with the exception of the pathogen *M. tuberculosis* and closely related slow-growing mycobacteria. In these bacteria, several lipids are associated with the external leaflet including – but not limited to – phthiocerol dimycocerosate (PDIM), phenolic glycolipid (PGL, phenolphthiocerol-based glycolipids that share a similar long-chain fatty acid backbone with PDIM), and lipooligosaccharides (LOS). These components seem to be important virulence factors (Reed et al., 2004; Forrellad et al., 2013) and have been shown to be involved in the infection of macrophages as well as in escape from the immune system (Cambier et al., 2014). The PDIM and PGL-associated genes (Rv2928 to Rv2963), are all co-located within the same cluster of the chromosome (Goude and Parish,

2008; **Supplementary Table S2**). LOS are common to several slow growing mycobacteria (including “*M. canettii*” from the *M. tuberculosis* complex) although they are not produced by *M. tuberculosis* due to the loss of Pks5.1 and truncation of PapA4. The remaining genes implicated in this pathway are present (**Figure 2**) which suggests micro-evolution in this species has led to the loss of LOS production (Boritsch et al., 2016; Brennan, 2016). This apparent evolutionary change correlates with a marked increase in whole cell hydrophobicity and enhanced aerosol transmission of current TB strains (Jankute et al., 2017).

The external layer of the mycomembrane also contains trehalose monomycolate – TMM, and trehalose dimycolate – TDM (also called “cord factor”) that also have crucial functions in the regulation of the host-symbiont relationship (Hunter et al., 2006). These molecules consist of glucose disaccharides (α -D-glucopyranosyl- α -D-glucopyranoside) esterified with MAs. TMM is generated in the cytoplasm, whereupon MmpL3 (Rv0206c) subsequently transports this molecule to the periplasm (Grzegorzewicz et al., 2016). Finally, the accepted model (for a review see Marrakchi et al., 2014) is that TMM in the periplasm serves as the MA donor for the mycolylation of arabinogalactan, and is also processed to give TDM. Both reactions involve the Ag85 enzyme complex (Belisle et al., 1997). Three genes (Rv3803c, Rv1886c, and Rv0129c) encode for the Ag85 complex and they are only present in the MA-positive species as seen in **Figure 2**. As TMM and TDM rely on the presence of MAs and Ag85, their distribution is therefore restricted to MA positive species. Indeed, they have been isolated from *Mycobacterium*, *Corynebacterium*, *Nocardia*, and *Rhodococcus* (Noll et al., 1956; Itoneda et al., 1970; Jean-Claude et al., 1976; Mompon et al., 1978; Lopes Silva et al., 1979; Pommier and Michel, 1979; Rapp et al., 1979; Batrakov et al., 1981). However, further characterization is necessary for other MA-positive species (such as *Segniliparus*).

WHAT IS THE EVOLUTIONARY ORIGIN OF THE MYCOBACTERIAL CELL ENVELOPE?

The biological functions and molecular mechanisms surrounding the biosynthesis of the mycomembrane present in the *Corynebacteriales* are being uncovered slowly, but surely. However, the precise origin of this feature that is unique amongst members of the *Actinobacteria* (otherwise composed essentially of monoderm bacteria) continues to be a mystery. Two main theories can potentially explain the biogenesis of the mycomembrane: (1) that it arose via the remodeling of an already existing outer membrane, or (2) that it has a *de novo* origin (**Graphical Abstract**).

The first theory was proposed based on the observation that a double membrane is generated as a byproduct of endospore formation in bacteria (although endospores have not been found in *Actinobacteria*) (Tocheva et al., 2011; Tocheva et al., 2013). Assuming that the primordial cell was monoderm, a double

membraned cell could have appeared via the retention of the second spore membrane, thus giving rise to a diderm common ancestor of all bacteria. This theory implies a bottleneck that selected for this ancestor but also that the current monoderm species appeared by independent loss of the outer membrane. In order to generate a mycomembrane, a significant re-engineering of the gene content (difficult to assess due to gene erosion over time) would have occurred in *Corynebacteriales* and could account for the atypical envelope characteristics when compared to other diderm species (Tocheva et al., 2016). This theory remains an open question in the field (Sutcliffe and Dover, 2016).

The second theory proposes that the double bacterial membrane is a homoplastic character (i.e., a similar trait from different evolutionary origins) that has evolved several times independently in a functionally convergent manner. With regard to the *Actinobacteria* phylum, the double membrane could have appeared “recently” by successive horizontal acquisition of genes allowing a step-by-step construction of the cell envelope that is present in *Mycobacterium*.

The distribution of the major genes implicated in the synthesis of the different layers of the mycomembrane is presented for the *Actinobacteria* in **Figure 2**. This figure needs to be interpreted carefully as the function of the different orthologous proteins has not been proven to be conserved across all the listed species. Nevertheless, one can observe a “phylogenetic gradient” in terms of the distribution of genes involved in the construction of the cell-envelope from inside to outside (**Figure 2**). In addition, one can observe a step-wise distribution in the evolution of the layers comprising the cell envelope. Both the gene content and the cell wall characteristics are well correlated. When investigating the genes involved in peptidoglycan synthesis throughout the genomes of the *Actinobacteria*, it can be observed that they are broadly distributed. On the other hand, arabinogalactan (and the genes implicated in this pathway) are restricted to bacteria that have diverged after the evolutionary node that we called “Node 1” (**Figure 2**). The MAs are even more narrowly distributed within bacteria that diverged after Node 2 (if we exclude the polyvalent FAS-II machinery). Finally, the genes associated with synthesis of the external leaflet are present in a sublineage-specific manner within the slow-growing mycobacteria that diverged after Node 3. This step-wise gradient of gene acquisition would support the theory in which the sequential gain-of-function has led to the successive evolution of the outer-membrane components in the ancestors of modern *M. tuberculosis*. The first step in this pathway appears to be the ability to attach and produce arabinogalactan that, in turn, supports the addition of the mycomembrane. Within this scenario, the final layer that corresponds to the external leaflet would have evolved most recently in a species-specific manner.

In this article, *M. tuberculosis* (and other slow growing mycobacteria) are used as our end point as they are the best characterized. However, we expect that with further characterization of the cell envelope of other *Corynebacteriales* and identification of the genes involved in their synthesis,

we will obtain a similar general pattern. This will be particularly interesting for the highly heterogeneous outer leaflet. In fact, *Corynebacteriales* colonize multiple ecological niches from extreme and diverse habitats including soil and the human microbiome (Ramakrishnan et al., 2013; Goodfellow and Jones, 2015). This diversity implies a specific adaptation for individual species. This phenomenon would involve a distinctive selection of cell envelope constituents and, more specifically, for the external leaflet of the outer-membrane that is in immediate contact with the environment. For example, **Figure 2** shows that several genes involved in PDIM formation are present in the genomes of members of the *Corynebacteriales* order that are assumed to be PDIM-negative. This is especially true for *M. gilvum*, which is a rapid-growing mycobacterium (Wee et al., 2017). It is important to note that a number of genes involved in PDIM and PGL synthesis are polyketide synthases, which are versatile enzymes involved in the production of various natural products (Quadri, 2014). The question remains whether these genes serve in the production of molecules localized in the outer leaflet of “DIM-negative” bacteria that may have a common origin with PDIM as we know it in the pathogenic slow-growing mycobacteria.

CONCLUSION

Regardless of whether the double membrane of *Corynebacteriales* represents a relict sharing a common origin with the double membrane present in typical Gram-negative species, or is the result of a more recent adaptation, it will undoubtedly be interesting and informative to attempt to experimentally reconstruct the double membrane of mycobacteria starting from an *Actinobacteria* species possessing a single membrane (such as *Turicella* sp.). This daring experiment will teach us more

about the mechanism of biogenesis of this double membrane and, perhaps, even inform on its molecular evolution and the natural selection of such an adaptation. In doing so, we could mimic the putative evolutionary process that has led to the *Mycobacterium* membrane as well as identify the functional differences linked to possible species-specific adaptation of the mycomembrane. This work may also highlight important enzyme functions that can be specifically targeted in vaccination or chemotherapeutic approaches aimed at killing pathogenic species such as *M. tuberculosis*.

AUTHOR CONTRIBUTIONS

ATV and FJV conceived and designed the experiments. ATV, FJV, MR, ET, SN, and IM contributed to the writing and editing of the manuscript. All authors read and approved the final manuscript.

FUNDING

This work was supported by the Natural Sciences and Engineering Research Council of Canada (NSERC) under Grant RGPIN-2016-04940. ATV received a Postdoctoral Fellowship from the NSERC. FJV is a research scholar of the Fonds de Recherche du Québec – Santé.

SUPPLEMENTARY MATERIAL

The Supplementary Material for this article can be found online at: <https://www.frontiersin.org/articles/10.3389/fmicb.2018.02341/full#supplementary-material>

REFERENCES

- Altschul, S. F., Madden, T. L., Schaffer, A. A., Zhang, J., Zhang, Z., Miller, W., et al. (1997). Gapped BLAST and PSI-BLAST: a new generation of protein database search programs. *Nucleic Acids Res.* 25, 3389–3402.
- Baek, I., Kim, M., Lee, I., Na, S. I., Goodfellow, M., and Chun, J. (2018). Phylogeny trumps chemotaxonomy: a case study involving *Turicella otitidis*. *Front. Microbiol.* 9:834. doi: 10.3389/fmicb.2018.00834
- Bansal-Mutalik, R., and Nikaido, H. (2014). Mycobacterial outer membrane is a lipid bilayer and the inner membrane is unusually rich in diacyl phosphatidylinositol dimannosides. *Proc. Natl. Acad. Sci. U.S.A.* 111, 4958–4963. doi: 10.1073/pnas.1403078111
- Barka, E. A., Vatsa, P., Sanchez, L., Gaveau-Vaillant, N., Jacquard, C., Meier-Kolthoff, J. P., et al. (2016). Taxonomy, physiology, and natural products of *Actinobacteria*. *Microbiol. Mol. Biol. Rev.* 80, 1–43. doi: 10.1128/MMBR.00019-15
- Barksdale, L., and Kim, K. S. (1977). *Mycobacterium*. *Bacteriol. Rev.* 41, 217–372.
- Barry, C. E., Lee, R. E., Mdluli, K., Sampson, A. E., Schroeder, B. G., Slayden, R. A., et al. (1998). Mycolic acids: structure, biosynthesis and physiological functions. *Prog. Lipid Res.* 37, 143–179.
- Basavannacharya, C., Robertson, G., Munshi, T., Keep, N. H., and Bhakta, S. (2010). ATP-dependent MurE ligase in *Mycobacterium tuberculosis*: biochemical and structural characterisation. *Tuberculosis* 90, 16–24. doi: 10.1016/j.tube.2009.10.007
- Batrakov, S. G., Rozynov, B. V., Koronelli, T. V., and Bergelson, L. D. (1981). Two novel types of trehalose lipids. *Chem. Phys. Lipids* 29, 241–266. doi: 10.1016/0009-3084(81)90055-4
- Baumgart, M., Schubert, K., Bramkamp, M., and Frunzke, J. (2016). Impact of LytR-CpsA-Psr proteins on cell wall biosynthesis in *Corynebacterium glutamicum*. *J. Bacteriol.* 198, 3045–3059. doi: 10.1128/JB.00406-16
- Becker, J., and Wittmann, C. (2016). “Industrial microorganisms: *Corynebacterium glutamicum*,” in *Industrial Biotechnology: Microorganisms*, Vol. 1, eds C. Wittmann and J. C. Liao (Hoboken, NJ: John Wiley & Sons), 183–220. doi: 10.1002/9783527807796.ch6
- Becker, K., and Sander, P. (2016). *Mycobacterium tuberculosis* lipoproteins in virulence and immunity - fighting with a double-edged sword. *FEBS Lett.* 590, 3800–3819. doi: 10.1002/1873-3468.12273
- Belisle, J. T., Vissa, V. D., Sievert, T., Takayama, K., Brennan, P. J., and Besra, G. S. (1997). Role of the major antigen of *Mycobacterium tuberculosis* in cell wall biogenesis. *Science* 276, 1420–1422.
- Boritsch, E. C., Frigui, W., Cascioferro, A., Malaga, W., Etienne, G., Laval, F., et al. (2016). pks5-recombination-mediated surface remodelling in *Mycobacterium tuberculosis* emergence. *Nat. Microbiol.* 1:15019. doi: 10.1038/nmicrobiol.2015.19
- Borowiec, M. L. (2016). AMAS: a fast tool for alignment manipulation and computing of summary statistics. *PeerJ* 4:e1660. doi: 10.7717/peerj.1660
- Brennan, P. J. (2016). Bacterial evolution: emergence of virulence in TB. *Nat. Microbiol.* 1:15031. doi: 10.1038/nmicrobiol.2015.31
- Burkovski, A. (2013). Cell envelope of corynebacteria: structure and influence on pathogenicity. *ISRN Microbiol.* 2013:935736. doi: 10.1155/2013/935736
- Cabruja, M., Mondino, S., Tsai, Y. T., Lara, J., Gramajo, H., and Gago, G. (2017). A conditional mutant of the fatty acid synthase unveils unexpected cross talks in mycobacterial lipid metabolism. *Open Biol.* 7:160277. doi: 10.1098/rsob.160277

- Cambier, C. J., Takaki, K. K., Larson, R. P., Hernandez, R. E., Tobin, D. M., Urdahl, K. B., et al. (2014). Mycobacteria manipulate macrophage recruitment through coordinated use of membrane lipids. *Nature* 505, 218–222. doi: 10.1038/nature12799
- Chiaraia, L., Lefebvre, C., Parra, J., Marcoux, J., Burlet-Schiltz, O., Etienne, G., et al. (2017). Dissecting the mycobacterial cell envelope and defining the composition of the native mycomembrane. *Sci. Rep.* 7:12807. doi: 10.1038/s41598-017-12718-4
- Christensen, H., Garton, N. J., Horobin, R. W., Minnikin, D. E., and Barer, M. R. (1999). Lipid domains of mycobacteria studied with fluorescent molecular probes. *Mol. Microbiol.* 31, 1561–1572.
- Contreras-Moreira, B., and Vinuesa, P. (2013). GET_HOMOLOGUES, a versatile software package for scalable and robust microbial pangenome analysis. *Appl. Environ. Microbiol.* 79, 7696–7701. doi: 10.1128/AEM.02411-13
- Coulombe, F., Divangahi, M., Veyrier, F., De Leseleuc, L., Gleason, J. L., Yang, Y., et al. (2009). Increased NOD2-mediated recognition of N-glycolyl muramyl dipeptide. *J. Exp. Med.* 206, 1709–1716. doi: 10.1084/jem.20081779
- Egan, A. J., Cleverley, R. M., Peters, K., Lewis, R. J., and Vollmer, W. (2017). Regulation of bacterial cell wall growth. *FEBS J.* 284, 851–867. doi: 10.1111/febs.13959
- Forrellad, M. A., Klepp, L. I., Gioffre, A., Sabio, Y., Garcia, J., Morbidoni, H. R., et al. (2013). Virulence factors of the *Mycobacterium tuberculosis* complex. *Virulence* 4, 3–66. doi: 10.4161/viru.22329
- Friedrich, M. J. (2017). Tuberculosis update 2017. *JAMA* 318:2287. doi: 10.1001/jama.2017.18477
- Fu, L. M., and Fu-Liu, C. S. (2002). Is *Mycobacterium tuberculosis* a closer relative to Gram-positive or Gram-negative bacterial pathogens? *Tuberculosis* 82, 85–90.
- Funke, G., Stubbs, S., Altwegg, M., Carlotti, A., and Collins, M. D. (1994). *Turicella otitidis* gen. nov., sp. nov., a coryneform bacterium isolated from patients with otitis media. *Int. J. Syst. Bacteriol.* 44, 270–273. doi: 10.1099/00207713-44-2-270
- Gomez-Escribano, J. P., Alt, S., and Bibb, M. J. (2016). Next generation sequencing of *Actinobacteria* for the discovery of novel natural products. *Mar. Drugs* 14:E78. doi: 10.3390/md14040078
- Goodfellow, M., and Jones, A. L. (2015). “Corynebacteriales ord. nov,” in *Bergey's Manual of Systematics of Archaea and Bacteria*, eds W. B. Whitman, F. Rainey, P. Kämpfer, M. Trujillo, J. Chun, P. DeVos, et al. (Hoboken, NJ: Wiley), doi: 10.1002/9781118960608.obm00009
- Goodfellow, M., Mordarski, M., and Williams, S. T. (1984). *The Biology of the Actinomycetes*. Cambridge, MA: Academic Press.
- Goude, R., and Parish, T. (2008). The genetics of cell wall biosynthesis in *Mycobacterium tuberculosis*. *Future Microbiol.* 3, 299–313. doi: 10.2217/17460913.3.3.299
- Grzegorzewicz, A. E., De Sousa-D'auria, C., Mcneil, M. R., Huc-Claustre, E., Jones, V., Petit, C., et al. (2016). Assembling of the *Mycobacterium tuberculosis* cell wall core. *J. Biol. Chem.* 291, 18867–18879. doi: 10.1074/jbc.M116.739227
- Hammes, W. P., Neukam, R., and Kandler, O. (1977). On the specificity of the uridine diphospho-N-acetylmuramyl-alanyl-D-glutamic acid: diamino acid ligase of *Bifidobacterium globosum*. *Arch. Microbiol.* 115, 95–102.
- Hansen, J. M., Golchin, S. A., Veyrier, F. J., Domenech, P., Boneca, I. G., Azad, A. K., et al. (2014). N-glycolylated peptidoglycan contributes to the immunogenicity but not pathogenicity of *Mycobacterium tuberculosis*. *J. Infect. Dis.* 209, 1045–1054. doi: 10.1093/infdis/jit622
- Harrison, J., Lloyd, G., Joe, M., Lowary, T. L., Reynolds, E., Walters-Morgan, H., et al. (2016). Lcp1 is a phosphotransferase responsible for ligating arabinogalactan to peptidoglycan in *Mycobacterium tuberculosis*. *MBio* 7:e00972-16. doi: 10.1128/mBio.00972-16
- Hasegawa, T., Lechevalier, M. P., and Lechevalier, H. A. (1978). New genus of the *Actinomycetales*: *Actinosynnema* gen. nov. *Int. J. Syst. Evol. Microbiol.* 28, 304–310. doi: 10.1099/00207713-28-2-304
- Hoang, D. T., Chernomor, O., Von Haeseler, A., Minh, B. Q., and Vinh, L. S. (2018). UFBoot2: improving the ultrafast bootstrap approximation. *Mol. Biol. Evol.* 35, 518–522. doi: 10.1093/molbev/msx281
- Hoffmann, C., Leis, A., Niederweis, M., Plitzko, J. M., and Engelhardt, H. (2008). Disclosure of the mycobacterial outer membrane: cryo-electron tomography and vitreous sections reveal the lipid bilayer structure. *Proc. Natl. Acad. Sci. U.S.A.* 105, 3963–3967. doi: 10.1073/pnas.0709530105
- Hunter, R. L., Olsen, M. R., Jagannath, C., and Actor, J. K. (2006). Multiple roles of cord factor in the pathogenesis of primary, secondary, and cavitary tuberculosis, including a revised description of the pathology of secondary disease. *Ann. Clin. Lab. Sci.* 36, 371–386.
- Ionedá, T., Lederer, E., and Rozanis, J. (1970). Sur la structure des diesters de tréhalose (“cord factors”) produits par *Nocardia asteroides* et *Nocardia rhodochrous*. *Chem. Phys. Lipids* 4, 375–392. doi: 10.1016/0009-3084(70)90037-X
- Jackson, M., Mcneil, M. R., and Brennan, P. J. (2013). Progress in targeting cell envelope biogenesis in *Mycobacterium tuberculosis*. *Future Microbiol.* 8, 855–875. doi: 10.2217/fmb.13.52
- Jankute, M., Cox, J. A., Harrison, J., and Besra, G. S. (2015). Assembly of the mycobacterial cell wall. *Annu. Rev. Microbiol.* 69, 405–423. doi: 10.1146/annurev-micro-091014-104121
- Jankute, M., Nataraj, V., Lee, O. Y., Wu, H. H. T., Ridell, M., Garton, N. J., et al. (2017). The role of hydrophobicity in tuberculosis evolution and pathogenicity. *Sci. Rep.* 7:1315. doi: 10.1038/s41598-017-01501-0
- Jean-Claude, P., Lacave, C., Ahibo-Coffy, A., and Savagnac, A. (1976). Séparation et étude structurale des espèces moléculaires de monomycolates et de dimycolates de α -D-tréhalose présents chez *Mycobacterium phlei*. *Eur. J. Biochem.* 63, 543–552. doi: 10.1111/j.1432-1033.1976.tb10258.x
- Kalyaanamoorthy, S., Minh, B. Q., Wong, T. K. F., Von Haeseler, A., and Jermini, L. S. (2017). ModelFinder: fast model selection for accurate phylogenetic estimates. *Nat. Methods* 14, 587–589. doi: 10.1038/nmeth.4285
- Katoh, K., and Standley, D. M. (2013). MAFFT multiple sequence alignment software version 7: improvements in performance and usability. *Mol. Biol. Evol.* 30, 772–780. doi: 10.1093/molbev/mst010
- Land, M., Hauser, L., Jun, S. R., Nookaew, I., Leuze, M. R., Ahn, T. H., et al. (2015). Insights from 20 years of bacterial genome sequencing. *Funct. Integr. Genomics* 15, 141–161. doi: 10.1007/s10142-015-0433-4
- Lechevalier, M. P., and Lechevalier, H. (1970). Chemical composition as a criterion in the classification of aerobic actinomycetes. *Int. J. Syst. Evol. Microbiol.* 20, 435–443. doi: 10.1099/00207713-20-4-435
- Lewin, G. R., Carlos, C., Chevrette, M. G., Horn, H. A., McDonald, B. R., Stankey, R. J., et al. (2016). Evolution and ecology of *Actinobacteria* and their bioenergy applications. *Annu. Rev. Microbiol.* 70, 235–254. doi: 10.1146/annurev-micro-102215-095748
- Liu, J., Rosenberg, E. Y., and Nikaido, H. (1995). Fluidity of the lipid domain of cell wall from *Mycobacterium chelonae*. *Proc. Natl. Acad. Sci. U.S.A.* 92, 11254–11258.
- Lopes Silva, C., Gesztes, J. L., and Ionedá, T. (1979). Thehalose mycolates from *Nocardia asteroides*, *Nocardia farcinica*, *Gordona lentifragmentia* and *Gordona bronchialis*. *Chem. Phys. Lipids* 24, 17–25. doi: 10.1016/0009-3084(79)90092-6
- Ludwig, W., Euzéby, J., Schumann, P., Busse, H., Trujillo, M. E., Kämpfer, P., et al. (2015). “Road map of the phylum *Actinobacteria*,” in *Bergey's Manual of Systematics of Archaea and Bacteria*, eds W. B. Whitman, F. Rainey, P. Kämpfer, M. Trujillo, J. Chun, P. DeVos, et al. (Hoboken, NJ: Wiley), doi: 10.1002/9781118960608.bm00029
- Marrakchi, H., Laneelle, M. A., and Daffe, M. (2014). Mycolic acids: structures, biosynthesis, and beyond. *Chem. Biol.* 21, 67–85. doi: 10.1016/j.chembiol.2013.11.011
- McNeil, M., Daffe, M., and Brennan, P. J. (1990). Evidence for the nature of the link between the arabinogalactan and peptidoglycan of mycobacterial cell walls. *J. Biol. Chem.* 265, 18200–18206.
- McNeil, M., Wallner, S. J., Hunter, S. W., and Brennan, P. J. (1987). Demonstration that the galactosyl and arabinosyl residues in the cell-wall arabinogalactan of *Mycobacterium leprae* and *Mycobacterium tuberculosis* are furanoid. *Carbohydr. Res.* 166, 299–308.
- Minnikin, D. E., Minnikin, S. M., Parlett, J. H., Goodfellow, M., and Magnusson, M. (1984). Mycolic acid patterns of some species of *Mycobacterium*. *Arch. Microbiol.* 139, 225–231.
- Mohammadipanah, F., and Dehghani, M. (2017). “Classification and taxonomy of *Actinobacteria*,” in *Biology and Biotechnology of Actinobacteria*, eds J. Wink, F. Mohammadipanah, and J. Hamed (Cham: Springer International Publishing), 51–77.
- Mompon, B., Federici, C., Toubiana, R., and Lederer, E. (1978). Isolation and structural determination of a “cord-factor” (trehalose 6,6' dimycolate) from

- Mycobacterium smegmatis*. *Chem. Phys. Lipids* 21, 97–101. doi: 10.1016/0009-3084(78)90057-9
- Nguyen, L. T., Schmidt, H. A., Von Haeseler, A., and Minh, B. Q. (2015). IQ-TREE: a fast and effective stochastic algorithm for estimating maximum-likelihood phylogenies. *Mol. Biol. Evol.* 32, 268–274. doi: 10.1093/molbev/msu300
- Noll, H., Bloch, H., Asselineau, J., and Lederer, E. (1956). The chemical structure of the cord factor of *Mycobacterium tuberculosis*. *Biochim. Biophys. Acta* 20, 299–309. doi: 10.1016/0006-3002(56)90289-X
- O'Callaghan, A., and van Sinderen, D. (2016). Bifidobacteria and their role as members of the human gut microbiota. *Front. Microbiol.* 7:925. doi: 10.3389/fmicb.2016.00925
- Pai, M., Behr, M. A., Dowdy, D., Dheda, K., Divangahi, M., Boehme, C. C., et al. (2016). Tuberculosis. *Nat. Rev. Dis. Primers* 2:16076. doi: 10.1038/nrdp.2016.76
- Parte, A., Whitman, W. B., Goodfellow, M., Kämpfer, P., Busse, H. J., Trujillo, M. E., et al. (2012). *Bergey's Manual of Systematic Bacteriology: The Actinobacteria*, Vol. 5. New York, NY: Springer.
- Pommier, M. T., and Michel, G. (1979). Glycolipides des *nocardiae*. Isolement et caractérisation de mononocardomycolates et de dinocardomycolates de tréhalose dans *Nocardia caviae*. *Chem. Phys. Lipids* 24, 149–155. doi: 10.1016/0009-3084(79)90084-7
- Quadri, L. E. (2014). Biosynthesis of mycobacterial lipids by polyketide synthases and beyond. *Crit. Rev. Biochem. Mol. Biol.* 49, 179–211. doi: 10.3109/10409238.2014.896859
- Radmacher, E., Alderwick, L. J., Besra, G. S., Brown, A. K., Gibson, K. J., Sahm, H., et al. (2005). Two functional FAS-I type fatty acid synthases in *Corynebacterium glutamicum*. *Microbiology* 151, 2421–2427. doi: 10.1099/mic.0.28012-0
- Ramakrishnan, V. R., Feazel, L. M., Gitomer, S. A., Ir, D., Robertson, C. E., and Frank, D. N. (2013). The microbiome of the middle meatus in healthy adults. *PLoS One* 8:e85507. doi: 10.1371/journal.pone.0085507
- Rapp, P., Bock, H., Wray, V., and Wagner, F. (1979). Formation, isolation and characterization of trehalose dimycolates from *Rhodococcus erythropolis* grown on N-Alkanes. *Microbiology* 115, 491–503. doi: 10.1099/00221287-115-2-491
- Raymond, J. B., Mahapatra, S., Crick, D. C., and Pavelka, M. S. Jr. (2005). Identification of the *namH* gene, encoding the hydroxylase responsible for the N-glycolylation of the mycobacterial peptidoglycan. *J. Biol. Chem.* 280, 326–333. doi: 10.1074/jbc.M411006200
- Reed, M. B., Domenech, P., Manca, C., Su, H., Barczak, A. K., Kreiswirth, B. N., et al. (2004). A glycolipid of hypervirulent tuberculosis strains that inhibits the innate immune response. *Nature* 431, 84–87. doi: 10.1038/nature02837
- Renaud, F. N., Gregory, A., Barreau, C., Aubel, D., and Freney, J. (1996). Identification of *Turicella otitidis* isolated from a patient with otorrhea associated with surgery: differentiation from *Corynebacterium afermentans* and *Corynebacterium auris*. *J. Clin. Microbiol.* 34, 2625–2627.
- Seemann, T. (2014). Prokka: rapid prokaryotic genome annotation. *Bioinformatics* 30, 2068–2069. doi: 10.1093/bioinformatics/btu153
- Song, S. H., Park, K. U., Lee, J. H., Kim, E. C., Kim, J. Q., and Song, J. (2009). Electrospray ionization-tandem mass spectrometry analysis of the mycolic acid profiles for the identification of common clinical isolates of mycobacterial species. *J. Microbiol. Methods* 77, 165–177. doi: 10.1016/j.mimet.2009.01.023
- Sutcliffe, I. C., and Dover, L. G. (2016). Comment on Tocheva et al. "Sporulation, bacterial cell envelopes and the origin of life". *Nat. Rev. Microbiol.* 14:600. doi: 10.1038/nrmicro.2016.113
- Tocheva, E. I., Lopez-Garrido, J., Hughes, H. V., Fredlund, J., Kuru, E., Vannieuwenhze, M. S., et al. (2013). Peptidoglycan transformations during *Bacillus subtilis* sporulation. *Mol. Microbiol.* 88, 673–686. doi: 10.1111/mmi.12201
- Tocheva, E. I., Matson, E. G., Morris, D. M., Moussavi, F., Leadbetter, J. R., and Jensen, G. J. (2011). Peptidoglycan remodeling and conversion of an inner membrane into an outer membrane during sporulation. *Cell* 146, 799–812. doi: 10.1016/j.cell.2011.07.029
- Tocheva, E. I., Ortega, D. R., and Jensen, G. J. (2016). Sporulation, bacterial cell envelopes and the origin of life. *Nat. Rev. Microbiol.* 14, 535–542. doi: 10.1038/nrmicro.2016.85
- Touchette, M. H., and Seeliger, J. C. (2017). Transport of outer membrane lipids in mycobacteria. *Biochim. Biophys. Acta* 1862, 1340–1354. doi: 10.1016/j.bbalip.2017.01.005
- Tul'skaya, E. M., Shashkov, A. S., Streshinskaya, G. M., Senchenkova, S. N., Potekhina, N. V., Kozlova, Y. I., et al. (2011). Teichuronic and teichulosonic acids of actinomycetes. *Biochemistry* 76, 736–744. doi: 10.1134/S0006297911070030
- Ventura, M., Canchaya, C., Tauch, A., Chandra, G., Fitzgerald, G. F., Chater, K. F., et al. (2007). Genomics of *Actinobacteria*: tracing the evolutionary history of an ancient phylum. *Microbiol. Mol. Biol. Rev.* 71, 495–548. doi: 10.1128/MMBR.00005-07
- Veyrier, F., Pletzer, D., Turenne, C., and Behr, M. A. (2009). Phylogenetic detection of horizontal gene transfer during the step-wise genesis of *Mycobacterium tuberculosis*. *BMC Evol. Biol.* 9:196. doi: 10.1186/1471-2148-9-196
- Vincent, A. T., Derome, N., Boyle, B., Culley, A. I., and Charette, S. J. (2017). Next-generation sequencing (NGS) in the microbiological world: how to make the most of your money. *J. Microbiol. Methods* 138, 60–71. doi: 10.1016/j.mimet.2016.02.016
- Vollmer, W., Blanot, D., and De Pedro, M. A. (2008). Peptidoglycan structure and architecture. *FEMS Microbiol. Rev.* 32, 149–167. doi: 10.1111/j.1574-6976.2007.00094.x
- Wee, W. Y., Dutta, A., and Choo, S. W. (2017). Comparative genome analyses of mycobacteria give better insights into their evolution. *PLoS One* 12:e0172831. doi: 10.1371/journal.pone.0172831
- Zuber, B., Chami, M., Houssin, C., Dubochet, J., Griffiths, G., and Daffe, M. (2008). Direct visualization of the outer membrane of mycobacteria and corynebacteria in their native state. *J. Bacteriol.* 190, 5672–5680. doi: 10.1128/JB.01919-07
- Zuber, B., Haenni, M., Ribeiro, T., Minnig, K., Lopes, F., Moreillon, P., et al. (2006). Granular layer in the periplasmic space of gram-positive bacteria and fine structures of *Enterococcus gallinarum* and *Streptococcus gordonii* septa revealed by cryo-electron microscopy of vitreous sections. *J. Bacteriol.* 188, 6652–6660. doi: 10.1128/JB.00391-06

Conflict of Interest Statement: The authors declare that the research was conducted in the absence of any commercial or financial relationships that could be construed as a potential conflict of interest.

Copyright © 2018 Vincent, Nyongesa, Morneau, Reed, Tocheva and Veyrier. This is an open-access article distributed under the terms of the Creative Commons Attribution License (CC BY). The use, distribution or reproduction in other forums is permitted, provided the original author(s) and the copyright owner(s) are credited and that the original publication in this journal is cited, in accordance with accepted academic practice. No use, distribution or reproduction is permitted which does not comply with these terms.



Distinct and Specific Role of NlpC/P60 Endopeptidases LytA and LytB in Cell Elongation and Division of *Lactobacillus plantarum*

Marie-Clémence Duchêne¹, Thomas Rolain¹, Adrien Knoops¹, Pascal Courtin², Marie-Pierre Chapot-Chartier², Yves F. Dufrêne¹, Bernard F. Hallet¹ and Pascal Hols^{1*}

¹ Louvain Institute of Biomolecular Science and Technology, Université Catholique de Louvain, Louvain-La-Neuve, Belgium,

² Micalis Institute, INRA, AgroParisTech, Université Paris-Saclay, Jouy-en-Josas, France

OPEN ACCESS

Edited by:

Tobias Dörr,
Cornell University, United States

Reviewed by:

Christoph Mayer,
University of Tübingen, Germany
Cara C. Boutte,
University of Texas at Arlington,
United States
Felipe Cava,
Umeå University, Sweden

*Correspondence:

Pascal Hols
pascal.hols@uclouvain.be

Specialty section:

This article was submitted to
Microbial Physiology and Metabolism,
a section of the journal
Frontiers in Microbiology

Received: 17 September 2018

Accepted: 21 March 2019

Published: 12 April 2019

Citation:

Duchêne M-C, Rolain T, Knoops A,
Courtin P, Chapot-Chartier M-P,
Dufrêne YF, Hallet BF and Hols P
(2019) Distinct and Specific Role of
NlpC/P60 Endopeptidases LytA and
LytB in Cell Elongation and Division of
Lactobacillus plantarum.
Front. Microbiol. 10:713.
doi: 10.3389/fmicb.2019.00713

Peptidoglycan (PG) is an essential lattice of the bacterial cell wall that needs to be continuously remodeled to allow growth. This task is ensured by the concerted action of PG synthases that insert new material in the pre-existing structure and PG hydrolases (PGHs) that cleave the PG meshwork at critical sites for its processing. Contrasting with *Bacillus subtilis* that contains more than 35 PGHs, *Lactobacillus plantarum* is a non-sporulating rod-shaped bacterium that is predicted to possess a minimal set of 12 PGHs. Their role in morphogenesis and cell cycle remains mostly unexplored, except for the involvement of the glucosaminidase Acm2 in cell separation and the NlpC/P60 D, L-endopeptidase LytA in cell shape maintenance. Besides LytA, *L. plantarum* encodes three additional NlpC/P60 endopeptidases (i.e., LytB, LytC and LytD). The *in silico* analysis of these four endopeptidases suggests that they could have redundant functions based on their modular organization, forming two pairs of paralogous enzymes. In this work, we investigate the role of each Lyt endopeptidase in cell morphogenesis in order to evaluate their distinct or redundant functions, and eventually their synthetic lethality. We show that the paralogous LytC and LytD enzymes are not required for cell shape maintenance, which may indicate an accessory role such as in PG recycling. In contrast, LytA and LytB appear to be key players of the cell cycle. We show here that LytA is required for cell elongation while LytB is involved in the spatio-temporal regulation of cell division. In addition, both PGHs are involved in the proper positioning of the division site. The absence of LytA activity is responsible for the asymmetrical positioning of septa in round cells while the lack of LytB results in a lateral misplacement of division planes in rod-shaped cells. Finally, we show that the co-inactivation of LytA and LytB is synthetically affecting cell growth, which confirms the key roles played by both enzymes in PG remodeling during the cell cycle of *L. plantarum*. Based on the large distribution of NlpC/P60 endopeptidases in low-GC Gram-positive bacteria, these enzymes are attractive targets for the discovery of novel antimicrobial compounds.

Keywords: *Lactobacillus*, cell cycle, cell wall, murepeptidase, NlpC/P60 endopeptidase, peptidoglycan hydrolase, morphogenesis

INTRODUCTION

The cell wall is a rigid structure that protects bacteria against external and internal pressures while giving them a proper shape (Delcour et al., 1999). A major component of the cell wall is the peptidoglycan (PG). The PG is a polymer composed of glycan strands linked together by peptide side chains to form a meshwork. The composition of the glycan strands is the same in all bacterial species: *N*-acetyl-muramic acid (MurNAc) alternating with *N*-acetyl-glucosamine (GlcNAc), which are connected by β -1,4 linkage (Vollmer, 2008). The composition of the peptide side chain is more flexible and can vary between bacterial species (Vollmer et al., 2008a). In *Lactobacillus plantarum*, the composition of the stem peptide is L-Ala, D-Glu, *meso*-diaminopimelate (*meso*-DAP), D-Ala, and D-lactate (Deghorain et al., 2007; Kleerebezem et al., 2010). The PG of *L. plantarum* is decorated with additional elements such as wall teichoic acids (WTA), *O*-acetylation of MurNAc (39%) and GlcNAc (9%) (Bernard et al., 2011a), and amidation of D-Glu (100%) and *meso*-DAP (94%) (Bernard et al., 2011b).

Bacteria have to continuously adapt the composition and organization of the PG in order to grow and divide properly. This task is performed by the concerted action between PG synthases and PG hydrolases (PGHs). While PG synthases mediate two main enzymatic reactions, i.e., transglycosylation and transpeptidation, PGHs have a broad range of enzymatic activities with respect to their role in PG processing (Vollmer et al., 2008b). They are separated into different families according to their PG cleavage sites (Vollmer et al., 2008b). Three families of enzymes cleave the glycan strand: glucosaminidases hydrolyze the sugar bond between GlcNAc and MurNAc (Litzinger et al., 2010); muramidases and lytic transglycosylases cleave between MurNAc and GlcNAc (Höltje et al., 1975; Barrett et al., 1984). Amidases cleave the amide bond between the glycan strand and the peptide side chain (Vollmer et al., 2008b). The last family is composed of endopeptidases (Vollmer et al., 2008b) and carboxypeptidases (Sauvage et al., 2008) that hydrolyze specific links in the peptide side chain or the interpeptide bridge.

In the last family, the NlpC/P60 D,L-endopeptidases deserves a special interest in Gram-positive bacteria since they were shown to have a major role in morphogenesis and cell cycle of *Bacillus subtilis*. In this species, seven NlpC/P60 endopeptidases were identified (Figure 1A). With the exception of PgdS that is strictly dedicated to the hydrolysis of poly- γ -glutamate, all the other D,L-endopeptidases were shown to hydrolyze PG (i.e., LytE, LytF, CwlS, CwlO, and CwlT) or PG fragments for their potential recycling (i.e., YkfC) (Schmidt et al., 2001; Fukushima et al., 2018). All of them were shown to display a γ -D-Glu-*meso*-DAP mureopeptidase activity (Ishikawa et al., 1998; Margot et al., 1999; Schmidt et al., 2001; Yamaguchi et al., 2004; Fukushima et al., 2006, 2007). With the exception of the bifunctional CwlT enzyme that is involved in the conjugation of ICEBs1 (Fukushima et al., 2007), LytE, LytF, CwlS, and CwlO are modular enzymes implicated in morphogenesis (Hashimoto et al., 2012). CwlO and LytE, whose co-inactivation is synthetically lethal, are required for cell elongation (Hashimoto et al., 2012). However, they perform specific roles and they are differentially controlled by

players of the elongation machinery (Domínguez-Cuevas et al., 2013; Meisner et al., 2013). Inactivation of CwlO leads to slightly bent and wider cells than the wild type while inactivation of LytE leads to slightly longer and thinner cells (Domínguez-Cuevas et al., 2013; Meisner et al., 2013). Besides its role in cell elongation, LytE was also reported to play a role in cell separation (Carballido-López et al., 2006). In addition, CwlO, which contains two coiled-coil domains, is activated by the membrane protein complex FtsEX (Domínguez-Cuevas et al., 2013; Meisner et al., 2013), while LytE, which contains three LysM PG-binding domains, was proposed to be guided by the actin-like cytoskeleton protein MreBH (Carballido-López et al., 2006; Domínguez-Cuevas et al., 2013; Meisner et al., 2013). Concerning the two last D,L-endopeptidases, LytF and CwlS, which contain five and four LysM domains, respectively, they were shown to be strictly implicated in the cell separation process (Yamamoto et al., 2003; Fukushima et al., 2006).

Lactobacillus plantarum is a commensal Gram-positive bacterium of the human gastrointestinal tract, which displays a *B. subtilis*-like rod shape (Kleerebezem et al., 2010). As a non-sporulating bacterium, *L. plantarum* only harbors 12 predicted PGHs, while *Bacillus subtilis* genome encodes at least 35 PGHs (Smith et al., 2000; Rolain et al., 2012). The predicted autolysome of *L. plantarum* contains 2 glucosaminidases (Acm1 and Acm2), 2 muramidases (Lys1 and Lys2), 3 lytic transglycosidases (MltA, MltB, MltC), 1 amidase (LytH), and 4 D,L-endopeptidases of the NlpC/P60 family (LytA, LytB, LytC, and LytD) (Rolain et al., 2012). In a previous work, we have investigated the functional role of these PGHs through systematic gene inactivation (Rolain et al., 2012). Knockout mutants of 9 out of the 12 predicted PGHs were successfully obtained (Rolain et al., 2012). Two PGHs, Acm2 and LytA, were shown to be differentially involved in the cell cycle. The glucosaminidase Acm2 is responsible of cell separation at a post-divisional stage, while the predicted D,L-endopeptidase LytA was identified as a morphogenic PGH given that its loss resulted in round cells (Rolain et al., 2012). Besides LytA, the function of the three other putative D,L-endopeptidases remain mostly unexplored (Figure 1B; Rolain et al., 2012). By comparison with the modular organization of *B. subtilis* D,L-endopeptidases, LytC and LytD display a similar organization as YkfC with SH3 PG-binding domains, while LytA and LytB possess interesting features such as the absence of coiled-coil domains, a limited number of LysM domains, and the presence of a glycosylated domain rich in alanine, serine, threonine (AST) (Figure 1B). Compared to *B. subtilis*, these specificities suggest that they could have different functions and/or be differently regulated.

The aim of this work is to dissect the role of the four Lyt endopeptidases of *L. plantarum*. To this end, cell morphogenesis was carefully examined in simple mutants of each individual *lyt* gene and double mutants of paralogous genes (i.e., *lytA lytB* and *lytC lytD*). While LytC and LytD did not seem to contribute to cell morphogenesis, LytA and LytB are key morphogenic PGHs. LytA is required for cell elongation, while LytB plays a role in the timing of cell division. Both PGHs are needed for the correct positioning of the division site and display a synthetic growth defect when co-inactivated.

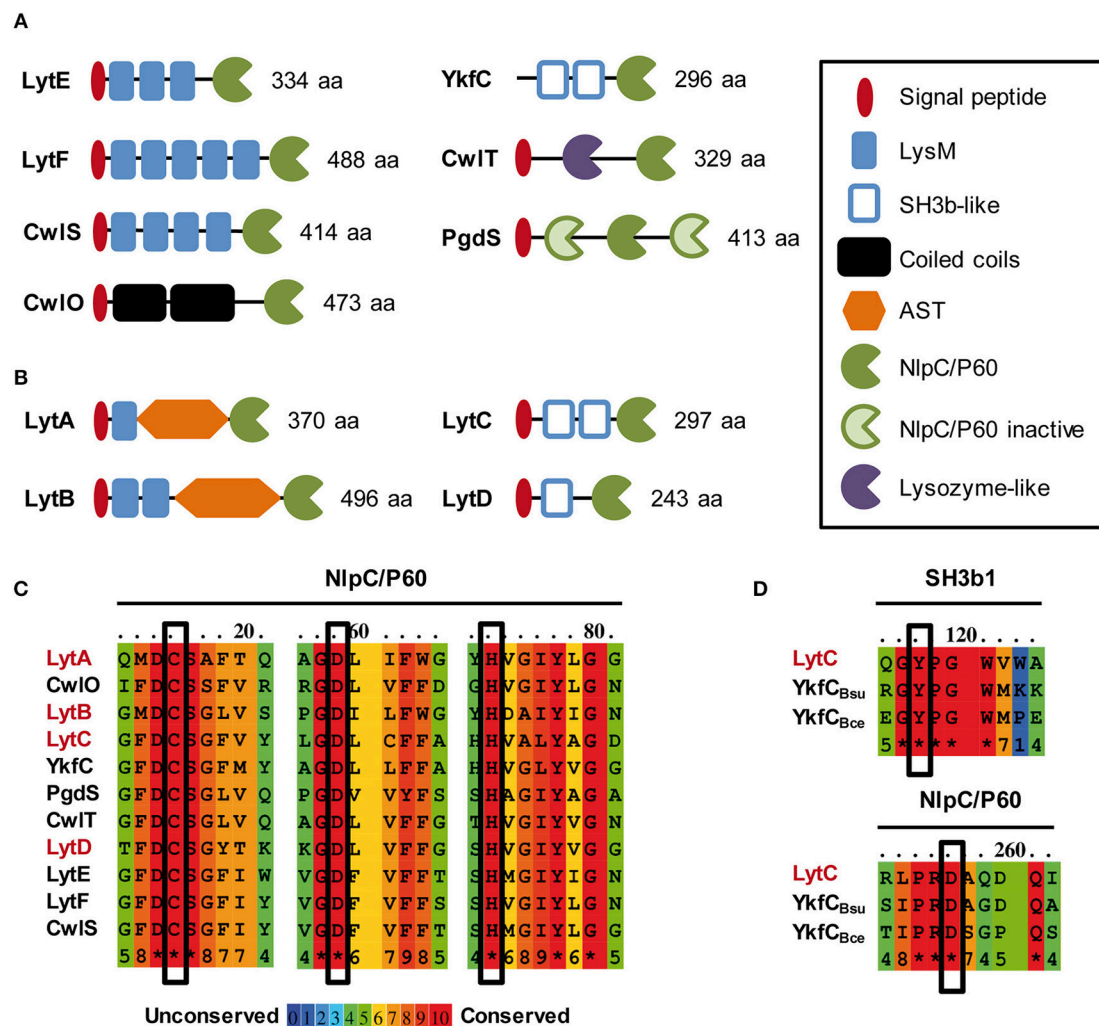


FIGURE 1 | *In silico* analysis of NlpC/P60 endopeptidases of *B. subtilis* and *L. plantarum*. Schematic representation of LytE, LytF, CwIS, CwIO, CwIT and PgdS from *B. subtilis* 168 (A) and LytA, LytB, LytC, and LytD from *L. plantarum* WCFS1 (B) Protein size (aa) corresponds to the precursor with its exportation signal-peptide. SH3b-like domain structures were predicted by Phyre 2.0 (www.sbg.bio.ic.ac.uk/phyre2/). (C) Alignment of conserved regions of NlpC/P60 domains that contain the essential residues for catalysis (Cys, His, Asp; boxed). NlpC/P60 endopeptidases of *B. subtilis* and *L. plantarum* are indicated in black and red, respectively. (D) Conserved regions between *L. plantarum* LytC, *B. subtilis* YkfC (YkfC_{Bsu}), and *B. cereus* YkfC (YkfC_{Bce}) that are involved in the selection of PG stem peptides ending with L-Ala. Key residues involved in substrate selection (Tyr and Asp) are boxed. Alignments in (C,D) were obtained with PRALINE (<http://www.ibi.vu.nl/programs/praline/www/>).

MATERIALS AND METHODS

Strains, Plasmids, and Growth Conditions

Strains and plasmids used in this work are listed in Table 1. Plasmid constructions were performed in *Escherichia coli* (strains AbleK and DH5 α). Functional study of Lyt enzymes was performed in *L. plantarum* NZ7100. *E. coli* strains were grown at 37°C with shaking in LB (LysoGeny Broth) medium and *L. plantarum* strains were grown at 30°C in MRS broth (Difco). When appropriate, antibiotics were added to the medium. Chloramphenicol was used at the concentration of 10 $\mu\text{g ml}^{-1}$ for *E. coli* and *L. plantarum*; and erythromycin was used at the concentration of 250 $\mu\text{g ml}^{-1}$ for *E. coli* and 12.5 $\mu\text{g ml}^{-1}$ for *L. plantarum*.

Nisin and ComS Induction

Nisin A (Sigma Aldrich) was used to induce *P_{nisA}* in the conditional mutants. Conditional mutant strains were cultured overnight in presence of nisin 25 ng ml^{-1} . Then, after dilution at an OD₆₀₀ of 0.1, strains were either not induced or induced with nisin (1 or 25 ng ml^{-1}).

The ComS-inducible system was used for complementation assays and localization of the FtsZ ring (fusion FtsZ-GFP⁺). ComS from *S. thermophilus* (LPYFAGCL) was synthesized by Peptide 2.0 (Chantilly, VA, USA). The dehydrated peptide was suspended in sterile milliQ water at a stock concentration of 100 μM . Complementation strains were diluted at an OD₆₀₀ of 0.1, induced 2 h later with 8 μM of ComS, and observed between 1 h 30 min and 6 h after induction. Strains producing FtsZ-GFP⁺

TABLE 1 | Strains and plasmids used in this study.

Strain/Plasmid	Characteristic(s)*	Reference/source
STRAINS		
<i>Lactobacillus plantarum</i>		
WCFS1	Single isolate of strain NCIMB8826	Kleerebezem et al., 2003
NZ7100	WCFS1 <i>lp_0076::nisRK</i>	Serrano et al., 2007
TR0015	NZ7100, <i>lytB::lox72</i> (Δ <i>lytB</i>)	Rolain et al., 2012
TR006	NZ7100, <i>Cm^R</i> , <i>lytA::lox66-P₃₂-cat-lox71</i> (Δ <i>lytA</i>)	Rolain et al., 2012
TR0016	NZ7100, <i>lytD::lox72</i> (Δ <i>lytD</i>)	Rolain et al., 2012
MCD202	NZ7100, <i>Cm^R</i> , <i>lytA::pGIMCD202</i> , <i>P_{nisA}-lytA</i>	This work
MCD20215	TR0015, <i>Cm^R</i> , <i>lytA::pGIMCD202</i> , Δ <i>lytB</i> <i>P_{nisA}-lytA</i>	This work
MCD203	NZ7100, <i>Cm^R</i> , <i>mreB1::pGIMCD203</i> , <i>P_{nisA}-mreB1CD</i>	This work
MCD206	NZ7100, <i>Cm^R</i> , <i>lytC::pGIMCD206</i> , <i>P_{nisA}-lytC</i>	This work
MCD208	NZ7100, <i>Cm^R</i> , <i>lytC::pGIMCD208</i> , <i>LytC⁻</i>	This work
MCD20616	TR0016, <i>Cm^R</i> , <i>lytC::pGIMCD206</i> , Δ <i>lytD</i> <i>P_{nisA}-lytC</i>	This work
<i>Streptococcus thermophilus</i>		
LMD-9	Wild type	American Type Culture Collection
<i>Escherichia coli</i>		
AbleK	Cloning host, <i>lac</i> (<i>LacZω-</i>) [<i>Kan^r</i> <i>McrA⁻</i> <i>McrCB⁻</i> <i>McrF⁻</i> <i>Mrr⁻</i> <i>HsdR</i> (<i>rK⁻</i> <i>mK⁻</i>)] [<i>F⁺</i> <i>proAB</i> <i>lacF⁺</i> Δ <i>M15</i> <i>Tn10</i> (<i>Tet^r</i>)]], decrease of the copy number of <i>colE1</i> plasmids	Stratagene
DH5 α	Cloning host, <i>F⁻</i> ϕ 80 <i>lacZ</i> Δ M15 Δ (<i>lacZYA-argF</i>)U169 <i>endA1</i> <i>recA1</i> <i>hsdR17</i> (<i>rK⁻</i> <i>mk⁺</i>) <i>phoA</i> <i>supE44</i> <i>thi-1</i> <i>gyrA96</i> <i>relA1</i> λ .	Thermo Fisher Scientific
PLASMIDS		
pSIP409 Derivatives		
pSIP409	<i>Erm^R</i> , low-copy expression vector, <i>rep256</i> , <i>colE1</i> , <i>P_{orfX}::gusA</i>	Sorvig et al., 2005
pSIP103-104	<i>Erm^R</i> , <i>rep256</i> , <i>colE1</i> , <i>gusA</i> , intergenic region between <i>lp0103</i> and <i>lp0104</i>	Desguin et al., 2015
pGIMCD101	<i>Erm^R</i> , <i>rep256</i> , <i>colE1</i> , <i>comR-P_{comS}-gusA</i>	This work
pGIMCD102	<i>Erm^R</i> , <i>rep256</i> , <i>colE1</i> , <i>comR-T_{ldhL}-gusA</i>	This work
pGIMCD106	<i>Erm^R</i> , <i>rep256</i> , <i>colE1</i> , <i>comR-T_{ldhL}-P_{shp0064}-gusA</i>	This work
pGIMCD107	<i>Erm^R</i> , <i>rep256</i> , <i>colE1</i> , <i>comR-T_{ldhL}-P_{shp0064}-MCS</i>	This work
pGIMCD110	<i>Erm^R</i> , <i>rep256</i> , <i>colE1</i> , <i>comR-T_{ldhL}-P_{shp0064}-ftsZ-gfp⁺</i>	This work
pGIMCD113	<i>Erm^R</i> , <i>rep256</i> , <i>colE1</i> , <i>comR-T_{ldhL}-P_{nisA}-gfp⁺</i>	This work
pGIMCD115	<i>Erm^R</i> , <i>rep256</i> , <i>colE1</i> , <i>comR-T_{ldhL}-P_{shp0064}-MCSbis</i>	This work
pGIMCD116	<i>Erm^R</i> , <i>rep256</i> , <i>colE1</i> , <i>comR-T_{ldhL}-P_{nisA}-ftsZ-gfp⁺</i>	This work
pGIMCD117	<i>Erm^R</i> , <i>rep256</i> , <i>colE1</i> , <i>comR-T_{ldhL}-P_{shp0064}-lytA</i>	This work
pGIMCD118	<i>Erm^R</i> , <i>rep256</i> , <i>colE1</i> , <i>comR-T_{ldhL}-P_{shp0064}-lytB</i>	This work
pGIMCD121	<i>Erm^R</i> , <i>rep256</i> , <i>colE1</i> , <i>comR-T_{ldhL}-P_{shp0064}-lytA*</i>	This work
pGIMCD122	<i>Erm^R</i> , <i>rep256</i> , <i>colE1</i> , <i>comR-T_{ldhL}-P_{shp0064}-lytAΔLysM</i>	This work
pGIMCD128	<i>Erm^R</i> , <i>rep256</i> , <i>colE1</i> , <i>comR-T_{ldhL}-P_{shp0064}-lytAΔAST</i>	This work
pGIMCD125	<i>Erm^R</i> , <i>rep256</i> , <i>colE1</i> , <i>comR-T_{ldhL}-P_{shp0064}-lytAΔNlpC/P60</i>	This work
pGIMCD123	<i>Erm^R</i> , <i>rep256</i> , <i>colE1</i> , <i>comR-T_{ldhL}-P_{shp0064}-lytA'-NlpC/P60_{LytB}</i> , swapping of NlpC/P60 domain, <i>LytA-NlpC/P60_{LytB}</i>	This work
pGIMCD132	<i>Erm^R</i> , <i>rep256</i> , <i>colE1</i> , <i>comR-T_{ldhL}-P_{shp0064}-lytBΔNlpC/P60</i>	This work
pGIMCD124	<i>Erm^R</i> , <i>rep256</i> , <i>colE1</i> , <i>comR-T_{ldhL}-P_{shp0064}-lytB'-NlpC/P60_{LytA}</i> , swapping of NlpC/P60 domain, <i>LytB-NlpC/P60_{LytA}</i>	This work
pUC18Cm Derivatives		
pUC18Cm	<i>Cm^R</i> , <i>colE1</i>	V. Ladero, laboratory collection
pGIMCD202	<i>Cm^R</i> , <i>colE1</i> , <i>T_{ldhL}-P_{nisA}-lytA'</i>	This work
pGIMCD203	<i>Cm^R</i> , <i>colE1</i> , <i>T_{ldhL}-P_{nisA}-mreB1'</i>	This work
pGIMCD206	<i>Cm^R</i> , <i>colE1</i> , <i>T_{ldhL}-P_{nisA}-lytC'</i>	This work
pGIMCD208	<i>Cm^R</i> , <i>colE1</i> , <i>'lytC'</i>	This work

(Continued)

TABLE 1 | Continued

Strain/Plasmid	Characteristic(s)*	Reference/source
pGIM008 Derivatives		
pGIM008	Cm ^R , pACYC184 derivative	Palumbo et al., 2006
pGIMCD700	Cm ^R , pGIM008 derivative, T _{Idh}	This work
pGIMCD702	Cm ^R , pGIM008 derivative, T _{Idh} -P _{nisA} -lytA'	This work
pGIMCD703	Cm ^R , pGIM008 derivative, T _{Idh} -P _{nisA} -mreB1'	
pGIMCD706	Cm ^R , pGIM008 derivative, T _{Idh} -P _{nisA} -lytC'	This work
pNZ8048 Derivatives		
pNZ8048	Cm ^R , P _{nisA}	Kuipers et al., 1997
pGIMCD301	Cm ^R , P _{nisA} -gfp ⁺	This work

*Cm^R and Erm^R, resistance to chloramphenicol and erythromycin, respectively.

were diluted at an OD₆₀₀ of 0.1, induced 2 h later as reported above, and shaken for improving GFP⁺ maturation until their observation 2 h later.

Growth Monitoring

Bacteria were cultured overnight in MRS supplemented with antibiotics and inducers when needed, diluted at an OD₆₀₀ of 0.05 in the same medium, and separated in 96-wells plates. The growth was monitored in a multi-plate reader Infinity Pro-200 (Tecan) every 10 min at 600 nm during 12 h.

Microscopy Observations

Cells were collected in exponential phase from MRS cultures (with antibiotics and inducers when needed) and resuspended in PBS buffer. Bacteria were observed on agarose pads composed of 1% agarose PBS buffer for static observations and of 1% agarose MRS for time-lapse observations. Cellular membranes were stained with FM4-64 (Life Technologies) as reported before (Andre et al., 2011). Images were obtained using an Axio I inverted microscope (Zeiss) equipped with an α Plan-Apochromat objective (100 \times /1.46 Oil DIC M27) (Zeiss), a HXP 120 C lighting unit (Zeiss) and C10600 ORCA-R2 camera (Hamamatsu). The fluorescence of FM4-64 and FtsZ-GFP⁺ was respectively detected with filter sets Cy3 (43 HE) and GFP (38 HE), displaying bandpass excitation (nm): 550/25 (Cy3) or 470/40 (GFP) and bandpass emission: 605/70 (Cy3) or 525/50 (GFP) (Zeiss). Images were analyzed using Axiovision 4.8 (Zeiss), MicrobeTracker (Sliusarenko et al., 2011), or MicrobeJ (Ducret et al., 2016).

Profiling of Muropeptides

PG from *L. plantarum* strains was prepared by treating a bacterial pellet with SDS, nucleases, and proteases solutions in order to eliminate all the cellular components except PG, according to a protocol previously described (Courtin et al., 2006). This protocol was slightly modified by applying DNase (50 μ g ml⁻¹) and RNase (50 μ g ml⁻¹) treatments before hydrofluoric acid extraction. PG was digested with mutanolysin from *Streptomyces globisporus* (Sigma-Aldrich). The resulting muropeptides were analyzed by RP-HPLC as previously reported (Courtin et al., 2006). Muropeptides were identified according to their retention

times by comparison to the previously published reference chromatogram for *L. plantarum* PG (Bernard et al., 2011a). In addition, disaccharide-dipeptide (Di) purified from *Lactobacillus casei* (Regulski et al., 2012) was used as standard. The relative abundance (in %) of Di (with or without O-acetylation) was calculated as the ratio of the areas of the two peaks over the sum of the areas of all the identified peaks on the chromatogram.

DNA Manipulations and Transformation

Classical methods of molecular biology were used as previously described (Sambrook et al., 1989). Preparation of electro-competent cells and transformation of *E. coli* and *L. plantarum* were performed as previously reported (Dower et al., 1988; Josson et al., 1989). The Phusion High Fidelity polymerase (NEB) was used for amplification by PCR of inserts used for plasmid constructions. PCR amplifications for validation were performed with the GoTaq polymerase (Promega) in a GeneAmp PCR system (Applied Biosystem). Primers were synthesized by Eurogentec (Belgium) and are listed in **Supplementary Table 1**.

General Strategy for the Construction of Plasmids and Mutant Strains

All expression and disruption plasmids were constructed in *E. coli* before their transfer by electroporation in *L. plantarum*. The correct construction of the vectors was validated by PCR (validation primers in **Supplementary Table 1**) and enzymatic digestion. DNA sequencing was performed to validate the final product (validation primers in **Supplementary Table 1**). Suicide vectors for gene inactivation were recombined by simple homologous recombination into the chromosome of *L. plantarum* as previously described (Palumbo et al., 2004). The conditional mutants contained a 3'-end truncated copy of the targeted gene (inactive, truncation of the NlpC/P60 domain for LytA and LytC) and a second intact copy under the control of the nisin-inducible promoter. The validation of mutant strains was performed by PCR amplification of regions flanking the site of vector integration and sequencing of the PCR product (validation primers in **Supplementary Table 1**).

Construction details of plasmids for conditional/disruption mutants, for complementation, for ComS-inducible expression,

and for expression of truncated/hybrid proteins and FtsZ-GFP⁺ fusion are presented in **Supplementary Text**.

RESULTS

In silico Analysis of NlpC/P60 Endopeptidases From *L. plantarum*

The four D,L-endopeptidases of *L. plantarum* can be separated in two groups based on their modular organization (**Figure 1B**). The first group contains LytA (Lp_3421, 370 aa) and LytB (Lp_2162, 496 aa). In their mature form, these two enzymes contain LysM domain(s) at the N-terminus; a low complexity AST central domain; and a catalytic domain of the NlpC/P60 family (pfam00877) at the C-terminus. The second group is composed of LytC (Lp_2520, 297 aa) and LytD (Lp_1242, 243 aa). These two proteins contain putative SH3b domains in their N-terminal part that were identified by a structural prediction (Phyre 2.0) and an NlpC/P60 catalytic domain at their C-terminus.

All members of the NlpC/P60 family contain three conserved residues involved in catalysis: Cys, His and a polar residue (His, Asp or Gln) (Anantharaman and Aravind, 2003). The alignment of the NlpC/P60 domains of the four *L. plantarum* Lyt enzymes and the 7 *B. subtilis* D,L-endopeptidases showed that Cys and His residues are fully conserved, as well as the third polar residue that is an Asp in this case (**Figure 1C**). The 3D structure prediction of the four Lyt catalytic domains suggests that the three conserved catalytic residues are in close proximity (**Supplementary Figure 1A**), consistent with their contribution to catalysis. Interestingly, LytC and LytD displayed a modular organization, which is similar to YkfC of *B. subtilis* and *Bacillus cereus* (Xu et al., 2010, 2015). Although YkfC of *B. subtilis* has been proposed to be intracellular due to the absence of a predicted signal-sequence, the *B. cereus* enzyme is predicted to be extracellular (Xu et al., 2010), as for LytC and LytD. YkfC is a γ -D-Glu-meso-DAP endopeptidase specific for PG peptides with free N-terminal L-Ala, suggesting a role in PG peptide recycling (Schmidt et al., 2001; Xu et al., 2010). Some NlpC/P60 endopeptidases were identified as recycling enzymes based on the presence of two conserved residues: an aspartate in their active site and a tyrosine at the junction between catalytic and SH3 PG-binding domains, which both restrict the access of the catalytic site to short PG peptides (Xu et al., 2015). Interestingly, LytC is the sole Lyt enzyme that contains these two conserved residues (**Figure 1C**). We also examined the phylogenetic proximity of NlpC/P60 domains between the D,L-endopeptidases of *L. plantarum* and *B. subtilis* (**Supplementary Figure 1B**). Interestingly, LytC clustered with YkfC while LytD clustered with the conjugation-related CwlT autolysin. In addition, the NlpC/P60 domains of LytA and LytB form a separate group, while LytE, LytF, CwlS, and CwlO involved in morphogenesis cluster altogether (**Supplementary Figure 1B**).

Finally, the accessory domains of LytA and LytB display interesting features compared to the morphogenic D,L-endopeptidases of *B. subtilis*. Both enzymes contain a central

AST domain of a different size (186 and 250 aa, respectively), which is predicted to be unstructured. Both domains were shown to be O-glycosylated, suggesting a regulation mechanism of the enzyme activity or stability (Fredriksen et al., 2013; Rolain et al., 2013). LytA and LytB also contain a lower number of LysM domains (i.e., 1 or 2) compared to the morphogenic endopeptidases of *B. subtilis* (i.e., 3–5) (**Figures 1A,B**). The LysM domain is a well-established PG-binding domain in PGHs that recognizes the GlcNAc – X – GlcNAc motif of PG glycan strands (Visweswaran et al., 2011; Mesnage et al., 2014). Interestingly, the LysM domains from LytA and LytB have different isoelectrical points (IP). The single LysM of LytA is basic (IP of 8.34) as found for LysM domains of *B. subtilis* D,L-endopeptidases (IP comprised between 9.22 and 10.14) while the two LysM of LytB are in the acidic range (IPs of 5.43 and 5.18). As the ability of LysM domains to bind PG is linked to their IP (Visweswaran et al., 2011), this could indicate that LytA and LytB bind PG under different pH conditions.

LytC and LytD Are Not Involved in Morphogenesis

In the first part of this work, we investigated the role of the putative D,L-endopeptidases LytC and LytD. A conditional mutant containing a chromosomal copy of the *lytC* gene under the control of the nisin-inducible promoter (*P_{nisA}-lytC* fusion) was constructed. Growth and cell morphology of the mutant strain was monitored in the absence of the nisin inducer (N0). The mutant strain did not show any obvious difference compared to the WT (strain NZ7100) (**Supplementary Figure 2**). Similar results were obtained for a mutant in which the chromosomal copy of *lytC* was disrupted by single crossover with a suicide plasmid carrying an internal fragment of the gene (data not shown). The stable deletion of *lytD* (Δ *lytD*) has previously been obtained (Rolain et al., 2012). The phenotype of the mutant strain was reinvestigated regarding growth and cell morphology. As previously reported, it was indistinguishable from the WT (**Supplementary Figure 2**; Rolain et al., 2012). Since LytC and LytD may have redundant functions due to their similar organization (**Figure 1B**), a double *lytC lytD* mutant was also constructed. Again, this mutant grown in absence of nisin behaved as the WT (**Supplementary Figure 2**).

Altogether, these data indicate that LytC and LytD are not involved in *L. plantarum* morphogenesis under the tested conditions.

LytA Is a Major Peptidoglycan Hydrolase in Cell Morphogenesis

We previously reported the construction of a stable *lytA* null mutant (Δ *lytA*) (Rolain et al., 2012). The cell morphology of this mutant was strongly affected, with round and aggregated cells instead of rod-shaped and well-separated cells observed for wild type (WT) cells (**Figure 2A**). In addition, this mutant displayed a growth defect and cannot be transformed to perform further analyses such as complementation studies (Rolain et al., 2012). For these reasons, we decided to construct a conditional *lytA* mutant by placing the chromosomal

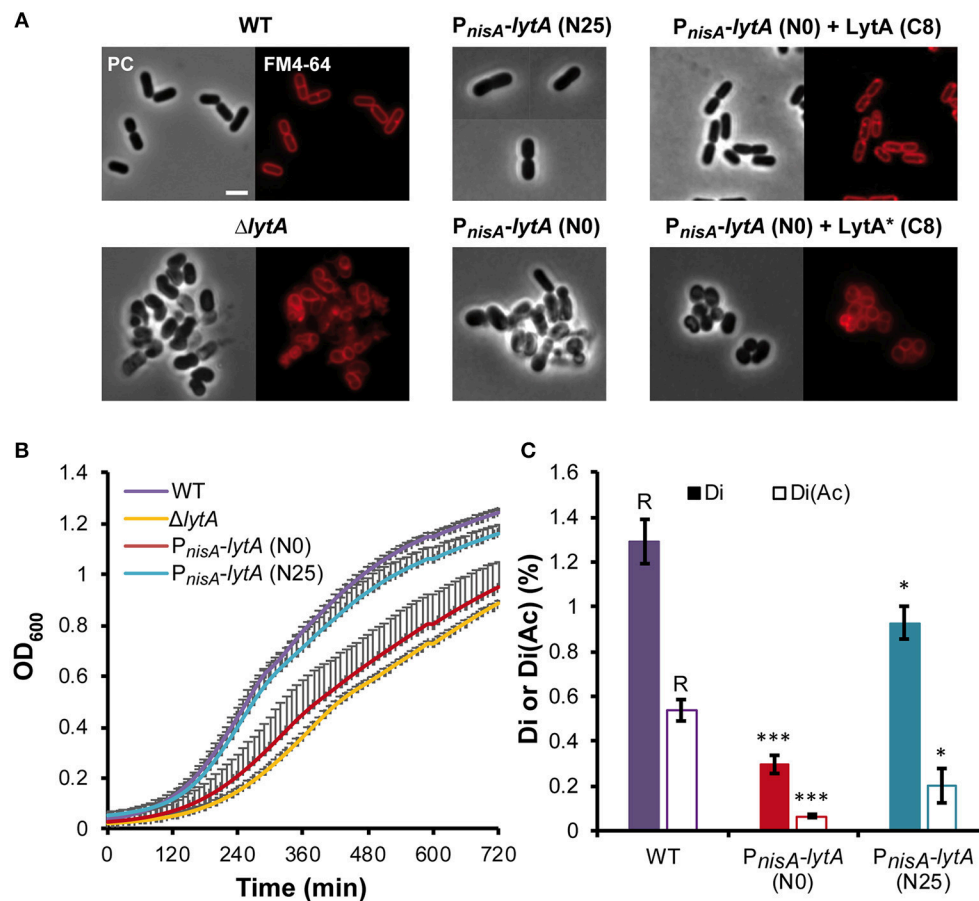


FIGURE 2 | Effect of LytA deficiency on cell morphology, growth, and PG composition. **(A)** Images of *L. plantarum* cells obtained by phase contrast (PC) microscopy and epifluorescence microscopy for membrane labeling with FM4-64. Left panel, WT and $\Delta lytA$ mutant; middle panel, conditional $P_{nisA-lytA}$ mutant without (N0) or with nisin 25 ng ml⁻¹ (N25); right panel, complementation of $P_{nisA-lytA}$ mutant with LytA ($P_{shp0064-lytA}$; + LytA) and a catalytic mutant of LytA ($P_{shp0064-lytA^*}$; + LytA*), grown without nisin (N0) in presence of ComS (8 μ M, C8). Cells were collected in exponential phase from MRS cultures (with chloramphenicol when needed) and observed on agarose pads after suspension in PBS. Similar observations were obtained from at least 3 independent experiments. The scale bar is 2 μ m. **(B)** Growth curves of WT, $\Delta lytA$ mutant, and $P_{nisA-lytA}$ mutant (N0 and N25) in MRS medium. Curves were generated from triplicates (mean values + standard deviations). **(C)** Percentage of disaccharides-dipeptides without and with *O*-acetylation (Di and Di+Ac, respectively) in the PG of WT and $P_{nisA-lytA}$ mutant (N0 and N25) after mutanolysin digestion. Mean values of three independent extractions \pm standard deviations. Significance with respect to the WT (R, reference) is based on Student's *t*-test. **P* < 0.05 and ****P* < 0.001, respectively.

copy of *lytA* under the control of P_{nisA} ($P_{nisA-lytA}$ fusion). In absence of nisin (N0), cell morphology and growth of this conditional mutant strain was similar to the stable $\Delta lytA$ mutant (Figures 2A,B). Under nisin induction (25 ng ml⁻¹, N25), the strain recovered a WT phenotype regarding growth and morphology, except for a slightly larger diameter (Figures 2A,B).

The conditional mutant strain was complemented by a copy of *lytA* expressed under the control of the ComS-inducible system ($P_{shp0064-lytA}$ fusion) carried by a low copy number plasmid (see Supplementary Text for details on the ComS-inducible system). In the presence of the inducer peptide ComS (8 μ M; C8), the LytA-depleted strain recovered the WT rod-shaped morphology (Figure 2A). In addition, we showed that LytA activity is crucial since complementation with a catalytic inactive mutant of LytA

[Cys₂₈₄ to Ala (Figure 1C); named LytA*] was unable to restore the WT rod-shaped morphology (Figure 2A).

Previous analyses of PG extracted from the $\Delta lytA$ mutant suggested that LytA was cleaving the bond between D-Glu and *meso*-DAP in the peptide side chains of the PG network (Rolain et al., 2012). To further correlate the observed morphological phenotypes with LytA activity, analyses of PG composition were performed in triplicates for the conditional mutant strain ($P_{nisA-lytA}$) in presence or absence of nisin (Figure 2C, Supplementary Figure 3, and Supplementary Table 2). PG analysis of the WT strain showed that the pool of disaccharides with two amino acids [GlcNAc-MurNAc-L-Ala-D-Glu with and without *O*-acetylation, (Di and Di+Ac, respectively)], which are potential products of D,L-endopeptidase activity on PG stem peptides, represents 1.83%

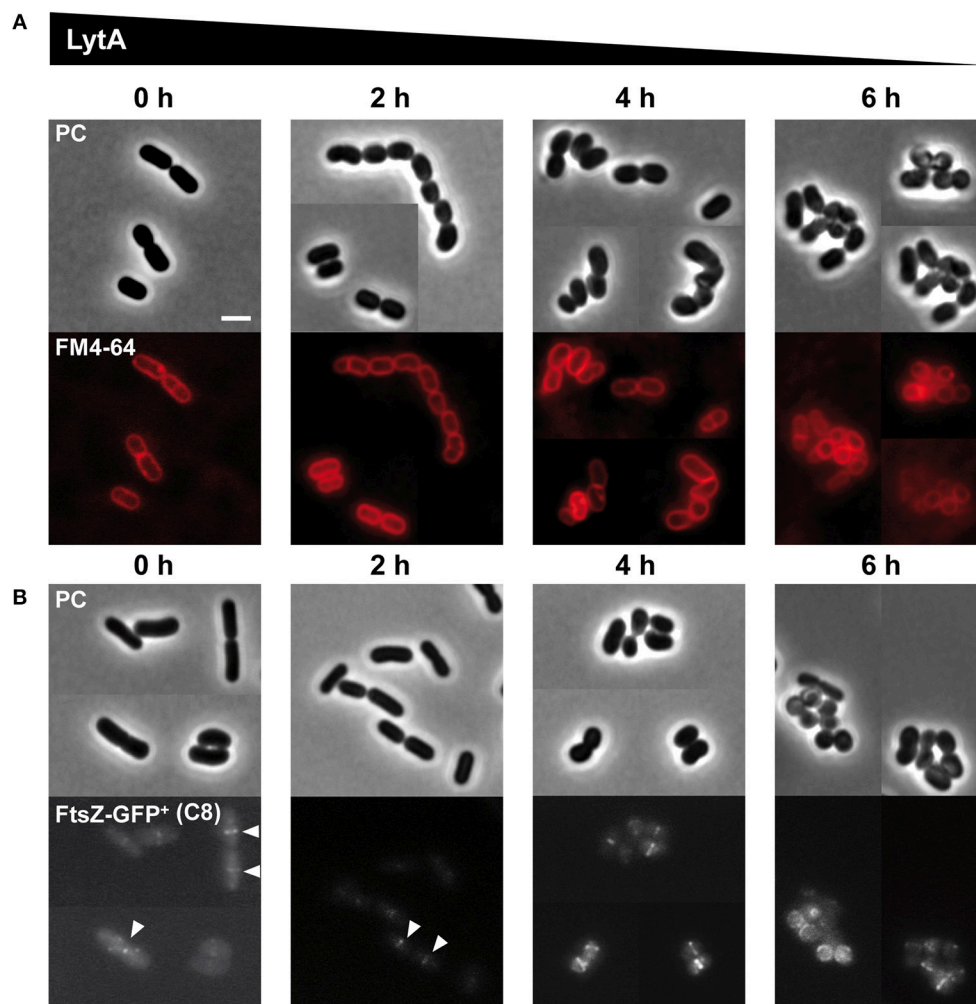


FIGURE 3 | Effect of progressive LytA depletion on cell morphology and division site positioning. **(A)** P_{nisA} -*lytA* mutant cells observed during nisin depletion (0, 2, 4, 6 h) by phase contrast (PC) microscopy and FM4-64 staining. The scale bar is 2 μ m. **(B)** P_{nisA} -*lytA* mutant cells expressing an FtsZ-GFP⁺ fusion ($P_{shp0064}$ -*ftsZ-gfp*⁺; + FtsZ-GFP⁺) observed during nisin depletion (0, 2, 4, 6 h) by phase contrast (PC) microscopy and epifluorescence microscopy for the localization of FtsZ-GFP⁺. White arrows indicate Z-rings in normal rod-shaped cells. Bacteria were cultured in MRS with erythromycin and chloramphenicol, and induced with ComS (8 μ M, C8). Cultures were moderately shaken after ComS induction. The scale bar is 2 μ m. For **(A,B)**, similar observations were obtained from at least two independent experiments.

of total soluble muropeptides. For the nisin-depleted strain (N0), the combined amount of Di and Di+Ac was 5-fold lower (0.37%), consistent with a lower production of LytA. When the conditional mutant strain was cultured in the presence of nisin (25 ng ml⁻¹, N25), the combined amount of Di and Di+Ac was 3-fold higher (1.13%) than in non-induced conditions, reaching a level close to the WT but remaining slightly lower. These data strongly suggest that LytA is a γ -D-Glu-*meso*-DAP endopeptidase that cleaves the bond between D-Glu and *meso*-DAP in the PG meshwork, and that its absence or decreased activity significantly alter the PG structure.

Altogether, these results demonstrate that LytA is a major PGH of *L. plantarum* morphogenesis and that its endopeptidase activity, more than its physical presence in a PG biosynthetic complex, is required for proper growth and cell cycle progression.

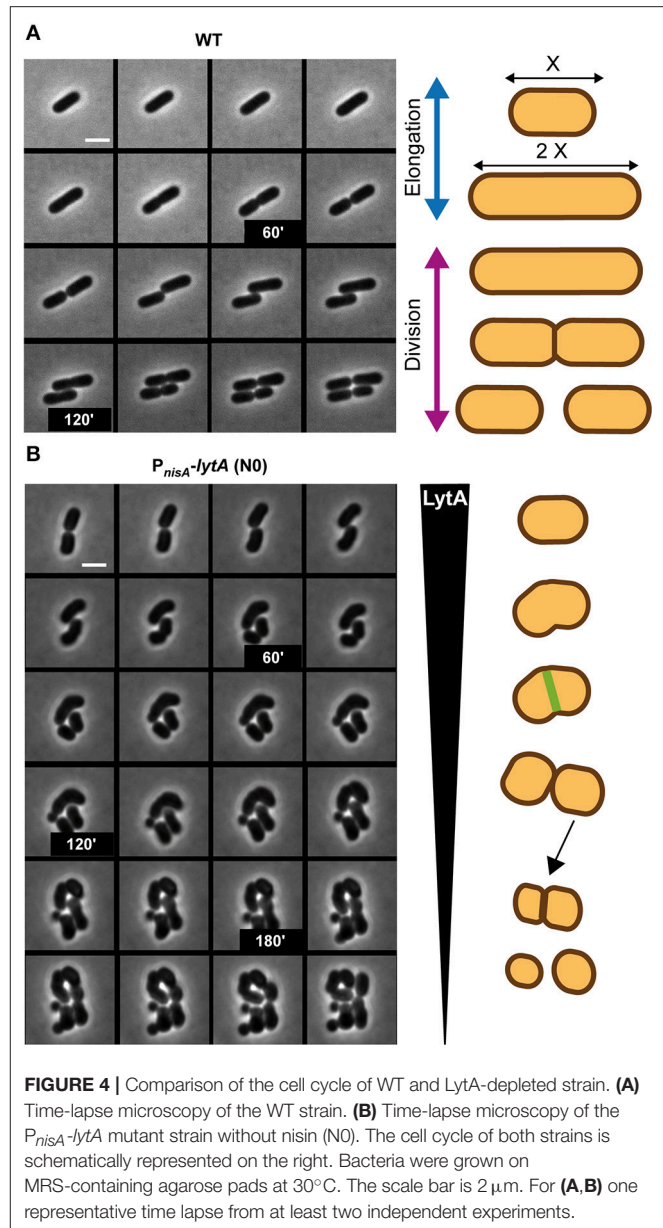
LytA Is Required for Cell Elongation and Septum Positioning

We previously reported that the morphology of the Δ *lytA* mutant was strongly affected with the presence of aggregated round cells of variable diameters and alterations of PG thickness at division sites (Rolain et al., 2012). Here, we used the conditional *lytA* mutant to understand the impact of a progressive depletion of LytA on cell morphogenesis. Cells were first stained with FM4-64 to observe membranes and septum position (**Figure 3A**) or labeled with an FtsZ-GFP⁺ fusion to visualize the divisional Z rings (**Figure 3B**). **Figure 3** shows the degenerative process of the conditional *lytA* mutant taken at different time points after nisin removal. In early steps (0–2 h), cells remained similar to WT, forming chains of rod-shaped bacteria with division planes and Z rings at mid-cell. After 4 h of depletion, cells formed short

chains of 2–3 deformed cells. Dividing cells started to bend and septa seemed to be placed in an abnormal orientation (**Figure 3**, **Supplementary Figure 4A**). After prolonged depletion (6 h), a large proportion of cells were round and aggregated. Membrane labeling appeared brighter and less homogenous, which may indicate that membrane biogenesis is altered [**Figure 3** (6 h), **Supplementary Figure 5A**]. In round cells, FtsZ does not seem to be correctly localized, forming dots or arcs at the cell periphery (**Figure 3**, 6 h). These observations show that LytA is required for cell elongation. In addition, population analysis showed that more than 70% of dividing cells ($n > 300$) have an altered positioning of the division plane after 6 h of LytA depletion (deviation $>10\%$ from the median position), while only $\sim 10\%$ of WT cells have slightly misplaced septa (a sample of LytA-depleted cells with misplaced septa is shown in **Supplementary Figures 4B**, **5A**). These asymmetrical division events likely account for the round cells of different diameters (**Supplementary Figure 5B**) that were previously reported for the stable $\Delta lytA$ mutant (Rolain et al., 2012). Mispositioning of division sites might be due to an indirect effect resulting from the lack of LytA-mediated PG remodeling activity, or from the absence of elongation.

Morphological alterations during the cell cycle of *lytA*-depleted cells were also followed by time-lapse microscopy. The conditional *lytA* mutant was cultured overnight in the presence of nisin and then diluted on an MRS-containing agarose pad in the absence of the inducer. The cell cycle of the LytA-depleted strain was compared to the cell cycle of the WT strain (**Figure 4**, **Supplementary Movies 1**, **2**). WT cells were shown to elongate until they reached twice their original length and then divided into two daughter cells of equal length (**Figure 4A**). For the LytA-depleted strain, cells started as rod-shaped bacteria and progressively reached the round and aggregated morphology after 2–3 generations (**Figure 4B**, left panel). Before the first division, a short elongation phase was observed but cells never doubled their length. Then, cells started to bend and division occurred like a break in the middle of the cell (V-shaped dividing cells). At the next generation, elongation is inhibited and new daughter cells were generated by asymmetrical division. This resulted in the formation of round cells of different diameters, including mini cells. At the end of the depletion process, only round and aggregated cells were observed due to absence of elongation, misplacement of division sites, and the lack of cell separation.

To get further insight into the role of LytA during the cell cycle, we chose to compare the LytA-depleted phenotype with that obtained from the conditional inactivation of the *mreB1CD* locus whose homolog from *B. subtilis* has been shown to be specifically involved in cell elongation (Formstone and Errington, 2005). To this end, the chromosomal copy of *L. plantarum* *mreB1CD* operon was placed under the control of the nisin-inducible promoter (P_{nisA} -*mreB1CD* fusion). The phenotype of the resulting MerB1CD-depleted cells was observed in time lapse (**Supplementary Figure 6** and **Supplementary Movie 3**). From these observations, it appeared that cells became rapidly unable to elongate, giving rise to small spherical cells after one or two division cycles. This phenotype is not exactly the same as that



observed for the LytA-depleted mutant in which impairment of elongation was accompanied with a defect in septum positioning. Thus, the data suggest that the lack of elongation for the *lytA* mutant is not, by itself, responsible for the mispositioning of the septum.

Altogether, the results demonstrate that LytA is a crucial player of *L. plantarum* cell cycle required for the elongation process. In addition, its absence has probably an indirect effect on the correct placement of the division site.

LytB Plays a Key Role in Septum Maturation and Timing of Division

We previously constructed a stable deletion mutant of *lytB* ($\Delta lytB$) (Rolain et al., 2012). Growth and overall cell morphology

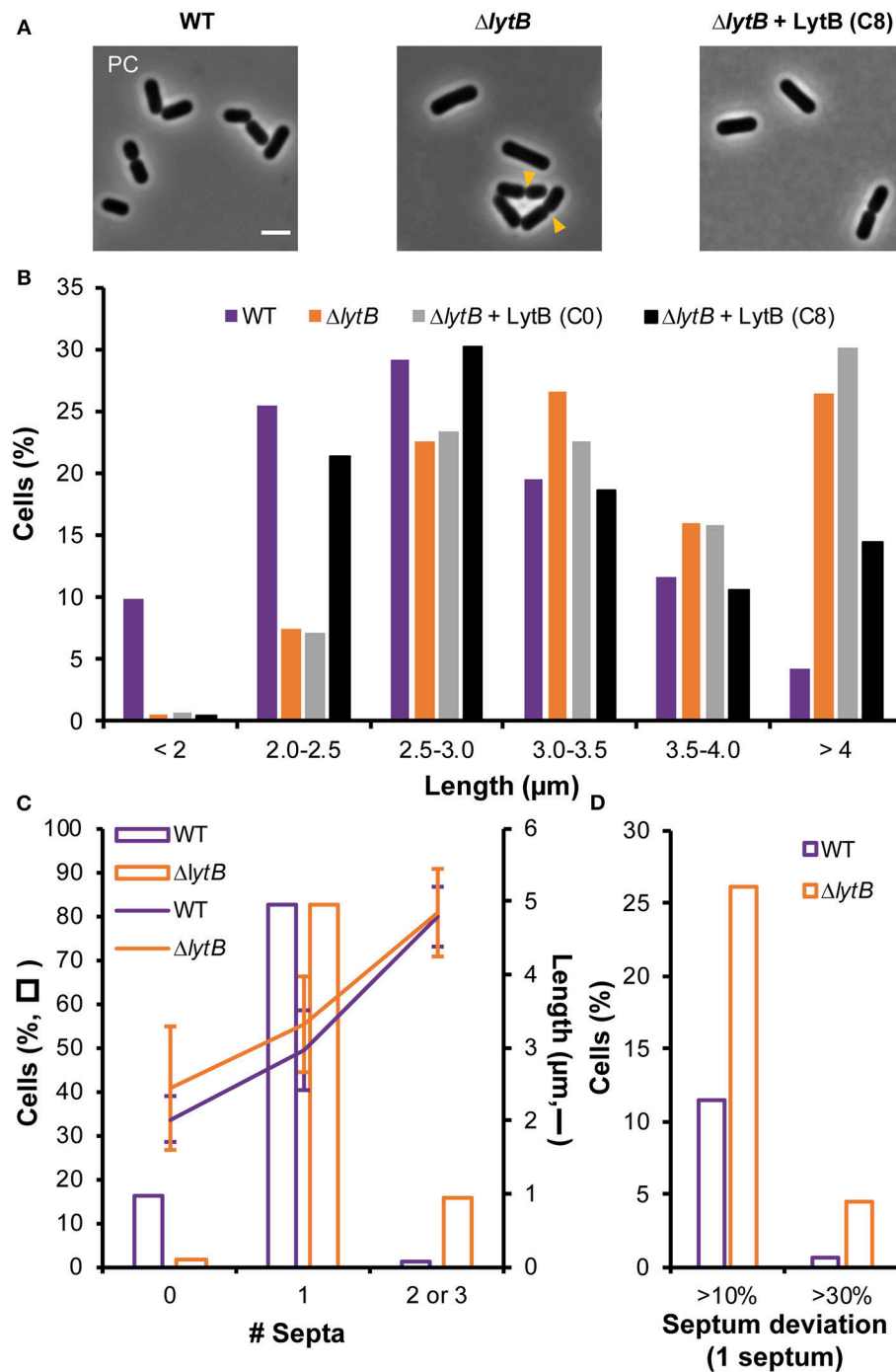


FIGURE 5 | Effect of LytB deficiency and its complementation on cell morphology and division site positioning. **(A)** Images of cells of WT, Δ lytB mutant, and Δ lytB mutant complemented with LytB ($P_{Shp0064}$ -lytB; + LytB) obtained by phase contrast (PC) microscopy. Yellow arrowheads show asymmetrical divisions in Δ lytB mutant cells. Bacteria were grown in MRS with erythromycin and ComS (8 μ M, C8) when needed. Scale bar is 2 μ m. **(B)** Cell length (μ m) of WT, Δ lytB mutant and Δ lytB mutant + LytB without (C0) and with ComS (C8) measured in exponential growth phase. Cells were cultured in MRS with erythromycin and ComS when needed. **(C)** Number of septa (0 to 3; bars) related to cell length (lanes; mean values \pm standard deviations) in WT and Δ lytB mutant cells. **(D)** Relative septum deviation (% of deviation from the median position of cells stained with FM4-64) in mono-septal cells of WT and Δ lytB mutant. For **(B–D)** measures were obtained from triplicates by using MicrobeJ with $n > 500$ cells.

of the mutant were initially reported to be similar to the WT (Figure 5A) (Rolain et al., 2012). However, a more thorough analysis of the cell size revealed that the mutant has a mean

cell length significantly longer than the WT [3.5 ± 0.85 vs. 2.8 ± 0.67 μ m, respectively; mean values \pm standard deviations, $n > 600$ cells from triplicates, Kolmogorov–Smirnov (KS) test, P

< 0.001], with a larger proportion of cells exceeding 4 μm (6-fold) and a lower proportion of cells shorter than 2 μm (16-fold) (**Figure 5B**). For the cell diameter, it remained unchanged in comparison to the WT (0.85 ± 0.12 vs. 0.82 ± 0.13 μm). The ΔlytB mutant was also complemented by a *lytB* copy under the control of the ComS-inducible system ($P_{\text{shp0064-lytB}}$ fusion). In the presence of ComS, the mean cell length of the complemented strain was significantly reduced compared to growth conditions without ComS (3.0 ± 0.80 vs. 3.6 ± 0.70 , respectively; $n > 900$ cells from triplicates, KS test, $P < 0.001$). However, the distribution of length frequencies of the complemented strain compared to the WT showed a partial complementation (**Figure 5B**), suggesting that the amount of LytB is inadequate for a full reversion of the phenotype.

The observed cell length increase in the LytB-deficient strain was correlated with septum positioning using FM4-64 labeling (**Figure 5C**, **Supplementary Figure 7**). LytB-deficient cells that are longer than 4 μm contained 2 or 3 septa (**Figure 5C**). The presence of two septa instead of three in more than 50% of long cells suggests that the formation of septa in daughter cells was not synchronized, while synchronization was observed in the WT (**Supplementary Figure 7**). In addition, lateral septa in WT daughter cells appeared at the end of the constriction of the median septum, while the maturation of the mid-cell septum seemed delayed in LytB-deficient cells (**Supplementary Figure 7**). This delayed maturation in dividing cells was confirmed by examining FtsZ positioning (FtsZ-GFP⁺). In WT, Z rings localized in daughter cells at the end of the constriction of the septum of the mother cell while the migration of Z rings in LytB-deficient cells took place at an earlier stage when maturation of the median septum was largely incomplete (**Supplementary Figure 8**). We also examined the lateral positioning of septa in dividing cells, which was affected in LytB-deficient cells compared to WT cells (**Figure 5D**, **Supplementary Figure 7**). In mono-septal cells, lateral mispositioning of the septum (>10% deviation from the median position) was observed in ~25% of mutant cells, including 5% of cells with major misplacement (>30% of deviation) (**Figure 5D**). In multi-septal cells, a similar situation was observed with numerous lateral misplacements of septa, leading in extreme cases to the production of minicells (**Supplementary Figure 7**). All these observations suggest that LytB is involved in septum maturation and that its absence affects the timing of division and the lateral positioning of the septum.

To further document the role of LytB in cell-cycle dynamics, the ΔlytB mutant was observed by time-lapse microscopy. In **Figure 6**, two behaviors of ΔlytB mutant cells are shown. In the first case (**Figure 6A**, **Supplementary Movie 4**), which is representative of the behavior of many cells, we observed that the cell elongated until it reached 6 μm prior to divide, which is 2 μm longer than the WT at the same pre-divisional state (**Figure 4A**). At the next generation, the daughter cells did not elongate significantly before starting division (**Figure 6A**). In an alternative rarer scenario, the left cell elongated until 5 μm and then a first asymmetrical division occurred, which gave rise to a mini cell (**Figure 6B**, **Supplementary Movie 5**). Then, a second asymmetrical division took place at the opposite pole

in the long daughter cell (**Figure 6B**). From various time-lapse experiments, ~25% of division events were asymmetrical ($n > 100$). In addition, we observed that some small cells stopped to grow and finally lysed, which may explain the lower proportion of short cells (<2 μm) at the whole population level of the ΔlytB mutant (**Figure 5B**, **Supplementary Figure 9**).

While elongation and division are well-separated processes in the WT (**Figure 4A**), the ΔlytB mutant is not able to regulate the timing of division during elongation. In addition, LytB deficiency affects the lateral placement of the division site, which could be asymmetrically localized in short or long cells (**Figure 6B**).

The Combined Inactivation of LytA and LytB Severely Affects Cell Growth

The above results suggest that LytA and LytB play different roles in the cell cycle of *L. plantarum*. This contrasts with the situation of *B. subtilis* where elongation is controlled by two D,L-endopeptidases (i.e., CwlO and LytE) (Dominguez-Cuevas et al., 2013; Meisner et al., 2013). Since LytB does not appear to be a rescuer of LytA, we decided to construct a double *lytA lytB* mutant to determine to what extent their activities interact with each other. Previous attempts to construct a stable mutant deleted for both *lytA* and *lytB* ($\Delta\text{lytB } \Delta\text{lytA}$) failed, which was an indirect indication that the combined presence of LytA and LytB is essential for growth (Rolain et al., 2012). To solve this issue, we transferred the $P_{\text{nisA-lytA}}$ conditional fusion into the ΔlytB mutant. The resulting double mutant ($P_{\text{nisA-lytA}} \Delta\text{lytB}$) was obtained in the presence of nisin. Compared to the singly depleted $P_{\text{nisA-lytA}}$ mutant, the double $P_{\text{nisA-lytA}} \Delta\text{lytB}$ mutant displayed a severe growth defect (**Figure 7A**). No growth of the double mutant was observed during the first 6 h while the simple mutant strain started to grow after 2 h post-inoculation (**Figure 7A**). The retarded growth of the double mutant is likely due to suppressor mutations since the corresponding cells displayed a typical rod-shape morphology (**Figure 7A** and data not shown). These suppressors are probably resulting from a reversion of the nisin-controlled expression system as previously observed for another conditional mutant of an essential gene (alanine racemase) in *L. plantarum* (unpublished data). So, this result indicates that the combined presence of LytA and LytB is (nearly) essential for growth and reinforces the key role played by both enzymes in PG remodeling during the cell cycle.

The cell morphology of the double mutant was then examined after 2 h of nisin depletion. Intriguingly, a mixed situation was observed with round aggregated cells and long cells forming chains, which is reminiscent of either LytA or LytB deficiency, respectively (**Figure 7B**). This mixed phenotype is likely due to cell-to-cell variations in the extent of LytA depletion. We also examined the positioning of septa and FtsZ-GFP⁺ in the double mutant under nisin depletion (**Figures 7B,C**). In the long cells, septa and Z ring-like structures formed perpendicularly to the long axis without being localized at mid-cell. This mispositioning is reminiscent of the abnormalities observed with the simple ΔlytB mutant (see **Figure 6B**). Akin to simple LytA-deficient cells, no clear positioning of FtsZ-GFP⁺ was observed in round cells. To investigate this heterogeneous cell morphology, we

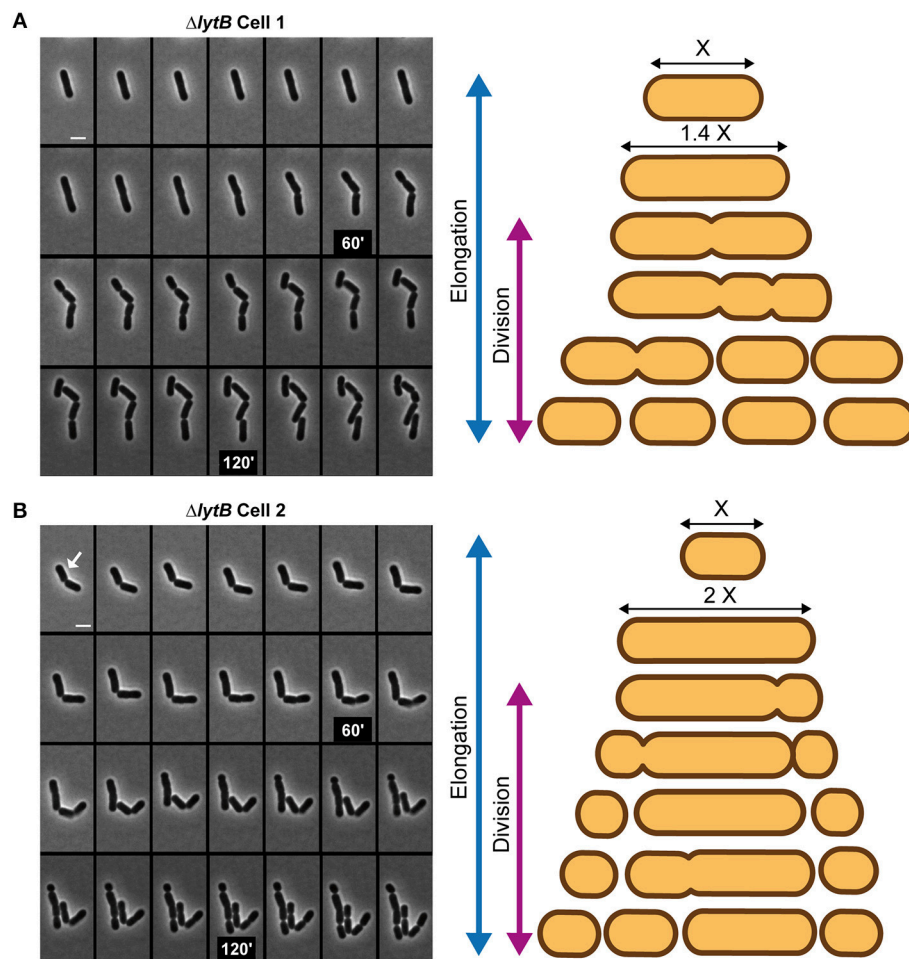


FIGURE 6 | Cell cycle of the LytB-deficient strain. Time-lapse microscopy of $\Delta lytB$ mutant cells showing a deregulation between elongation and division (**A**) and asymmetrical divisions (**B**). In (**B**) the selected cell for the scheme is indicated with a white arrow. Scheme of the cell cycle of two selected cells are displayed on the right. Bacteria were grown on MRS-containing agarose pads at 30°C. The scale bar is 2 μ m.

performed time-lapse experiments (**Supplementary Figure 10** and **Supplementary Movies 6, 7**). At the beginning of the depletion, cells were long and formed chains as found with the $\Delta lytB$ mutant. Then, they became twisted before their separation in round or unshaped cells resembling to LytA-deficient cells (**Supplementary Figure 10**). So, the initial observation of a mixed cell morphology under static conditions likely corresponds to different levels of LytA at the early stages of the depletion process.

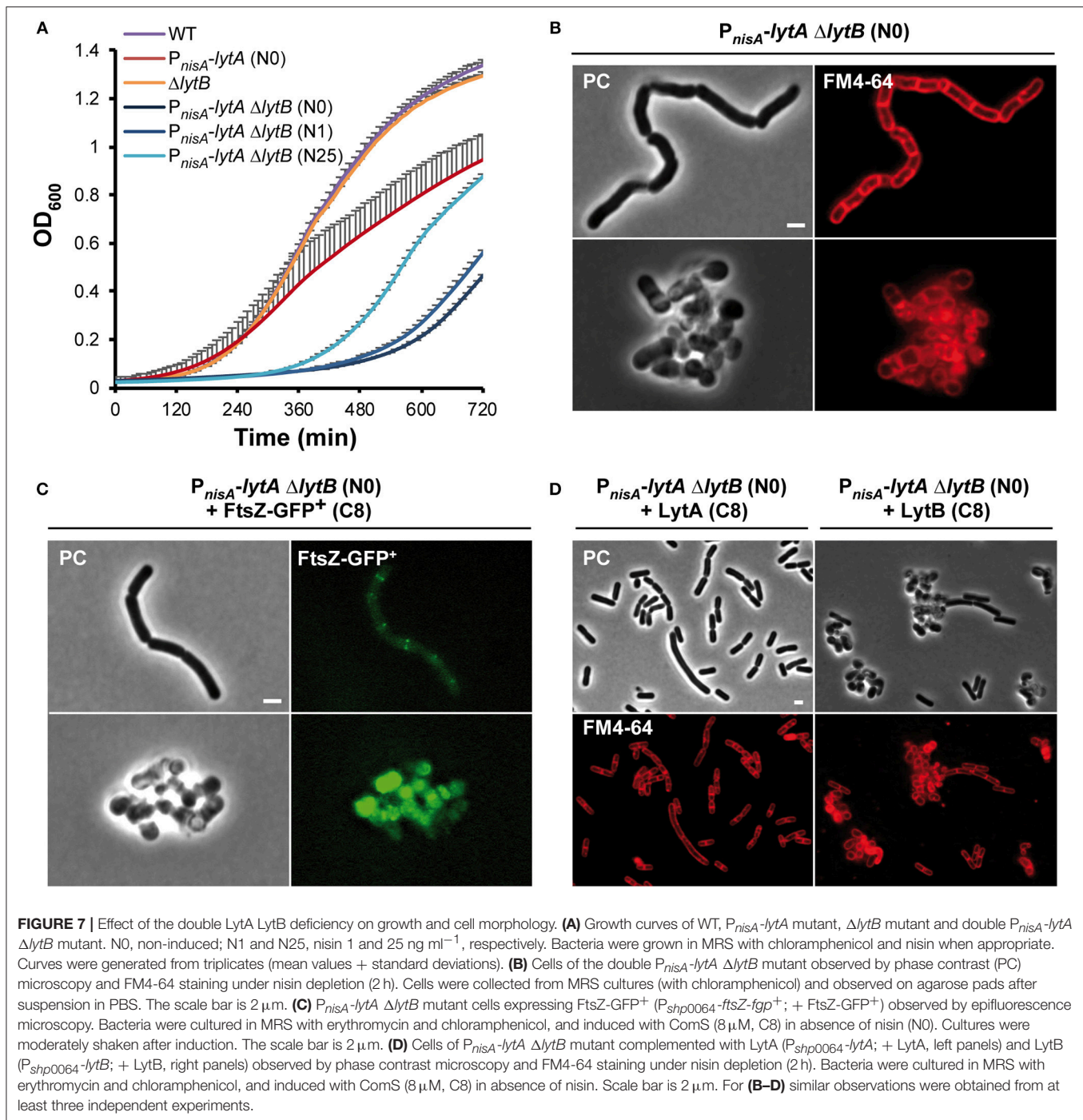
In order to validate that LytA and LytB have no overlapping function, the double P_{nisA} - $lytA$ $\Delta lytB$ mutant was complemented by either $lytA$ or $lytB$. When the double mutant was grown in the presence of ComS to express the complementing partner and under nisin depletion condition, $lytA$ -complemented cells recovered a rod shape but most cells were longer than WT cells (**Figure 7D**, left panels); whereas $lytB$ -complemented cells remained round and aggregated (**Figure 7D**, right panels). In addition, complementation assays of the simple P_{nisA} - $lytA$ mutant (N0) by $lytB$ or the simple $\Delta lytB$ mutant by

$lytA$ did not restore the morphology of WT cells (data not shown). Finally, complementation of the simple P_{nisA} - $lytA$ mutant by chimeric proteins where the catalytic domains (NlpC/P60 domains, see **Figure 1B**) were swapped between both proteins (i.e., LytA-NlpC/P60_{LytB} and LytB-NlpC/P60_{LytA}) revealed that the functionality of the LytA protein mainly relies on its accessory domains (**Supplementary Figure 11**). Indeed, the LytA-NlpC/P60_{LytB} hybrid restored cell elongation while the LytB-NlpC/P60_{LytA} fusion protein did not (**Supplementary Figure 11**).

Taken together, these results show that the combined PG hydrolytic activity of LytA and LytB is of major importance for *L. plantarum* growth. They also demonstrate that LytA and LytB play separate and non-redundant functions during the cell cycle.

DISCUSSION

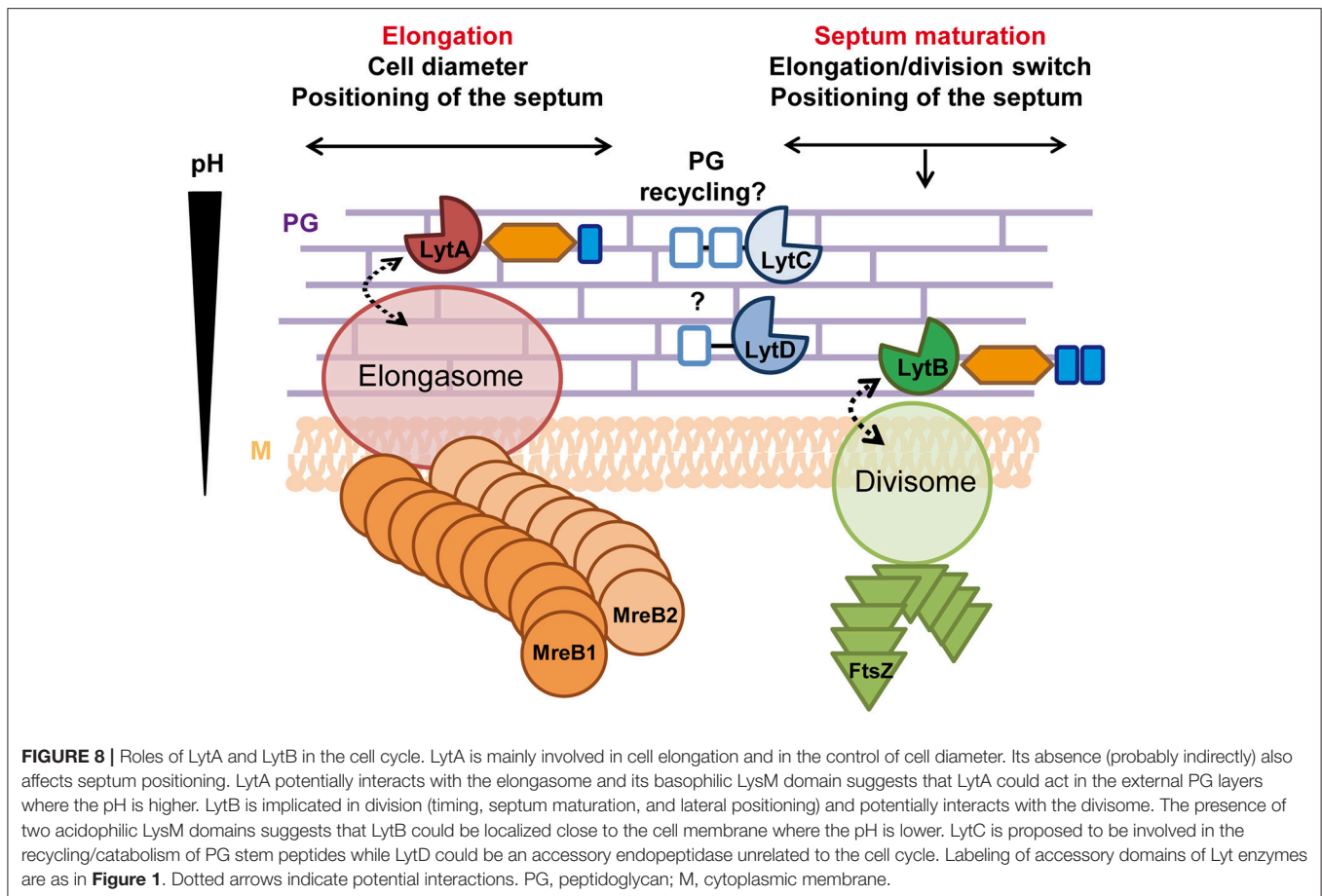
This work shed a new light on our understanding of the roles played by the four NlpC/P60 endopeptidases identified



in *L. plantarum*. While *LytC* and *LytD* do not appear to be involved in morphogenesis, the paralogous *LytA* and *lytB* enzymes play well-separated roles in the cell cycle (Figure 8). We reveal that *LytA* is a key PGH mainly dedicated to cell elongation while *LytB* is involved in the division process. Notably, the synthetic co-inhibition of these two processes showed that they are both important for *L. plantarum* growth.

LytC and LytD Are Not Implicated in Morphogenesis During Standard Growth Conditions

Mutant strains deficient for *LytC* and/or *LytD* did not show any observable defect in growth and cell morphology under the tested conditions (Supplementary Figure 1). *LytC* and *LytD* display a similar structural organization with accessory SH3b PG-binding domains (Figure 1B). Interestingly, *LytC* is predicted to be a



member of the YkfC subfamily of NlpC/P60 D,L-endopeptidases that only hydrolyze the γ -D-Glu-*meso*-DAP bond of free stem peptides ending with L-Ala (tri, tetra and pentapeptides) (Xu et al., 2015). This activity suggests that members of this subfamily are either involved in the recycling of stem peptide fragments for PG biosynthesis or for their catabolism under nutrient deprivation (Schmidt et al., 2001; Xu et al., 2015). While the physiological role of YkfC remains unknown in *B. subtilis*, the expression of its encoded gene seemed to be regulated and specifically induced in late vegetative growth phase (Smith et al., 2000). Similarly, the *lytC* gene was reported to be upregulated by stress conditions (i.e., T^o and NaCl) while the other *lyt* genes were stress-unresponsive (Rolain et al., 2012). In addition, in standard growth conditions, proteomic studies of surface proteins of *L. plantarum* WCFS1 did not reveal the presence of LytC while LytA, LytB and LytD were shown to be produced (Fredriksen et al., 2013). These observations suggest that LytC may play a physiological role in very specific conditions that remain to be determined and could explain the absence of phenotypes regarding growth and morphogenesis in our study.

Intriguingly, the NlpC/P60 domains of LytD and CwlT are closer compared to any other NlpC/P60 domain of *B. subtilis* D,L-endopeptidases (**Supplementary Figure 2B**). CwlT is not involved in the cell cycle as it is involved in the biogenesis of the DNA transfer machinery required for the conjugation of

ICEBs1 (Fukushima et al., 2007). The similarity of LytD with CwlT may indicate its involvement in an accessory process such as predation (e.g., fratricins) or the trans-envelope assembly of a secretion/uptake apparatus as previously reported for some members of the NlpC/P60 family (Xu et al., 2015). It is noteworthy that a range of streptococcal fratricins that are specifically induced during competence development are modular enzymes including SH3 domains and closely-related NlpC/P60 domains (Berg et al., 2012). Based on these *in silico* analyses, additional investigations are thus needed to determine the exact function of LytC and LytD.

LytA Is a Major NlpC/P60 Endopeptidase Involved in the Control of Cell Length

Conditional inactivation of *lytA* and time-lapse experiments revealed its major role in the cell elongation pathway of *L. plantarum* (**Figure 4**). The absence of LytA resulted in elongation arrest together with misplaced septa, leading to unseparated round cells of various sizes (**Figures 3, 4, Supplementary Figures 4, 5**). Interestingly, complementation studies of the conditional *lytA* mutant with LytA variants carrying the LytB NlpC/P60 domain, or deleted of either the LysM domain or the AST domain, showed a recovery of elongation without a restoration of cell width, which indicates an additional implication of LytA in the control of the cell

diameter (Supplementary Figures 11, 12). Moreover, these dramatic alterations of cell shape were more probably due to a lack of the LytA endopeptidase activity, as shown by complementation studies with a LytA catalytic inactive mutant (Figure 2). In addition, alterations of division planes and cell aggregation do not seem to be the consequence of a lack of elongation as the inactivation of MreBCD, a well-known player of elongation in other rod-shaped Gram-positive bacteria only leads to the formation of well-defined round cells in *L. plantarum* (Supplementary Figure 6). In *B. subtilis*, which displays a similar composition of the stem peptide and the same cross-linking (Vollmer et al., 2008a), CwlO and LytE were shown to, respectively control the cell longitudinal axis and cell diameter, being altogether required for the elongation process (Hashimoto et al., 2012; Domínguez-Cuevas et al., 2013; Meisner et al., 2013). Thus, the LytA enzyme of *L. plantarum* seems to recapitulate the combined activity of CwlO and LytE, which might be consistent with a lower level of PGH redundancy in *L. plantarum* (Smith et al., 2000; Rolain et al., 2012). However, an intriguing consequence of the absence of LytA activity is the misplacement of septa (Supplementary Figures 4, 5) and a lack of a clear localization of FtsZ in round cells (Figure 3). Apart from the Min system (Bernard et al., 2012), no positive or negative players regulating the positioning of the divisome have been identified in *L. plantarum*. Our analysis of PG composition suggests that LytA is responsible of the cleavage of most γ -D-Glu-meso-DAP bonds. As products of this hydrolysis represent around 10% of total disaccharides-peptides in the WT profile of muropeptides (Supplementary Table 2), this could indicate that LytA plays an important role in PG remodeling that could indirectly affect either the Min system or unknown players involved in the positioning of the division plane.

LytB Is Involved in Septum Maturation and Timing of Division

Cell measurements, positioning of septa, and time-lapse experiments showed that LytB is a key player in the regulation of cell division in *L. plantarum* (Figure 8). Indeed, LytB-deficient cells displayed heterogeneous lengths with misplaced division sites along the longitudinal cell axis (Figures 5, 6, Supplementary Figures 7, 8). Our results also suggest that the maturation of the septum is delayed as septa/Z-rings are present in daughter cells while the maturation of the mid-cell septum is still ongoing (Supplementary Figures 7, 8). This delayed septum maturation could contribute to the altered timing between elongation and division such as observed in time-lapse experiments (Figure 6). Moreover, the positioning of septa in daughter cells is laterally affected and seems desynchronized as bi-septal long cells were observed (see Supplementary Figures 7, 8). In *B. subtilis*, the individual inactivation of LytE, CwlS or LytE, yields filaments of unseparated cells (Fukushima et al., 2006), a phenotype that is reminiscent of that reported for the LytB inactivation in *L. plantarum*. Similarly, the inactivation of NlpC/P60 endopeptidases of *L. casei* BL23 (Lc-P75) and *L. rhamnosus* GG (P75/Msp1) lead to cell separation defects and cell chaining (Claes et al., 2012; Regulski et al., 2012). However,

the cell-cycle alterations observed for LytB inactivation seem more complex than a mere cell separation defect. By comparison with LytA inactivation, the absence of LytB did not reveal any alteration in the muropeptide profile compared to the WT (data not shown), which is compatible with a specific role of LytB in PG remodeling (e.g., septum maturation). In addition, we cannot exclude that LytB is intimately associated to the division machinery with a structural role. This could indirectly affect the synchronization and placement of division planes in daughter cells. Alternatively, a local remodeling of PG architecture by LytB could provide a specific signature important for the anchoring of early players and the correct placement of the division machinery. Intriguingly, cell-cycle alterations due to LytB depletion are reminiscent of those previously reported for the MurNac O-acetyl-transferase mutant of *L. plantarum* (OatA⁻) (Bernard et al., 2011a, 2012). As for LytB, the absence of OatA led to an altered timing between division and elongation while OatA overproduction resulted in misplaced septa (Bernard et al., 2012). This suggests that OatA and LytB might contribute to the same process. It is tempting to speculate that PG O-acetylation might locally disturb PG hydrolysis, for example, by affecting LysM-mediated binding of LytB to its substrate. Local PG O-acetylation and PG hydrolysis at mid-cell could in turn act as a cue for the initiation of cytokinesis.

Co-inactivation of LytA and LytB Leads to a Synthetic Growth Defect

Interestingly, co-inactivation of LytA and LytB severely affects growth, which might indicate a synthetic lethality (Figure 7). Time-lapse experiments of LytA depletion in the LytB-deficient strain clearly showed that LytA and LytB are involved in two separate processes (Supplementary Figure 10) since the cell morphology defect results in an evolving mixed phenotype with a dominance of LytA over LytB regarding cell shape alteration. In addition to a lack of cell elongation due to LytA deficiency, LytA is also involved in the correct positioning of the septum in round cells. Consequently, the combination of a second defect in the division process due to LytB inactivation (i.e., delayed septum maturation and altered selection of the division site) may thus explain the synthetic effect of a double mutation. It is well-established that rod-shaped cells can tolerate a defect in cell elongation but are much more sensitive to alterations in cell division (Szwedziak and Löwe, 2013). This severe growth defect is also reminiscent of the co-lethality observed for the co-inactivation of LytE and CwlO in *B. subtilis* (Hashimoto et al., 2012). In this case, while both LytE and CwlO are required for cell elongation, LytE is also involved in cell separation (Domínguez-Cuevas et al., 2013). Thus, the synthetic effect of LytA-LytB deficiency on growth in *L. plantarum* reinforces the essential role played by D,L-endopeptidases of the NlpC/P60 family during the cell cycle of rod-shaped Gram-positive bacteria.

How Are LytA and LytB Controlled?

Bacillus subtilis contains three actin-like cytoskeleton proteins (i.e., MreB, MreBH, and Mbl) that are involved in the control of cell elongation. The activity of the LysM-containing enzyme LytE was proposed to be guided by MreBH (and possibly MreB)

while the activity of the coiled-coil domain-containing enzyme CwlO was proposed to be associated to Mbl (Domínguez-Cuevas et al., 2013; Meisner et al., 2013). In addition, CwlO was shown to be under the control of the ABC transporter FtsEX, the latter being required for cell elongation in *B. subtilis* as opposed to cell division in *E. coli* (Yang et al., 2011; Domínguez-Cuevas et al., 2013; Meisner et al., 2013). PGHs (e.g., PcsB of *Streptococcus pneumoniae*) or PGH adaptor proteins (e.g., EnvC in *E. coli*) that are controlled by the FtsEX complex contain at least one coiled-coil domain that directly interacts with the surface-exposed FtsX protein (Sham et al., 2011; Yang et al., 2011). A similar interaction has been proposed between CwlO and FtsX (Domínguez-Cuevas et al., 2013). Intriguingly, none of the 12 putative PGHs of *L. plantarum* contains predicted coiled-coil domain (COILS prediction tool, <https://toolkit.tuebingen.mpg.de/#/tools/pcoils>). Moreover, no canonical FtsEX could be identified in the *L. plantarum* genome based on a search of conserved domains COG2884 and COG2177 for FtsE and FtsX, respectively. This suggests that LytA and/or LytB might be controlled by another mechanism or different players.

In this work, we also performed complementation experiments of the *lytA* mutant with chimeric proteins (i.e., LytA-NlpC/P60_{LytB} and LytB-NlpC/P60_{LytA}). The results showed that the accessory domains predominates over the catalytic domain to confer their specific function to the Lyt enzymes (Supplementary Figure 11). In various LysM-containing PGHs, it has been shown that deletion of LysM domain(s) leads to less active or even inactive enzymes (Steen et al., 2005; Layec et al., 2009; Frankel and Schneewind, 2012). In addition, it was observed that the number of LysM domains per PGH (cooperative binding) and their IPs play a major role in their PG-binding capacity (Visweswaran et al., 2011). The presence of one LysM domain with a basic IP in LytA compared to two LysM domains with acidic IPs in LytB may indicate that the LysM domain of LytA have a lower PG-binding capacity in vicinity of the cell membrane, which is more acidic compared to external PG layers (Jolliffe et al., 1981). In this case, LytA would be able to bind PG and be more active in external layers of the cell wall, where PG is more stretched and its hydrolysis required for cell elongation (Figure 8; Lee and Huang, 2013). Conversely, the presence of acidophilic LysM domains in LytB suggests that it could be active in close proximity with the cell membrane, which would be compatible with its role in the maturation and the positioning of the septum.

The roles of the glycosylated AST domains of LytA and LytB remains unexplored. In the Acm2 glucosaminidase of *L. plantarum*, the AST domain and more specifically its glycosyl residues were shown to negatively impact on the enzymatic activity (Rolain et al., 2013). The purification of glycosylated and non-glycosylated variants of LytA and LytB was attempted in different hosts but were unsuccessful so far (data not shown). Besides a direct impact on enzymatic activity, AST-related PGH domains were hypothesized to be involved in subcellular targeting (Huard et al., 2003; Eckert et al., 2006; Claes et al., 2012; Lebeer et al., 2012; Regulski et al., 2012). For instance, the AST domains of LytA or LytB and their glycolytic

decorations might interact with other cell-cycle proteins in order to associate LytA and/or LytB to specific complexes of cell wall biosynthesis.

AUTHOR CONTRIBUTIONS

PH, BH, M-PC-C, and YD conceived and designed the study. M-CD, TR, PC, and AK carried out the laboratory work. M-CD, PC, PH, BH, M-PC-C, and YD analyzed the data. M-CD, PH, and BH wrote the manuscript. All authors read and approved the final manuscript.

FUNDING

Work in the teams of PH, BH, and YD was supported by the National Foundation for Scientific Research (FNRS) and the Research Department of the Communauté française de Belgique (Concerted Research Action). Work in the team of M-PC-C was supported by INRA and Région Ile de France. M-CD and TR held a doctoral fellowship from FRIA. YD and PH are Research Director and Senior Research Associate of the FNRS.

ACKNOWLEDGMENTS

We are grateful to Dr. Johann Mignolet for his critical reading of the manuscript. We warmly thank Hervé Degand and Sylvie Derclaye for their technical assistance.

SUPPLEMENTARY MATERIAL

The Supplementary Material for this article can be found online at: <https://www.frontiersin.org/articles/10.3389/fmicb.2019.00713/full#supplementary-material>

Supplementary Text | Construction of strains and plasmids.

Supplementary Figure 1 | Structural prediction and phylogenetic relationships of NlpC/P60 catalytic domains.

Supplementary Figure 2 | Impact of LytC and LytD depletion on cell morphology and growth.

Supplementary Figure 3 | RP-HPLC separation of mucopeptides from *L. plantarum* WT and P_{nlsA}-*lytA* mutant (without, N0; and with nisin, N25).

Supplementary Figure 4 | Effect of LytA depletion on septum misplacement in dividing cells.

Supplementary Figure 5 | Effect of LytA depletion on septum misplacement in cell aggregates.

Supplementary Figure 6 | Cell cycle of the MreB1CD-deficient strain.

Supplementary Figure 7 | Effect of LytB inactivation on septum misplacement in dividing long cells.

Supplementary Figure 8 | Effect of LytB inactivation on Z rings positioning.

Supplementary Figure 9 | Time-lapse microscopy of Δ *lytB* mutant cells showing lysis of small non-growing cells.

Supplementary Figure 10 | Cell cycle of the double LytA LytB deficient strain.

Supplementary Figure 11 | Importance of accessory LytA domains for its morphogenic function.

Supplementary Figure 12 | Effect of the individual deletion of *LytA* domains on cell morphology.

Supplementary Table 1 | Primers used in this study.

Supplementary Table 2 | Disaccharide (Ds)-peptide composition of PG from *L. plantarum* WT and *P_{nlsA}-lytA* mutant (without, N0; and with nisin, N25).

Supplementary Movie 1 | Cell cycle of the WT (NZ7100).

Supplementary Movie 2 | Cell cycle of the conditional *lytA* mutant (MCD202, N0).

Supplementary Movie 3 | Cell cycle of the conditional *mreB1CD* mutant (MCD203, N0).

Supplementary Movie 4 | Cell cycle of the Δ *lytB* mutant (TR0015), Cell 1.

Supplementary Movie 5 | Cell cycle of the Δ *lytB* mutant (TR0015), Cell 2.

Supplementary Movie 6 | Cell cycle of the double *LytA-LytB* deficient strain (MCD20215, N0), Cell 1.

Supplementary Movie 7 | Cell cycle of the double *LytA-LytB* deficient strain (MCD20215, N0), Cell 2.

REFERENCES

- Anantharaman, V., and Aravind, L. (2003). Evolutionary history, structural features and biochemical diversity of the NlpC/P60 superfamily of enzymes. *Genome Biol.* 4:R11. doi: 10.1186/gb-2003-4-2-r11
- Andre, G., Deghorain, M., Bron, P. A., van Swam, I. I., Kleerebezem, M., Hols, P., et al. (2011). Fluorescence and atomic force microscopy imaging of wall teichoic acids in *Lactobacillus plantarum*. *ACS Chem. Biol.* 6, 366–376. doi: 10.1021/cb1003509
- Barrett, J. F., Dolinger, D. L., Schramm, V. L., and Shockman, G. D. (1984). The mechanism of soluble peptidoglycan hydrolysis by an autolytic muramidase. A processive exodisaccharidase. *J. Biol. Chem.* 259, 11818–11827.
- Berg, K. H., Bjørnstad, T. J., Johnsborg, O., and Håvarstein, L. S. (2012). Properties and biological role of streptococcal fratricins. *Appl. Environ. Microbiol.* 78, 3515–3522. doi: 10.1128/AEM.00098-12
- Bernard, E., Rolain, T., Courtin, P., Guillot, A., Langella, P., Hols, P., et al. (2011a). Characterization of O-acetylation of N-acetylglucosamine: a novel structural variation of bacterial peptidoglycan. *J. Biol. Chem.* 286, 23950–23958. doi: 10.1074/jbc.M111.241414
- Bernard, E., Rolain, T., Courtin, P., Hols, P., and Chapot-Chartier, M. P. (2011b). Identification of the amidotransferase AsnB1 as being responsible for meso-diaminopimelic acid amidation in *Lactobacillus plantarum* peptidoglycan. *J. Bacteriol.* 193, 6323–6330. doi: 10.1128/JB.05060-11
- Bernard, E., Rolain, T., David, B., André, G., Dupres, V., Dufrêne, Y. F., et al. (2012). Dual role for the O-acetyltransferase OatA in peptidoglycan modification and control of cell septation in *Lactobacillus plantarum*. *PLoS ONE* 7:e47893. doi: 10.1371/journal.pone.0047893
- Carballido-López, R., Formstone, A., Li, Y., Ehrlich, S. D., Noirot, P., and Errington, J. (2006). Actin homolog MreBH governs cell morphogenesis by localization of the cell wall hydrolase *LytE*. *Dev. Cell* 11, 399–409. doi: 10.1016/j.devcel.2006.07.017
- Claes, I. J., Schoofs, G., Regulski, K., Courtin, P., Chapot-Chartier, M. P., Rolain, T., et al. (2012). Genetic and biochemical characterization of the cell wall hydrolase activity of the major secreted protein of *Lactobacillus rhamnosus* GG. *PLoS ONE* 7:e31588. doi: 10.1371/journal.pone.0031588
- Courtin, P., Miranda, G., Guillot, A., Wessner, F., Mézange, C., Domakova, E., et al. (2006). Peptidoglycan structure analysis of *Lactococcus lactis* reveals the presence of an L,D-carboxypeptidase involved in peptidoglycan maturation. *J. Bacteriol.* 188, 5293–5298. doi: 10.1128/JB.00285-06
- Deghorain, M., Goffin, P., Fontaine, L., Mainardi, J. L., Daniel, R., Errington, J., et al. (2007). Selectivity for D-lactate incorporation into the peptidoglycan precursors of *Lactobacillus plantarum*: role of Aad, a VanX-like D-alanyl-D-alanine dipeptidase. *J. Bacteriol.* 189, 4332–4337. doi: 10.1128/JB.01829-06
- Delcour, J., Ferain, T., Deghorain, M., Palumbo, E., and Hols, P. (1999). The biosynthesis and functionality of the cell-wall of lactic acid bacteria. *Antonie Van Leeuwenhoek* 76, 159–184. doi: 10.1023/A:1002089722581
- Desguin, B., Goffin, P., Bakouche, N., Diman, A., Viaene, E., Dandoy, D., et al. (2015). Enantioselective regulation of lactate racemization by LarR in *Lactobacillus plantarum*. *J. Bacteriol.* 197, 219–230. doi: 10.1128/JB.02192-14
- Domínguez-Cuevas, P., Porcelli, I., Daniel, R. A., and Errington, J. (2013). Differentiated roles for MreB-actin isoforms and autolytic enzymes in *Bacillus subtilis* morphogenesis. *Mol. Microbiol.* 89, 1084–1098. doi: 10.1111/mmi.12335
- Dower, W. J., Miller, J. F., and Ragsdale, C. W. (1988). High efficiency transformation of *E. coli* by high voltage electroporation. *Nucleic Acids Res.* 16, 6127–6145. doi: 10.1093/nar/16.13.6127
- Ducet, A., Quardokus, E. M., and Brun, Y. V. (2016). MicrobeJ, a tool for high throughput bacterial cell detection and quantitative analysis. *Nat. Microbiol.* 1:16077. doi: 10.1038/nmicrobiol.2016.77
- Eckert, C., Lecerf, M., Dubost, L., Arthur, M., and Mesnage, S. (2006). Functional analysis of AtfA, the major N-acetylglucosaminidase of *Enterococcus faecalis*. *J. Bacteriol.* 188, 8513–8519. doi: 10.1128/JB.01145-06
- Formstone, A., and Errington, J. (2005). A magnesium-dependent *mreB* null mutant: implications for the role of *mreB* in *Bacillus subtilis*. *Mol. Microbiol.* 55, 1646–1657. doi: 10.1111/j.1365-2958.2005.04506.x
- Frankel, M. B., and Schneewind, O. (2012). Determinants of murein hydrolase targeting to cross-wall of *Staphylococcus aureus* peptidoglycan. *J. Biol. Chem.* 287, 10460–10471. doi: 10.1074/jbc.M111.336404
- Fredriksen, L., Moen, A., Adzhubei, A. A., Mathiesen, G., Eijssink, V. G., and Egge-Jacobsen, W. (2013). *Lactobacillus plantarum* WCFS1 O-linked protein glycosylation: an extended spectrum of target proteins and modification sites detected by mass spectrometry. *Glycobiology* 23, 1439–1451. doi: 10.1093/glycob/cwt071
- Fukushima, T., Afkham, A., Kurosawa, S., Tanabe, T., Yamamoto, H., and Sekiguchi, J. (2006). A new D,L-endopeptidase gene product, YojL (renamed CwLS), plays a role in cell separation with *LytE* and *LytF* in *Bacillus subtilis*. *J. Bacteriol.* 188, 5541–5550. doi: 10.1128/JB.00188-06
- Fukushima, T., Uchida, N., Ide, M., Kodama, T., and Sekiguchi, J. (2018). DL-endopeptidases function as both cell wall hydrolases and poly-gamma-glutamic acid hydrolases. *Microbiology* 164, 277–286. doi: 10.1099/mic.0.000609
- Fukushima, T., Yao, Y., Kitajima, T., Yamamoto, H., and Sekiguchi, J. (2007). Characterization of new L,D-endopeptidase gene product CwLK (previous YcdD) that hydrolyzes peptidoglycan in *Bacillus subtilis*. *Mol. Genet. Genomics* 278, 371–383. doi: 10.1007/s00438-007-0255-8
- Hashimoto, M., Ooiwa, S., and Sekiguchi, J. (2012). Synthetic lethality of the *lytE* *cwLO* genotype in *Bacillus subtilis* is caused by lack of D,L-endopeptidase activity at the lateral cell wall. *J. Bacteriol.* 194, 796–803. doi: 10.1128/JB.05569-11
- Höltje, J. V., Mirelman, D., Sharon, N., and Schwarz, U. (1975). Novel type of murein transglycosylase in *Escherichia coli*. *J. Bacteriol.* 124, 1067–1076.
- Huard, C., Miranda, G., Wessner, F., Bolotin, A., Hansen, J., Foster, S. J., et al. (2003). Characterization of AcMB, an N-acetylglucosaminidase autolysin from *Lactococcus lactis*. *Microbiology* 149, 695–705. doi: 10.1099/mic.0.25875-0
- Ishikawa, S., Hara, Y., Ohnishi, R., and Sekiguchi, J. (1998). Regulation of a new cell wall hydrolase gene, *cwLF*, which affects cell separation in *Bacillus subtilis*. *J. Bacteriol.* 180, 2549–2555.
- Jolliffe, L. K., Doyle, R. J., and Streips, U. N. (1981). The energized membrane and cellular autolysis in *Bacillus subtilis*. *Cell* 25, 753–763. doi: 10.1016/0092-8674(81)90183-5
- Josson, K., Scheirlinck, T., Michiels, F., Platteeuw, C., Stanssens, P., Joos, H., et al. (1989). Characterization of a gram-positive broad-host-range plasmid isolated from *Lactobacillus hilgardii*. *Plasmid* 21, 9–20. doi: 10.1016/0147-619X(89)90082-6
- Kleerebezem, M., Boekhorst, J., van Kranenburg R., Molenaar, D., Kuipers, O. P., Leer, R. et al. (2003). Complete genome sequence of *Lactobacillus plantarum* WCFS1. *Proc. Natl. Acad. Sci. U. S. A* 100, 1990–1995. doi: 10.1073/pnas.0337704100

- Kleerebezem, M., Hols, P., Bernard, E., Rolain, T., Zhou, M., Siezen, R. J., et al. (2010). The extracellular biology of the lactobacilli. *FEMS Microbiol. Rev.* 34, 199–230. doi: 10.1111/j.1574-6976.2009.00208.x
- Kuipers, O. P., de Ruyter, P. G., Kleerebezem, M., and de Vos, W. M. (1997). Controlled overproduction of proteins by lactic acid bacteria. *Trends Biotechnol.* 15, 135–140. doi: 10.1016/S0167-7799(97)01029-9
- Layec, S., Gérard, J., Legué, V., Chapot-Chartier, M. P., Courtin, P., Borges, F., et al. (2009). The CHAP domain of Cse functions as an endopeptidase that acts at mature septa to promote *Streptococcus thermophilus* cell separation. *Mol. Microbiol.* 71, 1205–1217. doi: 10.1111/j.1365-2958.2009.06595.x
- Lebeer, S., Claes, I. J., Balog, C. I., Schoofs, G., Verhoeven, T. L., Nys, K., et al. (2012). The major secreted protein Msp1/p75 is O-glycosylated in *Lactobacillus rhamnosus* GG. *Microb. Cell Fact.* 11:15. doi: 10.1186/1475-2859-11-15
- Lee, T. K., and Huang, K. C. (2013). The role of hydrolases in bacterial cell-wall growth. *Curr. Opin. Microbiol.* 16, 760–766. doi: 10.1016/j.mib.2013.08.005
- Litzinger, S., Fischer, S., Polzer, P., Diederichs, K., Welte, W., and Mayer, C. (2010). Structural and kinetic analysis of *Bacillus subtilis* N-acetylglucosaminidase reveals a unique Asp-His dyad mechanism. *J. Biol. Chem.* 285, 35675–35684. doi: 10.1074/jbc.M110.131037
- Margot, P., Pagni, M., and Karamata, D. (1999). *Bacillus subtilis* 168 gene *lytF* encodes a gamma-D-glutamate-meso-diaminopimelate murepeptidase expressed by the alternative vegetative sigma factor, sigmaD. *Microbiology* 145(Pt 1), 57–65. doi: 10.1099/13500872-145-1-57
- Meisner, J., Montero Llopis, P., Sham, L. T., Garner, E., Bernhardt, T. G., and Rudner, D. Z. (2013). FtsEX is required for CwlO peptidoglycan hydrolase activity during cell wall elongation in *Bacillus subtilis*. *Mol. Microbiol.* 89, 1069–1083. doi: 10.1111/mmi.12330
- Mesnager, S., Dellarole, M., Baxter, N. J., Rouget, J. B., Dimitrov, J. D., Wang, N., et al. (2014). Molecular basis for bacterial peptidoglycan recognition by LysM domains. *Nat. Commun.* 5:4269. doi: 10.1038/ncomms5269
- Palumbo, E., Deghorain, M., Coconcelli, P. S., Kleerebezem, M., Geyer, A., Hartung, T., et al. (2006). D-alanyl ester depletion of teichoic acids in *Lactobacillus plantarum* results in a major modification of lipoteichoic acid composition and cell wall perforations at the septum mediated by the Acm2 autolysin. *J. Bacteriol.* 188, 3709–3715. doi: 10.1128/JB.188.10.3709-3715.2006
- Palumbo, E., Favier, C. F., Deghorain, M., Coconcelli, P. S., Grangette, C., Mercenier, A., et al. (2004). Knockout of the alanine racemase gene in *Lactobacillus plantarum* results in septation defects and cell wall perforation. *FEMS Microbiol. Lett.* 233, 131–138. doi: 10.1016/j.femsle.2004.02.001
- Regulski, K., Courtin, P., Meyrand, M., Claes, I. J., Lebeer, S., Vanderleyden, J., et al. (2012). Analysis of the peptidoglycan hydrolase complement of *Lactobacillus casei* and characterization of the major gamma-D-glutamyl-L-lysyl-endopeptidase. *PLoS ONE* 7:e32301. doi: 10.1371/journal.pone.0032301
- Rolain, T., Bernard, E., Beaussart, A., Degand, H., Courtin, P., Egge-Jacobsen, W., et al. (2013). O-glycosylation as a novel control mechanism of peptidoglycan hydrolase activity. *J. Biol. Chem.* 288, 22233–22247. doi: 10.1074/jbc.M113.470716
- Rolain, T., Bernard, E., Courtin, P., Bron, P. A., Kleerebezem, M., Chapot-Chartier, M. P., et al. (2012). Identification of key peptidoglycan hydrolases for morphogenesis, autolysis, and peptidoglycan composition of *Lactobacillus plantarum* WCFS1. *Microb. Cell Fact.* 11:137. doi: 10.1186/1475-2859-11-137
- Sambrook, J., Fritsch, E. F., and Maniatis, T. (1989). *Molecular Cloning: A Laboratory Manual*. Cold Spring Harbor, NY: Cold Spring Harbor Laboratory.
- Sauvage, E., Kerff, F., Terrak, M., Ayala, J. A., and Charlier, P. (2008). The penicillin-binding proteins: structure and role in peptidoglycan biosynthesis. *FEMS Microbiol. Rev.* 32, 234–258. doi: 10.1111/j.1574-6976.2008.00105.x
- Schmidt, D. M., Hubbard, B. K., and Gerlt, J. A. (2001). Evolution of enzymatic activities in the enolase superfamily: functional assignment of unknown proteins in *Bacillus subtilis* and *Escherichia coli* as L-Ala-D/L-Glu epimerases. *Biochemistry* 40, 15707–15715. doi: 10.1021/bi011640x
- Serrano, L. M., Molenaar, D., Wels, M., Teusink, B., Bron, P. A., de Vos, W. M., et al. (2007). Thioredoxin reductase is a key factor in the oxidative stress response of *Lactobacillus plantarum* WCFS1. *Microb. Cell Fact.* 6:29. doi: 10.1186/1475-2859-6-29
- Sham, L. T., Barendt, S. M., Kopecky, K. E., and Winkler, M. E. (2011). Essential PcsB putative peptidoglycan hydrolase interacts with the essential FtsXSPn cell division protein in *Streptococcus pneumoniae* D39. *Proc. Natl. Acad. Sci. U. S. A.* 108, E1061–E1069. doi: 10.1073/pnas.1108323108
- Slusarenko, O., Heinritz, J., Emonet, T., and Jacobs-Wagner, C. (2011). High-throughput, subpixel precision analysis of bacterial morphogenesis and intracellular spatio-temporal dynamics. *Mol. Microbiol.* 80, 612–627. doi: 10.1111/j.1365-2958.2011.07579.x
- Smith, T. J., Blackman, S. A., and Foster, S. J. (2000). Autolysins of *Bacillus subtilis*: multiple enzymes with multiple functions. *Microbiology* 146(Pt 2), 249–262. doi: 10.1099/00221287-146-2-249
- Sørvig, E., Mathiesen, G., Naterstad, K., Eijnsink, V. G., and Axelsson, L. (2005). High-level, inducible gene expression in *Lactobacillus sakei* and *Lactobacillus plantarum* using versatile expression vectors. *Microbiology* 151, 2439–2449. doi: 10.1099/mic.0.28084-0
- Steen, A., Buist, G., Horsburgh, G. J., Venema, G., Kuipers, O. P., Foster, S. J., et al. (2005). AcmA of *Lactococcus lactis* is an N-acetylglucosaminidase with an optimal number of LysM domains for proper functioning. *FEBS J.* 272, 2854–2868. doi: 10.1111/j.1742-4658.2005.04706.x
- Szwedziak, P., and Löwe, J. (2013). Do the divisome and elongasome share a common evolutionary past? *Curr. Opin. Microbiol.* 16, 745–751. doi: 10.1016/j.mib.2013.09.003
- Visweswaran, G. R., Dijkstra, B. W., and Kok, J. (2011). Murein and pseudomurein cell wall binding domains of bacteria and archaea—a comparative view. *Appl. Microbiol. Biotechnol.* 92, 921–928. doi: 10.1007/s00253-011-3637-0
- Vollmer, W. (2008). Structural variation in the glycans strands of bacterial peptidoglycan. *FEMS Microbiol. Rev.* 32, 287–306. doi: 10.1111/j.1574-6976.2007.00088.x
- Vollmer, W., Blanot, D., and de Pedro, M. A. (2008a). Peptidoglycan structure and architecture. *FEMS Microbiol. Rev.* 32, 149–167. doi: 10.1111/j.1574-6976.2007.00094.x
- Vollmer, W., Joris, B., Charlier, P., and Foster, S. (2008b). Bacterial peptidoglycan (murein) hydrolases. *FEMS Microbiol. Rev.* 32, 259–286. doi: 10.1111/j.1574-6976.2007.00099.x
- Xu, Q., Abdubek, P., Astakhova, T., Axelrod, H. L., Bakolitsa, C., Cai, X., et al. (2010). Structure of the gamma-D-glutamyl-L-diamino acid endopeptidase YkfC from *Bacillus cereus* in complex with L-Ala-gamma-D-Glu: insights into substrate recognition by NlpC/P60 cysteine peptidases. *Acta Crystallogr. Sect. F. Struct. Biol. Cryst. Commun.* 66, 1354–1364. doi: 10.1107/S1744309110021214
- Xu, Q., Mengin-Lecreulx, D., Liu, X. W., Patin, D., Farr, C. L., Grant, J. C., et al. (2015). Insights into substrate specificity of NlpC/P60 cell wall hydrolases containing bacterial SH3 domains. *MBio.* 6:e02327-14. doi: 10.1128/mBio.02327-14
- Yamaguchi, H., Furuhashi, K., Fukushima, T., Yamamoto, H., and Sekiguchi, J. (2004). Characterization of a new *Bacillus subtilis* peptidoglycan hydrolase gene, *yvcE* (named *cwlO*), and the enzymatic properties of its encoded protein. *J. Biosci. Bioeng.* 98, 174–181. doi: 10.1016/S1389-1723(04)00262-2
- Yamamoto, H., Kurosawa, S., and Sekiguchi, J. (2003). Localization of the vegetative cell wall hydrolases LytC, LytE, and LytF on the *Bacillus subtilis* cell surface and stability of these enzymes to cell wall-bound or extracellular proteases. *J. Bacteriol.* 185, 6666–6677. doi: 10.1128/JB.185.22.6666-6677.2003
- Yang, D. C., Peters, N. T., Parzych, K. R., Uehara, T., Markovski, M., and Bernhardt, T. G. (2011). An ATP-binding cassette transporter-like complex governs cell-wall hydrolysis at the bacterial cytokinetic ring. *Proc. Natl. Acad. Sci. U.S.A.* 108, E1052–E1060. doi: 10.1073/pnas.1107780108

Conflict of Interest Statement: The authors declare that the research was conducted in the absence of any commercial or financial relationships that could be construed as a potential conflict of interest.

Copyright © 2019 Duchêne, Rolain, Knoop, Courtin, Chapot-Chartier, Dufrêne, Hallet and Hols. This is an open-access article distributed under the terms of the Creative Commons Attribution License (CC BY). The use, distribution or reproduction in other forums is permitted, provided the original author(s) and the copyright owner(s) are credited and that the original publication in this journal is cited, in accordance with accepted academic practice. No use, distribution or reproduction is permitted which does not comply with these terms.



Recovery of the Peptidoglycan Turnover Product Released by the Autolysin Atl in *Staphylococcus aureus* Involves the Phosphotransferase System Transporter MurP and the Novel 6-phospho-*N*-acetylmuramidase MupG

OPEN ACCESS

Edited by:

Marc Bramkamp,
Ludwig-Maximilians-Universität
München, Germany

Reviewed by:

Patrick Joseph Moynihan,
University of Birmingham,
United Kingdom
Volker F. Wendisch,
Bielefeld University, Germany

*Correspondence:

Christoph Mayer
christoph.mayer@uni-tuebingen.de
Marina Borisova
marina.borisova@uni-tuebingen.de

Specialty section:

This article was submitted to
Microbial Physiology and Metabolism,
a section of the journal
Frontiers in Microbiology

Received: 04 June 2018

Accepted: 24 October 2018

Published: 16 November 2018

Citation:

Kluj RM, Ebner P, Adamek M,
Ziemert N, Mayer C and Borisova M
(2018) Recovery of the Peptidoglycan
Turnover Product Released by
the Autolysin Atl in *Staphylococcus*
aureus Involves
the Phosphotransferase System
Transporter MurP and the Novel
6-phospho-*N*-acetylmuramidase
MupG. *Front. Microbiol.* 9:2725.
doi: 10.3389/fmicb.2018.02725

Robert Maria Kluj¹, Patrick Ebner², Martina Adamek¹, Nadine Ziemert¹,
Christoph Mayer^{1*} and Marina Borisova^{1*}

¹ Microbiology/Biotechnology, Department of Biology, Interfaculty Institute of Microbiology and Infection Medicine, University of Tübingen, Tübingen, Germany, ² Microbial Genetics, Department of Biology, Interfaculty Institute of Microbiology and Infection Medicine, University of Tübingen, Tübingen, Germany

The peptidoglycan of the bacterial cell wall undergoes a permanent turnover during cell growth and differentiation. In the Gram-positive pathogen *Staphylococcus aureus*, the major peptidoglycan hydrolase Atl is required for accurate cell division, daughter cell separation and autolysis. Atl is a bifunctional *N*-acetylmuramoyl-L-alanine amidase/endo- β -*N*-acetylglucosaminidase that releases peptides and the disaccharide *N*-acetylmuramic acid- β -1,4-*N*-acetylglucosamine (MurNAc-GlcNAc) from the peptidoglycan. Here we revealed the recycling pathway of the cell wall turnover product MurNAc-GlcNAc in *S. aureus*. The latter disaccharide is internalized and concomitantly phosphorylated by the phosphotransferase system (PTS) transporter MurP, which had been implicated previously in the uptake and phosphorylation of MurNAc. Since MurP mutant cells accumulate MurNAc-GlcNAc and not MurNAc in the culture medium during growth, the disaccharide represents the physiological substrate of the PTS transporter. We further identified and characterized a novel 6-phospho-*N*-acetylmuramidase, named MupG, which intracellularly hydrolyses MurNAc 6-phosphate-GlcNAc, the product of MurP-uptake and phosphorylation, yielding MurNAc 6-phosphate and GlcNAc. MupG is the first characterized representative of a novel family of glycosidases containing domain of unknown function 871 (DUF871). The corresponding gene *mupG* (SAUSA300_0192) of *S. aureus* strain USA300 is the first gene within a putative operon that also includes genes encoding the MurNAc 6-phosphate etherase MurQ,

MurP, and the putative transcriptional regulator MurR. Using mass spectrometry, we observed cytoplasmic accumulation of MurNac 6-phosphate-GlcNAc in $\Delta mupG$ and $\Delta mupGmurQ$ markerless non-polar deletion mutants, but not in the wild type or in the complemented $\Delta mupG$ strain. MurNac 6-phosphate-GlcNAc levels in the mutants increased during stationary phase, in accordance with previous observations regarding peptidoglycan recycling in *S. aureus*.

Keywords: peptidoglycan recycling, cell wall turnover, *Staphylococcus aureus*, Atl autolysin, peptidoglycan hydrolases, 6-phosphomuramidase, *exo-N*-acetylmuramidase, MurNac-GlcNAc

INTRODUCTION

Staphylococcus aureus is a small, spherical bacterium (~1 μm diameter) belonging to the phylum firmicutes that can cause life-threatening infections due to the emergence of multi-drug resistance (Hiramatsu et al., 2014). As a Gram-positive bacterium, *S. aureus* is encased in a thick layer of peptidoglycan (PGN), which maintains cell shape and protects the cells from rupture due to high turgor pressure (Cabeen and Jacobs-Wagner, 2005). The general structure of the PGN is conserved in all eubacteria, consisting of a glycan backbone of two alternating β -1,4-glycosidically linked sugars *N*-acetylmuramic acid (MurNac) and *N*-acetylglucosamine (GlcNAc) and polypeptides, connected to the D-lactyl moiety of MurNac, that are partially crosslinked (Vollmer et al., 2008). The PGN polymer is synthesized by glycosyltransferases and transpeptidases [involving shape, elongation, division and sporulation (SEDS) family peptidoglycan synthases and penicillin binding proteins (PBPs)] through polymerization of GlcNAc- β -1,4-MurNac-peptide building blocks, provided by lipid II precursors (Cho et al., 2016; Meeske et al., 2016). The overall peptidoglycan structure of *S. aureus* is different in some aspects compared to most other bacterial species. Firstly, pentaglycine (Gly₅) bridges are attached to the ϵ -NH₂ group of L-lysine (L-Lys) of the stem tetrapeptide L-alanine-D-isoglutamine-L-Lys-D-alanine (L-ala-D-isoGln-L-Lys-D-Ala) that are extensively cross-linked (degree of crosslinking of about 80%, dependent on the growth phase and growth conditions) with neighboring peptide stems via their carboxyl group of D-Ala (Gally and Archibald, 1993; Litzinger and Mayer, 2010). Secondly, the glycan chains are comparatively short. About 80% of the glycan chains of the mature cell wall have a predominant length of 3–10 disaccharides, the average degree of polymerization is 6 disaccharides, and only about 15% of the glycan chains have a degree of polymerization more than 25 (Boneca et al., 2000).

The coccus-shaped *S. aureus* divides sequentially in three orthogonal planes over three consecutive division cycles (Monteiro et al., 2015). Although elongation-specific cell wall synthesis machinery is absent, the cells elongate before initiation and after completion of the division septum (Monteiro et al., 2015). The final splitting of daughter cells is accompanied by fast reshaping of the flat septum to finally yield two coccoid offspring cells. Thus, the peptidoglycan is remarkably dynamic and it is constantly degraded during the

cell cycle of *S. aureus* by peptidoglycan hydrolases (potential autolysins) (Foster, 1995; Ramadurai et al., 1999; Takahashi et al., 2002; Kajimura et al., 2005; Biswas et al., 2006; Frankel et al., 2011; Wheeler et al., 2015; Chan et al., 2016). The major autolysin of *S. aureus*, called Atl, is a multi-domain enzyme, composed of a secretion signal peptide, a propeptide of still unclear function, and two catalytic domains, an N-terminal *N*-acetylmuramoyl-L-alanine amidase as well as a C-terminal endo- β -*N*-acetylglucosaminidase domain, which are interrupted by cell wall binding repeats (Sugai et al., 1995). The enzyme undergoes proteolytic processing to generate two extracellular peptidoglycan hydrolases, a 62 kDa *N*-acetylmuramoyl-L-alanine amidase (Atl_{AM}) and a 51 kDa endo- β -*N*-acetylglucosaminidase (Atl_{GL}), which localize in a ring-like structure on the cell surface at the septal region, most likely binding to lipoteichoic acids, extending from the cell membrane (Yamada et al., 1996; Götz et al., 2014). Both Atl hydrolase entities can also be secreted and are found in the culture supernatants of some strains (Sugai et al., 1995). Atl functions during cell expansion and division, and it is required for proper daughter cell separation (Sugai et al., 1995; Biswas et al., 2006). Furthermore, Atl is associated with autolysis processes, e.g., during biofilm formation (Biswas et al., 2006; Bose et al., 2012). Besides Atl_{GL}, *S. aureus* also possesses three other *N*-acetylglucosaminidases, SagA, SagB, and ScaH, which are important for proper septum formation at the final stage of cell division. SagB was also found to be responsible for shortening of newly synthesized glycan strands to their physiological length, thus ensuring flexibility during the cell elongation process (Wheeler et al., 2015; Chan et al., 2016). Interestingly, the *S. aureus* genome apparently does not encode any *N*-acetylmuramidases, with the exception of two putative lytic transglycosylases, IsaA and SceD (Stapleton et al., 2007), indicating that the processing of glycan strands in this organism involves endo-acting *N*-acetylglucosaminidases, besides peptidoglycan amidases and endopeptidases (Ramadurai et al., 1999; Kajimura et al., 2005; Frankel et al., 2011). The combined activities of these PGN hydrolases generate MurNac-GlcNAc and peptides as final peptidoglycan turnover products.

It was calculated that during the process of PGN turnover in *S. aureus*, 15% (Wong et al., 1974) or up to 25% (Blümel et al., 1979) of cell wall material fragments are released per generation in the culture medium. However,

the ability of Gram-positive bacteria in general to recycle these fragments was questioned for a long time. We recently elucidated that recycling occurs in different Gram-positive bacteria such as *S. aureus*, *Bacillus subtilis*, and *Streptomyces coelicolor* and revealed that the MurNac 6-phosphate (MurNac 6P) etherase MurQ (Borisova et al., 2016), responsible for the intracellular conversion of MurNac 6P to GlcNac 6-phosphate and D-lactate, is required for this process. In addition, we quantified the intracellular accumulation of MurNac 6P in the markerless $\Delta murQ$ mutant, showed that recycling of the MurNac portion of peptidoglycan occurs predominantly during nutrient limitation within transition and stationary phase (Borisova et al., 2016). Furthermore we discovered that peptidoglycan recycling is essential for bacterial survival in the late stationary phase (Borisova et al., 2016). In *S. aureus* strain USA300, the *murQ* etherase gene (SAUSA300_0193) is encoded in an operon together with SAUSA300_0194, encoding the enzyme IIB and IIC domains of the MurNac PTS-transporter MurP, SAUSA300_0195, encoding a MurR-like regulator, and SAUSA300_0192, encoding a protein with unknown function (Borisova et al., 2016).

We hypothesized that MurNac-GlcNac, the product of cell wall cleavage by Atl, rather than MurNac, might be taken up and recycled in *S. aureus* and proposed a role of the gene SAUSA300_0192 of unknown function in this process. To prove this hypothesis, we generated markerless gene deletion mutants and investigated the intracellular and extracellular accumulation of specific recycling products in different growth phases by mass spectrometry. Our study showed that MurNac 6P-GlcNac accumulates in SAUSA300_0192 mutant, predominantly during stationary phase, and that this compound is generated by the uptake and phosphorylation of MurNac-GlcNac by the PTS transporter MurP. The SAUSA300_0192 gene was shown to encode a novel 6-phospho-*N*-acetylmuramidase, named MupG that hydrolyses MurNac 6P-GlcNac yielding MurNac 6P and GlcNac. MupG is the first characterized protein of a so far unexplored family of proteins containing the domain of unknown function 871 (DUF871). Altogether in this study we revealed the recycling pathway of the peptidoglycan sugar turnover product of the Atl autolysin in *S. aureus*.

MATERIALS AND METHODS

Chemicals, Enzymes, and Oligonucleotides

Enzymes for DNA restriction and for cloning were purchased from New England Biolabs (Ipswich, USA) or Thermo Fischer Scientific (Waltham, MA, United States). The Gene JET plasmid miniprep kit, PCR purification kit, and Gene Ruler 1 kb marker were also purchased from Thermo Fisher Scientific and anhydrotetracycline was obtained from Biomol GmbH (Hamburg, Germany). Oligonucleotides were purchased from MWG Eurofins (Ebersberg, Germany) and are listed in **Supplementary Table 1**.

Bacterial Strains, Growth Conditions, and Plasmids

The bacterial strains and plasmids used in this study are listed in **Supplementary Table 2**. The construction of mutant strains and plasmids is also described in the **Supplementary Material**. *Staphylococcus aureus* USA300 JE2 strain was cultured aerobically in lysogeny broth (LB broth Lennox, Carl Roth) at 37°C and with continuous shaking at 160 rpm or on solid LB supplemented with 1.5% agar. *S. aureus* overnight cultures (~16 h) were used to inoculate fresh LB medium to yield an initial optical density at 600 nm (OD₆₀₀) of 0.05 for growth studies and for the determination of intracellular accumulation of *N*-acetylmuramic acid 6-phosphate-*N*-acetylglucosamine (MurNac 6P-GlcNac) at different growth phases. BM medium (10 g/l peptone, 5 g/l yeast extract, 1 g/l glucose, 5 g/l NaCl, 1 g/l K₂HPO₄) was used to prepare electrocompetent *S. aureus* JE2 cells and for the generation of the markerless $\Delta mupG$ and $\Delta mupGmurQ$ mutants (see **Supplementary Data** in the **Supplementary Material**). Antibiotics were used, when appropriate, at the following concentrations: 100 µg/ml ampicillin and 30 µg/ml kanamycin for *E. coli* and 10 µg/ml chloramphenicol for *S. aureus*.

Generation of Cytosolic Fractions and Reduction of Samples With NaBH₄

Overnight cultures of *S. aureus* JE2 wild type, $\Delta mupG$ and $\Delta mupGmurQ$ mutants were used to inoculate LB medium to an initial OD₆₀₀ of 0.05. Bacteria were grown at 37°C with constant shaking and harvested at mid-exponential growth phase (OD₆₀₀ of 2.4, grown for ~3–3.5 h), at transitional phase (OD₆₀₀ of 7.2, grown for 9 h) and stationary phase (OD₆₀₀ of 5.9, grown for 24 h). Afterward, 50 ml of the culture were transferred to Falcon tubes, bacteria were centrifuged at 4,000 × *g* for 10 min, washed with 20 ml deionized water, and pellets were frozen at –80°C. Bacterial samples were thawed at room temperature and suspended in different volumes of water to prepare cell suspensions with OD₆₀₀ of 250 per ml in the different growth phases. Seven hundred microliters of the bacterial suspensions were transferred to new tubes containing ~0.25 g glass beads (0.25–0.5 mm; Roth) and cells were disrupted in a cell homogeniser (Precellys Evolution, Bertin Technologies) at 6000 rpm for 30 s. This procedure was repeated 4 times, with cooling on ice for 1 min after the second cycle. Lysates were cooled briefly and subsequently centrifuged for 10 min at maximum speed in a microcentrifuge. Two hundred microliters of each supernatant was added to 800 µl of ice-cold acetone to precipitate remaining proteins. After centrifugation (12,000 × *g* for 10 min), the supernatant was transferred to a new tube, and samples were dried under vacuum for 2 h at 55°C and finally stored at 4°C prior to LC-MS measurements.

Reduction solution was freshly prepared for each experiment by adding 500 µl of 0.5 M borate buffer (pH 9) to 5 mg of sodium borohydride, as previously described (Schaub and Dillard, 2017). Thirty microliters of the cytosolic fractions or the culture supernatants were added to equal volumes

of the reduction solution and samples were incubated for 20 min at room temperature. Reactions were adjusted to pH between 3 and 4 by adding 10 μ l of 8.5% phosphoric acid. Samples were dried under vacuum at 45°C and pellets were solved in 30 μ l of deionized water prior to LC-MS analysis.

Analysis of MurNac 6P-GlcNAc Accumulation by LC-MS

Sample analysis of bacterial cytosolic fractions was conducted using an electrospray ionization-time of flight (ESI-TOF) mass spectrometer (MicroTOF II; Bruker Daltonics), operated in negative or positive ion-mode that was connected to an UltiMate 3000 high performance liquid chromatography (HPLC) system (Dionex). For HPLC-MS analysis cytosolic samples were dissolved in 50 μ l deionized water and 3 μ l were injected into a Gemini C18 column (150 by 4.6 mm, 5 μ m, 110 Å, Phenomenex). A 45 min program at a flow rate of 0.2 ml/min was used to separate compounds in the cytosolic fractions as previously described (Gisin et al., 2013). The mass spectra of the investigated samples were presented as base peak chromatograms (BPC), differential spectra (DS, obtained by subtraction of BPC_{mutant} minus BPC_{wildtype}) and extracted ion chromatograms (EIC) in DataAnalysis program and were presented in Prism 6 (GraphPad). The relative amounts of MurNac 6P-GlcNAc in different growth phases and in *mupG* complementation experiments were determined by calculating the area under the curve (AUC) of the respective EIC spectra for MurNac 6P-GlcNAc.

Construction of pET28a-*mupG* Plasmid and Heterologous Expression and Purification of MupG-His₆

For heterologous overexpression in *E. coli*, the *mupG* gene was cloned in a pET28a(+) expression vector as a recombinant protein with a C-terminal His₆-tag. Therefore, genomic DNA from *S. aureus* USA300 JE2 strain was used to amplify the *mupG* gene by PCR using primer pair MB-67 and MB-68. Both, the PCR product and vector were digested with NcoI and XhoI restriction enzymes, ligated by T4 DNA ligase and chemically competent *E. coli* DH5 α cells were transformed with the ligation reaction mixture. The pET28a-*mupG* recombinant plasmid was isolated from kanamycin-resistant *E. coli* cells and DNA sequence was verified by sequencing. BL21(DE3) cells were then transformed with the pET28a-*mupG* plasmid and protein was expressed by addition of IPTG (isopropyl- β -D-thiogalactopyranoside), controlling the T7 inducible promoter.

For expression of MupG, an overnight culture of *E. coli* BL21(DE3) pET28a-*mupG* cells was diluted to an OD₆₀₀ of 0.05 with LB medium supplemented with 30 μ g/ml kanamycin (final volume of 1 l) and cells were grown at 37°C with shaking. MupG expression was induced by addition of 1 mM IPTG after the culture reached an OD₆₀₀ of 0.75. Three hours after induction, bacteria were harvested by centrifugation (4,000 \times g, 4°C, 20 min) and frozen at -20°C. Then, cells were solved in phosphate buffer A (20 mM Na₂HPO₄, 500 mM NaCl, pH

8), disrupted by sonication (Branson Sonifier 250, 3 times for 2 min, output 5, duty cycle of 50%) and cell debris were removed by centrifugation (38,000 \times g, 4°C, 20 min). The soluble fraction was filtered (0.2 μ m, Sarstedt) and the His-tagged protein was purified by Ni²⁺ affinity chromatography system Äkta Purifier on a 1 ml HisTrap HP column (GE Healthcare). A linear gradient over 30 min from 96% buffer A and 4% buffer B (20 mM Na₂HPO₄, 500 mM NaCl, 500 mM imidazole, pH 8) to 100% buffer B was used to elute the His-tagged enzyme from the column. The UV_{280nm} active fractions were analyzed for MupG protein content on 13% SDS-PAGE gel. The MupG-His₆ containing fractions were pooled and further purified by size-exclusion chromatography (HiLoad 16/600 Superdex 75 pg, GE Healthcare) with buffer A for elution. Protein purity was analyzed by SDS-PAGE and the extinction coefficient at 280 nm of 20,860 M⁻¹ cm⁻¹ was calculated based on amino acid composition with the Expasy ProtParam tool. Protein was stored at -80°C in 10% glycerol solution.

Phylogenetic Analysis

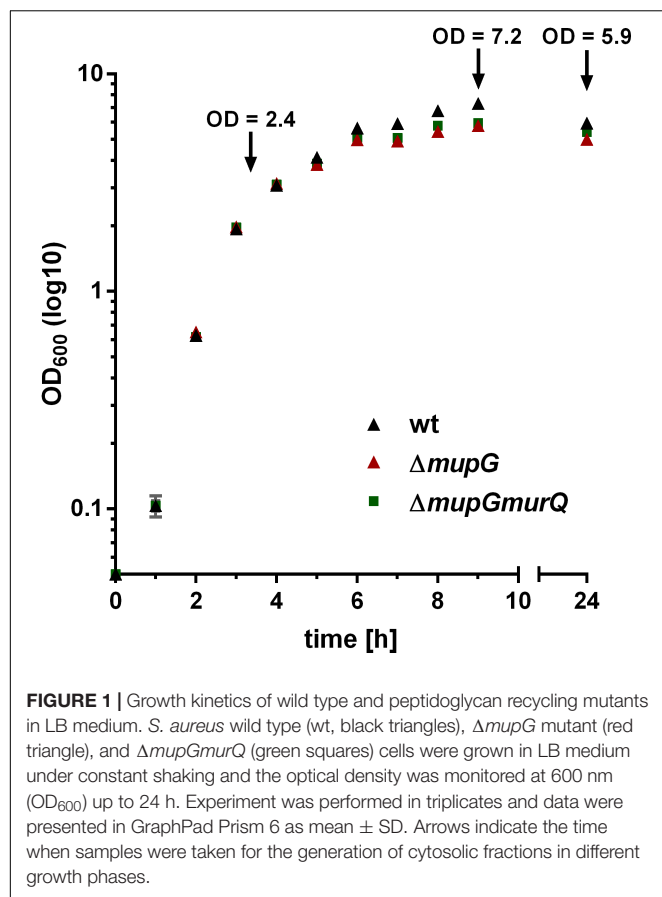
The phylogenetic tree was based on the Pfam entry PF05913. A set of 519 amino acid sequences in this entry (for a complete list of proteins see **Supplementary Table 3**) were aligned using MAFFT (Katoh and Standley, 2013) under default settings and subsequently trimmed with trimAl in automated1 mode (Capella-Gutiérrez et al., 2009). Pfam PF05913 sequences with less than 200 amino acids were removed from the analysis. The maximum likelihood phylogenetic tree was constructed with RaxML using the Gamma Blosum62 Protein model and rapid bootstrapping algorithm (Stamatakis, 2014). The visualization and annotation was done with the program interactive Tree Of Life (iTOL) v3: an online tool for the display and annotation of phylogenetic and other trees (Letunic and Bork, 2016).

RESULTS

Accumulation of MurNac 6-phosphate-GlcNAc in Δ *mupG* and Δ *mupGmurQ* Cells

The gene SAUSA300_0192, named *mupG*, encodes an uncharacterized, hypothetical protein that is classified as a member of a protein family of unknown function (DUF871). It is located upstream of *murQ*, *murP* and *murR*, encoded in an operon on the genome of *S. aureus* strain USA300_FPR3757 (according to the AureoWiki database¹) (Fuchs et al., 1990). We recently showed that the PTS transporter MurP and the MurNac 6-phosphate etherase MurQ are required for the recovery of the cell wall sugar *N*-acetylmuramic acid (MurNac) in *S. aureus* and other Gram-positive bacteria (Borisova et al., 2016). Thus, we assumed that the enzyme MupG of *S. aureus* might also be involved in the recycling of peptidoglycan turnover products, possibly acting sequentially with MurQ within a joint catabolic pathway. To prove this hypothesis, we generated markerless

¹http://aureowiki.med.uni-greifswald.de/SAUSA300_0192

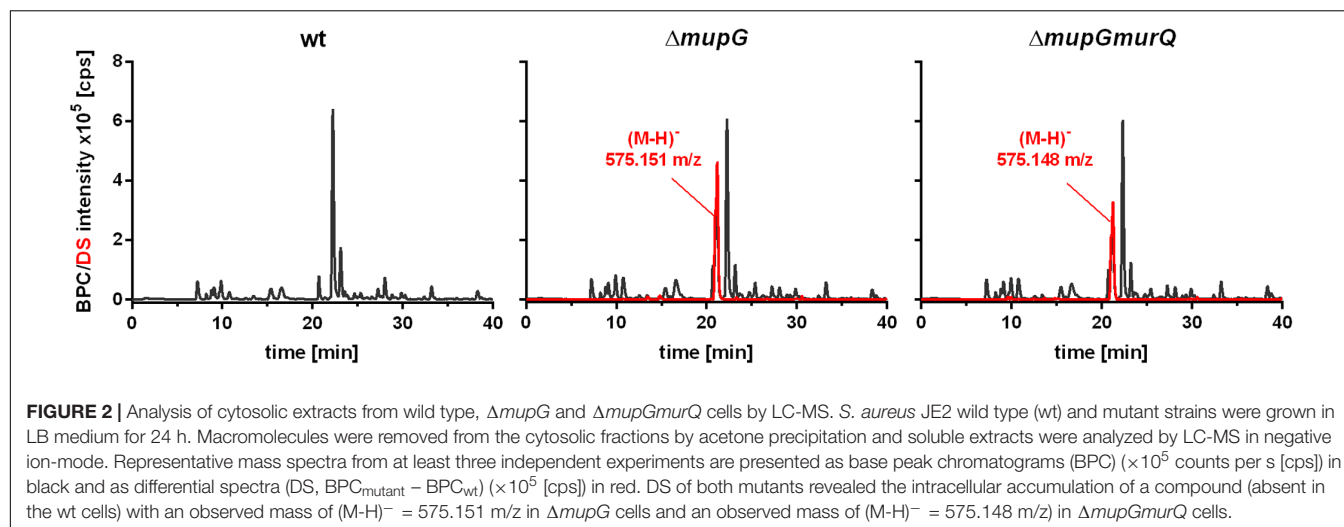


S. aureus $\Delta mupG$ and $\Delta mupGmurQ$ deletion mutants (see **Supplementary Data** and **Supplementary Figure 1**) and we analyzed growth of these mutant strains in comparison with the parental (wild type) strain in nutrient-rich LB medium for 24 h (**Figure 1**). No significant differences in growth were detectable in all three strains during exponential growth phase, when monitoring the optical density at 600 nm (OD_{600}). However, a slight reduction in OD_{600} was observed during late exponential and stationary phase for $\Delta mupG$ and $\Delta mupGmurQ$, compared to the wild type cultures. A *S. aureus* USA300 JE2 $\Delta murQ$ mutant, lacking the etherase encoding *murQ*, which is located in the same putative operon as *mupG* also showed a slight growth defect in these growth phases, as described previously in Borisova et al. (2016). Therefore, we also compared the growth of the $\Delta mupG$ mutant with the $\Delta murQ$ mutant. Interestingly, $\Delta mupG$ cultures reached slightly lower optical density compared to the $\Delta murQ$ cultures (see **Supplementary Figure 2**).

Mass spectrometric analyses of cytosolic cell fractions of $\Delta mupG$ and $\Delta mupGmurQ$ cells revealed the accumulation of an intracellular recycling product in both mutant strains, which was absent in wild type cells. The accumulation product in both mutant strains occurred at the same retention time of 21.2 min and had an identical mass within the error of mass analysis of <5 ppm ($\Delta mupG$ cells, $(M-H)^- = 575.151$ m/z and $\Delta mupGmurQ$ cells, $(M-H)^- = 575.148$ m/z) (**Figure 2**).

The accumulation of the same compound in both mutants and the absence of MurNac 6P accumulation in the double mutant, which has been reported to accumulate in a $\Delta murQ$ single mutant (Borisova et al., 2016), indicated that MupG and MurQ are indeed operating in the same peptidoglycan recovery pathway, with MupG presumably acting upstream of MurQ. The unknown accumulation product has a mass that is identical within the error of mass analysis with the theoretical mass of a phosphorylated disaccharide containing the sugars GlcNAc and MurNac (calculated mass in negative ion mode $(M-H)^- = 575.1495$ m/z and positive ion mode $(M+H)^+ = 577.164$ m/z). To identify the chemical structure of the phosphorylated disaccharide, i.e., which sugar resides at the reducing end and which sugar is phosphorylated, we analyzed the fragmentation patterns obtained by in-source decay during mass analysis. We analyzed the intact cytosolic extracts of the $\Delta mupG$ cells containing the accumulation product, as well as the same samples after reduction with $NaBH_4$ this time in positive ion-mode (**Figure 3**). As expected a mass shift of 2 Da occurred after treatment with $NaBH_4$, in agreement with the expected reduction of a sugar hemiacetal at the reducing end yielding a sugar alcohol. The accumulation product in the $\Delta mupG$ extract with a mass of $(M+H)^+ = 577.166$ m/z (non-reduced) was diminished [**Figure 3A**; calculated mass of a phosphorylated disaccharide containing GlcNAc and MurNac in positive ion mode: $(M+H)^+ = 577.164$ m/z], and a new mass appeared with $(M+H)^+ = 579.178$ m/z, corresponding to the same disaccharide reduced to sugar alcohol [calculated reduced form $(M+H)^+ = 579.1797$ m/z] (**Figure 3B**). The fact that the phosphorylated disaccharide is reduced at the anomeric position indicated that the C1 position is not phosphorylated, but most likely the C6 position carries the phosphate group. Thus, four different chemical structures are imaginable, which were presented in **Supplementary Figure 3A**.

In the non-reduced sample (**Figure 3A**), the recycling product with the mass of $(M+H)^+ = 577.166$ m/z was detected and also the Na^+ and K^+ adducts. Fragmentations included the neutral loss of GlcNAc (-221.092 Da; calculated exact mass loss of 221.089 Da), and a MurNac 6P elimination product (see **Supplementary Figure 3B**) with a mass of $(M+H)^+ = 356.074$ m/z (which is identical with the calculated m/z of this fragment). Besides, the loss of a phosphoryl group (-79.971 Da) and the loss of water (-18.013 Da), most likely at the anomeric site, was observed. The latter fragmentations caused the formation of a dephosphorylated recycling product [$(M+H)^+ = 497.195$ m/z] and a dehydrated product [$(M+H)^+ = 559.152$ m/z], respectively. From these MS result we could conclude that MurNac, but not GlcNAc, is phosphorylated. After sample reduction, the mass of the accumulation product changed to $(M+H)^+ = 579.178$ m/z (**Figure 3B**). Na^+ and K^+ adducts of the reduced compound were also detected. Compound fragmentation pattern included the neutral loss of GlcNAc, this time in a reduced form (measured and theoretical exact mass loss of 223.106 Da) and generated a compound, as seen in the non-reduced sample, with a m/z identical within error with a MurNac 6P elimination product (356.072 m/z) (**Figure 3B**; see also **Supplementary Figure 3B**).



Fragments indicating the loss of phosphate (-79.968 Da, resulting in 499.211 m/z, reduced MurNac-GlcNAc) were detected also in the reduced sample. However, a fragmentation product indicating the loss of water was absent, as expected for a compound reduced at the anomeric position. These latter results showed that after sample reduction with $NaBH_4$, the mass of the elimination product of MurNac 6P did not change, but the mass, corresponding to GlcNAc, was changed to the reduced form. Thus, we could conclude that the investigated phosphorylated disaccharide contains a MurNac at the non-reducing end that is phosphorylated and GlcNAc at the reducing end. Taken together, the fragmentation patterns of the non-reduced and reduced accumulation products, identified the accumulation of MurNac 6P-GlcNAc disaccharide in the $\Delta mupG$ cells.

MurNac 6P-GlcNAc Is Hydrolyzed by MupG Yielding MurNac 6P and GlcNAc

To characterize the *in vitro* functionality of MupG from *S. aureus*, we overexpressed the enzyme in *E. coli* BL21(DE3) in the presence of IPTG as a recombinant C-terminal His₆-fusion protein (Figure 4A) and purified the recombinant enzyme by Ni^{2+} -affinity and gel filtration chromatography (calculated mass of 41.5 kDa). After purification, a total amount of 3 and 5 mg protein, respectively, was obtained from 1 l bacterial culture in two different experiments and purity of the purified enzyme was confirmed with SDS-PAGE (Figure 4A). Addition of the recombinant MupG enzyme to cytosolic extracts, prepared from wild type and $\Delta mupG$ mutant cells revealed the specific cleavage of the $\Delta mupG$ recycling product $((M+H)^+ = 577.166$ m/z, measured in positive ion-mode, and a retention time of 21.2 min), yielding two new masses $(M+H)^+ = 222.098$ m/z and $(M+H)^+ = 374.083$ m/z (Figure 4B). These new masses correspond to the theoretical masses for GlcNAc $[(M+H)^+ = 222.097$ m/z] and MurNac P $[(M+H)^+ = 374.085$ m/z], respectively. However, MupG did not affect any other compound accumulating in the cytosol of the wild type cells or $\Delta mupG$ cells (data not shown). Notably, in extracts of the mutant, we detected a second peak with a mass

of $(M+H)^+ = 577.165$ m/z that eluted with a retention time of 25 min (Figure 4B). This compound was only detectable, when the MS analysis was conducted in the positive ion-mode, but was absent when samples were analyzed in negative ion-mode (see Figures 1, 2 for comparison). Recombinant MupG enzyme only diminished the compound with a retention time of 21.2 min but not the compound with the same m/z but a retention time of 25 min (Figure 4B). The identity of this compound is so far unclear, since the MS fragmentation pattern indicated that it is neither composed of non-phosphorylated nor of phosphorylated MurNac and GlcNAc sugars (data not shown).

To unequivocally identify MurNac 6P as the product of MupG cleavage, we incubated the MupG-treated cytosolic fraction, with the MurNac 6P etherase MurQ, which specifically converts MurNac 6P to GlcNAc 6P (Borisova et al., 2016). As expected, MurQ reduced the amount of MurNac 6P about 4 times, at the same time a mass with $(M+H)^+ = 302.062$ m/z, corresponding to the theoretical mass of GlcNAc 6P $((M+H)^+ = 302.064$ m/z) was generated (Figure 4B). MurQ treatment did not affect amounts of GlcNAc, the second product of MupG action. These results confirmed that the accumulating recycling product is indeed MurNac 6P-GlcNAc and that the MupG enzyme acts as a MurNac 6P-GlcNAc glycosidase. The recombinant enzyme was stable for several months at 4°C without losing significant activity, even in the absence of DTT reducing agent.

MurNac 6P-GlcNAc Accumulation Primarily Occurs in Transition and Stationary Phase and Is Abolished by Plasmid-Based Complementation of MupG

We previously showed that a *murQ* mutant of *S. aureus* accumulates intracellularly MurNac 6P predominantly in transition and stationary phases (Borisova et al., 2016). Here, we examined the growth phase-dependent accumulation of MurNac 6P-GlcNAc. The time points used for harvesting were mid

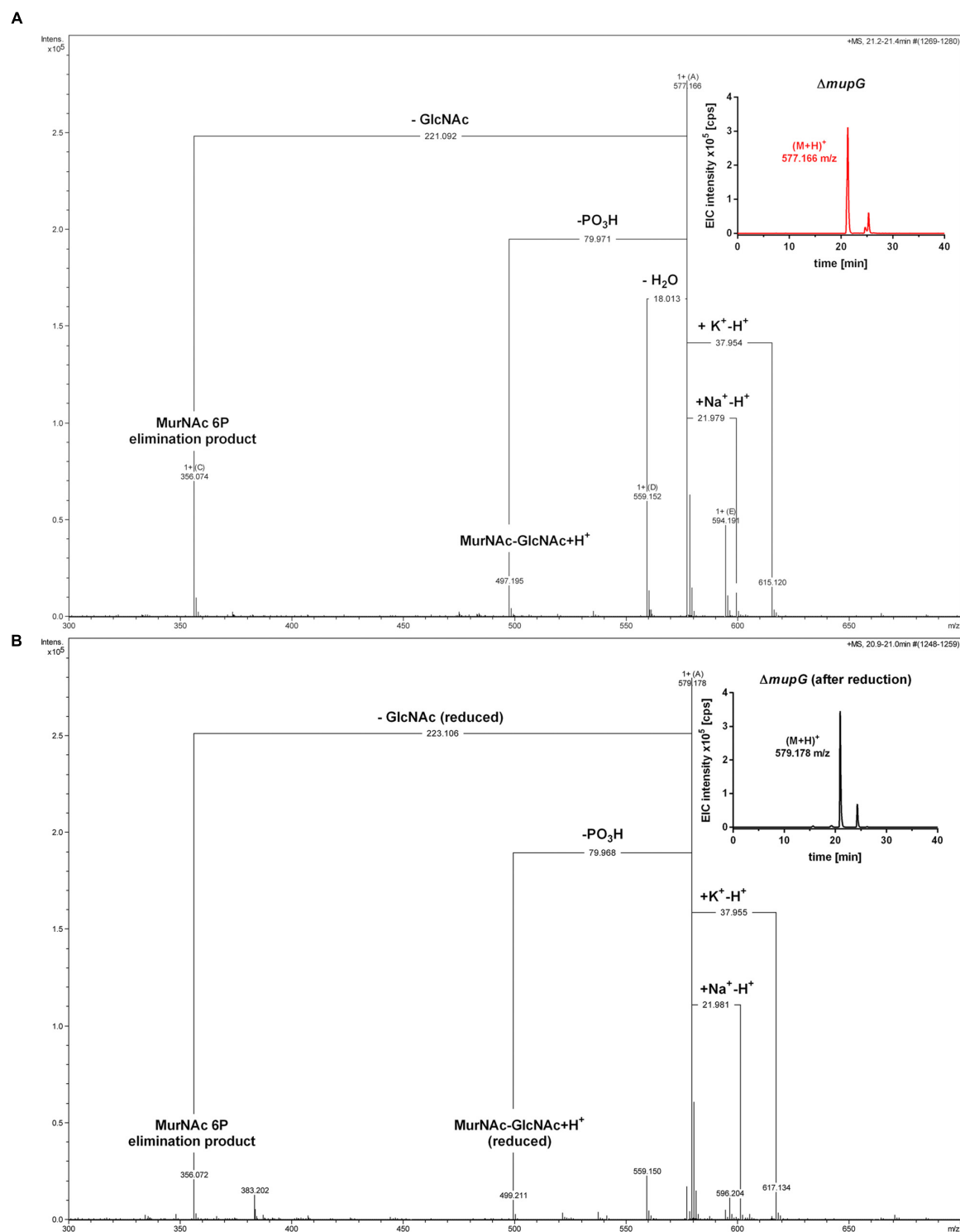
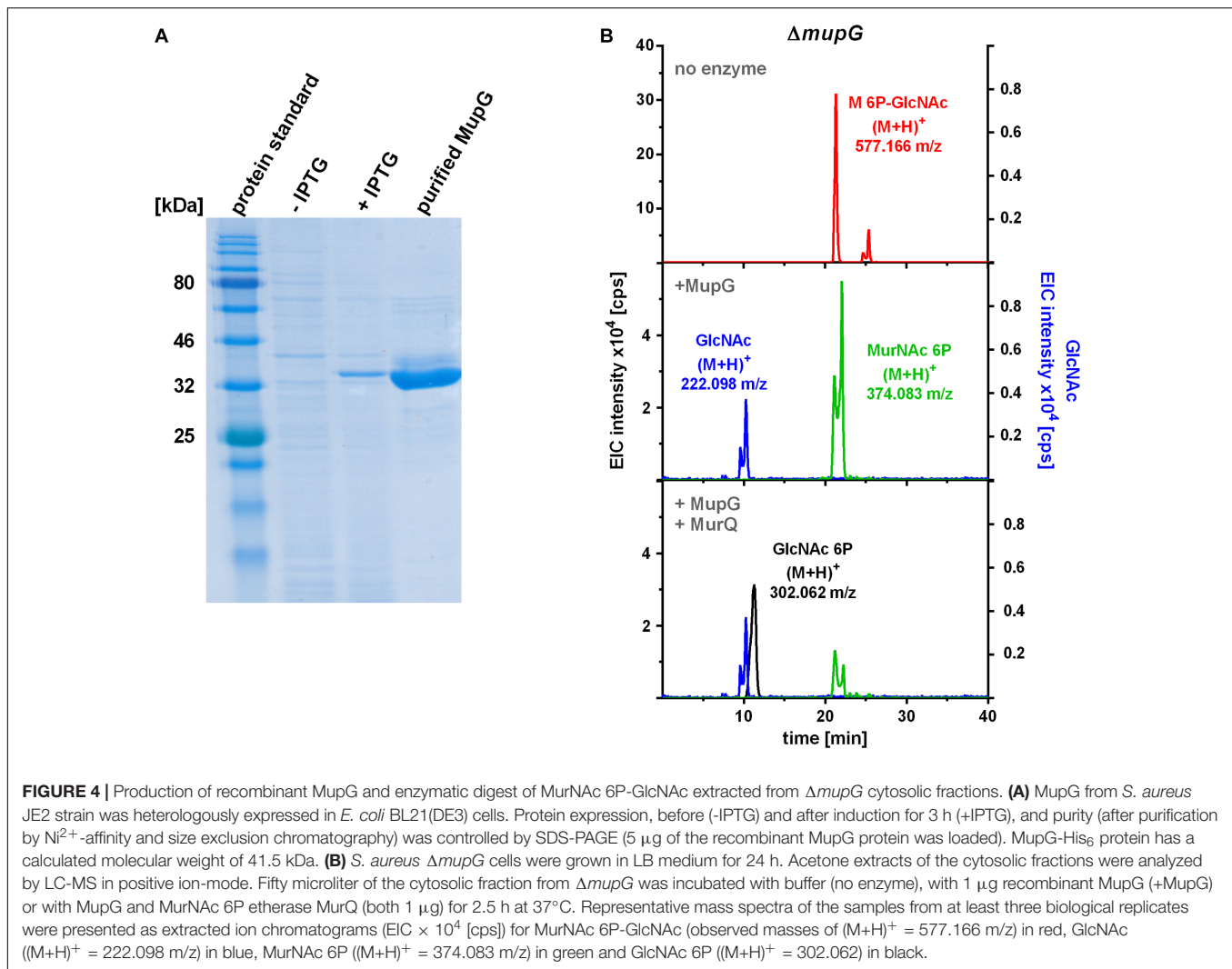


FIGURE 3 | Accumulation of MurNac 6P-GlcNAc in $\Delta mupG$ cells. *S. aureus* $\Delta mupG$ was grown in LB medium to stationary phase (24 h). Acetone extracts of the cytosolic fractions were analyzed by LC-MS in positive ion-mode, before **(A)** and after **(B)** $NaBH_4$ reduction. **(A)** Shown are the fragmentation patterns obtained by in-source decay of the compound that accumulates specifically in $\Delta mupG$ mutant cells and eluates at a retention time of 21.2–21.4 min, represented as extracted ion chromatogram with an observed mass of $(M+H)^+ = 577.166$ m/z ($EIC \times 10^5$ counts per s [cps], upper right corner). Representative mass spectra from three biological replicates are illustrated. **(B)** Shown are the fragmentation patterns after reduction of the sample with $NaBH_4$, which results in the formation of a new compound that elutes at 21.0 min, represented by an EIC with an observed mass of $(M+H)^+ = 579.178$ m/z (upper right corner). The mass spectra fragmentation patterns of both compounds were presented in Compass DataAnalysis program (Bruker) from 300 to 700 m/z. The obtained fragmentation pattern indicated that the substrate for MupG is MurNac 6P-GlcNAc.



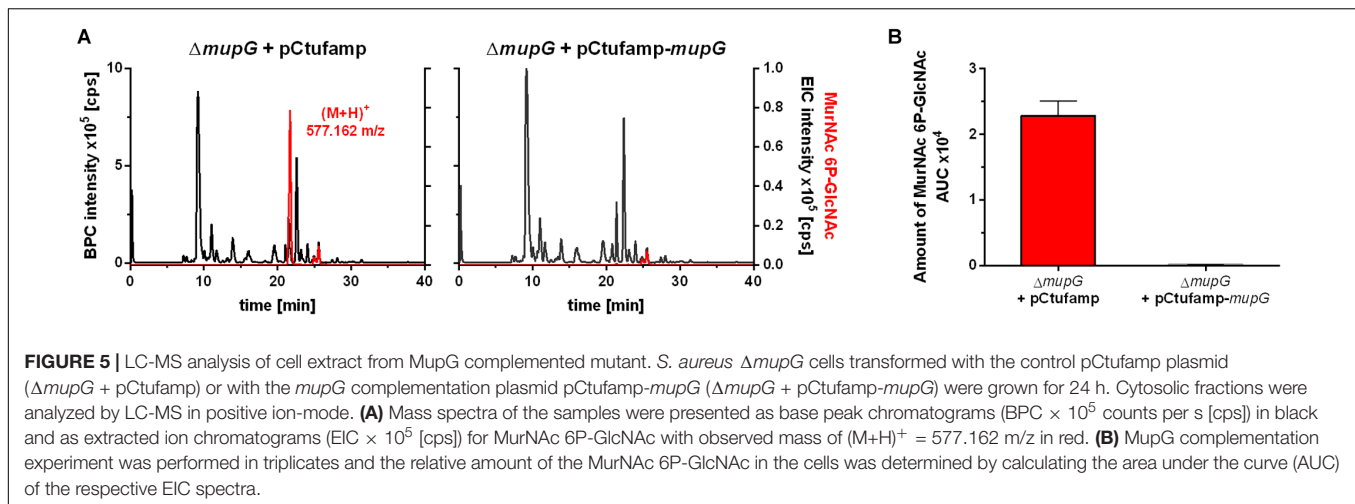
exponential growth phase (3 h), early stationary phase (9 h) and stationary phase (24 h). These growth phases were defined by a growth kinetics study with *S. aureus* wild type and $\Delta mupG$ mutant cells in LB medium (cf. Figure 1). The accumulation of MurNac 6P-GlcNAc was low at exponential phase, increased significantly at transition phase and reached the highest level after 24 h of growth (Supplementary Figure 4). Thus, accumulation of MurNac 6P-GlcNAc in $\Delta mupG$ cells confirmed that cell wall sugar recycling occurs predominantly in the transition and stationary phase.

We further investigated, whether accumulation of MurNac 6P-GlcNAc in the $\Delta mupG$ cells can be abolished by expressing MupG on a plasmid. We used stationary phase cells for this study, since highest levels of accumulation were obtained at this stage (Supplementary Figure 4). *S. aureus* $\Delta mupG$ cells were transformed with a plasmid (named pCtufamp-mupG; see Supplementary Data) constitutively expressing MupG, or with empty plasmid (pCtufamp) as a control. Analysis of the cytosolic fractions of the $\Delta mupG$ cells showed that MupG expression leads to complete disappearance of MurNac

6P-GlcNAc amounts in the cytosol after 24 h of growth (Figure 5).

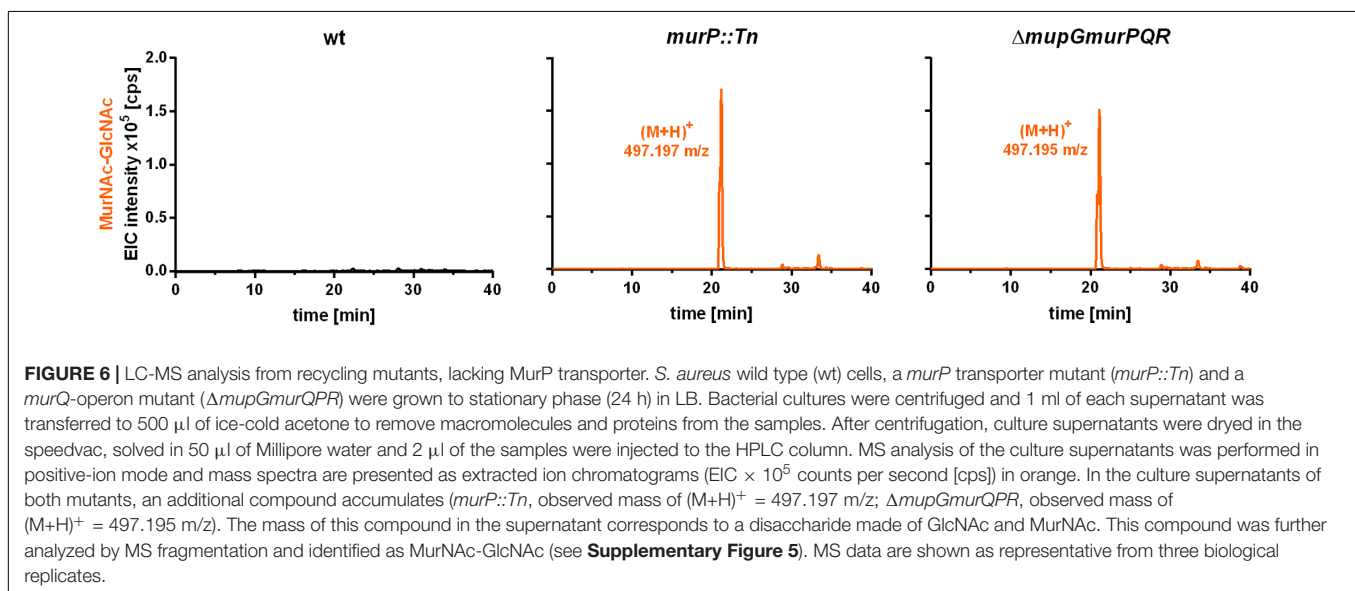
MurNac-GlcNAc Accumulates Extracellularly in *S. aureus* Cells Lacking the MurP Transporter

The PTS transporter MurP of *S. aureus* was shown to transport and concomitantly phosphorylate MurNac, yielding MurNac 6P (Borisova et al., 2016). However, MurNac-GlcNAc rather than MurNac is the main sugar released from the peptidoglycan by Atl and other autolysins during cell wall turnover in *S. aureus*. Thus, we proposed that MurNac-GlcNAc might be primary the natural substrates of MurP, thereby generating intracellular MurNac 6P-GlcNAc, the substrate of the MupG hydrolase. To test this hypothesis, we analyzed the extracellular extracts of *S. aureus* wild type and two *murP* mutant cells (*murP::Tn* insertion mutant and $\Delta mupGmurQPR$ markerless deletion mutant). The MS analysis of the culture supernatant indeed revealed the accumulation of a disaccharide turnover



product with a mass identical to MurNac-GlcNAc (observed $(M+H)^+ = 497.197$ and 497.195 m/z, respectively, theoretical mass of $(M+H)^+ = 497.198$ m/z), which was lacking in the culture supernatant of the wild type cells (**Figure 6**). To confirm the identity of the disaccharide, again MS fragmentation analyses before and after reduction were conducted, as summarized in **Supplementary Figure 5**. A compound with the mass of $(M+H)^+ = 497.197$ m/z was detected also as Na^+ and K^+ adducts, as well as it was characterized by the neutral loss of GlcNAc (-221.087 Da) and the formation of a MurNac elimination product [$(M+H)^+ = 276.111$ m/z]. In addition, we identified a fragmentation product in which water was eliminated (-18.004 Da) yielding a dehydration product [$(M+H)^+ = 479.192$ m/z] (**Supplementary Figure 5A**). After $NaBH_4$ reduction of the culture supernatant from the *murP::Tn* mutant, the mass of the disaccharide product $(M+H)^+ = 497.197$ m/z disappeared and a product in a

reduced form with a mass of $(M+H)^+ = 499.214$ m/z appeared. This product was also detected as Na^+ and K^+ adducts and, in addition, the fragmentation pattern revealed a mass corresponding to a MurNac elimination product (observed mass of 276.108 m/z) that lost a neutral mass, corresponding to the exact mass of reduced GlcNAc (-223.107 Da). The absence of a fragmentation product with a loss of water is in agreement with a reduction at the anomeric site, which precludes water elimination. The fragmentation pattern of the non-reduced and reduced extracellular accumulation products indicated that MurNac-GlcNAc, but not GlcNAc-MurNac, accumulates in the culture supernatant of $\Delta murP$ deletion mutants. This disaccharide was not cleaved by the recombinant β -1,4-*N*-acetylglucosaminidase NagZ from *B. subtilis* (Litzinger et al., 2010a,b) (data not shown), which provides a further evidence that GlcNAc-MurNac is not the recycling product in *S. aureus*. The same MS



fragmentation pattern was obtained in the culture supernatant of the $\Delta mupGmurQPR$ recycling mutant, before and after reduction of the supernatant (data not shown), showing that also in this mutant the recycling product MurNac-GlcNac accumulates. Interestingly, in the culture supernatant of the $\Delta mupGmurQPR$ mutant also other compounds accumulated and were absent in the supernatant of the wild type cells, which nature could not be identified so far (data not shown).

To conclude, the extracellular accumulation of MurNac-GlcNac in both *murP* mutants, as well as the intracellular accumulation of MurNac 6P-GlcNac in the *mupG* mutants and the absence of MurNac 6P-GlcNac and MurNac 6P in the cytosol of $\Delta mupGmurQPR$ operon mutant revealed that the disaccharide MurNac-GlcNac is the natural substrate internalized by the PTS transporter MurP, which intracellularly yields MurNac 6P-GlcNac, the substrate of MupG.

DISCUSSION

We discovered in this study how *S. aureus* reutilizes the sugar part of the peptidoglycan of its cell wall. The overall scheme of this novel peptidoglycan recycling pathway is depicted in **Figure 7**. Mass spectrometric analysis of sugars compounds, accumulating in the growth medium of $\Delta murP$ cells (MurNac-GlcNac) and in the cytoplasm of $\Delta mupG$ cells (MurNac 6P-GlcNac), measured directly or after reduction of the sugars, unequivocally demonstrated the chemical nature of these compounds and allowed to establish the pathway. Thus, the principle peptidoglycan turnover product of *S. aureus* is MurNac-GlcNac, which results from the peptidoglycan cleavage by muramoyl-L-Ala amidases and endo-N-acetylglucosaminidases, whereas lysozyme-like endo-N-acetylmuramidases would generate GlcNac-MurNac products. Remarkably, the peptidoglycan of *S. aureus* is frequently O-acetylated at the C6 hydroxyl group of MurNac, thereby rendered lysozyme-resistant (Bera et al., 2006; Sychantha et al., 2017). An endogenous lysozyme-like muramidase therefore would not be able to cleave the peptidoglycan of *S. aureus*. Accordingly, *S. aureus* possesses peptidoglycan-cleaving endo-N-acetylglucosaminidases: one of them is the well-studied major autolysin Atl (Sugai et al., 1995; Wheeler et al., 2015; Chan et al., 2016).

Since only MurNac-GlcNac and not MurNac was found in the spent medium of the *murP::Tn* and $\Delta mupGmurQPR$ mutants during growth, the disaccharide appears to be the general peptidoglycan turnover product of *S. aureus* and natural substrate of the PTS transporter MurP. However, MurP had been shown previously to take up and phosphorylate also MurNac, if added to the growth medium (Borisova et al., 2016). Thus, apparently MurP accepts both sugars, MurNac and MurNac-GlcNac as substrates. To our knowledge, this is the first report of a PTS system that is able to take up and to specifically phosphorylate a disaccharide as well as a monosaccharide (Postma et al., 1993). Since *murP* of *S. aureus* encodes only the enzyme IIBC components, an enzyme IIA (along with the general components EI and HPr of the PTS) is required to enable MurP functioning

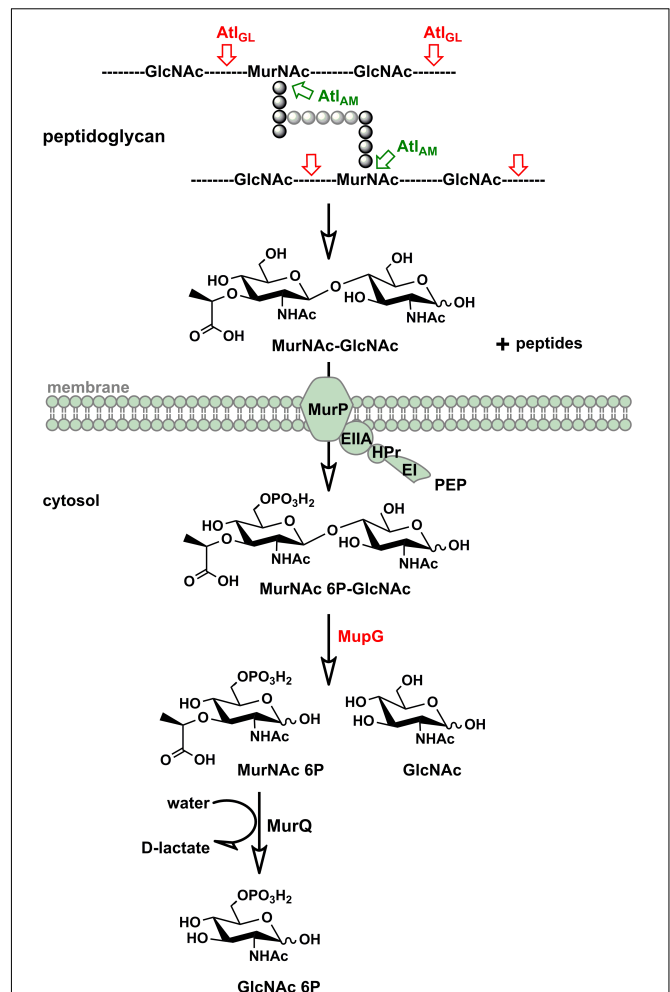


FIGURE 7 | Scheme of the peptidoglycan sugar recycling in *S. aureus*. During growth and division, *S. aureus* cells constantly degrade and resynthesize their peptidoglycan. The major autolysin Atl, a bifunctional muramoyl-L-alanine amidase and endo-N-acetylglucosaminidase, is able to cleave its peptidoglycan, generating MurNac-GlcNac and peptide turnover products. MurNac-GlcNac disaccharide is reutilized: transported in the cells and concomitantly phosphorylated by the MurP PTS transporter generating intracellularly MurNac 6P-GlcNac. Subsequently, the MurNac 6-phosphate-GlcNac glycosidase MupG cleaves this compound, generating the products MurNac 6P and GlcNac. The D-lactyl ether substituent of MurNac 6P is specifically cleaved off by the etherase MurQ, previously characterized in our lab, forming GlcNac 6P and D-lactate (Borisova et al., 2016). It is currently unclear how GlcNac, the second product of the MupG reaction, is further metabolized in *S. aureus* cells.

(**Figure 7**). So far, it is unclear which enzyme IIA operates together with MurP.

The most important result of this study is the identification of a novel 6-phosphomuramidase, encoded by *SAUSA300_0192* (strain USA300), which we named MupG, for MurNac-6P glycosidase. MurNac 6P-GlcNac accumulated in $\Delta mupG$ cells of *S. aureus* and recombinantly produced MupG cleaved MurNac 6P-GlcNac, releasing MurNac 6P and GlcNac. The former product is subsequently metabolized and was identified by

specific cleavage by the MurNAc 6P etherase MurQ, yielding GlcNAc 6P and D-lactate (Borisova et al., 2016). Moreover, accumulation of MurNAc 6P-GlcNAc in a $\Delta mupG$ mutant was abolished by complementation using a MupG-expressing plasmid. Since only accumulation of MurNAc 6P-GlcNAc and not of MurNAc 6P was observed in a $\Delta murGmurQ$ double mutant (please note that MurNAc 6P accumulates in $\Delta murQ$ cells; Borisova et al., 2016), it can be concluded that recycling of the sugar part of the peptidoglycan during growth of *S. aureus* in LB medium exclusively proceeds via the uptake of MurNAc-GlcNAc disaccharides.

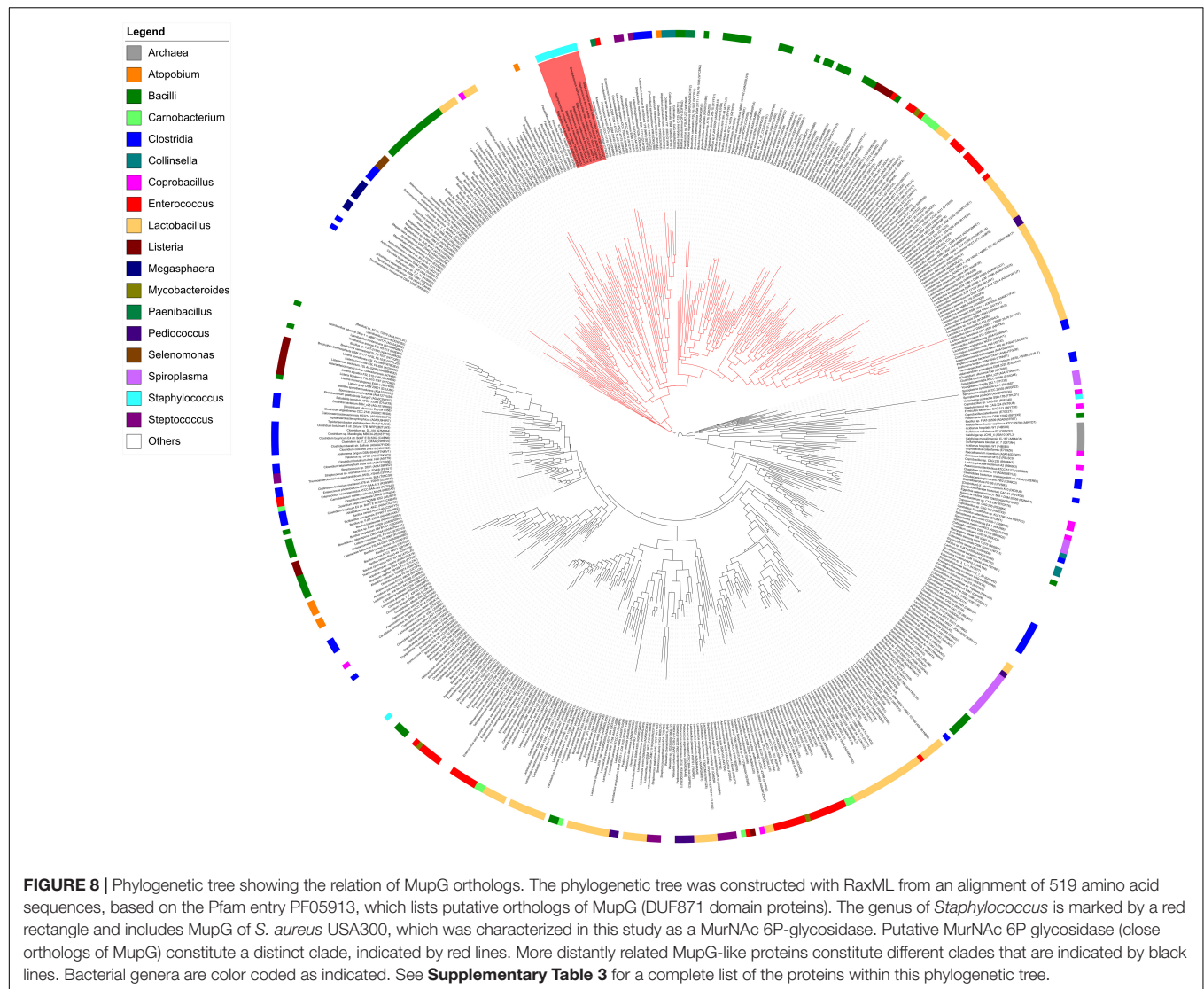
6-phosphoglycosidases commonly act in combination with PTS glycoside transporters. Such systems were characterized with specificities for α -glucosides such as maltose, sucrose, and trehalose (EC 3.2.1.122), or for β -glycosides (EC 3.2.1.86) or β -galactosides (EC 3.2.1.85), such as cellobiose, chitobiose, and lactose (Hengstenberg et al., 1993; Mokhtari et al., 2013). For example, *S. aureus* (as well as *Lactobacillus* and *Streptococcus* sp.) imports lactose via the specific PTS LacE (enzyme IIBC), which phosphorylates the disaccharide at the C6 hydroxyl group of the β -galactose moiety (Hengstenberg et al., 1993). In addition, it possesses a cytoplasmic 6-phospho- β -galactosidase (LacG) that hydrolyzes lactose 6P to galactose 6P and glucose (Staedtler et al., 1995; Yip et al., 2007; Hill and Reilly, 2008). All of the 6P-glycosidases characterized to date are classified within the CAZy glycosidase families 1 and 4 (Davies et al., 2005), which operate by very distinct mechanisms (Witt et al., 1993; Staedtler et al., 1995; Yip et al., 2007; Hill and Reilly, 2008). MupG, however, displays no significant similarity with these glycosidases, instead it founds an entirely new enzyme family. MupG and related proteins so far had been classified as domain of unknown function proteins (IPR008589; DUF871). Although they had been grouped within the glycoside hydrolase (IPR017853) and aldolase-type TIM barrel (IPR013785) superfamilies, no clear attribution to glycosidase function had been made by bioinformatic analyses. The mechanism of members of this novel glycosidase family, i.e., the stereochemical outcome and catalytic residues remain enigmatic. Our results, however, indicate that MupG has no requirement for NAD^+ as for family 4 glycosidases (Yip et al., 2007).

Proteins displaying significant amino acid sequence identities with MupG of *S. aureus* can be found in different bacterial species. Together with MupG these proteins constitute a family (Pfam PF05913) containing domain of unknown function (DUF) 871, with MupG representing the first characterized enzyme of this protein family. The distribution of putative orthologous proteins of MupG is surprisingly narrow and mostly restricted to the phylum firmicutes. The reason for this narrow phylogenetic distribution among the firmicutes and a very selective occurrence within organisms of other phyla, is currently unclear. It may suggest a recent evolutionary event and in addition the distribution by horizontal gene transfer, however, additional studies are required to confirm these assumptions. To learn more about the distribution of MupG orthologs within bacteria, we constructed a phylogenetic tree, based on an alignment of 519 amino acid sequences extracted from the protein family entry Pfam PF05913 (Figure 8) that includes proteins from 115

bacterial genera as well as from five Crenarcheotae and one nematode species (see **Supplementary Table 3** for a complete list of species or genera containing putative enzymes orthologous to MupG). Intriguingly, the phylogenetic tree revealed distinct clades of proteins that include close homologs of MupG and more distinct MupG-like proteins (Figure 8). Potential orthologs of MupG of *S. aureus* are found in various *Staphylococcus* sp. (red rectangle, Figure 8) and in many other Bacilli, e.g., Bacillales such as *Listeria*, *Paenibacillus*, and *Bacillus* sp., and also in Lactobacillales, e.g., *Streptococcus*, *Lactococcus*, *Enterococcus*, *Lactobacillus*, and *Pediococcus* sp., as well as in some Clostridiales. Intriguingly, also some few Fusobacteriales, Chlamydiales and Spirochetales species as well the nematode *Trichuris trichiura* possess a putative MupG ortholog. Some bacterial species, however, contain up to six putative paralogs of MupG (Supplementary Table 3), indicating that the PF05913/DUF871 protein family besides MupG orthologs might also contain proteins of distinct physiological function and with altered substrate specificity. For example, *Coprobacillus cateniformis* contains six putative paralogs, *Carnobacterium maltaromaticum* LMA28 five, *Lactobacillus plantarum* WCFS1 four, *Bacillus anthracis* and *Enterococcus faecalis* V583 three and *Lactococcus lactis* IL1403, *Bacillus megaterium* and many other bacteria contain two putative paralogs (cf. Supplementary Table 3). We assume that close homologs of MupG of *S. aureus* have identical function (MurNAc-6P glycosidases, see protein clade colored red in Figure 8) but more remotely related proteins (colored black in Figure 8) likely contain enzymes of different function. Remarkably, some archaea (e.g., *Sulfolobus solfataricus* and *Sulfurisphaera tokodaii*) contain putative MupG-like orthologs. Since archaea lack a peptidoglycan cell wall it seems likely that these enzymes have a function that differs from the hydrolysis of a peptidoglycan turnover product. Many firmicutes presumably contain a MupG ortholog and supposedly possess a recycling pathway for MurNAc-GlcNAc as that presented here for *S. aureus*. Notably, crystal structures of two putative orthologs of MupG [from *Bacillus cereus* (1×7f) and *Enterococcus faecalis* (2P0O)] were deposited to the protein structure database². We are currently investigating whether these enzymes and MupG have the same specificity and function.

For a long time, the need for cell wall recycling in Gram-positive bacteria, and particularly in coccoid bacteria such as *S. aureus*, had been questioned. Although, reports from the 1970s revealed a massive turnover of the cell wall in *S. aureus* (Wong et al., 1974; Blümel et al., 1979; reviewed in Doyle et al., 1988; Reith and Mayer, 2011). Recent studies, showed that the peptidoglycan of the cell wall in *S. aureus* undergoes a massive rearrangement during growth and division that involves glycan strand trimming by endo-N-acetylglucosaminidases (Wheeler et al., 2015; Chan et al., 2016), peptidoglycan degradation by autolysins such as Atl during cell division and separation (Yamada et al., 1996; Biswas, 2009; Götz et al., 2014) as well as autolysis during biofilm formation (Bose et al., 2012). We recently demonstrated that peptidoglycan recycling proceeds in Gram-positive organisms predominantly occurring during transition and stationary phases

²<https://www.rcsb.org/>



(Borisova et al., 2016). The results of the present study confirmed these previous observations. Notably, the *mupG* mutant and the $\Delta mupG \Delta murQ$ double mutant showed a weak disadvantage during growth in stationary phase (cf. **Supplementary Figure 2**). This growth defect was stronger than previously observed for the $\Delta murQ$ mutant (Borisova et al., 2016), which might be explained by the inability of the former mutants to recycle both sugars of the peptidoglycan, GlcNAc and MurNac, whereas the latter mutant has a defect only in the recovery of MurNac. So far, it remains unclear how the GlcNAc part of MurNac 6P-GlcNAc is recovered, after cleavage by MupG in the cytoplasm. GlcNAc reutilization would require either a GlcNAc kinase, or alternatively the secretion and a re-import by the GlcNAc PTS of *S. aureus*, in both cases yielding GlcNAc 6P, which can be shuttled into the amino sugar catabolic pathway (Komatsuzawa et al., 2004). Moreover, the fate of the peptide part of the peptidoglycan is currently unknown.

CONCLUSION

Here we elucidated a novel pathway for the uptake and catabolism of the disaccharide MurNac-GlcNAc, which is a specific peptidoglycan turnover product generated by the joint action of peptidoglycan amidases and endo-*N*-acetylglucosamidases, e.g., by the bifunctional autolysin Atl of *S. aureus*. The pathway in *S. aureus* involves the PTS transporter MurP, required for the uptake and phosphorylation of the disaccharide yielding MurNac 6-phosphate-GlcNAc, and MupG, a unique glycosidase with 6-phospho-*N*-acetylmuramidase activity. MupG is the first characterized representative of a so far unexplored protein family containing domain of unknown function DUF871, which is distributed mostly among firmicutes. As many of these organisms also possess peptidoglycan-cleaving endo-*N*-acetylglucosaminidases and MurP-like transporters, besides MupG orthologs, recycling of the peptidoglycan turnover product MurNac-GlcNAc

is presumably a common feature among these firmicutes. Peptidoglycan recycling is crucial for stationary phase survival of Gram-positive bacteria (Borisova et al., 2016) and thus, the pathway identified in this study may serve as a novel target to treat persistent infections by *S. aureus* and selectively other bacteria.

AUTHOR CONTRIBUTIONS

RK, MB, and PE cloned MupG. RK and MB expressed and biochemically characterized MupG. RK and MB performed HPLC-MS experiments and analyzed the data. MA, RK, and NZ aligned the MupG-like protein family, constructed the phylogenetic tree based on this alignment, and prepared the **Figure 8**. MB and CM formulated the original problem and provided guidance throughout the study. MB, CM, RK, and PE designed the experiments and developed the methodology. MB, CM, and RK wrote the manuscript. MB approved the final version to be published.

REFERENCES

- Bera, A., Biswas, R., Herbert, S., and Götz, F. (2006). The presence of peptidoglycan O-acetyltransferase in various staphylococcal species correlates with lysozyme resistance and pathogenicity. *Infect. Immun.* 74, 4598–4604. doi: 10.1128/IAI.00301-06
- Biswas, R. (2009). Characterization of *Staphylococcus aureus* peptidoglycan hydrolases and isolation of defined peptidoglycan structures. Ph.D. thesis, University of Tübingen, Tübingen.
- Biswas, R., Voggu, L., Simon, U. K., Hentschel, P., Thumm, G., and Götz, F. (2006). Activity of the major staphylococcal autolysin Atl. *FEMS Microbiol. Lett.* 259, 260–268. doi: 10.1111/j.1574-6968.2006.00281.x
- Blümel, P., Uecker, W., and Giesbrecht, P. (1979). Zero order kinetics of cell wall turnover in *Staphylococcus aureus*. *Arch. Microbiol.* 121, 103–110. doi: 10.1007/BF00689972
- Boneca, I. G., Huang, Z. H., Gage, D. A., and Tomasz, A. (2000). Characterization of *Staphylococcus aureus* cell wall glycan strands, evidence for a new β -N-acetylglucosaminidase activity. *J. Biol. Chem.* 275, 9910–9918. doi: 10.1074/jbc.275.14.9910
- Borisova, M., Gaupp, R., Duckworth, A., Schneider, A., Dalügge, D., Mühleck, M., et al. (2016). Peptidoglycan recycling in Gram-positive bacteria is crucial for survival in stationary phase. *mBio* 7:e00923-16. doi: 10.1128/mBio.00923-16
- Bose, J. L., Lehman, M. K., Fey, P. D., and Bayles, K. W. (2012). Contribution of the *Staphylococcus aureus* Atl AM and GL murein hydrolase activities in cell division, autolysis, and biofilm formation. *PLoS One* 7:e42244. doi: 10.1371/journal.pone.0042244
- Cabeen, M. T., and Jacobs-Wagner, C. (2005). Bacterial cell shape. *Nat. Rev. Microbiol.* 3, 601–610. doi: 10.1038/nrmicro1205
- Capella-Gutiérrez, S., Silla-Martínez, J. M., and Gabaldón, T. (2009). trimAl: a tool for automated alignment trimming in large-scale phylogenetic analyses. *Bioinformatics* 25, 1972–1973. doi: 10.1093/bioinformatics/btp348
- Chan, Y. G., Frankel, M. B., Missiakas, D., and Schneewind, O. (2016). SagB glucosaminidase is a determinant of *Staphylococcus aureus* glycan chain length, antibiotic susceptibility, and protein secretion. *J. Bacteriol.* 198, 1123–1136. doi: 10.1128/JB.00983-15
- Cho, H., Wivagg, C. N., Kapoor, M., Barry, Z., Rohs, P. D., Suh, H., et al. (2016). Bacterial cell wall biogenesis is mediated by SEDS and PBP polymerase families functioning semi-autonomously. *Nat. Microbiol.* 1:16172 doi: 10.1038/nmicrobiol.2016.172

FUNDING

This work was financed by the German Research Foundation (DFG; Grants SFB766/A15 and GRK1708/B2 to CM). We further acknowledge support by the DFG and the Open Access Publishing Fund of the University of Tübingen.

ACKNOWLEDGMENTS

We are very grateful to Rosmarie Gaupp, Friedrich Götz, and Heike Brötz-Oesterheld for providing plasmids, strains, and working space.

SUPPLEMENTARY MATERIAL

The Supplementary Material for this article can be found online at: <https://www.frontiersin.org/articles/10.3389/fmicb.2018.02725/full#supplementary-material>

- Davies, G. J., Gloster, T. M., and Henrissat, B. (2005). Recent structural insights into the expanding world of carbohydrate-active enzymes. *Curr. Opin. Struct. Biol.* 15, 637–645. doi: 10.1016/j.sbi.2005.10.008
- Doyle, R. J., Chaloupka, J., and Vinter, V. (1988). Turnover of cell walls in microorganisms. *Microbiol. Rev.* 52, 554–567.
- Foster, S. J. (1995). Molecular characterization and functional analysis of the major autolysin of *Staphylococcus aureus* 8325/4. *J. Bacteriol.* 177, 5723–5725. doi: 10.1128/jb.177.19.5723-5725.1995
- Frankel, M. B., Hendrickx, A. P., Missiakas, D. M., and Schneewind, O. (2011). LytN, a murein hydrolase in the cross-wall compartment of *Staphylococcus aureus*, is involved in proper bacterial growth and envelope assembly. *J. Biol. Chem.* 286, 32593–32605. doi: 10.1074/jbc.M111.258863
- Fuchs, R., Stoehr, P., Rice, P., Omond, R., and Cameron, G. (1990). New services of the EMBL data library. *Nucleic Acids Res.* 18, 4319–4323. doi: 10.1093/nar/18.15.4319
- Gally, D., and Archibald, A. R. (1993). Cell wall assembly in *Staphylococcus aureus*: proposed absence of secondary crosslinking reactions. *J. Gen. Microbiol.* 139, 1907–1913. doi: 10.1099/00221287-139-8-1907
- Gisin, J., Schneider, A., Nagele, B., Borisova, M., and Mayer, C. (2013). A cell wall recycling shortcut that bypasses peptidoglycan de novo biosynthesis. *Nat. Chem. Biol.* 9, 491–493. doi: 10.1038/nchembio.1289
- Götz, F., Heilmann, C., and Stehle, T. (2014). Functional and structural analysis of the major amidase (Atl) in *Staphylococcus*. *Int. J. Med. Microbiol.* 304, 156–163. doi: 10.1016/j.ijmm.2013.11.006
- Hengstenberg, W., Kohlbrecher, D., Witt, E., Kruse, R., Christiansen, I., Peters, D., et al. (1993). Structure and function of proteins of the phosphotransferase system and of 6-phospho-beta-glycosidases in Gram-positive bacteria. *FEMS Microbiol. Rev.* 12, 149–163.
- Hill, A. D., and Reilly, P. J. (2008). Computational analysis of glycoside hydrolase family 1 specificities. *Biopolymers* 89, 1021–1031. doi: 10.1002/bip.21052
- Hiramatsu, K., Katayama, Y., Matsuo, M., Sasaki, T., Morimoto, Y., Sekiguchi, A., et al. (2014). Multi-drug-resistant *Staphylococcus aureus* and future chemotherapy. *J. Infect. Chemother.* 20, 593–601. doi: 10.1016/j.jiac.2014.08.001
- Kajimura, J., Fujiwara, T., Yamada, S., Suzawa, Y., Nishida, T., Oyamada, Y., et al. (2005). Identification and molecular characterization of an N-acetylmuramyl-L-alanine amidase Sle1 involved in cell separation of *Staphylococcus aureus*. *Mol. Microbiol.* 58, 1087–1101. doi: 10.1111/j.1365-2958.2005.04881.x
- Katoh, K., and Standley, D. M. (2013). MAFFT multiple sequence alignment software version 7: improvements in performance and usability. *Mol. Biol. Evol.* 30, 772–780. doi: 10.1093/molbev/mst010

- Komatsuzawa, H., Fujiwara, T., Nishi, H., Yamada, S., Ohara, M., McCallum, N., et al. (2004). The gate controlling cell wall synthesis in *Staphylococcus aureus*. *Mol. Microbiol.* 53, 1221–1231. doi: 10.1111/j.1365-2958.2004.04200.x
- Letunic, I., and Bork, P. (2016). Interactive tree of life (iTOL) v3: an online tool for the display and annotation of phylogenetic and other trees. *Nucleic Acids Res.* 44, W242–W245. doi: 10.1093/nar/gkw290
- Litzinger, S., Duckworth, A., Nitzsche, K., Risinger, C., Wittmann, V., and Mayer, C. (2010a). Muropeptide rescue in *Bacillus subtilis* involves sequential hydrolysis by beta-N-acetylglucosaminidase and N-acetylmuramyl-L-alanine amidase. *J. Bacteriol.* 192, 3132–3143. doi: 10.1128/JB.01256-09
- Litzinger, S., Fischer, S., Polzer, P., Diederichs, K., Welte, W., and Mayer, C. (2010b). Structural and kinetic analysis of *Bacillus subtilis* N-acetylglucosaminidase reveals a unique Asp-His dyad mechanism. *J. Biol. Chem.* 285, 35675–35684. doi: 10.1074/jbc.M110.131037
- Litzinger, S., and Mayer, C. (2010). “Chapter 1: the murein sacculus,” in *Prokaryotic Cell Wall Compounds - Structure and Biochemistry*, eds H. König, H. Claus, and A. Varma (New York, NY: Springer), 3–52.
- Meeske, A. J., Riley, E. P., Robins, W. P., Uehara, T., Mekalanos, J. J., Kahne, D., et al. (2016). SEDS proteins are a widespread family of bacterial cell wall polymerases. *Nature* 537, 634–638. doi: 10.1038/nature19331
- Mokhtari, A., Blacato, V. S., Repizo, G. D., Henry, C., Pikis, A., Bourand, A., et al. (2013). *Enterococcus faecalis* utilizes maltose by connecting two incompatible metabolic routes via a novel maltose 6'-phosphate phosphatase (MapP). *Mol. Microbiol.* 88, 234–253. doi: 10.1111/mmi.12183
- Monteiro, J. M., Fernandes, P. B., Vaz, F., Pereira, A. R., Tavares, A. C., Ferreira, M. T., et al. (2015). Cell shape dynamics during the staphylococcal cell cycle. *Nat. Commun.* 6:8055. doi: 10.1038/ncomms9055
- Postma, P. W., Lengeler, J. W., and Jacobson, G. R. (1993). Phosphoenolpyruvate:carbohydrate phosphotransferase systems of bacteria. *Microbiol. Rev.* 57, 543–594.
- Ramadurai, L., Lockwood, K. J., Nadakavukaren, M. J., and Jayaswal, R. K. (1999). Characterization of a chromosomally encoded glycylglycine endopeptidase of *Staphylococcus aureus*. *Microbiology* 145(Pt 4), 801–808. doi: 10.1099/13500872-145-4-801
- Reith, J., and Mayer, C. (2011). Peptidoglycan turnover and recycling in Gram-positive bacteria. *Appl. Microbiol. Biotechnol.* 92, 1–11. doi: 10.1007/s00253-011-3486-x
- Schaub, R. E., and Dillard, J. P. (2017). Digestion of peptidoglycan and analysis of soluble fragments. *Bio Protoc.* 7:e2438. doi: 10.21769/BioProtoc.2438
- Staedtler, P., Hoenig, S., Frank, R., Withers, S. G., and Hengstenberg, W. (1995). Identification of the active-site nucleophile in 6-phospho-beta-galactosidase from *Staphylococcus aureus* by labelling with synthetic inhibitors. *Eur. J. Biochem.* 232, 658–663. doi: 10.1111/j.1432-1033.1995.tb20857.x
- Stamatakis, A. (2014). RAxML version 8: a tool for phylogenetic analysis and post-analysis of large phylogenies. *Bioinformatics* 30, 1312–1313. doi: 10.1093/bioinformatics/btu033
- Stapleton, M. R., Horsburgh, M. J., Hayhurst, E. J., Wright, L., Jonsson, I. M., Tarkowski, A., et al. (2007). Characterization of IsaA and ScaD, two putative lytic transglycosylases of *Staphylococcus aureus*. *J. Bacteriol.* 189, 7316–7325. doi: 10.1128/JB.00734-07
- Sugai, M., Komatsuzawa, H., Akiyama, T., Hong, Y. M., Oshida, T., Miyake, Y., et al. (1995). Identification of endo-beta-N-acetylglucosaminidase and N-acetylmuramyl-L-alanine amidase as cluster-dispersing enzymes in *Staphylococcus aureus*. *J. Bacteriol.* 177, 1491–1496. doi: 10.1128/jb.177.6.1491-1496.1995
- Sychantha, D., Jones, C. S., Little, D. J., Moynihan, P. J., Robinson, H., Galley, N. F., et al. (2017). In vitro characterization of the antivirulence target of Gram-positive pathogens, peptidoglycan O-acetyltransferase A (OatA). *PLoS Pathog.* 13:e1006667. doi: 10.1371/journal.ppat.1006667
- Takahashi, J., Komatsuzawa, H., Yamada, S., Nishida, T., Labischinski, H., Fujiwara, T., et al. (2002). Molecular characterization of an atl null mutant of *Staphylococcus aureus*. *Microbiol. Immunol.* 46, 601–612. doi: 10.1111/j.1348-0421.2002.tb02741.x
- Vollmer, W., Blanot, D., and De Pedro, M. A. (2008). Peptidoglycan structure and architecture. *FEMS Microbiol. Rev.* 32, 149–167. doi: 10.1111/j.1574-6976.2007.00094.x
- Wheeler, R., Turner, R. D., Bailey, R. G., Salamaga, B., Mesnage, S., Mohamad, S. A., et al. (2015). Bacterial cell enlargement requires control of cell wall stiffness mediated by peptidoglycan hydrolases. *mBio* 6:e00660. doi: 10.1128/mBio.00660-15
- Witt, E., Frank, R., and Hengstenberg, W. (1993). 6-Phospho-beta-galactosidases of gram-positive and 6-phospho-beta-glucosidase B of gram-negative bacteria: comparison of structure and function by kinetic and immunological methods and mutagenesis of the lacG gene of *Staphylococcus aureus*. *Protein Eng.* 6, 913–920. doi: 10.1093/protein/6.8.913
- Wong, W., Young, F. E., and Chatterjee, A. N. (1974). Regulation of bacterial cell walls: turnover of cell wall in *Staphylococcus aureus*. *J. Bacteriol.* 120, 837–843.
- Yamada, S., Sugai, M., Komatsuzawa, H., Nakashima, S., Oshida, T., Matsumoto, A., et al. (1996). An autolysin ring associated with cell separation of *Staphylococcus aureus*. *J. Bacteriol.* 178, 1565–1571. doi: 10.1128/jb.178.6.1565-1571.1996
- Yip, V. L., Thompson, J., and Withers, S. G. (2007). Mechanism of GlvA from *Bacillus subtilis*: a detailed kinetic analysis of a 6-phospho-alpha-glucosidase from glycoside hydrolase family 4. *Biochemistry* 46, 9840–9852. doi: 10.1021/bi700536p

Conflict of Interest Statement: The authors declare that the research was conducted in the absence of any commercial or financial relationships that could be construed as a potential conflict of interest.

Copyright © 2018 Kluj, Ebner, Adamek, Ziemert, Mayer and Borisova. This is an open-access article distributed under the terms of the Creative Commons Attribution License (CC BY). The use, distribution or reproduction in other forums is permitted, provided the original author(s) and the copyright owner(s) are credited and that the original publication in this journal is cited, in accordance with accepted academic practice. No use, distribution or reproduction is permitted which does not comply with these terms.



Functional Characterization of Enzymatic Steps Involved in Pyruvylation of Bacterial Secondary Cell Wall Polymer Fragments

Fiona F. Hager¹, Arturo López-Guzmán¹, Simon Krauter², Markus Blaukopf², Mathias Polter¹, Inka Brockhausen³, Paul Kosma² and Christina Schäffer^{1*}

¹ NanoGlycobiology Unit, Department of NanoBiotechnology, Universität für Bodenkultur Wien, Vienna, Austria, ² Division of Organic Chemistry, Department of Chemistry, Universität für Bodenkultur Wien, Vienna, Austria, ³ Department of Biomedical and Molecular Sciences, Queen's University, Kingston, ON, Canada

OPEN ACCESS

Edited by:

Stephane Mesnage,
University of Sheffield,
United Kingdom

Reviewed by:

Evguenii Vinogradov,
National Research Council Canada,
Canada

Antonio Molinaro,
Università degli Studi di Napoli
Federico II, Italy

*Correspondence:

Christina Schäffer
christina.schaeffer@boku.ac.at

Specialty section:

This article was submitted to
Microbial Physiology and Metabolism,
a section of the journal
Frontiers in Microbiology

Received: 04 May 2018

Accepted: 05 June 2018

Published: 27 June 2018

Citation:

Hager FF, López-Guzmán A, Krauter S, Blaukopf M, Polter M, Brockhausen I, Kosma P and Schäffer C (2018) Functional Characterization of Enzymatic Steps Involved in Pyruvylation of Bacterial Secondary Cell Wall Polymer Fragments. *Front. Microbiol.* 9:1356. doi: 10.3389/fmicb.2018.01356

Various mechanisms of protein cell surface display have evolved during bacterial evolution. Several Gram-positive bacteria employ S-layer homology (SLH) domain-mediated sorting of cell-surface proteins and concomitantly engage a pyruvylated secondary cell-wall polymer as a cell-wall ligand. Specifically, pyruvate ketal linked to β -D-ManNAc is regarded as an indispensable epitope in this cell-surface display mechanism. That secondary cell wall polymer (SCWP) pyruvylation and SLH domain-containing proteins are functionally coupled is supported by the presence of an ortholog of the predicted pyruvyltransferase CsaB in bacterial genomes, such as those of *Bacillus anthracis* and *Paenibacillus alvei*. The *P. alvei* SCWP, consisting of pyruvylated disaccharide repeats [\rightarrow 4)- β -D-GlcNAc-(1 \rightarrow 3)-4,6-Pyr- β -D-ManNAc-(1 \rightarrow)] serves as a model to investigate the widely unexplored pyruvylation reaction. Here, we reconstituted the underlying enzymatic pathway *in vitro* in combination with synthesized compounds, used mass spectrometry, and nuclear magnetic resonance spectroscopy for product characterization, and found that CsaB-catalyzed pyruvylation of β -D-ManNAc occurs at the stage of the lipid-linked repeat. We produced the *P. alvei* TagA (PAV_RS07420) and CsaB (PAV_RS07425) enzymes as recombinant, tagged proteins, and using a synthetic 11-phenoxyundecyl-diphosphoryl- α -GlcNAc acceptor, we uncovered that TagA is an inverting UDP- α -D-ManNAc:GlcNAc-lipid carrier transferase, and that CsaB is a pyruvyltransferase, with synthetic UDP- α -D-ManNAc and phosphoenolpyruvate serving as donor substrates. Next, to substitute for the UDP- α -D-ManNAc substrate, the recombinant UDP-GlcNAc-2-epimerase MnaA (PAV_RS07610) of *P. alvei* was included in this *in vitro* reconstitution system. When all three enzymes, their substrates and the lipid-linked GlcNAc primer were combined in a one-pot reaction, a lipid-linked SCWP repeat precursor analog was obtained. This work highlights the biochemical basis of SCWP biosynthesis and bacterial pyruvyl transfer.

Keywords: secondary cell wall polymer, SLH domain, glycosyltransferase, pyruvyltransferase, multi-enzyme assay

INTRODUCTION

The cell surface influences the physicochemical properties of a bacterium, its physiology, life-style, and fitness in a competitive habitat. While the cell surface of any bacterium is composition- and structure-wise unique and, thus, can be regarded as a “bacterial bar code,” distinct mechanisms for the robust and, frequently, multivalent display of proteins have evolved. Cell surface display mechanisms are usually based on the fusion of a cell wall targeting motif to the proteins deemed for display, working in concert with a cell wall ligand (Lee et al., 2003; Desvaux et al., 2006).

Several Gram-positive bacteria employ SLH domain-mediated sorting of cell surface proteins and concomitantly engage a pyruvylated SCWP (also known as cell wall glycopolymer) as a cell wall ligand. Specifically, pyruvate ketal linked to β -D-ManNAc is regarded an indispensable and ancestral epitope in this cell surface display mechanism (Mesnage et al., 2000; Cava et al., 2004; Kern et al., 2010). There are over 54,000 specific hits within the conserved protein domain family SLH (pfam00395) (Marchler-Bauer et al., 2015), widely in the phyla firmicutes, cyanobacteria, and actinobacteria, among others, underlining the prevalence of this protein domain in bacteria. The functional coupling of SLH domain containing proteins (SLH proteins) and SCWP pyruvylation is substantiated by the finding that several bacteria – including, e.g., *Bacillus anthracis* (Forsberg et al., 2012), *Bacillus cereus* strains (Forsberg et al., 2011), *Lysinibacillus sphaericus* (Ilk et al., 1999), *Thermoanaerobacterium thermosulfurigenes* (May et al., 2006), and *Paenibacillus alvei* (Schäffer et al., 2000), all synthesize a suite of SLH proteins, contain pyruvate in their cell wall and have an ortholog of the CsaB enzyme predicted to catalyze the transfer of pyruvate ketal to β -D-ManNAc (Mesnage et al., 2000). Experimental data on CsaB is available for *B. anthracis* (Mesnage et al., 2000; Kern et al., 2010) and *Thermus thermophilus* (Cava et al., 2004), where *csaB* deficient mutants revealed a drastically reduced pyruvic acid content (by ~98%) in comparison to the parent strain supporting pyruvyl transfer activity of CsaB.

Considering the predictably wide-spread occurrence of this protein cell surface display mechanism – in both pathogenic and non-pathogenic bacteria – it is surprising how little is known about the biosynthesis of pyruvylated SCWPs and the involved enzymes. Pyruvylated SCWPs are covalently linked to muramic acid residues of the peptidoglycan backbone and differ structurally from the well investigated teichoic/teichuronic acids (Archibald et al., 1993; Mesnage et al., 2000; Messner et al., 2009; Schade and Weidenmaier, 2016; Rajagopal and Walker, 2017), with the lack of repetitive alditol phosphates and phosphodiester

bonds as the most evident differences (Sára, 2001; Schäffer and Messner, 2005).

The SCWP of *P. alvei* CCM 2051^T (referred to as *P. alvei* throughout the manuscript) – the model organism of the current study – is composed of, on average, 11 pyruvylated disaccharide repeats with the structure $[\rightarrow 4)\text{-}\beta\text{-D-GlcNAc-(1}\rightarrow 3)\text{-4,6-Pyr-}\beta\text{-D-ManNAc-(1}\rightarrow]$ (Schäffer et al., 2000). This SCWP is pivotal to the integrity of the bacterium's cell wall due to its interaction with *P. alvei*'s abundant S-layer protein SpaA (Janesch et al., 2013b) and the cell surface protein SlhA (Janesch et al., 2013a), both possessing three dedicated SLH domains, each, involved in SCWP binding interactions (Ryan J. Blackler, Arturo López-Guzmán, Fiona F. Hager, Gudrun Martinz, Susannah M. L. Gagnon, Omid Haji-Ghassemi, Bettina Janesch, Paul Messner, Paul Kosma, Christina Schäffer and Stephen V. Evans, unpublished data). In close vicinity to the *P. alvei* *spaA* and *slhA* genes on the bacterial genome, five ORFs – named, based on a pBLAST search in relation to the sequenced genome of *P. alvei* DSM 29, *orf1* (PAV_RS07430), *csaB* (PAV_RS07425), *tagA* (PAV_RS07420), *tagO* (PAV_RS07415), and *orf7* (PAV_RS07395) – were identified, which we predicted to constitute an SCWP biosynthesis gene locus (Zarschler et al., 2010). While *P. alvei* does not harbor teichoic acids in its cell wall, TagA and TagO from that gene locus show amino acid sequence similarity to the TagA and TagO enzymes from the polyribitol wall teichoic acid biosynthesis pathway in *Staphylococcus aureus* (Tag A, 36.9% and Tag O, 42.0%) and *Bacillus subtilis* (Tag A, 37.2% and Tag O, 32.0%) (Ginsberg et al., 2006; Brown et al., 2010, 2013). The first enzyme in this pathway, TagO, is an integral membrane protein that transfers GlcNAc-phosphate from UDP-GlcNAc to an undecaprenylphosphate carrier lipid embedded in the cytoplasmic membrane (Weidenmaier et al., 2004; D'Elia et al., 2006b). The lipid-linked monosaccharide is then elongated to a disaccharide by the UDP-ManNAc transferase TagA (Zhang et al., 2006; Brown et al., 2008; D'Elia et al., 2009). While this lipid-linked disaccharide constitutes the platform for the subsequent steps of wall teichoic acid biosynthesis (Lazarevic et al., 2002; Swoboda et al., 2010; Kawai et al., 2011; Zilla et al., 2015; Schaefer et al., 2017), it is equivalent to the disaccharide substrate needed to generate the repeat backbone of the *P. alvei* SCWP (Schäffer et al., 2000).

Information on the pyruvylation step in SCWP biosynthesis, or pyruvylation of sugars in general, is scarce. Pyruvyl transfer activity of CsaB in the context of bacterial cell wall synthesis can be indirectly inferred from data on a few bacteria, in which *csaB* deletion mutants could be created by using sophisticated strategies. A *B. anthracis* Δ *csaB* mutant, for instance, showed S-layer deficiency – probably due to the loss of the pyruvylated motif in the SCWP cell wall ligand – and atypical cell morphology forming long chains of incompletely separated cells (Mesnage et al., 2000; Kern et al., 2010). However, while the structure of the *B. anthracis* SCWP is known (Forsberg et al., 2012), loss of SCWP pyruvylation in a *B. anthracis* mutant has not been demonstrated experimentally. Further, Wang et al. (2013) described *csaB* mutant cells of *B. cereus* G9241, which showed reduced pathogenicity in causing anthrax-like disease in mice.

Abbreviations: cDNA, copy DNA; COSY, correlation spectroscopy; gDNA, genomic DNA; GlcNAc-PP-UndPh, 11-phenoxyundecyl-diphosphoryl- α -GlcNAc; His₆-tag, hexahistidine tag; HMBC, heteronuclear multiple-bond correlation spectroscopy; HSQC, heteronuclear single-quantum coherence spectroscopy; IPTG, isopropyl- β -D-thiogalactopyranoside; ORE, open reading frame; PEP, phosphoenolpyruvate; PvGal, 4,6-ketal-linked galactose; RT, room temperature (22°C); SCWP, secondary cell wall polymer; SDS-PAGE, sodium dodecyl sulfate-polyacrylamide gel electrophoresis; S-layer, bacterial cell surface layer; SLH domain, S-layer homology domain; TOCSY, total correlation spectroscopy.

In contrast, in *P. alvei*, attempts to delete *csaB* have not been successful (Bettina Janesch, Fiona F. Hager, Christina Schäffer, unpublished data), potentially indicating essentiality of the enzyme.

Recent data comes from the pyruvyltransferase Pvg1p of the fission yeast *Schizosaccharomyces pombe*, which carries pyruvic acid 4,6-ketal-linked to galactose (PvGal) as decoration of its *N*-glycans (Gemmill and Trimble, 1996). The recombinant Pvg1p enzyme transferred pyruvyl residues from PEP specifically to β -linked galactose as present in *p*-nitrophenyl- β -Gal (pNP- β -Gal) or pNP- β -lactose (Yoritsune et al., 2013). The crystal structure of the pyruvyltransferase Pvg1p was obtained at a resolution of 2.46 Å, which served as a basis for enzyme/substrate modeling (Higuchi et al., 2016). PvGal biosynthesis was also studied *in vitro* in the context of the therapeutic potential of the *Bacteroides fragilis* capsular polysaccharide A (Sharma et al., 2017).

The current study focuses on the predicted UDP-ManNAc transferase TagA and the predicted pyruvyltransferase CsaB from the *P. alvei* SCWP biosynthesis gene locus. We produced these enzymes, and also the bacterium's cognate UDP-GlcNAc-2-epimerase MnaA, in *Escherichia coli* and used the recombinant, purified proteins in *in vitro* enzyme assays, together with a chemically synthesized GlcNAc-PP-UndPh acceptor (Wang et al., 2014) and PEP as donor substrates, and, in some assays, UDP-ManNAc. In a one-pot reaction, a nature-analogous, lipid-linked SCWP repeat could be obtained, as was confirmed by mass spectrometry and NMR spectroscopy. It was found that pyruvylation of the β -D-ManNAc residue occurs at the lipid-linked disaccharide stage. This study contributes to our understanding of how SCWPs other than teichoic acids/teichuronic acids are biosynthesized and specifically sheds light on the pyruvylation step. Pyruvylation might constitute a valuable target for interfering with the bacterial cell wall composition and, thereby, also bacterial pathogenicity.

MATERIALS AND METHODS

Bacterial Strains and Culture Conditions

Paenibacillus alvei CCM 2051^T (wild-type strain; Czech Collection of Microorganisms, CCM; Brno, Czech Republic) was grown at 37°C and 160 rpm in Luria-Bertani (LB) broth or on LB agar plates. *E. coli* DH5 α and BL21 (DE3) (Invitrogen) were cultivated in selective LB medium (agar or broth) supplemented with 100 μ g/ml ampicillin (Amp) at 37°C with 180 rpm.

RNA Purification and Reverse Transcription-PCR

Total RNA was extracted from *P. alvei* using the PureLink RNA Mini Kit (Thermo Fisher Scientific) and subsequently on-column purified with Purelink DNase (Thermo Fisher Scientific) and TurboDNase (Ambion) to remove DNA contamination. cDNA was then generated using the MultiScribe Reverse Transcriptase from the High-Capacity cDNA Reverse Transcription Kit (Thermo Fisher Scientific) using 500 ng of total RNA. One-twentieth of the cDNA reaction mixture was used as template

for PCR using the Phusion High-Fidelity DNA polymerase (Thermo Fisher Scientific). The produced cDNA was amplified by PCR using primer pairs *csaB*_for/*tagA*_rev and *tagA*_for/*tagO*_rev spanning, from 5' to 3', the genes *csaB* and *tagA*, and *tagA* and *tagO*, respectively. Further, the region spanning *csaB* and *tagO* was bridged using *csaB*_for/*tagO*_rev. As a positive control, gDNA was used, whereas DNase I-treated RNA without the cDNA-generating step as well as NRT (reverse transcription reaction missing reverse transcriptase) served as a control for contamination of total RNA with chromosomal DNA. PCR reaction products were investigated by agarose gel electrophoresis. Primers for RT-PCR were purchased from ThermoFisher Scientific and are listed in Table 1.

DNA Techniques and Plasmid Construction

Genomic DNA of *P. alvei* was isolated from 5 ml of bacterial culture (Cheng and Jiang, 2006). For the purification of DNA fragments and digested plasmids from agarose gels, the GeneJETTM Gel Extraction Kit (Fermentas) was used. Isolation of plasmid DNA from transformed *E. coli* cells was done using the GeneJETTM Plasmid Miniprep Kit (Fermentas). Primers for PCR and DNA sequencing were purchased from ThermoFisher Scientific and are listed in Table 1. For the amplification of genes from gDNA of *P. alvei*, the Phusion High-Fidelity DNA Polymerase (Fermentas) and the thermal cycler My CyclerTM (Bio-Rad) were used.

For recombinant protein expression in *E. coli* BL21 (DE3) cells, plasmids encoding MnaA and CsaB as C-terminal His₆-tag fusion constructs were created by PCR using *P. alvei* gDNA as a template and the primer pairs *MnaA*_fwd_*NdeI*/*MnaA*_rev_*XhoI* and *CsaB*_fwd_*NdeI*/*CsaB*_rev_*XhoI* (Table 1), respectively, to amplify the 1175-bp *mnaA* (PAV_RS07420) and the 1209-bp *csaB* (PAV_RS07425) genes. The amplification products were digested with *NdeI*/*XhoI* and cloned into *NdeI*/*XhoI*-linearized pET22b(+) (Novagen) for expression of His₆-tagged proteins. Recombinant TagA was produced as a fusion protein with the maltose binding protein (MBP) located at its N-terminus, because of a 10-fold higher protein expression rate in comparison to His₆-tagged TagA (Fiona

TABLE 1 | Oligonucleotide primers used for PCR amplification reactions.

Gene	Primer	Sequence (5'–3')
<i>csaB</i>	<i>csaB</i> _for	GGCGCAAGTGATGAAGAAGC
<i>tagA</i>	<i>tagA</i> _rev	GAAGCTGCCCCGACACCCA
<i>tagA</i>	<i>tagA</i> _for	GCTGTTCGTTGCTCGTGGAG
<i>tagO</i>	<i>tagO</i> _rev	CCAGAGTCCCCCATAAAGAT
<i>mnaA</i> -His ₆	<i>MnaA</i> _fwd_ <i>NdeI</i>	GCGCGGGCATATGTCCAAAGTGAAAGTA
<i>mnaA</i> -His ₆	<i>MnaA</i> _rev_ <i>XhoI</i>	GCGCGGGCTCGAGATTTGTGAACTTTGT
MBP- <i>tagA</i>	<i>TagA</i> _fwd_ <i>EcoRI</i>	CGATGGAATTCATGTTAGAAATGAAGGAT
MBP- <i>tagA</i>	<i>TagA</i> _rev_ <i>PstI</i>	CGATGCTGCAGTTACTGCACTTTTGTGGG
<i>csaB</i> -His ₆	<i>CsaB</i> _fwd_ <i>NdeI</i>	CTGTGGCATATGGCGTCCAAAGCTAC AAGAATAGTACTTTCCGGATATTACGGATTCT
<i>csaB</i> -His ₆	<i>CsaB</i> _rev_ <i>XhoI</i>	GACCTACTCGAGCGCCTTATGACGCAGCCAC TTCACAATTTGTTGCGCTGGCTGTTCTGCTT

F. Hager, Christina Schäffer, unpublished observation). The primer pair TagA_fwd_EcoRI/TagA_rev_PstI was used to produce the 781-bp tagA (PAV_RS07420) amplicon, which was digested with EcoRI/PstI and cloned into EcoRI/PstI-linearized pMAL_c2E vector (NEB). All three constructs were chemically transformed into *E. coli* DH5 α cells for the amplification of plasmid DNA. Transformants were screened by colony PCR using RedTaq ReadyMix PCR mix (Sigma-Aldrich) and confirmed by restriction mapping and sequencing (Microsynth).

Heterologous Overexpression and Purification of Recombinant Enzymes

The plasmids encoding *P. alvei* MnaA-His₆, CsaB-His₆, and MBP-TagA, and named pET22b_mnaA, pET22b_csaB, and pMAL_tagA, respectively, were heat-shock-transformed into *E. coli* BL21 (DE3) cells. Selected transformed cells were grown in LB medium to the mid-exponential growth phase (OD₆₀₀ 0.5–0.8), and protein expression was induced with a final concentration of 0.6 mM isopropyl- β -D-thiogalactopyranoside (IPTG). After induction, the bacterial cultures were grown for 4 h at 37°C and 180 rpm followed by harvest through centrifugation (5,500 \times g, 20 min, 8°C).

For nickel affinity chromatography of MnaA-His₆ and CsaB-His₆, the cell pellets of 500 ml bacterial culture containing the C-terminally His₆-tagged enzymes were resuspended in lysis buffer (50 mM sodium phosphate, pH 7.5, 200 mM NaCl, supplemented with 10 mM imidazole and EDTA-free protease inhibitor mixture; cOmplete, Roche Applied Science). Cells were disrupted by sonication applying nine pulses of 20 s (Branson Sonifier 250; output 8, duty cycle 45%, 10 s breaks), each, and lysates were ultra-centrifuged (80,695 \times g, 20 min, 4°C) to remove cell debris. The supernatant fraction (cell crude extract) was incubated for 30 min with 2 ml of nickel-nitrilotriacetic acid resin in a column (Qiagen) equilibrated in lysis buffer using a flow rate of 1.0 ml/min. After recovery of the flow through, the column was washed with lysis buffer containing increasing imidazole concentrations of 20 and 50 mM, 10 column volumes, each. Finally, the protein of interest was eluted with 5 ml of 250 mM imidazole in lysis buffer. Fractions containing MnaA-His₆ and CsaB-His₆, respectively, as determined by 10% SDS-PAGE (Laemmli, 1970) after Coomassie Brilliant Blue G250 staining, were pooled and extensively dialyzed against 25 mM sodium phosphate buffer, pH 7.5, at RT, to remove imidazole.

The MBP-TagA fusion protein was purified over an amylose resin (NEB; 5 ml of resin per liter of bacterial culture) according to the manufacturer's protocol. Protein elution was done with 20 mM Tris/HCl, pH 7.5, containing 200 mM NaCl, 1 mM EDTA, and 10 mM maltose. Fractions containing the protein of interest according to Coomassie Brilliant Blue G250-stained 10% SDS-PAGE were pooled and extensively dialyzed at RT against 25 mM bis(2-hydroxyethyl)amino-Tris(hydroxymethyl)methane (bis-Tris-propane), pH 7.8, for the TagA *in vitro* activity assay, and against 25 mM sodium phosphate buffer, pH 7.5, for MnaA/TagA co-incubation, to remove maltose.

Protein Analytical Methods

The recombinant proteins were verified by Western-blotting using in the case of MnaA-His₆ and CsaB-His₆ an anti-His₆ antibody (Sigma-Aldrich) and for MBP-TagA, an anti-MBP antibody (Thermo Scientific). The protein concentration of the recombinant, tagged enzymes was measured spectrophotometrically and calculated using the A₂₈₀ extinction coefficient and molecular weight obtained from the expASY ProtParam tool¹ and by the Bradford protein assay (Bradford, 1976).

Chemical Synthesis of UDP- α -D-ManNAc

UDP- α -D-ManNAc was chemically synthesized as a donor substrate for the TagA reaction, essentially following established protocols (Yamazaki et al., 1980; Freese and Vann, 1996; Ginsberg et al., 2006) (Supplementary Scheme S1). Starting from 2-acetamido-2-deoxy-D-mannopyranose (compound 6), the triethylammonium salt compound 7 (triethylammonium 2-acetamido-2-deoxy- α -D-mannopyranosyl phosphate) was synthesized. Compound 7 (46 mg, 0.092 mmol) was reacted with uridine 5'-monophosphomorpholidate (153 mg, 0.223 mmol) in 8 ml of freshly distilled dried pyridine under argon atmosphere at RT for 7 days and then concentrated *in vacuo* at 30°C. The product was purified by using a Bio-Scale Mini Macro-Prep High Q anion exchange cartridge (Bio-Rad) with a gradient (0–100%) of 0.25 M triethylammonium bicarbonate buffer, pH 8.0, and lyophilized to give compound 8 [triethylammonium uridine 5'-(2-acetamido-2-deoxy- α -D-mannopyranosyl diphosphate)].

Enzymatic Synthesis of UDP- α -D-ManNAc Using *P. alvei* UDP-GlcNAc Epimerase MnaA

The enzymatic assay of MnaA was set up based on a published protocol (Blume, 2003), with several modifications. Briefly, purified *P. alvei* MnaA-His₆ (45 μ g) was incubated with UDP-GlcNAc (Sigma-Aldrich) at a concentration of 1.3 or 0.5 mM, in 46 mM sodium phosphate buffer, pH 7.5, supplemented with 11 mM MgCl₂, in a total reaction volume of 192.5 μ l at 37°C for up to 30 min; individual reactions were done and stopped in intervals of 5 min. After heat-inactivation (100°C, 1 min), the mixture was centrifuged (10,000 \times g, 5 min, RT), and the supernatant was analyzed by reversed-phase (RP) HPLC (Thermo Scientific/Dionex; Ultimate 3000 Standard LC System) on a Hyperclone 5 μ ODS column (Phenomenex, 150 mm \times 4.6 mm, 5 μ) using 0.4 M sodium phosphate buffer, pH 6.1, with a flow rate of 0.6 ml/min as eluent (Zolghadr et al., 2015). Peaks were identified using UDP (1 nmol), UDP-GlcNAc (5 nmol), and UDP-ManNAc (5 nmol) as standards; detection was done at 254 nm. Epimerization rates by MnaA were calculated from the integrated peak areas using software provided by the Ultimate 3000 Standard LC System.

¹<http://web.expasy.org/protparam>

Sep-Pak Purification of Enzyme Products

Purification of products from *in vitro* enzyme reactions (as described below) was done using a (C18) Sep-Pak classic cartridge (Waters; 360 mg sorbens). The cartridge was equilibrated with 3 ml of methanol followed by 6 ml of H₂O immediately prior to application of the reaction mixture. The samples were loaded on the cartridge by gravity flow, and the flow-through was collected. Subsequently, the cartridge was eluted with 4 ml of H₂O (1-ml fractions) for removal of excess of UDP-ManNAc and hydrophilic components (bis-Tris-propane, sodium phosphate, MgCl₂, or potential enzyme products that are more hydrophilic than the initial acceptor substrate), followed by 3 ml of methanol (1.5 ml fractions); fractions were collected and dried *in vacuo* using a SpeedVac centrifuge (Thermo Fisher Scientific).

LC-ESI-MS of Purified Enzyme Products

Fractions obtained after (C18) Sep-Pak purification were dissolved in a 1:1-solution of H₂O and acetonitrile, and 10 μ l of the sample solutions were analyzed by LC (C4)-ESI-MS using a Phenomenex Jupiter 5 μ C₄, 300 Å, 150 mm \times 2 mm column coupled to an LC-MS device (Shimadzu LC 10 system, Shimadzu 2020 mass spectrometer, Alltech ELSD 3300). The elution profile used during analysis was a gradient of 5–100% CH₃CN (0–2 min: 5% CH₃CN; 2–10 min: 5–100%, 15–16 min: 100–5%, 16–22 min: 5%) at a flow of 0.5 ml/min and a column temperature of 40°C. The eluate was directed into the ESI source for mass detection in the range of 50–2000 with a scan speed of 2143 μ s, and the masses were evaluated using the integrated software, Shimadzu – LabSolutions V. 5.42 SP4.

NMR Spectroscopy of Enzyme Products

NMR spectra of enzyme products were recorded at 297 K in 99.9% D₂O (0.4 ml) in a Shigemi tube with a Bruker Avance III 600 spectrometer (¹H at 600.13 MHz, ¹³C at 150.9 MHz, ³¹P at MHz at 242.9 MHz), using standard Bruker NMR software. ¹H NMR spectra were referenced to 2,2-dimethyl-2-silapentane-5-sulfonic acid (δ 0.0), ¹³C NMR spectra were referenced to external dioxane (δ 67.40), and ³¹P spectra were referenced to external ortho-phosphoric acid (δ 0.0) for solutions in D₂O. COSY experiments and gradient-selected ¹H, ¹H total correlation spectroscopy (TOCSY, mixing time 80 ms) were recorded by use of the pulse programs cosygpqf and mlevph, respectively, with 2048 \times 256 data points and 16 and 8 scans, respectively per t₁-increment. By use of the pulse program hsqcedetgp with 2048 \times 1024 data points and 16 scans per t₁-increment multiplicity edited heteronuclear single quantum coherence spectra (HSQC) (Schleucher et al., 1994) were obtained. Heteronuclear multiple bond correlation spectra (HMBC) (Bax and Summers, 1986) were acquired using the pulse program hmbcgpndqf with 4096 \times 512 data points and 64 scans per t₁-increment and using spectral widths of 9.0 ppm for ¹H and 222 ppm for ¹³C to check for carbonyl correlated signals.

TagA *In Vitro* Activity Assay

To analyze the *P. alvei* TagA enzyme for its activity to transfer ManNAc from UDP- α -D-ManNAc to a α -D-GlcNAc residue as provided by the natural acceptor mimic GlcNAc-PP-(CH₂)₁₁-OPh (Xu et al., 2011), donor to acceptor ratios of 2.5:1, 1.25:1, and 1:1 were used, and MBP-TagA concentrations ranged from 50 nM to 1 μ M. For this purpose, a 5-mM stock solution of UDP- α -D-ManNAc, a 2-mM stock solution of acceptor, in H₂O, each, and a 1- μ M protein solution in 25 mM bis-Tris-propane buffer, pH 7.8, were prepared. Enzymatic reactions were performed in 25 mM bis-Tris-propane buffer with addition of 250 mM NaCl (TagA reaction buffer), for 1 h at 37°C, followed by overnight-incubation at RT (Zhang et al., 2006). As controls, reaction mixtures without acceptor or enzyme were used.

For the reaction set-up, Eppendorf tubes and reagents were kept on ice throughout the pipetting procedure. A master mixture was prepared in TagA reaction buffer, containing MBP-TagA and UDP- α -D-ManNAc (0.5 mM per 40 μ l of assay volume). To start the enzymatic reaction, the master mixture was added to varying volumes of the GlcNAc-PP-UndPh acceptor solution, followed by incubation as described above. The reaction was stopped by quenching with 700 μ l of ice-cold H₂O and dried *in vacuo*. Subsequently, the reactions were resuspended in 10 μ l of H₂O, each, and analyzed by thin layer chromatography (TLC), using silica G60 plates (10 cm \times 5 cm; Merck) and ethyl acetate/methanol/H₂O/acetic acid at a ratio of 4:1.5:0.7:0.1 (v/v/v/v) as solvent. The TLC plates were stained for carbohydrates with anisaldehyde-sulfuric acid dip-solution, containing ethanol/H₂SO₄/acetone/*p*-anisaldehyde = 100/5/3/2 (v/v/v/v) and developed at 250°C (Stahl and Kaltenbach, 1961).

For the characterization of the TagA reaction product, the assay was scaled up, using 250 nM MBP-TagA, 2.4 mM acceptor, and 0.5 mM UDP-ManNAc. After incubation and stopping the reaction as described above, the reaction mixture was purified over a (C18) Sep-Pak cartridge (see above). Dried fractions from the MeOH elution step were once dissolved in a 1:1-solution of H₂O and acetonitrile and analyzed by LC (C4)-ESI-MS and, second, dissolved in D₂O for final characterization by NMR spectroscopy.

Coupled MnaA/TagA *In Vitro* Activity Assay

MnaA-His₆ (38 μ g) and MBP-TagA (20 μ g) were co-incubated for 1 h at 37°C with 2.5 mM UDP-GlcNAc in sodium phosphate buffer, pH 7.5, supplemented with 11 mM MgCl₂, in a total reaction volume of 190 μ l. The reaction was stopped by addition of 700 μ l of ice-cold H₂O, purified over a (C18) Sep-Pak cartridge and analyzed by LC(C4)-ESI-MS (see above).

Determination of a Donor Substrate for Pyruvyltransfer by CsaB

To determine, if PEP can serve as a substrate for the *P. alvei* CsaB enzyme, *in situ* NMR measurements were performed using 10 μ M CsaB-His₆, 1.5 mM UDP- α -D-ManNAc, and 1.5 mM phospho(enol)pyruvic acid monopotassium salt, in a total volume of 600 μ l of deuterated sodium phosphate buffer,

pD 7.9, at 27°C. ^1H NMR and ^{31}P NMR spectra were recorded *in situ* for up to 15 h (see above).

Enzymatic One-Pot Reaction for the *in Vitro* Reconstitution of a Complete SCWP Repeat

To reconstitute a complete, lipid-linked repeat precursor of the *P. alvei* SCWP *in vitro* by means of the bacterium's native enzymes, 45 $\mu\text{g}/50\ \mu\text{g}$ (the first value refers to MS analysis, the second to NMR spectroscopy) of MnaA-His₆, 13.5 $\mu\text{g}/45\ \mu\text{g}$ of MBP-TagA and 14 $\mu\text{g}/45\ \mu\text{g}$ of CsaB-His₆ were incubated for 1 h at 37°C together with UDP-GlcNAc (8.1 mM/8.5 mM), PEP monopotassium salt (4.2 mM/4.3 mM, Sigma-Aldrich) and GlcNAc-PP-UndPh (300 $\mu\text{M}/1.4\ \text{mM}$; **Scheme 1**, compound **3**), in a total volume of 295 $\mu\text{l}/1175\ \mu\text{l}$ of 30 mM sodium phosphate buffer, pH 7.5, supplemented with 5.6 mM/5.3 mM MgCl_2 . Product formation was analyzed after (C18) Sep-Pak purification either by LC(C4)-ESI-MS or by NMR spectroscopy.

RESULTS

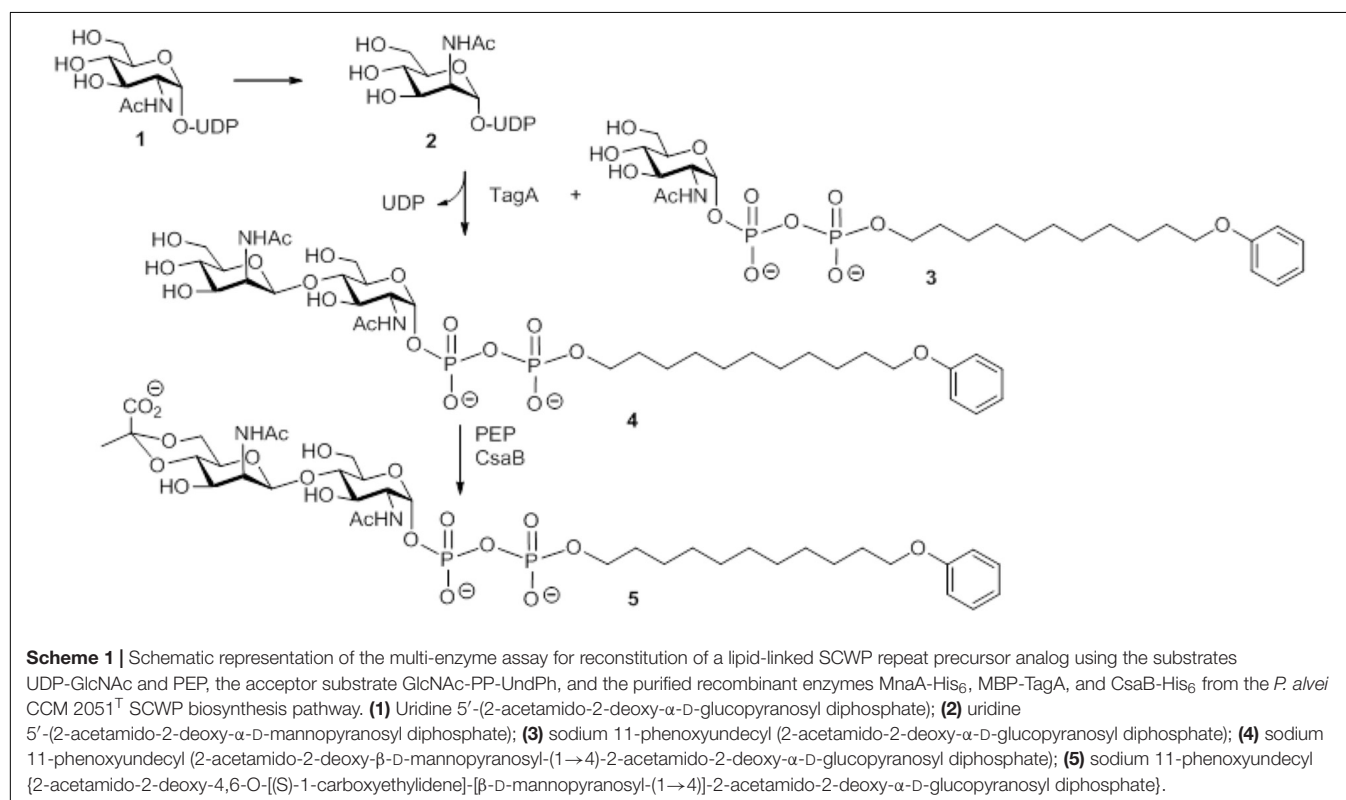
Transcription Analysis of *csaB*, *tagA*, and *tagO* Encoded in the *P. alvei* SCWP Biosynthesis Locus

To analyze whether the *csaB* (PAV_RS07425; coding for a putative pyruvyltransferase), *tagA* (PAV_RS07420; coding for a putative β -1,4 ManNAc transferase), and *tagO* (PAV_RS07415;

coding for a putative initiation enzyme of SCWP biosynthesis) genes from the predicted *P. alvei* SCWP biosynthesis gene locus (Zarschler et al., 2010) are co-transcribed on a polycistronic mRNA, total RNA from *P. alvei* cells was extracted, and co-transcription of the genes was analyzed using RT-PCR as outlined in **Figure 1**. The results showed that *csaB*, *tagA*, and *tagO* are co-transcribed as a single RNA transcript (**Figure 1**), since a PCR product of the expected size was obtained with the primer pairs *csaB*_for/*tagA*_rev (1.072 kb) and *tagA*_for/*tagO*_rev (1.065 kb), respectively, designed to bridge the ends between the ORFs of neighboring genes yielding amplification products only when co-transcription was happening. Further, primer pair *csaB*_for/*tagO*_rev yielded a 2037 bp transcript corresponding to the size of all three genes together. This confirmed that the *P. alvei* *tagO*, *tagA*, and *csaB* genes are transcriptionally linked.

Overexpression and Purification of Recombinant *mnaA*, *tagA*, and *csaB*

The *mnaA* and *csaB* genes from *P. alvei* were cloned into pET22-b(+), the *tagA* gene into pMALc2e. The enzymes were produced in *E. coli* BL21(DE3) as either C-terminally His₆-tagged proteins or, in the case of TagA, as an N-terminal MBP fusion protein, which enabled purification via nickel affinity chromatography or over an amylose resin, respectively. According to a Coomassie Brilliant Blue G250-stained 10% SDS-PAGE gel, the enzymes were purified to a high degree and revealed molecular weights of 44.5 kDa (MnaA-His₆), 43.6 kDa (CsaB-His₆), and 71.8 kDa (MBP-TagA), respectively (**Figure 2**), which corresponded to the



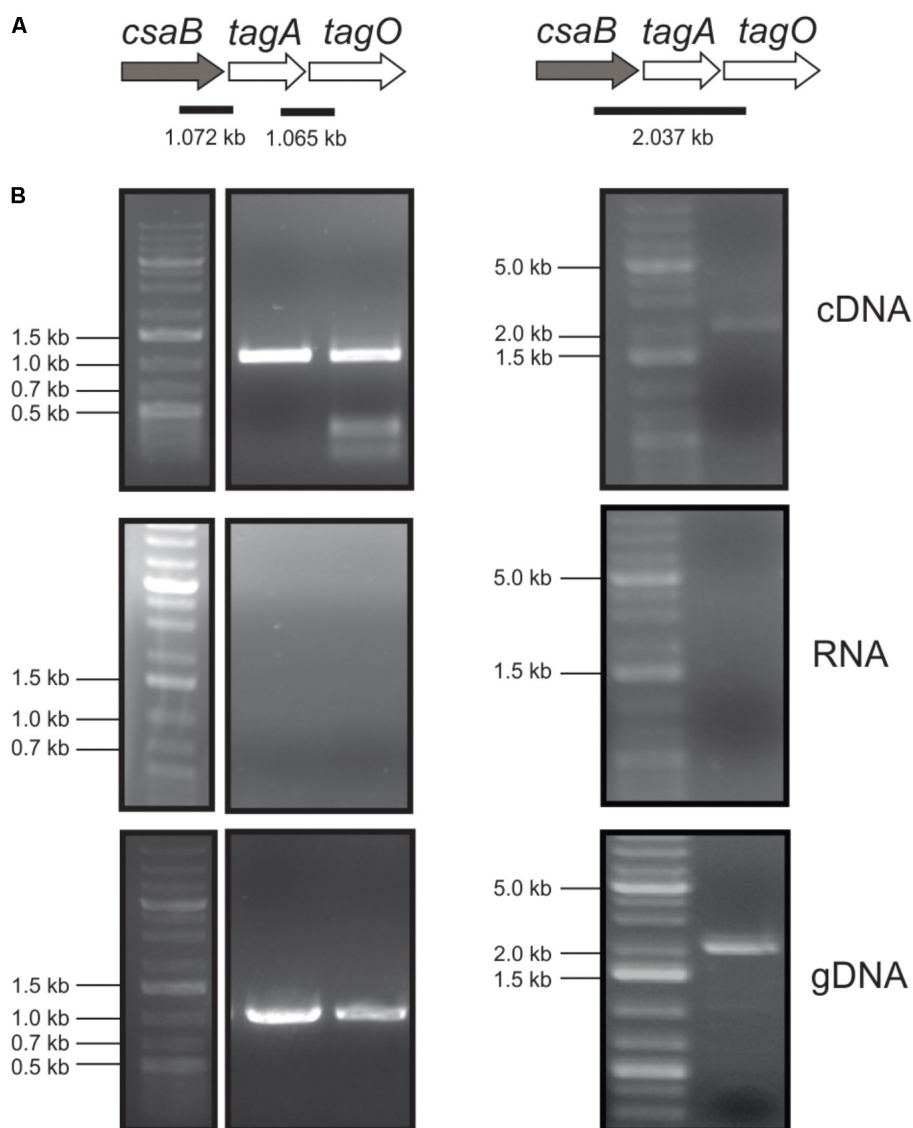


Figure 1 | Co-transcription analysis of the *tagO*, *tagA*, and *csaB* genes from the *P. alvei* CCM 2051 SCWP biosynthesis gene locus. **(A)** SCWP gene locus with expected PCR fragment sizes indicated. **(B)** Agarose gel electrophoresis analyses of co-transcription of genes from cDNA (upper panel), total RNA (middle panel; negative control) and gDNA (lower panel; positive control). All samples were run with a standard on the same gel. Primers used are listed in **Table 1**. O'Gene Ruler 1 kb Plus DNA Ladder (Thermo Fisher Scientific) was used as a gene ladder and is indicated on the left.

values as calculated based on amino acid sequences. Proteins were verified by Western-blotting (not shown). The recombinant enzymes were stored at a concentration of 0.3 mg/ml in 20 mM sodium phosphate buffer, pH 7.5, at -20°C (MnaA-His₆) or, in the case of enzyme inactivation upon freezing, at 4°C (MBP-TagA and CsaB-His₆).

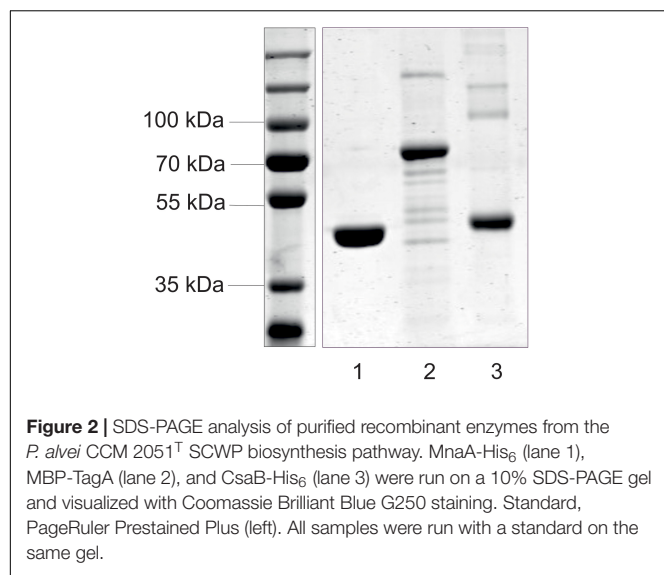
Chemical Synthesis of UDP- α -D-ManNAc

For the envisaged *in vitro* reconstitution of the lipid-linked $\rightarrow 3$)-4,6-Pyr- β -D-ManNAc-(1 \rightarrow 4)- β -D-GlcNAc-(1 \rightarrow repeat of the *P. alvei* SCWP, UDP- α -D-ManNAc as the predicted donor substrate for the TagA enzyme was chemically synthesized, since it is not commercially available (Supplementary Scheme S1).

Starting from 2-(acetylamido)-2-deoxy-D-mannopyranose (ManNAc) (Supplementary Scheme S1, compound **6**), UDP- α -D-ManNAc (Supplementary Scheme S1, compound **8**) was chemically synthesized in five steps and was obtained after purification via ion exchange chromatography (Ginsberg et al., 2006).

Recombinant *P. alvei* MnaA Shows UDP-GlcNAc-2-Epimerase Activity

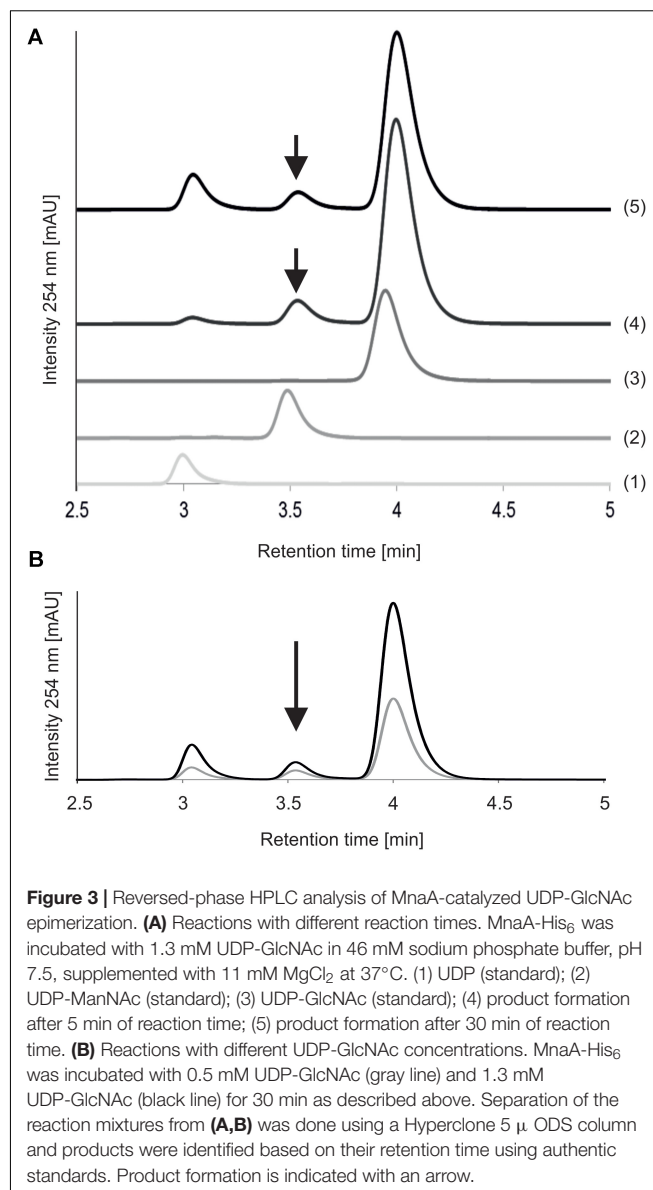
Purified, His₆-tagged MnaA was mixed with the UDP-GlcNAc substrate at different concentrations in phosphate buffer, pH 7.5, supplemented with MgCl₂, and incubated at 37°C up to 30 min; reactions were stopped in 5-min intervals.



MnaA-catalyzed epimerization of UDP-GlcNAc – which had a retention time of 3.9 min on the RP(C18)-HPLC column under the given conditions – was compared after 5 and 30 min of reaction time, using an authentic UDP- α -D-ManNAc standard (retention time, 3.4 min) for product identification (**Figure 3A**). Already after 5 min of incubation with the epimerase, two new peaks were detected, at 3.0 and 3.5 min, respectively, with the former corresponding to UDP and the latter to the UDP- α -D-ManNAc product. While the UDP peak increased upon prolonged reaction time, the peaks of UDP-GlcNAc and produced UDP-ManNAc decreased. Neither peak was detected when MnaA was omitted from the reaction (not shown). MnaA-catalyzed formation of UDP- α -D-ManNAc slightly increased when more substrate was provided (0.5 mM compared to 1.3 mM UDP-GlcNAc; **Figure 3B**). For further investigations, UDP-ManNAc production was established using *P. alvei* MnaA and 1.3 mM UDP-GlcNAc, revealing an epimerization rate of 9.5%, which was within the published range (Morgan et al., 1997; Murkin et al., 2004; Mann et al., 2016). Despite MnaA is annotated as non-hydrolyzing 2-epimerase, increasing amounts of UDP emerged over time as a reaction intermediate (**Figure 3A**). This was also observed by others (Morgan et al., 1997) and can be explained by the proposed mechanism B of co-factor independent epimerases involving acetamidoglucal and UDP as intermediates (Samuel and Tanner, 2002).

Recombinant *P. alvei* TagA Shows UDP-ManNAc:GlcNAc-Pyrophosphate-R Transferase Activity

Next, the option of pyruvylation at the disaccharide stage was studied, which required the presence of a biosynthetic surrogate of the undecaprenyl diphosphate activated substrates. Previously, it had been shown that synthetic GlcNAc-PP-UndPh (**Scheme 1**, compound 3) served as glycosyl acceptor for a UDP-Gal:GlcNAc- α -pyrophosphate-R β (1,3)-galactosyltransferase WbbD from



E. coli strain VW187 (O7:K1) involved in the biosynthesis of O7-specific lipopolysaccharide (Riley et al., 2005) and was, thus, selected to analyze whether it would also serve as an acceptor for the UDP-ManNAc transferase TagA from *P. alvei* to produce the lipid-linked disaccharide β -D-ManNAc-(1 \rightarrow 4)- α -GlcNAc-PP-UndPh (**Scheme 1**, compound 4). TagA was tested for its ManNAc transfer activity and shown to be active in a concentration range of 1 μ M to 50 nM. The activity was visualized by TLC showing complete conversion to product species with a donor (synthetically prepared UDP- α -ManNAc) to acceptor (**Scheme 1**, compound 3) ratio of 2.5:1, whereas ratios of 1.25:1 and 1:1 still showed unused substrate (data not shown). LC-MS data of the (C18) SepPak-purified product mixture obtained with the 2.5:1-reaction (optimal ratio) in the negative ion mode indicated the presence of the glycosylated product (**Scheme 1**, compound 4, m/z = 829.3;

Supplementary Figure S1B) as well as, with suboptimal donor to acceptor ratio, unreacted substrate (compound 3 of **Scheme 1**, $m/z = 626.6$; Supplementary Figure S1A); the latter was confirmed by NMR spectroscopic data and indicated a $\sim 2:1$ ratio for compound 3 to compound 4 (**Scheme 1**).

Furthermore, a HSQC spectrum (data not shown) identified a downfield-shifted signal at 79.0 ppm consistent with a 4-*O*-glycosylated α -GlcNAc moiety. The presence of a product mixture and of residual bis-Tris-propane buffer, however, precluded a full assignment of the ^1H and ^{13}C NMR signals, although several correlations could be established on the basis of COSY and HSQC data (**Table 2**).

Recombinant CsaB Shows Interaction With PEP but No Pyruvyl Transfer to Free UDP-ManNAc

Possessing a high-energy phosphate bond and being involved in bacterial cell metabolism, PEP was chosen as the donor substrate for the pyruvyl transfer reaction. Studies of the pyruvyltransferase Pvlgp from *S. pombe* (Yoritsune et al., 2013) confirmed that PEP could be an appropriate substrate.

To examine, if pyruvylation occurs at the nucleotide sugar level, 1.5 mM synthetic UDP-ManNAc (Supplementary Scheme S1, compound 8) was incubated with 10 μM CsaB and 1.5 mM PEP at pD 7.9 and 27°C in an *in situ* NMR experiment. Over the course of several hours, signals arising from UDP-ManNAc remained unchanged, but PEP was subject to a slow deuterium exchange reaction. Whereas both olefinic protons of PEP were readily seen at 5.33 and 5.15 ppm at the start of the measurement, a steady decrease of signal intensities was observed with concomitant increase of two slightly high-field shifted singlets corresponding to the monodeuterated PEP derivatives. After 14 h of reaction time, signals of protonated PEP species were almost completely absent (**Figure 4**), whereas in the control experiment without addition of enzyme, deuteration of PEP was not observed. These observations indicated an interaction of PEP with CsaB, but lack of pyruvylation of UDP-ManNAc, obviously due to the absence of an appropriate acceptor substrate.

Choice of an Appropriate Acceptor Substrate Enables CsaB-Mediated Pyruvyl Transfer *in Vitro*

Based on the successful functional proof of the UDP-ManNAc transferase TagA by MS and NMR data, a three-step enzymatic transformation was carried out (**Scheme 1**). In a multi-enzyme assay, a one-pot reaction of the epimerase MnaA, the UDP-ManNAc transferase TagA, and the pyruvyltransferase CsaB together with UDP-GlcNAc, PEP, and the GlcNAc-PP-UndPh acceptor (**Scheme 1**, compound 3) was set up, with the three enzymes predicted to work in a cascade reaction in nature (**Scheme 1**). The reaction product - 4,6-Pyr- β -D-ManNAc- α -D-GlcNAc-diphosphoryl-phenoxyundecyl (**Scheme 1**, compound 5) - was purified via a (C18) Sep-Pak

column, from which it eluted with water - while ManNAc-GlcNAc-PP-UndPh and remaining acceptor were eluted with methanol - and was analyzed by LC-(C4)-ESI-MS. The earlier elution of the pyruvylated product species can be explained by its higher polarity than the initial acceptor (**Scheme 1**, compound 3) and the TagA product (**Scheme 1**, compound 4). The mass ion $m/z = 899.3$ detected in negative ion mode in LC-(C4)-ESI-MS analysis indicated the presence of a lipid-linked pyruvylated disaccharide species (Supplementary Figure S1C).

Structural analysis of the CsaB product (**Scheme 1**, compound 5) was performed by one- and two-dimensional NMR spectroscopy of a scaled-up reaction. Briefly, the 600 MHz ^1H NMR spectrum (**Figure 5**) recorded in D_2O in a Shigemi tube showed *inter alia* five aromatic signals corresponding to the undecyl terminal phenyl protons, the anomeric proton of the GlcNAc unit at 5.46 ppm (as broad signal due to spin coupling with the adjacent phosphate) and the anomeric signal of the ManNAc residue at 4.90 ppm, which was correlated to H-2 of ManNAc seen at 4.51 ppm. The anomeric configurations were confirmed on the basis of the heteronuclear coupling constants $J_{\text{C}-1,\text{H}-1}$ (174.2 Hz for the α -GlcNAc unit and 164.7 Hz for the β -ManNAc residue), thereby also confirming that TagA had reacted as an inverting glycosyltransferase. TOCSY correlations then allowed tracking down the spin systems originating from both anomeric protons (see **Table 2**). The high-field region showed two methyl group signals attributed to the two *N*-acetyl amino groups as well as two vicinal methylene groups, each connected to an OCH_2 signal occurring at 4.08 and 3.91 ppm, respectively. Additional CH_2 signals were observed at 1.43 ppm and in the range of 1.34–1.27 ppm. Notably, a singlet signal corresponding to the methyl group of the pyruvyl moiety was detected at 1.44 ppm.

Carbon 4 of the GlcNAc residue was observed at 79.2 ppm which, again, identified this position as the glycosylation site. In addition, the signals of carbon 6 and carbon 4 of the ManNAc residue were shifted downfield (64.7 and 74.7 ppm, respectively), which indicated that both positions had been substituted. By contrast, carbon 5 of ManNAc was significantly shifted to higher field (67.6 ppm), again in agreement with a 4,6-*O*-substitution pattern (**Figure 6**). Further structural proof was derived from HMBC measurements (data not shown), which allowed to assign the spacer-linked OCH_2 group at 4.08 ppm as the phenoxy-linked methylene group (based on the HMBC-correlation to the quaternary aromatic carbon at 158.9 ppm), whereas the second OCH_2 group at 3.91 ppm showed HMBC connectivity to the anomeric carbon of the GlcNAc unit at 94.9 ppm. Eventually, the pyruvic acetal group was unambiguously confirmed on the basis of HMBC-correlations of the pyruvyl methyl group to a quaternary carbon signal at 102.6 ppm and the carboxylate signal at 176.2 ppm. Moreover, an HMBC connectivity of H-6a of the ManNAc unit to C-2 of the pyruvic acid acetal was observed. The (*S*) stereochemistry of the pyruvic acid acetal was determined on the basis of the characteristic ^1H NMR chemical shift of the methyl group at 1.44 ppm in agreement with literature data (Jansson et al., 1993).

TABLE 2 | NMR data of compounds **4** and **5** recorded in D₂O.

	H-1 <i>J</i> C-1	H-2 <i>J</i> C-2	H-3 <i>J</i> C-3	H-4 <i>J</i> C-4	H-5 <i>J</i> C-5	H-6a <i>J</i> C-6	H-6b <i>J</i>
Compound 4							
β-D-ManNAcp-(1→	4.87	4.575	~3.80	3.48	3.39	n.d.	n.d.
	<1.0	4.2	n.d.	9.8	2.0, 4.9		
	99.9	54.3		67.3	77.2		
CH ₃		2.03/0.04					
		22.7					
NHC = O	n.d.						
→4)-α-D-GlcNAcp-(1→PP	5.45	3.99	~3.94	~3.78	3.92	n.d.	n.d.
	3.1, 7.1	2.6	n.d.	n.d.	n.d.		
	94.9	54.2	72.15	79.0	72.2		
CH ₃		2.03 /0.04					
		22.7					
NHC = O	n.d.						
PP→OCH ₂ CH ₂ CH ₂ -	~3.90	1.60	n.d.				
	n.d.	6.2					
	67.6	30.7					
PhOCH ₂ CH ₂ CH ₂ -	4.08	1.75	1.42				
	n.d.	6.6	6.6				
	69.5	28.8	25.9				
Additional signals (CH ₂) ₂	1.37–1.20						
	29.3						
Ph	–	7.01	7.36	7.02	7.36	7.01	
		7.1	7.3	7.6	7.3	7.1	
		115.7	130.6	122.0	130.6	115.7	
Compound 5							
4,6-Pyr-β-D-ManpNAC-(1→	4.90	4.51	3.93	3.58	3.39	4.01	~3.72
	<1.0	4.3	4.5, 10.1	9.8	5.0, 9.9	4.9, 10.8	
	100.5	54.0	70.3	74.6	67.6	64.7	
CH ₃		2.05					
		22.75					
NHC = O	176.15						
Pyruvic acetal	–	–	1.44				
	176.2	102.6	25.5				
→4)-α-D-GlcpNAC-(1→PP	5.46	3.98	3.85	3.74	3.92	3.81	~3.72
	br s	10.5	9.4, 9.4	9.0	n.d.	12.4	
	94.9	54.4	70.2	79.2	72.2	60.45	
CH ₃		2.05					
		22.75					
NHC = O	176.15						
PP→OCH ₂ CH ₂ CH ₂	3.91	1.60	1.33				
	n.d.	6.7	n.d.				
	67.6	30.5	29.3				
PhOCH ₂ CH ₂ CH ₂	4.08	1.74	1.43				
	6.6	6.8,	7.1				
	69.6	29.0					
Additional (CH ₂) ₂ signals	1.35–1.27						
	29.4						
Ph	–	7.02	7.37	7.04	7.37	7.02	
		8.3	8.0	7.5	8.0	8.3	
	158.9	115.7	130.5	122.2	130.5	115.7	

Chemical shifts are given in ppm and coupling constants in Hz. n.d., not determined.

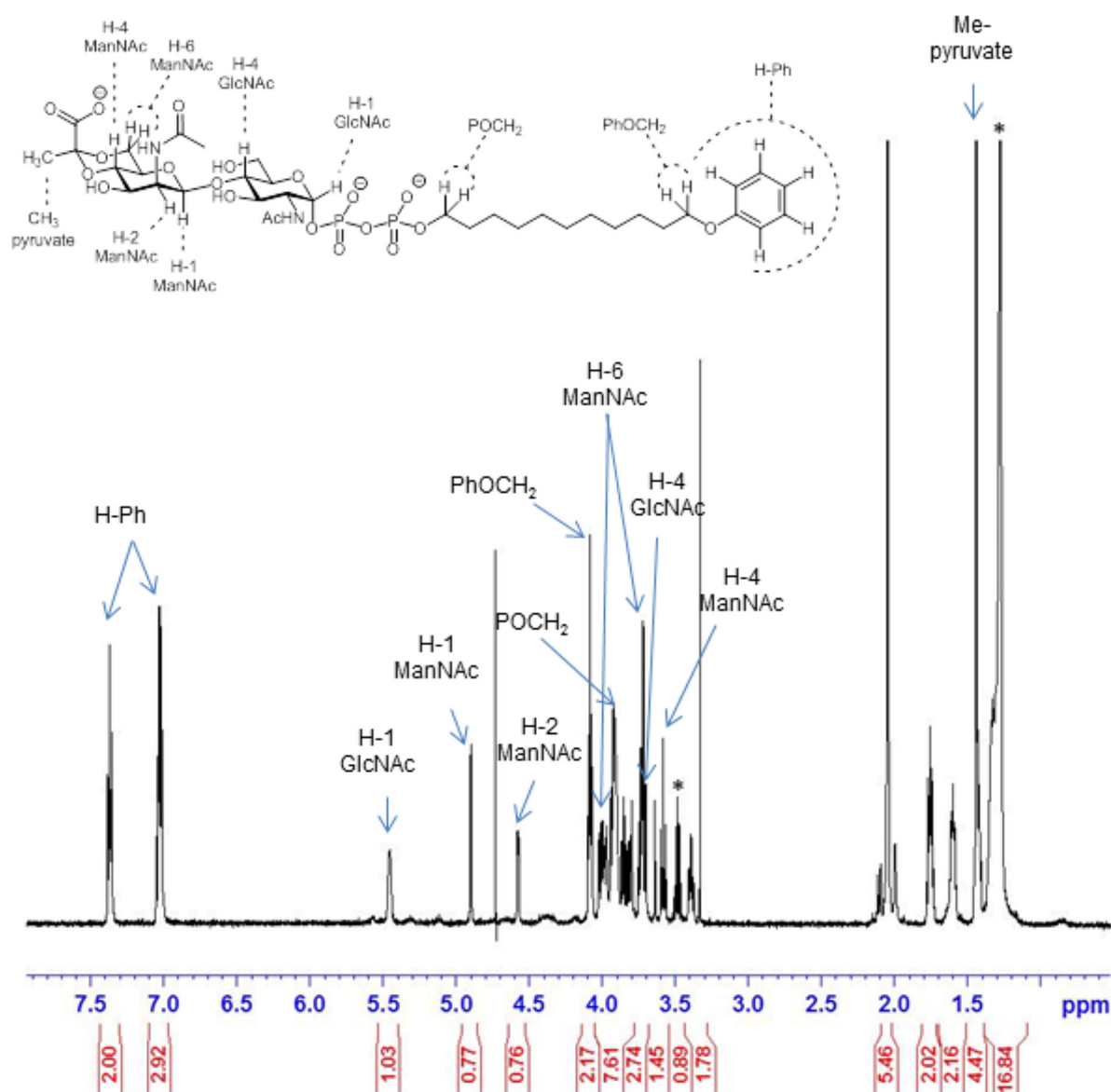


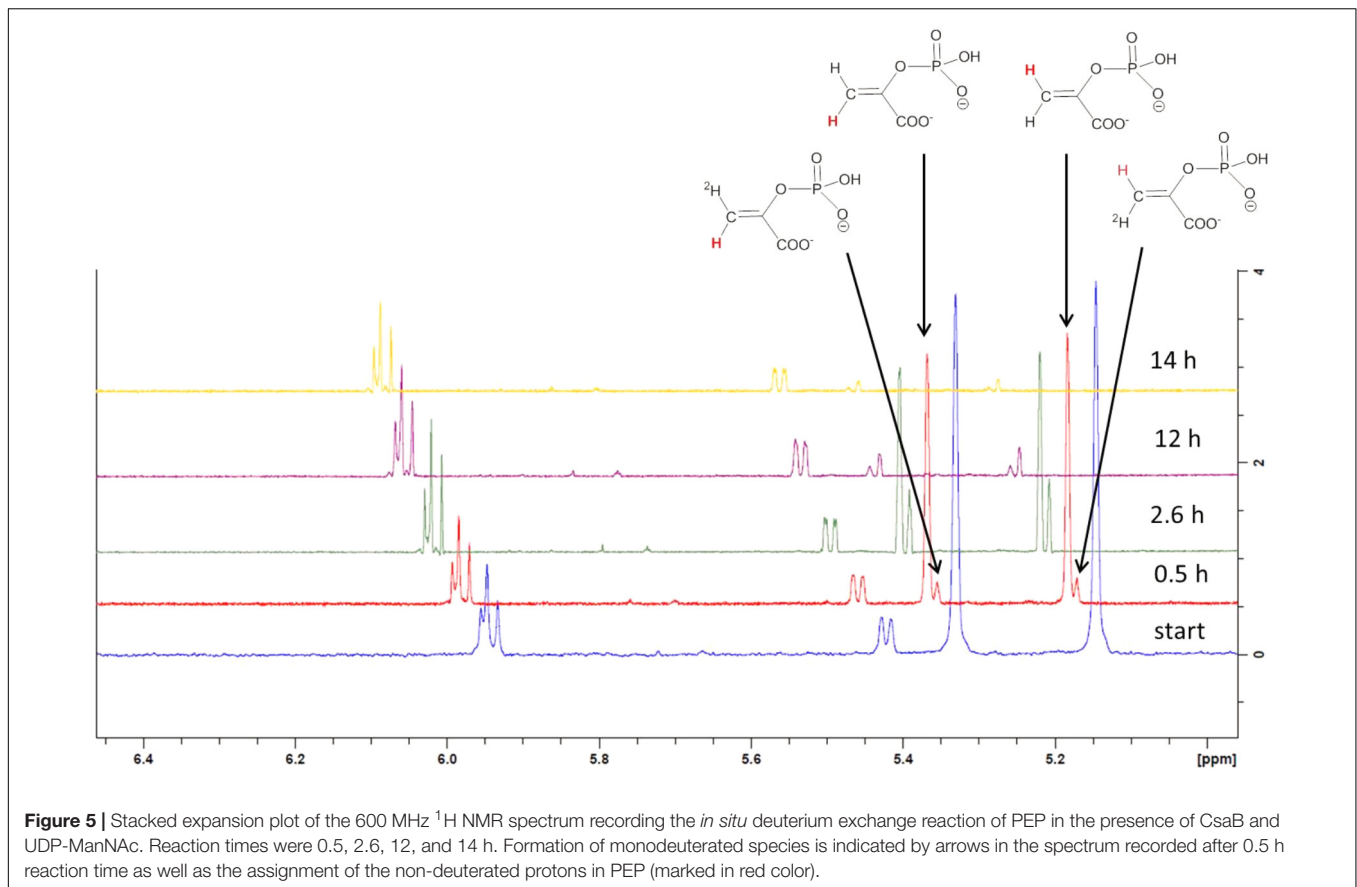
Figure 4 | 600 MHz ^1H NMR spectrum of the pyruvylated disaccharide product 5 (from **Scheme 1**). Signals corresponding to key parts of the structure are indicated by arrows. Asterisk “*” denotes residuals.

DISCUSSION

Several Gram-positive bacteria, including *B. anthracis*, *B. cereus* (Forsberg et al., 2011, 2012; van Sorge et al., 2014) and the herein described non-pathogenic model organism *P. alvei* CCM 2051^T (Schäffer et al., 2000), attach a SCWP to their peptidoglycan cell wall. SCWPs are of strain-specific composition and typically comprise saccharide repeats (Schäffer and Messner, 2005). They are predicted to share distinct structural features with wall teichoic acids such as the murein linkage unit, and they presumably fulfill similar functions during the bacterial cell cycle (Xia et al., 2010; Brown et al., 2013). Some SCWPs are modified with pyruvate ketal groups, which endows them to serve as a cell

wall ligand for SLH domains present in various Gram-positive bacterial cell surface proteins; among those and most abundant, the S-layer proteins which self-assemble into 2-dimensional crystalline arrays on the bacterial cell surface (Sleytr et al., 2010). Intriguingly, this pyruvate ketal modification is, in all investigated cases, present on a β -D-ManNAc residue (Sára, 2001). The 4,6-Pyr- β -D-ManNAc epitope might be more prevalent in SCWPs than is currently anticipated, since a frequently applied strategy for SCWP isolation is its cleavage from peptidoglycan with 48% hydrofluoric acid, which is known to liberate acid-labile pyruvate-ketal groups (Schäffer and Messner, 2017).

In *P. alvei*, the SCWP consists of pyruvylated $[\rightarrow 3)\text{-}\beta\text{-D-ManpNAc-(1}\rightarrow 4)\text{-}\beta\text{-D-GlcpNAc-(1}\rightarrow]$ disaccharide repeats



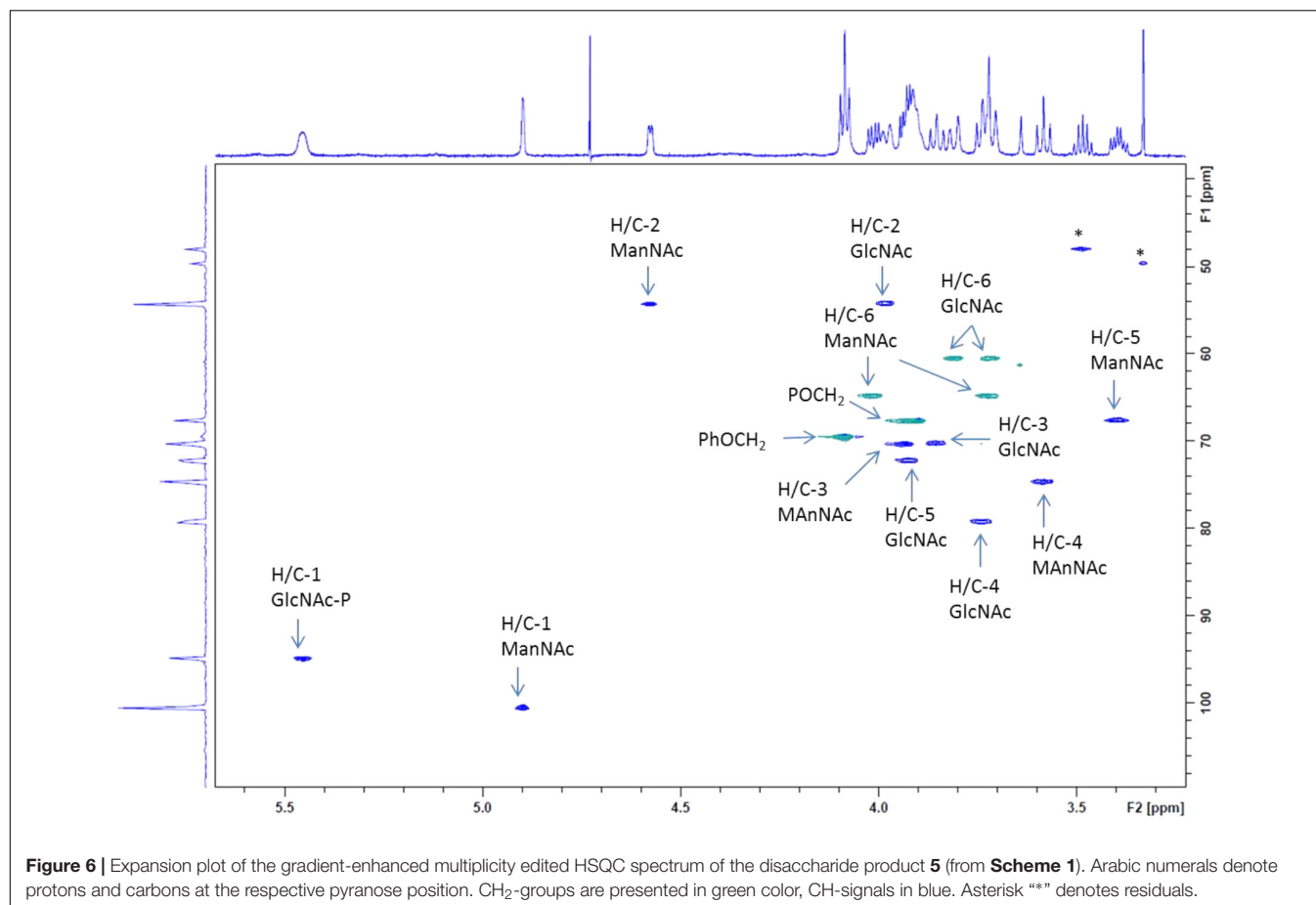
(Schäffer and Messner, 2005; Janesch et al., 2013a). The SCWP repeats of *B. anthracis* (Mesnage et al., 2000; Forsberg et al., 2012) and *B. cereus* strains (Choudhury et al., 2006; Forsberg et al., 2011) as analyzed from hydrofluoric acid-treated material are extensions of the disaccharide motif by one α -D-GlcNAc residue yielding $[\rightarrow 4)\text{-}\beta\text{-D-ManpNAc-(1}\rightarrow 4)\text{-}\beta\text{-D-GlcpNAc-(1}\rightarrow 6)\text{-}\alpha\text{-D-GlcpNAc-(1}\rightarrow]$ and include additional non-stoichiometric galactosyl (Chateau et al., 2018) and acetyl modifications; in these SCWPs, exclusively the non-reducing-end β -D-ManNAc residue carries a 4,6-linked pyruvate ketal modification.

Given that SCWPs comprise a large fraction of the Gram-positive cell wall - where approximately every fourth *N*-acetylmuramic acid residue of the peptidoglycan backbone is modified with an SCWP (Schäffer et al., 2000), understanding how these polymers are made and, especially, how the pyruvate ketal modification is elaborated, are necessary steps in exploring their potential as antimicrobial targets. For studying SCWP biosynthesis, *P. alvei* is an ideal model organism, since we have exact knowledge of its SCWP structure (Schäffer et al., 2000) and prediction of a genomic SCWP biosynthesis gene locus (Zarschler et al., 2010), which makes a chemo-enzymatic approach feasible.

Pyruvylated SCWPs fall into the category of anionic cell wall glycopolymers - to which also wall teichoic and lipoteichoic acids belong - the presence of which seems to be essential for the Gram-positive cell wall (Chapot-Chartier and Kulakauskas, 2014). This

is substantiated by the failure to create a viable knock-out mutant of the *tagO* gene predictably encoding the initiation enzyme of SCWP biosynthesis, in both *B. anthracis* (Lunderberg et al., 2015; Oh et al., 2017) and *P. alvei* (Fiona F. Hager and Christina Schäffer, unpublished data); in both of these bacteria, the SCWP is the only known anionic cell wall glycopolymer. In contrast, for *B. subtilis*, a viable *tagO* knock-out mutant affecting wall teichoic acid biosynthesis could be obtained; albeit, this mutant experienced morphological changes and was unable to colonize host tissue (D'Elia et al., 2006a). Remarkably, the creation of a *B. subtilis* mutant with simultaneous deficiency in wall teichoic acid and lipoteichoic acid was lethal, probably due to complete charge depletion of the cell wall (D'Elia et al., 2006a).

We have obtained evidence that the principle of TagO and TagA catalyzed formation of a undecaprenylpyrophosphate-linked ManNAc-GlcNAc disaccharide as known from teichoic acid biosynthesis (Brown et al., 2013) is also valid for SCWP biosynthesis, supporting bioinformatic predictions (Zarschler et al., 2010; Oh et al., 2017). In the current study, this picture is even extended by shedding light on the pyruvylation step, using the *P. alvei* SCWP biosynthesis enzymes TagA and CsaB in conjunction with MnaA and a GlcNAc-PP-UndPh precursor. We succeeded in producing in a multi-enzyme *in vitro* assay a complete, pyruvylated, lipid-linked SCWP repeat precursor derivative, thereby obtaining insight into the biochemical basis of CsaB activity. Earlier we proposed that the *P. alvei* genome



harbors a dedicated SCWP biosynthesis gene locus. Here, we show that *csaB* (PAV_RS07425), *tagA* (PAV_RS07420), and *tagO* (PAV_RS07415) are indeed linked as one transcriptional unit (**Figure 1B**), which makes their concerted action a likely scenario; the *mnaA* gene (PAV_RS07610) is located elsewhere on the genome. The UDP-GlcNAc-2-epimerase MnaA was included in our biosynthetic *in vitro* study, since *in vivo*, UDP-GlcNAc epimerization is a necessary prerequisite for provision of the UDP-ManNAc donor substrate to TagA. For each of these genes, a single copy was identified in the *P. alvei* genome.

Despite its indispensability for assembling the cell wall of many Gram-positive bacteria, the pyruvylation reaction to obtain the 4,6-Pyr-β-D-ManNAc epitope has not been biochemically investigated, thus far. This might be due to the lack of available substrates for *in vitro* studies of the predicted pyruvyltransferase CsaB, and missing knowledge of the biosynthetic stage of pyruvylation. In an initial *in situ* NMR measurement of recombinant *P. alvei* CsaB together with PEP, interaction of the enzyme and PEP could be observed (**Figure 4**), confirming PEP as donor substrate for pyruvylation. Searching for an appropriate acceptor candidate, notably, pyruvyltransfer could not be detected with synthetic pNP-β-ManNAc (kindly provided by Stephen Withers; Fiona F. Hager, unpublished data) mimicking the disaccharide linkage, nor with synthetic UDP-ManNAc, although a nucleotide binding

site is predicted for CsaB based on its amino acid sequence (Fiona F. Hager, Arturo López-Guzmán, Christina Schäffer, unpublished data). These findings let us conclude that either a longer SCWP building block, or a lipid-linked precursor was needed. Since more likely from a biosynthetic perspective and supported by the current model of SCWP biosynthesis in *B. anthracis*, where non-stoichiometric modifications of the repeats would occur at the lipid-linked stage (Missiakos and Schneewind, 2017), we decided for the latter option and set up a stepwise enzymatic cascade to reach our target molecule.

An *in vitro* enzymatic assay using recombinant UDP-ManNAc:GlcNAc-lipid transferase TagA in combination with a synthetic 11-phenoxyundecyl-diphosphoryl-α-GlcNAc (GlcNAc-PP-UndPh, **Scheme 1**, compound **3**) acceptor (with the undecyl moiety mimicking the natural undecaprenyl carrier lipid) and chemically synthesized UDP-ManNAc or UDP-ManNAc produced by MnaA catalysis as donor resulting in a ManNAc-GlcNAc-PP-UndPh product species (**Scheme 1**, compound **4**), was established. Importantly, in a co-incubation assay of MnaA and TagA, apparently enough UDP-GlcNAc was epimerized for subsequent TagA-catalyzed ManNAc transfer to produce compound **4**. While TagA is a predicted cytosolic protein, fluorescence microscopy studies with a TagA-GFP chimera showed its localization near the cytoplasmic membrane

supporting the necessity of a lipid tail on the acceptor substrate; further, the TagA-GFP chimera was shown to accumulate at cellular septation sites underlining its activity in cell wall metabolism (Fiona F. Hager, Christina Schäffer unpublished data). It is very likely that in the native host, the TagA reaction is preceded by a TagO reaction initiating SCWP biosynthesis by transferring GlcNAc-phosphate to an undecaprenylphosphate carrier lipid (Weidenmaier et al., 2004; D'Elia et al., 2006b).

With compound **4** (Scheme 1) in hands we had a suitable acceptor substrate for the pyruvyl transfer reaction to generate the pyruvylated, lipid-linked disaccharide repeat precursor constituting the *P. alvei* SCWP. The product was fully elucidated by NMR analysis providing the first functional proof of a bacterial pyruvyltransferase *in vitro*. Altogether, our data suggests a mechanism where pyruvylation occurs most likely at the stage of the lipid-linked disaccharide. Currently, it is still unclear, if polymerization of the complete SCWP chain occurs in the cytoplasm prior to export followed by, predictably, LytR-CpsA-Psr family ligase-mediated (Kawai et al., 2011; Zilla et al., 2015; Schaefer et al., 2017) linkage to the C6-hydroxyl of MurNAc in the glycan strands of peptidoglycan. While during biosynthesis of wall teichoic biosynthesis, polymerization occurs at a single lipid-carrier (Xia and Peschel, 2008; Kawai et al., 2011; Chan et al., 2013), this scenario is questionable in the case of SCWP biosynthesis of *P. alvei*, where we have shown *in vitro* that the disaccharide lipid-carrier serves as a substrate for CsaB (this study). Alternatives, as known from LPS biosynthesis pathways (Raetz and Whitfield, 2002) would be the assembly of individually synthesized pyruvylated repeats and step-wise transfer of repeats to the non-reducing end of a lipid-linked primer or, polymerization after export. The requirement of a lipid carrier for pyruvyltransferase activity is supported by studies of the pyruvyltransferase WcfO from the capsular polysaccharide A biosynthesis gene cluster of *B. fragilis*. There, according to MS evidence, the enzyme is active on an undecaprenyl-pyrophosphate-linked disaccharide for producing a PvGal residue prior to final assembly of the capsular polysaccharide A tetrasaccharide repeat precursor (Sharma et al., 2017).

Another scenario is known from polyribitol wall teichoic acid biosynthesis in *S. aureus* and *B. subtilis*. It involves a primase, TagB, which attaches a single glycerol-phosphate (GroP) unit to the non-reducing end of the lipid-linked GlcNAc-ManNAc disaccharide platform (Brown et al., 2008). Following assembly of the disaccharide linkage unit, the pathway for polyribitol wall teichoic acid requires the enzymes TarF, TarK, and TarL to complete the polymeric main chain (Lazarevic et al., 2002). Once polyribitol wall teichoic acid has been completed, still attached to the undecaprenyl carrier lipid, it is flipped to the external surface of the cytoplasmic membrane (Swoboda et al., 2010) where it is linked to peptidoglycan involving a LytR-CpsA-Psr (LCP) family ligase (Kawai et al., 2011; Zilla et al., 2015; Schaefer et al., 2017).

Generally, polymerization of SCWP repeats and SCWP ligation to peptidoglycan are remaining challenging open questions in SCWP biosynthesis pathways. According to a recent model of *B. anthracis* SCWP biosynthesis

(Missiakas and Schneewind, 2017; Oh et al., 2017), an undecaprenyl-pyrophosphate linked GlcNAc-GlcNAc-ManNAc trisaccharide repeat would be preassembled in a cytoplasmic, TagO and TagA1/-2 catalyzed reaction followed by membrane flipping involving the multidrug and toxin extrusion-like protein Bas5279. At the outer surface of the cytoplasmic membrane, the lipid-bound SCWP would be ligated onto murein linkage units and the final polymer would be attached to peptidoglycan by a LytR-CpsA-Psr ligase. The newly identified WpaA and WpaB proteins are anticipated to be involved in both polymerization and ligation reactions, however, without experimental evidence of activity. These proteins are categorized as Pfam protein family PF13425, which belongs to clan CL0499 that also encompasses Wzy (polymerases) and WaaL (ligases) proteins involved in bacterial polysaccharide biosynthesis, such as LPS (Raetz and Whitfield, 2002). Depletion of either protein was shown to affect vegetative growth, cell shape, and S-layer assembly, supportive of a role of these proteins in *B. anthracis* cell wall metabolism (Oh et al., 2017). Strikingly, the *B. anthracis* SCWP biosynthesis model does not take into account the pyruvylation reaction.

We provided the first functional proof of a bacterial pyruvyltransferase CsaB by a stepwise enzymatic synthesis of the required acceptor substrate, taking the structurally defined SCWP of *P. alvei* as a model system. In a one pot reaction applying a reaction cascade of UDP-GlcNAc epimerization and ManNAc transfer, a lipid-pyrophosphate linked ManNAc-GlcNAc disaccharide species was generated whereon CsaB-catalyzed pyruvyl transfer was executed. This is a key step in deciphering the biosynthesis of pyruvylated SCWPs as found not only in our model organism but also in Gram-positive pathogens, where due to the essentiality of the SCWP, the mechanistic characterization of the involved enzymes may reveal possible antimicrobial targets.

AUTHOR CONTRIBUTIONS

FH, PK, and CS conceived and designed the experiments. FH, MP, SK, and AL-G performed the experiments and developed methodology. FH, SK, MB, MP, PK, and CS analyzed the data. SK and IB contributed reagents, materials, and analysis tools. FH, PK, and CS wrote the manuscript. All authors revised and approved the manuscript.

FUNDING

Funding was provided by the Austrian Science Fund FWF Project P27374-B22 (to CS) and the Ph.D. Program "Biomolecular Technology of Proteins" W1224.

ACKNOWLEDGMENTS

The authors would like to thank Prof. Stephen G. Withers (University of British Columbia, Vancouver, BC, Canada) for provision of pNP- β -ManNAc, Prof. Walter A. Szarek

(Queen's University, Kingston, ON, Canada) for synthesis of the 11-phenoxyundecyl-diphosphoryl- α -GlcNAc acceptor, Dr. Andreas Hofinger-Horvath (Universität für Bodenkultur Wien) for NMR recordings, and Sebastian Löffler for help with the characterization of the UDP-GlcNAc-2-epimerase.

REFERENCES

- Archibald, A. R., Hancock, I. C., and Harwood, C. R. (1993). "Cell wall structure, synthesis and turnover," in *Bacillus subtilis and Other Gram-Positive Bacteria*, eds A. Sonenshein, J. A. Hoch, and R. Losick (Washington, DC: ASM Press), 381–410.
- Bax, A., and Summers, M. F. (1986). Proton and carbon-13 assignments from sensitivity-enhanced detection of heteronuclear multiple-bond connectivity by 2D multiple quantum NMR. *J. Am. Chem. Soc.* 108, 2093–2094. doi: 10.1021/ja00268a061
- Blume, A. (2003). *Expression and Functional Characterisation of the Key Enzyme of the Sialic acid Biosynthesis, UDP-GlcNAc 2-Epimerase/MannNAc Kinase*. Berlin: Freie Universität of Berlin.
- Bradford, M. M. (1976). A rapid and sensitive method for the quantitation of microgram quantities of protein utilizing the principle of protein-dye binding. *Anal. Biochem.* 72, 248–254. doi: 10.1016/0003-2697(76)90527-3
- Brown, S., Meredith, T., Swoboda, J., and Walker, S. (2010). *Staphylococcus aureus* and *Bacillus subtilis* W23 make polyribitol wall teichoic acids using different enzymatic pathways. *Chem. Biol.* 17, 1101–1110. doi: 10.1016/j.chembiol.2010.07.017
- Brown, S., Santa Maria, J. P., and Walker, S. (2013). Wall teichoic acids of Gram-positive bacteria. *Annu. Rev. Microbiol.* 67, 313–336. doi: 10.1146/annurev-micro-092412-155620
- Brown, S., Zhang, Y. H., and Walker, S. (2008). A revised pathway proposed for *Staphylococcus aureus* wall teichoic acid biosynthesis based on in vitro reconstitution of the intracellular steps. *Chem. Biol.* 15, 12–21. doi: 10.1016/j.chembiol.2007.11.011
- Cava, F., De Pedro, M. A., Schwarz, H., Henne, A., and Berenguer, J. (2004). Binding to pyruvylated compounds as an ancestral mechanism to anchor the outer envelope in primitive bacteria. *Mol. Microbiol.* 52, 677–690. doi: 10.1111/j.1365-2958.2004.04011.x
- Chan, Y. G., Frankel, M. B., Dengler, V., Schneewind, O., and Missiakas, D. (2013). *Staphylococcus aureus* mutants lacking the LytR-CpsA-Psr family of enzymes release cell wall teichoic acids into the extracellular medium. *J. Bacteriol.* 195, 4650–4659. doi: 10.1128/JB.00544-13
- Chapot-Chartier, M. P., and Kulakauskas, S. (2014). Cell wall structure and function in lactic acid bacteria. *Microb. Cell Fact.* 13(Suppl. 1):S9. doi: 10.1186/1475-2859-13-S1-S9
- Chateau, A., Lunderberg, J. M., Oh, S. Y., Abshire, T., Friedlander, A., Quinn, C. P., et al. (2018). Galactosylation of the secondary cell wall polysaccharide of *Bacillus anthracis* and its contribution to anthrax pathogenesis. *J. Bacteriol.* 200:e00562-17. doi: 10.1128/JB.00562-17
- Cheng, H. R., and Jiang, N. (2006). Extremely rapid extraction of DNA from bacteria and yeasts. *Biotechnol. Lett.* 28, 55–59. doi: 10.1007/s10529-005-4688-z
- Choudhury, B., Leoff, C., Saile, E., Wilkins, P., Quinn, C. P., Kannenberg, E. L., et al. (2006). The structure of the major cell wall polysaccharide of *Bacillus anthracis* is species-specific. *J. Biol. Chem.* 281, 27932–27941. doi: 10.1074/jbc.M605768200
- D'Elia, M. A., Henderson, J. A., Beveridge, T. J., Heinrichs, D. E., and Brown, E. D. (2009). The N-acetylmannosamine transferase catalyzes the first committed step of teichoic acid assembly in *Bacillus subtilis* and *Staphylococcus aureus*. *J. Bacteriol.* 191, 4030–4034. doi: 10.1128/JB.00611-08
- D'Elia, M. A., Millar, K. E., Beveridge, T. J., and Brown, E. D. (2006a). Wall teichoic acid polymers are dispensable for cell viability in *Bacillus subtilis*. *J. Bacteriol.* 188, 8313–8316.
- D'Elia, M. A., Pereira, M. P., Chung, Y. S., Zhao, W., Chau, A., Kenney, T. J., et al. (2006b). Lesions in teichoic acid biosynthesis in *Staphylococcus aureus* lead to a lethal gain of function in the otherwise dispensable pathway. *J. Bacteriol.* 188, 4183–4189.
- Desvaux, M., Dumas, E., Chafsey, I., and Hébraud, M. (2006). Protein cell surface display in Gram-positive bacteria: from single protein to macromolecular protein structure. *FEMS Microbiol. Lett.* 256, 1–15. doi: 10.1111/j.1574-6968.2006.00122.x
- Forsberg, L. S., Abshire, T. G., Friedlander, A., Quinn, C. P., Kannenberg, E. L., and Carlson, R. W. (2012). Localization and structural analysis of a conserved pyruvylated epitope in *Bacillus anthracis* secondary cell wall polysaccharides and characterization of the galactose-deficient wall polysaccharide from avirulent *B. anthracis* CDC 684. *Glycobiology* 22, 1103–1117. doi: 10.1093/glycob/cws080
- Forsberg, L. S., Choudhury, B., Leoff, C., Marston, C. K., Hoffmaster, A. R., Saile, E., et al. (2011). Secondary cell wall polysaccharides from *Bacillus cereus* strains G9241, 03BB87 and 03BB102 causing fatal pneumonia share similar glycosyl structures with the polysaccharides from *Bacillus anthracis*. *Glycobiology* 21, 934–948. doi: 10.1093/glycob/cwr026
- Freese, S. J., and Vann, W. F. (1996). Synthesis of 2-acetamido-3-O-acetyl-2-deoxy-d-mannose phosphoramidites. *Carbohydr. Res.* 281, 313–319. doi: 10.1016/0008-6215(95)00345-2
- Gemmill, T. R., and Trimble, R. B. (1996). *Schizosaccharomyces pombe* produces novel pyruvate-containing N-linked oligosaccharides. *J. Biol. Chem.* 271, 259452594–259452599. doi: 10.1074/jbc.271.42.25945
- Ginsberg, C., Zhang, Y. H., Yuan, Y., and Walker, S. (2006). In vitro reconstitution of two essential steps in wall teichoic acid biosynthesis. *ACS Chem. Biol.* 1, 25–28. doi: 10.1021/cb0500041
- Higuchi, Y., Yoshinaga, S., Yoritsune, K., Tateno, H., Hirabayashi, J., Nakakita, S., et al. (2016). A rationally engineered yeast pyruvyltransferase Pvg1p introduces sialylation-like properties in neo-human-type complex oligosaccharide. *Sci. Rep.* 6:26349. doi: 10.1038/srep26349
- Ilk, N., Kosma, P., Puchberger, M., Egelseer, E. M., Mayer, H. F., Sleytr, U. B., et al. (1999). Structural and functional analyses of the secondary cell wall polymer of *Bacillus sphaericus* CCM 2177 that serves as an S-layer-specific anchor. *J. Bacteriol.* 181, 7643–7646.
- Janesch, B., Koerd, A., Messner, P., and Schäffer, C. (2013a). The S-layer homology domain-containing protein SlhA from *Paenibacillus alvei* CCM 2051T is important for swarming and biofilm formation. *PLoS One* 8:e76566. doi: 10.1371/journal.pone.0076566
- Janesch, B., Messner, P., and Schäffer, C. (2013b). Are the surface layer homology domains essential for cell surface display and glycosylation of the S-layer protein from *Paenibacillus alvei* CCM 2051T? *J. Bacteriol.* 195, 565–575. doi: 10.1128/JB.01487-12
- Jansson, P. E., Lindberg, J., and Widmalm, G. (1993). Syntheses and NMR-studies of Pyruvic acid 4,6-acetals of some methyl hexopyranosides. *Acta Chem. Scand.* 47, 711–715. doi: 10.3891/acta.chem.scand.47-0711
- Kawai, Y., Marles-Wright, J., Cleverley, R. M., Emmins, R., Ishikawa, S., Kuwano, M., et al. (2011). A widespread family of bacterial cell wall assembly proteins. *EMBO J.* 30, 4931–4941. doi: 10.1038/emboj.2011.358
- Kern, J., Ryan, C., Faull, K., and Schneewind, O. (2010). *Bacillus anthracis* surface-layer proteins assemble by binding to the secondary cell wall polysaccharide in a manner that requires *csaB* and *tagO*. *J. Mol. Biol.* 401, 757–775. doi: 10.1016/j.jmb.2010.06.059
- Laemmli, U. K. (1970). Cleavage of structural proteins during the assembly of the head of bacteriophage T4. *Nature* 227, 680–685. doi: 10.1038/227680a0
- Lazarevic, V., Abellan, F. X., Moller, S. B., Karamata, D., and Mauel, C. (2002). Comparison of ribitol and glycerol teichoic acid genes in *Bacillus subtilis* W23 and 168: identical function, similar divergent organization, but different regulation. *Microbiology* 148, 815–824. doi: 10.1099/00221287-148-3-815
- Lee, S. Y., Choi, J. H., and Xu, Z. (2003). Microbial cell-surface display. *Trends Biotechnol.* 21, 45–52. doi: 10.1016/S0167-7799(02)00006-9
- Lunderberg, J. M., Zilla, M. L., Missiakas, D., and Schneewind, O. (2015). *Bacillus anthracis tagO* is required for vegetative growth and secondary cell wall polysaccharide synthesis. *J. Bacteriol.* 197, 3511–3520. doi: 10.1128/JB.00494-15
- Mann, P. A., Müller, A., Wolff, K. A., Fischmann, T., Wang, H., Reed, P., et al. (2016). Chemical genetic analysis and functional characterization of

SUPPLEMENTARY MATERIAL

The Supplementary Material for this article can be found online at: <https://www.frontiersin.org/articles/10.3389/fmicb.2018.01356/full#supplementary-material>

- Staphylococcal* wall teichoic acid 2-epimerases reveals unconventional antibiotic drug targets. *PLoS Pathog.* 12:e1005585. doi: 10.1371/journal.ppat.1005585
- Marchler-Bauer, A., Derbyshire, M. K., Gonzales, N. R., Lu, S. N., Chitsaz, F., Geer, L. Y., et al. (2015). CDD: NCBI's conserved domain database. *Nucleic Acids Res.* 43, D222–D226. doi: 10.1093/nar/gku1221
- May, A., Pusztahelyi, T., Hoffmann, N., Fischer, R.-J., and Bahl, H. (2006). Mutagenesis of conserved charged amino acids in SLH domains of *Thermoanaerobacterium thermosulfurigenes* EM1 affects attachment to cell wall sacculi. *Arch. Microbiol.* 185, 263–269. doi: 10.1007/s00203-006-0092-x
- Mesnager, S., Fontaine, T., Mignot, T., Delepierre, M., Mock, M., and Fouet, A. (2000). Bacterial SLH domain proteins are non-covalently anchored to the cell surface via a conserved mechanism involving wall polysaccharide pyruvylation. *EMBO J.* 19, 4473–4484. doi: 10.1093/emboj/19.17.4473
- Messner, P., Egelseer, E. M., Sleytr, U. B., and Schäffer, C. (2009). "Bacterial surface layer glycoproteins and "non-classical" secondary cell wall polymers," in *Microbial Glycobiology: Structures, Relevance and Applications*, eds A. P. Moran, P. J. Brennan, O. Holst, and M. Von Itzstein (San Diego, CA: Academic Press), 109–128.
- Missiakas, D., and Schneewind, O. (2017). Assembly and Function of the *Bacillus anthracis* S-Layer. *Annu. Rev. Microbiol.* 71, 79–98. doi: 10.1146/annurev-micro-090816-093512
- Morgan, P. M., Sala, R. F., and Tanner, M. E. (1997). Eliminations in the reactions catalyzed by UDP-N-acetylglucosamine 2-epimerase. *J. Am. Chem. Soc.* 119, 10269–10277. doi: 10.1021/ja971718q
- Murkin, A. S., Chou, W. K., Wakarchuk, W. W., and Tanner, M. E. (2004). Identification and mechanism of a bacterial hydrolyzing UDP-N-acetylglucosamine 2-epimerase. *Biochemistry* 43, 14290–14298. doi: 10.1021/bi048606d
- Oh, S. Y., Lunderberg, J. M., Chateau, A., Schneewind, O., and Missiakas, D. (2017). Genes required for *Bacillus anthracis* secondary cell wall polysaccharide synthesis. *J. Bacteriol.* 199:e00613–16. doi: 10.1128/JB.00613-16
- Raetz, C. R., and Whitfield, C. (2002). Lipopolysaccharide endotoxins. *Annu. Rev. Biochem.* 71, 635–700. doi: 10.1146/annurev.biochem.71.110601.135414
- Rajagopal, M., and Walker, S. (2017). Envelope structures of Gram-positive bacteria. *Curr. Top. Microbiol. Immunol.* 404, 1–44. doi: 10.1007/82_2015_5021
- Riley, J. G., Menggad, M., Montoya-Peleaz, P. J., Szarek, W. A., Marolda, C. L., Valvano, M. A., et al. (2005). The *wbbD* gene of *E. coli* strain VW187 (O7:K1) encodes a UDP-Gal: GlcNAc α -pyrophosphate-R β 1,3-galactosyltransferase involved in the biosynthesis of O7-specific lipopolysaccharide. *Glycobiology* 15, 605–613. doi: 10.1093/glycob/cwi038
- Samuel, J., and Tanner, M. E. (2002). Mechanistic aspects of enzymatic carbohydrate epimerization. *Nat. Prod. Rep.* 19, 261–277. doi: 10.1039/b100492l
- Sára, M. (2001). Conserved anchoring mechanisms between crystalline cell surface S-layer proteins and secondary cell wall polymers in Gram-positive bacteria? *Trends Microbiol.* 9, 47–49; discussion 49–50. doi: 10.1016/S0966-842X(00)01905-3
- Schade, J., and Weidenmaier, C. (2016). Cell wall glycopolymers of Firmicutes and their role as nonprotein adhesins. *FEMS Microbiol. Lett.* 590, 3758–3771. doi: 10.1002/1873-3468.12288
- Schaefer, K., Matano, L. M., Qiao, Y., Kahne, D., and Walker, S. (2017). *In vitro* reconstitution demonstrates the cell wall ligase activity of LCP proteins. *Nat. Chem. Biol.* 13, 396–401. doi: 10.1038/nchembio.2302
- Schäffer, C., and Messner, P. (2005). The structure of secondary cell wall polymers: how Gram-positive bacteria stick their cell walls together. *Microbiology* 151, 643–651. doi: 10.1099/mic.0.27749-0
- Schäffer, C., and Messner, P. (2017). Emerging facets of prokaryotic glycosylation. *FEMS Microbiol. Rev.* 41, 49–91. doi: 10.1093/femsre/fuw036
- Schäffer, C., Müller, N., Mandal, P. K., Christian, R., Zayni, S., and Messner, P. (2000). A pyrophosphate bridge links the pyruvate-containing secondary cell wall polymer of *Paenibacillus alvei* CCM 2051 to muramic acid. *Glycoconj. J.* 17, 681–690. doi: 10.1023/A:1011062302889
- Schleucher, J., Schwendinger, M., Sattler, M., Schmidt, P., Schedletzky, O., Glaser, S. J., et al. (1994). A general enhancement scheme in heteronuclear multidimensional NMR employing pulsed field gradients. *J. Biomol. NMR* 4, 301–306. doi: 10.1007/BF00175254
- Sharma, S., Erickson, K. M., and Troutman, J. M. (2017). Complete tetrasaccharide repeat unit biosynthesis of the immunomodulatory *Bacteroides fragilis* capsular polysaccharide A. *ACS Chem. Biol.* 12, 92–101. doi: 10.1021/acscchembio.6b00931
- Sleytr, U. B., Egelseer, E. M., Ilk, N., Messner, P., Schäffer, C., Pum, D., et al. (2010). "Nanobiotechnological applications of S-layers," in *Prokaryotic Cell Wall Compounds - Structure and Biochemistry*, eds H. König, H. Claus, and A. Varma (Berlin: Springer-Verlag), 459–481. doi: 10.1007/978-3-642-05062-6_16
- Stahl, E., and Kaltenbach, U. (1961). Dünnschicht-Chromatographie: VI. Mitteilung. Spurenanalyse von Zuckergemischen auf Kieselgur G-Schichten. *J. Chromatogr.* 5, 351–355. doi: 10.1016/S0021-9673(01)92868-7
- Swoboda, J. G., Campbell, J., Meredith, T. C., and Walker, S. (2010). Wall teichoic acid function, biosynthesis, and inhibition. *ChemBiochem* 11, 35–45. doi: 10.1002/cbic.200900557
- van Sorge, N. M., Cole, J. N., Kuipers, K., Henningham, A., Aziz, R. K., Kasirer-Friede, A., et al. (2014). The classical lancefield antigen of group A *Streptococcus* is a virulence determinant with implications for vaccine design. *Cell Host Microbe* 15, 729–740. doi: 10.1016/j.chom.2014.05.009
- Wang, S., Czuchry, D., Liu, B., Vinnikova, A. N., Gao, Y., Vlahakis, J. Z., et al. (2014). Characterization of Two UDP-Gal: GalNAc-diphosphate-lipid b 1,3-galactosyltransferases WbWc from *Escherichia coli* serotypes O104 and O5. *J. Bacteriol.* 196, 3122–3133. doi: 10.1128/JB.01698-14
- Wang, Y. T., Oh, S. Y., Hendrickx, A. P., Lunderberg, J. M., and Schneewind, O. (2013). *Bacillus cereus* G9241 S-layer assembly contributes to the pathogenesis of anthrax-like disease in mice. *J. Bacteriol.* 195, 596–605. doi: 10.1128/JB.02005-12
- Weidenmaier, C., Kokai-Kun, J. F., Kristian, S. A., Chanturiya, T., Kalbacher, H., Gross, M., et al. (2004). Role of teichoic acids in *Staphylococcus aureus* nasal colonization, a major risk factor in nosocomial infections. *Nat. Med.* 10, 243–245. doi: 10.1038/nm991
- Xia, G., Kohler, T., and Peschel, A. (2010). The wall teichoic acid and lipoteichoic acid polymers of *Staphylococcus aureus*. *Int. J. Med. Microbiol.* 300, 148–154. doi: 10.1016/j.ijmm.2009.10.001
- Xia, G., and Peschel, A. (2008). Toward the pathway of *S. aureus* WTA biosynthesis. *Chem. Biol.* 15, 95–96. doi: 10.1016/j.chembiol.2008.02.005
- Xu, C., Liu, B., Hu, B., Han, Y., Feng, L., Allingham, J. S., et al. (2011). Biochemical characterization of UDP-Gal:GlcNAc-pyrophosphate-lipid beta-1,4-galactosyltransferase WfeD, a new enzyme from *Shigella boydii* type 14 that catalyzes the second step in O-antigen repeating-unit synthesis. *J. Bacteriol.* 193, 449–459. doi: 10.1128/JB.00737-10
- Yamazaki, T., Warren, C. D., Herscovics, A., and Jeanloz, R. W. (1980). Convenient synthesis of uridine 5'-2-acetamido-2-deoxy- α -D-mannopyranosyluronic acid pyrophosphate. *Carbohydr. Res.* 79, C9–C12.
- Yoritsune, K., Matsuzawa, T., Ohashi, T., and Takegawa, K. (2013). The fission yeast Pvg1p has galactose-specific pyruvyltransferase activity. *FEBS Lett.* 587, 917–921. doi: 10.1016/j.febslet.2013.02.016
- Zarschler, K., Janesch, B., Kainz, B., Ristl, R., Messner, P., and Schäffer, C. (2010). Cell surface display of chimeric glycoproteins via the S-layer of *Paenibacillus alvei*. *Carbohydr. Res.* 345, 1422–1431. doi: 10.1016/j.carres.2010.04.010
- Zhang, Y. H., Ginsberg, C., Yuan, Y., and Walker, S. (2006). Acceptor substrate selectivity and kinetic mechanism of *Bacillus subtilis* TagA. *Biochemistry* 45, 10895–10904. doi: 10.1021/bi060872z
- Zilla, M. L., Chan, Y. G. Y., Lunderberg, J. M., Schneewind, O., and Missiakas, D. (2015). LytR-CpsA-Psr enzymes as determinants of *Bacillus anthracis* secondary cell wall polysaccharide assembly. *J. Bacteriol.* 197, 343–353. doi: 10.1128/JB.02364-14
- Zolghadr, B., Gasselhuber, B., Windwarder, M., Pabst, M., Kracher, D., Kernl, M., et al. (2015). UDP-sulfoquinovose formation by *Sulfolobus acidocaldarius*. *Extremophiles* 19, 451–467. doi: 10.1007/s00792-015-0730-9

Conflict of Interest Statement: The authors declare that the research was conducted in the absence of any commercial or financial relationships that could be construed as a potential conflict of interest.

Copyright © 2018 Hager, López-Guzmán, Krauter, Blaukopf, Polter, Brockhausen, Kosma and Schäffer. This is an open-access article distributed under the terms of the Creative Commons Attribution License (CC BY). The use, distribution or reproduction in other forums is permitted, provided the original author(s) and the copyright owner are credited and that the original publication in this journal is cited, in accordance with accepted academic practice. No use, distribution or reproduction is permitted which does not comply with these terms.



Activation of the PhoPR-Mediated Response to Phosphate Limitation Is Regulated by Wall Teichoic Acid Metabolism in *Bacillus subtilis*

Kevin M. Devine*

Smurfit Institute of Genetics, Trinity College Dublin, Dublin, Ireland

OPEN ACCESS

Edited by:

Christoph Mayer,
Universität Tübingen, Germany

Reviewed by:

Fabian Moritz Commichau,
Georg-August-Universität Göttingen,
Germany
Boris Görke,
Universität Wien, Austria

*Correspondence:

Kevin M. Devine
kdevine@tcd.ie

Specialty section:

This article was submitted to
Microbial Physiology and Metabolism,
a section of the journal
Frontiers in Microbiology

Received: 16 August 2018

Accepted: 19 October 2018

Published: 06 November 2018

Citation:

Devine KM (2018) Activation
of the PhoPR-Mediated Response
to Phosphate Limitation Is Regulated
by Wall Teichoic Acid Metabolism
in *Bacillus subtilis*.
Front. Microbiol. 9:2678.
doi: 10.3389/fmicb.2018.02678

Phosphorous is essential for cell viability. To ensure an adequate supply under phosphate limiting conditions, bacteria induce a cohort of enzymes to scavenge for phosphate, and a high affinity transporter for its uptake into the cell. This response is controlled by a two-component signal transduction system named PhoBR in *Escherichia coli* and PhoPR in *Bacillus subtilis*. PhoR is a sensor kinase whose activity is responsive to phosphate availability. Under phosphate limiting conditions, PhoR exists in kinase mode that phosphorylates its cognate response regulator (PhoB, PhoP). When activated, PhoB~P /PhoP~P execute changes in gene expression that adapt cells to the phosphate limited state. Under phosphate replete conditions, PhoR exists in phosphatase mode that maintains PhoB/PhoP in an inactive, non-phosphorylated state. The mechanism by which phosphate availability is sensed and how it controls the balance between PhoR kinase and phosphatase activities has been studied in *E. coli* and *B. subtilis*. Two different mechanisms have emerged. In the most common mechanism, PhoR activity is responsive to phosphate transport through a PstSCAB/PhoU signaling complex that relays the conformational status of the transporter to PhoR. In the second mechanism currently confined to *B. subtilis*, PhoR activity is responsive to wall teichoic acid metabolism whereby biosynthetic intermediates can promote or inhibit PhoR autokinase activity. Variations of both mechanisms are found that allow each bacterial species to adapt to phosphate availability in their particular environmental niche.

Keywords: phosphate limitation, PhoBR *Escherichia coli*, PhoPR *Bacillus subtilis*, control of PhoR activity, phosphate transport mechanism, wall teichoic acid metabolism mechanism

INTRODUCTION

Phosphorous containing biomolecules participate in a wide range of cellular activities, including information processing, energy metabolism, signaling, regulation of protein activity, and maintenance of acid-base homeostasis. Furthermore, the cell envelopes of some bacteria (e.g., *Bacilli* and *Staphylococci*) contain lipoteichoic acid (LTA) and wall teichoic acid (WTA), anionic

polymers with a high phosphorous content. LTA is a polymer of glycerol phosphate that extends into the cell wall from a lipid anchored in the cell membrane. WTA is a polymer of glycerol- or ribitol-phosphate that is covalently attached to peptidoglycan (Weidenmaier and Peschel, 2008; Percy and Gründling, 2014). These anionic polymers play important roles in cellular morphology and cell division (Swoboda et al., 2010; Percy and Gründling, 2014).

An adequate supply of phosphorous is therefore a prerequisite for cell viability. This is a challenge for bacteria especially those in habitats such as soil where the level of free phosphate can be low due to pH dependent formation of precipitates (Batjes, 1997). Bacteria adopt two general strategies to maintain an adequate phosphorous supply: (i) intracellular storage and (ii) scavenging for phosphate with enzymes induced under phosphorous limiting conditions. Many bacteria store phosphorous as polyphosphate, a polymer of hundreds of phosphate residues linked by high energy phosphoanhydride bonds that is synthesized by polyphosphate kinase (PPK1) using nucleotide triphosphates (Brown and Kornberg, 2008; Rao et al., 2009; Jiménez et al., 2017). Phosphate is released from the polyphosphate store by degradation with exo- and endo-polyphosphate phosphatases (Brown and Kornberg, 2008; Achbergerová and Nahálka, 2011). However, *Bacillus subtilis* subspecies *subtilis* (hereafter called *B. subtilis*) cannot synthesize polyphosphate but instead uses WTA as the store from which phosphate is released by the combined activities of the GlpQ and PhoD phosphodiesterases, whose expression is increased upon phosphate limitation in a PhoPR dependent manner (Eder et al., 1996; Antelmann et al., 2000; Myers et al., 2016).

Adaptation to phosphate limitation is often mediated by a two-component signal transduction system (TCS) named PhoBR in *Escherichia coli* and PhoPR in *B. subtilis* (hereafter called the PHO response). PhoR is a sensor kinase whose activity is responsive to phosphate availability. When activated, PhoR phosphorylates its cognate response regulator (PhoB or PhoP) that in turn directs a program of gene expression to adapt bacteria to the phosphate limited state. The PHO responses of these bacteria are characterized by (i) increased expression and secretion of enzymes that scavenge for phosphate; (ii) increased expression of a high affinity ABC-type phosphate transporter (PstSCAB), and (iii) amplification of the response by positive autoregulation of the *phoBR* and *phoPR* operons.

How PhoR senses phosphate and how its activity is controlled in a manner that is responsive to phosphate availability has been investigated mainly in *E. coli* and *B. subtilis*. Two different mechanisms have emerged that control the balance between the autokinase and phosphatase activities of PhoR. The first mechanism, exemplified by PhoBR activation in *E. coli*, is responsive to phosphate transport and is mediated by the PstSCAB transporter and PhoU adaptor protein (Hsieh and Wanner, 2010). The second mechanism, exemplified by PhoPR in *B. subtilis*, is responsive to WTA metabolism and is mediated by intermediates in WTA biosynthesis (Botella et al., 2014; Prunty et al., 2018). Variation of both mechanisms is observed that

enable bacteria to ensure an adequate phosphorous supply in their particular ecological niches.

ACTIVATION OF PhoBR IS RESPONSIVE TO PHOSPHATE TRANSPORT BY PstSCAB IN *E. coli*

Seven proteins are necessary and sufficient for induction of the PHO response in *E. coli*: the PhoBR TCS, the PstSCAB ABC-type phosphate transporter and the PhoU protein that is encoded in the *pstSCABphoU* operon (Hsieh and Wanner, 2010). PhoBR is a classical TCS. PhoR is membrane associated and composed of two transmembrane domains and a cytoplasmically located PAS (Per Arndt Sim) domain that interacts with PhoU. The PhoB response regulator is activated by PhoR-mediated phosphorylation and binds to PHO boxes located in the promoter region of PhoBR regulon genes (Blanco et al., 2002). The PstSCAB ABC-type transporter is composed of a periplasmically located PstS protein that binds phosphate, PstCA proteins located within the membrane that form the transport channel and a PstB dimer that binds ATP and provides energy for the transport process. The PhoU protein is a membrane-associated metal binding protein composed of two three-alpha helical bundles that forms multimers (Liu et al., 2005; Oganessian et al., 2005). Genetic analysis has shown that the PHO response is constitutively activated when either the PstSCAB transporter or PhoU is deleted (Figure 1A; Hsieh and Wanner, 2010). This implies that PhoR is in default autokinase mode under phosphate limiting conditions and that the PstSCAB high affinity transporter and PhoU are both required for its conversion to phosphatase mode under phosphate replete conditions (Hsieh and Wanner, 2010). The PhoU protein interacts with the PAS domain of PhoR and the PstB protein of the PstSCAB transporter to form a membrane bound signaling complex that converts PhoR to phosphatase activity mode (Gardner et al., 2014, 2015). The PhoU protein also modulates the activity of the PstSCAB transporter (Rice et al., 2009). Results show that the balance between the autokinase and phosphatase modes of PhoR activity is controlled neither by intracellular phosphate concentration nor by transport of phosphate *per se* (Cox et al., 1988, 1989; Rao et al., 1993). Instead, there is evidence from a genetic approach stabilizing PstB in two different conformations, that conformational changes in the PstSCAB transporter are important in determining the balance between the autokinase and phosphatase modes of PhoR activity (Vuppada et al., 2018). When the transporter is present in an outward facing 'closed' structure, the PstSCAB/PhoU signaling complex either does not interact with PhoR (Figure 1A, PhoU solid lines) or interacts with PhoR (Figure 1A, PhoU broken lines) to promote autokinase activity, the state that exists under phosphate limiting conditions. However, when the transporter is present in an inward facing 'open' structure, the PstSCAB/PhoU signaling complex interacts with PhoR to promote phosphatase activity, the state that exists under conditions of phosphate sufficiency (Figure 1B). Thus phosphate availability in *E. coli* is sensed indirectly through conformational changes in the PstSCAB transporter (Gardner et al., 2015; Vuppada et al., 2018).

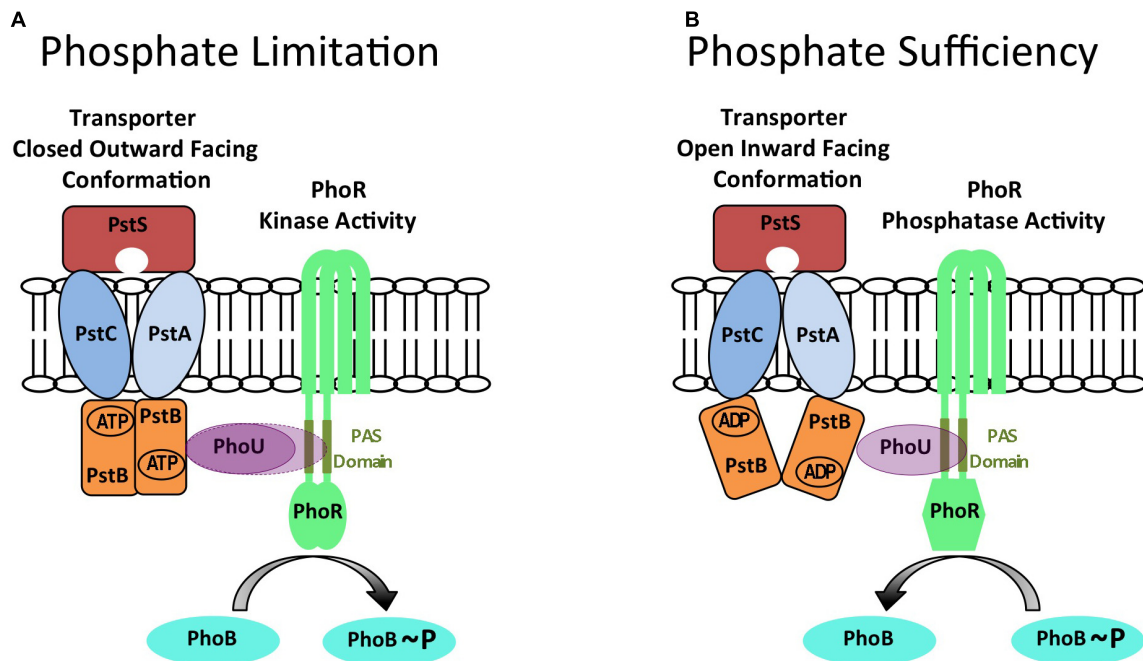


FIGURE 1 | A model for controlling the balance between PhoR autokinase and phosphatase activities in *E. coli* generated by conformational changes in the PstSCAB phosphate transporter. The PhoR protein can exist in either autokinase mode during conditions of phosphate limitation (**A**) or in phosphatase mode during conditions of phosphate sufficiency (**B**). It is proposed that these alternate states are determined by different conformations of the PstSCAB transporter that are relayed to PhoR by PhoU to determine its activity. When PstSCAB is in a closed outward facing conformation (**A**) the PhoU adaptor protein is either unable to interact with PhoR (PhoU solid lines), or interacts with the PAS domain of PhoR to promote autokinase activity (PhoU broken lines) during conditions of phosphate limitation. The cognate PhoB response regulator is phosphorylated in this condition. However, when PstSCAB is in an open inward facing conformation (**B**) the PhoU adaptor protein interacts with the PAS domain of PhoR to promote phosphatase activity during conditions of phosphate sufficiency. The cognate PhoB response regulator is dephosphorylated in this condition. This diagram is an adaptation of the models and figures presented in Hsieh and Wanner (2010) and Vuppada et al. (2018).

In fact, transporters have now been shown to have a signaling role in controlling the activity of several TCS (for reviews see Tetsch and Jung, 2009; Piepenbreier et al., 2017).

VARIATIONS OF THE PhoBR/PstSCAB/PhoU REGULATORY THEME PRESENT IN OTHER BACTERIA

The PhoBR/PstSCAB/PhoU theme of regulation is widely used to control phosphate metabolism and related cellular processes (e.g., virulence) in bacteria (Lamarche et al., 2008; Chekabab et al., 2014; Santos-Beneit, 2015). However, the theme can be varied by alteration of the number, activities or interactions of the constituent components as illustrated by these selected examples. In *Caulobacter crescentus*, PhoU is an essential protein that does not control PhoR activity but regulates intracellular phosphate metabolism (Lubin et al., 2015). There are two PhoU proteins encoded in *Staphylococcus epidermidis*: the *phoU1* gene is located within the *pstSCABphoU1* operon while *phoU2* is located upstream of a gene with homology to the PitA phosphate transporter (Wang et al., 2017). Genetic analysis indicates that only PhoU2 controls PhoPR activity (Wang et al., 2017). *Streptococcus pneumoniae* encodes a single two-component system PnpRS located upstream of a phosphate

transporter Pst1 (*pstS1CIA1B1phoU1*) but encodes a second phosphate transporter Pst2 (*pstS2C2A2B2phoU2*) at a distinct chromosomal locus (Zheng et al., 2016). Expression of Pst2 is constitutive and PhoU2 inhibits Pst2 transporter activity. Expression of Pst1 is induced by phosphate limitation in a PnpRS dependent manner while PhoU1 inhibits Pst1 transporter activity (Zheng et al., 2016). However, PhoU2, but not PhoU1, controls PnpRS activity in a manner similar to that in *E. coli* (Zheng et al., 2016). These selected examples indicate the versatility of the PhoBR/PstSCAB/PhoU regulatory theme and show how it can be varied in bacteria to respond to phosphate availability in their particular ecological niche.

ACTIVATION OF PhoPR IN *B. subtilis* IS RESPONSIVE TO WALL TEICHOIC ACID METABOLISM

Several features of the PHO response in *B. subtilis* indicate that it differs from that of *E. coli*. The *B. subtilis* genome does not encode a PhoU homologue and the PHO response is induced normally in a strain with the high-affinity phosphate transporter (*pstSCAB_{1B2}*) deleted (Qi et al., 1997). Furthermore unlike *E. coli*, the composition and metabolism of cell wall anionic polymers is changed in a PhoPR-dependent manner during the PHO

response in *B. subtilis* (Liu and Hulett, 1998; Liu et al., 1998; Allenby et al., 2005; Botella et al., 2011, 2014; Salzberg et al., 2015). When activated, PhoP~P represses transcription of the *tagAB* operon thereby reducing WTA synthesis, and activates transcription of the *tuaA-H* operon thereby increasing synthesis

of teichuronic acid, a replacement non-phosphate containing anionic polymer (Figure 2; Liu and Hulett, 1998; Liu et al., 1998; Allenby et al., 2005; Botella et al., 2011). In addition, PhoPR regulon genes encode a plethora of enzymes for scavenging phosphate including the GlpQ and PhoD phosphodiesterases that

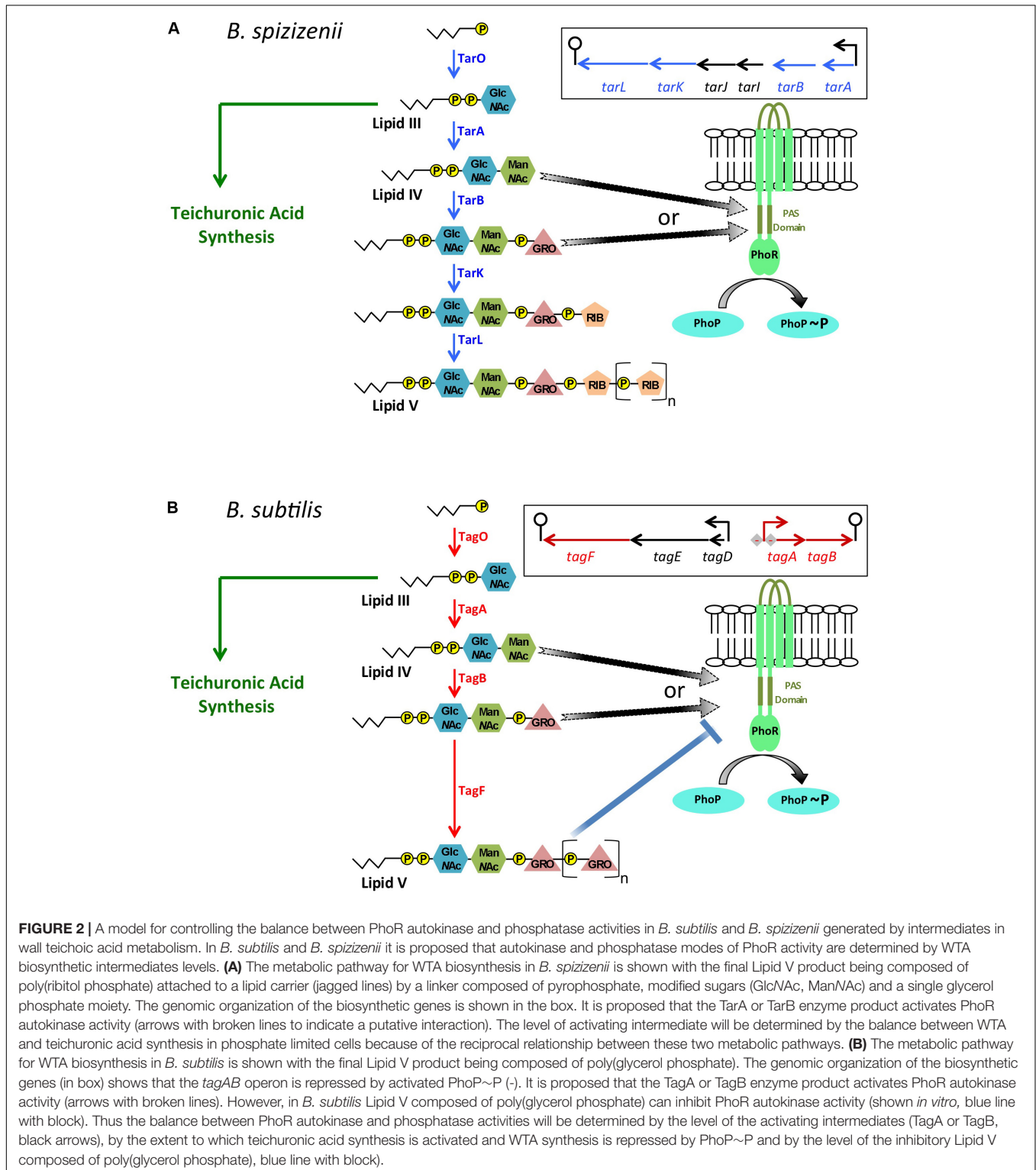


FIGURE 2 | A model for controlling the balance between PhoR autokinase and phosphatase activities in *B. subtilis* and *B. spizizenii* generated by intermediates in wall teichoic acid metabolism. In *B. subtilis* and *B. spizizenii* it is proposed that autokinase and phosphatase modes of PhoR activity are determined by WTA biosynthetic intermediates levels. **(A)** The metabolic pathway for WTA biosynthesis in *B. spizizenii* is shown with the final Lipid V product being composed of poly(ribitol phosphate) attached to a lipid carrier (jagged lines) by a linker composed of pyrophosphate, modified sugars (GlcNAc, ManNAc) and a single glycerol phosphate moiety. The genomic organization of the biosynthetic genes is shown in the box. It is proposed that the TarA or TarB enzyme product activates PhoR autokinase activity (arrows with broken lines to indicate a putative interaction). The level of activating intermediate will be determined by the balance between WTA and teichuronic acid synthesis in phosphate limited cells because of the reciprocal relationship between these two metabolic pathways. **(B)** The metabolic pathway for WTA biosynthesis in *B. subtilis* is shown with the final Lipid V product being composed of poly(glycerol phosphate). The genomic organization of the biosynthetic genes (in box) shows that the *tagAB* operon is repressed by activated PhoP~P (-). It is proposed that the TagA or TagB enzyme product activates PhoR autokinase activity (arrows with broken lines). However, in *B. subtilis* Lipid V composed of poly(glycerol phosphate) can inhibit PhoR autokinase activity (shown *in vitro*, blue line with block). Thus the balance between PhoR autokinase and phosphatase activities will be determined by the level of the activating intermediates (TagA or TagB, black arrows), by the extent to which teichuronic acid synthesis is activated and WTA synthesis is repressed by PhoP~P and by the level of the inhibitory Lipid V composed of poly(glycerol phosphate), blue line with block).

function in WTA degradation (Eder et al., 1996; Antelmann et al., 2000; Allenby et al., 2005; Botella et al., 2011; Myers et al., 2016). Furthermore, *B. subtilis* is unable to synthesize polyphosphate.

PhoR in *B. subtilis* also differs from that in *E. coli* in having an extracytoplasmic loop capable of forming a PAS domain that is not required for induction of the PHO response under laboratory conditions (Figure 2; Shi and Hulett, 1999; Chang et al., 2010; Botella et al., 2014). Amplification of the PHO response by positive autoregulation of *phoPR* transcription is augmented by PhoP~P binding to PhoP-boxes located between the *phoR* stop codon and the operon terminator, by an as yet unknown mechanism (Salzberg et al., 2015). It is perhaps not surprising therefore that activation of the PHO response in *B. subtilis* differs from that in *E. coli* and that it involves WTA metabolism.

The link between anionic polymer metabolism and PhoR activity was established in *B. subtilis* by the finding that amplification of the PHO response is delayed and attenuated in cells unable to synthesize teichuronic acid (Botella et al., 2014). Since transcription of the *tuaA-H* operon requires activated PhoP~P, this result indicates that teichuronic acid biosynthesis amplifies the PHO response by a positive feedback mechanism to increase PhoR autokinase activity (Botella et al., 2014). This observation is especially significant since WTA synthesis is reduced by PhoP~P mediated repression of *tagAB* expression. Furthermore, there is a reciprocal relationship between WTA and teichuronic acid synthesis in *B. subtilis* (the TagO enzyme product is a precursor in both metabolic pathways) implying that an increase in teichuronic acid synthesis will cause a decrease in WTA synthesis (Figure 2; Botella et al., 2014). Therefore, we sought to establish if increased PhoR activity during amplification of the PHO response is caused by an increase in the level of a teichuronic acid biosynthetic intermediate that promotes autokinase activity or by a decrease in the level of a WTA biosynthetic intermediate that inhibits autokinase activity. Genetic and biochemical evidence shows that (i) attenuation of the PHO response in strains unable to synthesize teichuronic acid can be suppressed by a concomitant reduction in WTA synthesis and (ii) PhoR autokinase activity is inhibited *in vitro* by a derivative of the WTA biosynthetic intermediate produced by the TagF enzyme (Botella et al., 2014). These data show that PhoR autokinase activity is responsive to WTA metabolism in *B. subtilis*, being inhibited by the product of the TagF enzyme (Botella et al., 2014).

Since the PHO response is amplified in *B. subtilis* by two processes that require activated PhoP~P (i.e., reduction of WTA synthesis and activation of teichuronic synthesis), it is evident that it must be initiated by a different PhoP~P-independent mechanism. Thus, initiation of the PHO response was addressed in *Bacillus subtilis* subspecies *spizizenii* (hereafter called *B. spizizenii*) that synthesizes WTA composed of poly(ribitol phosphate) (*tarABIJKL* genes) (Prunty et al., 2018). Investigation of the PHO response in *B. spizizenii* has the advantage that it is not amplified as in *B. subtilis* [i.e., WTA intermediates composed of poly(ribitol phosphate) do not inhibit PhoR autokinase activity], and expression of WTA biosynthetic enzymes is not repressed by PhoP~P (Prunty et al., 2018). Three pieces of evidence indicate that the PHO response is activated by

an intermediate in WTA synthesis in *B. spizizenii*. (1) In a strain with inducible expression of the *tarABIJKL* operon encoding the WTA biosynthetic enzymes, the magnitude of the PHO response is directly proportional to the level of added inducer (Prunty et al., 2018). (2) The PHO response is increased in a strain of *B. spizizenii* unable to synthesize teichuronic acid, indicating that the onset of teichuronic acid synthesis reduces the level of a WTA intermediate that activates the PHO response (Prunty et al., 2018). (3) The increased PHO response in a strain unable to synthesize teichuronic acid is reduced by lowering expression of the genes that encode the WTA biosynthetic enzymes (Prunty et al., 2018). Similar results were obtained in *B. spizizenii* strains expressing either the homologous PhoR kinase or the PhoR kinase from *B. subtilis* showing that activation occurs by the same mechanism in both subspecies (Prunty et al., 2018). These results suggest that an intermediate in WTA synthesis activates PhoR autokinase activity in both *B. subtilis* and *B. spizizenii* (Prunty et al., 2018). Since only the TagA/TarA and TagB/TarB enzymatic steps of the WTA biosynthetic pathways are common in *B. subtilis* and *B. spizizenii*, we conclude that one or other of their enzyme products promotes PhoR autokinase activity (Prunty et al., 2018).

A model for activation of the PHO response in *B. spizizenii* and *B. subtilis* (Figures 2A,B, respectively) proposes that upon phosphate limitation (i) there is a surge in the cellular level of WTA intermediates caused by a reduction in growth rate and lowered cell wall synthesis and (ii) the increased level of TagA/TarA or TagB/TarB enzyme product promotes PhoR autokinase activity (Prunty et al., 2018). In addition, PhoR autokinase activity is controlled in *B. subtilis* only by the level of the TagF enzyme product composed of poly (glycerol phosphate) (Figure 2B; Botella et al., 2014).

In summary, the balance of PhoR autokinase and phosphatase activities is responsive to WTA metabolism in *B. subtilis* and *B. spizizenii* (Prunty et al., 2018).

VARIATIONS OF THE PhoPR/WALL TEICHOIC ACID METABOLISM REGULATORY THEME

The kinetics of the PHO responses of *B. subtilis* and *B. spizizenii* are different (Botella et al., 2014; Prunty et al., 2018). In *B. subtilis*, the PHO response is activated, then amplified and maintained while phosphate limitation persists (Botella et al., 2014). In *B. spizizenii* the PHO response is activated but then gradually turned off even with persistence of phosphate limiting conditions (Prunty et al., 2018). These separate responses are not due to differences in the PhoR kinases, which are highly homologous and experimentally shown to be functionally equivalent (Prunty et al., 2018). Instead, the different PHO responses derive from the fact that the TagF enzyme product composed of poly(glycerol phosphate) inhibits PhoR autokinase activity in *B. subtilis* but the corresponding TarL enzyme product composed of poly(ribitol phosphate) does not inhibit PhoR autokinase activity in *B. spizizenii* (Figure 2; Botella et al., 2014; Prunty et al., 2018). Therefore, host features that impact on expression of WTA biosynthetic enzymes and the level of WTA intermediates

will influence the PHO responses of these two subspecies. These host features include genomic organization of WTA biosynthetic genes, regulation of their expression and their cellular mRNA level (Prunty et al., 2018). All WTA biosynthetic enzymes are encoded in a single operon (*tarABIJKL*) in *B. spizizenii* (Figure 2A) but are separated into two operons (*tagAB* and *tagDEF*) in *B. subtilis* (Figure 2B). Expression of the *tarABIJKL* operon is not regulated by PhoPR in *B. spizizenii* (Figure 2A) whereas expression of the *tagAB* operon is negatively regulated by activated PhoP~P in *B. subtilis* (Figure 2B). In *B. spizizenii*, mRNA levels of the *tarABIJKL* genes are uniformly reduced to ~15% of that found in exponentially growing phosphate replete cells (Prunty et al., 2018). However, in *B. subtilis*, mRNA levels of the *tagAB* genes are reduced to <1%, while that of *tagF* is only reduced to 27%, of that found in exponentially growing, phosphate replete cells. Thus, these different host features direct distinct PHO responses in *B. subtilis* and *B. spizizenii* by altering WTA metabolism, allowing adaptation to phosphate availability to be optimized in particular ecological niches.

CONCLUDING REMARKS

The bacterial PHO response is widely conserved among bacteria. However, two different mechanisms have emerged by which PhoR activity is controlled in a manner that is responsive to phosphate availability. A mechanism responsive to the conformation of the PstSCAB phosphate transporter in conjunction with PhoU, exemplified by PhoBR in *E. coli*, that is widespread among Gram-positive and Gram-negative bacteria. A distinct mechanism that is responsive to WTA synthesis is exemplified by PhoPR in *B. subtilis*. It is unclear why such a

distinct mechanism has evolved in *B. subtilis*, but it may relate to the high phosphate composition of cell wall anionic polymers, the ability to alter anionic polymer composition during phosphate limitation, the inability to synthesize polyphosphate and the use of WTA as a phosphate store. It is likely that PhoPR is activated in a PhoU-type mechanism in Staphylococcal species suggesting that phosphorous containing WTA is not a determining feature in evolution of the novel mechanism in *B. subtilis*. However, differences in phosphorous availability in their natural habits may have played a significant role, with its availability in soil being especially problematical for Bacillus species. Therefore it will be interesting to establish how strains of *B. subtilis* and *Staphylococcus aureus* expressing the PhoPR activation mechanism of the other bacterium adapt to phosphate limiting conditions and survive in their natural habitat.

AUTOR CONTRIBUTIONS

KD designed the review and drafted the manuscript.

FUNDING

These projects were funded by Science Foundation Ireland, Principal Investigator Awards 08/IN.1/B1859 and 12/1A/1570 to KD.

ACKNOWLEDGMENTS

The author thanks CM, Michael Prunty, Joan Geoghegan, and Abigail O'Brien for critically reading the manuscript.

REFERENCES

- Achbergerová, L., and Nahálka, J. (2011). Polyphosphate—an ancient energy source and active metabolic regulator. *Microb. Cell. Fact.* 10:63. doi: 10.1186/1475-2859-10-63
- Allenby, N. E., O'Connor, N., Prágai, Z., Ward, A. C., Wipat, A., and Harwood, C. R. (2005). Genome-wide transcriptional analysis of the phosphate starvation stimulon of *Bacillus subtilis*. *J. Bacteriol.* 187, 8063–8080. doi: 10.1128/JB.187.23.8063-8080.2005
- Antelmann, H., Scharf, C., Hecker, M. (2000). Phosphate starvation-inducible proteins of *Bacillus subtilis*: proteomics and transcriptional analysis. *J. Bacteriol.* 182, 4478–4490. doi: 10.1128/JB.182.16.4478-4490.2000
- Batjes, N. H. (1997). A world data set for derived soil properties by FAO-UNESCO soil unit for global modelling. *Soil Use Manag.* 13, 9–16.
- Blanco, A. G., Sola, M., Gomis-Rüth, F. X., and Coll, M. (2002). Tandem DNA recognition by PhoB, a two-component signal transduction transcriptional activator. *Structure* 10, 701–713. doi: 10.1016/S0969-2126(02)00761-X
- Botella, E., Devine, S. K., Hubner, S., Salzberg, L. I., Gale, R. T., Brown, E. D., et al. (2014). PhoR autokinase activity is controlled by an intermediate in wall teichoic acid metabolism that is sensed by the intracellular PAS domain during the PhoPR-mediated phosphate limitation response of *Bacillus subtilis*. *Mol. Microbiol.* 94, 1242–1259. doi: 10.1111/mmi.12833
- Botella, E., Hübner, S., Hokamp, K., Hansen, A., Bisicchia, P., Noone, D., et al. (2011). Cell envelope gene expression in phosphate-limited *Bacillus subtilis* cells. *Microbiology* 157, 2470–2484. doi: 10.1099/mic.0.049205-0
- Brown, M. R., and Kornberg, A. (2008). The long and short of it-polyphosphate, PPK and bacterial survival. *Trends Biochem. Sci.* 33, 284–290. doi: 10.1016/j.tibs.2008.04.005
- Chang, C., Tesar, C., Gu, M., Babnigg, G., Joachimiak, A., Pokkuluri, P. R., et al. (2010). Extracytoplasmic PAS-like domains are common in signal transduction proteins. *J. Bacteriol.* 192, 1156–1159. doi: 10.1128/JB.01508-09
- Chekabab, S. M., Jubelin, G., Dozois, C. M., and Harel, J. (2014). PhoB activates *Escherichia coli* O157:H7 virulence factors in response to inorganic phosphate limitation. *PLoS One* 9:e94285. doi: 10.1371/journal.pone.0094285
- Cox, G. B., Webb, D., Godovac-Zimmermann, J., and Rosenberg, H. (1988). Arg-220 of the PstA protein is required for phosphate transport through the phosphate specific transport system in *Escherichia coli* but not for alkaline phosphatase repression. *J. Bacteriol.* 170, 2283–2286. doi: 10.1128/jb.170.5.2283-2286.1988
- Cox, G. B., Webb, D., and Rosenberg, H. (1989). Specific amino acid residues in both the PstB and PstC proteins are required for phosphate transport by the *Escherichia coli* Pst system. *J. Bacteriol.* 171, 1531–1534. doi: 10.1128/jb.171.3.1531-1534.1989
- Eder, S., Shi, L., Jensen, K., Yamane, K., and Hulett, F. M. (1996). A *Bacillus subtilis* secreted phosphodiesterase/alkaline phosphatase is the product of a Pho regulon gene, phoD. *Microbiology* 142, 2041–2047. doi: 10.1099/13500872-142-8-2041
- Gardner, S. G., Johns, K. D., Tanner, R., and McCleary, W. R. (2014). The PhoU protein from *Escherichia coli* interacts with PhoR, PstB, and metals to form a phosphate-signaling complex at the membrane. *J. Bacteriol.* 196, 1741–1752. doi: 10.1128/JB.00029-14

- Gardner, S. G., Miller, J. B., Dean, T., Robinson, T., Erickson, M., Ridge, P. G., et al. (2015). Genetic analysis, structural modeling, and direct coupling analysis suggest a mechanism for phosphate signaling in *Escherichia coli*. *BMC Genet.* 16(Suppl. 2):S2. doi: 10.1186/1471-2156-16-S2-S2
- Hsieh, Y. J., and Wanner, B. L. (2010). Global regulation by the seven-component Pi signaling system. *Curr. Opin. Microbiol.* 13, 198–203. doi: 10.1016/j.mib.2010.01.014
- Jiménez, J., Bru, S., Ribeiro, M. P., and Clotet, J. (2017). Polyphosphate: popping up from oblivion. *Curr. Genet.* 63, 15–18. doi: 10.1007/s00294-016-0611-5
- Lamarche, M. G., Wanner, B. L., Crépin, S., and Harel, J. (2008). The phosphate regulon and bacterial virulence: a regulatory network connecting phosphate homeostasis and pathogenesis. *FEMS Microbiol. Rev.* 32, 461–473. doi: 10.1111/j.1574-6976.2008.00101.x
- Liu, W., and Hulett, F. M. (1998). Comparison of PhoP binding to the *tuaA* promoter with PhoP binding to other Pho-regulon promoters establishes a *Bacillus subtilis* Pho core binding site. *Microbiology* 144, 1443–1450. doi: 10.1099/00221287-144-5-1443
- Liu, W., Eder, S., and Hulett, F. M. (1998). Analysis of *Bacillus subtilis* tagAB and tagDEF expression during phosphate starvation identifies a repressor role for PhoP-P. *J. Bacteriol.* 180, 753–738.
- Liu, J., Lou, Y., Yokota, H., Adams, P. D., Kim, R., and Kim, S. H. (2005). Crystal structure of a PhoU protein homologue: a new class of metalloprotein containing multinuclear iron clusters. *J. Biol. Chem.* 280, 15960–15966. doi: 10.1074/jbc.M414117200
- Lubin, E. A., Henry, J. T., Fiebigm, A., Crosson, S., and Laub, M. T. (2015). Identification of the PhoB regulon and role of PhoU in the phosphate starvation response of *Caulobacter crescentus*. *J. Bacteriol.* 198, 187–200. doi: 10.1128/JB.00658-15
- Myers, C. L., Li, F. K., Koo, B. M., El-Halfawy, O. M., French, S., Gross, C. A., et al. (2016). Identification of two phosphate starvation-induced wall teichoic acid hydrolases provides first insights into the degradative pathway of a key bacterial cell wall component. *J. Biol. Chem.* 291, 26066–26082. doi: 10.1074/jbc.M116.760447
- Oganesyan, V., Oganesyan, N., Adams, P. D., Jancarik, J., Yokota, H. A., and Kim, R., et al. (2005). Crystal structure of the “PhoU-like” phosphate uptake regulator from *Aquifex aeolicus*. *J. Bacteriol.* 187, 4238–4244. doi: 10.1128/JB.187.12.4238-4244.2005
- Percy, M. G., and Gründling, A. (2014). Lipoteichoic acid synthesis and function in gram-positive bacteria. *Annu. Rev. Microbiol.* 68, 81–100. doi: 10.1146/annurev-micro-091213-112949
- Piepenbreier, H., Fritz, G., and Gebhard, S. (2017). Transporters are information processors in bacterial signalling pathways. *Mol. Microbiol.* 104, 1–15. doi: 10.1111/mmi.13633
- Prunty, M. P., Noone, D., and Devine, K. M. (2018). The distinct PhoPR mediated responses to phosphate limitation in *Bacillus subtilis* subspecies *subtilis* and *spizizenii* stem from differences in wall teichoic acid composition and metabolism. *Mol. Microbiol.* 109, 23–40. doi: 10.1111/mmi.13965
- Qi, Y., Kobayashi, Y., and Hulett, F. M. (1997). The *pst* operon of *Bacillus subtilis* has a phosphate-regulated promoter and is involved in phosphate transport but not in regulation of the *pho* regulon. *J. Bacteriol.* 179, 2534–2539. doi: 10.1128/jb.179.8.2534-2539.1997
- Rao, N. N., Gómez-García, M. R., and Kornberg A. (2009). Inorganic polyphosphate: essential for growth and survival. *Annu. Rev. Biochem.* 78, 605–647. doi: 10.1146/annurev.biochem.77.083007.093039
- Rao, N. N., Roberts, M. F., Torriani, A., and Yashphe, J. (1993). Effect of *glpT* and *glpD* mutations on expression of the *phoA* gene in *Escherichia coli*. *J. Bacteriol.* 175, 74–79. doi: 10.1128/jb.175.1.74-79.1993
- Rice, C. D., Pollard, J. E., Lewis, Z. T., and McCleary, W. R. (2009). Employment of a promoter-swapping technique shows that PhoU modulates the activity of the PstSCAB2 ABC transporter in *Escherichia coli*. *Appl. Environ. Microbiol.* 75, 573–582. doi: 10.1128/AEM.01046-1048
- Santos-Beneit, F. (2015). The Pho regulon: a huge regulatory network in bacteria. *Front. Microbiol.* 6:402. doi: 10.3389/fmicb.2015.00402
- Salzberg, L. I., Botella, E., Hokamp, K., Antelmann, H., Maaß, S., Becher, D., et al. (2015). Genome-wide analysis of phosphorylated PhoP binding to chromosomal DNA reveals several novel features of the PhoPR-mediated phosphate limitation response in *Bacillus subtilis*. *J. Bacteriol.* 197, 1492–1506. doi: 10.1128/JB.02570-2514
- Shi, L., and Hulett, F. M. (1999). The cytoplasmic kinase domain of PhoR is sufficient for the low phosphate-inducible expression of *pho* regulon genes in *Bacillus subtilis*. *Mol. Microbiol.* 31, 211–222. doi: 10.1046/j.1365-2958.1999.01163.x
- Swoboda, J. G., Campbell, J., Meredith, T. C., and Walker, S. (2010). Wall teichoic acid function, biosynthesis, and inhibition. *ChemBiochem* 11, 35–45. doi: 10.1002/cbic.200900557
- Tetsch, L., and Jung, K. (2009). The regulatory interplay between membrane-integrated sensors and transport proteins in bacteria. *Mol. Microbiol.* 73, 982–991. doi: 10.1111/j.1365-2958.2009.06847.x
- Vuppada, R. K., Hansen, C. R., Strickland, K. A. P., Kelly, K. M., and McCleary, W. R. (2018). Phosphate signaling through alternate conformations of the PstSCAB phosphate transporter. *BMC Microbiol.* 18:8. doi: 10.1186/s12866-017-1126-z
- Wang, X., Han, H., Lv, Z., Lin, Z., Shang, Y., Xu, T., et al. (2017). PhoU2 but not PhoU1 as an important regulator of biofilm formation and tolerance to multiple stresses by participating in various fundamental metabolic processes in *Staphylococcus epidermidis*. *J. Bacteriol.* 199:e00219-17. doi: 10.1128/JB.00219-17
- Weidenmaier, C., and Peschel, A. (2008). Teichoic acids and related cell-wall glycopolymers in gram-positive physiology and host interactions. *Nat. Rev. Microbiol.* 6, 276–287. doi: 10.1038/nrmicro1861
- Zheng, J. J., Sinha, D., Wayne, K. J., and Winkler, M. E. (2016). Physiological roles of the dual phosphate transporter systems in low and high phosphate conditions and in capsule maintenance of *Streptococcus pneumoniae* D39. *Front. Cell. Infect. Microbiol.* 6:63. doi: 10.3389/fcimb.2016.00063

Conflict of Interest Statement: The author declares that the research was conducted in the absence of any commercial or financial relationships that could be construed as a potential conflict of interest.

Copyright © 2018 Devine. This is an open-access article distributed under the terms of the Creative Commons Attribution License (CC BY). The use, distribution or reproduction in other forums is permitted, provided the original author(s) and the copyright owner(s) are credited and that the original publication in this journal is cited, in accordance with accepted academic practice. No use, distribution or reproduction is permitted which does not comply with these terms.



Cell Wall Hydrolases in Bacteria: Insight on the Diversity of Cell Wall Amidases, Glycosidases and Peptidases Toward Peptidoglycan

Aurore Vermassen¹, Sabine Leroy¹, Régine Talon¹, Christian Provot², Magdalena Popowska³ and Mickaël Desvaux^{1*}

¹ Université Clermont Auvergne, INRA, MEDIS, Clermont-Ferrand, France, ² BioFilm Control SAS, Saint-Beauzire, France,

³ Department of Applied Microbiology, Faculty of Biology, Institute of Microbiology, University of Warsaw, Warsaw, Poland

OPEN ACCESS

Edited by:

Patrick Joseph Moynihan,
University of Birmingham,
United Kingdom

Reviewed by:

Christopher Davies,
Medical University of South Carolina,
United States
Johann Peltier,
Institut Pasteur, France
Sheena McGowan,
Monash University, Australia

*Correspondence:

Mickaël Desvaux
mickael.desvaux@inra.fr

Specialty section:

This article was submitted to
Microbial Physiology and Metabolism,
a section of the journal
Frontiers in Microbiology

Received: 09 August 2018

Accepted: 08 February 2019

Published: 28 February 2019

Citation:

Vermassen A, Leroy S, Talon R,
Provot C, Popowska M and
Desvaux M (2019) Cell Wall
Hydrolases in Bacteria: Insight on the
Diversity of Cell Wall Amidases,
Glycosidases and Peptidases Toward
Peptidoglycan.
Front. Microbiol. 10:331.
doi: 10.3389/fmicb.2019.00331

The cell wall (CW) of bacteria is an intricate arrangement of macromolecules, at least constituted of peptidoglycan (PG) but also of (lipo)teichoic acids, various polysaccharides, polyglutamate and/or proteins. During bacterial growth and division, there is a constant balance between CW degradation and biosynthesis. The CW is remodeled by bacterial hydrolases, whose activities are carefully regulated to maintain cell integrity or lead to bacterial death. Each cell wall hydrolase (CWH) has a specific role regarding the PG: (i) cell wall amidase (CWA) cleaves the amide bond between N-acetylmuramic acid and L-alanine residue at the N-terminal of the stem peptide, (ii) cell wall glycosidase (CWG) catalyses the hydrolysis of the glycosidic linkages, whereas (iii) cell wall peptidase (CWP) cleaves amide bonds between amino acids within the PG chain. After an exhaustive overview of all known conserved catalytic domains responsible for CWA, CWG, and CWP activities, this review stresses that the CWHs frequently display a modular architecture combining multiple and/or different catalytic domains, including some lytic transglycosylases as well as CW binding domains. From there, direct physiological and collateral roles of CWHs in bacterial cells are further discussed.

Keywords: bacterial cell wall, peptidoglycan (PG) hydrolases, protein modules, cell wall binding domains, bacterial division and growth, cell lysis, cell wall remodeling

INTRODUCTION

The first bacterial cell wall hydrolase (CWH) was discovered in 1921 by the Scottish bacteriologist Sir Alexander Fleming, who is well known for his 1928 discovery of the antibiotic penicillin (Fleming, 1929). He had observed “a remarkable bacteriolytic element,” which caused bacterial lysis on an agar plate and which he called “lysozyme” in 1922. Lysozyme cleaves the β -(1-4)-glycosidic bond between N-acetylmuramic acid (MurNAc) and N-acetylglucosamine (GlcNAc) in peptidoglycan (PG) (Chipman et al., 1967). This hydrolytic enzyme has served as a model in protein biochemistry and its contribution to antibacterial defense is well recognized.

The bacterial cell wall (CW) is a complex arrangement of macromolecules that varies depending on the species of bacteria and whether they are parietal monoderm bacteria (archetypal Gram-positive bacteria), lipopolysaccharidic diderm bacteria (archetypal Gram-negative bacteria) or mycolate diderm bacteria (archetypal acid-fast bacteria)

(Desvaux et al., 2018; **Figure 1**). While the PG is the major polymer of the CW, teichoic and lipoteichoic acids as well as other macromolecular components like polysaccharides, polyglutamate or proteins can also be (Neuhaus and Baddiley, 2003; Dramsi et al., 2008; Vollmer et al., 2008a). In resisting to internal turgor pressure to maintain bacterial cell integrity and shape, the CW is essential to bacterial growth under various environmental conditions (Weidel and Pelzer, 1964; Vollmer et al., 2008a). Besides, it needs to be remodeled to accommodate cell elongation and division for proper bacterial growth. In CW-monoderm bacteria, the CW is an interface between the cell and its environment and participates in interactions with abiotic surfaces, bacteriophages and eukaryotic host cells (Silhavy et al., 2010).

Depending on the CW bonds they specifically cleave, CWHs can be discriminated into three types of enzymes, namely amidases, glycosidases or peptidases (Rigden et al., 2003; Fenton et al., 2010; Szweda et al., 2012). CWHs were historically described as lysins and classified as endolysins, exolysins and/or autolysins based on their origin and role (Vollmer et al., 2008b; Schmelcher et al., 2012). In fact, endolysins referred to bacteriophage encoded CWHs degrading the CW of the host bacterium upon activation of the lytic cycle. Exolysins referred to secreted bacterial CWHs aiming at killing bacterial cells of different species or even strains within the same species. Rather than bacterial cell lysis, autolysins referred to hydrolases mainly involved in CW remodeling in the course of bacterial cell division (Vollmer et al., 2008b; Vollmer, 2012). However, advances in biochemical and structural characterization indicate that these lysins include amidases, glycosidases and peptidases. In function, endolysins are similar to exolysins and autolysins, except that these two latter hydrolases are not encoded by bacteriophages (Schmelcher et al., 2012). Moreover, a so-called autolysin can induce cell lysis (and not just CW remodeling) when its expression is not tightly controlled (Typas et al., 2012). For these reasons, in this manuscript, we will favor the term CWHs over lysins, and describe them with respect to their catalytic activity into CW amidases, CW glycosidases and/or CW peptidases rather than endolysins, exolysins and autolysins. This nomenclature highlights the importance of the modular architecture of the polypeptide for its function. Since the PG is the only CW component targeted by CWHs characterized to date, they can be interchangeably called PG hydrolases (PGHs).

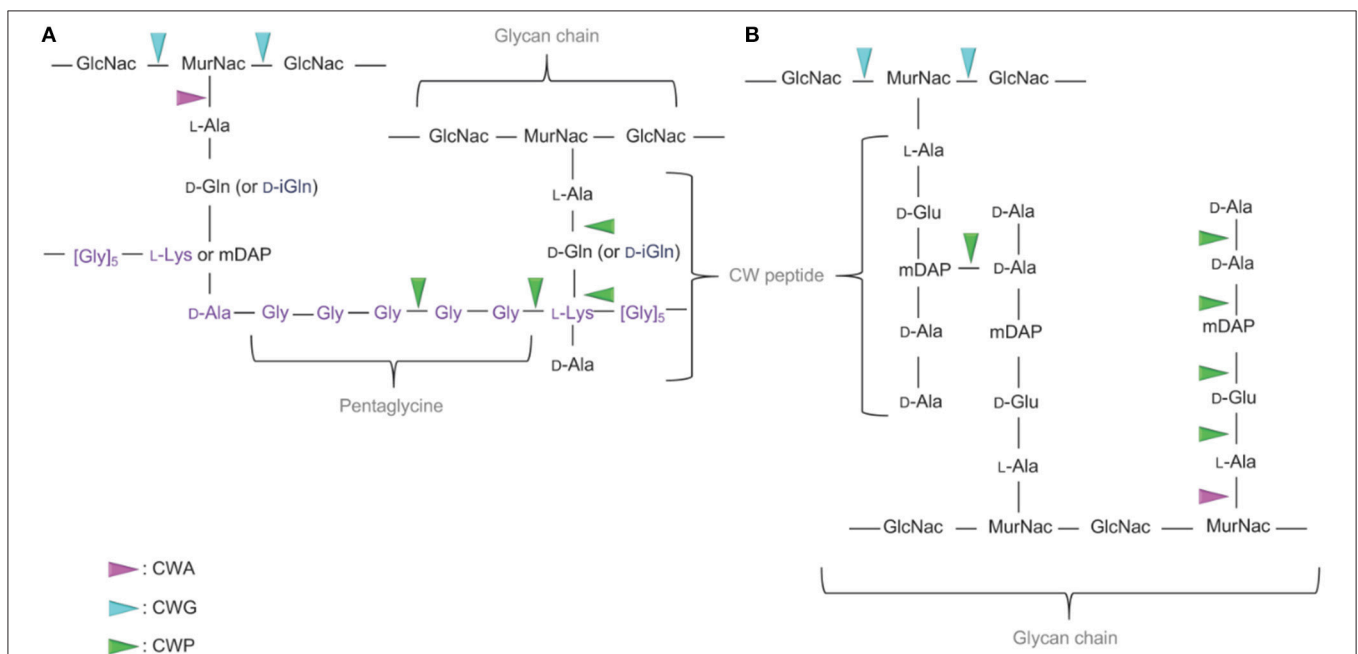
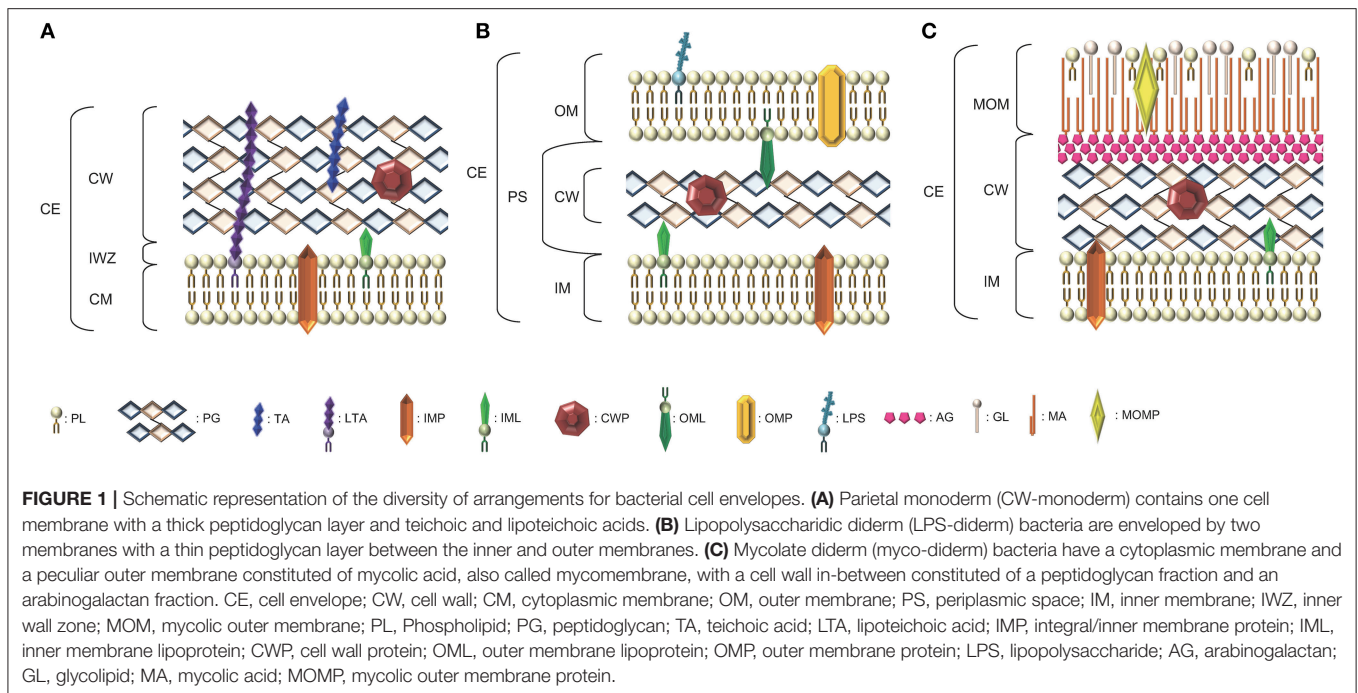
After a brief reminding of the CW structure and organization in bacteria, the different conserved domains related to bacterial CWHs are here exhaustively overviewed in order to further stress the diversity of their modular architecture and their physiological relevance is further discussed.

THE CELL WALL: COMPOSITION, STRUCTURE AND ORGANIZATION

Bacteria have developed a complex cell envelope, which helps them to survive in various environments (Vollmer et al., 2008a;

Silhavy et al., 2010). The CW is a macromolecule with an elastic-plastic behavior that defines the shape of the bacterium (Amir et al., 2014). It enables the bacterial cell to resist lysis as a result of its high intracellular osmotic pressure. In CW-monoderm bacteria, the cytoplasmic membrane is surrounded by a thick CW (10–20 layers thick) composed of PG, to which secondary polymers are covalently attached (e.g., teichoic acids (**Figure 1**; Vollmer et al., 2008a); in addition, lipoteichoic acids are anchored to the cytoplasmic membrane via their diacylglycerol moiety. Some polysaccharides, namely teichuronic acids or polyglutamate, and surface proteins can be covalently or non-covalently linked to the PG. Actually, the totality of the molecular components found at the bacterial cell surface refers to the surfaceome and its protein subset constitutes the proteosurfaceome (Desvaux et al., 2018). When displayed at the surface of CW-monoderm bacteria, proteins can either be associated with the cytoplasmic membrane, i.e., IMPs (integral membrane proteins) or lipoproteins, or with the CW (Popowska and Markiewicz, 2004; Desvaux et al., 2006). At the CW, proteins can either be covalently anchored (LPXTG-proteins) or specifically associated with some CW components through weak interactions thanks to the presence of conserved motifs, e.g., LysM (lysine motif), CWB1 (CW binding repeat of type 1) or PGB1 (peptidoglycan binding domain of type 1) (Desvaux et al., 2006, 2018). In the cell envelope of LPS-diderm bacteria, the CW is located between the cytoplasmic membrane (then also called inner membrane) and the outer membrane, i.e., within the periplasmic space. It consists of a thin layer of PG (only 1–3 layers thick) linked to some lipoproteins anchored to the outer membrane (**Figure 1**; Torti and Park, 1976).

The molecular organization, variations in the primary structure and description of the different types of the PG in bacteria has been extensively described in dedicated reviews readily available for in-depth details (Schleifer and Kandler, 1972; Turner et al., 2014; Desvaux et al., 2018). In CW-monoderm bacteria, the PG polymer results from the cross-linking of glycan strands through peptide stems. While peptide stems originate from the lactyl moiety of the MurNAc saccharide, the glycan strands are composed of alternating MurNAc and GlcNAc saccharides (**Figure 2**; Bourhis and Werts, 2007; Johnson et al., 2013). In the stem peptide, the first two residues of are generally L-Ala and D-Gln or iGln, whereas D-Ala is typically the last one (Humann and Lenz, 2009). In many rod-shaped CW-monoderm bacteria, e.g., *Listeria* or *Bacillus*, a meso-diaminopimelate (mDAP) constitutes the third residue of the stem peptide. In cocci species, though, a lysine residue is found at this position (Vollmer et al., 2008a). The *Staphylococcus aureus* PG comprises 20 or more layers of linear glycan chains with alternating MurNAc and GlcNAc, and a L-Ala-D-iGln-L-Lys-D-Ala stem peptide (Dmitriev et al., 2004). To connect PG chains, a pentaglycine interpeptide branches off the amino group of the L-Lys of the stem peptide to the D-Ala in the position of a neighboring chain (**Figure 2**). In *S. aureus*, the PG chains have a maximum length of 23–26 disaccharide units but the majority of chains ranges between 3 and 10 (Boneca et al., 2000). Actually, most of the diversity in the PG composition



occurs with the nature of the crosslinking of the stem peptides (Schleifer and Kandler, 1972).

In LPS-diderm bacteria, the composition of PG is quite similar with alternating MurNAc and GlcNAc (**Figure 2**). However, a 1,6-anhydro modification is present at the end of the strand in MurNAc residue (Vollmer and Holtje, 2004). Of note, such modification can also be detected in some CW-monoderm bacteria, like *B. subtilis* (Atrih et al., 1999). The L-Ala-D-Glu-mDAP-D-Ala-D-Ala stem peptides is linked to the lactyl group of MurNAc (**Figure 2**). Most cross-links result from the mDAP at position 3 of one stem peptide with the D-Ala at position 4 of a second stem peptide of a neighboring glycan strand (Vollmer and Holtje, 2004). In *Escherichia coli*, the length of glycan chains is around 25–35 disaccharide units in average but the length distribution is quite broad (Harz et al., 1990).

In myco-diderm bacteria, the mycolic outer membrane (MOM) or mycomembrane has been intensively investigated (Niederweis et al., 2010; Jackson, 2014) and the CW located between the MOM and the IM is constituted of two main fractions, the PG and arabinogalactan (AG), which are covalently attached (Alderwick et al., 2015). The AG is actually connected to mycolic acids at the MOM then forming the so-called mycolyl-arabinogalactan-peptidoglycan complex. Regarding the PG and compared to CW-monoderm or LPS-diderm bacteria, much less information is available but it is generally assumed its synthesis is similar to that of *E. coli* (Schleifer and Kandler, 1972; Van Heijenoort, 2001; Alderwick et al., 2015). Briefly, the PG in myco-diderm bacteria is composed of alternating GlcNAc and MurNAc, linked in a β -1,4 configuration (Alderwick et al., 2015). Besides MurNAc, N-glycolyl derivatives of the muramic acid (MurNGly) are also present as a result of the oxidation of the N-acetyl group to a N-glycolyl group. Regarding the stem peptides, the proportion of cross-linking is also significantly higher in myco-diderm bacteria compared to LPS-diderm bacteria as observed for *Mycobacterium* species vs. *E. coli* (Alderwick et al., 2015).

In both CW-monoderm and LPS-diderm bacteria, modifications to the basic PG structure such as N-glycosylation, O-acetylation and/or N-deacetylation occur frequently and many of them are species-specific (Markiewicz and Popowska, 2011). Moreover, in response to environmental conditions, the PG structure of a given bacterium may also change. Such modifications could enhance resistance to antibiotics and host degradative enzymes targeting the CW. Modifications to the basic PG structure occur at several levels, namely in the disaccharide backbone, the bridge regions, and the peptide stem (Humann and Lenz, 2009).

CELL WALL HYDROLASES IN BACTERIA

The classification of a CWH as CW amidase, CW glycosidase and/or CW peptidase is associated with the presence of conserved catalytic domains respective to these different enzymatic activities (Alcorlo et al., 2017). These functionally important domains can be identified in proteins following searches against Interpro (IPR) (Mitchell et al., 2019), the most renown

and reliable integrative protein signature databank regrouping different specialist member databases, such as Pfam (Finn et al., 2016), SMART (Letunic and Bork, 2018) or CDD (Marchler-Bauer et al., 2017). In fact, the identification of a conserved motif based on a probabilistic match against HMM (hidden Markov model) or even PSSM (position-specific scoring matrix) profiles is more effective, relevant and robust than a percentage of identity or similarity against regular expressions (Nagl, 2003). The cleavage sites of the PG by the different CWHs are shown in **Figure 2**. To date, only CWHs involved in the degradation of PG have been reported, and consequently they can be synonymously and more precisely called PGHs, at least until CWHs targeting other components of the CW are reported and characterized. Regarding the structure of solved CWHs readers can refer to recent review for further in-depth knowledge (Alcorlo et al., 2017; Broendum et al., 2018).




Cell Wall Amidases (CWA, E.C.3.5.1)

CWAs actually correspond to N-acetylmuramoyl-L-alanine amidases (NALAAs) and can also be called PG amidases (PGAs) or amidases in the scientific literature (Young, 1992; Shockman et al., 1996). They hydrolyse the amide bond separating the glycan strand from the stem peptide, that is between the MurNAc and L-alanine residues (Holtje, 1995; Vollmer et al., 2008b). In bacteria, three different types of catalytic domains are currently reported as responsible for a NALAA activity, namely (i) N-acetylmuramoyl-L-alanine amidase of type 2 (NALAA-2; IPR002502), (ii) N-acetylmuramoyl-L-alanine amidase of type 3 (NALAA-3; IPR002508), and (iii) N-acetylmuramoyl-L-alanine amidase of type 5 (NALAA-5; IPR008044) (**Table 1** and **Figure 3**).

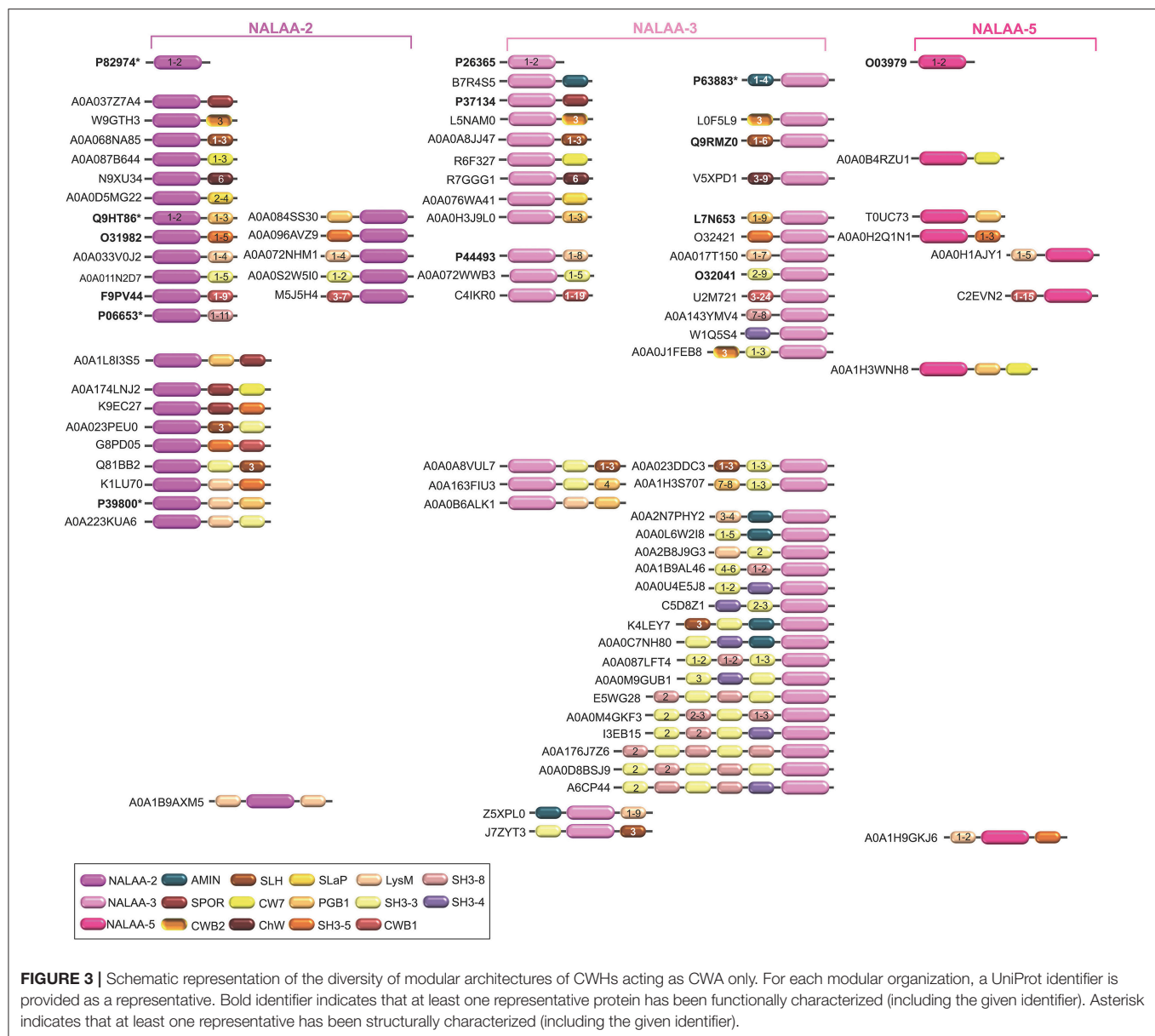
N-acetylmuramoyl-L-alanine amidase of Type 2 (NALAA-2)

The NALAA-2 domain is about 125 amino acids long (IPR002502). *E. coli* AmpD is one of the most investigated CWHs with a NALAA-2 domain (Holtje et al., 1994; Van Heijenoort, 2001). This enzyme rapidly cleaves 1,6-anhydro-MurNAc-L-Ala bonds in MurNAc-tri and tetrapeptides. Amid (amidase D) has a broader substrate specificity in cleaving both 1,6-anhydro-MurNAc-L-Ala and MurNAc-L-Ala bonds (Pennartz et al., 2009). In some *Bacillus* species, a truncated version of this domain can be found, that is the NALAA-2C (N-acetylmuramoyl-L-alanine amidase domain of type 2 C-terminal; IPR021976), which remains poorly understood (Yang et al., 2013). The structure of NALAA-2 catalytic domain has been extensively investigated (**Table 1**; Firczuk and Bochtler, 2007; Alcorlo et al., 2017). The catalysis is zinc-dependent and occurs in a L-shape cavity where the Zn^{2+} cation is located at the intersection of the region for the glycan binding and the region for the peptide stem binding (Lee et al., 2013; Martinez-Caballero et al., 2013). NALAA-2 has an open and closed conformation as the enzyme activation involves important structural rearrangements at the substrate and peptide-stem binding sites (Liepinsh et al., 2003; Carrasco-Lopez et al., 2011).

TABLE 1 | Conserved catalytic domains responsible for cell wall amidase (CWA) activity in bacterial cell wall hydrolases (CWHs).

Catalytic domain ^a	Abbreviation	InterPro	Other databases ^b	Structure ^c	Additional catalytic domain ^{a,d}	Cell wall binding domain ^e	Bacteria ^f
Cell wall amidase	CWA						
N-acetylmuramoyl-L-alanine amidase of type 2	NALAA-2	IPR002502	PF01510 SM00644 SSF55846 G3DSA:3.40.80.10 CD06583	1J3G, 2Y28, 2Y2B, 2Y2C, 2Y2D, 2Y2E, 4IW, 4X36, 3D2Z, 5CTV, 4BOL, 4BJ4, 4BPA, 4BXJ, 4BXD, 3RDR, 3HMB, 4BXE, 2BH7, 2WKX, 2D2Y, 3D2Z, 4QLS		PGB1, SPOR, SH3-3, SH3-5, SH3-8, SLAP, LysM, CWT, SLH, CWB1, CWB2, ChW	Proteobacteria (<i>Pseudomonas</i> , <i>Acinetobacter</i>), Actinobacteria (<i>Streptomyces</i> , <i>Mycobacterium</i> , <i>Micromonospora</i>), Firmicutes (<i>Clostridium</i> , <i>Bacillus</i> , <i>Lactobacillus</i> , <i>Paenibacillus</i> , <i>Staphylococcus</i> , <i>Enterococcus</i> , <i>Selenomonas</i>), Bacteroidetes (<i>Flavobacterium</i> , <i>Chryseobacterium</i> , <i>Bacteroides</i> , <i>Prevotella</i> , <i>Chitinophaga</i>), Cyanobacteria (<i>Synechococcus</i>), Chloroflexi (<i>Chloroflexus</i>), Fusobacteria (<i>Fusobacterium</i> , <i>Leptotrichia</i>)
N-acetylmuramoyl-L-alanine amidase of type 3	NALAA-3	IPR002508	PF01520 SM00646 G3DSA:3.40.630.40 CD02696	4BIN, 4KNK, 4KNL, 3LAT, 4EPC		LysM, AMIN, PGB1, SPOR, SH3-3, SH3-4, SH3-8, SLAP, CWB2, SLH, CWB1, CWT, ChW	Firmicutes (<i>Clostridium</i> , <i>Bacillus</i> , <i>Paenibacillus</i> , <i>Lactobacillus</i> , <i>Eubacterium</i> , <i>Desulfatovacuum</i>), Proteobacteria (<i>Pseudomonas</i> , <i>Vibrio</i> , <i>Sphingomonas</i>), Bacteroidetes (<i>Flavobacterium</i> , <i>Bacteroides</i> , <i>Prevotella</i>), Actinobacteria (<i>Mycobacterium</i> , <i>Streptomyces</i> , <i>Corynebacterium</i>), Cyanobacteria (<i>Nostoc</i> , <i>Calothrix</i> , <i>Synechococcus</i>)
N-acetylmuramoyl-L-alanine amidase of type 5	NALAA-5	IPR008044	PF05382	n.d.		SH3-5, PGB1, LysM, CWT, CWB1	Firmicutes (<i>Lactobacillus</i> , <i>Streptococcus</i> , <i>Enterococcus</i> , <i>Clostridium</i> , <i>Anaerococcus</i> , <i>Fructobacillus</i> , <i>Lactococcus</i>), Proteobacteria (<i>Acinetobacter</i> , <i>Actinobacteria</i> (<i>Blifidobacterium</i>))

^aColoured highlighting indicate the type of cell wall hydrolase (CWH), namely cell wall amidase (CWA; pink), cell wall glycosidase (CWG; cyan) or cell wall peptidase (CWP; green).
^bDatabases used to construct the InterPro entry, namely Pfam (PF), SMART (SM), Conserved Domain database (CD), Prosite (PS), Superfamily (SF), Protein Information Resource System (PIRSF), TIGRFam (TIGR), HAMAP (MF), CATH-Gene3D (G3DSA).
^cIdentifier from the Protein DataBase (PDB), n.d.: structure not determined.
^dAdditional catalytic domains that can be associated with the catalytic domain under consideration in a given monopolyptide along the modular architecture of the protein. Catalytic domains corresponding to CWA are shaded in pink, to CWG in blue, and to CWP in green. Unshaded catalytic domains correspond to non-hydrolytic enzymes, namely N-acetylmuramidases (lytic transglycosylases), namely the TG (transglycosylase; IPR010618), RipA (rare lipoprotein A; IPR034718), MltG (membrane-bound lytic transglycosylase of type G; IPR003770), SleB (Spore cortex-lytic enzyme of *Bacillus*; IPR011105), SLT1 (soluble lytic murein transglycosylase of type 1; IPR008258) or SLT2 (IPR031304) domains.
^eAdditional cell wall binding domains that can be found along the modular architecture of a monopolyptide. LysM: lysin motif (IPR018392), PGB1: peptidoglycan binding domain of type 1 (IPR002477), PGB3 (IPR018537), PGB4 (IPR022029), SLH: S-layer homology domain (IPR001119), LysM: lysin motif (IPR018392), SPOR: sporulation-related (IPR007730), CWB1: cell wall binding repeat of type 1 (IPR018337), CWB2 (IPR007253), ChW: clostridial hydrophobic repeat with a conserved W residue (IPR006637), CWT: cell wall binding domain of Cpl-7 (IPR013168), SLAP: S-layer protein (IPR024968), AMIN: N-terminal nonamidase (IPR021731), SH3-1: sarcoma [src] homology 3 of type 1 (IPR00018), SH3-2 (PF07653), SH3-3 (PF08239), SH3-4 (PF06347), SH3-5 (PF08460), SH3-6 (PF12913), SH3-7 (PF12914), SH3-8 (PF13457) and SH3-9 (PF14604).
^fMain phyla of the kingdom Bacteria and examples of some of the main bacterial genera (in brackets and in italics) with bacterial genomes encoding protein harboring the CWA catalytic domain as recorded in InterPro and Pfam databases.



N-acetylmuramoyl-L-alanine amidase of Type 3 (NALAA-3)

The NALAA-3 domain is approximately 175 amino acids long (IPR002508). In *E. coli*, the NALAA-3 AmiA and AmiC were shown to result in the release of the L-Ala-D-Glu-mDAP tripeptide and L-Ala-D-Glu-mDAP-D-Ala tetrapeptide. Like NALAA-2, NALAA-3 is a zinc-dependent amidase, which structure has been solved (Zoll et al., 2012; Rocaboy et al., 2013; Buttner et al., 2014).

N-acetylmuramoyl-L-alanine amidase of Type 5 (NALAA-5)

The NALAA-5 domain is around 140 amino acids long (IPR008044). Dp-1, a bacteriophage of *Streptococcus pneumoniae* belonging to Siphoviridae family, encodes a NALAA-5 CW

degrading enzyme (Lopez et al., 1981; Garcia et al., 1983). It was the first pneumococcal CWH to be purified and biochemically characterized as a CWA, which was further demonstrated to require choline for full enzymatic activity (Garcia et al., 1983). No structural information is as yet available for this CWA family.

Cell Wall Glycosidases (CWG, EC 3.2.1)

Glycosidases catalyse the hydrolysis of the glycosidic linkage (O-, N-, and S-linked), leading to the formation of a glucide hemiacetal or hemiketal (Holtje, 1995; Vollmer et al., 2008b). Glycosidases can also be called glycoside or glycosyl hydrolases. Over the years, the number of families of glycosidases has grown steadily and currently there are 135 families according to the CAZyme (Carbohydrate Active Enzymes) database (CAZy; <http://www.cazy.org>). CW glycosidases (CWGs), also called PG glycosidases (PGGs), can be broadly differentiated

TABLE 2 | Conserved catalytic domains responsible for cell wall glycosidase (CWG) activity in bacterial cell wall hydrolases (CWHs).

Catalytic domain ^a	Abbreviation	InterPro	Other databases ^b	Structure ^c	Additional catalytic domain ^{d,e}	Cell wall binding domain ^e	Bacteria ^f
Cell wall glycosidase	CWG						
N-acetylglucosaminidase							
Glycoside hydrolase family 3	GHF-3	IPR002772 IPR001764	PF01915 SSF52279 G3DSA:3.40.50.1700 PF00933 PR00133 G3DSA:3.20.20.300	3NVD, 3BMX, 4GYJ, 4GYK, 20XN, 1TR8, 3LK6, 3TEV, 4GVG, 4GVI, 4GVF, 4GVH, 3NVD	PM15	SLH, CWBD1, LPXTG	Actinobacteria (<i>Streptomyces</i> , <i>Bifidobacterium</i> , <i>Microbacterium</i> , <i>Cellulomonas</i>), Bacteroidetes (<i>Flavobacterium</i> , <i>Prevotella</i> , <i>Bacteroides</i> , <i>Chryseobacterium</i> , <i>Mucilaginibacter</i>), Firmicutes (<i>Clostridium</i> , <i>Paenibacillus</i> , <i>Bacillus</i> , <i>Enterococcus</i> , <i>Butyrivibrio</i> , <i>Lactobacillus</i>), Proteobacteria (<i>Sphingomonas</i> , <i>Pseudomonas</i> , <i>Sphingobium</i>)
Glycoside hydrolase family 73	GHF-73	IPR002901	PF01832 SM00047	2Q2W, 4KVK, 4KNL, 3LAT, 4EPC, 3F7, 5JQC, 2ZYC, 3WVO, 3K3T	NALAA-2 NALAA-3 NALAA-5 GHF-24 GHF-25 CHAP Nlp/P60 PM23 MITG	LysM, AMIN, SLH, SH3-3, SH3-5, SH3-8, CWB1, CWBD2, PGB1, CHW, LPXTG	Firmicutes (<i>Lactobacillus</i> , <i>Enterococcus</i> , <i>Clostridium</i> , <i>Bacillus</i> , <i>Staphylococcus</i> , <i>Paenibacillus</i> , <i>Streptococcus</i> , <i>Carnobacterium</i>), Proteobacteria (<i>Pseudomonas</i> , <i>Vibrio</i> , <i>Pseudomonas</i> , <i>Shewanella</i> , <i>Burkholderia</i> , <i>Moraxella</i>), Bacteroidetes (<i>Flavobacterium</i> , <i>Chryseobacterium</i> , <i>Capnocytophaga</i> , <i>Parabacteroides</i> , <i>Pedobacter</i> , <i>Sphingobacterium</i> , <i>Mucilaginibacter</i> , <i>Chitinophaga</i> , <i>Levinella</i>), Actinobacteria (<i>Actinomyces</i> , <i>Olsenella</i> , <i>Tessaracoccus</i>), Cyanobacteria (<i>Nostoc</i> , <i>Calothrix</i>)
Lysozymes							
Glycoside hydrolase family 22	GHF-22	IPR001916	PF00062	n.d.	none	PGB1	Proteobacteria (<i>Labilithrix</i>), Actinobacteria (<i>Frankia</i>), Firmicutes (<i>Enterococcus</i>)
Glycoside hydrolase family 24	GHF-24	IPR002196	PF00959	2ANV, 2ANX	NALAA-5 GHF-73 GHF-25 CHAP PM23 PM15	PGB1, SH3-3, CW7, LysM, SLH	Proteobacteria (<i>Burkholderia</i> , <i>Paraburkholderia</i> , <i>Pantoea</i> , <i>Erwinia</i> , <i>Xenorhabdus</i> , <i>Acinetobacter</i> , <i>Sodalis</i> , <i>Pseudomonas</i> , <i>Vibrio</i> , <i>Pseudomonas</i> , <i>Bartonella</i> , <i>Rhizobium</i> , <i>Sphingomonas</i> , <i>Novosphingobium</i> , <i>Erythrobacter</i> , <i>Azospirillum</i> , <i>Paracoccus</i>), Cyanobacteria (<i>Nostoc</i> , <i>Calothrix</i> , <i>Leptolyngbyaceae</i> , <i>Microcoleaceae</i> , <i>Oscillatoriaceae</i>), Bacteroidetes (<i>Chryseobacterium</i> , <i>Prevotella</i> , <i>Sphingobacterium</i> , <i>Chitinophaga</i>), Firmicutes (<i>Clostridium</i> , <i>Paenibacillus</i>), Plantomycetes (<i>Fimbrilglobus</i> , <i>Physcisphaerae</i>), Actinobacteria (<i>Mycobacterium</i> , <i>Corynebacterium</i>), Acidobacteria (<i>Granulicella</i> , <i>Bryocella</i> , <i>Candidatus</i>), Fusobacteria (<i>Fusobacterium</i> , <i>Bryocella</i>)
Glycoside hydrolase family 25	GHF-25	IPR002053	PF01183	2WWD, 2WVW, 2WWD, 5JUP	NALAA-2 GHF-73 GHF-24 CHAP PM15 PM23	LysM, AMIN, SLH, PGB1, SH3-3, SH3-5, SH3-8, CWB1, CWB2, CW7, SPOR, SLAP, CHW	Firmicutes (<i>Lactobacillus</i> , <i>Clostridium</i> , <i>Streptococcus</i> , <i>Enterococcus</i> , <i>Ruminococcus</i> , <i>Butyrivibrio</i> , <i>Eubacterium</i> , <i>Bacillus</i> , <i>Erysipelatoclostridium</i>), Actinobacteria (<i>Streptomyces</i> , <i>Corynebacterium</i> , <i>Rhodococcus</i> , <i>Nocardia</i> , <i>Arthrobacter</i> , <i>Micromonospora</i> , <i>Amycolatopsis</i> , <i>Bifidobacterium</i> , <i>Saccharopolyspora</i>), Proteobacteria (<i>Mesorhizobium</i> , <i>Rhizobium</i> , <i>Sphingomonas</i> , <i>Acinetobacter</i>), Bacteroidetes (<i>Flavobacterium</i> , <i>Chryseobacterium</i> , <i>Prevotella</i> , <i>Bacteroides</i> , <i>Pedobacter</i> , <i>Chitinophaga</i>), Cyanobacteria (<i>Plankthotrix</i> , <i>Nostoc</i>), Chloroflexi (<i>Chloroflex</i> , <i>Anaerolineaceae</i> , <i>Pelotinea</i>)

^aColored highlighting indicate the type of cell wall hydrolase (CWH), namely cell wall amidase (CWA; pink), cell wall glycosidase (CWG; cyan) or cell wall peptidase (CWP; green).

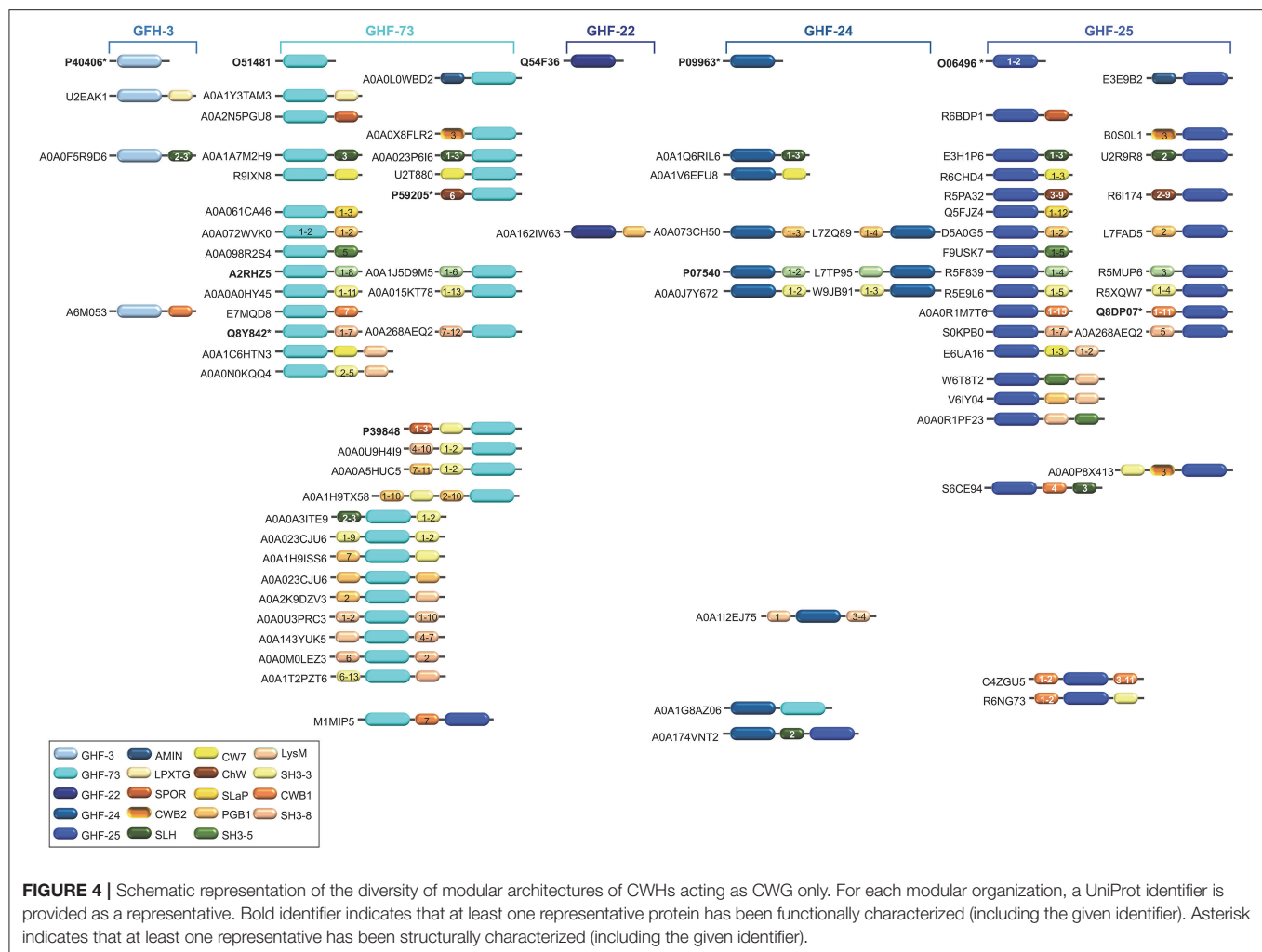
^bDatabases used to construct the InterPro entry, namely Pfam (PF), SMART (SM), Conserved Domain database (CD), Prosite (PS), Superfamily (SF), Protein Information Resource System (PIRSF), TIGRfam (TIGR), HAMAP (MF), CATH-Gene3D (G3DSA).

^cIdentifier from the Protein DataBank (PDB). n.d.: structure not determined.

^dAdditional catalytic domains that can be associated with the catalytic domain under consideration in a given monopeptide along the modular architecture of the protein. Catalytic domains corresponding to CWA are shaded in pink, to CWG in blue, and to CWP in green. Unshaded catalytic domains correspond to non-hydrolytic enzymes, namely N-acetylmuramidases (lytic transglycosylases), namely the TG (transglycosylase; IPR010618), RipA (rare lipoprotein A; IPR034718), MITG (membrane-bound lytic transglycosylase of type G; IPR003770), SleB (Spore cortex-lytic enzyme of Bacillus; IPR011105), SLT1 (soluble lytic murein transglycosylase of type 1; IPR008258) or SLT2 (IPR031304) domains.

^eAdditional cell wall binding domains that can be found along the modular architecture of a monopeptide. LysM: lysin motif (IPR018392), PGB1: peptidoglycan binding domain of type 1 (IPR002477), PGB2 (IPR014927), PGB3 (IPR018537), PGB4 (IPR020209), SLH: S-layer homology domain (IPR001119), LysM: lysin motif (IPR018392), SPOR: sporulation-related (IPR007730), CWB1: cell wall binding repeat of type 1 (IPR018337), CWB2 (IPR007253), CHW: clostridial hydrophobic repeat with a conserved W residue (IPR006637), CW7: cell wall binding domain of Cwp-7 (IPR013168), SLAP: S-layer protein (IPR024968), AMIN: N-terminal nonamidine (IPR021731), SH3-1: sarcosine [src] homology 3 of type 1 (PF00018), SH3-2 (PF07653), SH3-3 (PF08239), SH3-4 (PF06347), SH3-5 (PF08460), SH3-6 (PF12913), SH3-7 (PF12914), SH3-8 (PF13457) and SH3-9 (PF14604).

^fMain phyla of the kingdom Bacteria and examples of some of the main bacterial genera (in brackets and in italics) with bacterial genomes encoding protein harboring the CWA catalytic domain as recorded in InterPro and Pfam databases.



into (i) N-acetylglucosaminidases, and (ii) lysozymes (Table 2 and Figure 4).

N-acetylglucosaminidases

N-acetylglucosaminidases hydrolyse the glycosidic bond in different oligosaccharide substrates including the CW, chitin and N-glycans by cleaving specifically between N-acetyl- β -D-glucosamine residues and contiguous monosaccharides (Karamanos, 1997). To date, two domains have been reported as involved in N-acetylglucosaminidase activity, the (i) glycosyl hydrolase family 3 (GHF-3; IPR001764), and (ii) glycosyl hydrolase family 73 (GHF-73; IPR001764) (Table 2).

Glycosyl hydrolase family 3 (GHF-3)

The GHF-3 domain is about 300 amino acids long (IPR001764) with a conserved Asp-His dyad is involved in CW lysis (Litzinger et al., 2010). NagZ (N-acetylglucosaminidase Z) from *E. coli* is one of the best characterized GHF-3 CWGs, which cleaves the GlcNAc-(1-4)-1,6-anhydro-MurNAc disaccharide (Cheng et al., 2000; Votsch and Templin, 2000; Van Heijenoort, 2001). It is active on both monomer and dimer mucopeptides and is specific for the β linkage. In *B. subtilis*, the NagZ ortholog requires CWA

AmiE to release MurNAc efficiently by sequential hydrolysis of mucopeptides (Litzinger et al., 2010). NagZ from *Vibrio cholerae* was the first GHF-3 enzyme to be solved at structural level (Stubbs et al., 2007). As in many glycosyl hydrolases, it features a $(\beta/\alpha)_8$ barrel fold, known as a TIM barrel, with a large cavity containing the active catalytic site formed of an Asp-Glu dyad. However, structural investigation with NagZ from *B. subtilis* revealed a unique Asp-His catalytic mechanism (Litzinger et al., 2010). Interestingly, this enzyme contains an additional GHF-3 C-terminal domain (IPR002772) but the catalysis appears to rely only on N-terminal TIM-barrel domain (Varghese et al., 1999). Besides, the loop, where the catalytic His is located, undergoes significant structural changes during the binding of the substrate and catalysis (Bacik et al., 2012).

Glycosyl hydrolase family 73 (GHF-73)

The GHF-73 domain is around 80 amino acids long (IPR002901) where the active catalytic site is formed by a tetrad of Tyr-Ala-Thr-Asp amino acid residues together with a highly conserved glutamic acid residue (Huard et al., 2004; Inagaki et al., 2009). The first structure of a GHF-73 enzyme was obtained from Auto (autolysin) from *Listeria monocytogenes* (Bublitz et al., 2009). It

revealed the mechanism of autoinhibition via the occlusion of the substrate binding cleft by an N-terminal α -helix. As confirmed in the other solved structures for this glycosyl hydrolase family (Hashimoto et al., 2009; Maruyama et al., 2010), Glu appears as the catalytic residue in the active site of LytB in *S. pneumoniae* (Bai et al., 2014).

Lysozymes

Lysozymes (also sometimes referred as N-acetylmuramidases) and lytic transglycosylases (LTGs) cleave the same β 1,4-glycosidic bond but in two different ways. While its hydrolysis by lysozymes result in a product with a terminal reducing MurNAc residue without a ring, LTGs are not hydrolases but cleave the bond between MurNAc and GlcNAc with the concomitant formation of a 1,6-anhydro ring at the MurNAc residue (Herlihey and Clarke, 2017). Lysozymes are generally categorized into at least five different classes, i.e., C (chicken type), G (goose type), P (Bacteriophage lambda), F (fungi), and B (bacteria) (Jolles, 1996; Pei and Grishin, 2005; Vollmer et al., 2008b; Callewaert and Michiels, 2010; Callewaert et al., 2012). In bacteria, lysozymes remain poorly characterized but three conserved domains are currently recognized, i.e., the (i) glycosyl hydrolase family 22 (GHF-22; IPR001916), (ii) glycosyl hydrolase family 24 (GHF-24; IPR002190) and (iii) glycosyl hydrolase family 25 (GHF-25; IPR002053) (Table 2).

Glycoside hydrolase family 22 (GHF-22)

The GHF-22 domain is about 120 amino acids long (IPR001916) and corresponds to lysozymes of type C almost uniquely found in species of the superkingdom Eukaryota (Mckenzie, 1996; Callewaert and Michiels, 2010). However, homologous sequences were recently identified in some bacterial species (Yamamoto et al., 2014; D'angelo et al., 2016) (Table 2).

Glycoside hydrolase family 24 (GHF-24)

The GHF-24 domain is approximately 110 amino acids long (IPR002190) and corresponds to phage lysozymes (type P), which structure has been solved only for the bacteriophage P22 lysozyme (Mooers and Matthews, 2006). Together with GHF-22, the function and activity of GHF-24 enzymes still await to be investigated in bacteria.

Glycoside hydrolase family 25 (GHF-25)

The GHF-25 domain is about 180 amino acid long (IPR002053) and corresponds to the lysozymes of type B such as Cpl-1, produced by the phage Cp-1, which specifically lyses several serotypes of *S. pneumoniae* (Perez-Dorado et al., 2007; Doehn et al., 2013). LytC from *S. pneumoniae* was the first GHF-25 enzyme whose structure has been solved (Perez-Dorado et al., 2010). Conformational changes appear to play a key role in PG hydrolysis, especially in the control of the enzymatic activity. In SleM from *Clostridium perfringens*, dimerisation was demonstrated to be of great importance for the enzymatic activity, most certainly by facilitating the positioning of substrate respective to the catalytic site (Al-Riyami et al., 2016).

Cell Wall Peptidases (CWPs, EC 3.4)

A CW peptidase (CWP) cleaves the amide bonds between amino acids in PG (Holtje, 1995). CWPs, also called PG peptidases (PGPs), can be discriminated between endopeptidases or carboxypeptidases depending on their substrate specificity, as they respectively cleave within the PG peptide or remove the C-terminal amino acids. While D,L- and L,D-peptidases cleave between L- and D-amino acids, D,D-peptidases cleave between two D-amino acids (Smith et al., 2000). To date, 10 different types of domains have been reported for CWPs, the (i) cysteine histidine-dependent amidohydrolases/peptidases (CHAP; IPR007921), (ii) new lipoprotein C/protein of 60-kDa (NlpC/P60; IPR000064), (iii) peptidase M14 (PM14; IPR005073), (iv) peptidase M15 (PM15; IPR000755), (v) peptidase M23 (PM23; IPR016047), (vi) peptidase M74 (PM74; IPR005073), (vii) peptidase S11 (PS11; IPR001967), (viii) peptidase S13 (PS13; IPR000667), (ix) transpeptidase (TP, IPR005490), and (x) peptidase S66 (PS66; IPR003507) (Table 3 and Figure 5).

Cysteine Histidine-Dependent Amidohydrolases/Peptidases (CHAP)

The CHAP domain is around 120 amino acids long (IPR007921) with the unique feature to be potentially involved in two different CW cleavage activities (Bateman and Rawlings, 2003; Rigden et al., 2003). As a peptidase, it cleaves between D-alanine and the first glycine of the pentaglycine cross-bridge, but it can also act as an amidase by cleaving the chemical bond between MurNAc and L-alanine at the N-terminal of the stem peptide (Bateman and Rawlings, 2003; Rigden et al., 2003). Depending on the CHAP-proteins, some have been described as having only a peptidase activity (e.g., LysK), only amidase activity (e.g., Skl), or both (e.g., LytN) (Llull et al., 2006; Becker et al., 2009; Frankel and Schneewind, 2012). In phage proteins, the CHAP domain is mostly positioned in the N-terminal region, whereas in bacterial proteins it is systematically positioned at the C-terminal (Zou and Hou, 2010). The bacteriophage LysK was active on purified PG of a number of pathogenic strains including a wide range of staphylococci (O'flaherty et al., 2005; Becker et al., 2009). Resolution of the CHAP structure revealed a calcium-binding site, where calcium ion appeared to play a key role in the switch from active to inactive states (Gu et al., 2014; Sanz-Gaitero et al., 2014; Keary et al., 2016; Broendum et al., 2018). In CHAP SSP0609 from *S. saprophyticus*, a highly-conserved Cys-His-Glu-Asn tetrad relaying the active site was further evidenced (Rossi et al., 2009). While a set of hydrophobic residues forming a large cavity that would confer specificity to the binding site was lacking in the immediate vicinity of the active site, two Tyr aromatic residues likely play a role in substrate anchoring.

New Lipoprotein C/Protein of 60-kDa (NlpC/P60)

The NlpC/P60 domain is about 100 amino acids long (IPR000064) and proteins of this superfamily are ubiquitous papain-like cysteine peptidases involved in the catalysis of the N-acetylmuramate-L-alanine or D- γ -glutamyl-mesodiaminopimelate linkages (Anantharaman and Aravind, 2003). Four major families have been identified, namely (i) the P60-like family, (ii) the Acmb/LytN-like family, (iii) the YaeF/Poxvirus

TABLE 3 | Conserved catalytic domains responsible for cell wall peptidase (CWP) activity in bacterial cell wall hydrolases (CWHs).

Catalytic domain ^a	Abbreviation	InterPro	Other databases ^b	Structure ^c	Additional catalytic domain ^{a,d}	Cell wall binding domain ^e	Bacteria ^f
Cell wall peptidase	CWP						
Cysteine histidine-dependent amidohydrolases/peptidase	CHAP	IPR007921	PF05257 PS50911	2K3A, 4CSH, 4QT3, 4OLK	NALAA-2 NALAA-3 NALAA-5 GHF-73 GHF-24 NlpC/P60 PM23 SieB SLT1 SLT2	LysM, PGB1, SH3-3, SH3-5, SH3-8, SLH, CWB1, SLAP, CWB2	Firmicutes (Clostridium, Staphylococcus, Streptococcus, Enterococcus, Lactococcus, Lactobacillus, Paenibacillus, Ruminococcus), Actinobacteria (Bifidobacterium, Streptomyces, Nonomuraea, Arthrobacter, Mycobacterium, Rhodococcus, Actinomadura, Nocardioides), Proteobacteria (Sphingomonas, Sphingobium, Sphingopyxis, Nonosporobium, Bradyrhizobium, Rhizobium, Acetobacter, Brevindimonas, Burkholderia, Klebsiella, Psychrobacter, Moraxella), Bacteroidetes (Sphingobacterium, Flavobacterium, Mucilaginibacter), Chloroflexi (Ktedonobacter), Cyanobacteria (Scytonema)
New lipoprotein C/protein of 60-kDa	NlpC/P60	IPR000064	PF00877 G3DSA:3.90.1720.10	2HBW, 3NPF, 3H41, 3M1U, 4FDY, 4HPE	NALAA-2 NALAA-3 GHF-73 CHAP PM15 PM23 SieB SLT1 SLT2 TG	PGB1, PGB2, LysM, SH3-1, SH3-2, SH3-3, SH3-4, SH3-5, SH3-6, SH3-7, SH3-8, SLH, SPOR, SLAP, CWB2, CWB1, ChW	Actinobacteria (Streptomyces, Mycobacterium, Corynebacterium, Rhodococcus, Nocardia, Gordonia, Arthrobacter, Micromonospora, Amycolatopsis, Actinomyces, Geodermatophilus, Blastococcus, Pseudonocardia), Firmicutes (Bacillus, Lactobacillus, Paenibacillus, Clostridium, Lachnoclostridium, Eubacterium, Ruminiclostridium, Faecalibacterium, Lysinibacillus), Proteobacteria (Pseudomonas, Helicobacter, Desulfovibrio, Rhizobium, Bacteroides, Burkholderia, Acidovorax, Variovorax, Vibrio, Halomonas, Xenorhabdus, Pantoea), Bacteroidetes (Flavobacterium, Chryseobacterium, Bacteroides, Pedobacter, Sphingobacterium, Mucilaginobacterium), Cyanobacteria (Synechococcus, Nostoc), Spirochaetes (Treponema, Leptospira), Chloroflexi (Chloroflexus, Chloroflexi)
Peptidase M14	PM14	IPR000834	PF00246 PS00132 PR00765 SM00631	5HXD	none	LysM, PGB1, LPXTG, SLH, CWB2, ChW	Proteobacteria (Sphingomonas, Pseudomonas, Shewanella, Vibrio, Pseudomonas, Lysobacter, Brevindimonas), Bacteroidetes (Flavobacterium, Chryseobacterium, Polaribacter, Cellulophaga, Pedobacter, Algoriphagus, Chitinophaga, Spirosoma, Maribacter), Actinobacteria (Streptomyces, Micromonospora, Monomuraea, Nocardioides, Lentzea, Amycolatopsis), Firmicutes (Bacillus, Paenibacillus, Clostridium, Ruminococcus, Halobacillus, Virgibacillus), Ignavibacteriae (Ignavibacterium), Chloroflexi (Anaerolineaceae, Anaerolineae)

(Continued)

TABLE 3 | Continued

Catalytic domain ^a	Abbreviation	InterPro	Other databases ^b	Structure ^c	Additional catalytic domain ^{a,d}	Cell wall binding domain ^e	Bacteria ^f
Peptidase M15	PM15	IPR000755	PF01427 MF01924 PIRSF026671	1R44, 4OXD, 4OX5, 4MUR, 4MUS, 4MUT, 4OAK	NALAA-2 NALAA-3 GHF-3 GHF-25 NlpC/P60 PS11 TP SieB	PGB3, SH3-3, SH3-4	Proteobacteria (<i>Legionella</i> , <i>Pseudomonas</i> , <i>Halomonas</i> , <i>Burkholderia</i> , <i>Bradyrhizobium</i> , <i>Desulfovibrio</i> , <i>Calobacter</i>), Actinobacteria (<i>Streptomyces</i> , <i>Mycobacterium</i> , <i>Micronospora</i> , <i>Amycolatopsis</i> , <i>Nonomuraea</i> , <i>Nocardoides</i>), Bacteroidetes (<i>Flavobacterium</i> , <i>Prevotella</i> , <i>Bacteroides</i> , <i>Pedobacter</i> , <i>Chitinophaga</i> , <i>Hymenobacter</i>), Cyanobacteria (<i>Synechococcus</i> , <i>Calothrix</i> , <i>Nostoc</i> , <i>Planktothrix</i>)
Peptidase M23	PM23	IPR016047	PF01551	1QWY, 4ZYB	NALAA-2 NALAA-3 NALAA-5 GHF-24 GHF-73 NlpC/P60 TP SieB SLT1 SLT2 TG	LysM, AMIN, SH3-3, SH3-4, SH3-9, CWB1, CWB2, SLH, SPOR, CW7, PGB1	Proteobacteria (<i>Pseudomonas</i> , <i>Helicobacter</i> , <i>Desulfovibrio</i> , <i>Sphingomonas</i> , <i>Novosphingobium</i> , <i>Rhizobium</i> , <i>Vibrio</i> , <i>Pseudalteromonas</i> , <i>Burkholderia</i> , Actinobacteria (<i>Streptomyces</i> , <i>Mycobacterium</i> , <i>Arthrobacter</i> , <i>Micronospora</i> , <i>Corynebacterium</i>), Firmicutes (<i>Bacillus</i> , <i>Clostridium</i> , <i>Paenibacillus</i> , <i>Eubacterium</i> , <i>Ruminococcus</i>), Bacteroidetes (<i>Flavobacterium</i> , <i>Bacteroides</i> , <i>Prevotella</i> , <i>Chryseobacterium</i>), Cyanobacteria (<i>Synechococcus</i> , <i>Calothrix</i> , <i>Nostoc</i>), Spirochaetes (<i>Leptospira</i> , <i>Treponema</i>), Chloroflexi (<i>Chloroflexus</i> , <i>Anaerolinea</i>), Deinococcus-Thermus (<i>Melothermus</i> , <i>Deinococcus</i>)
Peptidase M74	PM74	IPR005073	PF03411 MF01623, PIRSF018455	1U10, 1TPZP	RipA NALAA-2 NALAA-3 SLT1	LysM, PGB1	Proteobacteria (<i>Bradyrhizobium</i> , <i>Ochrobactrum</i> , <i>Brucella</i> , <i>Methylobacterium</i> , <i>Mesorhizobium</i> , <i>Rhizobium</i> , <i>Paracoccus</i> , <i>Rhodobacter</i> , <i>Roseovarius</i> , <i>Sulfitobacter</i> , <i>Escherichia</i> , <i>Klebsiella</i> , <i>Salmonella</i> , <i>Pantoea</i> , <i>Serratia</i> , <i>Sorangium</i> , <i>Bdellovibrio</i>), Actinobacteria (<i>Streptomyces</i>), Bacteroidetes (<i>Fluviicola</i>)
Peptidase S11	PS11	IPR001967	PF00768	1SKF, 1ES4, 1ES5, 1ES2, 3A3J, 1TVF, 3IT9	PM15 TP PS13 SLT1	SPOR, CWB1, LysM, SLH, SH3-3	Proteobacteria (<i>Pseudomonas</i> , <i>Acinetobacter</i> , <i>Vibrio</i> , <i>Rhizobium</i> , <i>Mesorhizobium</i> , <i>Sphingomonas</i> , <i>Bordetella</i> , <i>Burkholderia</i> , <i>Marinobacter</i> , <i>Bradyrhizobium</i> , <i>Devosia</i> , <i>Acetobacter</i>), Firmicutes (<i>Clostridium</i> , <i>Bacillus</i> , <i>Eubacterium</i> , <i>Lachnospirillum</i> , <i>Ruminococcus</i> , <i>Paenibacillus</i> , <i>Lactobacillus</i> , <i>Streptococcus</i> , <i>Ruminiclostridium</i>), Actinobacteria (<i>Mycobacterium</i> , <i>Mycobacterium</i> , <i>Microbacterium</i> , <i>Micromonospora</i> , <i>Amycolatopsis</i> , <i>Streptomyces</i> , <i>Olsenella</i>), Chloroflexi (<i>Kleidonobacter</i>), Fusobacteria (<i>Fusobacterium</i> , <i>Leptotrichia</i>), Verrucomicrobia (<i>Akkermansia</i> , <i>Roseibacillus</i>)

(Continued)

TABLE 3 | Continued

Catalytic domain ^a	Abbreviation	InterPro	Other databases ^b	Structure ^c	Additional catalytic domain ^{a,d}	Cell wall binding domain ^e	Bacteria ^f
Peptidase S13	PS13	IPR000667	PF02113 TIGR00666 PR00922	3A3D, 2EX2,	PS11	SPOR, LysM, SLH	Proteobacteria (<i>Pseudomonas</i> , <i>Vibrio</i> , <i>Haemomonas</i> , <i>Marinobacter</i> , <i>Legionella</i> , <i>Sphingomonas</i> , <i>Paraburkholderia</i> , <i>Caballeronia</i> , <i>Acidovorax</i> , <i>Bordetella</i>), Actinobacteria (<i>Streptomyces</i> , <i>Mycobacterium</i> , <i>Arthrobacter</i> , <i>Corynebacterium</i> , <i>Micromonospora</i> , <i>Nocardoides</i> , <i>Bifidobacterium</i> , <i>Actinomyces</i> , <i>Rhodococcus</i>), <i>Bacteroidetes</i> (<i>Prevotella</i> , <i>Chryseobacterium</i> , <i>Pedobacter</i> , <i>Bacteroides</i> , <i>Sphingobacterium</i> , <i>Mucilaginibacter</i> , <i>Chitinophaga</i>), Cyanobacteria (<i>Synechococcus</i> , <i>Cyanothece</i> , <i>Calothrix</i> , <i>Nostoc</i> , <i>Leptolyngbya</i>), Firmicutes (<i>Bacillus</i> , <i>Virgibacillus</i> , <i>Lysinibacillus</i>), Acidobacteria (<i>Chloracidobacterium</i> , <i>Granulicella</i>), Ignavibacteriae (<i>Meliobacter</i>), Planctomycetes (<i>Singulisphaera</i> , <i>Gemmata</i>)
Peptidase S66	PS66	IPR003507	PF02016 PIRSF028757	n.d.	none	none	Proteobacteria (<i>Burkholderia</i> , <i>Paraburkholderia</i> , <i>Limnhabitans</i> , <i>Achromobacter</i> , <i>Acidovorax</i> , <i>Pseudomonas</i> , <i>Escherichia</i> , <i>Klebsiella</i> , <i>Salmonella</i> , <i>Desulfohalobium</i>), Firmicutes (<i>Clostridium</i> , <i>Eubacterium</i> , <i>Veillonella</i> , <i>Megasphaera</i> , <i>Megamonas</i>), Actinobacteria (<i>Streptomyces</i> , <i>Nonomuraea</i> , <i>Microbacterium</i> , <i>Micromonospora</i>)
Transpeptidase	TP	IPR005490	PF03734	4XZZ, 4Y4V, 3VYP, 5D7H, 5DU7, 4GSQ, 5DVP, 5DUJ	PM15 PM23 PS11 SLT1 TG	PGB1, PGB4, LysM, SLH, SH3-3, SH3-4, SH3-8, SPOR, CWP1, ChW, CWP2	Proteobacteria (<i>Pseudomonas</i> , <i>Rhizobium</i> , <i>Mesorhizobium</i> , <i>Bradyrhizobium</i> , <i>Methylobacterium</i> , <i>Sphingomonas</i> , <i>Loktanella</i> , <i>Paracoccus</i> , <i>Roseovarius</i> , <i>Geobacter</i>), Actinobacteria (<i>Streptomyces</i> , <i>Mycobacterium</i> , <i>Micromonospora</i> , <i>Corynebacterium</i> , <i>Rhodococcus</i> , <i>Pseudonocardia</i>), Firmicutes (<i>Clostridium</i> , <i>Lactobacillus</i> , <i>Bacillus</i> , <i>Paenibacillus</i> , <i>Lachnospirillum</i> , <i>Propionispora</i>), Bacteroidetes (<i>Bacteroides</i> , <i>Flavobacterium</i> , <i>Pedobacter</i> , <i>Hymenobacter</i> , <i>Chitinophaga</i>), <i>Prevotella</i> , <i>Parabacteroides</i> , <i>Porphyromonas</i> , <i>Odoribacter</i> , <i>Dysgonomonas</i>), Cyanobacteria (<i>Synechococcus</i> , <i>Nostoc</i>), Verrucomicrobia (<i>Akkermansia</i> , <i>Roseibacillus</i>), Chloroflexi (<i>Anaerolinea</i> , <i>Chloroflexus</i> , <i>Ktedonobacter</i>)

^aColored highlighting indicate the type of cell wall hydrolase (CWH), namely cell wall amidase (CWA; pink), cell wall glycosidase (CWG; cyan) or cell wall peptidase (CWP; green).
^bDatabases used to construct the InterPro entry, namely Pfam (PF), SMART (SM), Conserved Domain database (CD), Prosite (PS), Superfamily (SF), Protein Information Resource System (PIRSF), TIGRfam (TIGR), HAMAP (MF), CATH-Gene3D (G3DSA).
^cIdentifier from the Protein DataBank (PDB). n.d.: structure not determined.
^dAdditional catalytic domains that can be associated with the catalytic domain under consideration in a given monopolypeptide. LysM: lysin motif (IPR018392), PGB1: peptidoglycan binding domain of type 1 (IPR002477), PGB2 (IPR014927), PGB3 (IPR018537), PGB4 (IPR020209), SLH: S-layer homology domain (IPR001119), LysM: lysin motif (IPR018392), SPOR: sporulation-related (IPR007730), CWP1: cell wall binding repeat of type 1 (IPR018337), CWP2 (IPR007253), ChW: clostridial hydrophobic repeat with a conserved W residue (IPR006637), CWP7: cell wall binding domain of Cpl-7 (IPR013168), SLAP: S-layer protein (IPR024968), AMIN: N-terminal nonamidase (IPR021731), SH3-1: sarcosine [src] homology 3 of type 1 (IPR00018), SH3-2 (PF07653), SH3-3 (PF08239), SH3-4 (PF06347), SH3-5 (PF08460), SH3-6 (PF12913), SH3-7 (PF12914), SH3-8 (PF13457) and SH3-9 (PF14604).
^fMain phyla of the kingdom Bacteria and examples of some of the main bacterial genera (in brackets and in italics) with bacterial genomes encoding protein harboring the CWA catalytic domain as recorded in InterPro and Pfam databases.

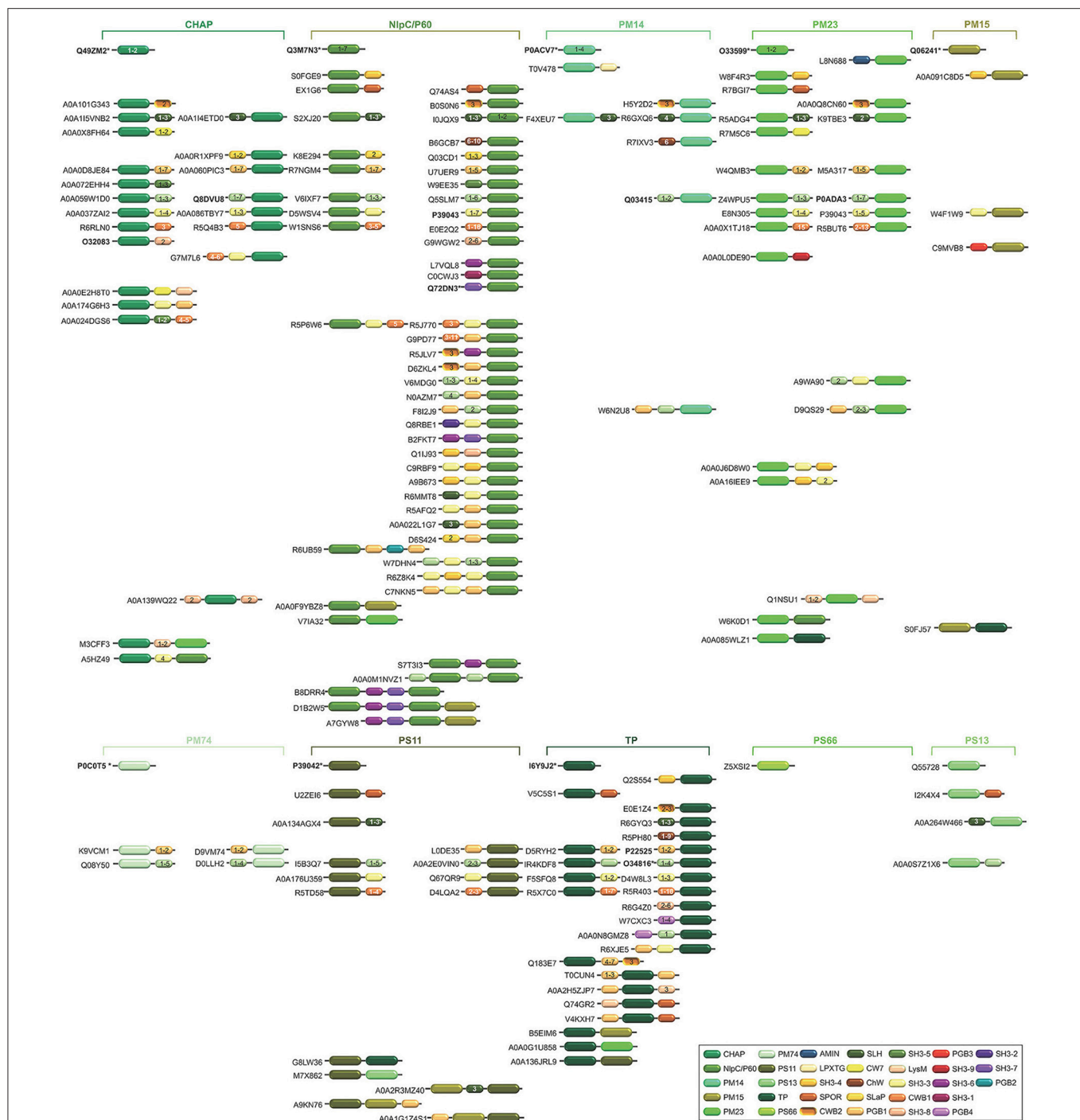


FIGURE 5 | Schematic representation of the diversity of modular architectures of CWHs acting as CWP only. For each modular organization, a UniProt identifier is provided as a representative. Bold identifier indicates that at least one representative protein has been functionally characterized (including the given identifier). Asterisk indicates that at least one representative has been structurally characterized (including the given identifier).

G6R family, and (iv) the lecithin retinol acyltransferase-like (LRAT-like) family (Anantharaman and Aravind, 2003). These two latter enzyme families contain a circularly permuted catalytic domain where the relative positions of the cysteine and histidine/polar residue of the conserved catalytic triad are swapped in the primary sequence (Anantharaman and

Aravind, 2003). In *B. subtilis*, LytF and LytE, which belong to the P60-like family, break the linkage of m-diaminopimelic acid of the PG (Yu et al., 2016). Structure determination of NlpC/P60 domain in CwlT from *Clostridioides difficile*, previously known as *Clostridium difficile* or *Peptoclostridium difficile* (Yutin and Galperin, 2013; Lawson et al., 2016),

revealed a conserved Cys-His-His-Tyr active site specific to tetrapeptide (Xu et al., 2014). Switch between catalysis in the closed state to the substrate entry or product release in the open state is likely regulated by a side chain above the catalytic Cys residue.

Peptidase M15 (PM15)

The PM15 domain is approximately 200 amino acids long (IPR000755) and can be further discriminated into four subfamilies, namely from PM15A to PM15D. In *Enterococcus faecium*, the structure of the D-Ala-D-Ala dipeptidase VanX has been solved and revealed a Zn-dependent catalytic mechanism (Bussiere et al., 1998). In contrast, the D,D-carboxypeptidase VanY is active against pentapeptide but lacks activity against dipeptides (Wright et al., 1992). The D,D-carboxypeptidase VanXYc from *Enterococcus gallinarum*, however, can further hydrolyse pentapeptides (Meziane-Cherif et al., 2014). Following structural and biochemical analyses, the molecular basis of this dual specificity was unraveled and appeared to result from the flexibility of a mobile cap region over the catalytic site, which allows the switch between di- and pentapeptide hydrolysis (Meziane-Cherif et al., 2014). Such a structural element would be lacking from VanY enzymes. While structure comparison revealed similarity in the catalytic sites of VanXY and VanX, differences were pinpointed at the D-Ala-D-Ala binding sites especially for a second cavity present in VanXY but with no equivalent in VanX.

Peptidase M23 (PM23)

The PM23 domain is around 100 amino acids long (IPR016047). Lysostaphin from *Staphylococcus simulans* is one of the best studied PM23. In its active form, lysostaphin cuts the peptide bond between the third and fourth glycine residues of the pentaglycine cross-link in the PG of *Staphylococcus* (Schneewind et al., 1995). The active enzyme shares structural similarity with Ale-1 and LytM (Sabala et al., 2014). In *Staphylococcus capitis*, however, the N-terminal repeats of the lysostaphin homolog Ale-1 are not processed post-translationally (Sugai et al., 1997; Lu et al., 2006). In *S. aureus*, LytM is produced as a latent CWH, where the occluding region and N-terminal domain need to be removed for its activation (Sabala et al., 2012). Following resolution of the enzyme structure (Odintsov et al., 2004), the importance of Zn²⁺ cation in the catalysis was confirmed, whereas the active site appeared to be located at the bottom of an extended, long and narrow groove, partially filled up by a loop, which would constitute the substrate-binding cleft (Firczuk et al., 2005; Grabowska et al., 2015). Beside the preferential glycine-glycine bonds, characterization of several PM23 suggested that they can also be less frequently active against alanine-glutamine bonds (Schindler and Schuhradt, 1964; Horsburgh et al., 2003a).

Peptidase M74 (PM74)

The PM74 domain is about 230 amino acids long (IPR005073). The PM74 D,D-endopeptidase MepA from *E. coli* cleaves the D-alanyl-meso-2,6-diamino-pimelyl amide bond in PG (Keck et al., 1990; Van Heijenoort, 2001). Structural investigations further revealed the enzymatic activity of MepA was Zn dependent and

consequently sensitive to metal chelators (Keck et al., 1990; Van Heijenoort, 2001; Marcyjaniak et al., 2004).

Peptidase S11 (PS11)

The PS11 domain is approximately 235 amino acids long (IPR001967) and is systematically associated with another C-terminal domain (IPR012907), which is organized into a sandwich of two anti-parallel β -sheets. The function of this C-terminal domain is unknown, but it could mediate interaction with other CW synthesizing enzymes (Davies et al., 2001). The PS11 is involved in hydrolysis of the D-Ala-D-Ala bond and is present in several penicillin-binding proteins (PBPs) (Van Heijenoort, 2001; Macheboeuf et al., 2006). Investigation of the enzymatic mechanism stressed the importance of the Lys-Ser-Cys at the catalytic site (Fonze et al., 1999; Rhazi et al., 2003).

Peptidase M14 (PM14)

The PM14 domain is about 270 amino acids long (IPR005073). Together with PS13 and PS66 domains, little experimental work has been dedicated to PM14 domain. In *E. coli*, the PM14 MpaA hydrolyses the γ -D-glutamyl-diaminopimelic acid bond in the murein tripeptide L-alanyl- γ -D-glutamyl-meso-diaminopimelic acid (Uehara and Park, 2003). Structural analysis revealed the entrance and binding of the substrate into the active groove was mediated by a loop with critical Tyr-Asp residues (Ma et al., 2017).

Peptidase S13 (PS13)

The PS13 domain is around 430 amino acids long (IPR000667). The PS13 PBP4 from *E. coli* exhibits both D,D-carboxypeptidase and D,D-endopeptidase activities (Van Heijenoort, 2011).

Peptidase S66 (PS66)

The PS66 domain is about 315 amino acids long (IPR003507). The PS66 LdcA from *E. coli* is a L,D-carboxypeptidase releasing the terminal D-alanine residue from the tetrapeptide L-Ala- γ -D-Glu-meso-A₂pm-D-Ala (Templin et al., 1999).

Transpeptidase (TP)

The TP domain is approximately 120 amino acids long (IPR005490). The L,D-transpeptidase LdtMt2 from *Mycobacterium tuberculosis* harbors a TP domain and has been the subject of intense structural investigations, especially for the study of drugs blocking the enzyme activity through PG cross-linking (Kim et al., 2013; Li et al., 2013; Bianchet et al., 2017; Kumar et al., 2017; Gokulan et al., 2018). In *E. coli*, YbiS, ErfK, YcfS, YcbB, and YnhG also harbor a TP domain but exhibit both L,D-transpeptidase and L,D-carboxypeptidase activities (Magnet et al., 2008; Van Heijenoort, 2011). These five enzymes possess a sole Cys residue essential for activity. While YbiS, ErfK and YcfS enable to cross-link lipoprotein to PG, YcbB and YnhG catalyse the cross-linking of mDAP to form direct meso-diaminopimelate (DAP-DAP, also called linkage of 3-3 type) (Sanders and Pavelka, 2013). Actually, the majority of the cross-linking of the stem peptides involves penicillin-binding proteins (PBPs) with D,D-transpeptidase activity (IPR001460) and corresponds to the 4-3 type, where a D-alanine residue at the fourth position of the peptide stem links at a mDAP at

the third position of an adjacent peptide stem (Glauner et al., 1988; Arbeloa et al., 2004). While Csd6 from *Helicobacter pylori* clearly possesses a TP domain, it would not function as a L,D-transpeptidase at all but as a L,D-carboxypeptidase (Kim et al., 2015). This stresses the need for further investigations to gain insight in the diversity of the TP domain, most certainly into subfamilies and probably a redefinition of this domain family.

The Diversity of the Modular Architecture of Cell Wall Hydrolases

Besides the different catalytic domains involved in PG hydrolysis and reviewed here above, numerous CWHs have CW binding domains (Table 1 and Figures 3–5). In bacteria, several conserved domains have been reported as involved in covalent or non-covalent binding of proteins to CW components (Desvaux et al., 2006, 2018; Tables 1–3). The optimal type and number of anchoring domains required for maximum binding differs from one protein to another (Visweswaran et al., 2014). As a general rule, these domains allow binding of the enzymes to the CW at an adequate concentration and properly position the active site toward the PG substrate site for formation of an efficient enzyme-substrate complex (Steen et al., 2005; Bosma et al., 2006; Shao et al., 2012). Because of close spatial proximity, the released hydrolysed products can be readily and efficiently transported into the cell for recycling (Ozdemir et al., 2012).

LysM (IPR018392), one of the most frequent CW binding domains found in CWHs, is found at the N- or C-terminal of a protein (Buist et al., 2008). The number of domains found in a CWH varies from one to 12, and these domains are generally separated by serine-threonine-asparagine rich intervening sequences (Bateman and Bycroft, 2000; Visweswaran et al., 2014). When present, PGB1 (IPR002477) is usually found in a single copy at the N- or C-terminal; although up to nine repeats can be found in some proteins (Desvaux et al., 2006). The SLH (S-layer homology domain; IPR001119) is generally found at the C-terminal of CWHs. In the NALAA-3 AmiC from *E. coli*, the AMIN (N-terminal nonamidase; IPR021731) domain allows proper localization of the enzyme at the division site through binding to the PG (Rocaboy et al., 2013).

In CWHs, nine different types of SH3 (sarcoma [src] homology 3; IPR003646) domains can be found, from SH3 of type 1 (SH3-1) to SH3-9 (Tables 1–3). The SH3 domains can be found in the N- or C-terminal region of a CWH (Figures 3–6). This domain contains five β -strands forming two orthogonal anti-parallel β -sheets of two and three β -strands each (D'aquino and Ringe, 2003; Desvaux et al., 2006, 2018). In PlyTW (phage Twort endolysin), it has been demonstrated that loss of SH3 domain results in an \sim 10-fold reduction in enzymatic activity (Becker et al., 2015). Deletion analysis of SpAE (staphylococcal phage 2638A endolysin) indicates that the NALAA-2 domain confers most of the lytic activity and requires the full SH3 domain for maximal activity (Abaev et al., 2013). Actually, loops from SH3 domains can dock into the ends of the active site groove of the catalytic site, remodel the substrate binding site and modulate substrate specificity (Xu et al., 2015).

Actually, more than one CW binding domain can be found in some CWHs (Figures 3–6). While it can be hypothesized that such combinations are beneficial for catalysis, much remains to be learned about their effect on PG hydrolysis. Studies have yet to be made of the structure-function relationships and structural constraints regarding the large varieties of combinations between different catalytic domains and/or CW binding domains (Alcorlo et al., 2017; Broendum et al., 2018).

The different catalytic domains reviewed above can be found individually or in combination in various CWHs (Tables 1–3 and Figure 6). CWHs with only one catalytic domain do not necessarily have a CW binding domain but very often CWHs harboring an additional catalytic domain also have a CW binding domain (Visweswaran et al., 2014). Numerous different combinations of CWA, CWG, and CWP domains can be found, although the diversity of associations of CWA or CWG domains with CWP domains or the simultaneous presence of CWA, CWG, and CWP domains in a single CWH is rare (Figure 6).

Most CWAs exhibit only one catalytic domain, either NALAA-2, NALAA-3, or NALAA-5 (Figure 3); no CWA combining two types of amidase catalytic domain has been reported to date (Table 1). However, in some CWHs, these CWA domains can be found in association with either a CWG domain, especially GHF-73, or a peptidase domain, such as PM23 (Albrecht et al., 2012) (Figure 6). As in CwlA from *B. subtilis* (Foster, 1993), NAALA-2 can be found in association with GHF-25. The major CWHs AtlA from *S. aureus* and AtlE from *S. epidermidis* are synthesized as propeptides with a NALAA-2 domain together with a GHF-73 domain (Oshida et al., 1995; Heilmann et al., 1997; Albrecht et al., 2012). The propeptide is cleaved off by an extracellular protease generating two extracellular CWHs, namely a 51 kDa endo- β -N-acetylglucosaminidase and a 62 kDa N-acetylmuramoyl-L-alanine amidase, which are independently involved in the partitioning of daughter cells after cell division (Yamada et al., 1996; Götz et al., 2014). Regarding peptidase domains associated with an amidase domain, SpAE has a N-terminal PM23 domain together with a central NALAA-2 domain (Abaev et al., 2013). Deletion analysis indicates that the NALAA-2 domain confers most of the lytic activity (Abaev et al., 2013). In contrast, in LytA from *S. aureus* where a N-terminal CHAP domain is associated with a central NALAA-2 domain, the lytic activity is prominently conferred by the CHAP domain (Havarstein et al., 2006). By generating a truncation in the homologous CWH LysK (from bacteriophage K in *Lactococcus lactis*), where only the first 165 amino acids are kept, an activity twofold higher than that of the native protein was observed (Rigden et al., 2003; Horgan et al., 2009). The endolysin PlyTW from bacteriophage Twort has a similar architecture to LytA and LysK, and its CHAP domain alone is sufficient and necessary for cell lysis but the NALAA-2 domain alone is insufficient (Becker et al., 2015).

CWG can either display one glycosidase domain alone or in association with a peptidase domain (Figure 6). While only the GHF-25 and GHF-73 glycosidase domains can be found in association with an amidase domain, several peptidase domains can be associated with glycosidase. Among the four CWHs from *L. lactis*, AcmbB (N-acetylmuramidase type B) harbors a central



FIGURE 6 | Schematic representation of the diversity of modular architectures of multifunctional CWHs, i.e., acting as CWA-CWG, CWA-CWP, CWG-CWP, CWA-CWP, or CWH-LTG. For each modular organization, a UniProt identifier is provided as a representative. Bold identifier indicates that at least one representative protein has been functionally characterized (including the given identifier). Asterisk indicates that at least one representative has been structurally characterized (including the given identifier).

GHF-73 domain and a C-terminal CHAP domain (Huard et al., 2003, 2004; Visweswaran et al., 2013). Qualitatively, a truncated version of the enzyme lacking the CHAP domain seems less efficient than the enzyme with the dual catalytic sites for CW hydrolysis (Huard et al., 2003). Considering the low *pI* (5.03) of the mature protein, and that a hydrolytic activity can only be detected at acidic pH in renaturing conditions, this suggests that interaction with the negatively charged CW is favored by a positive or neutral charge of the protein. Unlike CWAs, some CWGs and CWPAs can combine two different types of glycosidase or peptidase catalytic domains, e.g., PS11 and PS13 (Tables 2, 3 and Figure 7). However, the functional characterization and benefit for enzymes with such a modular architecture has not been yet investigated. With regards the wealth of diverse combinations, much remains to be learned about the inhibiting and synergistic effects of the interactions between amidase, glucosidase and peptidase domains in a monopeptidic CWH.

Of interest, some CWHs can also harbor additional catalytic domains involved in CW degradation but unrelated to hydrolases, namely the LTGs (Figure 6). In fact, the molecular reaction mechanism for LTGs does not involve water (Höltje et al., 1975). Based on conserved sequence motifs (Herlihey and Clarke, 2017), LTGs are discriminated between SLT1 (soluble lytic murein transglycosylase of type 1; IPR008258), SLT2 (IPR031304), SleB (Spore cortex-lytic enzyme of *Bacillus*; IPR011105), TG (transglycosylase; IPR010618), MltA (membrane-bound lytic transglycosylase of type A; IPR005300), MltG (previously known as YceG; IPR003770) and RlpA (rare lipoprotein A; IPR034718) domains (Blackburn and Clarke, 2001; Scheurwater et al., 2008; Vollmer et al., 2008b; Li et al., 2012). Of note, LysG (IPR023346; PF13702) constitutes an additional LTG domain but further biochemical characterisations are still required to confirm this (Xu et al., 2014). While MltA catalytic domain could never be found associated with any CWH domain, SLT1 can be found together with some CWA domains, namely NALAA-2 or NALAA-3, and/or some CWP domains, namely CHAP, NlpC/P60, PM23, and TP (Table 1). SLT2, TG and RlpA could only be found in some CWPs. Among CWGs, only MltG could be found in association with GHF-73.

CELL WALL HYDROLASES FROM CELL DIVISION, THROUGH CELL WALL REARRANGEMENT, TO RECYCLING AND CELL LYSIS, UP TO COLLATERAL EFFECTS

CWHs are an essential part of bacterial cell physiology. These ubiquitous enzymes have important roles in cell division and CW rearrangement in creating space within the PG to accommodate supramolecular structures for the secretion and assembly of flagella or pili (Scheurwater et al., 2008). PG recycling is tightly coordinated with its biosynthesis in a carefully controlled manner to prevent the loss of CW integrity, which would lead to cell lysis and bacterial death (Figure 7). Beyond bacterial growth and cell lysis, CWH activity can have side effects on a wide range of physiological functions from bacterial adhesion,

biofilm formation, protein secretion, conjugation, virulence and immune response.

Cell Division and Cell Wall Rearrangement

In the course of bacterial cell growth, PG is biosynthesised through well-known anabolic pathways, including (i) the synthesis of MurNAc pentapeptide precursor (Barreteau et al., 2008; Sobhanifar et al., 2013), (ii) the attachment of the precursor to the membrane anchored lipid carrier completing the formation of the PG precursor lipid II (Bouhss et al., 2008), and (iii) the polymerisation of the PG by PBPs, glycosyltransferases, L,D- and D,D-transpeptidases after translocation of lipid II across the cytoplasmic membrane (Sauvage et al., 2008; Typas et al., 2012). The majority of low molecular weight PBPs acts as D,D-carboxypeptidases that help to control the extent of cross-linking through hydrolysis of the carboxy D-Ala-D-Ala peptide bond of a stem peptide (Scheffers and Pinho, 2005). D,D-carboxypeptidases remove terminal D-Ala residues at position 5 of pentapeptides in the PG and regulate PG synthesis (Egan et al., 2015). For example, a *S. pneumoniae* mutant lacking the D,D-carboxypeptidase PBP3 forms aberrant septa and has a thickened CW, whereas an *E. coli* mutant lacking PBP5 has bent or even branched cell shapes (Nelson and Young, 2001; Vollmer et al., 2008b). PG growth or elongation requires the cleavage of covalent bonds by hydrolases to allow the newly attached material to be inserted in the layer without increasing its thickness (Typas et al., 2012; Vollmer, 2012). In *E. coli*, the three CWPs, Spr, YdhO (belonging to NlpC/P60) and YebA (belonging to PM23), are collectively required for cell growth and PG incorporation (Singh et al., 2012). The depletion of these endopeptidases results in growth arrest and lysis in *E. coli* and prevents further incorporation of new PG (Vollmer, 2012).

In *B. subtilis*, the disruption of two D,L-endopeptidase genes *cwlo* and *lytE* (belonging to NlpC/P60) is lethal (Bisicchia et al., 2007). Inactivation of the LytF CWP harboring a NlpC/P60 domain lead to slightly filamentous cells, whereas the *lytF lytE* double mutant forms extra-long chains (Ohnishi et al., 1999). In *S. aureus*, the Sle1 CWP with a CHAP is required for cell separation (Kajimura et al., 2005). However, it is not yet known how the CWHs required for cell growth are positioned and regulated and how their depletion results in a halt in PG incorporation. In accordance with the “make-before-break” strategy (Koch and Doyle, 1985), a new three-for-one growth mechanism has been proposed (Holtje, 1996, 1998), namely for every three new PG strands inserted in the CW, one old strand is replaced. The existence of multienzyme complexes in *E. coli* was proposed to combine the activities of PG synthases (transpeptidases and transglycosidases) and PG hydrolases (Holtje, 1996, 1998; Scheffers and Pinho, 2005). Affinity chromatography with immobilized lytic enzymes such as MltA, Slt70 or MltB has indeed identified interactions with PG synthases (Vollmer et al., 2008a).

PG cleavage is also required for reductive cell division and cell separation. *E. coli* has 13 periplasmic CWHs that can collectively cleave almost any glycoside, peptide or amide bond (Vollmer et al., 2008b). No single hydrolase gene knockout prevents growth of *E. coli*, probably owing to high redundancy. In fact, multiple

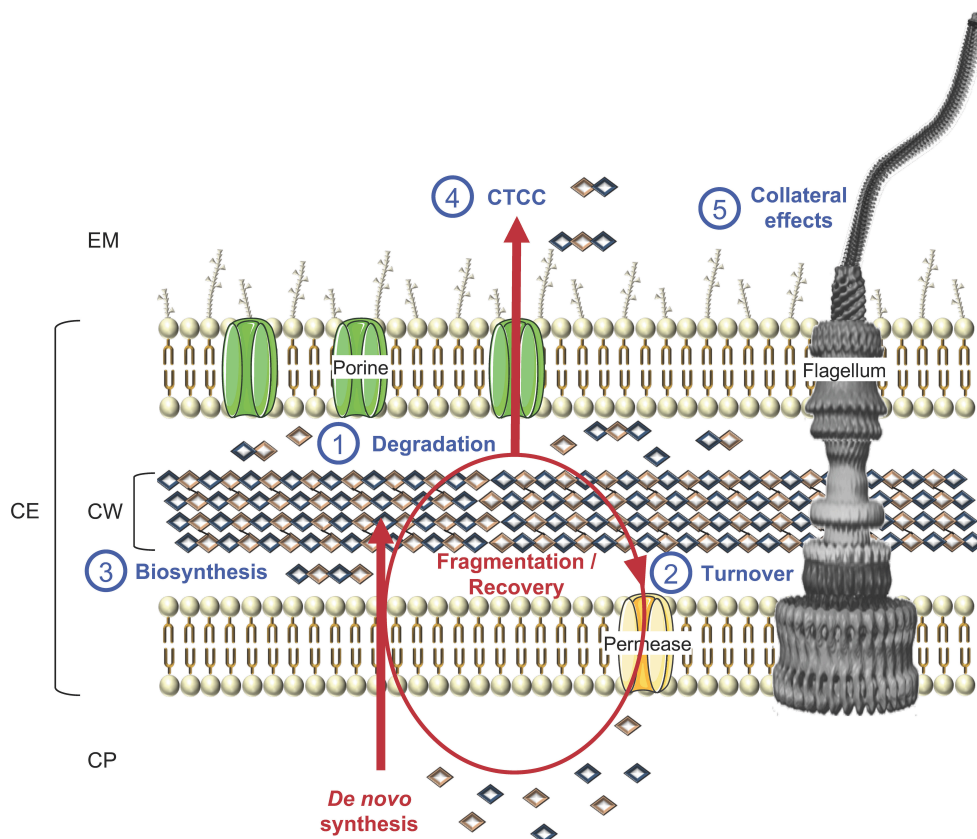


FIGURE 7 | Schematic representation of cell wall biosynthesis and recycling, exemplified in a LPS-diderm bacterial cell. Besides (1) degradation, which can lead to cell lysis, CWHs also participate to cell wall rearrangement and other key physiological functions, namely (2) turnover of cell wall material through their recycling to (3) biosynthesis, as well as (4) cell-to-cell communication (CTCC) since some released peptidoglycan fragments can act as signaling molecules or have (5) side effects on final protein subcellular localization, e.g., flagella, with consequences on motility, bacterial adhesion, biofilm formation, protein secretion, conjugation, virulence and/or immune response. CP, cytoplasm; CE, cell envelope; CW, cell wall; EM, extracellular milieu.

hydrolases genes have to be deleted to form chains of non-separated cells (Vollmer et al., 2008b). CWAs have a prominent role in septum cleavage, in comparison with that of glycosidases and peptidases (Heidrich et al., 2001, 2002; Priyadarshini et al., 2006; Typas et al., 2012). The AmiA, AmiB, and AmiC CWAs play an important role in releasing daughter cells after cell division (Heidrich et al., 2001). AmiC appears to be the principal septum-cleaving enzyme in *E. coli*. Indeed, mutants inactivated in AmiC separate poorly, with about 30% of the population existing as chains of 3–6 unseparated cells, vs. 5–10% of the population in chains of 3–4 cells when only *amiA* is deleted, and no chaining effect upon deletion of *amiB* (Heidrich et al., 2001). In a mutant lacking AmiA, AmiB and AmiC CWAs, more than 90% of the cells exist as unseparated chains from 6 to 24 cells long (Priyadarshini et al., 2006). The cumulative effect of deleting all CWAs and CWP as well as the Slt70 CWG is even more severe (Priyadarshini et al., 2006). The endopeptidases of the M23-LytM family are also implicated in the septation of *E. coli* cells (Typas et al., 2012). *E. coli* has four LytM paralogues, namely EnvC, NlpD, YgeR, and YebA, and their inactivation results in default in cell separation (Typas et al., 2012). In CW-monoderm

bacteria, cleavage of the septum occurs simultaneously with cell division (Vollmer et al., 2008a). Several hydrolases contribute to this step, for example, an *atl* mutant of *S. aureus* and a *lytB* mutant of *S. pneumoniae* form clusters of non-separated cells (Vollmer et al., 2008a). Both hydrolases are localized at the sites of cell division.

In addition, CWs can interact with each other and modulate their catalytic activity. In *E. coli*, the cell division proteins FtsN and FtsEX activate paralogs of LytM endopeptidases, namely EnvC and NlpD respectively, which further activate three amidases involved in the splitting of septum (Uehara et al., 2010; Typas et al., 2012); NlpD activates AmiC and EnvC activates AmiA and AmiB. In *B. subtilis*, FtsEX has also been shown to regulate the activity of CwlO (Dominguez-Cuevas et al., 2013; Meisner et al., 2013). Similarly, in *S. pneumoniae*, FtsEX activates the hydrolase PcsB (Sham et al., 2011). This hydrolase is essentially controlled by the sensor regulator YycFG (Ng et al., 2003). The allosteric activation of *E. coli* amidase AmiB requires structural modification of the active site for substrate binding, and this mechanism seems to be conserved in amidases cleaving the septum (Yang et al., 2012). Similar activation by one or more

protein(s) could also be applied to the *E. coli* D,D-endopeptidases Spr, YdhO, and YebA, which have low *in vitro* activity against PG (Singh et al., 2012). In the case of *B. subtilis*, the expression of the muramidase YocH and of the endopeptidases CwlO, CwlF and LytE is controlled by the YycFG two-component system, which plays a key role in synchronizing CW metabolism and division (Bisicchia et al., 2007). The PG lipid II precursor or the process of its incorporation could be the signal sensed by YycFG (Bisicchia et al., 2007). In LPS-diderm bacteria, CWH activity is controlled by incorporation into multi enzyme complexes that span the periplasm, extending from inner membrane-anchored synthases to the hydrolases, some of which are associated with the outer membrane (Typas et al., 2012). Hydrolases in the complex may be localized at sites of PG synthesis, preventing them from hydrolysing PG elsewhere (Typas et al., 2012). In CW-monoderm bacteria, a direct interaction between PG synthases and hydrolases is generally not possible because they are physically separated; the synthases act in the inner face and the hydrolases on the outer layers (Carballido-Lopez et al., 2006). As already mentioned in *B. subtilis*, though, CwlO is activated by the membrane protein complex FtsEX, it has been suggested that its activity is restricted to the inner part of the PG layers (Dominguez-Cuevas et al., 2013). In this species, PG synthesis is controlled by the actin-like cytoplasmic protein MreBH, which forms filaments at the cytoplasmic membrane and directs the PG synthesis by co-localization of the synthases and the hydrolases (Carballido-Lopez et al., 2006). While colocalisation of synthases and hydrolases was proposed as model for the control of PG synthesis by the MreB cytoskeleton, later work in the field rather suggests that the localization of PG synthases and hydrolases is uncoupled (Dominguez-Cuevas et al., 2013; Meisner et al., 2013).

LTGs are involved in the assembly of large *trans*-envelope structures such as the secretion system of type II (T2SS), T3SS and T4SS, as well as surface organelles, including type 4 pili (T4P) and flagella (Koraimann, 2003; Zahrl et al., 2005; Scheurwater and Burrows, 2011; Herlihey and Clarke, 2017). They are required to enlarge gaps locally in the PG to allow the efficient assembly and anchoring of transport complexes in the cell envelope (Koraimann, 2003). For examples, VirB1 is involved in the assembly of the T4SS (Hoppner et al., 2005), FlgJ in the flagellum (Nambu et al., 1999; Hirano et al., 2001), and EtgA in the T3SS (Garcia-Gomez et al., 2011). While PilT is considered as involved in T2SS assembly, including T4P (Koraimann, 2003), its role remains to be ascertained. In *B. subtilis*, LytC and LytD CWHs have mutually compensatory roles in CW turnover and cell separation as well as motility (Horsburgh et al., 2003b). Besides cellular lysis, the AcmA CWG is involved in cell remodeling in *L. lactis* (Huard et al., 2004; Steen et al., 2005). In *Salmonella* Typhimurium, FlgJ (flagellar protein J) exhibits a GHF-73, whose CWG activity is essential for flagella assembly as it degrades the PG locally to enable the formation of the rod structure in the periplasmic space (Nambu et al., 1999).

Recycling and Cell Lysis

It has been established that a turnover of around 45% of the CW material occurs over one generation in bacteria (Goodell, 1985). In CW-monoderm bacteria, where PG generally accounts

for more than 20% of the cell mass, vs. 2% in LPS-diderm bacteria, this would result in a significant loss of resources (Johnson et al., 2013). By providing the building blocks for CW biosynthesis, recycling is an energy saver mechanism for bacterial growth (Figure 7). Besides, when the bacterial cells are faced with a sudden loss of carbon, recycling of CW material would allow bacterial survival by completing a last round of cell division before growth arrest (Park and Uehara, 2008). While few data are available for CW-monoderm bacteria, *E. coli* has been widely used to investigate the processes of CW recycling (Park and Uehara, 2008). The major pathway involves the uptake of the anhydromuropeptides released in the periplasm from PG hydrolysis by the transporter AmpG specific for GlcNAc-1,6-anhMurNAc and GlcNAc-1,6-anhMurNAc-peptides (Park and Uehara, 2008). These anhydromuropeptides are further degraded in the cytoplasm by the N-acetylglucosaminidase NagZ, the anhMurNAc-Lala amidase AmpD and the L,D-carboxypeptidase LdcA, and then join the PG synthesis pathway (Holtje et al., 1994; Templin et al., 1999; Cheng et al., 2000; Reith and Mayer, 2011; Johnson et al., 2013). While AmpD and AmpG are absent from CW-monoderm bacteria, CWGs of the lysozyme family play a more prominent role than N-acetylglucosaminidase or LTGs (Reith and Mayer, 2011). Rather than anhydromuropeptides, lysozymes release MurNAc-containing muropeptides. In addition, hydrolysis of the stem peptides by amidases and peptidases plays a crucial role in PG degradation in CW-monoderm bacteria (Reith and Mayer, 2011). It has been shown that the CW of *S. aureus* must be pre-digested first with amidase before it becomes a good substrate for the glucosaminidase (Götz et al., 2014). Muropeptide cleavage occurs in the extracellular space of the CW compartment. Uptake of CW amino sugars will occur through the phosphotransferase system PTS permeases (NagP, MurP) and uptake of CW peptides through Mpp/Opp-like ABC transporters (Johnson et al., 2013). In *S. aureus* and *B. subtilis*, respectively, about 5 and 10% of the MurNAc of the CW is recycled per generation (Borisova et al., 2016).

Autolysis can be induced by the inhibition of PG synthesis in growing cells (Vollmer et al., 2008b; Van Heijenoort, 2011). In this case, the autolysis in *E. coli* is not due to any specific induction of hydrolases but rather to an uncoupling between synthesis and degradation owing to an absence of control of the turnover CWHs (Van Heijenoort, 2011). Treatment of growing cells of *E. coli* with penicillin reduces the rate of PG synthesis and increases net lysis; a correlation has been established between induction of autolysis and inhibition of synthesis and degradation of PG by CWHs (Vollmer et al., 2008b). Autolysis of *E. coli* is low for non-growing cells and this can be attributed to PBP7 endopeptidase involvement in D-Ala-D-meso-A2pm cross-linkage, which contributes to structural changes of PG (Van Heijenoort, 2011). The activity of DdpX CWP exhibiting PM15 is considered as potentially lethal and owes to the hydrolysis of the D-Ala-D-Ala bond (Lessard et al., 1998). Overproduction of PBP5 CWP encoded by *dacA* and harboring a PS11 domain appeared to be lethal, causing *E. coli* cells to grow as spherically before lysing (Markiewicz et al., 1982). PBP5 regulates the availability of pentapeptide subunits for the formation of the

cross-linkages by transpeptidation (Broome-Smith et al., 1988; Potluri et al., 2010; Van Heijenoort, 2011).

The myxobacteria, which are predatory bacteria, produce extracellular lytic agents including CWHs such as lysozyme and endo- β -N-acetylglucosaminidase (Bourgerie et al., 1994). Similarly, *Pseudomonas aeruginosa* and other LPS-diderm bacteria deliver NlpC/P60 type endopeptidases via T4SS into the periplasm of adjacent bacterial cells causing their lysis (Chou et al., 2012). The production of bacteriolytic exo-enzymes is also a property of many species of actinomycetes, in particular streptomycetes (Vollmer et al., 2008b). Lysis phenomena have been observed in the sporulation stage of myxobacteria and *Bacillus*, and will result in the release of nutrients (Vollmer et al., 2008b). In *B. subtilis*, the CwlB and CwlC CWAs with a NALAA-3 domain are present in large amounts at the time of mother cell lysis (Smith and Foster, 1995). While single inactivation of *cwlB* or *cwlC* does not affect mother cell lysis, it was found to be blocked upon double gene knock-out (Nugroho et al., 1999). The CwlH CWA with a NALAA-2 domain was shown to be required for mother cell lysis and acts in a compensatory manner with CwlC (Nugroho et al., 1999; Yang et al., 2013). As CwlC, LytC is expressed only late in sporulation but is also involved in mother lysis (Smith and Foster, 1995).

Competent cells of *S. pneumoniae* are able to lyse non-competent cells during co-cultivation, a phenomenon termed allolysis (Guiral et al., 2005). The mechanism involves the two-peptide bacteriocin CibAB and its immunity factor CibC, as well as the LytA, LytC, and CbpD CWHs (Guiral et al., 2005). The bacteriocin activates the hydrolases, which disrupt the CW of the non-competent cells. Regulated bacterial death and lysis have been characterized in studies on the control of the lytic cycle during bacteriophage infection (Rice and Bayles, 2008). The mechanism controlling the bacteriophage-induced lysis involves a holin and a cognate CWH (Desvaux, 2012). In a first mechanism, upon activation of the holin, the membrane becomes leaky and allows the escape of the CWH to the PG and thus its degradation. The second mechanism involves bacteriophages-encoded CWH containing signal arrest release (SAR) domains (Rice and Bayles, 2008). This SAR-type hydrolase is transported in a Sec-dependant manner and anchors in the outer face of the membrane in an inactive form until the holin releases it.

CWHs must be highly regulated to prevent cell lysis. This regulation occurs at both the transcriptional and post-translational levels. In *B. subtilis*, the transcription of the two hydrolases LytT and LytD is regulated by the sigma factor SigD, whereas LytE is regulated by SigA, SigH, and SigI (Serizawa et al., 2004). In *S. aureus*, perturbation of CW synthesis resulted in the modulation of the expression of the major CWH Atl by the two-component regulation system VraSR (vancomycin resistance-associated sensor/regulator) (Kuroda et al., 2003). In *S. aureus*, another two-component system LytSR controls the rate of autolysis by regulating the expression of *lrgAB* encoding an antiholin that interacts with holin to prevent cell lysis (Rice and Bayles, 2008). The interaction between the hydrolases and the CW is crucial for their activity, and their subcellular localization regulated at the post-translational level reflects their targeting mechanisms (Vollmer et al., 2008b).

Furthermore, most of these hydrolases have a binding domain for PG or other CW components that greatly enhances their enzymatic activity. Proteolytic processing of CWHs is common both for their activity and their stability in response to different environments. For example, the hydrolase Atl of *S. aureus* is produced as a proenzyme that undergoes proteolysis resulting in mature cell-surface and extracellular glucosamidase and amidase (Komatsuzawa et al., 1997). In LytC from *S. pneumoniae*, conformational changes in the GHF-25 domain play a key role in the control of the enzymatic activity to avoid self-lysis during bacterial growth and division (Perez-Dorado et al., 2010).

Finally, the activity of the hydrolases is regulated by their environment, such as the presence or not of other CW polymers, as illustrated by the teichoic acids that modify the activity of the amidase in *B. subtilis* or the growth at acidic pH that inhibits lysis (Vollmer et al., 2008b).

Collateral Physiological Effects

As reviewed above, the primary role of CWHs is the degradation of PG. The digestion can occur in a sparing manner for cleavage of the septum during cell division or spore maturation, enlargement of the sacculus, and assembly of supramolecular structures such as secretion systems, pili, or flagella (Vollmer et al., 2008b). The degradation can be more drastic in the case of the cell lysis, whether autolysis, allolysis, or exolysis (that is lysis of non-sibling prey cells). As a result of these CWH activities, several collateral effects of significance to bacterial physiology can further occur (Wyckoff et al., 2012). The expression of CWHs can affect the assembly of the supramolecular structure and indirectly modulate their affiliated function. For flagella, motility can be indirectly mitigated by FlgJ (Nambu et al., 1999), which could subsequently affect chemotaxis or surface colonization. By disturbing the assembly of pili, some CWHs could have side effects on bacterial aggregation, adhesion, biofilm formation, twitching motility or conjugation. For the secretion systems, some CWHs could incidentally modify the transport of proteins localized at the membrane, CW, periplasm, extracellular milieu or even injected into a host cell. Depending on the secreted proteins, a wide range of side effects could occur from substrate transport and cell adhesion to bacterial virulence.

In *L. monocytogenes*, CwhA (cell wall hydrolase A) was originally considered as a virulence factor *per se*, named Iap (invasion-associated protein) or P60 (protein of 60 KDa) at the time. Actually, it appeared to be primarily a CWH inducing septation defect and consequently mislocalisation of key cell-surface virulence factors, namely the internalin InlA and the actin polymerisation factor ActA (Pilgrim et al., 2003; Desvaux and Hebraud, 2006). In addition, reduced secretion of both the CWHs CwhA and MurA via the SecA2 export pathway promotes extensive cell aggregation and sedimentation, as well as cell elongation inducing the formation of low-adherent filamentous biofilm (Machata et al., 2005; Renier et al., 2011, 2014). Regarding sessile development, the CWH activities can alter the global charge of the bacterial cell surface and/or modify the exposure of adhesin, which in turn modifies the bacterial aggregation/adhesion properties and/or

biofilm formation abilities, as shown for AcmA from *L. lactis* (Mercier et al., 2002).

Besides recycling for CW biosynthesis, PG fragments released by the CWH activity could have messenger functions and act as signaling molecules (Boudreau et al., 2012) (**Figure 7**). In *E. coli*, muropeptides were shown to induce β -lactamase at the transcriptional level via the regulator AmpR (Jacobs et al., 1997). PG fragments could also initiate regrowth of dormant cells in the viable but nonculturable state (Keep et al., 2006). In the course of infection, these fragments can have proinflammatory activity and are recognized by PGRPs (peptidoglycan recognition proteins), which activate the immune response, especially the Toll or immune deficiency signal transduction pathways, or induce a proteolytic cascade generating antimicrobial compounds that induce phagocytosis or hydrolysis (Dziarski, 2003; Dziarski and Gupta, 2006; Markiewicz and Popowska, 2011). In *Neisseria gonorrhoeae* for instance, it is known for some times that PG fragments are cytotoxic to human ciliated Fallopian tube cells by causing their death and sloughing (Melly et al., 1984; Dillard, 2014). Besides, PG fragments from the neisserial CW influence the host innate immune response as they recognize and activate the NOD1 and NOD2 receptors (Mavrogiorgos et al., 2014; Knilans et al., 2017).

CONCLUDING REMARKS

While the biochemical composition of the bacterial CW is now well-known, its supramolecular organization and the interaction of the different constituents still require further studies. Biophysical investigations with state-of-the-art approaches have been performed on a handful of model bacteria, namely *B. subtilis*, *S. aureus*, or *S. pneumoniae* for CW-monoderm bacteria but quite restricted to *E. coli* for LPS-diderm bacteria (Vollmer et al., 2008a; Turner et al., 2010; Beaussart et al., 2014). Beyond the simplistic dichotomy of Gram-positive vs. Gram-negative bacteria, there is a need to encompass the full biodiversity of the bacterial kingdom considering the divergent molecular compositions and structural arrangements of the CW. As presented in this review, this can be more effectively embraced by considering the trichotomy of CW-monoderm, LPS-diderm and myco-diderm bacteria.

Rather than the designations of autolysin, endolysin and exolysin, which are confusing, ambiguous and quite often used misleadingly in the scientific literature, this review stresses the relevance of using instead the global term CWH (or PGH) and the more specific designations of CWA, CWG, and CWP, for which conserved motifs and/or three-dimensional structures are clearly established. Besides, the combination of these latter terms, such as CWA-CWG or CWA-CWG-CWP, better reflect the modular organization of the numerous CWHs exhibiting multiple catalytic sites. This comprehensive review of the diversity of conserved domains exhibiting CWH catalytic activity will help scientists in the field to describe the enzymes at hand. While the association of different catalytic properties generally results in synergistic effects, the CW binding motifs that can be found along the monopeptide, generally improve the efficiency of the enzymatic activity (Shoseyov et al., 2006). While some CWHs attracted a lot of interest very early, e.g. the

lysostaphin (Schindler and Schuhardt, 1964), this review also stresses numerous domains that have yet to be fully characterized and that only a handful of investigations have been dedicated to the biochemical, catalytic, molecular, structural and/or physiological characterization of enzymes with multiple catalytic sites and/or CW binding domains (**Figures 3–6**). In other words, the synergistic and processive effects of such combinations of domains have yet to be elucidated. Of note and besides LTG domains, some CWHs can exhibit additional catalytic domains unrelated to CW degradation or CW biosynthesis but this aspect has not been really explored yet. Interestingly, lysozyme activity was recently uncovered in the *Ruminococcus champellensis* cellulosome (Morais et al., 2016) and several dockerin-containing CWHs enable to associate to the cohesion domains of a scaffoldin were further reported (Bensoussan et al., 2017). Beyond the cellulosome dedicated to the degradation of plant materials (Shoham et al., 1999; Desvaux, 2005; Smith et al., 2017), a new concept could emerge, that is an extracellular multi-enzymes complex dedicated to bacterial cell lysis, i.e. the lyticome. Clearly, our knowledge of the full diversity of CWHs is still incomplete and new conserved domains will most likely be uncovered in the years to come. Yet more complex are the regulation and modulation of expression as well as activity of CWHs. These secreted enzymes are not only regulated at the transcriptional level but also at different translational and post-translational levels, including translocational and conformational levels, which are the first regulatory levels. A complete understanding of their interactions with CW components and of enzymatic interplay is most certainly the next frontier for breakthroughs in the field, without counting on the many side effects of these enzymes on the bacterial ecophysiology, a topic of much current interest (Wyckoff et al., 2012).

AUTHOR CONTRIBUTIONS

AV and MD wrote the first overall draft of the manuscript and drew the original pictures. SL, RT, MP, and CP wrote sections of the manuscript. MD, SL, and RT contributed to conceptualize the overarching aims. MD had management as well as coordination responsibility for the execution of the work. MD and CP contributed to the acquisition of the financial supports and resources leading to this publication. All authors contributed to the critical revision of the manuscript, read and approved the submitted version.

ACKNOWLEDGMENTS

This work was supported in part by INRA (Institut National de la Recherche Agronomique), the DéESse project from the Région Auvergne and FEDER (Fonds Européen de Développement Régional), the Polish National Center of Science (n°2013/09/B/NZ6/00710), and the Campus France PHC (Programme Hubert Curien) France-Poland POLONIUM (n°28298ZE). AV was a post-doctoral research fellow supported by a Bourse Innovation Transfert de Technologie. We are very grateful to David Marsh (djmarsh@wanadoo.fr) for correcting the European English of the manuscript.

REFERENCES

- Abaev, I., Foster-Frey, J., Korobova, O., Shishkova, N., Kiseleva, N., Kopylov, P., et al. (2013). Staphylococcal Phage 2638A endolysin is lytic for *Staphylococcus aureus* and harbors an inter-lytic-domain secondary translational start site. *Appl. Microbiol. Biotechnol.* 97, 3449–3456. doi: 10.1007/s00253-012-4252-4
- Albrecht, T., Raue, S., Rosenstein, R., Nieselt, K., and Götz, F. (2012). Phylogeny of the staphylococcal major autolysin and its use in genus and species typing. *J. Bacteriol.* 194, 2630–2636. doi: 10.1128/JB.06609-11
- Alcorlo, M., Martínez-Caballero, S., Molina, R., and Hermoso, J. A. (2017). Carbohydrate recognition and lysis by bacterial peptidoglycan hydrolases. *Curr. Opin. Struct. Biol.* 44, 87–100. doi: 10.1016/j.sbi.2017.01.001
- Alderwick, L. J., Harrison, J., Lloyd, G. S., and Birch, H. L. (2015). The mycobacterial cell wall–peptidoglycan and arabinogalactan. *Cold Spring Harb. Perspect. Med.* 5:a021113. doi: 10.1101/cshperspect.a021113
- Al-Riyami, B., Ustok, F. I., Stott, K., Chirgadze, D. Y., and Christie, G. (2016). The crystal structure of *Clostridium perfringens* SleM, a muramidase involved in cortical hydrolysis during spore germination. *Proteins* 84, 1681–1689. doi: 10.1002/prot.25112
- Amir, A., Babaepour, F., McIntosh, D. B., Nelson, D. R., and Jun, S. (2014). Bending forces plastically deform growing bacterial cell walls. *Proc. Natl. Acad. Sci. USA* 111, 5778–5783. doi: 10.1073/pnas.1317497111
- Anantharaman, V., and Aravind, L. (2003). Evolutionary history, structural features and biochemical diversity of the NlpC/P60 superfamily of enzymes. *Genome Biol.* 4:R11. doi: 10.1186/gb-2003-4-5-p3
- Arbeloa, A., Hugonnet, J. E., Sentilhes, A. C., Josseume, N., Dubost, L., Monsempes, C., et al. (2004). Synthesis of mosaic peptidoglycan cross-bridges by hybrid peptidoglycan assembly pathways in Gram-positive bacteria. *J. Biol. Chem.* 279, 41546–41556. doi: 10.1074/jbc.M407149200
- Atrih, A., Bacher, G., Allmaier, G., Williamson, M. P., and Foster, S. J. (1999). Analysis of peptidoglycan structure from vegetative cells of *Bacillus subtilis* 168 and role of PBP 5 in peptidoglycan maturation. *J. Bacteriol.* 181, 3956–3966.
- Bacik, J. P., Whitworth, G. E., Stubbs, K. A., Vocado, D. J., and Mark, B. L. (2012). Active site plasticity within the glycoside hydrolase NagZ underlies a dynamic mechanism of substrate distortion. *Chem. Biol.* 19, 1471–1482. doi: 10.1016/j.chembiol.2012.09.016
- Bai, X. H., Chen, H. J., Jiang, Y. L., Wen, Z., Huang, Y., Cheng, W., et al. (2014). Structure of pneumococcal peptidoglycan hydrolase LytB reveals insights into the bacterial cell wall remodeling and pathogenesis. *J. Biol. Chem.* 289, 23403–23416. doi: 10.1074/jbc.M114.579714
- Barreteau, H., Kovac, A., Boniface, A., Sova, M., Gobec, S., and Blanot, D. (2008). Cytoplasmic steps of peptidoglycan biosynthesis. *FEMS Microbiol. Rev.* 32, 168–207. doi: 10.1111/j.1574-6976.2008.00104.x
- Bateman, A., and Bycroft, M. (2000). The structure of a LysM domain from *Escherichia coli* membrane-bound lytic murein transglycosylase D (MltD). *J. Mol. Biol.* 299, 1113–1119. doi: 10.1006/jmbi.2000.3778
- Bateman, A., and Rawlings, N. D. (2003). The CHAP domain: a large family of amidases including GSP amidase and peptidoglycan hydrolases. *Trends Biochem. Sci.* 28, 234–237. doi: 10.1016/S0968-0004(03)00061-6
- Beaussart, A., Pechoux, C., Trieu-Cuot, P., Hols, P., Mistou, M. Y., and Dufrene, Y. F. (2014). Molecular mapping of the cell wall polysaccharides of the human pathogen *Streptococcus agalactiae*. *Nanoscale* 6, 14820–14827. doi: 10.1039/C4NR05280C
- Becker, S. C., Dong, S., Baker, J. R., Foster-Frey, J., Pritchard, D. G., and Donovan, D. M. (2009). LysK CHAP endopeptidase domain is required for lysis of live staphylococcal cells. *FEMS Microbiol. Lett.* 294, 52–60. doi: 10.1111/j.1574-6968.2009.01541.x
- Becker, S. C., Swift, S., Korobova, O., Schischkova, N., Kopylov, P., Donovan, D. M., et al. (2015). Lytic activity of the staphylococcal Twort phage endolysin CHAP domain is enhanced by the SH3b cell wall binding domain. *FEMS Microbiol. Lett.* 362, 1–8. doi: 10.1093/femsle/fnu019
- Bensoussan, L., Morais, S., Dassa, B., Friedman, N., Henrissat, B., Lombard, V., et al. (2017). Broad phylogeny and functionality of cellulosomal components in the bovine rumen microbiome. *Environ. Microbiol.* 19, 185–197. doi: 10.1111/1462-2920.13561
- Bianchet, M. A., Pan, Y. H., Basta, L. A. B., Saavedra, H., Lloyd, E. P., Kumar, P., et al. (2017). Structural insight into the inactivation of *Mycobacterium tuberculosis* non-classical transpeptidase LdtMt2 by biapenem and tebipenem. *BMC Biochem.* 18:8. doi: 10.1186/s12858-017-0082-4
- Bisicchia, P., Noone, D., Lioliou, E., Howell, A., Quigley, S., Jensen, T., et al. (2007). The essential YycFG two-component system controls cell wall metabolism in *Bacillus subtilis*. *Mol. Microbiol.* 65, 180–200. doi: 10.1111/j.1365-2958.2007.05782.x
- Blackburn, N. T., and Clarke, A. J. (2001). Identification of four families of peptidoglycan lytic transglycosylases. *J. Mol. Evol.* 52, 78–84. doi: 10.1007/s002390010136
- Boneca, I. G., Huang, Z. H., Gage, D. A., and Tomasz, A. (2000). Characterization of *Staphylococcus aureus* cell wall glycan strands, evidence for a new β -N-acetylglucosaminidase activity. *J. Biol. Chem.* 275, 9910–9918. doi: 10.1074/jbc.275.14.9910
- Borisova, M., Gaupp, R., Duckworth, A., Schneider, A., Dalügge, D., Mühleck, M., et al. (2016). Peptidoglycan recycling in Gram-Positive bacteria is crucial for survival in stationary phase. *mBio* 7:e00923-16. doi: 10.1128/mBio.00923-16
- Bosma, T., Kanninga, R., Neef, J., Audouy, S. A. L., Van Roosmalen, M. L., Steen, A., et al. (2006). Novel surface display system for proteins on non-genetically modified Gram-positive bacteria. *Appl. Environ. Microbiol.* 72, 880–889. doi: 10.1128/AEM.72.1.880-889.2006
- Boudreau, M. A., Fisher, J. F., and Mobashery, S. (2012). Messenger functions of the bacterial cell wall-derived muropeptides. *Biochemistry* 51, 2974–2990. doi: 10.1021/bi300174x
- Bouhss, A., Trunkfield, A. E., Bugg, T. D., and Mengin-Lecreux, D. (2008). The biosynthesis of peptidoglycan lipid-linked intermediates. *FEMS Microbiol. Rev.* 32, 208–233. doi: 10.1111/j.1574-6976.2007.00089.x
- Bourgerie, S., Karamanos, Y., Grard, T., and Julien, R. (1994). Purification and characterization of an endo-N-acetyl- β -D-glucosaminidase from the culture medium of *Stigmatella aurantiaca* DW4. *J. Bacteriol.* 176, 6170–6174. doi: 10.1128/jb.176.20.6170-6174.1994
- Bourhis, L. L., and Werts, C. (2007). Role of Nods in bacterial infection. *Microbes Infect.* 9, 629–636. doi: 10.1016/j.micinf.2007.01.014
- Broendum, S. S., Buckle, A. M., and McGowan, S. (2018). Catalytic diversity and cell wall binding repeats in the phage-encoded endolysins. *Mol. Microbiol.* 110, 879–896. doi: 10.1111/mmi.14134
- Broome-Smith, J. K., Ioannidis, I., Edelman, A., and Spratt, B. G. (1988). Nucleotide sequences of the penicillin-binding protein 5 and 6 genes of *Escherichia coli*. *Nucleic Acids Res.* 16:1617. doi: 10.1093/nar/16.4.1617
- Bublitz, M., Polle, L., Holland, C., Heinz, D. W., Nimtz, M., and Schubert, W. D. (2009). Structural basis for autoinhibition and activation of Auto, a virulence-associated peptidoglycan hydrolase of *Listeria monocytogenes*. *Mol. Microbiol.* 71, 1509–1522. doi: 10.1111/j.1365-2958.2009.06619.x
- Buist, G., Steen, A., Kok, J., and Kuipers, O. P. (2008). LysM, a widely distributed protein motif for binding to (peptido)glycans. *Mol. Microbiol.* 68, 838–847. doi: 10.1111/j.1365-2958.2008.06211.x
- Bussiere, D. E., Pratt, S. D., Katz, L., Severin, J. M., Holzman, T., and Park, C. H. (1998). The structure of VanX reveals a novel amino-dipeptidase involved in mediating transposon-based vancomycin resistance. *Mol. Cell* 2, 75–84. doi: 10.1016/S1097-2765(00)80115-X
- Buttner, F. M., Zoll, S., Nega, M., Gotz, F., and Stehle, T. (2014). Structure-function analysis of *Staphylococcus aureus* amidase reveals the determinants of peptidoglycan recognition and cleavage. *J. Biol. Chem.* 289, 11083–11094. doi: 10.1074/jbc.M114.557306
- Callear, L., and Michiels, C. W. (2010). Lysozymes in the animal kingdom. *J. Biosci.* 35, 127–160. doi: 10.1007/s12038-010-0015-5
- Callear, L., Van Herreweghe, J. M., Vanderkelen, L., Leysen, S., Voet, A., and Michiels, C. W. (2012). Guards of the great wall: bacterial lysozyme inhibitors. *Trends Microbiol.* 20, 501–510. doi: 10.1016/j.tim.2012.06.005
- Carballido-Lopez, R., Formstone, A., Li, Y., Ehrlich, S. D., Noirot, P., and Errington, J. (2006). Actin homolog MreBH governs cell morphogenesis by localization of the cell wall hydrolase LytE. *Dev. Cell* 11, 399–409. doi: 10.1016/j.devcel.2006.07.017
- Carrasco-Lopez, C., Rojas-Altuve, A., Zhang, W., Hesk, D., Lee, M., Barbe, S., et al. (2011). Crystal structures of bacterial peptidoglycan amidase AmpD and an unprecedented activation mechanism. *J. Biol. Chem.* 286, 31714–31722. doi: 10.1074/jbc.M111.264366

- Cheng, Q., Li, H., Merdek, K., and Park, J. T. (2000). Molecular characterization of the β -N-acetylglucosaminidase of *Escherichia coli* and its role in cell wall recycling. *J. Bacteriol.* 182, 4836–4840. doi: 10.1128/JB.182.17.4836-4840.2000
- Chipman, D. M., Grisaro, V., and Sharon, N. (1967). The binding of oligosaccharides containing N-acetylglucosamine and N-acetylmuramic acid to lysozyme. The specificity of binding subsites. *J. Biol. Chem.* 242, 4388–4394.
- Chou, S., Bui, N. K., Russell, A. B., Lexa, K. W., Gardiner, T. E., Leroux, M., et al. (2012). Structure of a peptidoglycan amidase effector targeted to Gram-negative bacteria by the Type VI secretion system. *Cell Rep.* 1, 656–664. doi: 10.1016/j.celrep.2012.05.016
- D'angelo, T., Oshone, R., Abebe-Akele, F., Simpson, S., Morris, K., Thomas, W. K., et al. (2016). Permanent draft genome sequence for Frankia sp. strain EI5c, a single-spore isolate of a nitrogen-fixing Actinobacterium, isolated from the root nodules of *Elaeagnus angustifolia*. *Genome Announc.* 4:e00660-16. doi: 10.1128/genomeA.00660-16
- D'aquino, J. A., and Ringe, D. (2003). Determinants of the Src Homology Domain 3-Like Fold. *J. Bacteriol.* 185, 4081–4086. doi: 10.1128/JB.185.14.4081-4086.2003
- Davies, C., White, S. W., and Nicholas, R. A. (2001). Crystal structure of a deacylation-defective mutant of penicillin-binding protein 5 at 2.3-Å resolution. *J. Biol. Chem.* 276, 616–623. doi: 10.1074/jbc.M004471200
- Desvaux, M. (2005). The cellulosome of *Clostridium cellulolyticum*. *Enz Microbiol Technol* 37, 373–385. doi: 10.1016/j.enzmictec.2004.04.025
- Desvaux, M. (2012). Contribution of holins to protein trafficking: secretion, leakage or lysis? *Trends Microbiol.* 20, 259–261. doi: 10.1016/j.tim.2012.03.008
- Desvaux, M., Candela, T., and Serró, P. (2018). Surfaceome and proteosurfaceome in parietal monoderm bacteria: focus on protein cell-surface display. *Front. Microbiol.* 9:100. doi: 10.3389/fmicb.2018.00100
- Desvaux, M., Dumas, E., Chafsey, I., and Hebraud, M. (2006). Protein cell surface display in Gram-positive bacteria: from single protein to macromolecular protein structure. *FEMS Microbiol Lett.* 256, 1–15. doi: 10.1111/j.1574-6968.2006.00122.x
- Desvaux, M., and Hebraud, M. (2006). The protein secretion systems in *Listeria*: inside out bacterial virulence. *FEMS Microbiol. Rev.* 30, 774–805. doi: 10.1111/j.1574-6976.2006.00035.x
- Dillard, J. P. (2014). "Peptidoglycan metabolism and fragment production," in *Pathogenic Neisseria: Genomics, Molecular Biology and Disease Intervention*, eds. J. K. Davies, C. M. Kahler (Norfolk: Caister Academic Press), 97–114.
- Dmitriev, B. A., Toukach, F. V., Holst, O., Rietschel, E. T., and Ehlers, S. (2004). Tertiary structure of *Staphylococcus aureus* cell wall murein. *J. Bacteriol.* 186, 7141–7148. doi: 10.1128/JB.186.21.7141-7148.2004
- Doehn, J. M., Fischer, K., Reppe, K., Gutbier, B., Tschernig, T., Hocke, A. C., et al. (2013). Delivery of the endolysin Cpl-1 by inhalation rescues mice with fatal pneumococcal pneumonia. *J. Antimicrob. Chemother.* 68, 2111–2117. doi: 10.1093/jac/dkt131
- Dominguez-Cuevas, P., Porcelli, I., Daniel, R. A., and Errington, J. (2013). Differentiated roles for MreB-actin isologues and autolytic enzymes in *Bacillus subtilis* morphogenesis. *Mol. Microbiol.* 89, 1084–1098. doi: 10.1111/mmi.12335
- Dramsi, S., Magnet, S., Davison, S., and Arthur, M. (2008). Covalent attachment of proteins to peptidoglycan. *FEMS Microbiol. Rev.* 32, 307–320. doi: 10.1111/j.1574-6976.2008.00102.x
- Dziarski, R. (2003). Recognition of bacterial peptidoglycan by the innate immune system. *Cell. Mol. Life Sci.* 60, 1793–1804. doi: 10.1007/s00018-003-3019-6
- Dziarski, R., and Gupta, D. (2006). The peptidoglycan recognition proteins (PGRPs). *Genome Biol.* 7:232. doi: 10.1186/gb-2006-7-8-232
- Egan, A. J., Biboy, J., Van't Veer, I., Breukink, E., and Vollmer, W. (2015). Activities and regulation of peptidoglycan synthases. *Philos. Trans. R. Soc. Lond.* 370:20150031. doi: 10.1098/rstb.2015.0031
- Fenton, M., Ross, P., McAuliffe, O., O'mahony, J., and Coffey, A. (2010). Recombinant bacteriophage lysins as antibacterials. *Bioeng. Bugs* 1, 9–16. doi: 10.4161/bbug.1.1.9818
- Finn, R. D., Coghill, P., Eberhardt, R. Y., Eddy, S. R., Mistry, J., Mitchell, A. L., et al. (2016). The Pfam protein families database: towards a more sustainable future. *Nucleic Acids Res.* 44, D279–285. doi: 10.1093/nar/gkv1344
- Firczuk, M., and Bochtler, M. (2007). Folds and activities of peptidoglycan amidases. *FEMS Microbiol. Rev.* 31, 676–691. doi: 10.1111/j.1574-6976.2007.00084.x
- Firczuk, M., Mucha, A., and Bochtler, M. (2005). Crystal structures of active LytM. *J. Mol. Biol.* 354, 578–590. doi: 10.1016/j.jmb.2005.09.082
- Fleming, A. (1929). On the antibacterial action of cultures of a penicillium, with special reference to their use in the isolation of *B. influenzae*. *Bull. World Health Organ.* 79, 780–790.
- Fonze, E., Vermeire, M., Nguyen-Disteche, M., Brasseur, R., and Charlier, P. (1999). The crystal structure of a penicilloyl-serine transferase of intermediate penicillin sensitivity. The DD-transpeptidase of *Streptomyces* K15. *J. Biol. Chem.* 274, 21853–21860. doi: 10.1074/jbc.274.31.21853
- Foster, S. J. (1993). Analysis of *Bacillus subtilis* 168 prophage-associated lytic enzymes; identification and characterization of CWLA-related prophage proteins. *J. Gen. Microbiol.* 139, 3177–3184. doi: 10.1099/00221287-139-12-3177
- Frankel, M. B., and Schneewind, O. (2012). Determinants of murein hydrolase targeting to cross-wall of *Staphylococcus aureus* peptidoglycan. *J. Biol. Chem.* 287, 10460–10471. doi: 10.1074/jbc.M111.336404
- Garcia, P., Garcia, E., Ronda, C., Lopez, R., and Tomas, A. (1983). A phage-associated murein hydrolase in *Streptococcus pneumoniae* infected with bacteriophage Dp-1. *J. Gen. Microbiol.* 129, 489–497.
- Garcia-Gomez, E., Espinosa, N., De La Mora, J., Dreyfus, G., and Gonzalez-Pedrajo, B. (2011). The muramidase EtpA from enteropathogenic *Escherichia coli* is required for efficient Type III secretion. *Microbiology* 157, 1145–1160. doi: 10.1099/mic.0.045617-0
- Glauner, B., Holtje, J. V., and Schwarz, U. (1988). The composition of the murein of *Escherichia coli*. *J. Biol. Chem.* 263, 10088–10095.
- Gokulan, K., Khare, S., Cerniglia, C. E., Foley, S. L., and Varughese, K. I. (2018). Structure and inhibitor specificity of L,D-transpeptidase (LdtMt2) from *Mycobacterium tuberculosis* and antibiotic resistance: calcium binding promotes dimer formation. *AAPS J.* 20:44. doi: 10.1208/s12248-018-0193-x
- Goodell, E. W. (1985). Recycling of murein by *Escherichia coli*. *J. Bacteriol.* 163, 305–10.
- Götz, F., Heilmann, C., and Stehle, T. (2014). Functional and structural analysis of the major amidase (Atl) in *Staphylococcus*. *Int. J. Med. Microbiol.* 304, 156–163. doi: 10.1016/j.ijmm.2013.11.006
- Grabowska, M., Jagielska, E., Czapinska, H., Bochtler, M., and Sabala, I. (2015). High resolution structure of an M23 peptidase with a substrate analogue. *Sci. Rep.* 5:14833. doi: 10.1038/srep14833
- Gu, J., Feng, Y., Feng, X., Sun, C., Lei, L., Ding, W., et al. (2014). Structural and biochemical characterization reveals LysGH15 as an unprecedented "EF-hand-like" calcium-binding phage lysin. *PLoS Pathog.* 10:e1004109. doi: 10.1371/journal.ppat.1004109
- Guiral, S., Mitchell, T. J., Martin, B., and Claverys, J. P. (2005). Competence-programmed predation of noncompetent cells in the human pathogen *Streptococcus pneumoniae*: genetic requirements. *Proc. Natl. Acad. Sci. U.S.A.* 102, 8710–8715. doi: 10.1073/pnas.0500879102
- Harz, H., Burgdorf, K., and Holtje, J. V. (1990). Isolation and separation of the glycane strands from murein of *Escherichia coli* by reversed-phase high-performance liquid chromatography. *Anal. Biochem.* 190, 120–128. doi: 10.1016/0003-2697(90)90144-X
- Hashimoto, W., Ochiai, A., Momma, K., Itoh, T., Mikami, B., Maruyama, Y., et al. (2009). Crystal structure of the glycosidase family 73 peptidoglycan hydrolase FlgJ. *Biochem. Biophys. Res. Commun.* 381, 16–21. doi: 10.1016/j.bbrc.2009.01.186
- Havarstein, L. S., Martin, B., Johnsborg, O., Granadel, C., and Claverys, J. P. (2006). New insights into the pneumococcal fratricide: relationship to clumping and identification of a novel immunity factor. *Mol. Microbiol.* 59, 1297–1307. doi: 10.1111/j.1365-2958.2005.05021.x
- Heidrich, C., Templin, M. F., Ursinus, A., Merdanovic, M., Berger, J., Schwarz, H., et al. (2001). Involvement of N-acetylmuramyl-L-alanine amidases in cell separation and antibiotic-induced autolysis of *Escherichia coli*. *Mol. Microbiol.* 41, 167–178. doi: 10.1046/j.1365-2958.2001.02499.x
- Heidrich, C., Ursinus, A., Berger, J., Schwarz, H., and Holtje, J. V. (2002). Effects of multiple deletions of murein hydrolases on viability, septum cleavage, and sensitivity to large toxic molecules in *Escherichia coli*. *J. Bacteriol.* 184, 6093–6099. doi: 10.1128/JB.184.22.6093-6099.2002
- Heilmann, C., Hussain, M., Peters, G., and Gotz, F. (1997). Evidence for autolysin-mediated primary attachment of *Staphylococcus*

- epidermidis* to a polystyrene surface. *Mol. Microbiol.* 24, 1013–1024. doi: 10.1046/j.1365-2958.1997.4101774.x
- Herlihey, F. A., and Clarke, A. J. (2017). Controlling autolysis during flagella insertion in gram-negative bacteria. *Adv. Exp. Med. Biol.* 925, 41–56. doi: 10.1007/5584_2016_52
- Hirano, T., Minamino, T., and Macnab, R. M. (2001). The role in flagellar rod assembly of the N-terminal domain of *Salmonella* FlgJ, a flagellum-specific muramidase. *J. Mol. Biol.* 312, 359–369. doi: 10.1006/jmbi.2001.4963
- Holtje, J. V. (1995). From growth to autolysis: the murein hydrolases in *Escherichia coli*. *Arch. Microbiol.* 164, 243–254. doi: 10.1007/BF02529958
- Holtje, J. V. (1996). A hypothetical holoenzyme involved in the replication of the murein sacculus of *Escherichia coli*. *Microbiology* 142, 1911–1918. doi: 10.1099/13500872-142-8-1911
- Holtje, J. V. (1998). Growth of the stress-bearing and shape-maintaining murein sacculus of *Escherichia coli*. *Microbiol. Mol. Biol. Rev.* 62, 181–203.
- Holtje, J. V., Kopp, U., Ursinus, A., and Wiedemann, B. (1994). The negative regulator of β -lactamase induction AmpD is a N-acetyl-anhydromuramyl-L-alanine amidase. *FEMS Microbiol. Lett.* 122, 159–164. doi: 10.1111/j.1574-6968.1994.tb07159.x
- Höltje, J. V., Mirelman, D., Sharon, N., and Schwarz, U. (1975). Novel type of murein transglycosylase in *Escherichia coli*. *J. Bacteriol.* 124, 1067–1076.
- Hoppner, C., Carle, A., Sivanesan, D., Hoepfner, S., and Baron, C. (2005). The putative lytic transglycosylase VirB1 from *Brucella suis* interacts with the Type IV secretion system core components VirB8, VirB9 and VirB11. *Microbiology* 151, 3469–3482. doi: 10.1099/mic.0.28326-0
- Horgan, M., O'Flynn, G., Garry, J., Cooney, J., Coffey, A., Fitzgerald, G. F., et al. (2009). Phage lysin LysK can be truncated to its CHAP domain and retain lytic activity against live antibiotic-resistant staphylococci. *Appl. Environ. Microbiol.* 75, 872–874. doi: 10.1128/AEM.01831-08
- Horsburgh, G. J., Atrih, A., and Foster, S. J. (2003a). Characterization of LytH, a differentiation-associated peptidoglycan hydrolase of *Bacillus subtilis* involved in endospore cortex maturation. *J. Bacteriol.* 185, 3813–3820. doi: 10.1128/JB.185.13.3813-3820.2003
- Horsburgh, G. J., Atrih, A., Williamson, M. P., and Foster, S. J. (2003b). LytG of *Bacillus subtilis* is a novel peptidoglycan hydrolase: the major active glucosaminidase. *Biochemistry* 42, 257–264. doi: 10.1021/bi020498c
- Huard, C., Miranda, G., Redko, Y., Wessner, F., Foster, S. J., and Chapot-Chartier, M. P. (2004). Analysis of the peptidoglycan hydrolase complement of *Lactococcus lactis*: identification of a third N-acetylglucosaminidase, AcmC. *Appl. Environ. Microbiol.* 70, 3493–3499. doi: 10.1128/AEM.70.6.3493-3499.2004
- Huard, C., Miranda, G., Wessner, F., Bolotin, A., Hansen, J., Foster, S. J., et al. (2003). Characterization of AcmB, an N-acetylglucosaminidase autolysin from *Lactococcus lactis*. *Microbiology* 149, 695–705. doi: 10.1099/mic.0.25875-0
- Humann, J., and Lenz, L. L. (2009). Bacterial peptidoglycan degrading enzymes and their impact on host muropeptide detection. *J. Innate Immun.* 1, 88–97. doi: 10.1159/000181181
- Inagaki, N., Iguchi, A., Yokoyama, T., Yokoi, K. J., Ono, Y., Yamakawa, A., et al. (2009). Molecular properties of the glucosaminidase AcmA from *Lactococcus lactis* MG1363: mutational and biochemical analyses. *Gene* 447, 61–71. doi: 10.1016/j.gene.2009.08.004
- Jackson, M. (2014). The mycobacterial cell envelope-lipids. *Cold Spring Harb. Perspect. Med.* 4:a021105. doi: 10.1101/cshperspect.a021105
- Jacobs, C., Frere, J. M., and Normark, S. (1997). Cytosolic intermediates for cell wall biosynthesis and degradation control inducible β -lactam resistance in Gram-negative bacteria. *Cell* 88, 823–832. doi: 10.1016/S0092-8674(00)81928-5
- Johnson, J. W., Fisher, J. F., and Mobashery, S. (2013). Bacterial cell-wall recycling. *Ann. N. Y. Acad. Sci.* 1277:54–75. doi: 10.1111/j.1749-6632.2012.06813.x
- Jolles, P. (1996). From the discovery of lysozyme to the characterization of several lysozyme families. *EXS*. 1996:75:3–5. doi: 10.1007/978-3-0348-9225-4_1
- Kajimura, J., Fujiwara, T., Yamada, S., Suzawa, Y., Nishida, T., Oyama, Y., et al. (2005). Identification and molecular characterization of an N-acetylmuramyl-L-alanine amidase Sle1 involved in cell separation of *Staphylococcus aureus*. *Mol. Microbiol.* 58, 1087–1101. doi: 10.1111/j.1365-2958.2005.04881.x
- Karamanos, Y. (1997). Endo-N-acetyl- β -D-glucosaminidases and their potential substrates: structure/function relationships. *Res. Microbiol.* 148, 661–671. doi: 10.1016/S0923-2508(99)80065-5
- Keary, R., Sanz-Gaitero, M., Van Raaij, M. J., O'mahony, J., Fenton, M., McAuliffe, O., et al. (2016). Characterization of a Bacteriophage-Derived Murein Peptidase for Elimination of Antibiotic-Resistant *Staphylococcus aureus*. *Curr. Protein Pept. Sci.* 17, 183–190. doi: 10.2174/1389203716666151102105515
- Keck, W., Van Leeuwen, A. M., Huber, M., and Goodell, E. W. (1990). Cloning and characterization of mepA, the structural gene of the penicillin-insensitive murein endopeptidase from *Escherichia coli*. *Mol. Microbiol.* 4, 209–219. doi: 10.1111/j.1365-2958.1990.tb00588.x
- Keep, N. H., Ward, J. M., Cohen-Gonsaud, M., and Henderson, B. (2006). Wake up! Peptidoglycan lysis and bacterial non-growth states. *Trends Microbiol.* 14, 271–276. doi: 10.1016/j.tim.2006.04.003
- Kim, H. S., Im, H. N., An, D. R., Yoon, J. Y., Jang, J. Y., Mobashery, S., et al. (2015). The cell shape-determining Csd6 protein from *Helicobacter pylori* constitutes a new family of L,D-carboxypeptidase. *J. Biol. Chem.* 290, 25103–25117. doi: 10.1074/jbc.M115.658781
- Kim, H. S., Kim, J., Im, H. N., Yoon, J. Y., An, D. R., Yoon, H. J., et al. (2013). Structural basis for the inhibition of *Mycobacterium tuberculosis* L,D-transpeptidase by meropenem, a drug effective against extensively drug-resistant strains. *Acta Crystallogr. D Biol. Crystallogr.* 69, 420–431. doi: 10.1107/S0907444912048998
- Knillans, K. J., Hackett, K. T., Anderson, J. E., Weng, C., Dillard, J. P., and Duncan, J. A. (2017). *Neisseria gonorrhoeae* lytic transglycosylases LtgA and LtgD reduce host innate immune signaling through TLR2 and NOD2. *ACS Infect Dis* 3, 624–633. doi: 10.1021/acsinfecdis.6b00088
- Koch, A. L., and Doyle, R. J. (1985). Inside-to-outside growth and turnover of the wall of gram-positive rods. *J. Theor. Biol.* 117, 137–157. doi: 10.1016/S0022-5193(85)80169-7
- Komatsuzawa, H., Sugai, M., Nakashima, S., Yamada, S., Matsumoto, A., Oshida, T., et al. (1997). Subcellular localization of the major autolysin, ATL and its processed proteins in *Staphylococcus aureus*. *Microbiol. Immunol.* 41, 469–479. doi: 10.1111/j.1348-0421.1997.tb01880.x
- Koraimann, G. (2003). Lytic transglycosylases in macromolecular transport systems of Gram-negative bacteria. *Cell. Mol. Life Sci.* 60, 2371–2388. doi: 10.1007/s00018-003-3056-1
- Kumar, P., Kaushik, A., Lloyd, E. P., Li, S. G., Mattoo, R., Ammerman, N. C., et al. (2017). Non-classical transpeptidases yield insight into new antibacterials. *Nat. Chem. Biol.* 13, 54–61. doi: 10.1038/nchembio.2237
- Kuroda, M., Kuroda, H., Oshima, T., Takeuchi, F., Mori, H., and Hiramatsu, K. (2003). Two-component system VraSR positively modulates the regulation of cell-wall biosynthesis pathway in *Staphylococcus aureus*. *Mol. Microbiol.* 49, 807–821. doi: 10.1046/j.1365-2958.2003.03599.x
- Lawson, P. A., Citron, D. M., Tyrrell, K. L., and Finegold, S. M. (2016). Reclassification of *Clostridium difficile* as *Clostridioides difficile* (Hall and O'Toole 1935) Prevot 1938. *Anaerobe* 40, 95–99. doi: 10.1016/j.anaerobe.2016.06.008
- Lee, M., Artola-Recolons, C., Carrasco-Lopez, C., Martinez-Caballero, S., Heseck, D., Spink, E., et al. (2013). Cell-wall remodeling by the zinc-protease AmpDh3 from *Pseudomonas aeruginosa*. *J. Am. Chem. Soc.* 135, 12604–12607. doi: 10.1021/ja407445x
- Lessard, I. A., Pratt, S. D., McCafferty, D. G., Bussiere, D. E., Hutchins, C., Wanner, B. L., et al. (1998). Homologs of the vancomycin resistance D-Ala-D-Ala dipeptidase VanX in *Streptomyces toyocaensis*, *Escherichia coli* and *Synechocystis*: attributes of catalytic efficiency, stereoselectivity and regulation with implications for function. *Chem. Biol.* 5, 489–504. doi: 10.1016/S1074-5521(98)90005-9
- Letunic, I., and Bork, P. (2018). 20 years of the SMART protein domain annotation resource. *Nucleic Acids Res.* 46, D493–D496. doi: 10.1093/nar/gkx922
- Li, W. J., Li, D. F., Hu, Y. L., Zhang, X. E., Bi, L. J., and Wang, D. C. (2013). Crystal structure of L,D-transpeptidase LdtMt2 in complex with meropenem reveals the mechanism of carbapenem against *Mycobacterium tuberculosis*. *Cell Res.* 23, 728–731. doi: 10.1038/cr.2013.53
- Li, Y., Jin, K., Setlow, B., Setlow, P., and Hao, B. (2012). Crystal structure of the catalytic domain of the *Bacillus cereus* SleB protein, important in cortex peptidoglycan degradation during spore germination. *J. Bacteriol.* 194, 4537–4545. doi: 10.1128/JB.00877-12
- Liepinsh, E., Genereux, C., Dehareng, D., Joris, B., and Otting, G. (2003). NMR structure of *Citrobacter freundii* AmpD, comparison with bacteriophage T7

- lysozyme and homology with PGRP domains. *J. Mol. Biol.* 327, 833–842. doi: 10.1016/S0022-2836(03)00185-2
- Litzinger, S., Fischer, S., Polzer, P., Diederichs, K., Welte, W., and Mayer, C. (2010). Structural and kinetic analysis of *Bacillus subtilis* N-acetylglucosaminidase reveals a unique Asp-His dyad mechanism. *J. Biol. Chem.* 285, 35675–35684. doi: 10.1074/jbc.M110.131037
- Llull, D., Lopez, R., and Garcia, E. (2006). Skl, a novel choline-binding N-acetylmuramoyl-L-alanine amidase of *Streptococcus mitis* SK137 containing a CHAP domain. *FEBS Lett.* 580, 1959–1964. doi: 10.1016/j.febslet.2006.02.060
- Lopez, R., Garcia, E., and Concepcion, R. (1981). Bacteriophages of *Streptococcus pneumoniae*. *Rev. Infect. Dis.* 3, 212–223. doi: 10.1093/clinids/3.2.212
- Lu, J. Z., Fujiwara, T., Komatsuzawa, H., Sugai, M., and Sakon, J. (2006). Cell wall-targeting domain of glycylglycine endopeptidase distinguishes among peptidoglycan cross-bridges. *J. Biol. Chem.* 281, 549–558. doi: 10.1074/jbc.M509691200
- Ma, Y., Bai, G., Cui, Y., Zhao, J., Yuan, Z., and Liu, X. (2017). Crystal Structure of Murein-Tripeptide Amidase MpaA from *Escherichia coli* O157 at 2.6 Å Resolution. *Protein Pept. Lett.* 24, 181–187. doi: 10.2174/0929866523666161128153128
- Machata, S., Hain, T., Rohde, M., and Chakraborty, T. (2005). Simultaneous deficiency of both MurA and p60 proteins generates a rough phenotype in *Listeria monocytogenes*. *J. Bacteriol.* 187, 8385–8394. doi: 10.1128/JB.187.24.8385-8394.2005
- Macheboeuf, P., Contreras-Martel, C., Job, V., Dideberg, O., and Dessen, A. (2006). Penicillin binding proteins: key players in bacterial cell cycle and drug resistance processes. *FEMS Microbiol. Rev.* 30, 673–691. doi: 10.1111/j.1574-6976.2006.00024.x
- Magnet, S., Dubost, L., Marie, A., Arthur, M., and Gutmann, L. (2008). Identification of the L,D-transpeptidases for peptidoglycan cross-linking in *Escherichia coli*. *J. Bacteriol.* 190, 4782–4785. doi: 10.1128/JB.00025-08
- Marchler-Bauer, A., Bo, Y., Han, L., He, J., Lanczycki, C. J., Lu, S., et al. (2017). CDD/SPARCLE: functional classification of proteins via subfamily domain architectures. *Nucleic Acids Res.* 45, D200–D203. doi: 10.1093/nar/gkw1129
- Marcyjanik, M., Odintsov, S. G., Sabala, I., and Bochtler, M. (2004). Peptidoglycan amidase MepA is a LAS metallopeptidase. *J. Biol. Chem.* 279, 43982–43989. doi: 10.1074/jbc.M406735200
- Markiewicz, Z., Broome-Smith, J. K., Schwarz, U., and Spratt, B. G. (1982). Spherical *Escherichia coli* due to elevated levels of D-alanine carboxypeptidase. *Nature* 297, 702–704. doi: 10.1038/297702a0
- Markiewicz, Z., and Popowska, M. (2011). An update on some structural aspects of the mighty miniwall. *Pol. J. Microbiol.* 60, 181–186.
- Martinez-Caballero, S., Lee, M., Artola-Recolons, C., Carrasco-Lopez, C., Heseck, D., Spink, E., et al. (2013). Reaction products and the X-ray structure of AmpDh2, a virulence determinant of *Pseudomonas aeruginosa*. *J. Am. Chem. Soc.* 135, 10318–10321. doi: 10.1021/ja405464b
- Maruyama, Y., Ochiai, A., Itoh, T., Mikami, B., Hashimoto, W., and Murata, K. (2010). Mutational studies of the peptidoglycan hydrolase FlgJ of *Sphingomonas* sp. strain A1. *J. Basic Microbiol.* 50, 311–317. doi: 10.1002/jobm.200900249
- Mavroggiorgos, N., Mekasha, S., Yang, Y., Kelliher, M. A., and Ingalls, R. R. (2014). Activation of NOD receptors by *Neisseria gonorrhoeae* modulates the innate immune response. *Innate Immun.* 20, 377–389. doi: 10.1177/1753425913493453
- Mckenzie, H. A. (1996). alpha-Lactalbumins and lysozymes. *EXS* 75, 365–409. doi: 10.1007/978-3-0348-9225-4_19
- Meisner, J., Montero Llopis, P., Sham, L. T., Garner, E., Bernhardt, T. G., and Rudner, D. Z. (2013). FtsEX is required for CwlO peptidoglycan hydrolase activity during cell wall elongation in *Bacillus subtilis*. *Mol. Microbiol.* 89, 1069–1083. doi: 10.1111/mmi.12330
- Melly, M. A., Mcgee, Z. A., and Rosenthal, R. S. (1984). Ability of monomeric peptidoglycan fragments from *Neisseria gonorrhoeae* to damage human fallopian-tube mucosa. *J. Infect. Dis.* 149, 378–386. doi: 10.1093/infdis/149.3.378
- Mercier, C., Durrieu, C., Briandet, R., Domakova, E., Tremblay, J., Buist, G., et al. (2002). Positive role of peptidoglycan breaks in lactococcal biofilm formation. *Mol. Microbiol.* 46, 235–243. doi: 10.1046/j.1365-2958.2002.03160.x
- Meziane-Cherif, D., Stogios, P. J., Evdokimova, E., Savchenko, A., and Courvalin, P. (2014). Structural basis for the evolution of vancomycin resistance D,D-peptidases. *Proc. Natl. Acad. Sci. U.S.A.* 111, 5872–5877. doi: 10.1073/pnas.1402259111
- Mitchell, A. L., Attwood, T. K., Babbitt, P. C., Blum, M., Bork, P., Bridge, A., et al. (2019). InterPro in 2019: improving coverage, classification and access to protein sequence annotations. *Nucleic Acids Res.* 47, D351–D360. doi: 10.1093/nar/gky1100
- Mooers, B. H., and Matthews, B. W. (2006). Extension to 2268 atoms of direct methods in the ab initio determination of the unknown structure of bacteriophage P22 lysozyme. *Acta Crystallogr. D Biol. Crystallogr.* 62, 165–176. doi: 10.1107/S0907444905037212
- Morais, S., Cockburn, D. W., Ben-David, Y., Koropatkin, N. M., Martens, E. C., Duncan, S. H., et al. (2016). Lysozyme activity of the *Ruminococcus champanellensis* cellulosome. *Environ. Microbiol.* 18, 5112–5122. doi: 10.1111/1462-2920.13501
- Nagl, S. B. (2003). “Function prediction from protein sequence,” in *Bioinformatics: Genes, Proteins and Computers*, eds. C. Orenco, D. Jones, J. Thornton (Oxford: BIOS scientific Publishers), 64–78.
- Nambu, T., Minamino, T., Macnab, R. M., and Kutsukake, K. (1999). Peptidoglycan-hydrolyzing activity of the FlgJ protein, essential for flagellar rod formation in *Salmonella Typhimurium*. *J. Bacteriol.* 181, 1555–1561.
- Nelson, D. E., and Young, K. D. (2001). Contributions of PBP5 and DD-carboxypeptidase penicillin binding proteins to maintenance of cell shape in *Escherichia coli*. *J. Bacteriol.* 183, 3055–3064. doi: 10.1128/JB.183.10.3055-3064.2001
- Neuhaus, F. C., and Baddiley, J. (2003). A continuum of anionic charge: structures and functions of d-alanyl-teichoic acids in Gram-positive bacteria. *Microbiol. Mol. Biol. Rev.* 67, 686–723. doi: 10.1128/MMBR.67.4.686-723.2003
- Ng, W. L., Robertson, G. T., Kazmierczak, K. M., Zhao, J., Gilmour, R., and Winkler, M. E. (2003). Constitutive expression of PcsB suppresses the requirement for the essential VicR (YycF) response regulator in *Streptococcus pneumoniae* R6. *Mol. Microbiol.* 50, 1647–1663. doi: 10.1046/j.1365-2958.2003.03806.x
- Niederweis, M., Danilchanka, O., Huff, J., Hoffmann, C., and Engelhardt, H. (2010). Mycobacterial outer membranes: in search of proteins. *Trends Microbiol.* 18, 109–116. doi: 10.1016/j.tim.2009.12.005
- Nugroho, F. A., Yamamoto, H., Kobayashi, Y., and Sekiguchi, J. (1999). Characterization of a new sigma-K-dependent peptidoglycan hydrolase gene that plays a role in *Bacillus subtilis* mother cell lysis. *J. Bacteriol.* 181, 6230–6237.
- Odintsov, S. G., Sabala, I., Marcyjanik, M., and Bochtler, M. (2004). Latent LytM at 1.3 Å resolution. *J. Mol. Biol.* 335, 775–785. doi: 10.1016/j.jmb.2003.11.009
- O’flaherty, S., Coffey, A., Meaney, W., Fitzgerald, G. F., and Ross, R. P. (2005). The recombinant phage lysin LysK has a broad spectrum of lytic activity against clinically relevant staphylococci, including methicillin-resistant *Staphylococcus aureus*. *J. Bacteriol.* 187, 7161–7164. doi: 10.1128/JB.187.20.7161-7164.2005
- Ohnishi, R., Ishikawa, S., and Sekiguchi, J. (1999). Peptidoglycan hydrolase LytF plays a role in cell separation with CwlF during vegetative growth of *Bacillus subtilis*. *J. Bacteriol.* 181, 3178–3184.
- Oshida, T., Sugai, M., Komatsuzawa, H., Hong, Y. M., Suganaka, H., and Tomasz, A. (1995). A *Staphylococcus aureus* autolysin that has an N-acetylmuramoyl-L-alanine amidase domain and an endo-β-N-acetylglucosaminidase domain: cloning, sequence analysis, and characterization. *Proc. Natl. Acad. Sci.* 92, 285–289. doi: 10.1073/pnas.92.1.285
- Ozdemir, I., Blumer-Schuetz, S. E., Kelly, R. M. (2012). S-layer homology domain proteins CsaC_0678 and CsaC_2722 are implicated in plant polysaccharide deconstruction by the extremely thermophilic bacterium *Caldicellulosiruptor saccharolyticus*. *Appl. Environ. Microbiol.* 78, 768–777. doi: 10.1128/AEM.07031-11
- Park, J. T., and Uehara, T. (2008). How bacteria consume their own exoskeletons (turnover and recycling of cell wall peptidoglycan). *Microbiol. Mol. Biol. Rev.* 72, 211–227. doi: 10.1128/MMBR.00027-07
- Pei, J., and Grishin, N. V. (2005). COG3926 and COG5526: a tale of two new lysozyme-like protein families. *Protein Sci.* 14, 2574–2581. doi: 10.1110/ps.051656805
- Pennartz, A., G  n  reux, C., Parquet, C., Mengin-Lecreux, D., and Joris, B. (2009). Substrate-induced inactivation of the *Escherichia coli* AmiD N-acetylmuramoyl-L-alanine amidase highlights a new strategy to inhibit

- p>
this class of enzyme.
- Antimicrob. Agents Chemother.*
- 53, 2991–2997. doi: 10.1128/AAC.01520-07
- Perez-Dorado, I., Campillo, N. E., Monterroso, B., Heseck, D., Lee, M., Paez, J. A., et al. (2007). Elucidation of the molecular recognition of bacterial cell wall by modular pneumococcal phage endolysin CPL-1. *J. Biol. Chem.* 282, 24990–24999. doi: 10.1074/jbc.M704317200
- Perez-Dorado, I., Gonzalez, A., Morales, M., Sanles, R., Striker, W., Vollmer, W., et al. (2010). Insights into pneumococcal fratricide from the crystal structures of the modular killing factor LytC. *Nat. Struct. Mol. Biol.* 17, 576–581. doi: 10.1038/nsmb.1817
- Pilgrim, S., Kolb-Maurer, A., Gentschev, I., Goebel, W., and Kuhn, M. (2003). Deletion of the gene encoding p60 in *Listeria monocytogenes* leads to abnormal cell division and loss of actin-based motility. *Infect. Immun.* 71, 3473–3484. doi: 10.1128/IAI.71.6.3473-3484.2003
- Popowska, M., and Markiewicz, Z. (2004). Classes and functions of *Listeria monocytogenes* surface proteins. *Pol. J. Microbiol.* 53, 75–88.
- Potluri, L., Karczmarek, A., Verheul, J., Piette, A., Wilkin, J. M., Werth, N., et al. (2010). Septal and lateral wall localization of PBP5, the major D,D-carboxypeptidase of *Escherichia coli*, requires substrate recognition and membrane attachment. *Mol. Microbiol.* 77, 300–323. doi: 10.1111/j.1365-2958.2010.07205.x
- Priyadarshini, R., Popham, D. L., and Young, K. D. (2006). Daughter cell separation by penicillin-binding proteins and peptidoglycan amidases in *Escherichia coli*. *J. Bacteriol.* 188, 5345–5355. doi: 10.1128/JB.00476-06
- Reith, J., and Mayer, C. (2011). Peptidoglycan turnover and recycling in Gram-positive bacteria. *Appl. Microbiol. Biotechnol.* 92, 1–11. doi: 10.1007/s00253-011-3486-x
- Renier, S., Chagnot, C., Deschamps, J., Caccia, N., Szlavik, J., Joyce, S. A., et al. (2014). Inactivation of the SecA2 protein export pathway in *Listeria monocytogenes* promotes cell aggregation, impacts biofilm architecture and induces biofilm formation in environmental condition. *Environ. Microbiol.* 16, 1176–1192. doi: 10.1111/1462-2920.12257
- Renier, S., Hebraud, M., and Desvaux, M. (2011). Molecular biology of surface colonization by *Listeria monocytogenes*: an additional facet of an opportunistic Gram-positive foodborne pathogen. *Environ. Microbiol.* 13, 835–850. doi: 10.1111/j.1462-2920.2010.02378.x
- Rhazi, N., Charlier, P., Dehareng, D., Engner, D., Vermeire, M., Frere, J. M., et al. (2003). Catalytic mechanism of the *Streptomyces* K15 DD-transpeptidase/penicillin-binding protein probed by site-directed mutagenesis and structural analysis. *Biochemistry* 42, 2895–2906. doi: 10.1021/bi027256x
- Rice, K. C., and Bayles, K. W. (2008). Molecular control of bacterial death and lysis. *Microbiol. Mol. Biol. Rev.* 72, 85–109. doi: 10.1128/MMBR.00030-07
- Rigden, D. J., Jedrzejewski, M. J., and Galperin, M. Y. (2003). Amidase domains from bacterial and phage autolysins define a family of gamma-D,L-glutamate-specific amidohydrolases. *Trends Biochem. Sci.* 28, 230–234. doi: 10.1016/S0968-0004(03)00062-8
- Rocabay, M., Herman, R., Sauvage, E., Remaut, H., Moonens, K., Terrak, M., et al. (2013). The crystal structure of the cell division amidase AmiC reveals the fold of the AMIN domain, a new peptidoglycan binding domain. *Mol. Microbiol.* 90, 267–277. doi: 10.1111/mmi.12361
- Rossi, P., Aramini, J. M., Xiao, R., Chen, C. X., Nwosu, C., Owens, L. A., et al. (2009). Structural elucidation of the Cys-His-Glu-Asn proteolytic relay in the secreted CHAP domain enzyme from the human pathogen *Staphylococcus saprophyticus*. *Proteins* 74, 515–519. doi: 10.1002/prot.22267
- Sabala, I., Jagielska, E., Bardelang, P. T., Czapinska, H., Dahms, S. O., Sharpe, J. A., et al. (2014). Crystal structure of the antimicrobial peptidase lysostaphin from *Staphylococcus simulans*. *FEBS J.* 281, 4112–4122. doi: 10.1111/febs.12929
- Sabala, I., Jonsson, I.-M., Tarkowski, A., and Bochtler, M. (2012). Anti-staphylococcal activities of lysostaphin and LytM catalytic domain. *BMC Microbiol.* 12:97. doi: 10.1186/1471-2180-12-97
- Sanders, A. N., and Pavelka, M. S. (2013). Phenotypic analysis of *Escherichia coli* mutants lacking L,D-transpeptidases. *Microbiology* 159, 1842–1852. doi: 10.1099/mic.0.069211-0
- Sanz-Gaitero, M., Keary, R., Garcia-Doval, C., Coffey, A., and Van Raaij, M. J. (2014). Crystal structure of the lytic CHAP(K) domain of the endolysin LysK from *Staphylococcus aureus* bacteriophage K. *Virology* 11:133. doi: 10.1186/1743-422X-11-133
- Sauvage, E., Kerff, F., Terrak, M., Ayala, J. A., and Charlier, P. (2008). The penicillin-binding proteins: structure and role in peptidoglycan biosynthesis. *FEMS Microbiol. Rev.* 32, 234–258. doi: 10.1111/j.1574-6976.2008.00105.x
- Scheffers, D. J., and Pinho, M. G. (2005). Bacterial cell wall synthesis: new insights from localization studies. *Microbiol. Mol. Biol. Rev.* 69, 585–607. doi: 10.1128/MMBR.69.4.585-607.2005
- Scheurwater, E., Reid, C. W., and Clarke, A. J. (2008). Lytic transglycosylases: bacterial space-making autolysins. *Int. J. Biochem. Cell Biol.* 40, 586–591. doi: 10.1016/j.biocel.2007.03.018
- Scheurwater, E. M., and Burrows, L. L. (2011). Maintaining network security: how macromolecular structures cross the peptidoglycan layer. *FEMS Microbiol. Lett.* 318, 1–9. doi: 10.1111/j.1574-6968.2011.02228.x
- Schindler, C. A., and Schuhardt, V. T. (1964). Lysostaphin: a new bacteriolytic agent for the staphylococcus. *Proc. Natl. Acad. Sci. U.S.A.* 51, 414–421. doi: 10.1073/pnas.51.3.414
- Schleifer, K. H., and Kandler, O. (1972). Peptidoglycan types of bacterial cell walls and their taxonomic implications. *Bacteriol. Rev.* 36, 407–477.
- Schmelcher, M., Donovan, D. M., and Loessner, M. J. (2012). Bacteriophage endolysins as novel antimicrobials. *Future Microbiol.* 7, 1147–1171. doi: 10.2217/fmb.12.97
- Schneewind, O., Fowler, A., and Faull, K. F. (1995). Structure of the cell wall anchor of surface proteins in *Staphylococcus aureus*. *Science* 268, 103–106. doi: 10.1126/science.7701329
- Serizawa, M., Yamamoto, H., Yamaguchi, H., Fujita, Y., Kobayashi, K., Ogasawara, N., et al. (2004). Systematic analysis of SigD-regulated genes in *Bacillus subtilis* by DNA microarray and Northern blotting analyses. *Gene* 329, 125–136. doi: 10.1016/j.gene.2003.12.024
- Sham, L.-T., Barendt, S. M., Kopecky, K. E., and Winkler, M. E. (2011). Essential PcsB putative peptidoglycan hydrolase interacts with the essential FtsX(Spn) cell division protein in *Streptococcus pneumoniae* D39. *Proc. Natl. Acad. Sci. U.S.A.* 108, E1061–E1069. doi: 10.1073/pnas.1108323108
- Shao, X., Ni, H., Lu, T., Jiang, M., Li, H., Huang, X., et al. (2012). An improved system for the surface immobilisation of proteins on *Bacillus thuringiensis* vegetative cells and spores through a new spore cortex-lytic enzyme anchor. *N. Biotechnol.* 29, 302–310. doi: 10.1016/j.nbt.2011.09.003
- Shockman, G. D., Daneo-Moore, L., Kariyama, R., and Massidda, O. (1996). Bacterial walls, peptidoglycan hydrolases, autolysins, and autolysis. *Microbiol. Drug Resistance* 2, 95–98. doi: 10.1089/mdr.1996.2.95
- Shoham, Y., Lamed, R., and Bayer, E. A. (1999). The cellulosome concept as an efficient microbial strategy for the degradation of insoluble polysaccharides. *Trends Microbiol.* 7, 275–281. doi: 10.1016/S0966-842X(99)01533-4
- Shoseyov, O., Shani, Z., and Levy, I. (2006). Carbohydrate binding modules: biochemical properties and novel applications. *Microbiol. Mol. Biol. Rev.* 70, 283–295. doi: 10.1128/MMBR.00028-05
- Silhavy, T. J., Kahne, D., and Walker, S. (2010). The bacterial cell envelope. *Cold Spring Harb. Perspect. Biol.* 2:a000414. doi: 10.1101/cshperspect.a000414
- Singh, S. K., Saisree, L., Amrutha, R. N., and Reddy, M. (2012). Three redundant murein endopeptidases catalyse an essential cleavage step in peptidoglycan synthesis of *Escherichia coli* K12. *Mol. Microbiol.* 86, 1036–1051. doi: 10.1111/mmi.12058
- Smith, S. P., Bayer, E. A., and Czejek, M. (2017). Continually emerging mechanistic complexity of the multi-enzyme cellulosome complex. *Curr. Opin. Struct. Biol.* 44, 151–160. doi: 10.1016/j.sbi.2017.03.009
- Smith, T. J., Blackman, S. A., and Foster, S. J. (2000). Autolysins of *Bacillus subtilis*: multiple enzymes with multiple functions. *Microbiology* 146, 249–262. doi: 10.1099/00221287-146-2-249
- Smith, T. J., and Foster, S. J. (1995). Characterization of the involvement of two compensatory autolysins in mother cell lysis during sporulation of *Bacillus subtilis* 168. *J. Bacteriol.* 177, 3855–3862. doi: 10.1128/jb.177.13.3855-3862.1995
- Sobhanifar, S., King, D. T., and Strynadka, N. C. (2013). Fortifying the wall: synthesis, regulation and degradation of bacterial peptidoglycan. *Curr. Opin. Struct. Biol.* 23, 695–703. doi: 10.1016/j.sbi.2013.07.008
- Steen, A., Buist, G., Horsburgh, G. J., Venema, G., Kuipers, O. P., Foster, S. J., et al. (2005). AcmA of *Lactococcus lactis* is an N-acetylglucosaminidase with an optimal number of LysM domains for proper functioning. *FEBS J.* 272, 2854–2868. doi: 10.1111/j.1742-4658.2005.04706.x
- Stubbs, K. A., Balcewich, M., Mark, B. L., and Vocadlo, D. J. (2007). Small molecule inhibitors of a glycoside hydrolase attenuate inducible

- AmpC-mediated β -lactam resistance. *J. Biol. Chem.* 282, 21382–21391. doi: 10.1074/jbc.M700084200
- Sugai, M., Fujiwara, T., Akiyama, T., Ohara, M., Komatsuzawa, H., Inoue, S., et al. (1997). Purification and molecular characterization of glycylglycine endopeptidase produced by *Staphylococcus capitis* EPK1. *J. Bacteriol.* 179, 1193–1202. doi: 10.1128/jb.179.4.1193-1202.1997
- Szweda, P., Schiellmann, M., Kotlowski, R., Gorczyca, G., Zalewska, M., and Milewski, S. (2012). Peptidoglycan hydrolases-potential weapons against *Staphylococcus aureus*. *Appl. Microbiol. Biotechnol.* 96, 1157–1174. doi: 10.1007/s00253-012-4484-3
- Templin, M. F., Ursinus, A., and Höltje, J.-V. (1999). A defect in cell wall recycling triggers autolysis during the stationary growth phase of *Escherichia coli*. *EMBO J.* 18, 4108–4117. doi: 10.1093/emboj/18.15.4108
- Torti, S. V., and Park, J. T. (1976). Lipoprotein of Gram-negative bacteria is essential for growth and division. *Nature* 263, 323–326. doi: 10.1038/263323a0
- Turner, R. D., Ratcliffe, E. C., Wheeler, R., Golestanian, R., Hobbs, J. K., and Foster, S. J. (2010). Peptidoglycan architecture can specify division planes in *Staphylococcus aureus*. *Nat. Commun.* 1:26. doi: 10.1038/ncomms1025
- Turner, R. D., Vollmer, W., and Foster, S. J. (2014). Different walls for rods and balls: the diversity of peptidoglycan. *Mol. Microbiol.* 91, 862–874. doi: 10.1111/mmi.12513
- Typas, A., Banzhaf, M., Gross, C. A., and Vollmer, W. (2012). From the regulation of peptidoglycan synthesis to bacterial growth and morphology. *Nat. Rev. Microbiol.* 10, 123–136. doi: 10.1038/nrmicro2677
- Uehara, T., and Park, J. T. (2003). Identification of MpaA, an amidase in *Escherichia coli* that hydrolyzes the γ -D-Glutamyl-meso-Diaminopimelate bond in murein peptides. *J. Bacteriol.* 185, 679–682. doi: 10.1128/JB.185.2.679-682.2003
- Uehara, T., Parzych, K. R., Dinh, T., and Bernhardt, T. G. (2010). Daughter cell separation is controlled by cytokinetic ring-activated cell wall hydrolysis. *EMBO J.* 29, 1412–1422. doi: 10.1038/emboj.2010.36
- Van Heijenoort, J. (2001). Formation of the glycan chains in the synthesis of bacterial peptidoglycan. *Glycobiology* 11, 25R–36R. doi: 10.1093/glycob/11.3.25R
- Van Heijenoort, J. (2011). Peptidoglycan Hydrolases of *Escherichia coli*. *Microbiol. Mol. Biol. Rev.* 75, 636–663. doi: 10.1128/MMBR.00022-11
- Varghese, J. N., Hrmova, M., and Fincher, G. B. (1999). Three-dimensional structure of a barley β -D-glucan exohydrolase, a family 3 glycosyl hydrolase. *Structure* 7, 179–190. doi: 10.1016/S0969-2126(99)80024-0
- Visweswaran, G. R., Steen, A., Leenhouts, K., Szeliga, M., Ruban, B., Hesselting-Meinders, A., et al. (2013). AcMD, a homolog of the major autolysin AcMA of *Lactococcus lactis*, binds to the cell wall and contributes to cell separation and autolysis. *PLoS ONE* 8:e72167. doi: 10.1371/journal.pone.0072167
- Visweswaran, G. R. R., Leenhouts, K., Van Roosmalen, M., Kok, J., and Buist, G. (2014). Exploiting the peptidoglycan-binding motif, LysM, for medical and industrial applications. *Appl. Microbiol. Biotechnol.* 98, 4331–4345. doi: 10.1007/s00253-014-5633-7
- Vollmer, W. (2012). Bacterial growth does require peptidoglycan hydrolases. *Mol. Microbiol.* 86, 1031–1035. doi: 10.1111/mmi.12059
- Vollmer, W., Blanot, D., and De Pedro, M. A. (2008a). Peptidoglycan structure and architecture. *FEMS Microbiol. Rev.* 32, 149–167. doi: 10.1111/j.1574-6976.2007.00094.x
- Vollmer, W., and Holtje, J. V. (2004). The architecture of the murein (peptidoglycan) in gram-negative bacteria: vertical scaffold or horizontal layer(s)? *J. Bacteriol.* 186, 5978–5987. doi: 10.1128/JB.186.18.5978-5987.2004
- Vollmer, W., Joris, B., Charlier, P., and Foster, S. (2008b). Bacterial peptidoglycan (murein) hydrolases. *FEMS Microbiol. Rev.* 32, 259–286. doi: 10.1111/j.1574-6976.2007.00099.x
- Votsch, W., and Templin, M. F. (2000). Characterization of a β -N-acetylglucosaminidase of *Escherichia coli* and elucidation of its role in mureopeptide recycling and β -lactamase induction. *J. Biol. Chem.* 275, 39032–39038. doi: 10.1074/jbc.M004797200
- Weidel, W., and Pelzer, H. (1964). Bagshaped macromolecules—a new outlook on bacterial cell walls. *Adv. Enzymol. Relat. Subj. Biochem. J.* 26, 193–232. doi: 10.1002/9780470122716.ch5
- Wright, G. D., Molinas, C., Arthur, M., Courvalin, P., and Walsh, C. T. (1992). Characterization of VanY, a DD-carboxypeptidase from vancomycin-resistant *Enterococcus faecium* BM4147. *Antimicrob. Agents Chemother.* 36, 1514–1518. doi: 10.1128/AAC.36.7.1514
- Wyckoff, T. J., Taylor, J. A., and Salama, N. R. (2012). Beyond growth: novel functions for bacterial cell wall hydrolases. *Trends Microbiol.* 20, 540–547. doi: 10.1016/j.tim.2012.08.003
- Xu, Q., Chiu, H. J., Farr, C. L., Jaroszewski, L., Knuth, M. W., Miller, M. D., et al. (2014). Structures of a bifunctional cell wall hydrolase CwIT containing a novel bacterial lysozyme and an NlpC/P60 DL-endopeptidase. *J. Mol. Biol.* 426, 169–184. doi: 10.1016/j.jmb.2013.09.011
- Xu, Q., Mengin-Lecreux, D., Liu, X. W., Patin, D., Farr, C. L., Grant, J. C., et al. (2015). Insights into substrate specificity of NlpC/P60 cell wall hydrolases containing bacterial SH3 domains. *MBio* 6, e02327–e02314. doi: 10.1128/mBio.02327-14
- Yamada, S., Sugai, M., Komatsuzawa, H., Nakashima, S., Oshida, T., Matsumoto, A., et al. (1996). An autolysin ring associated with cell separation of *Staphylococcus aureus*. *J. Bacteriol.* 178, 1565–1571. doi: 10.1128/jb.178.6.1565-1571.1996
- Yamamoto, E., Muramatsu, H., and Nagai, K. (2014). *Vulgatibacter incomptus* gen. nov., sp. nov. and *Labilithrix luteola* gen. nov., sp. nov., two myxobacteria isolated from soil in Yakushima Island, and the description of *Vulgatibacteraceae* fam. nov., *Labilithricaceae* fam. nov. and *Anaeromyxobacteraceae* fam. nov. *Int. J. Syst. Evol. Microbiol.* 64, 3360–3368. doi: 10.1099/ij.s.0.063198-0
- Yang, D. C., Tan, K., Joachimiak, A., and Bernhardt, T. G. (2012). A conformational switch controls cell wall-remodelling enzymes required for bacterial cell division. *Mol. Microbiol.* 85, 768–781. doi: 10.1111/j.1365-2958.2012.08138.x
- Yang, J., Peng, Q., Chen, Z., Deng, C., Shu, C., Zhang, J., et al. (2013). Transcriptional regulation and characteristics of a novel N-acetylmuramoyl-L-alanine amidase gene involved in *Bacillus thuringiensis* mother cell lysis. *J. Bacteriol.* 195, 2887–2897. doi: 10.1128/JB.00112-13
- Young, R. (1992). Bacteriophage lysis: mechanism and regulation. *Microbiol. Rev.* 56, 430–481.
- Yu, M., Yang, J., and Guo, M. (2016). Is the LysM domain of *Listeria monocytogenes* p60 protein suitable for engineering a protein with high peptidoglycan binding affinity? *Bioengineered* 7, 406–410. doi: 10.1080/21655979.2016.1200772
- Yutin, N., and Galperin, M. Y. (2013). A genomic update on clostridial phylogeny: Gram-negative spore formers and other misplaced clostridia. *Environ. Microbiol.* 15, 2631–2641. doi: 10.1111/1462-2920.12173
- Zahl, D., Wagner, M., Bischof, K., Bayer, M., Zavec, B., Beranek, A., et al. (2005). Peptidoglycan degradation by specialized lytic transglycosylases associated with Type III and Type IV secretion systems. *Microbiology* 151, 3455–3467. doi: 10.1099/mic.0.28141-0
- Zoll, S., Schlag, M., Shkumatov, A. V., Rautenberg, M., Svergun, D. I., Gotz, F., et al. (2012). Ligand-binding properties and conformational dynamics of autolysin repeat domains in staphylococcal cell wall recognition. *J. Bacteriol.* 194, 3789–3802. doi: 10.1128/JB.00331-12
- Zou, Y., and Hou, C. (2010). Systematic analysis of an amidase domain CHAP in 12 *Staphylococcus aureus* genomes and 44 staphylococcal phage genomes. *Comput. Biol. Chem.* 34, 251–257. doi: 10.1016/j.compbiolchem.2010.07.001

Conflict of Interest Statement: CP is permanent employee of BioFilm Control and declare his company provided support in the form of salary.

The remaining authors declare that the research was conducted in the absence of any commercial or financial relationships that could be construed as a potential conflict of interest.

Copyright © 2019 Vermassen, Leroy, Talon, Provot, Popowska and Desvaux. This is an open-access article distributed under the terms of the Creative Commons Attribution License (CC BY). The use, distribution or reproduction in other forums is permitted, provided the original author(s) and the copyright owner(s) are credited and that the original publication in this journal is cited, in accordance with accepted academic practice. No use, distribution or reproduction is permitted which does not comply with these terms.



Peptidoglycan Muropeptides: Release, Perception, and Functions as Signaling Molecules

Oihane Irazoki, Sara B. Hernandez and Felipe Cava*

Laboratory for Molecular Infection Medicine Sweden, Department of Molecular Biology, Umeå Centre for Microbial Research, Umeå University, Umeå, Sweden

OPEN ACCESS

Edited by:

Patrick Joseph Moynihan,
University of Birmingham,
United Kingdom

Reviewed by:

Joseph P. Dillard,
University of Wisconsin-Madison,
United States
Jonathan Dworkin,
Columbia University,
United States

*Correspondence:

Felipe Cava
felipe.cava@molbiol.umu.se

Specialty section:

This article was submitted to
Microbial Physiology and Metabolism,
a section of the journal
Frontiers in Microbiology

Received: 09 October 2018

Accepted: 27 February 2019

Published: 28 March 2019

Citation:

Irazoki O, Hernandez SB and Cava F
(2019) Peptidoglycan Muropeptides:
Release, Perception, and Functions
as Signaling Molecules.
Front. Microbiol. 10:500.
doi: 10.3389/fmicb.2019.00500

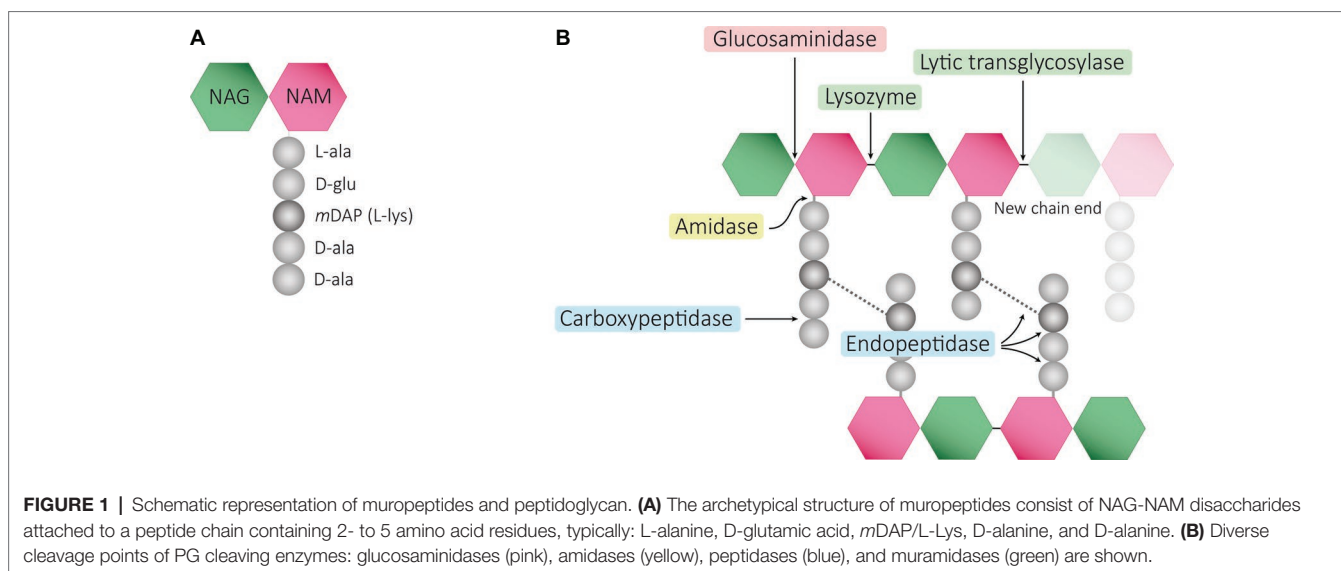
Peptidoglycan (PG) is an essential molecule for the survival of bacteria, and thus, its biosynthesis and remodeling have always been in the spotlight when it comes to the development of antibiotics. The peptidoglycan polymer provides a protective function in bacteria, but at the same time is continuously subjected to editing activities that in some cases lead to the release of peptidoglycan fragments (i.e., muropeptides) to the environment. Several soluble muropeptides have been reported to work as signaling molecules. In this review, we summarize the mechanisms involved in muropeptide release (PG breakdown and PG recycling) and describe the known PG-receptor proteins responsible for PG sensing. Furthermore, we overview the role of muropeptides as signaling molecules, focusing on the microbial responses and their functions in the host beyond their immunostimulatory activity.

Keywords: peptidoglycan, PG cleaving enzymes, PG recycling, PG receptors, signaling functions, bacterial interactions

INTRODUCTION

Most bacteria surround themselves with a protective cell wall to repel environmental challenges. These tough cell walls are primarily composed of a peptidoglycan (PG) exoskeleton, also called the murein sacculus (Vollmer et al., 2008a; de Pedro and Cava, 2015). PG is a highly dynamic macromolecule subjected to constant remodeling in response to changing environmental conditions (Horcajo et al., 2012). It counteracts osmotic pressure, maintains cell shape and integrity, and serves as a protective barrier against physical, chemical, and biological threats (Holtje, 1998; Vollmer et al., 2008a). PG is found on the outside of the cytoplasmic membrane of almost all bacteria (Nanninga, 1998; Mengin-Lecreulx and Lemaitre, 2005) and presents a conserved overall composition and biogenesis, although the complexity and thickness of the structure vary (Cava and de Pedro, 2014). Peptidoglycan also serves as a scaffold for anchoring other cell envelope components such as proteins (Dramsı et al., 2008) and teichoic acids (Neuhaus and Baddiley, 2003).

Structurally speaking, the PG sacculus is made up of linear glycan strands cross-linked to each other by short peptide chains forming a continuous layer. The glycan backbone generally consists of repeating disaccharides of *N*-acetylglucosamine (NAG) and *N*-acetylmuramic acid (NAM) covalently attached to a peptide chain containing 2–5 amino acid residues. The archetypical peptide stem structure is L-alanine, D-glutamic acid, a dibasic amino acid [typically



meso-diaminopimelic acid (*mDAP*) or L-lysine], D-alanine, and D-alanine (**Figure 1A**). Some of the peptide chains from adjacent glycan strands are cross-linked, resulting in a thick three-dimensional multi-layered meshwork. This arrangement is widely conserved across most bacterial species; however, the chemistry of the residues of the peptide stem, the glycan chains, and the type of crosslinking can vary (Vollmer et al., 2008a). These variations alter the properties of the cell wall and allow for great diversity in fine structure and architecture (Schleifer and Kandler, 1972; Vollmer and Bertsche, 2008; Cava and de Pedro, 2014; Turner et al., 2014). For more detailed information about PG structure, synthesis, and regulation, we refer to extended reviews (Vollmer et al., 2008a; Typas et al., 2011; Egan et al., 2017).

During growth and maturation, PG is degraded by dedicated enzymes, which shed PG fragments (or mucopeptides) in a process termed PG turnover. In *E. coli*, in a single generation of growth, as much as 50% of the PG is excised from the cell wall as anhydromucopeptides, suggesting a robust turnover of the cell wall (Doyle et al., 1988). Around the 95% of these are efficiently recovered and reused through the PG-recycling pathway (Goodell and Schwarz, 1985; Park and Uehara, 2008).

In recent years, PG has been of much interest not only because it is one of the major antibiotic targets (Kohanski et al., 2010) but also due to its importance in host physiology and metabolism since it presents immunostimulatory activities (Girardin et al., 2003a,b). Some PG-derived fragments are recycled for cell wall biosynthesis but they are also used in bacterial communication and are detected by eukaryotes to initiate an immune response (Girardin et al., 2003a,b; Boudreau et al., 2012; Woodhams et al., 2013; Dworkin, 2014). Recent data suggest that mucopeptides have many diverse roles, including involvement in symbiotic associations, microbial interactions, and pathogenesis in animals and plants. In this review, we focus on the signaling functions of PG fragments, describing the mechanisms involved in the release of these molecules and the means by which they are sensed by bacterial and host cells.

MUROPEPTIDES RELEASE

It is well documented that the PG sacculus is remodeled during bacterial growth and that this process causes the release of mucopeptides. The discharge of PG fragments can occur as a consequence of the disruption of PG during growth or by the complete lysis of cells.

PG Cleaving Enzymes

Cleavage of PG is required for fundamental physiological processes in bacteria such as enlargement of the PG sacculus during bacterial growth and cell separation during cell division (Holtje, 1998; Layec et al., 2008; Uehara et al., 2010; Typas et al., 2011; Uehara and Bernhardt, 2011; Waldemar, 2012); incorporation and assembly of protein complexes into the cell wall (e.g., secretion, conjugation, and flagellum systems) (Dijkstra and Keck, 1996; Koraimann, 2003; Scheurwater et al., 2008; Scheurwater and Burrows, 2011; Stohl et al., 2013); or sporulation and resuscitation of dormant states (Keep et al., 2006; Wyckoff et al., 2012; Popham and Bernhards, 2015). Enzymes cleaving the bonds that exist within PG are generally known as PG hydrolases (PGHs), and although some (i.e., lytic transglycosylases) do not present chemical hydrolytic activity, from now on we will refer to all them as PGHs. Despite the large number and diversity of proteins cleaving the PG, they can be grouped accordingly to the type of the bond cleaved such as glycosidases (cleaving glycosidic bonds of the glycan strands), amidases (hydrolyzing the amide bond between the first amino acid of the stem peptide and the NAM), and peptidases (cleaving bonds between amino acids present in the stem peptides) (**Figure 1B**). They often act on a particular type of PG, cleaving intact high-molecular-weight murein sacculi and its soluble fragments (Vollmer et al., 2008b).

PG glycan chains contain two glycosidic bonds sensitive to the activity of glycosidases: the bond between a NAG and the

adjacent NAM is hydrolyzed by *N*-Acetyl- β -glucosaminidases (*N*-acetylglucosaminidases), while muramidases (or muralytic enzymes) cleave the bond between sequential NAM and NAG residues (**Figure 1B**). Muramidases are divided into two subgroups depending on their catalytic mechanism: lysozymes are hydrolytic enzymes that add water across the glycosidic bond during the cleavage generating a reducing NAM product; while lytic transglycosylases (LTs) catalyze an intramolecular rearrangement involving the C-6 hydroxyl group of the NAM resulting in the formation of unique 1,6-anhydro-*N*-acetylmuramic acid products, the so-called anhydromuropeptides (Holtje et al., 1975; Thunnissen et al., 1995; Callewaert and Michiels, 2010). PG peptidases can be classified into two groups: carboxypeptidases (removing the C-terminal amino acid of peptide stems) and endopeptidases (cleaving within the peptide cross-links), and both can be referred to as DD-, LD-, or DL-peptidases based on the isomeric form of the two amino acids that are split (Vollmer et al., 2008b).

PGHs are ubiquitous among all eubacteria (Shockman et al., 1996; Firczuk and Bochtler, 2007; Layec et al., 2008; Sharma et al., 2016). Many species present a large number of PG cleaving enzymes, and while for some of them, functional redundancy has been observed under laboratory conditions (van Heijenoort, 2011; Rolain et al., 2012; Singh et al., 2012), and specific functions have been demonstrated for others (Schaub et al., 2016; Santin and Cascales, 2017). During growth, PGHs are capable of fulfilling the PG-remodeling demands acting on the murein sacculus without disrupting the structural

integrity of the cell wall, but a regulatory failure of their activity could easily lead to uncontrolled PG degradation and consequent cell lysis (autolysis) (van Heijenoort, 2011). Therefore, bacterial PGHs (so-called autolysins) must be regulated in order to prevent accidental lysis (Rice and Bayles, 2008). Regulation of bacterial PGH activity has been characterized at different levels including gene expression, subcellular localization, the formation of multi-enzyme catalytic complexes, or modification of the PG substrate (Holtje and Tuomanen, 1991; Vollmer et al., 2008b; Chapot-Chartier, 2010; Morlot et al., 2010).

The cleavage of covalent bonds in the murein sacculus during cell wall metabolism leads to the release of PG-derived material. Depending on the cleaving enzyme, different fragments can be released from the PG sacculus: both lysozymes and lytic transglycosylases release disaccharide-peptides, but while the hydrolytic reaction of lysozymes generates a terminal reducing NAM (Callewaert and Michiels, 2010), lytic transglycosylases produce anhydromuropeptides which present a 1,6-anhydro ring at the NAM (anhNAM) (Holtje et al., 1975); monosaccharide-peptides (named here muramyl peptides) can also be produced by the activity of *N*-acetylglucosaminidases (Votsch and Templin, 2000). Even though peptidase or amidase activities do not release muropeptides or muramyl-peptides themselves, their role remodeling the high-molecular-weight murein sacculus or its soluble fragments (e.g., amidase activity releases NOD1-stimulatory free peptides) certainly shape the number and the chemical composition of the released molecules (Lenz et al., 2016).

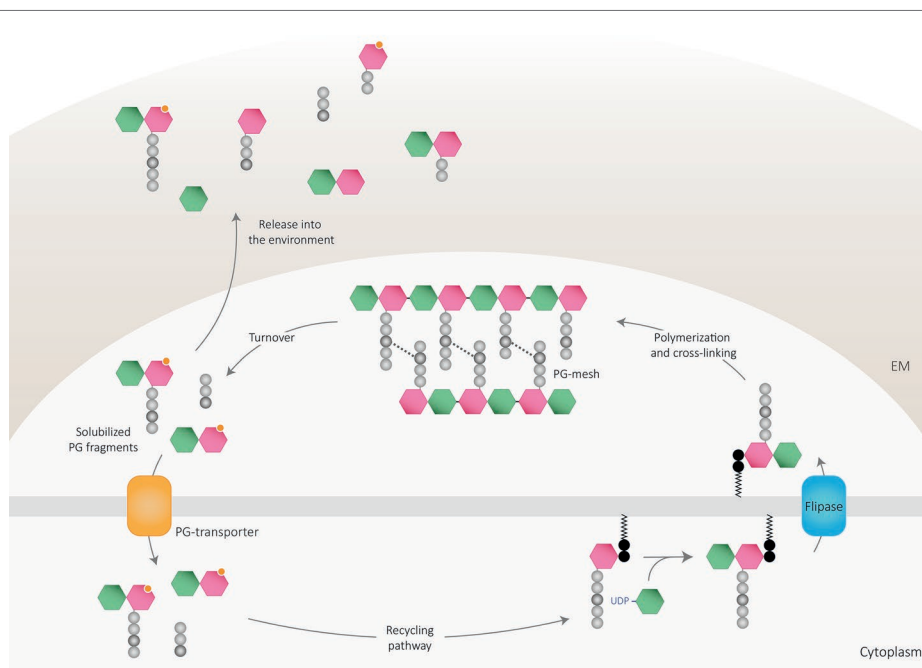


FIGURE 2 | Peptidoglycan recycling and muropeptide release. PG cleaving enzymes digest the sacculi delivering PG fragments to the periplasm, which can be either released to the environment or transported into the cytoplasm through PG transporters. Once in the cytosol, PG fragments might enter the recycling pathway to finally be reincorporated into the newly polymerized PG mesh or used as an own-energy source by the cell. Part of PG-turnover products is released to the environment, where are detected by other cells and can act as signaling molecules. EM: extracellular matrix.

PG fragments are solubilized from the murein sacculus in active bacteria by a process termed cell wall turnover (**Figure 2**) that leads to the excision of muropeptides, shedding, and cell wall catabolism (Chaloupka, 1962; Doyle et al., 1988). As mentioned, up to half of the pre-existing PG is turned over and discharged from the wall every generation in both Gram-positive and Gram-negative bacteria (Mauck et al., 1971; Wong et al., 1974; Dworkin, 2014). The released material can be reimported into the bacterial cytoplasm and reused for PG synthesis or as nutrient or energy sources through an efficient PG recycling pathway (Chaloupka and Strnadova, 1972; Goodell and Schwarz, 1985; Park and Uehara, 2008; Borisova et al., 2016) or liberated to the environment. Accordingly, the bacterial PG recycling pathway modulates to some extent the bioavailability of soluble fragments (Johnson et al., 2013).

PG Recycling

Historically, it has been assumed that PG recycling was limited to Gram-negative bacteria since, in comparison, larger amounts of PG turnover products were isolated from the growth medium of several Gram-positives (Mauck et al., 1971). Nevertheless, orthologs of some recycling enzymes are present in most Gram-positive bacteria (Park and Uehara, 2008; Litzinger et al., 2010; Reith and Mayer, 2011). In fact, recent studies have shown that PG recycling also occurs in different Gram-positives (Borisova et al., 2016; Kluj et al., 2018), although reuse of PG sugars and peptide turnover products for murein synthesis in these organisms is currently unclear. PG recycling has been more extensively studied in Gram-negative bacteria (Johnson et al., 2013; Dhar et al., 2018) where recycling begins with degradation of the PG by the activity of PGHs. LTs are the main enzymes involved in high-molecular-weight sacculus degradation and therefore play a key role in PG recycling (Dominguez-Gil et al., 2016).

Most bacteria encode multiple LTs (e.g., 8 have been described in *E. coli* and 11 in *P. aeruginosa*), which can be divided into soluble periplasmic LTs (named SltS) or membrane-attached LTs (named MltS), and can perform the cleavage at the end of the glycan strands (exolytic) and/or in the middle of the PG chains (endolytic) (Dik et al., 2017). Although redundancy in generating soluble anhydromuropeptides has been observed by single and multiple deletion analysis (Korsak et al., 2005; Lamers et al., 2015), a unique contribution from some hydrolytic enzymes has also been proven (Kraft et al., 1999). Particularly, Slt70 of *E. coli* is considered to be the major LT involved in PG-turnover, as it has been shown to be the main enzyme following β -lactam treatment (Cho et al., 2014).

Depending on the efficiency and regulation of the PG-recycling pathway of the bacterium, anhydromuropeptides can either be transported to the cytoplasm (where they are subsequently processed by the activity of several enzymes) or released to the environment by a currently unknown mechanism (**Figure 2**). In *E. coli*, the gate of entry for the internalization of soluble anhydromuropeptide monomers (NAG-anhNAM-peptides) into the cytoplasm is the AmpG permease, an inner transmembrane

protein that specifically takes up anhydromuropeptides or free anhydrodisaccharides (Cheng and Park, 2002). Deletion of the gene encoding AmpG prevents the uptake of anhydromuropeptides leading to their accumulation in the medium (Jacobs et al., 1994; Wiedemann et al., 1998; Garcia and Dillard, 2008; Nyholm, 2009) revealing the importance of recycling as a limiting factor for PG-fragment release. Once in the cytosol, anhydromuropeptides are further hydrolyzed by a mechanism involving a set of dedicated enzymes (extensively reviewed in Johnson et al., 2013; Dhar et al., 2018). The specific activities of NagZ (*N*-acetylglucosaminidase) and AmpD (*N*-L-alanine amidase) on molecules presenting anhNAM structure yield NAG, anhNAM, and free peptides in the cytoplasm (Holtje et al., 1994; Cheng et al., 2000; Votsch and Templin, 2000; Lee et al., 2009). Resulting tetrapeptides are hydrolyzed by the action of the L,D-carboxypeptidase LdcA (Templin et al., 1999) into tripeptides, which can be degraded into individual amino acids for utilization as nutrient or energy sources (Schroeder et al., 1994; Schmidt et al., 2001; Uehara and Park, 2003) or attached directly to UDP-NAM by the murein peptide ligase Mpl (Mengin-Lecreulx et al., 1996; Das et al., 2011). Ligated UDP-NAM-tripeptides and processed sugar products can then be recycled by entering the pathway for *de novo* PG synthesis (White and Pasternak, 1967; Uehara et al., 2005, 2006).

The internalization of anhydromuropeptides and subsequent breakdown in order to supply a demanding nutrient or energy sources seems unlikely under favorable growth conditions (Uehara and Park, 2008), and even if enzymes involved in PG degradation are expressed during growth (Park and Uehara, 2008; Maqbool et al., 2012), it has been estimated that 97% of the recovered material is reutilized for new PG synthesis (Goodell, 1985). Furthermore, even if the switching control between PG recycling and catabolism is not clear yet, some genes encoding for enzymes involved in degradation of the peptide have been shown to be de-repressed under nutrient starvation (Shimada et al., 2013) pointing out a tight control between these two processes.

Distribution and Function(s) of PG Recycling

While PG turnover is widespread in bacteria, it remains unclear how prevalent PG recycling is. Since this pathway relies upon the transport of anhydromuropeptides into the cytosol, the existence of AmpG-like permeases may be required for PG recycling. Though PG recycling has only been experimentally proven in certain species, AmpG is present in diverse Gram-negatives (Uehara and Park, 2008) but apparently absent in Gram-positives (Reith and Mayer, 2011). This observation may fit with a limited number of known LTs in Gram-positives (Dik et al., 2017) and their apparently restricted function to PG enlargement (Tsui et al., 2016), spore formation/germination (Heffron et al., 2009), or induction of autolysis (Wydaud-Dematteis et al., 2018). On the other hand, abundant lysozyme-like enzymes, *N*-acetylglucosaminidases and amidases, have been described to act at the cell wall compartment in Gram-positive bacteria (Lopez et al., 1997; Smith et al., 2000; Vollmer and Bertsche, 2008). These activities liberate PG fragments

presenting terminal-reducing NAM and free peptides, which can be taken up by other specific transporters, offsetting the lack of an AmpG permease (Reith and Mayer, 2011).

The presence of orthologs of other genes involved in the pathway also points toward the existence of a dedicated route for recycling PG-degradation products. In this regard, genes involved in the processing and reutilization of PG sugars are widespread among both Gram-negative and Gram-positive bacteria (Jaeger and Mayer, 2008; Borisova et al., 2014), suggesting an extensive role and consequently important function(s) of PG recycling. Though the primary function of PG recycling is not clear (it is not essential under experimental conditions) (Jacobs et al., 1994; Cheng et al., 2000), it has been reported to be involved in a range of diverse processes. It is still widely thought that reutilization of PG fragments as carbon and energy sources is potentially critical to promote growth under nutrient-limiting conditions, but for *E. coli* there is no clear evidence supporting this hypothesis. Nevertheless, reutilization of PG recycled products has been observed to be essential in particular cases. The use of recycled NAM for cell wall synthesis apparently increases survival of *Bacillus subtilis* and *Staphylococcus aureus* under starvation conditions during stationary phase (Borisova et al., 2016), which is consistent with previous findings showing that in Gram-positive bacteria MurQ and NagZ expression is higher in stationary phase (Litzinger et al., 2010; Botella et al., 2011). In the Gram-negative oral anaerobe *Tannerella forsythia*, which is unable to synthesize its own PG sugars, scavenging environmental muropeptides (released by cohabiting bacteria) through an AmpG-like transporter is vital for PG-synthesis (Ruscitto et al., 2017). Additionally, in two Cyanobacteria species, PG recycling has been suggested to be an energy-saving strategy to promote growth under light-limiting conditions (Jiang et al., 2010).

Aside from the importance of the reutilization of PG products, other functions proposed for PG recycling are more related to the production and accumulation of solubilized cell wall fragments when the pathway is not working efficiently. In this regard, a variety of messenger functions have been attributed to PG fragments, which are compiled below.

Alternative Ways to Produce Soluble PG Fragments

The essentiality and uniqueness of the bacterial PG make this structure an excellent antibacterial target (Kohanski et al., 2010; Muller et al., 2017). It is therefore not surprising that lysozymes, which exhibit a highly specific cleavage activity on PG, are widespread (Callewaert and Michiels, 2010). Although the antimicrobial action of lysozymes is also intimately related to their structure (Ibrahim et al., 2001), their catalytic activity disrupts PG by hydrolyzing the β -1,4 glycosidic bonds linking adjacent PG monomers, resulting in cell lysis and successive release of muropeptides. Production of lysozymes constitutes a natural defence mechanism against bacterial pathogens (Bertsche et al., 2015), and consequently, pathogenic bacteria have developed different mechanisms to evade lysozyme action such as modification of the PG (Yadav et al., 2018), alteration

of the charge, and strength of the envelope or the production of lysozyme inhibitors (Ragland and Criss, 2017).

As a defence mechanism, plants and animals have exploited PG structure and developed mechanisms to monitor the presence of bacteria through PG recognition proteins (PGRPs) (Royet et al., 2011; Gust, 2015), some of which also present PG-cleavage activity separate from their ability to sense bacterial PG (Royet and Dziarski, 2007; Royet et al., 2011). These PGRPs present *N*-acetylmuramoyl-L-alanine amidase activity that hydrolyzes the amide bond between NAG and L-alanine in peptidoglycan and removes the stem peptides from the glycan chain, contributing to the release of PG fragments to the environment.

Furthermore, many Gram-negative bacteria can interact with other microbes and the host by releasing outer membrane vesicles (OMVs) to the environment (Kulp and Kuehn, 2010). Formation of OMVs has also been suggested as another mechanism of delivering peptidoglycan in several Gram-negative human pathogens (Kaparakis et al., 2010; Bielig et al., 2011).

DETECTION OF RELEASED MUROPEPTIDES

Specific roles for a variety of soluble PG fragments as messenger molecules have been known for decades (Adam and Lederer, 1984) and have come into focus more recently. Microbe-associated molecular patterns (MAMPs) are defined as molecular signatures highly conserved in bacteria but absent from the host cells (Boller and Felix, 2009). MAMPs are detected by specific receptors termed pattern recognition receptors (PRRs) that are able to bind PG among other molecules (including lipopolysaccharides, lipoteichoic acids, lipoproteins, microbial DNA and RNA, flagellin, fungal cell wall glucans, or chitin) (Strober et al., 2006; Cinel and Opal, 2009; Mogensen, 2009; Diacovich and Gorvel, 2010). In the host, MAMP recognition leads to the activation of PRR-induced signal pathways that trigger the expression of a broad range of molecules, including adaptor molecules, cytokines, chemokines, cell adhesion molecules, and immunoreceptors, which induce proinflammatory and antimicrobial responses (Akira et al., 2006).

Despite the abundance of PG-containing microbiota and the numerous studies implicating PG as an immunostimulatory signal (Boneca, 2005), little is known about the systemic concentration of PG fragments in the environment or host, even though it is well documented that muropeptides serve also as signaling molecules and that a collection of receptor systems have evolved to detect these molecules.

PG Sensors

In the last two decades, multiple structural motifs and proteins have been described to bind PG. Interestingly, not a single class of microorganism is sensed by only one type of receptor, hence ensuring a rapid and potent response while allowing for some specificity during, for example, infection. In this review, we summarize those receptors that recognize and bind PG.

Lysin Motif

LysM (LysM) is considered a general PG-binding domain that binds specifically to molecules containing repetitions of NAG such as chitin, peptidoglycan, and short oligosaccharides (Buist et al., 2008; Mesnage et al., 2014). The LysM, usually 42–48 amino acids in length, is an ubiquitous modular cassette present across all kingdoms except for Archaea (Zhang et al., 2009). Usually, multiple motifs within one LysM domain are separated by spacing sequences (typically Ser-Thr-Asp/Pro) forming a flexible region in-between (Buist et al., 2008; Ohnuma et al., 2008). While it was initially identified in bacterial cell wall degrading enzymes [e.g., *E. coli* lytic transglycosylase MltD (Bateman and Bycroft, 2000), *Enterococcus faecalis* N-acetylglucosaminidase AtlA (Mesnage et al., 2014), *B. subtilis* D,L-endopeptidase CwlS (Wong et al., 2014), or *Lactococcus lactis* N-acetylglucosaminidase AcmA (Steen et al., 2005)], LysM is also present in many other proteins involved in PG synthesis or remodeling (Buist et al., 2008; Buendia et al., 2018). The study of several proteins involved in bacterial peptidoglycan synthesis and remodeling has shown that even when PG peptide stems are not necessary for LysM binding, they modulate the binding affinity (Mesnage et al., 2014). In plants, the recognition of PG by LysM containing proteins initiates a signaling cascade that can suppress the host immune response (Gust, 2015). Furthermore, several LysM-containing proteins have been described to be involved in diverse processes, including recognition of bacteria, during bacteria-plant symbiosis, bacteriophage infection, and assembly of bacterial spores (Andre et al., 2008; Buist et al., 2008; Zipfel, 2014; Gust, 2015; Dworkin, 2018).

PASTA Domain

Penicillin-binding and Ser/Thr kinase-associated (PASTA) proteins are essential tools for bacteria to sense and respond to the host environment and antibiotic stress as they play a central role in virulence and β -lactam resistance *via* their ability to regulate metabolism, cell division, and cell wall homeostasis through the recognition of mucopeptides (Shah et al., 2008; Pensinger et al., 2018). The PASTA motif is involved in recognizing not only self-PG fragments but also exogenous mucopeptides (Shah et al., 2008). Ligands are mostly species-specific, but a preference for mucopeptides from species producing cell walls of similar composition (for example, containing *m*DAP in the third position in the peptide stem) has also been described (Lee et al., 2010; Mir et al., 2011).

NOD-Like Receptors

Nucleotide binding and oligomerization domain proteins (NODs) are intracellular regulatory proteins that respond to a variety of signaling molecules including PG-derived fragments (Girardin et al., 2003c; Martinon and Tschopp, 2005; McDonald et al., 2005; Dziarski and Gupta, 2006; Strober et al., 2006; Le Bourhis et al., 2007; Sorbara and Philpott, 2011; Keestra-Gounder and Tsolis, 2017). NLRs show a conserved architecture, containing a C-terminal leucine-rich repeat domain, a central nucleotide binding and oligomerization domain, and N-terminal caspase activation and recruitment domain (Inohara and Nunez, 2003; Martinon and Tschopp, 2005). NOD1 and

NOD2 are the best characterized NLRs, so far. NOD1 recognizes molecules containing D-Glu-*m*DAP (including PG free, mono-, and disaccharide peptides) (Girardin et al., 2003a), which are primarily found in Gram-negative bacteria with some exceptions such as *Bacillus* spp., *Mycobacterium* sp., *Listeria* spp., and *Lactobacillus plantarum* (Girardin et al., 2003c; Bourhis et al., 2007; Mahapatra et al., 2008; Bernard et al., 2011), while NOD2 senses NAM-D-Ala-D-Glu unit, ubiquitously present in both Gram-positive and Gram-negative mono- and disaccharide di-, tri-, and tetrapeptides (Girardin et al., 2003b; Dagil et al., 2016). PG fragments from non-invasive bacteria are transported into the eukaryotic cytosol through bacterial secretion systems, endocytosis, or specific membrane transport systems [PEPT: PepT1, PepT2, and pannexin (Vavricka et al., 2004; Charrier and Merlin, 2006; Kanneganti et al., 2007; Swaan et al., 2008)] or are delivered *via* OMVs (Philpott et al., 2014; Kaparakis-Liaskos and Ferrero, 2015; Canas et al., 2018), where they are sensed by both NOD receptors. The detection of PG by NOD proteins results in the activation of intracellular signaling cascades that triggers the nuclear factor- κ B (NF- κ B), innate response involved in inflammatory responses, and antimicrobial activity (Fritz et al., 2006; Meylan et al., 2006; Franchi et al., 2009).

Peptidoglycan Recognition Proteins

Peptidoglycan recognition proteins (PGRPs) are evolutionarily conserved innate immunity molecules homologous to bacteriophage type 2 amidases found in animals and humans that present bactericidal activity (Dziarski, 2004; Royet and Dziarski, 2007). All PGRPs have a carboxy-terminal amidase domain (named PGRP domain) with a specific binding site for muramyl penta-, tetra-, or tri-peptides (Royet and Dziarski, 2007), but some mammalian PGRPs also have an additional binding site specific for bacterial lipopolysaccharide (Tydell et al., 2006; Sharma et al., 2011). So far, diverse PGRPs have been identified in insects [e.g., *Drosophila* has 13 PGRPs (Royet et al., 2011; Kurata, 2014)] and mammals [e.g., humans and mice have four (PGLYRP 1–4) (Liu et al., 2000; Lu et al., 2006; Cho et al., 2007; Dziarski and Gupta, 2010)] that recognize diverse PG fragments depending on their affinity and have a function in antibacterial immunity and inflammation. Instead of activating the innate system, PGRPs directly kill bacterial cells by binding PG, either to muramyl-peptides exposed by lytic endopeptidases in Gram-positive bacteria or uniformly to the outer membrane in Gram-negative bacteria (Kashyap et al., 2017). PGRP-PG interaction activates bacterial two-component systems (CsrR-CsrS and CpxA-CpxR in Gram-positive and Gram-negative bacteria, respectively) that induce bacterial lysis by membrane depolarization and the simultaneous induction of oxidative, thiol, and metal stresses, which produce bacterial killing (Royet et al., 2011; Kashyap et al., 2014, 2017). Some data also suggest that the amidase domain acts as a scavenger to degrade PG and control the immune response (Mellroth et al., 2003).

C-Type Lectin-Like Receptors

C-type lectin-like receptors (CTLRs) are a major class of PRR that present an extracellular carbohydrate recognition domain that putatively binds sugar moieties within the glycan backbone

of bacterial PG or the fungal glucan mannan, in a calcium-dependent manner (Plato et al., 2013; Sukhithasri et al., 2013). Upon ligand recognition, specialized CTLRs trigger or inhibit a variety of signaling pathways, thus initiating pathogen phagocytosis, cytokine production, and activating diverse immune responses (Mayer et al., 2017). CTLRs bind to various pathogens, including viruses, fungi, parasites, and bacteria, and little is known about their specific role (if any) in PG detection. Regenerating gene family protein 3A (Reg3A) and mannose-binding lectin (MBL) protein are the only ones proven so far to bind PG (Sukhithasri et al., 2013). Reg3A is a lectin family protein that recognizes bacterial PG and presents bactericidal activity against Gram-positive bacteria (Lehotzky et al., 2010; van Ampting et al., 2012), while MBL is an oligomeric, calcium-dependent serum protein that recognizes both bacterial and fungal cell wall components leading to the activation of the lectin complement pathway (Shi et al., 2004; Nadesalingam et al., 2005).

Hexokinases

Known as the first enzyme involved in glycolysis that catalyzes the phosphorylation of glucose to glucose-6-phosphate, hexokinases are also eukaryotic cytosolic sensors for PG. Recently, it has been suggested that the monomeric sugar NAG, generated during PG hydrolysis, can trigger the activation of the inflammatory programs in immune cells through binding and dissociating the cytosolic hexokinase (Gerriets et al., 2015; Wolf et al., 2016). Active hexokinases are associated with the mitochondrial outer membrane but are released when inhibited by NAG, similar to when glucose-6-phosphate (the product of hexokinase) accumulates the cytosol and promotes activation of the NLRP3 inflammasome, which regulates the processing and secretion of interleukin (IL)-1 β and IL-18 (Shimada et al., 2010). Although the mechanism by which this occurs has not yet been described, a model has been proposed in which

hexokinase acts as a pattern recognition receptor, alerting the cell to the degradation of bacterial PG in phagosomes and activating an inflammatory response *via* disruption of the glycolytic pathway and the mitochondrial function (Wolf et al., 2016).

MECHANISMS TO AVOID PG RECOGNITION

Bacteria have evolved sophisticated molecular strategies to subvert host defences by interfering with molecules involved in pathogen recognition and signaling. Both pathogenic and commensal bacteria are able to modify their PG in order to change the interaction with receptors and therefore avoid triggering the host immune responses (Boneca, 2005; Davis and Weiser, 2011). PG modifications fall into two main groups: (1) modification of glycan backbone to resist catalytic activity of PG-hydrolytic enzymes (*N*-deacetylation, *N*-glycosylation, O-acetylation) and (2) modifications of the stem peptides to evade immune recognition (L-Ala peptide substitutions, D-Glu and *m*DAP amidation, and *m*DAP substitution by L-ornithine). Thus, these modifications constitute a tactic that provides resistance to cell lysis and helps bacteria to evade the host immune system. For specificities about PG modifications, we refer to excellent reviews on the topic (Moynihan et al., 2014; Ragland and Criss, 2017; Yadav et al., 2018).

MUROPEPTIDES AS SIGNALING MOLECULES

PG remodeling produces soluble PG fragments that can have a role in bacteria-bacteria and bacteria-host communication and act as signaling molecules that trigger adaptive responses (Figure 3, Table 1).

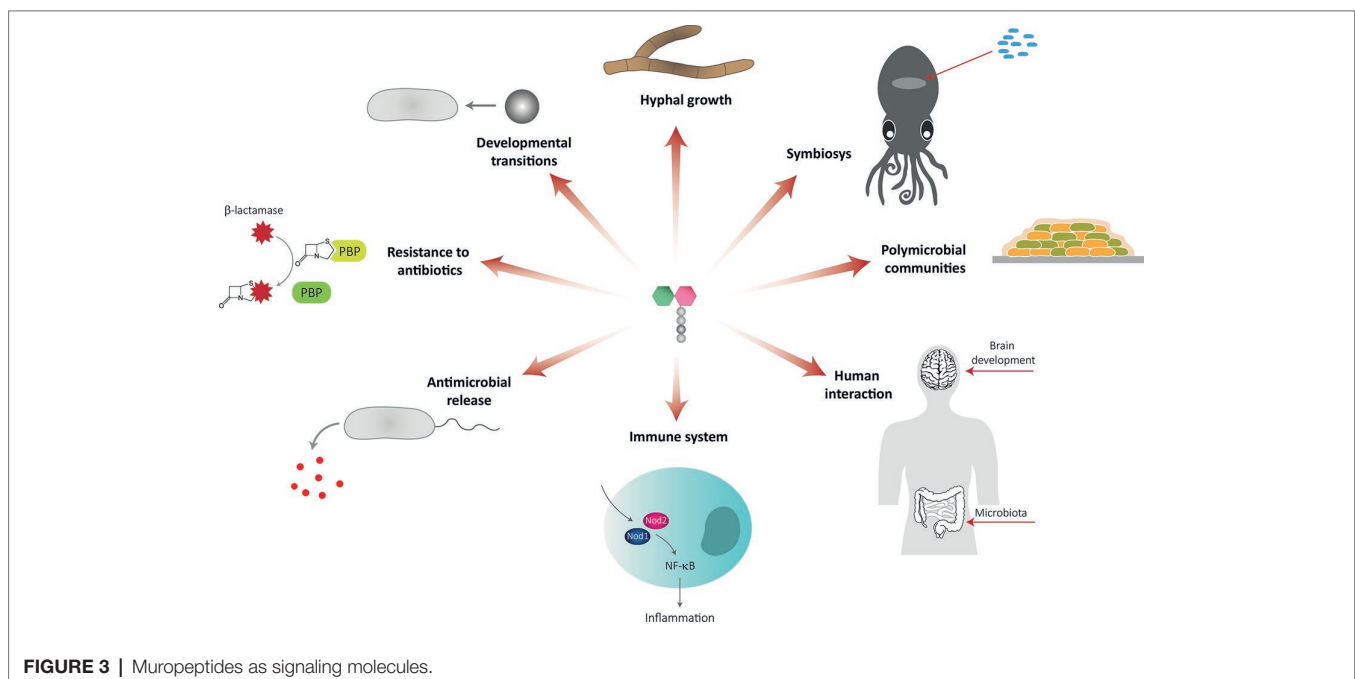
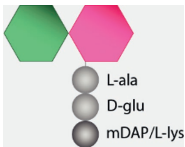

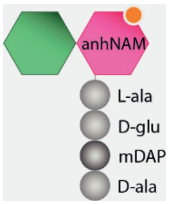


TABLE 1 | Messenger functions of mucopeptides.

PG fragment	Structure	Sensing molecule	Function
Dissacharide tripeptide		PrkC and homologs (STPKs)	Induction of germination (Shah et al., 2008; Dworkin and Shah, 2010) Exit from dormancy (Keep et al., 2006; Mukamolova et al., 2006)
mDAP-type PG (tri-, tetra-, pentapeptides)		NA	Induction of rippling in <i>M. xanthus</i> (Shimkets and Kaiser, 1982)
Monomeric NAG sugar		Ngt1 NA NA	Hyphal growth induction (Alvarez and Konopka, 2007) Antimicrobial induction in <i>P. aeruginosa</i> (Korgaonkar and Whiteley, 2011) and <i>Streptomyces coelicolor</i> (Rigali et al., 2006) CURLI fiber expression in <i>E. coli</i> (Konopka, 2012; Naseem et al., 2012)
Muramyl-dipeptide		Cyr1p	Hyphal growth induction (Xu et al., 2008)
Anhydro-murotetrapeptide (Tracheal cytotoxin, TCT)		NA PGRP2 PGRP3-4	Signaling for morphogenesis (Koropatnick et al., 2004) Hydrolysis of pro-inflammatory PG fragments (Troll et al., 2010) Induction of inflammatory response (Goodson et al., 2005)
Anhydro-muramyltri-peptide		AmpR	β -Lactamase induction: AmpC (Uehara and Park, 2002, 2008)
Disaccharide pentapeptide		BlrB	β -Lactamase induction: Amp, Cep, Imi (Tayler et al., 2010)
Dipeptide		Blal/MecI	β -Lactamase induction: BlaZ, BlaP, MecA (Amoroso et al., 2012)
Dipeptide D-Glu-mDAP (mono and disaccharide peptides containing this structure)		NOD1	NF- κ B Innate response activation (Girardin et al., 2003a,b)
Muramyl-dipeptide (disaccharide di-, tri-, tetrapeptides)		NOD2	NF- κ B Innate response activation (Fritz et al., 2006; Meylan et al., 2006; Franchi et al., 2009)

Developmental Transitions

Many bacteria have sophisticated mechanisms to undergo morphological changes in response to environmental stress including the formation of spores, dormant cells, persisters, or viable but non-culturable cells (Oliver, 2005; Wood et al., 2013; Li et al., 2014; Huang and Hull, 2017). Cells in these states monitor their environment seeking for improved conditions to reverse non-active states and reinitiate growth. Taking into account the quantity of PG release by bacteria (Doyle et al., 1988), it is plausible that muropeptides play a role as interspecies signal molecules to promote microbial growth under favorable conditions (Keep et al., 2006).

For example, *B. subtilis* spores are able to germinate in the presence of low concentration of muropeptides (disaccharide tripeptides containing *m*DAP) released by actively growing cells (Shah et al., 2008; Dworkin and Shah, 2010). Muropeptide-driven exit from dormancy requires the PrkC kinase, a member of the serine/threonine kinase (STPK) family, which has an intracellular kinase domain and an extracellular PG binding domain with multiple PASTA repeats (Yeats et al., 2002; Squeglia et al., 2011). PrkC binds PG, initiating a signal cascade that leads to spore germination (Shah et al., 2008). STPKs have a variety of roles in bacteria and are found in most Gram-positive bacteria. To date, PrkC homologues have been identified in *S. pneumoniae* (StkP), *S. mutans* (PknB), *M. tuberculosis* (PknB), *C. difficile* (PrkC), and *S. aureus* (PknB) (Fernandez et al., 2006; Sebaihia et al., 2006; Donat et al., 2009; Maestro et al., 2011; Mir et al., 2011). Interestingly, *S. aureus* PknB homolog responds not only to *m*DAP PG-type but also to the L-Lys-containing muropeptides (Dworkin and Shah, 2010), suggesting that bacteria expressing this kinase can react to signals from all species that produce PG.

Muropeptides are also implicated in the exit from dormancy of *Micrococcus* and *Mycobacterium* through the resuscitation-promoting factor (Rpf), a muralytic enzyme that cleaves the β -1,4 glycosidic bond in the glycan backbone of PG (Mukamolova et al., 2002, 2006). Combined with other hydrolytic enzymes, Rpf might generate *m*DAP-containing muropeptides, which can bind to STPKs and trigger resuscitation in an analogous manner to spore germination in *B. subtilis* (Shah et al., 2008; Kana and Mizrahi, 2010). Furthermore, these *m*DAP-muropeptides might be detected by other receptors like Nod1 (Girardin et al., 2003a,c), suggesting that mycobacteria may, in addition, utilize those to modulate host innate immune responses during infection (Jo, 2008).

The predatory bacterium *Myxococcus xanthus* is able to respond to prey signals and alter its chemotactic and developmental pattern by forming fruiting bodies, where the vegetative cell differentiates into spores (Berleman et al., 2006; Keane and Berleman, 2016). One key phenomenon during fruiting body formation is the establishment of rhythmically advancing waves of cells (known as rippling) that has been shown to be induced by PG (Shimkets and Kaiser, 1982). This behavior is stimulated not only by *M. xanthus* PG fragments but also by a variety of proteobacteria and Gram-positive bacteria PG (e.g., *E. coli*, *B. subtilis*) (Shimkets and Kaiser, 1982).

Altogether, these findings suggest a pathway for bacterial resuscitation from a non-growing state *via* the detection of

cell wall fragments in the environment, which seems to be a widely used strategy in the microbial world (Keep et al., 2006).

Interspecies Interactions

PG fragments serve as signals in a range of host interactions (both pathogenic and symbiotic relationship of bacteria with plants and animals) and also in prokaryote-prokaryote encounters. For example, *Bacillus cereus* mediates commensalism with bacteria from the Cytophaga-Flavobacterium group in the soybean rhizosphere (Peterson et al., 2006). PG isolated from *B. cereus* stimulates the growth of *Flavobacterium johnsoniae* *in vitro*, pointing out to a beneficial relationship between these rhizosphere microorganisms. It has been suggested that *F. johnsoniae* secretes a cell wall degrading enzyme that permits the mobilization of *B. cereus* PG fragments as a carbon source for their growth, although the responsible enzyme and mechanism are still unknown (Peterson et al., 2006).

In *C. albicans*, muramyl dipeptides exhibit a potent hypha-inducing activity by directly binding to adenylyl cyclase Cyr1p LRR domain that stimulates cAMP production and subsequent hyphal growth (Xu et al., 2008). In addition, when *C. albicans* undergoes hyphal morphogenesis as a response to the presence of PG, *P. aeruginosa* is able to form a dense biofilm on the filamentous hyphal cells and kill them. Interestingly, *C. albicans* has developed a mechanism to protect itself by responding to the quorum factor 3-oxo-C12 homoserine lactone produced by *Pseudomonas*, which restricts its growth to a budding pattern that is not attacked by the bacteria (Hogan and Kolter, 2002; Naseem et al., 2012).

There are also several examples of PG fragments triggering the production of antimicrobial compounds within bacterial communities. *P. aeruginosa* is found in acute and chronic wounds forming a biofilm resistant to antimicrobials. Recent studies proved that exogenous NAG and other PG fragments derived from commensal Gram-positive bacteria elevate the virulence of *P. aeruginosa*, which is able to respond to the presence of PG fragments by producing pyocyanin, a potent antimicrobial phenazine (Korgaonkar and Whiteley, 2011; Korgaonkar et al., 2013). As *Pseudomonas* lives in polymicrobial communities, this mechanism might be of advantage to monitor surrounding microorganisms in order to eliminate competitors or provide additional nutrients for growth. In a similar way, NAG also induces the production of antimicrobials in the soil bacterium *Streptomyces coelicolor* (Rigali et al., 2006).

Another pathogenic bacterium, *E. coli*, also responds to NAG molecules derived from PG degradation by reducing CURLI fibers and type 1 fimbriae synthesis, both being essential for pathogenesis (Konopka, 2012; Naseem et al., 2012). In this case, regulation of these bacterial structures could balance the interaction between the pathogen and the host immune response, delaying the inflammation and allowing the dissemination of the bacteria within the host.

Induction of Antibiotic Resistance

Some bacteria are able to induce β -lactamases expression in the presence of high levels of antibiotics (e.g., *Citrobacter freundii*, *P. aeruginosa*, and *Stenotrophomonas*), a phenomenon that is

tightly linked to PG recycling (Dietz et al., 1997b; Zeng and Lin, 2013; Yin et al., 2014). In Gram-negative bacteria, two major mechanisms have been characterized: the AmpG-AmpR-AmpC pathway and the BlrAB two-component system. Regulation of the β -lactamase AmpC relies on the relative concentrations of cytoplasmic anhydromuropeptides. In the absence of β -lactam pressure, the UDP-muramyl-pentapeptide PG precursor is bound to the transcriptional regulator AmpR, inhibiting the expression of the *ampC* gene (Jacoby, 2009). However, in the presence of β -lactams, PG synthesis is blocked due to the inhibition of PBPs transpeptidase activity (Moya et al., 2009; Cho et al., 2014) leading to dysfunctionality of PBPs and resulting in an accumulation of anhydromuropeptides (mainly anhydromuramyl-tripeptides) in the periplasm (Cho et al., 2014). This accumulation displaces UDP-muramyl-pentapeptide from AmpR (Uehara and Park, 2002, 2008), and thus, *ampC* is expressed and β -lactamases are secreted to the periplasm, where they hydrolyze the antibiotic (Holtje et al., 1994; Jacobs et al., 1994; Jacobs, 1997; Dietz et al., 1997a). Similarly, in *S. aureus* and *Bacillus licheniformis*, accumulation of cytoplasmic dipeptides, D-Glu-L-Lys or D-Glu-*m*DAP, respectively, is responsible for triggering the inactivation of Blal/MecI repressors, leading to the synthesis of β -lactamases BlaZ, BlaP, and MecaA (Amoroso et al., 2012). In *Aeromonas hydrophila*, β -lactamase production is regulated by a different system in which expression of AmpC is controlled through the two-component system BlrAB. Upon β -lactam exposure, disaccharide pentapeptides accumulate in the periplasm, inducing the autophosphorylation of BlrB, which phosphorylates BlrA, activating the transcription of the AmpC, Cep, and Imi β -lactamases simultaneously (Tayler et al., 2010). Additionally, the BlrAB two-component system (also known as CreBC) has been associated with β -lactam resistance in *P. aeruginosa* and *Stenotrophomonas maltophilia* (Moya et al., 2009; Huang et al., 2015).

In the past years, the use of combination therapy with β -lactams and vancomycin to treat methicillin-resistant *Staphylococcus aureus* (MRSA)-infected patients has caused the emergence of β -lactam-induced vancomycin-resistant MRSA (BIVR-MRSA). The presence of β -lactams inhibits PG biosynthesis, producing the accumulation of large amounts of PG precursors (specifically lipid II) with free D-Ala-D-Ala terminals that bind with vancomycin, depleting its concentration. Even if it is well characterized that the muropeptide NAG-NAM-L-Ala-D-Gln-L-Lys-(ϵ -amino-4Gly)-D-Ala-2Gly triggers vancomycin resistance (Ikeda et al., 2010), the mechanism underlying BIVR phenomenon remains to be elucidated.

Though induction mechanisms differ, all mentioned pathways are controlled by the amount of soluble PG fragments and so are linked to cell wall turnover and PG recycling.

BACTERIA-HOST INTERACTIONS

The interaction of bacteria with host cells through PG signaling molecules is well known, and the PG-mediated responses have been characterized in the past years. In mammals, plants, and

some insects, PG-derived fragments are recognized by the innate immune system and promote host defence against bacterial infections (Royet et al., 2011; Gust, 2015; Capo et al., 2016; Pashenkov et al., 2018; Wolf and Underhill, 2018), indicating that PG recognition is an evolutionarily conserved process.

PG is involved in establishing symbiosis during *Vibrio fischeri* colonization of the *Euprymna scolopes* squid light organ (Koropatnick et al., 2004). In this marine mutualism, the squid uses light produced by *V. fischeri* to avoid predators during its nocturnal behavior. Juvenile squids make use of the ciliated epithelial cells in the light organ to acquire the *V. fischeri* symbiont from the environment in each generation. Bacterial cells swim through ciliated ducts to gain access to deep crypt spaces, where they lose the flagellum and establish a permanent association with the host. Once colonized, *V. fischeri* releases tracheal cytotoxin (TCT, 1,6-anhydro-disaccharide tetrapeptides containing *m*DAP), which in synergy with LPS derivatives triggers the normal morphogenesis of the light organ. Morphogenesis involves the loss of ciliated epithelium, the shortening and eventual loss of appendages (Koropatnick et al., 2004, 2007; Brennan et al., 2014), and the reduction of mucus secretion (Nyholm et al., 2000), which prevents the entry of other bacteria. *E. scolopes* has four known PGRPs that are expressed in the light organ, which could be responsible for TCT sensing (Goodson et al., 2005; Royet et al., 2011). PGRP3 and PGRP4 are proposed to function as PG receptors on the surface of light organ cells, while PGRP2 is thought to be secreted into the lumen of the crypts helping maintain an appropriate level of *V. fischeri*. PGRP2 also hydrolyzes PG fragments preventing the inflammatory response activation, which allows the beneficial coexistence of the symbiont with the host (Troll et al., 2010).

The two Gram-negative pathogens *Neisseria gonorrhoeae* and *Bordetella pertussis* also release high amounts of muropeptides during infection: a mixture of 1,6-anhydrodisaccharide tri- and tetrapeptides (Sinha and Rosenthal, 1980, 1981) and TCT (Rosenthal et al., 1987), respectively. PG fragments are sensed by the intracellular NOD1 and NOD2 proteins that trigger the NF- κ B and the mitogen-activated protein kinase pathways, finally stimulating the activation of the innate immune response, the release of proinflammatory cytokines, and cell damage. In *B. pertussis* infection, the release of TCT causes the death and detachment of ciliated cells from the epithelium of the trachea (Goldman et al., 1982; Heiss et al., 1993), while a similar pathology is observed during gonococcal infection of human fallopian tubes (Melly et al., 1984; Woodhams et al., 2013; Chan and Dillard, 2017). Likewise, detection of PG fragments of other pathogens (e.g., *Shigella* spp.) by NOD proteins can stimulate the innate immune response too (Philpott et al., 2000; Girardin et al., 2001; Nigro et al., 2008).

Moreover, it has been proposed that in humans, PG fragments might present other signaling functions apart from modulating the inflammatory response. Aside from defending the host against pathogens, the immune system is also involved in accommodating host colonization by symbiotic microorganisms and maintaining microbiota-host homeostasis. PG fragments are therefore part of the mechanism that controls interactions between the microbiota and host and has effects on host

physiology and development outside the gastrointestinal system (Royet et al., 2011). Gut microbiota is a source of PG that can be translocated from the intestinal mucosa into circulation in the absence of pathogens (Clarke et al., 2010).

For example, recent studies strongly suggest that PG fragments from the intestinal microbiota have the potential to affect the immune system and govern the inflammatory response through NOD proteins (Hergott et al., 2016). In a similar way, and even though the underlying mechanisms remain to be elucidated, gut microbiota has been proposed to modulate brain development and behavior. PG fragments derived from commensal gut microbiota can be translocated into the brain by crossing the blood-brain barrier and can induce inflammation (Fillon et al., 2006; Arentsen et al., 2017). During mice brain development, PG fragments are sensed by pattern recognition receptors (PRRs) expressed during a specific temporal window, in concordance with the PG accumulation observed in the cerebellum and in parallel with the bacterial colonization process (Arentsen et al., 2017). Interestingly, any perturbation of the gut microbiota (e.g., antibiotic treatment) alters the expression of those PRRs in the brain, suggesting that this disruption may alter the developing brain, making it more susceptible to disorders or increasing the risk for immune diseases (Arentsen et al., 2017, 2018). Still, little is known about the structure of the PG molecule that generates these effects or the mechanism behind it.

Finally, somnogenic activity has been attributed to some PG fragments derived from gut microbiota, such as muramyl peptides containing DAP (Krueger, 1985; Krueger and Opp, 2016). According to the reported data, this somnogenic property is structure-dependent, with muramyl-tripeptide being the smallest active molecule able to induce sleep.

CONCLUSIONS

The role of PG as a MAMP has long been recognized, especially as signaling molecules that modulate the innate immune response in some animals and plants. As during normal cell growth, bacteria release PG turnover products to the environment, and different organisms have developed sophisticated mechanisms to detect and respond to these molecules. Besides their role in infection or immune response development, bacteria use PG fragments as signaling cues to track the state of their cell wall or to monitor surrounding microorganisms. As many bacteria live within polymicrobial communities, this might be a

beneficial mechanism to eliminate competitors or to obtain additional nutrients for growth. As a result of these functions, PG-fragments can be considered as signaling molecules.

The amount of PG turnover products released to the environment is dependent on the PG recycling pathway, and so, it is expected that bacteria regulate this process. Information regarding the regulation of AmpG or other transporters with similar activity is therefore crucial for a complete understanding of the function(s) of released anhydromuropeptides and other PG fragments; however, few studies have focused on this kind of protein (Cheng and Park, 2002; Chahboune et al., 2005; Zhang et al., 2010; Chan and Dillard, 2016; Li et al., 2016). A recently described assay to quantify AmpG-mediated transport (Perley-Robertson et al., 2016) may help to understand important aspects regarding the regulation of this permease in years to come. Likewise, other interesting tools have recently been developed to investigate PG recycling by studying other enzymes involved in this pathway (DeMeester et al., 2018).

The development of highly sensitive analytical methods and the use of synthetic muropeptides could help to elucidate the specific receptors that are able to bind PG as much as to determine the agonist PG structures and their role as signaling molecules. Overall, PG sensing seems to be a global mechanism that leads to different responses, so it is conceivable the existence of multiple PG-sensing pathways. More research is needed to clarify the different sensing mechanisms, to determine the interplay level of the different receptors (or to identify new ones), or understand the responses generated by muropeptides during bacteria-bacteria or bacteria-host interactions.

AUTHOR CONTRIBUTIONS

All authors listed have made a substantial, direct and intellectual contribution to the work, and approved it for publication.

FUNDING

OI and SH are thankful to the Swedish Research Council, Laboratory for Molecular Infection Medicine Sweden (MIMS) and UCMR for the financial support. Research in the Cava lab was supported by MIMS, the Knut and Alice Wallenberg Foundation (KAW), the Swedish Research Council, and the Kempe Foundation.

REFERENCES

- Adam, A., and Lederer, E. (1984). Muramyl peptides: immunomodulators, sleep factors, and vitamins. *Med. Res. Rev.* 4, 111–152. doi: 10.1002/med.2610040202
- Akira, S., Uematsu, S., and Takeuchi, O. (2006). Pathogen recognition and innate immunity. *Cell* 124, 783–801. doi: 10.1016/j.cell.2006.02.015
- Alvarez, F. J., and Konopka, J. B. (2007). Identification of an N-acetylglucosamine transporter that mediates hyphal induction in *Candida albicans*. *Mol. Biol. Cell.* 18, 965–975. doi: 10.1091/mbc.E06-10-0931
- Amoroso, A., Boudet, J., Berzigotti, S., Duval, V., Teller, N., Mengin-Lecreulx, D., et al. (2012). A peptidoglycan fragment triggers beta-lactam resistance in *Bacillus licheniformis*. *PLoS Pathog.* 8:e1002571. doi:10.1371/journal.ppat.1002571
- Andre, G., Leenhouts, K., Hols, P., and Dufrene, Y. F. (2008). Detection and localization of single LysM-peptidoglycan interactions. *J. Bacteriol.* 190, 7079–7086. doi: 10.1128/JB.00519-08
- Arentsen, T., Khalid, R., Qian, Y., and Diaz Heijtz, R. (2018). Sex-dependent alterations in motor and anxiety-like behavior of aged bacterial peptidoglycan sensing molecule 2 knockout mice. *Brain Behav. Immun.* 67, 345–354. doi: 10.1016/j.bbi.2017.09.014

- Arentsen, T., Qian, Y., Gkotzis, S., Femenia, T., Wang, T., Udekwu, K., et al. (2017). The bacterial peptidoglycan-sensing molecule Pglyrp2 modulates brain development and behavior. *Mol. Psychiatry* 22, 257–266. doi: 10.1038/mp.2016.182
- Bateman, A., and Bycroft, M. (2000). The structure of a LysM domain from *E. coli* membrane-bound lytic murein transglycosylase D (MltD). *J. Mol. Biol.* 299, 1113–1119. doi: 10.1006/jmbi.2000.3778
- Berleman, J. E., Chumley, T., Cheung, P., and Kirby, J. R. (2006). Rippling is a predatory behavior in *Myxococcus xanthus*. *J. Bacteriol.* 188, 5888–5895. doi: 10.1128/JB.00559-06
- Bernard, E., Rolain, T., Courtin, P., Hols, P., and Chapot-Chartier, M. P. (2011). Identification of the amidotransferase AsnB1 as being responsible for meso-diaminopimelic acid amidation in *Lactobacillus plantarum* peptidoglycan. *J. Bacteriol.* 193, 6323–6330. doi: 10.1128/JB.05060-11
- Bertsche, U., Mayer, C., Gotz, F., and Gust, A. A. (2015). Peptidoglycan perception-sensing bacteria by their common envelope structure. *Int. J. Med. Microbiol.* 305, 217–223. doi: 10.1016/j.ijmm.2014.12.019
- Bielig, H., Rompikuntal, P. K., Dongre, M., Zurek, B., Lindmark, B., Ramstedt, M., et al. (2011). NOD-like receptor activation by outer membrane vesicles from *Vibrio cholerae* non-O1 non-O139 strains is modulated by the quorum-sensing regulator HapR. *Infect. Immun.* 79, 1418–1427. doi: 10.1128/IAI.00754-10
- Boller, T., and Felix, G. (2009). A renaissance of elicitors: perception of microbe-associated molecular patterns and danger signals by pattern-recognition receptors. *Annu. Rev. Plant Biol.* 60, 379–406. doi: 10.1146/annurev.arplant.57.032905.105346
- Boneca, I. G. (2005). The role of peptidoglycan in pathogenesis. *Curr. Opin. Microbiol.* 8, 46–53. doi: 10.1016/j.mib.2004.12.008
- Borisova, M., Gaupp, R., Duckworth, A., Schneider, A., Dalugge, D., Muhleck, M., et al. (2016). Peptidoglycan recycling in gram-positive bacteria is crucial for survival in stationary phase. *MBio* 7, 1–10. doi: 10.1128/mBio.00923-16
- Borisova, M., Gisin, J., and Mayer, C. (2014). Blocking peptidoglycan recycling in *Pseudomonas aeruginosa* attenuates intrinsic resistance to fosfomycin. *Microb. Drug Resist.* 20, 231–237. doi: 10.1089/mdr.2014.0036
- Botella, E., Hubner, S., Hokamp, K., Hansen, A., Bisicchia, P., Noone, D., et al. (2011). Cell envelope gene expression in phosphate-limited *Bacillus subtilis* cells. *Microbiology* 157, 2470–2484. doi: 10.1099/mic.0.049205-0
- Boudreau, M. A., Fisher, J. E., and Mobashery, S. (2012). Messenger functions of the bacterial cell wall-derived muropeptides. *Biochemistry* 51, 2974–2990. doi: 10.1021/bi300174x
- Bourhis, L. L., Benko, S., and Girardin, S. E. (2007). Nod1 and Nod2 in innate immunity and human inflammatory disorders. *Biochem. Soc. Trans.* 35, 1479–1784. doi: 10.1042/BST0351479
- Brennan, C. A., Hunt, J. R., Kremer, N., Krasity, B. C., Apicella, M. A., McFall-Ngai, M. J., et al. (2014). A model symbiosis reveals a role for sheathed-flagellum rotation in the release of immunogenic lipopolysaccharide. *elife* 3:e01579. doi: 10.7554/eLife.01579
- Buendia, L., Girardin, A., Wang, T., Cottret, L., and Lefebvre, B. (2018). LysM receptor-like kinase and LysM receptor-like protein families: an update on phylogeny and functional characterization. *Front. Plant Sci.* 9:1531. doi: 10.3389/fpls.2018.01531
- Buist, G., Steen, A., Kok, J., and Kuipers, O. P. (2008). LysM, a widely distributed protein motif for binding to (peptidoglycans. *Mol. Microbiol.* 68, 838–847. doi: 10.1111/j.1365-2958.2008.06211.x
- Callewaert, L., and Michiels, C. W. (2010). Lysozymes in the animal kingdom. *J. Biosci.* 35, 127–160. doi: 10.1007/s12038-010-0015-5
- Canas, M. A., Fabrega, M. J., Gimenez, R., Badia, J., and Baldoma, L. (2018). Outer membrane vesicles from probiotic and commensal *Escherichia coli* activate NOD1-mediated immune responses in intestinal epithelial cells. *Front. Microbiol.* 9:498. doi: 10.3389/fmicb.2018.00498
- Capo, F., Charroux, B., and Royet, J. (2016). Bacteria sensing mechanisms in *Drosophila* gut: local and systemic consequences. *Dev. Comp. Immunol.* 64, 11–21. doi: 10.1016/j.dci.2016.01.001
- Cava, F., and de Pedro, M. A. (2014). Peptidoglycan plasticity in bacteria: emerging variability of the murein sacculus and their associated biological functions. *Curr. Opin. Microbiol.* 18, 46–53. doi: 10.1016/j.mib.2014.01.004
- Chahboune, A., Decaffmeyer, M., Brasseur, R., and Joris, B. (2005). Membrane topology of the *Escherichia coli* AmpG permease required for recycling of cell wall anhydromuropeptides and AmpC beta-lactamase induction. *Antimicrob. Agents Chemother.* 49, 1145–1149. doi: 10.1128/AAC.49.3.1145-1149.2005
- Chaloupka, J., Kreckova, P., and Rihova, L. (1962). The mucopeptide turnover in the cell walls of growing cultures of *Bacillus megaterium* KM. *Experientia* 18, 362–363. doi: 10.1007/BF02172250
- Chaloupka, J., and Strnadova, M. (1972). Turnover of murein in a diaminopimelic acid dependent mutant of *Escherichia coli*. *Folia. Microbiol.* 17, 446–455. doi: 10.1007/BF02872729
- Chan, J. M., and Dillard, J. P. (2016). *Neisseria gonorrhoeae* crippled its peptidoglycan fragment permease to facilitate toxic peptidoglycan monomer release. *J. Bacteriol.* 198, 3029–3040. doi: 10.1128/JB.00437-16
- Chan, J. M., and Dillard, J. P. (2017). Attention seeker: production, modification, and release of inflammatory peptidoglycan fragments in *Neisseria* species. *J. Bacteriol.* 199, 1–13. doi: 10.1128/JB.00354-17
- Chapot-Chartier, M.-P. (2010). “Bacterial autolysins,” in *Prokaryotic cell wall compounds: Structure and biochemistry*. eds. H. König, H. Claus, and A. Varma (Berlin, Heidelberg: Springer Berlin Heidelberg), 383–406.
- Charrier, L., and Merlin, D. (2006). The oligopeptide transporter hPepT1: gateway to the innate immune response. *Lab. Invest.* 86, 538–546. doi: 10.1038/labinvest.3700423
- Cheng, Q., Li, H., Merdek, K., and Park, J. T. (2000). Molecular characterization of the beta-N-acetylglucosaminidase of *Escherichia coli* and its role in cell wall recycling. *J. Bacteriol.* 182, 4836–4840. doi: 10.1128/JB.182.17.4836-4840.2000
- Cheng, Q., and Park, J. T. (2002). Substrate specificity of the AmpG permease required for recycling of cell wall anhydro-muropeptides. *J. Bacteriol.* 184, 6434–6436. doi: 10.1128/JB.184.23.6434-6436.2002
- Cho, H., Uehara, T., and Bernhardt, T. G. (2014). Beta-lactam antibiotics induce a lethal malfunctioning of the bacterial cell wall synthesis machinery. *Cell* 159, 1300–1311. doi: 10.1016/j.cell.2014.11.017
- Cho, S., Wang, Q., Swaminathan, C. P., Heseck, D., Lee, M., Boons, G. J., et al. (2007). Structural insights into the bactericidal mechanism of human peptidoglycan recognition proteins. *Proc. Natl. Acad. Sci. USA* 104, 8761–8766. doi: 10.1073/pnas.0701453104
- Cinel, I., and Opal, S. M. (2009). Molecular biology of inflammation and sepsis: a primer. *Crit. Care Med.* 37, 291–304. doi: 10.1097/CCM.0b013e31819267fb
- Clarke, T. B., Davis, K. M., Lysenko, E. S., Zhou, A. Y., Yu, Y., and Weiser, J. N. (2010). Recognition of peptidoglycan from the microbiota by Nod1 enhances systemic innate immunity. *Nat. Med.* 16, 228–231. doi: 10.1038/nm.2087
- Dagil, Y. A., Arbatsky, N. P., Alkhazova, B. I., L'Vov, V. L., Mazurov, D. V., and Pashenkov, M. V. (2016). The dual NOD1/NOD2 agonism of muropeptides containing a meso-diaminopimelic acid residue. *PLoS One* 11:e0160784. doi: 10.1371/journal.pone.0160784
- Das, D., Herve, M., Feuerhelm, J., Farr, C. L., Chiu, H. J., Elsliger, M. A., et al. (2011). Structure and function of the first full-length murein peptide ligase (Mpl) cell wall recycling protein. *PLoS One* 6:e17624. doi: 10.1371/journal.pone.0017624
- Davis, K. M., and Weiser, J. N. (2011). Modifications to the peptidoglycan backbone help bacteria to establish infection. *Infect. Immun.* 79, 562–570. doi: 10.1128/IAI.00651-10
- de Pedro, M. A., and Cava, F. (2015). Structural constraints and dynamics of bacterial cell wall architecture. *Front. Microbiol.* 6:449. doi: 10.3389/fmicb.2015.00449
- DeMeester, K. E., Liang, H., Jensen, M. R., Jones, Z. S., D'Ambrosio, E. A., Scinto, S. L., et al. (2018). Synthesis of functionalized N-acetyl muramic acids to probe bacterial cell wall recycling and biosynthesis. *J. Am. Chem. Soc.* 140, 9458–9465. doi: 10.1021/jacs.8b03304
- Dhar, S., Kumari, H., Balasubramanian, D., and Mathee, K. (2018). Cell-wall recycling and synthesis in *Escherichia coli* and *Pseudomonas aeruginosa*—their role in the development of resistance. *J. Med. Microbiol.* 67, 1–21. doi: 10.1099/jmm.0.000636
- Diacovich, L., and Gorvel, J. P. (2010). Bacterial manipulation of innate immunity to promote infection. *Nat. Rev. Microbiol.* 8, 117–128. doi: 10.1038/nrmicro2295
- Dietz, H., Pfeifle, D., and Wiedemann, B. (1997a). The signal molecule for beta-lactamase induction in enterobacter cloacae is the anhydromuramyl-pentapeptide. *Antimicrob. Agents Chemother.* 41, 2113–2120.
- Dietz, H., Pfeifle, D., and Wiedemann, B. (1997b). The signal molecule for beta-lactamase induction in *Enterobacter cloacae* is the anhydromuramyl-pentapeptide. *Antimicrob. Agents Chemother.* 41, 2113–2120. doi: 10.1128/Aac.41.10.2113

- Dijkstra, A. J., and Keck, W. (1996). Peptidoglycan as a barrier to transenvelope transport. *J. Bacteriol.* 178, 5555–5562. doi: 10.1128/jb.178.19.5555-5562.1996
- Dik, D. A., Marous, D. R., Fisher, J. F., and Mobashery, S. (2017). Lytic transglycosylases: concinnity in concision of the bacterial cell wall. *Crit. Rev. Biochem. Mol. Biol.* 52, 503–542. doi: 10.1080/10409238.2017.1337705
- Dizierski, R., and Gupta, D. (2010). Mammalian peptidoglycan recognition proteins (PGRPs) in innate immunity. *Innate Immun.* 16, 168–174. doi: 10.1177/1753425910366059
- Dominguez-Gil, T., Molina, R., Alcorlo, M., and Hermoso, J. A. (2016). Renew or die: the molecular mechanisms of peptidoglycan recycling and antibiotic resistance in Gram-negative pathogens. *Drug Resist. Updat.* 28, 91–104. doi: 10.1016/j.drug.2016.07.002
- Donat, S., Streker, K., Schirmeister, T., Raket, S., Stehle, T., Liebeck, M., et al. (2009). Transcriptome and functional analysis of the eukaryotic-type serine/threonine kinase PknB in *Staphylococcus aureus*. *J. Bacteriol.* 191, 4056–4069. doi: 10.1128/JB.00117-09
- Doyle, R. J., Chaloupka, J., and Vinter, V. (1988). Turnover of cell walls in microorganisms. *Microbiol. Rev.* 52, 554–567.
- Drams, S., Magnet, S., Davison, S., and Arthur, M. (2008). Covalent attachment of proteins to peptidoglycan. *FEMS Microbiol. Rev.* 32, 307–320. doi: 10.1111/j.1574-6976.2008.00102.x
- Dworkin, J. (2014). The medium is the message: interspecies and interkingdom signaling by peptidoglycan and related bacterial glycans. *Annu. Rev. Microbiol.* 68, 137–154. doi: 10.1146/annurev-micro-091213-112844
- Dworkin, J. (2018). Detection of fungal and bacterial carbohydrates: do the similar structures of chitin and peptidoglycan play a role in immune dysfunction? *PLoS Pathog.* 14:e1007271. doi: 10.1371/journal.ppat.1007271
- Dworkin, J., and Shah, I. M. (2010). Exit from dormancy in microbial organisms. *Nat. Rev. Microbiol.* 8, 890–896. doi: 10.1038/nrmicro2453
- Dziarski, R. (2004). Peptidoglycan recognition proteins (PGRPs). *Mol. Immunol.* 40, 877–886. doi: 10.1016/j.molimm.2003.10.011
- Dziarski, R., and Gupta, D. (2006). Mammalian PGRPs: novel antibacterial proteins. *Cell. Microbiol.* 8, 1059–1069. doi: 10.1111/j.1462-5822.2006.00726.x
- Egan, A. J., Cleverley, R. M., Peters, K., Lewis, R. J., and Vollmer, W. (2017). Regulation of bacterial cell wall growth. *FEBS J.* 284, 851–867. doi: 10.1111/febs.13959
- Fernandez, P., Saint-Joanis, B., Barilone, N., Jackson, M., Gicquel, B., Cole, S. T., et al. (2006). The Ser/Thr protein kinase PknB is essential for sustaining mycobacterial growth. *J. Bacteriol.* 188, 7778–7784. doi: 10.1128/JB.00963-06
- Fillon, S., Soulis, K., Rajasekaran, S., Benedict-Hamilton, H., Radin, J. N., Orihuela, C. J., et al. (2006). Platelet-activating factor receptor and innate immunity: uptake of gram-positive bacterial cell wall into host cells and cell-specific pathophysiology. *J. Immunol.* 177, 6182–6191. doi: 10.4049/jimmunol.177.9.6182
- Firczuk, M., and Bochtler, M. (2007). Folds and activities of peptidoglycan amidases. *FEMS Microbiol. Rev.* 31, 676–691. doi: 10.1111/j.1574-6976.2007.00084.x
- Franchi, L., Warner, N., Viani, K., and Nunez, G. (2009). Function of Nod-like receptors in microbial recognition and host defense. *Immunol. Rev.* 227, 106–128. doi: 10.1111/j.1600-065X.2008.00734.x
- Fritz, J. H., Ferrero, R. L., Philpott, D. J., and Girardin, S. E. (2006). Nod-like proteins in immunity, inflammation and disease. *Nat. Immunol.* 7, 1250–1257. doi: 10.1038/ni1412
- Garcia, D. L., and Dillard, J. P. (2008). Mutations in ampG or ampD affect peptidoglycan fragment release from *Neisseria gonorrhoeae*. *J. Bacteriol.* 190, 3799–3807. doi: 10.1128/JB.01194-07
- Gerriets, V. A., Kishton, R. J., Nichols, A. G., Macintyre, A. N., Inoue, M., Ilkayeva, O., et al. (2015). Metabolic programming and PDHK1 control CD4+ T cell subsets and inflammation. *J. Clin. Invest.* 125, 194–207. doi: 10.1172/JCI76012
- Girardin, S. E., Boneca, I. G., Carneiro, L. A., Antignac, A., Jehanno, M., Viala, J., et al. (2003a). Nod1 detects a unique muropeptide from gram-negative bacterial peptidoglycan. *Science* 300, 1584–1587. doi: 10.1126/science.1084677
- Girardin, S. E., Boneca, I. G., Viala, J., Chamaillard, M., Labigne, A., Thomas, G., et al. (2003b). Nod2 is a general sensor of peptidoglycan through muramyl dipeptide (MDP) detection. *J. Biol. Chem.* 278, 8869–8872. doi: 10.1074/jbc.C200651200
- Girardin, S. E., Tournebise, R., Mavris, M., Page, A. L., Li, X., Stark, G. R., et al. (2001). CARD4/Nod1 mediates NF- κ B and JNK activation by invasive *Shigella flexneri*. *EMBO Rep.* 2, 736–742. doi: 10.1093/embo-reports/kve155
- Girardin, S. E., Travassos, L. H., Herve, M., Blanot, D., Boneca, I. G., Philpott, D. J., et al. (2003c). Peptidoglycan molecular requirements allowing detection by Nod1 and Nod2. *J. Biol. Chem.* 278, 41702–41708. doi: 10.1074/jbc.M307198200
- Goldman, W. E., Klapper, D. G., and Baseman, J. B. (1982). Detection, isolation, and analysis of a released *Bordetella pertussis* product toxic to cultured tracheal cells. *Infect. Immun.* 36, 782–794.
- Goodell, E. W. (1985). Recycling of murein by *Escherichia coli*. *J. Bacteriol.* 163, 305–310.
- Goodell, E. W., and Schwarz, U. (1985). Release of cell-wall peptides into culture-medium by exponentially growing *Escherichia coli*. *J. Bacteriol.* 162, 391–397.
- Goodson, M. S., Kojadinovic, M., Troll, J. V., Scheetz, T. E., Casavant, T. L., Soares, M. B., et al. (2005). Identifying components of the NF- κ B pathway in the beneficial *Euprymna scolopes*-*Vibrio fischeri* light organ symbiosis. *Appl. Environ. Microbiol.* 71, 6934–6946. doi: 10.1128/AEM.71.11.6934-6946.2005
- Gust, A. A. (2015). Peptidoglycan perception in plants. *PLoS Pathog.* 11:e1005275. doi: 10.1371/journal.ppat.1005275
- Heffron, J. D., Orsburn, B., and Popham, D. L. (2009). Roles of germination-specific lytic enzymes CwlJ and SleB in *Bacillus anthracis*. *J. Bacteriol.* 191, 2237–2247. doi: 10.1128/JB.01598-08
- Heiss, L. N., Moser, S. A., Unanue, E. R., and Goldman, W. E. (1993). Interleukin-1 is linked to the respiratory epithelial cytopathology of pertussis. *Infect. Immun.* 61, 3123–3128.
- Hergott, C. B., Roche, A. M., Tamashiro, E., Clarke, T. B., Bailey, A. G., Laughlin, A., et al. (2016). Peptidoglycan from the gut microbiota governs the lifespan of circulating phagocytes at homeostasis. *Blood* 127, 2460–2471. doi: 10.1182/blood-2015-10-675173
- Hogan, D. A., and Kolter, R. (2002). *Pseudomonas candida* interactions: an ecological role for virulence factors. *Science* 296, 2229–2232. doi: 10.1126/science.1070784
- Holtje, J. V. (1998). Growth of the stress-bearing and shape-maintaining murein sacculus of *Escherichia coli*. *Microbiol. Mol. Biol. Rev.* 62, 181–203.
- Holtje, J. V., Kopp, U., Ursinus, A., and Wiedemann, B. (1994). The negative regulator of beta-lactamase induction AmpD is a N-acetyl-anhydromuramyl-L-alanine amidase. *FEMS Microbiol. Lett.* 122, 159–164. doi: 10.1111/j.1574-6968.1994.tb07159.x
- Holtje, J. V., Mirelman, D., Sharon, N., and Schwarz, U. (1975). Novel type of murein transglycosylase in *Escherichia coli*. *J. Bacteriol.* 124, 1067–1076.
- Holtje, J. V., and Tuomanen, E. I. (1991). The murein hydrolases of *Escherichia coli*: properties, functions and impact on the course of infections in vivo. *J. Gen. Microbiol.* 137, 441–454. doi: 10.1099/00221287-137-3-441
- Horcajo, P., de Pedro, M. A., and Cava, F. (2012). Peptidoglycan plasticity in bacteria: stress-induced peptidoglycan editing by noncanonical D-amino acids. *Microb. Drug Resist.* 18, 306–313. doi: 10.1089/mdr.2012.0009
- Huang, M., and Hull, C. M. (2017). Sporulation: how to survive on planet Earth (and beyond). *Curr. Genet.* 63, 831–838. doi: 10.1007/s00294-017-0694-7
- Huang, Y.-W., Wu, C.-J., Hu, R.-M., Lin, Y.-T., and Yang, T.-C. (2015). Interplay among membrane-bound lytic transglycosylase D1, the CreBC two-component regulatory system, the AmpNG-AmpDI-NagZ-AmpR regulatory circuit, and L1/L2 β -lactamase expression in *Stenotrophomonas maltophilia*. *Antimicrob. Agents Chemother.* 59, 6866–6872. doi: 10.1128/aac.05179-14
- Ibrahim, H. R., Matsuzaki, T., and Aoki, T. (2001). Genetic evidence that antibacterial activity of lysozyme is independent of its catalytic function. *FEBS Lett.* 506, 27–32. doi: 10.1016/S0014-5793(01)02872-1
- Ikeda, S., Hanaki, H., Yanagisawa, C., Ikeda-Dantsuji, Y., Matsui, H., Iwatsuki, M., et al. (2010). Identification of the active component that induces vancomycin resistance in MRSA. *J. Antibiot.* 63, 533–538. doi: 10.1038/ja.2010.75
- Inohara, N., and Nunez, G. (2003). NODs: intracellular proteins involved in inflammation and apoptosis. *Nat. Rev. Immunol.* 3, 371–382. doi: 10.1038/nri1086
- Jacobs, C. (1997). Pharmacia Biotech & Science prize. 1997 grand prize winner. Life in the balance: cell walls and antibiotic resistance. *Science* 278, 1731–1732. doi: 10.1126/science.278.5344.1731b
- Jacobs, C., Huang, L. J., Bartowsky, E., Normark, S., and Park, J. T. (1994). Bacterial-cell wall recycling provides cytosolic muropeptides as effectors for beta-lactamase induction. *EMBO J.* 13, 4684–4694. doi: 10.1002/j.1460-2075.1994.tb06792.x
- Jacoby, G. A. (2009). AmpC beta-lactamases. *Clin. Microbiol. Rev.* 22, 161–182. doi: 10.1097/AOG.0b013e3181b9d222

- Jaeger, T., and Mayer, C. (2008). N-acetylmuramic acid 6-phosphate lyases (MurNac etherases): role in cell wall metabolism, distribution, structure, and mechanism. *Cell. Mol. Life Sci.* 65, 928–939. doi: 10.1007/s00018-007-7399-x
- Jiang, H., Kong, R., and Xu, X. (2010). The N-acetylmuramic acid 6-phosphate etherase gene promotes growth and cell differentiation of cyanobacteria under light-limiting conditions. *J. Bacteriol.* 192, 2239–2245. doi: 10.1128/JB.01661-09
- Jo, E. K. (2008). Mycobacterial interaction with innate receptors: TLRs, C-type lectins, and NLRs. *Curr. Opin. Infect. Dis.* 21, 279–286. doi: 10.1097/QCO.0b013e3282f88b5d
- Johnson, J. W., Fisher, J. F., and Mobashery, S. (2013). Bacterial cell-wall recycling. *Ann. N. Y. Acad. Sci.* 1277, 54–75. doi: 10.1111/j.1749-6632.2012.06813.x
- Kana, B. D., and Mizrahi, V. (2010). Resuscitation-promoting factors as lytic enzymes for bacterial growth and signaling. *FEMS Immunol. Med. Microbiol.* 58, 39–50. doi: 10.1111/j.1574-695X.2009.00606.x
- Kanneganti, T. D., Lamkanfi, M., and Nunez, G. (2007). Intracellular NOD-like receptors in host defense and disease. *Immunity* 27, 549–559. doi: 10.1016/j.immuni.2007.10.002
- Kaparakis, M., Turnbull, L., Carneiro, L., Firth, S., Coleman, H. A., Parkington, H. C., et al. (2010). Bacterial membrane vesicles deliver peptidoglycan to NOD1 in epithelial cells. *Cell. Microbiol.* 12, 372–385. doi: 10.1111/j.1462-5822.2009.01404.x
- Kaparakis-Liaskos, M., and Ferrero, R. L. (2015). Immune modulation by bacterial outer membrane vesicles. *Nat. Rev. Immunol.* 15, 375–387. doi: 10.1038/nri3837
- Kashyap, D. R., Kuzma, M., Kowalczyk, D. A., Gupta, D., and Dziarski, R. (2017). Bactericidal peptidoglycan recognition protein induces oxidative stress in *Escherichia coli* through a block in respiratory chain and increase in central carbon catabolism. *Mol. Microbiol.* 105, 755–776. doi: 10.1111/mmi.13733
- Kashyap, D. R., Rompca, A., Gaballa, A., Helmann, J. D., Chan, J., Chang, C. J., et al. (2014). Peptidoglycan recognition proteins kill bacteria by inducing oxidative, thiol, and metal stress. *PLoS Pathog.* 10:e1004280. doi: 10.1371/journal.ppat.1004280
- Keane, R., and Berleman, J. (2016). The predatory life cycle of *Myxococcus xanthus*. *Microbiology* 162, 1–11. doi: 10.1099/mic.0.000208
- Keep, N. H., Ward, J. M., Cohen-Gonsaud, M., and Henderson, B. (2006). Wake up! Peptidoglycan lysis and bacterial non-growth states. *Trends Microbiol.* 14, 271–276. doi: 10.1016/j.tim.2006.04.003
- Keestra-Gounder, A. M., and Tsois, R. M. (2017). NOD1 and NOD2: beyond peptidoglycan sensing. *Trends Immunol.* 38, 758–767. doi: 10.1016/j.it.2017.07.004
- Kluj, R. M., Ebner, P., Adamek, M., Ziemert, N., Mayer, C., and Borisova, M. (2018). Recovery of the peptidoglycan turnover product released by the autolysin Atl in *Staphylococcus aureus* involves the phosphotransferase system transporter MurP and the novel 6-phospho-N-acetylmuramidase MupG. *Front. Microbiol.* 9, 1–14. doi: 10.3389/fmicb.2018.02725
- Kohanski, M. A., Dwyer, D. J., and Collins, J. J. (2010). How antibiotics kill bacteria: from targets to networks. *Nat. Rev. Microbiol.* 8, 423–435. doi: 10.1038/nrmicro2333
- Konopka, J. B. (2012). N-acetylglucosamine (GlcNAc) functions in cell signaling. *Scientifica* 2012, 1–15. doi: 10.6064/2012/489208
- Koraimann, G. (2003). Lytic transglycosylases in macromolecular transport systems of Gram-negative bacteria. *Cell. Mol. Life Sci.* 60, 2371–2388. doi: 10.1007/s00018-003-3056-1
- Korgaonkar, A., Trivedi, U., Rumbaugh, K. P., and Whiteley, M. (2013). Community surveillance enhances *Pseudomonas aeruginosa* virulence during polymicrobial infection. *Proc. Natl. Acad. Sci. USA* 110, 1059–1064. doi: 10.1073/pnas.1214550110
- Korgaonkar, A. K., and Whiteley, M. (2011). *Pseudomonas aeruginosa* enhances production of an antimicrobial in response to N-acetylglucosamine and peptidoglycan. *J. Bacteriol.* 193, 909–917. doi: 10.1128/JB.01175-10
- Koropatnick, T. A., Engle, J. T., Apicella, M. A., Stabb, E. V., Goldman, W. E., and McFall-Ngai, M. J. (2004). Microbial factor-mediated development in a host-bacterial mutualism. *Science* 306, 1186–1188. doi: 10.1126/science.1102218
- Koropatnick, T. A., Kimbell, J. R., and McFall-Ngai, M. J. (2007). Responses of host hemocytes during the initiation of the squid-Vibrio symbiosis. *Biol. Bull.* 212, 29–39. doi: 10.2307/25066578
- Korsak, D., Liebscher, S., and Vollmer, W. (2005). Susceptibility to antibiotics and beta-lactamase induction in murein hydrolase mutants of *Escherichia coli*. *Antimicrob. Agents Chemother.* 49, 1404–1409. doi: 10.1128/AAC.49.4.1404-1409.2005
- Kraft, A. R., Prabhu, J., Ursinus, A., and Holtje, J. V. (1999). Interference with murein turnover has no effect on growth but reduces beta-lactamase induction in *Escherichia coli*. *J. Bacteriol.* 181, 7192–7198.
- Krueger, J. M. (1985). Somnogenic activity of muramyl peptides. *Trends Pharmacol. Sci.* 6, 218–221. doi: 10.1016/0165-6147(85)90099-9
- Krueger, J. M., and Opp, M. R. (2016). Sleep and microbes. *Int. Rev. Neurobiol.* 131, 207–225. doi: 10.1016/bs.irn.2016.07.003
- Kulp, A., and Kuehn, M. J. (2010). Biological functions and biogenesis of secreted bacterial outer membrane vesicles. *Annu. Rev. Microbiol.* 64, 163–184. doi: 10.1146/annurev.micro.091208.073413
- Kurata, S. (2014). Peptidoglycan recognition proteins in *Drosophila* immunity. *Dev. Comp. Immunol.* 42, 36–41. doi: 10.1016/j.dci.2013.06.006
- Lamers, R. P., Nguyen, U. T., Nguyen, Y., Buensuceso, R. N., and Burrows, L. L. (2015). Loss of membrane-bound lytic transglycosylases increases outer membrane permeability and beta-lactam sensitivity in *Pseudomonas aeruginosa*. *Microbiol. Biotechnol.* 4, 879–895. doi: 10.1002/mbo3.286
- Layec, S., Decaris, B., and Leblond-Bourget, N. (2008). Diversity of Firmicutes peptidoglycan hydrolases and specificities of those involved in daughter cell separation. *Res. Microbiol.* 159, 507–515. doi: 10.1016/j.resmic.2008.06.008
- Le Bourhis, L., Benko, S., and Girardin, S. E. (2007). Nod1 and Nod2 in innate immunity and human inflammatory disorders. *Biochem. Soc. Trans.* 35, 1479–1484. doi: 10.1042/BST0351479
- Lee, M., Heseck, D., Shah, I. M., Oliver, A. G., Dworkin, J., and Mobashery, S. (2010). Synthetic peptidoglycan motifs for germination of bacterial spores. *Chembiochem* 11, 2525–2529. doi: 10.1002/cbic.201000626
- Lee, M., Zhang, W., Heseck, D., Noll, B. C., Boggess, B., and Mobashery, S. (2009). Bacterial AmpD at the crossroads of peptidoglycan recycling and manifestation of antibiotic resistance. *J. Am. Chem. Soc.* 131, 8742–8743. doi: 10.1021/ja9025566
- Lehotzky, R. E., Partch, C. L., Mukherjee, S., Cash, H. L., Goldman, W. E., Gardner, K. H., et al. (2010). Molecular basis for peptidoglycan recognition by a bactericidal lectin. *Proc. Natl. Acad. Sci. USA* 107, 7722–7727. doi: 10.1073/pnas.0909449107
- Lenz, J. D., Stohl, E. A., Robertson, R. M., Hackett, K. T., Fisher, K., Xiong, K., et al. (2016). Amidase activity of amic controls cell separation and stem peptide release and is enhanced by NlpD in *Neisseria gonorrhoeae*. *J. Biol. Chem.* 291, 10916–10933. doi: 10.1074/jbc.M116.715573
- Li, L., Mendis, N., Trigui, H., Oliver, J. D., and Faucher, S. P. (2014). The importance of the viable but non-culturable state in human bacterial pathogens. *Front. Microbiol.* 5:258. doi: 10.3389/fmicb.2014.00258
- Li, P., Ying, J., Yang, G., Li, A., Wang, J., Lu, J., et al. (2016). Structure-function analysis of the transmembrane protein AmpG from *Pseudomonas aeruginosa*. *PLoS One* 11:e0168060. doi: 10.1371/journal.pone.0168060
- Litzinger, S., Duckworth, A., Nitzsche, K., Risinger, C., Wittmann, V., and Mayer, C. (2010). Muropeptide rescue in *Bacillus subtilis* involves sequential hydrolysis by beta-N-acetylglucosaminidase and N-acetylmuramyl-L-alanine amidase. *J. Bacteriol.* 192, 3132–3143. doi: 10.1128/JB.01256-09
- Liu, C., Gelius, E., Liu, G., Steiner, H., and Dziarski, R. (2000). Mammalian peptidoglycan recognition protein binds peptidoglycan with high affinity, is expressed in neutrophils, and inhibits bacterial growth. *J. Biol. Chem.* 275, 24490–24499. doi: 10.1074/jbc.M001239200
- Lopez, R., Garcia, E., Garcia, P., and Garcia, J. L. (1997). The pneumococcal cell wall degrading enzymes: a modular design to create new lysins? *Microb. Drug Resist.* 3, 199–211. doi: 10.1089/mdr.1997.3.199
- Lu, X., Wang, M., Qi, J., Wang, H., Li, X., Gupta, D., et al. (2006). Peptidoglycan recognition proteins are a new class of human bactericidal proteins. *J. Biol. Chem.* 281, 5895–5907. doi: 10.1074/jbc.M511631200
- Maestro, B., Novakova, L., Heseck, D., Lee, M., Leyva, E., Mobashery, S., et al. (2011). Recognition of peptidoglycan and beta-lactam antibiotics by the extracellular domain of the Ser/Thr protein kinase StkP from *Streptococcus pneumoniae*. *FEBS Lett.* 585, 357–363. doi: 10.1016/j.febslet.2010.12.016
- Mahapatra, S., Crick, D. C., McNeil, M. R., and Brennan, P. J. (2008). Unique structural features of the peptidoglycan of *Mycobacterium leprae*. *J. Bacteriol.* 190, 655–661. doi: 10.1128/JB.00982-07

- Maqbool, A., Herve, M., Mengin-Lecreulx, D., Wilkinson, A. J., and Thomas, G. H. (2012). MpaA is a murein-tripeptide-specific zinc carboxypeptidase that functions as part of a catabolic pathway for peptidoglycan-derived peptides in gamma-proteobacteria. *Biochem. J.* 448, 329–341. doi: 10.1042/BJ20121164
- Martinon, F., and Tschopp, J. (2005). NLRs join TLRs as innate sensors of pathogens. *Trends Immunol.* 26, 447–454. doi: 10.1016/j.it.2005.06.004
- Mauck, J., Chan, L., and Glaser, L. (1971). Turnover of the cell wall of Gram-positive bacteria. *J. Biol. Chem.*
- Mayer, S., Raulf, M. K., and Lepenies, B. (2017). C-type lectins: their network and roles in pathogen recognition and immunity. *Histochem. Cell Biol.* 147, 223–237. doi: 10.1007/s00418-016-1523-7
- McDonald, C., Inohara, N., and Nunez, G. (2005). Peptidoglycan signaling in innate immunity and inflammatory disease. *J. Biol. Chem.* 280, 20177–20180. doi: 10.1074/jbc.R500001200
- Mellroth, P., Karlsson, J., and Steiner, H. (2003). A scavenger function for a *Drosophila* peptidoglycan recognition protein. *J. Biol. Chem.* 278, 7059–7064. doi: 10.1074/jbc.M208900200
- Melly, M. A., McGee, Z. A., and Rosenthal, R. S. (1984). Ability of monomeric peptidoglycan fragments from *Neisseria gonorrhoeae* to damage human fallopian-tube mucosa. *J. Infect. Dis.* 149, 378–386. doi: 10.1093/infdis/149.3.378
- Mengin-Lecreulx, D., and Lemaitre, B. (2005). Structure and metabolism of peptidoglycan and molecular requirements allowing its detection by the *Drosophila* innate immune system. *J. Endotoxin Res.* 11, 105–111. doi: 10.1179/096805105X35233
- Mengin-Lecreulx, D., van Heijenoort, J., and Park, J. T. (1996). Identification of the mpl gene encoding UDP-N-acetylmuramate: L-alanyl-gamma-D-glutamyl-meso-diaminopimelate ligase in *Escherichia coli* and its role in recycling of cell wall peptidoglycan. *J. Bacteriol.* 178, 5347–5352. doi: 10.1128/jb.178.18.5347-5352.1996
- Mesnage, S., Dellarole, M., Baxter, N. J., Rouget, J. B., Dimitrov, J. D., Wang, N., et al. (2014). Molecular basis for bacterial peptidoglycan recognition by LysM domains. *Nat. Commun.* 5, 4269. doi: 10.1038/ncomms5269
- Meylan, E., Tschopp, J., and Karin, M. (2006). Intracellular pattern recognition receptors in the host response. *Nature* 442, 39–44. doi: 10.1038/nature04946
- Mir, M., Asong, J., Li, X., Cardot, J., Boons, G. J., and Husson, R. N. (2011). The extracytoplasmic domain of the *Mycobacterium tuberculosis* Ser/Thr kinase PknB binds specific muopeptides and is required for PknB localization. *PLoS Pathog.* 7:e1002182. doi: 10.1371/journal.ppat.1002182
- Mogensen, T. H. (2009). Pathogen recognition and inflammatory signaling in innate immune defenses. *Clin. Microbiol. Rev.* 22, 240–273. doi: 10.1186/1471-2180-9-281
- Morlot, C., Uehara, T., Marquis, K. A., Bernhardt, T. G., and Rudner, D. Z. (2010). A highly coordinated cell wall degradation machine governs spore morphogenesis in *Bacillus subtilis*. *Genes Dev.* 24, 411–422. doi: 10.1101/gad.1878110
- Moya, B., Dotsch, A., Juan, C., Blazquez, J., Zamorano, L., Haussler, S., et al. (2009). Beta-lactam resistance response triggered by inactivation of a nonessential penicillin-binding protein. *PLoS Pathog.* 5:e1000353. doi: 10.1371/journal.ppat.1000353
- Moynihan, P. J., Sychantha, D., and Clarke, A. J. (2014). Chemical biology of peptidoglycan acetylation and deacetylation. *Bioorg. Chem.* 54, 44–50. doi: 10.1016/j.bioorg.2014.03.010
- Mukamolova, G. V., Murzin, A. G., Salina, E. G., Demina, G. R., Kell, D. B., Kaprelyants, A. S., et al. (2006). Muralytic activity of *Micrococcus luteus* Rpf and its relationship to physiological activity in promoting bacterial growth and resuscitation. *Mol. Microbiol.* 59, 84–98. doi: 10.1111/j.1365-2958.2005.04930.x
- Mukamolova, G. V., Turapov, O. A., Kazarian, K., Telkov, M., Kaprelyants, A. S., Kell, D. B., et al. (2002). The rpf gene of *Micrococcus luteus* encodes an essential secreted growth factor. *Mol. Microbiol.* 46, 611–621. doi: 10.1046/j.1365-2958.2002.03183.x
- Muller, A., Klockner, A., and Schneider, T. (2017). Targeting a cell wall biosynthesis hot spot. *Nat. Prod. Rep.* 34, 909–932. doi: 10.1039/c7np00012j
- Nadesalingam, J., Dodds, A. W., Reid, K. B. M., and Palaniyar, N. (2005). Mannose-binding lectin recognizes peptidoglycan via the N-acetyl glucosamine moiety, and inhibits ligand-induced proinflammatory effect and promotes chemokine production by macrophages. *J. Immunol.* 175, 1785–1794. doi: 10.4049/jimmunol.175.3.1785
- Nanninga, N. (1998). Morphogenesis of *Escherichia coli*. *Microbiol. Mol. Biol. Rev.* 62, 110–129.
- Naseem, S., Parrino, S. M., Buenten, D. M., and Konopka, J. B. (2012). Novel roles for GlcNAc in cell signaling. *Commun. Integr. Biol.* 5, 156–159. doi: 10.4161/cib.19034
- Neuhaus, F. C., and Baddiley, J. (2003). A continuum of anionic charge: structures and functions of d-alanyl-teichoic acids in gram-positive bacteria. *Microbiol. Mol. Biol. Rev.* 67, 686–723. doi: 10.1128/mmbr.67.4.686-723.2003
- Nigro, G., Fazio, L. L., Martino, M. C., Rossi, G., Tattoli, I., Liparoti, V., et al. (2008). Muramylpeptide shedding modulates cell sensing of *Shigella flexneri*. *Cell. Microbiol.* 10, 682–695. doi: 10.1111/j.1462-5822.2007.01075.x
- Nyholm, S. V. (2009). Peptidoglycan monomer release and *Vibrio fischeri*. *J. Bacteriol.* 191, 1997–1999. doi: 10.1128/JB.01801-08
- Nyholm, S. V., Stabb, E. V., Ruby, E. G., and McFall-Ngai, M. J. (2000). Establishment of an animal–bacterial association: recruiting symbiotic vibrios from the environment. *PNAS* 97, 10231–10235.
- Ohnuma, T., Onaga, S., Murata, K., Taira, T., and Katoh, E. (2008). LysM domains from *Pteris ryukyuensis* chitinase-A: a stability study and characterization of the chitin-binding site. *J. Biol. Chem.* 283, 5178–5187. doi: 10.1074/jbc.M707156200
- Oliver, J. D. (2005). The viable but nonculturable state in bacteria. *J. Microbiol.* 43, 93–100. doi: 10.1016/j.jns.2004.11.042
- Park, J. T., and Uehara, T. (2008). How bacteria consume their own exoskeletons (turnover and recycling of cell wall peptidoglycan). *Microbiol. Mol. Biol. Rev.* 72, 211–227. doi: 10.1128/MMBR.00027-07
- Pashenkov, M. V., Dagil, Y. A., and Pinegin, B. V. (2018). NOD1 and NOD2: molecular targets in prevention and treatment of infectious diseases. doi: 10.1016/j.intimp.2017.11.036
- Pensing, D. A., Schaenzer, A. J., and Sauer, J. D. (2018). Do shoot the messenger: PASTA kinases as virulence determinants and antibiotic targets. *Trends Microbiol.* 26, 56–69. doi: 10.1016/j.tim.2017.06.010
- Perley-Robertson, G. E., Yadav, A. K., Winogrodzki, J. L., Stubbs, K. A., Mark, B. L., and Voadlo, D. J. (2016). A fluorescent transport assay enables studying AmpG permeases involved in peptidoglycan recycling and antibiotic resistance. *ACS Chem. Biol.* 11, 2626–2635. doi: 10.1021/acschembio.6b00552
- Peterson, S. B., Dunn, A. K., Klimowicz, A. K., and Handelsman, J. (2006). Peptidoglycan from *Bacillus cereus* mediates commensalism with rhizosphere bacteria from the Cytophaga-Flavobacterium group. *Appl. Environ. Microbiol.* 72, 5421–5427. doi: 10.1128/AEM.02928-05
- Philpott, D. J., Sorbara, M. T., Robertson, S. J., Croitoru, K., and Girardin, S. E. (2014). NOD proteins: regulators of inflammation in health and disease. *Nat. Rev. Immunol.* 14, 9–23. doi: 10.1038/nri3565
- Philpott, D. J., Yamaoka, S., Israel, A., and Sansonetti, P. J. (2000). Invasive *Shigella flexneri* activates NF- κ B through a lipopolysaccharide-dependent innate intracellular response and leads to IL-8 expression in epithelial cells. *J. Immunol.* 165, 903–914. doi: 10.4049/jimmunol.165.2.903
- Plato, A., Willment, J. A., and Brown, G. D. (2013). C-type lectin-like receptors of the dectin-1 cluster: ligands and signaling pathways. *Int. Rev. Immunol.* 32, 134–156. doi: 10.3109/08830185.2013.777065
- Popham, D. L., and Bernhards, C. B. (2015). Spore peptidoglycan. *Microbiol. Spectr.* 3. doi: 10.1128/microbiolspec.TBS-0005-2012
- Ragland, S. A., and Criss, A. K. (2017). From bacterial killing to immune modulation: recent insights into the functions of lysozyme. *PLoS Pathog.* 13:e1006512. doi: 10.1371/journal.ppat.1006512
- Reith, J., and Mayer, C. (2011). Peptidoglycan turnover and recycling in Gram-positive bacteria. *Appl. Microbiol. Biotechnol.* 92, 1–11. doi: 10.1007/s00253-011-3486-x
- Rice, K. C., and Bayles, K. W. (2008). Molecular control of bacterial death and lysis. *Microbiol. Mol. Biol. Rev.* 72, 85–109. doi: 10.1128/MMBR.00030-07
- Rigali, S., Nothaft, H., Noens, E. E., Schlicht, M., Colson, S., Muller, M., et al. (2006). The sugar phosphotransferase system of *Streptomyces coelicolor* is regulated by the GntR-family regulator DasR and links N-acetylglucosamine metabolism to the control of development. *Mol. Microbiol.* 61, 1237–1251. doi: 10.1111/j.1365-2958.2006.05319.x
- Rolain, T., Bernard, E., Courtin, P., Bron, P. A., Kleerebezem, M., Chapot-Chartier, M. P., et al. (2012). Identification of key peptidoglycan hydrolases for morphogenesis, autolysis, and peptidoglycan composition of

- Lactobacillus plantarum* WCFS1. *Microb. Cell Factories* 11, 137. doi: 10.1186/1475-2859-11-137
- Rosenthal, R. S., Nogami, W., Cookson, B. T., Goldman, W. E., and Folkner, W. J. (1987). Major fragment of soluble peptidoglycan released from growing bordetella-pertussis is tracheal cytotoxin. *Infect. Immun.* 55, 2117–2120.
- Royet, J., and Dziarski, R. (2007). Peptidoglycan recognition proteins: pleiotropic sensors and effectors of antimicrobial defences. *Nat. Rev. Microbiol.* 5, 264–277. doi: 10.1038/nrmicro1620
- Royet, J., Gupta, D., and Dziarski, R. (2011). Peptidoglycan recognition proteins: modulators of the microbiome and inflammation. *Nat. Rev. Immunol.* 11, 837–851. doi: 10.1038/nri3089
- Ruscitto, A., Honma, K., Veeramachineni, V. M., Nishikawa, K., Stafford, G. P., and Sharma, A. (2017). Regulation and molecular basis of environmental mureptide uptake and utilization in fastidious oral anaerobe *Tannerella forsythia*. *Front. Microbiol.* 8:648. doi: 10.3389/fmicb.2017.00648
- Santin, Y. G., and Cascales, E. (2017). Domestication of a housekeeping transglycosylase for assembly of a Type VI secretion system. *EMBO Rep.* 18, 138–149. doi: 10.15252/embr.201643206
- Schaub, R. E., Chan, Y. A., Lee, M., Heseck, D., Mobashery, S., and Dillard, J. P. (2016). Lytic transglycosylases LtgA and LtgD perform distinct roles in remodeling, recycling and releasing peptidoglycan in *Neisseria gonorrhoeae*. *Mol. Microbiol.* 102, 865–881. doi: 10.1111/mmi.13496
- Scheurwater, E. M., and Burrows, L. L. (2011). Maintaining network security: how macromolecular structures cross the peptidoglycan layer. *FEMS Microbiol. Lett.* 318, 1–9. doi: 10.1111/j.1574-6968.2011.02228.x
- Scheurwater, E., Reid, C. W., and Clarke, A. J. (2008). Lytic transglycosylases: bacterial space-making autolysins. *Int. J. Biochem. Cell Biol.* 40, 586–591. doi: 10.1016/j.biocel.2007.03.018
- Schleifer, K. H., and Kandler, O. (1972). Peptidoglycan types of bacterial cell-walls and their taxonomic implications. *Bacteriol. Rev.* 36, 407–477.
- Schmidt, D. M., Hubbard, B. K., and Gerlt, J. A. (2001). Evolution of enzymatic activities in the enolase superfamily: functional assignment of unknown proteins in *Bacillus subtilis* and *Escherichia coli* as L-Ala-D/L-Glu epimerases. *Biochemistry* 40, 15707–15715. doi: 10.1021/bi011640x
- Schroeder, U., Henrich, B., Fink, J., and Plapp, R. (1994). Peptidase D of *Escherichia coli* K-12, a metallopeptidase of low substrate specificity. *FEMS Microbiol. Lett.* 123, 153–159.
- Sebahia, M., Wren, B. W., Mullany, P., Fairweather, N. E., Minton, N., Stabler, R., et al. (2006). The multidrug-resistant human pathogen *Clostridium difficile* has a highly mobile, mosaic genome. *Nat. Genet.* 38, 779–786. doi: 10.1038/ng1830
- Shah, I. M., Laaberki, M. H., Popham, D. L., and Dworkin, J. (2008). A eukaryotic-like Ser/Thr kinase signals bacteria to exit dormancy in response to peptidoglycan fragments. *Cell* 135, 486–496. doi: 10.1016/j.cell.2008.08.039
- Sharma, P., Dube, D., Singh, A., Mishra, B., Singh, N., Sinha, M., et al. (2011). Structural basis of recognition of pathogen-associated molecular patterns and inhibition of proinflammatory cytokines by camel peptidoglycan recognition protein. *J. Biol. Chem.* 286, 16208–16217. doi: 10.1074/jbc.M111.228163
- Sharma, A. K., Kumar, S., K. H., Dhakan, D. B., and Sharma, V. K. (2016). Prediction of peptidoglycan hydrolases- a new class of antibacterial proteins. *BMC Genomics* 17, 411. doi: 10.1186/s12864-016-2753-8
- Shi, L., Takahashi, K., Dundee, J., Shahroor-Karni, S., Thiel, S., Jensenius, J. C., et al. (2004). Mannose-binding lectin-deficient mice are susceptible to infection with *Staphylococcus aureus*. *J. Exp. Med.* 199, 1379–1390. doi: 10.1084/jem.20032207
- Shimada, T., Park, B. G., Wolf, A. J., Brikos, C., Goodridge, H. S., Becker, C. A., et al. (2010). *Staphylococcus aureus* evades lysozyme-based peptidoglycan digestion that links phagocytosis, inflammasome activation, and IL-1 β secretion. *Cell Host Microbe* 7, 38–49. doi: 10.1016/j.chom.2009.12.008
- Shimada, T., Yamazaki, K., and Ishihama, A. (2013). Novel regulator PgrR for switch control of peptidoglycan recycling in *Escherichia coli*. *Genes Cells* 18, 123–134. doi: 10.1111/gtc.12026
- Shimkets, L. J., and Kaiser, D. (1982). Induction of coordinated movement of *Myxococcus xanthus* cells. *J. Bacteriol.* 152, 451–461.
- Shockman, G. D., Daneo-Moore, L., Kariyama, R., and Massidda, O. (1996). Bacterial walls, peptidoglycan hydrolases, autolysins, and autolysis. *Microb. Drug Resist.* 2, 95–98. doi: 10.1089/mdr.1996.2.95
- Singh, S. K., SaiSree, L., Amrutha, R. N., and Reddy, M. (2012). Three redundant murein endopeptidases catalyse an essential cleavage step in peptidoglycan synthesis of *Escherichia coli* K12. *Mol. Microbiol.* 86, 1036–1051. doi: 10.1111/mmi.12058
- Sinha, R. K., and Rosenthal, R. S. (1980). Release of soluble peptidoglycan from growing conococci: demonstration of anhydro-muramyl-containing fragments. *Infect. Immun.* 29, 914–925.
- Sinha, R. K., and Rosenthal, R. S. (1981). Effect of penicillin G on release of peptidoglycan fragments by *Neisseria gonorrhoeae*: characterization of extracellular products. *Antimicrob. Agents Chemother.* 20, 98–103. doi: 10.1128/AAC.20.1.98
- Smith, T. J., Blackman, S. A., and Foster, S. J. (2000). Autolysins of *Bacillus subtilis*: multiple enzymes with multiple functions. *Microbiology* 146, 249–262. doi: 10.1099/00221287-146-2-249
- Sorbara, M. T., and Philpott, D. J. (2011). Peptidoglycan: a critical activator of the mammalian immune system during infection and homeostasis. *Immunol. Rev.* 243, 40–60. doi: 10.1111/j.1600-065X.2011.01047.x
- Squeglia, F., Marchetti, R., Ruggiero, A., Lanzetta, R., Marasco, D., Dworkin, J., et al. (2011). Chemical basis of peptidoglycan discrimination by PrkC, a key kinase involved in bacterial resuscitation from dormancy. *J. Am. Chem. Soc.* 133, 20676–20679. doi: 10.1021/ja208080r
- Steen, A., Buist, G., Horsburgh, G. J., Venema, G., Kuipers, O. P., Foster, S. J., et al. (2005). AcmA of *Lactococcus lactis* is an N-acetylglucosaminidase with an optimal number of LysM domains for proper functioning. *FEBS J.* 272, 2854–2868. doi: 10.1111/j.1742-4658.2005.04706.x
- Stohl, E. A., Dale, E. M., Criss, A. K., and Seifert, H. S. (2013). *Neisseria gonorrhoeae* metalloprotease NGO1686 is required for full piliation, and piliation is required for resistance to H₂O₂- and neutrophil-mediated killing. *MBio* 4, 1–9. doi: 10.1128/mBio.00399-13
- Strober, W., Murray, P. J., Kitani, A., and Watanabe, T. (2006). Signalling pathways and molecular interactions of NOD1 and NOD2. *Nat. Rev. Immunol.* 6, 9–20. doi: 10.1038/nri1747
- Sukhithasri, V., Nisha, N., Biswas, L., Anil Kumar, V., and Biswas, R. (2013). Innate immune recognition of microbial cell wall components and microbial strategies to evade such recognitions. *Microbiol. Res.* 168, 396–406. doi: 10.1016/j.micres.2013.02.005
- Swaan, P. W., Bensman, T., Bahadduri, P. M., Hall, M. W., Sarkar, A., Bao, S., et al. (2008). Bacterial peptide recognition and immune activation facilitated by human peptide transporter PEPT2. *Am. J. Respir. Cell Mol. Biol.* 39, 536–542. doi: 10.1165/rcmb.2008-0059OC
- Taylor, A. E., Ayala, J. A., Niumsup, P., Westphal, K., Baker, J. A., and Zhang, L., et al. (2010). Induction of beta-lactamase production in *Aeromonas hydrophila* is responsive to beta-lactam-mediated changes in peptidoglycan composition. *Microbiology* 156, 2327–2335. doi: 10.1099/mic.0.035220-0
- Templin, M. F., Ursinus, A., and Holtje, J. V. (1999). A defect in cell wall recycling triggers autolysis during the stationary growth phase of *Escherichia coli*. *EMBO J.* 18, 4108–4117. doi: 10.1093/emboj/18.15.4108
- Thunnissen, A. M., Rozeboom, H. J., Kalk, K. H., and Dijkstra, B. W. (1995). Structure of the 70-kDa soluble lytic transglycosylase complexed with bulgecin A. Implications for the enzymatic mechanism. *Biochemistry* 34, 12729–12737. doi: 10.1021/bi00039a032
- Troll, J. V., Bent, E. H., Pacquette, N., Wier, A. M., Goldman, W. E., Silverman, N., et al. (2010). Taming the symbiont for coexistence: a host PGRP neutralizes a bacterial symbiont toxin. *Environ. Microbiol.* 12, 2190–2203. doi: 10.1111/j.1462-2920.2009.02121.x
- Tsui, H. C., Zheng, J. J., Magallon, A. N., Ryan, J. D., Yunc, R., Rued, B. E., et al. (2016). Suppression of a deletion mutation in the gene encoding essential PBP2b reveals a new lytic transglycosylase involved in peripheral peptidoglycan synthesis in *Streptococcus pneumoniae* D39. *Mol. Microbiol.* 100, 1039–1065. doi: 10.1111/mmi.13366
- Turner, R. D., Vollmer, W., and Foster, S. J. (2014). Different walls for rods and balls: the diversity of peptidoglycan. *Mol. Microbiol.* 91, 862–874. doi: 10.1111/mmi.12513
- Tydel, C. C., Yuan, J., Tran, P., and Selsted, M. E. (2006). Bovine peptidoglycan recognition protein-S: antimicrobial activity, localization, secretion, and binding properties. *J. Immunol.* 176, 1154–1162. doi: 10.4049/jimmunol.176.2.1154

- Typas, A., Banzhaf, M., Gross, C. A., and Vollmer, W. (2011). From the regulation of peptidoglycan synthesis to bacterial growth and morphology. *Nat. Rev. Microbiol.* 10, 123–136. doi: 10.1038/nrmicro2677
- Uehara, T., and Bernhardt, T. G. (2011). More than just lysins: peptidoglycan hydrolases tailor the cell wall. *Curr. Opin. Microbiol.* 14, 698–703. doi: 10.1016/j.mib.2011.10.003
- Uehara, T., and Park, J. T. (2002). Role of the murein precursor UDP-N-acetylmuramyl-L-Ala- D-Glu- meso-diaminopimelic acid-D-Ala-D-Ala in repression of -lactamase induction in cell division mutants. *J. Bacteriol.* 184, 4233–4239. doi: 10.1128/jb.184.15.4233-4239.2002
- Uehara, T., and Park, J. T. (2003). Identification of MpaA, an amidase in *Escherichia coli* that hydrolyzes the gamma-D-glutamyl-meso-diaminopimelate bond in murein peptides. *J. Bacteriol.* 185, 679–682. doi: 10.1128/JB.185.2.679-682.2003
- Uehara, T., and Park, J. T. (2008). Peptidoglycan recycling. *EcoSal Plus* 3, 1–8. doi: 10.1128/ecosalplus.4.7.1.5
- Uehara, T., Parzych, K. R., Dinh, T., and Bernhardt, T. G. (2010). Daughter cell separation is controlled by cytokinetic ring-activated cell wall hydrolysis. *EMBO J.* 29, 1412–1422. doi: 10.1038/emboj.2010.36
- Uehara, T., Suefuji, K., Jaeger, T., Mayer, C., and Park, J. T. (2006). MurQ etherase is required by *Escherichia coli* in order to metabolize anhydro-N-acetylmuramic acid obtained either from the environment or from its own cell wall. *J. Bacteriol.* 188, 1660–1662. doi: 10.1128/JB.188.4.1660-1662.2006
- Uehara, T., Suefuji, K., Valbuena, N., Meehan, B., Donegan, M., and Park, J. T. (2005). Recycling of the anhydro-N-acetylmuramic acid derived from cell wall murein involves a two-step conversion to N-acetylglucosamine-phosphate. *J. Bacteriol.* 187, 3643–3649. doi: 10.1128/JB.187.11.3643-3649.2005
- van Ampting, M. T., Loonen, L. M., Schonewille, A. J., Konings, I., Vink, C., Iovanna, J., et al. (2012). Intestinally secreted C-type lectin Reg3b attenuates salmonellosis but not listeriosis in mice. *Infect. Immun.* 80, 1115–1120. doi: 10.1128/IAI.06165-11
- van Heijenoort, J. (2011). Peptidoglycan hydrolases of *Escherichia coli*. *Microbiol. Mol. Biol. Rev.* 75, 636–663. doi: 10.1128/MMBR.00022-11
- Vavricka, S. R., Musch, M. W., Chang, J. E., Nakagawa, Y., Phanvijitsiri, K., Waypa, T. S., et al. (2004). hPepT1 transports muramyl dipeptide, activating NF- κ B and stimulating IL-8 secretion in human colonic Caco2/bbe cells. *Gastroenterology* 127, 1401–1409. doi: 10.1053/j.gastro.2004.07.024
- Vollmer, W., and Bertsche, U. (2008). Murein (peptidoglycan) structure, architecture and biosynthesis in *Escherichia coli*. *Biochim. Biophys. Acta* 1778, 1714–1734. doi: 10.1016/j.bbame.2007.06.007
- Vollmer, W., Blanot, D., and de Pedro, M. A. (2008a). Peptidoglycan structure and architecture. *FEMS Microbiol. Rev.* 32, 149–167. doi: 10.1111/j.1574-6976.2007.00094.x
- Vollmer, W., Joris, B., Charlier, P., and Foster, S. (2008b). Bacterial peptidoglycan (murein) hydrolases. *FEMS Microbiol. Rev.* 32, 259–286. doi: 10.1111/j.1574-6976.2007.00099.x
- Votsch, W., and Templin, M. F. (2000). Characterization of a beta -N-acetylglucosaminidase of *Escherichia coli* and elucidation of its role in muropeptide recycling and beta -lactamase induction. *J. Biol. Chem.* 275, 39032–39038. doi: 10.1074/jbc.M004797200
- Waldemar, V. (2012). Bacterial growth does require peptidoglycan hydrolases. *Mol. Microbiol.* 86, 1031–1035. doi: 10.1111/mmi.12059
- White, R. J., and Pasternak, C. A. (1967). The purification and properties of N-acetylglucosamine 6-phosphate deacetylase from *Escherichia coli*. *Biochem. J.* 105, 121–125. doi: 10.1042/bj1050121
- Wiedemann, B., Dietz, H., and Pfeifle, D. (1998). Induction of beta-lactamase in *Enterobacter cloacae*. *Clin. Infect. Dis.* 27(Suppl. 1), S42–S47.
- Wolf, A. J., Reyes, C. N., Liang, W., Becker, C., Shimada, K., Wheeler, M. L., et al. (2016). Hexokinase is an innate immune receptor for the detection of bacterial peptidoglycan. *Cell* 166, 624–636. doi: 10.1016/j.cell.2016.05.076
- Wolf, A. J., and Underhill, D. M. (2018). Peptidoglycan recognition by the innate immune system. *Nat. Rev. Immunol.* 18, 243–254. doi: 10.1038/nri.2017.136
- Wong, J. E., Alsarraf, H. M., Kaspersen, J. D., Pedersen, J. S., Stougaard, J., Thirup, S., et al. (2014). Cooperative binding of LysM domains determines the carbohydrate affinity of a bacterial endopeptidase protein. *FEBS J.* 281, 1196–1208. doi: 10.1111/febs.12698
- Wong, W., Young, F. E., and Chatterjee, A. N. (1974). Regulation of bacterial cell walls: turnover of cell wall in *Staphylococcus aureus*. *J. Bacteriol.* 120, 837–843.
- Wood, T. K., Knabel, S. J., and Kwan, B. W. (2013). Bacterial persister cell formation and dormancy. *Appl. Environ. Microbiol.* 79, 7116–7121. doi: 10.1128/AEM.02636-13
- Woodhams, K. L., Chan, J. M., Lenz, J. D., Hackett, K. T., and Dillard, J. P. (2013). Peptidoglycan fragment release from *Neisseria meningitidis*. *Infect. Immun.* 81, 3490–3498. doi: 10.1128/IAI.00279-13
- Wyckoff, T. J., Taylor, J. A., and Salama, N. R. (2012). Beyond growth: novel functions for bacterial cell wall hydrolases. *Trends Microbiol.* 20, 540–547. doi: 10.1016/j.tim.2012.08.003
- Wydau-Dematteis, S., El Meouche, I., Courtin, P., Hamiot, A., Lai-Kuen, R., Saubaméa, B., et al. (2018). Cwp19 is a novel lytic transglycosylase involved in stationary-phase autolysis resulting in toxin release in *Clostridium difficile*. *mBio* 9, e00648–e00618. doi: 10.1128/mBio.00648-18
- Xu, X. L., Lee, R. T., Fang, H. M., Wang, Y. M., Li, R., Zou, H., et al. (2008). Bacterial peptidoglycan triggers *Candida albicans* hyphal growth by directly activating the adenylyl cyclase Cyr1p. *Cell Host Microbe* 4, 28–39. doi: 10.1016/j.chom.2008.05.014
- Yadav, A., Espallat, A., and Cava, F. (2018). Bacterial strategies to preserve cell wall integrity against environmental threats. *Front. Microbiol.* 9:2064. doi: 10.3389/FMICB.2018.02064
- Yeats, C., Finn, R. D., and Bateman, A. (2002). The PASTA domain: a beta-lactam-binding domain. *Trends Biochem. Sci.* 27, 438. doi: 10.1016/S0968-0004(02)02164-3
- Yin, J., Mao, Y., Ju, L., Jin, M., Sun, Y., Jin, S., et al. (2014). Distinct roles of major peptidoglycan recycling enzymes in beta-Lactamase production in *Shewanella oneidensis*. *Antimicrob. Agents Chemother.* 58, 6536–6543. doi: 10.1128/AAC.03238-14
- Zeng, X., and Lin, J. (2013). Beta-lactamase induction and cell wall metabolism in Gram-negative bacteria. *Front Microbiol.* 4:128. doi: 10.3389/fmicb.2013.00128
- Zhang, Y., Bao, Q., Gagnon, L. A., Huletsky, A., Oliver, A., Jin, S., et al. (2010). ampG gene of *Pseudomonas aeruginosa* and its role in beta-lactamase expression. *Antimicrob. Agents Chemother.* 54, 4772–4779. doi: 10.1128/AAC.00009-10
- Zhang, X. C., Cannon, S. B., and Stacey, G. (2009). Evolutionary genomics of LysM genes in land plants. *BMC Evol. Biol.* 9, 183. doi: 10.1186/1471-2148-9-183
- Zipfel, C. (2014). Plant pattern-recognition receptors. *Trends Immunol.* 35, 345–351. doi: 10.1016/j.it.2014.05.004

Conflict of Interest Statement: The authors declare that the research was conducted in the absence of any commercial or financial relationships that could be construed as a potential conflict of interest.

Copyright © 2019 Irazoki, Hernandez and Cava. This is an open-access article distributed under the terms of the Creative Commons Attribution License (CC BY). The use, distribution or reproduction in other forums is permitted, provided the original author(s) and the copyright owner(s) are credited and that the original publication in this journal is cited, in accordance with accepted academic practice. No use, distribution or reproduction is permitted which does not comply with these terms.



The Pathogenic *Neisseria* Use a Streamlined Set of Peptidoglycan Degradation Proteins for Peptidoglycan Remodeling, Recycling, and Toxic Fragment Release

Ryan E. Schaub and Joseph P. Dillard*

Department of Medical Microbiology and Immunology, School of Medicine and Public Health, University of Wisconsin-Madison, Madison, WI, United States

OPEN ACCESS

Edited by:

Christoph Mayer,
University of Tübingen, Germany

Reviewed by:

Allison H. Williams,
Institut Pasteur, France
André Zapun,
UMR5075 Institut de Biologie
Structurale (IBS), France

*Correspondence:

Joseph P. Dillard
joe.dillard@wisc.edu

Specialty section:

This article was submitted to
Microbial Physiology and Metabolism,
a section of the journal
Frontiers in Microbiology

Received: 06 October 2018

Accepted: 15 January 2019

Published: 31 January 2019

Citation:

Schaub RE and Dillard JP (2019)
The Pathogenic *Neisseria* Use
a Streamlined Set of Peptidoglycan
Degradation Proteins
for Peptidoglycan Remodeling,
Recycling, and Toxic
Fragment Release.
Front. Microbiol. 10:73.
doi: 10.3389/fmicb.2019.00073

Neisseria gonorrhoeae and *Neisseria meningitidis* release peptidoglycan (PG) fragments from the cell as the bacteria grow. For *N. gonorrhoeae* these PG fragments are known to cause damage to human Fallopian tube tissue in organ culture that mimics the damage seen in patients with pelvic inflammatory disease. *N. meningitidis* also releases pro-inflammatory PG fragments, but in smaller amounts than those from *N. gonorrhoeae*. It is not yet known if PG fragment release contributes to the highly inflammatory conditions of meningitis and meningococcemia caused by *N. meningitidis*. Examination of the mechanisms of PG degradation and recycling identified proteins required for these processes. In comparison to the model organism *E. coli*, the pathogenic *Neisseria* have far fewer PG degradation proteins, and some of these proteins show differences in subcellular localization compared to their *E. coli* homologs. In particular, some *N. gonorrhoeae* PG degradation proteins were demonstrated to be in the outer membrane while their homologs in *E. coli* were found free in the periplasm or in the cytoplasm. The localization of two of these proteins was demonstrated to affect PG fragment release. Another major factor for PG fragment release is the allele of *ampG*. Gonococcal AmpG was found to be slightly defective compared to related PG fragment permeases, thus leading to increased release of PG. A number of additional PG-related factors affect other virulence functions in *Neisseria*. Endopeptidases and carboxypeptidases were found to be required for type IV pilus production and resistance to hydrogen peroxide. Also, deacetylation of PG was required for virulence of *N. meningitidis* as well as normal cell size. Overall, we describe the processes involved in PG degradation and recycling and how certain characteristics of these proteins influence the interactions of these pathogens with their host.

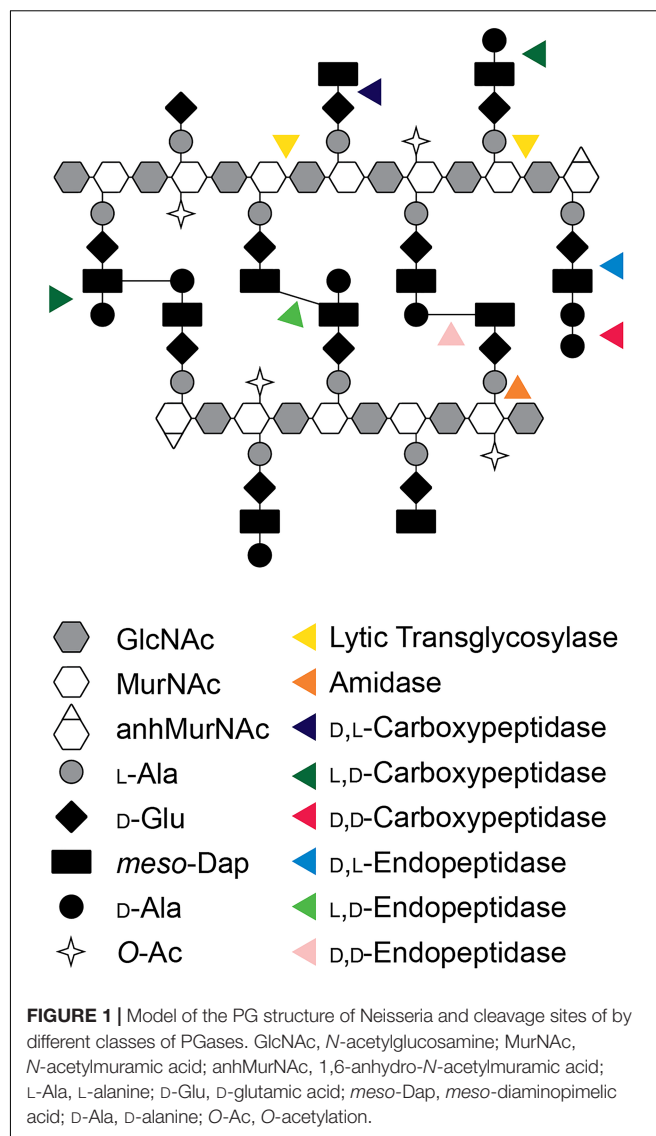
Keywords: peptidoglycan (PG), *Neisseria*, peptidoglycan (PG) hydrolases, lytic transglycosylase, O-acetylation, lipoproteins, NOD1

PEPTIDOGLYCAN (PG) STRUCTURE IN NEISSERIA

The pathogenic *Neisseria* attracted the attention of peptidoglycan (PG) researchers due to the propensity of these bacteria to release small PG fragments during growth (Rosenthal, 1979; Sinha and Rosenthal, 1980). During gonococcal infections, these released PG fragments induce an inflammatory response in the human host that causes tissue damage in the Fallopian tubes and may exacerbate the pathology of urethral, uterine, and disseminated infections. However, the structure of *Neisseria* PG is not unusual. In *N. gonorrhoeae* and *N. meningitidis*, known as gonococci (GC) and meningococci (MC), the PG composition is highly similar to that seen in *Escherichia coli* and many other Gram-negative bacterial species (Dougherty, 1985; Glauner et al., 1988; Antignac et al., 2003b). The glycan strands are composed of repeating β -(1,4)-linked disaccharides of GlcNAc- β -(1,4)-MurNAc. Peptides are attached to the MurNAc and consist of two to five amino acids of the sequence L-Ala-D-Glu-*meso*-Dap-D-Ala-D-Ala (Figure 1). In *N. gonorrhoeae*, approximately 40% of the peptides are crosslinked to peptides on adjacent PG strands to form the cell wall, although there is some variation in the degree of crosslinking between strains (Rosenthal et al., 1980). The crosslinks are formed between the fourth amino acid D-Ala on one strand and the third amino acid *meso*-Dap on the other for a majority of the crosslinks. Crosslinks are also formed between *meso*-Dap on one strand and *meso*-Dap on the other strand. It was reported that *N. meningitidis* cell wall does not contain Dap-Dap crosslinks (Antignac et al., 2003b), but more recent experiments indicate that Dap-Dap crosslinks occur in both *N. gonorrhoeae* and *N. meningitidis* (Woodhams, 2013). The peptide chains in the intact cell wall are mostly tetrapeptides (75%) or tripeptides (25%), with dipeptides and pentapeptides making up a small fraction (Dougherty, 1985). There are two significant differences between *Neisseria* PG and that of *E. coli*. *Neisseria* have O-acetylation at the C6-hydroxyl on about 50% of the MurNAc residues (Rosenthal et al., 1982). This modification controls the function of lytic transglycosylases (LTs) and serves to limit PG degradation by host lysozyme (Blundell et al., 1980; Rosenthal et al., 1982). The second difference is that *E. coli* has proteins covalently attached to the PG such as Braun's lipoprotein (Lpp), whereas GC and MC do not have proteins covalently attached to PG (Wolf-Watz et al., 1975).

RELEASE OF PEPTIDOGLYCAN FRAGMENTS INTO THE MILIEU

Raoul S. (Randy) Rosenthal found that *N. gonorrhoeae* had a high rate of PG turnover, and for over a decade he worked to characterize the PG fragments released and their effects on infection. The most abundant PG fragments released from GC are the PG monomers (GlcNAc-anhMurNAc-tripeptide and GlcNAc-anhMurNAc tetrapeptide) and the free peptides (Ala-Glu-Dap and Ala-Glu-Dap-Ala). The free tripeptide and the tripeptide monomer are agonists for the pattern-recognition receptor NOD1 in humans, and these molecules likely contribute



to the large inflammatory responses seen in a variety of *N. gonorrhoeae* infections (Girardin et al., 2003a). In the *ex vivo* model of gonococcal pelvic inflammatory disease, PG fragments from GC were shown to be sufficient to cause death and sloughing of ciliated cells in human Fallopian tubes and to recapitulate the tissue damage seen in patients with pelvic inflammatory disease (Melly et al., 1984). In addition to the release of PG monomers and free peptides, *N. gonorrhoeae* and *N. meningitidis* release a variety of other PG fragments. These include both glycosidically linked and peptide-linked PG dimers, a tetrasaccharide with a single attached peptide, free disaccharide, and anhydroMurNAc (Rosenthal, 1979; Sinha and Rosenthal, 1980; Woodhams et al., 2013) (see Table 1 and Figure 2).

Neisseria are not the only bacterial species that release PG fragments during growth. Work from Bill Goldman et al. (1982) over many years described the release of the PG monomer GlcNAc-anhMurNAc tetrapeptide by *Bordetella pertussis* (Rosenthal et al., 1987). Known as tracheal cytotoxin

TABLE 1 | PG degradation enzymes required for release of specific PG fragments.

	PG fragment	AKA	Required enzymes	Significance
A	G-aM-3	Anhydro-tripeptide monomer	LtgA or LtgD, PBP3 or PBP4, LdcA	Toxic to FTOC, NOD1 agonist
B	G-aM-4	Anhydro-tetrapeptide monomer	LtgA or LtgD	Mouse NOD1 agonist, TCT
C	L-Ala-D-Glu-mDAP	Free tripeptide	AmiC, PBP3 or PBP4, LdcA	NOD1 agonist
D	L-Ala-D-Glu-mDAP-D-Ala	Free tetrapeptide	AmiC, PBP3 or PBP4	Mouse NOD1 agonist
E	G-M(4)-G-aM(4)	Glycosidic dimer	LTs	Converted by host lysozyme to NOD2 agonist
F	G-aM-4-4-aM-G	Peptide-linked dimer	LTs	
G	G-M-G-aM(4)	Tetrasaccharide-peptide	AmiC, LtgC	
H	G-aM	Free disaccharide	AmiC, LtgC	
I	aM	Anhydro-MurNAc	NagZ, AmiC	

G, *N*-acetylglucosamine; M, *N*-acetyl muramic acid; aM, 1,6-anhydro-*N*-acetyl muramic acid; 3, tripeptide; 4, tetrapeptide. Ltg indicates an unspecified lytic transglycosylase. FTOC, human fallopian tube tissue in organ culture.

or TCT, the PG monomer was found to lead to loss of ciliated cells in hamster tracheal organ culture and production of inflammatory cytokines and nitric oxide by primary tracheal cells from that tissue (Heiss et al., 1993). In *E. coli*, PG fragments are released, but in much smaller amounts than in *Neisseria* or *Bordetella*. *E. coli* release 3–8% of their glycan-containing PG fragments generated during growth. The fragments that are released are the smaller, more broken down pieces of PG and consist of GlcNAc-anhMurNAc and free peptides (Goodell and Schwarz, 1985; Park and Uehara, 2008). *Vibrio fischeri* was shown to release PG monomers, and these PG fragments serve to stimulate tissue remodeling in the Hawaiian bobtail squid (*Euprymna scolopes*) that is in a mutualistic relationship with the bacteria (Koropatnick et al., 2004). It is interesting to note that in *V. fischeri* symbiosis, the PG fragments cause the loss of ciliated cell appendages, which is reminiscent of the loss of ciliated cells in the *B. pertussis* and *N. gonorrhoeae* infections. A number of other bacterial species stimulate a NOD1 response during bacterial infections, which suggests that those species also release PG fragments. *Shigella flexneri*, *Helicobacter pylori*, and *Chlamydia trachomatis* among other species, have been shown to stimulate NOD1 responses, suggesting that those bacteria release PG fragments (Viala et al., 2004; Welter-Stahl et al., 2006; Nigro et al., 2008).

NEISSERIA HAVE A SMALL SET OF PEPTIDOGLYCANASES

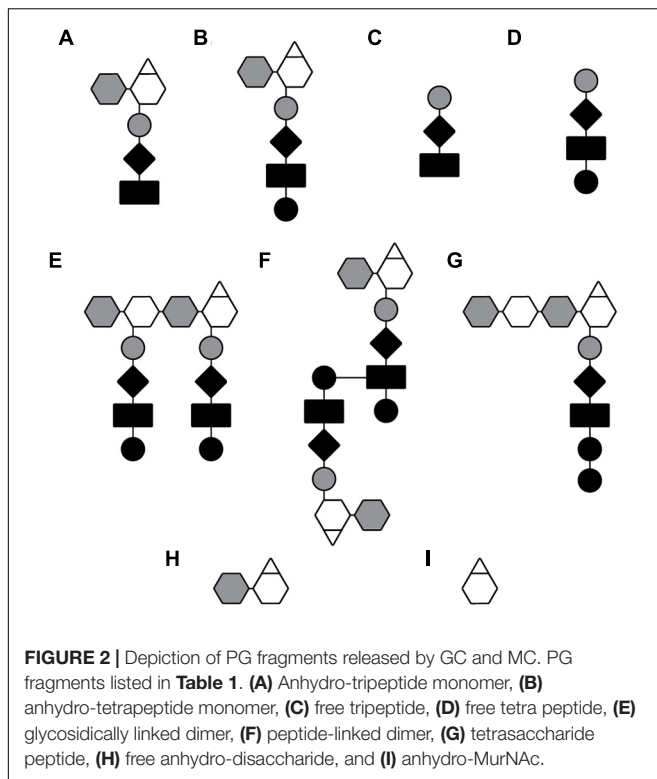
Peptidoglycan degrading enzymes, broadly called peptidoglycanases (PGases), continuously act to modify and degrade PG. Some of these PGases act to modify PG by trimming peptide stems in ways that affect crosslinking and maturation. Others act to cleave PG to allow for the insertion of new glycan strands and to allow dividing cells to separate. GC and MC have a reduced set of PGases compared to most other Gram-negative bacteria. The reduction extends over many different classes of PGases that include LTs, endopeptidases/carboxypeptidases (EPs/), *N*-acetylmuramoyl-L-alanine amidases (amidases), and other activator or accessory proteins. With fewer PGases there is less redundancy of PG degradation functions. A consequence of

having a simplified set of PGases is that single gene mutations can present phenotypic differences.

A prime example of the simplified nature of *Neisseria* PGases is the amidases. The amidases are responsible for removing the peptide stem from the glycan backbone. *E. coli* and many other Gram-negatives have four periplasmic amidases. In *E. coli* three amidases, AmiA, AmiB, and AmiC, are cell separation amidases. These three amidases have two activators. EnvC activates AmiA and AmiB, and NlpD activates AmiC (Uehara et al., 2010). The inactivation of one or two amidases has little or no effect of cell separation. However, if genes for all three cell separation amidases are mutated then the cells form long chains of unseparated cells (Priyadarshini et al., 2006). In contrast, *N. gonorrhoeae* has only a single cell separation amidase, AmiC. A single mutation of either *amiC*, or *nlpD*, which encodes the activator protein, results in a separation phenotype that causes cells to form clumps sharing cell walls (Garcia and Dillard, 2006).

A similar reduction has been observed for LTs, the enzymes that cleave the MurNAc- β -(1,4)-GlcNAc bond of the glycan backbone. As of a current count, the core genome of *Neisseria* includes at seven putative LTs, while the *E. coli* genome encodes nine LTs (Dik et al., 2017). Single LT mutant phenotypes have been observed for the many LTs in GC, but not in *E. coli* (Lommatzsch et al., 1997). Mutation of *ltgC* in GC, or its homolog *gna33* in MC, causes cell separation defects similar to what is observed in an *amiC* mutant (Adu-Bobie et al., 2004; Cloud and Dillard, 2004). The same is not true of the *E. coli* homolog MltA. Mutation of *mltA* alone or in combination of two other LT genes, *slt* and *mltB*, showed no phenotype (Lommatzsch et al., 1997).

Neisseria have two LTs responsible for the production of PG monomers. These LTs, LtgA and LtgD, are homologs of Slt70 and MltB in *E. coli*. LtgA and LtgD are responsible for creating nearly all of the tripeptide and tetrapeptide PG monomers released by GC (Cloud-Hansen et al., 2008). Mutation of *ltgA* results in a 38% decrease in PG monomers while mutation of *ltgD* results in 62% decrease (Cloud and Dillard, 2002). Mutation of both *ltgA* and *ltgD* results in the absence of released of PG monomers including the NOD1 agonist, tripeptide monomer (Cloud-Hansen et al., 2008).



Other single gene mutation phenotypes include increased release of peptide-linked PG dimers and a reduction in tripeptide monomers observed when deleting the L,D-carboxypeptidase gene, *ldcA* (Lenz et al., 2017). Deletion of the D,D-carboxy/endopeptidase gene *dacB* causes the accumulation of pentapeptide in the sacculi and the release of more pentapeptide monomer (Oberfell et al., 2018). Similar results were seen for an *ldcA* mutant in MC and are expected to occur in the MC *dacB* mutant (Woodhams, 2013; Lenz et al., 2017).

Gonococci appears to be missing a number of Class C PBPs known to be peptidases. A class of strict D,D-carboxypeptidases, called Type-5 PBPs, is present in many Gram-negatives. *E. coli* has three members of this family of proteins encoded by *dacA*, *dacC*, and *dacD* (Sauvage et al., 2008). Of these genes, only *dacC* is present in *Neisseria*, but the conserved active site residues are missing (Oberfell et al., 2018). AmpH-like PBPs are also absent in the pathogenic *Neisseria* (GenBank: AE004969.1) (Benson et al., 2018).

Peptidoglycan synthesis proteins are reduced in the GC and MC in a similar trend as PG degrading proteins. GC has only one Class A bifunctional transglycosylase/transpeptidase PBP and one Class B transpeptidase PBP in contrast to *E. coli* that has three Class A PBPs and two Class B (Sauvage et al., 2008). This difference in high molecular mass (HMM) PBPs could be due to the absence of elongation-related proteins in coccoid bacteria. A similar reduction of HMM PBPs is also observed in coccoid Gram-positive bacteria. *Bacillus subtilis* has four Class A PBPs and six Class B PBPs while *Staphylococcus aureus* has only one

Class A PBP, and three Class B PBPs. The reduced number of PG synthesis genes in *Neisseria* and other coccoid bacteria that do not undergo elongation suggests that the genes necessary for a cell elongation complex are absent in these bacteria.

PGase LOCALIZATION IN NEISSERIA

In addition to a reduction of PGases some of the PGases in *Neisseria* have unique subcellular localization compared to other species. This is especially true of the LTs with four of seven core LTs predicted to have localizations different than what has been observed in *E. coli* (Table 2). The cellular localization of periplasmic proteins is determined by the signal sequence. Lipoproteins have a signal sequence that contains a “lipobox” consisting of the protein sequence LxxC where x represents a small amino acid (Kovacs-Simon et al., 2011). The cysteine of the lipobox is lipidated, and then the protein is either transferred to the outer membrane or retained in the inner membrane depending of the amino acid following the cysteine by what is known as the +2 rule (Seydel et al., 1999).

LtgD is the LT responsible for creating the majority of PG monomers that are released from GC (Schaub et al., 2016). LtgD has been classified as a Family 3A LT (Dik et al., 2017). One characteristic of this family of LTs is that they are present as both membrane-bound and soluble proteins. In *E. coli*, membrane-bound lytic transglycosylase B (MltB) is anchored to the outer membrane by a lipidated cysteine residue (Ehlert et al., 1995). Proteolytic cleavage of MltB results in a soluble derivative called Slt35. *Pseudomonas aeruginosa* also has multiple Family 3A LTs (Dik et al., 2017). In this case there is no cleavage of the protein to create two forms of the protein, but there are two paralogs, one that gets anchored to the membrane and a more efficient form that is soluble (Blackburn and Clarke, 2002). In GC there is only one form of LtgD, and it is always anchored to the outer membrane (Schaub et al., 2016). If a mutation is made that results in the absence of the anchoring cysteine of LtgD to the outer membrane, then there is a decrease in the amount of PG monomers released from GC (Schaub et al., 2016). The purpose of having multiple localizations for Family 3A LTs is still unclear, but it appears that membrane localization of LtgD favors the release of PG fragments.

The localization of LtgA to the outer membrane is different in *Neisseria* and related species than it is in most other bacteria such as the periplasmically localized homolog in *E. coli* known as Slt70 (for soluble LT 70 kDa). The septally localized LtgA produces the majority of monomers produced in the cell with most monomers being taken up by the cytoplasmic membrane permease AmpG to be recycled. Conversely, LtgD is distributed throughout the cell and the majority of monomers produced by LtgD are released from the cell. When the lipobox cysteine of LtgA was mutated there was no change in the abundance of released monomer (Schaub et al., 2016). This result either means that outer membrane localization is not important for LtgA's function in PG fragment release or that removal of the lipid is not a sufficient change to prevent LtgA association with the outer membrane.

Other LTs are localized differently in *Neisseria*. In *E. coli* MltC is a lipoprotein that localizes to the inner leaflet of the outer membrane. The *Neisseria* MltC homolog, LtgB, does not have a lipobox motif and is predicted to be an unanchored periplasmic protein. LtgB also lacks an N-terminal DUF3393 domain usually associated with Family 1B LTs (Dik et al., 2017). Single mutants do not have a known phenotype in either GC or *E. coli*, but the true function of these LTs may be masked by a redundant LT.

Bioinformatics indicates that other LT localizations are also different in *Neisseria*. The Family 1D LT, LtgE, is predicted to be a periplasmic protein unlike its *E. coli* homolog, MltD, that is predicted to be anchored to the outer membrane (Bateman and Bycroft, 2000) (Table 2). It is possible that LtgE in fact an inner membrane protein. It has a lipobox (LSVCP) with the proline at the +2 position predicting that the protein would be retained in the inner membrane (Seydel et al., 1999). This prediction is similar to what was found for the *Pseudomonas aeruginosa* LtgE homolog that is also a lipoprotein retained in the inner membrane (Lewenza et al., 2008). The SPOR-domain-containing LT named RlpA (for rare lipoprotein A) is a lipoprotein in *E. coli* as the name suggests. In GC and MC RlpA does not contain a cysteine and is not predicted to be lipidated (GenBank: AAW90349.1).

The localization of another PGase functions to create more tripeptide monomer, as mentioned above. In other bacteria LdcA is a cytoplasmic protein that functions in recycling to remove the D-Ala at the fourth position of the peptide stem (Templin et al., 1999). It is this removal of the D-Ala that allows this tripeptide to be reused. Mpl adds the tripeptide to UDP-MurNAc and then MurF then adds D-Ala-D-Ala to UDP-MurNAc tripeptide to form the PG precursor UDP-MurNAc-pentapeptide (Johnson et al., 2013). It is presumed that LdcA has the same cytoplasmic function in *Neisseria*. Lenz et al. (2017) found that LdcA is also present as an outer-membrane

lipoprotein in GC in addition to being present in the cytoplasm. LdcA was found to be functional in the periplasm since an *ldcA* signal sequence deletion, that keeps LdcA in the cytoplasm, has the same effect on sacculi composition and PG fragment release as an *ldcA* deletion. Mutation of *ldcA* eliminated the presence of tripeptides in the sacculi while increasing the abundance of tetrapeptides. The mutation of *ldcA* altered the ratio of released PG fragments from 3:1 tripeptide to tetrapeptide monomers to nearly only tetrapeptide monomers. The *ldcA* mutants released significantly more peptide-linked PG dimer, suggesting that LdcA also cuts the L,D-Dap-Dap crosslinks. The localization of LdcA to the periplasm is necessary for the observed phenotypes (Lenz et al., 2017). Consequently, the unusual periplasmic localization of LdcA is necessary for the production of NOD1 agonists.

Another way that *Neisseria* cell wall proteins localize differently is within protein complexes. Recently the cell division interactome, or divisome, of *N. gonorrhoeae* has been investigated and was found to have two unique interactions and a number of interactions missing (Zou et al., 2017). An instance where interactions are missing is with the cell division transpeptidase PBP2 encoded by the gene *penA*. The *E. coli* homolog, known as PBP3 or FtsI, has been found to interact with seven different proteins during cell division. Intriguingly, gonococcal PBP2 was only found to interact with one cell separation protein, FtsW. PBP2 is the essential target of many β -lactam antibiotics. Consequently, *penA* alleles conferring β -lactam resistance are becoming common in clinical isolates. Up to 60 amino acid changes have been observed in *penA* mutants (Tomberg et al., 2017). The mutations resulting in antibiotic resistance have been found to decrease the affinity of PBP2 to β -lactams and result in less transpeptidation that causes an increase in pentapeptide stems in the sacculi of resistant strains in GC and MC (Garcia-Bustos and Dougherty, 1987; Antignac et al., 2003a). Some alleles, such as *penA41*, confer a 300-fold increase in the minimum inhibitory concentration (MIC) for ceftriaxone

TABLE 2 | Subcellular localization of LTs and peptidases in GC and *E. coli*.

Type	GC protein	Locus	SignalP ^a	LipoP ^b	EC protein	SignalP ^a	LipoP ^b
LTs	LtgA	NGO_2135	Y	SpII+2=S	Slit70	Y	Spl
	LtgB	NGO_1033	Y	Spl	MltC	Y	SpII+2=S
	LtgC	NGO_2048	Y	SpII+2=Q	MltA	Y	SpII+2=S
	LtgD	NGO_0626	Y	SpII+2=T	MltB	Y	SpII+2=S
	LtgE	NGO_0608	Y	Spl	MltD	Y	SpII+2=Q
	LtgG	NGO_0238	Y	Spl	MltG	Y	Spl
	RlpA	NGO_1728	Y	Spl	RlpA	Y	SpII+2=T
GGI LTs	AtlA	NGrG_00979 ^c	N	Cyt	Lambda R ^d	N	Cyt
	LtgX	NGrG_01000 ^c	Y	Cyt	F orf169 ^e	Y	Spl
Peptidases	PBB3	NGO_0107	Y	Spl	PBP4	Y	Spl
	PBP4	NGO_0327	Y	Spl	PBP7	Y	Spl
	DacC	NGO_0443	Y	Spl	PBP6	Y	Spl
	LdcA	NGO_1274	Y	SpII+2=G	LdcA	N	CYT

^aPrediction of a signal peptide using SignalP 3.0. Y, periplasmic localization; N, cytoplasmic localization. ^bPrediction of subcellular localization and lipidation by LipoP. Cyt, cytoplasm; Spl, periplasmic; SpII, lipidated protein with +2 amino acid influencing inner membrane or outer membrane localization. ^cLocus from GC strain MS11 due to the reference strain FA 1090 not possessing a GGI. ^d*E. coli* lambda phage LT. ^eLT from *E. coli* F-plasmid.

(Tomberg et al., 2013). It is possible that the absence of many of the PBP2 interactions observed in other organisms has allowed the incorporation of beneficial *penA* mutations that would otherwise not be viable.

MACHINE-RELATED PGases

One of the main functions of PG is to provide act as a barrier to macromolecules. The mesh-like structure of PG has been shown to exclude proteins larger than 50 kDa (Demchick and Koch, 1996). Larger proteins and protein complexes need to modify the PG to get past the barrier in a way that does not compromise the integrity of the PG and the cell. Several PGases only act on specific localized substrates and are often associated with larger protein complexes. One of these complexes is the Type IV pilus (Tfp). This organelle is essential for infection and is used by *Neisseria* for attachment to epithelial cells, twitching motility, resistance to oxidative killing, and for DNA uptake (Stohl et al., 2013; Kolappan et al., 2016). It is composed of sub-complexes that allow for the Tfp to extend through the periplasm and extend and retract the pili fibers with molecular motors. The Tfp can extend micrometers beyond the surface of the cell, and each motor has a force exceeding 100 pN (Maier et al., 2002).

An M23B zinc metalloprotease known as NGO1686 or Mpg (for metalloprotease active against PG) was originally found in a screen for genes upregulated during oxidative stress (Stohl et al., 2005, 2012). The connection of a PGase to oxidative stress was originally unclear. Later observations from Dillard and Seifert (2001) found that *mpg* mutants had altered colony morphology and led to an investigation of the Tfp. The *mpg* mutants were found to be defective in piliation, having only about one fifth as many pili as the wild-type, and the mutant exhibited low-piliation phenotypes such as lower levels of natural transformation (Stohl et al., 2013). Further investigation revealed that only functioning pili protected from oxidative stress. A series of pili mutations led to the hypothesis that *mpg* mutants do not have wild-type pili anti-retraction properties, and that Mpg acts to remodel PG to allow for the formation of an anti-retraction complex (Stohl et al., 2013).

Other PGases are also necessary for the assembly of the multi-protein Type IV pili complex (Tfp). Other PGases that influence pili formation are the low-molecular-mass penicillin-binding proteins PBP3 (aka DacB) and DacC, homologs of *E. coli* PBP4 and PBP6. It was found that the bifunctional carboxy/endopeptidase PBP3 drastically alters the composition of the sacculi with *dacB* mutant sacculi having almost no tripeptide monomers, less tetrapeptide monomers, and more pentapeptide monomers and dimers (Oberfell et al., 2018). Mutation of *dacC* had little effect on sacculi composition. Mutation of *dacB* or *dacC* individually did not affect pilus production, but a double *dacB dacC* mutant had drastically reduced piliation that corresponded with a 94% reduction in transformation efficiency (Oberfell et al., 2018). It is clear that PGases are important for the assembly/stability of Tfp, especially PGases possessing carboxy/endopeptidase activity. The modifications are arguably necessary for allowing the insertion of the large Tfp apparatus

with its many associated proteins. Mpg and PBP3 are both D,D-endo/carboxypeptidases. Homologs of DacC are also D,D-endopeptidases, but many *Neisseria* species have mutations in their three active site motifs (SXXK, SXN, and KTG) all of which are necessary for peptidase activity. *N. meningitidis* DacC only has an intact SXN motif, while *N. gonorrhoeae* DacC lacks all three active site motifs (Oberfell et al., 2018). Perhaps in *Neisseria*, DacC acts in a complex with PBP3 and directs its activity. Apparently enzymatically functional DacC is present in Gram-negative rods, including the *Neisseria* species *N. weaveri* and *N. elongata*. The deletion or mutation of multiple genes or gene clusters has been observed in the evolution from a rod to coccoid shape (Veyrier et al., 2015). It is possible that DacC evolved to function as an endopeptidase during elongation but now functions as a scaffold protein to direct Tfp assembly.

Another example of PGases directing the insertion of large protein complexes in the cell wall are those PGases involved with the type IV secretion system (T4SS) that is encoded in the gonococcal genetic island (GGI). The majority of gonococcal strains identified, around 64–80%, have a GGI (Dillard and Seifert, 2001; Pachulec and van der Does, 2010; Wu et al., 2011). The GGI has been identified in 17.5% of *N. meningitidis* strains, and is present in at least two other *Neisseria* spp. (Woodhams et al., 2012; Pachulec et al., 2014; Callaghan et al., 2017). The GGI encodes a T4SS with homology to the *E. coli* F-plasmid in addition to a number of uncharacterized proteins (Callaghan et al., 2017). The *Neisseria* T4SS functions by secreting single-stranded DNA (Salgado-Pabon et al., 2007). In order for the T4SS to be made and secrete DNA, PGases within the GGI are necessary for the insertion and assembly of the multi-protein secretion system complex into the cell wall. Even though there are multiple LTs and endopeptidases encoded on the chromosome, specific PGases are needed for the T4SS to function. Most GGIs encode two LTs, AtlA and LtgX, both of which are necessary for DNA secretion. Some GGIs have been found to have *eppA*, encoding an M23 endopeptidase, instead of *atlA*. Strains with *eppA* instead of *atlA* are not able to secrete DNA even though other T4SSs, such as that of the F-plasmid, do not require an AtlA homolog (Kohler et al., 2013). It is curious that the T4SS requires multiple LTs while the Tfp requires multiple peptidases for proper assembly and function.

HOW NEISSERIA DIFFER FROM THE *E. coli* MODEL

The pathogenic *Neisseria* differ from the model Gram-negative bacterial species, *E. coli*, in important ways in respect to their PG composition and associated proteins. Some of these differences are due to their respective shapes and the lack in GC of many of the elongation complex proteins. Other differences may be due to differences in classes of proteobacteria. For example, the PG synthesis regulatory proteins, LpoA and LpoB, are only found in γ -proteobacteria (Paradis-Bleau et al., 2010; Typas et al., 2010).

Gonococci and MC are thought to have evolved from rod-shaped bacteria and to have lost the multiple genes encoding

parts of the elongation complex (Veyrier et al., 2015). MreB, the filamentous actin-like protein necessary for directing PG synthesis machinery, is absent in GC and MC. Also absent is the *E. coli* PBP2 homolog, a monofunctional D,D-transpeptidase, often associated with MreB that is essential for cell elongation (Zapun et al., 2008). Other MreB-associated proteins absent in GC and MC are the membrane associated proteins MreC, MreD, and RodZ, as well as a glycosyl transferase RodA (Veyrier et al., 2015).

The pathogenic *Neisseria* lack other PG synthesis proteins or their activators. In *E. coli* the periplasmic outer membrane lipoproteins LpoA and LpoB activate the major bifunctional PG synthases PBP1a and PBP1b, respectively (Typas et al., 2010). GC and MC do not possess LpoA, LpoB, or PBP1b. Lpo homologs are restricted to γ -proteobacteria, which makes the absence of these in β -proteobacteria unsurprising. However, there may be an undiscovered regulator of PBP1 in *Neisseria*. Interestingly, PBP1, the only bifunctional PBP in *Neisseria*, is a homolog of PBP1a in *E. coli*. PBP1a is mainly involved with elongation, whereas PBP1b is involved in cell division.

Gram-negative bacteria anchor their outer membrane (OM) to PG. These PG-OM connections have been shown to stabilize the outer membrane and influence the production of outer membrane vesicles. *E. coli* has three known strategies for connecting the OM to PG: one covalent attachment and two types of non-covalent interactions. Braun's lipoprotein (Lpp) is one of the most abundant proteins in *E. coli*. Lpp is inserted in the inner leaflet of outer membrane at the N-terminus by a lipidated cysteine, and the C-terminus of Lpp is covalently linked to Dap residues in PG by a conserved C-terminal lysine (Braun and Sieglin, 1970; Samsudin et al., 2017). MC and GC lack homologs of Lpp and no other covalent attachments have been reported (Wolf-Watz et al., 1975; Dougherty, 1985; Hill and Judd, 1989). GC and MC also lack the L,D-transpeptidases ErfK, YbiS, YcfS that are thought to link Lpp to PG (Sanders and Pavelka, 2013). Another related system lacking in GC and MC is the Rcs, or regulator of capsule synthesis system (*rcsBCDF* and *igaA*), that together with Lpp, sense stress by monitoring the size of the periplasmic space (Guo and Sun, 2017; Miller and Salama, 2018).

Non-covalent OM-PG interactions are made in two different ways in *E. coli*, through OmpA and through the Tol-Pal system. The N-terminal domain of OmpA forms an outer membrane porin, while the periplasmic C-terminal domain binds Dap of the macromolecular PG layer. The other interaction is made by a PG-associated lipoprotein, Pal. The N-terminal cysteine of Pal is lipidated and structurally related to the C-terminal PG-binding domain of OmpA (Yamada et al., 1984). Pal is able to further anchor to the inner membrane by binding to the periplasmic TolB that binds to TolA, which is anchored in the inner membrane (Clavel et al., 1998). *Neisseria* have neither OmpA nor the Tol-Pal system, but they do have two OmpA C-terminal domain containing proteins (OmpA_C-like). One of these OmpA_C-like proteins is NGO1559 and is a predicted outer membrane lipoprotein. Little is known about NGO1559 except that its expression is regulated by iron, and that the protein is found in the outer membrane of GC (Ducey et al., 2005; Zielke et al., 2014).

RmpM (reduction-modifiable protein M) in MC and GC (also called protein III or PIII in GC) defines the other class of OmpA_C-like proteins found in pathogenic *Neisseria*. RmpM protein was demonstrated to stabilize the outer membrane in MC, specifically through its OmpA_C-like domain (Maharjan et al., 2016). It has been shown to crystalize with outer membrane porin PorB from GC (Zeth et al., 2013). It was also shown to be necessary for localizing the LysM-domain containing protein NGO1873 to the outer membrane, and binds to epithelial cells of the male and female genital tracts (Leuzzi et al., 2013). These proteins could function in alternative pathways to compensate for those absent in *Neisseria* (e.g., Tol-Pal, Lpp) or they may have other unknown influences on cell wall synthesis, PG remodeling, protein localization, or host attachment.

O-ACETYLATION OF PG

Modification of PG has been observed in many of the bacteria where PG has been analyzed. O-Acetylation of the C6 carbon of MurNAc has been observed in both Gram-positive and Gram-negative bacteria, although the acetylation occurs by different families of proteins (Moynihan and Clarke, 2011). In Gram-negative bacteria, including MC and GC, two acetyltransferase proteins are necessary for PG O-acetylation. The first protein is a transmembrane acetyltransferase that functions to transfer an acetyl group past the cytoplasmic membrane to a second acetyltransferase. This second periplasmic acetyltransferase then O-acetylates the PG. Both the transmembrane acetyltransferase (PacA) and the periplasmic acetyltransferase (PacB) are necessary for PG O-acetylation (Dillard and Hackett, 2005). O-Acetylation is known to block host lysozyme from cleaving the PG backbone (Rosenthal, 1979). Another consequence of O-acetylation is that it blocks the ability of endogenous LTs to degrade the PG sugar backbone and may thus affect where new PG synthesis occurs.

When O-acetylation is blocked by the mutation of *pacA* and/or *pacB* the overall physiology of MC and GC are mostly unchanged. In GC, the absence of PG O-acetylation did not affect resistance to human serum, resistance to lysozyme, or PG turnover, but it did increase lysis in the presence of EDTA (Dillard and Hackett, 2005). In MC, the absence of acetylation was shown to have no effect on PG chain length or virulence in a murine sepsis model (Veyrier et al., 2013).

Gram-negative bacteria with O-acetylated PG also have an esterase, Ape1, that is able to remove O-acetyl groups from PG (Weadge et al., 2005). The ability to de-O-acetylate PG is seemingly of greater importance than the ability to O-acetylate. In GC, roughly 40% of PG is O-acetylated in wild type cells. Deletion of *ape1* did not affect the overall amount of acetylated PG (Dillard and Hackett, 2005). MC cells with an *ape1* deletion had little change in overall O-acetylation, but were shown to be significantly larger than wild type or cells with triple *pacA*, *pacB*, and *ape1* mutations and had longer glycan strands (Veyrier et al., 2013). Virulence in a murine sepsis model was also significantly decreased in an *ape1* single mutant, but not in an O-acetylation triple mutant in MC (Veyrier et al., 2013). The same study also showed that Ape1 preferentially acetylates glycans linked

to tripeptides (L-Ala-D-Glu-meso-Dap). The reason that *apeI* mutants are defective in virulence is not clear, but it could be that the inability to degrade glycan strands leads to this phenotype. In *ltgA ltgD* mutants, which are also defective in degradation of glycan strands, the cells have a defect in envelope integrity and are sensitive to killing by neutrophils and neutrophil-produced elastase and lysozyme (Ragland et al., 2017).

O-Acetylation of PG has been observed to be important for a number of other Gram-negative human pathogens such as *Campylobacter jejuni*, *Helicobacter pylori*, and *Proteus mirabilis*, but is not common in many bacteria of a healthy microbiome (Dupont and Clarke, 1991; Wang et al., 2012; Ha et al., 2016). O-Acetylation has also been shown to provide lysozyme resistance in the Gram-positive *Enterococcus faecalis*, *Listeria monocytogenes*, *Staphylococcus aureus*, and *Streptococcus pneumoniae* (Moynihan and Clarke, 2011). This process represents a viable option for targeted antimicrobials that do not dramatically alter the microbiome. It also allows for an even more targeted approach by blocking the de-O-acetylase of Gram-negative bacteria.

PG RECYCLING

Despite releasing significant amounts of PG fragments into the milieu, *N. gonorrhoeae* and *N. meningitidis* have functional PG recycling systems and recycle a majority of the PG fragments generated during growth. The PG monomers and free disaccharide are taken up into the cytoplasm by the permease AmpG. The amount of PG fragment release vs. PG recycling is one area where these two pathogens have substantial differences in PG metabolism. While *N. gonorrhoeae* releases 15% of the PG monomers generated during growth, *N. meningitidis* only releases 4% of PG monomers (Garcia and Dillard, 2008; Woodhams et al., 2013). That increased PG fragment release is sufficient to increase NOD1 signaling in epithelial cells and the production of IL-8 in human Fallopian tube tissue (Woodhams et al., 2013). The differences in recycling efficiency between *N. gonorrhoeae* and *N. meningitidis* are partly explained by sequence differences in the C-terminal region of AmpG. Three amino acid differences in gonococcal AmpG compared to meningococcal AmpG result in decreased recycling in GC (Chan and Dillard, 2016). The reason these amino acid substitutions affect PG recycling is not clear, but they are not in the region of the protein expected to act in PG fragment binding.

In addition to AmpG, *Neisseria* also contain the following proteins needed for PG fragment recycling: LdcA, NagZ, AnmK, AmpD, and Mpl. No homolog of MurQ is present, but in other bacteria it has been found that there is an alternative pathway mediated by MupP that converts MurNAc 6-phosphate to MurNAc, bypassing *de novo* synthesis (Borisova et al., 2017). MupP is present in GC (GenBank: EEZ47171.1). Of these enzymes, only AmpD, NagZ, and LdcA have been studied in *Neisseria* (Garcia and Dillard, 2008; Bhoopalan et al., 2016; Lenz et al., 2017). As mentioned above, LdcA is found as an outer-membrane lipoprotein and thus performs at least some of its functions in the periplasm. However, it was also noted that a

smaller soluble form of the protein is produced, and that form of the protein may be in the cytoplasm. Mutation of *ampD* was shown to lead to a build up of MurNAc-peptides in the gonococcal cytoplasm, confirming AmpD's role in PG recycling (Garcia and Dillard, 2008). NagZ's role in recycling in GC has not been fully assessed. However, it was shown that purified NagZ was able to remove GlcNAc from PG monomers and free disaccharide. Interestingly, a gonococcal *nagZ* mutant was found to produce thicker biofilms than the wild type, and a moonlighting role was proposed for NagZ in biofilm disassembly as an extracellular glycosidase (Bhoopalan et al., 2016).

Circumstantial evidence suggests that PG breakdown products may be sensed in the gonococcal cytoplasm and their levels may influence PG fragment production or release. We noted that certain PG recycling mutants failed to release free disaccharide even though they were producing free disaccharide in the periplasm. The first example noted was the *ampD* mutant. In this strain, free disaccharide release was nearly abolished. However, an *ampD ampG* double mutant released wild-type levels of free disaccharide, demonstrating that free disaccharide generation in the periplasm was unaffected by the *ampD* mutation (Garcia and Dillard, 2008). Similar results with disaccharide release were obtained with *ltgA* or *ltgD* mutants (Cloud and Dillard, 2002; Cloud-Hansen et al., 2008). Interestingly, PG monomer release was also found to be affected in certain mutants unable to recycle. An *ltgA ltgD* mutant was compared to an *ltgA ltgD ampG* mutant. The *ltgA ltgD* mutant releases little or no PG monomer or free disaccharide, and it is reduced in recycling due to producing less of the anhydro-disaccharide-containing PG fragments recognized by AmpG. When the *ltgA ltgD ampG* mutant was analyzed for fragment release, significant amounts of PG monomers were released indicating that some of this material was generated in the periplasm, but release had somehow been prevented (Schaub et al., 2016). These results suggest that GC are able to regulate PG release and PG uptake into the cytoplasm. Such regulation could be useful for controlling cell wall metabolism or for releasing more or less of the inflammatory PG fragments under different infection conditions.

PG AND HOST IMMUNE RESPONSE

The pathology of *N. gonorrhoeae* and *N. meningitidis* infections is due to the host inflammatory response. The bacteria release multiple pro-inflammatory molecules including lipooligosaccharide, porin protein PorB (a TLR2 agonist), heptose-1,7-bisphosphate, and PG fragments (Sinha and Rosenthal, 1980; Kattner et al., 2014; Packiam et al., 2014; Gaudet et al., 2015). The inflammatory response must be advantageous for the bacteria, and for *N. gonorrhoeae*, the ability to attract neutrophils and infect them may be an important step in the disease (Criss et al., 2009). Both NOD1 and NOD2 responses to PG fragments have been observed in the inflammatory responses to *N. gonorrhoeae*. A NOD2 response was described for mice infected with *N. gonorrhoeae*, and a NOD1 response

was implicated in human Fallopian tube or epithelial cell studies *in vitro* (Woodhams et al., 2013; Mavrogiorgos et al., 2014).

For humans, NOD1 agonists must contain the second and third amino acids of the PG peptide chain, and the peptide must terminate with DAP (Girardin et al., 2003a; Magalhaes et al., 2005). For GC, the released NOD1 agonists are disaccharide-tripeptide monomer and the free tripeptide (Sinha and Rosenthal, 1980; Chan and Dillard, 2017). Production of the free tripeptide requires AmiC to cleave the peptide from the glycan strand (Lenz et al., 2016). In order for there to be significant amounts of tripeptides in the sacculus, LdcA has to cleave the fourth amino acid (D-Ala) from some of the peptide chains (Lenz et al., 2017). Not surprisingly, AmiC and LdcA were both demonstrated to act in producing NOD1 agonists (Lenz et al., 2016, 2017). However, the requirement for peptidases for NOD1 agonist production was not quite so obvious. Mutations affecting *dacB* (encoding PBP3) and *pbpG* (encoding PBP4) were also demonstrated to decimate NOD1 activation by *N. gonorrhoeae* (Schaub et al., 2019). These enzymes both cleave the common peptide crosslinks (Ala-DAP) and remove the fifth amino acid (D-Ala) (Stefanova et al., 2003; Schaub et al., 2019). When the fifth amino acid is not removed, LdcA cannot cleave the fourth amino acid to leave a strand terminating in DAP (Schaub et al., 2019). Also, the L,D-transpeptidase cannot act to make DAP-DAP crosslinks and in the process cleave an Ala-DAP bond. Thus, no NOD1 agonist is made.

NOD2 is generally described as responding to macromolecular PG such as the whole sacculus or as recognizing muramyl-dipeptide (MurNAc-L-Ala-D-Glu) (Girardin et al., 2003b). *N. gonorrhoeae* and *N. meningitidis* are prone to autolysis, making macromolecular PG available for immune recognition (Bos et al., 2005; Chan et al., 2012). Furthermore, large PG fragments have been demonstrated to induce pathology in a rat model of gonococcal arthritis (Fleming et al., 1986). O-Acetylation of PG decreases its destruction by lysozyme and may explain its greater effects on arthritis (Fleming et al., 1986; Dillard and Hackett, 2005). *N. gonorrhoeae* and *N. meningitidis* do not release muramyl dipeptide (Sinha and Rosenthal, 1980). However, they do release a soluble PG molecule that is converted by the host into a NOD2 agonist. Glycosidically linked dimers are released by both pathogens, and when these molecules are digested by host lysozyme, the PG monomers carrying a reducing end on MurNAc are potent agonists for NOD2 (Woodhams et al., 2013; Dagil et al., 2016; Knilans et al., 2017). When PG dimers are degraded by the bacterial glycosidases, such as LtgA or LtgD, the products all have a 1,6-anhydro bond on the MurNAc and do not stimulate NOD2 (Knilans et al., 2017). It is interesting to note that commensal *Neisseria* species *N. sicca* and *N. mucosa* do not produce PG dimers, suggesting that the lack of a NOD2 response may be helpful for these bacteria to maintain a non-pathogenic lifestyle (Chan and Dillard, 2016).

We recently made the observation that one common *N. gonorrhoeae* strain induces an unusually high NOD2 response. Strain FA19 was found to cause a large NOD2 response in epithelial cells both to soluble PG fragments released by the bacteria during growth and to purified sacculi. Compositional analyses demonstrated that both the sacculus and the released

fragments contained much larger amounts of dipeptide chains compared to other gonococcal strains (Schaub et al., 2019). This observation suggests that *Neisseria* have another, yet uncharacterized, endopeptidase and that this enzyme may differ between strains or may be regulated to give larger or smaller NOD2 responses.

CONCLUDING REMARKS

All *N. gonorrhoeae* strains analyzed to date have a somewhat defective version of the PG fragment permease AmpG, making it likely that all GC release a substantial amount of their PG fragments generated during growth (Chan and Dillard, 2016). Understanding the roles of these PG fragments in infections and the host responses to them will continue to progress as more sophisticated infection models are developed and as we learn more from *ex vivo* human organ culture models. Even without considering effects on infection, the *Neisseria* make an attractive model for understanding PG metabolism generally. With the ability to do natural transformation and the small number of PG metabolism genes, the *Neisseria* make a promising system for revealing the functions of PG degradation and synthesis proteins. *N. gonorrhoeae* and *N. meningitidis* are coccal in shape, but they have close relatives that are rod shaped including *N. elongata* and *N. bacilliformis*. Thus the evolution and advantages of coccal shape might be further explored as has begun with the studies by Veyrier et al. (2015). The tendency of the bacteria to undergo autolysis adds another area of interest for understanding phenomena related to infection and inflammation as well as release of DNA for natural transformation (Hebel and Young, 1975; Hamilton and Dillard, 2006). Key areas for future investigation involve understanding protein-protein interactions and mechanisms of regulation and sensing of PG synthesis and degradation. The AmpR-based method of PG sensing in the cytoplasm is not present in many bacterial species and is not present in *Neisseria* (Jacobs et al., 1994; Chan and Dillard, 2017). However, there is evidence of PG fragment sensing, suggesting an unexplored mechanism exists (Cloud-Hansen et al., 2008; Garcia and Dillard, 2008). As mentioned above, the LpoA-LpoB mechanism of regulating PG biosynthesis is also absent in many bacterial species, so an unknown mechanism is likely to be identified for that process as well. Protein-protein interactions for *Neisseria* PG metabolism proteins have been found as in other bacteria, and it is likely that further investigation of this simplified system will reveal more information about coordinated activities, enzyme activation, and regulation (Lenz et al., 2016; Chan and Dillard, 2017; Perez Medina and Dillard, 2018).

AUTHOR CONTRIBUTIONS

This review was written with contributions from RS and JD.

FUNDING

This work was supported by NIH grant R01AI097157.

REFERENCES

- Adu-Bobie, J., Lupetti, P., Brunelli, B., Granoff, D., Norais, N., Ferrari, G., et al. (2004). GNA33 of *Neisseria meningitidis* is a lipoprotein required for cell separation, membrane architecture, and virulence. *Infect. Immun.* 72, 1914–1919. doi: 10.1128/IAI.72.4.1914-1919.2004
- Antignac, A., Boneca, I. G., Rousselle, J. C., Namane, A., Carlier, J. P., Vazquez, J. A., et al. (2003a). Correlation between alterations of the penicillin-binding protein 2 and modifications of the peptidoglycan structure in *Neisseria meningitidis* with reduced susceptibility to penicillin G. *J. Biol. Chem.* 278, 31529–31535. doi: 10.1074/jbc.M304607200
- Antignac, A., Rousselle, J. C., Namane, A., Labigne, A., Taha, M. K., and Boneca, I. G. (2003b). Detailed structural analysis of the peptidoglycan of the human pathogen *Neisseria meningitidis*. *J. Biol. Chem.* 278, 31521–31528. doi: 10.1074/jbc.M304749200
- Bateman, A., and Bycroft, M. (2000). The structure of a LysM domain from *E. coli* membrane-bound lytic murein transglycosylase D (MltD). *J. Mol. Biol.* 299, 1113–1119. doi: 10.1006/jmbi.2000.3778
- Benson, D. A., Cavanaugh, M., Clark, K., Karsch-Mizrachi, I., Ostell, J., Pruitt, K. D., et al. (2018). GenBank. *Nucleic Acids Res.* 46, D41–D47. doi: 10.1093/nar/gkx1094
- Bhoopalan, S. V., Piekarowicz, A., Lenz, J. D., Dillard, J. P., and Stein, D. C. (2016). nagZ triggers gonococcal biofilm disassembly. *Sci. Rep.* 6:22372. doi: 10.1038/srep22372
- Blackburn, N. T., and Clarke, A. J. (2002). Characterization of soluble and membrane-bound family 3 lytic transglycosylases from *Pseudomonas aeruginosa*. *Biochemistry* 41, 1001–1013. doi: 10.1021/bi011833k
- Blundell, J. K., Smith, G. J., and Perkins, H. R. (1980). The peptidoglycan of *Neisseria gonorrhoeae*: O-acetyl groups and lysozyme sensitivity. *FEMS Microbiol. Lett.* 9, 259–261. doi: 10.1111/j.1574-6968.1980.tb05648.x
- Borisova, M., Gisin, J., and Mayer, C. (2017). The N-acetylmuramic acid 6-phosphate phosphatase MupP completes the *Pseudomonas* peptidoglycan recycling pathway leading to intrinsic fosfomycin resistance. *mBio* 8:e00092-17. doi: 10.1128/mBio.00092-17
- Bos, M. P., Tefsen, B., Voet, P., Weynants, V., van Putten, J. P., and Tommassen, J. (2005). Function of neisserial outer membrane phospholipase A in autolysis and assessment of its vaccine potential. *Infect. Immun.* 73, 2222–2231. doi: 10.1128/IAI.73.4.2222-2231.2005
- Braun, V., and Sieglin, U. (1970). The covalent murein-lipoprotein structure of the *Escherichia coli* cell wall. The attachment site of the lipoprotein on the murein. *Eur. J. Biochem.* 13, 336–346. doi: 10.1111/j.1432-1033.1970.tb00936.x
- Callaghan, M. M., Heilers, J. H., van der Does, C., and Dillard, J. P. (2017). Secretion of chromosomal DNA by the *Neisseria gonorrhoeae* type IV secretion system. *Curr. Top. Microbiol. Immunol.* 413, 323–345. doi: 10.1007/978-3-319-75241-9_13
- Chan, J. M., and Dillard, J. P. (2016). *Neisseria gonorrhoeae* crippled its peptidoglycan fragment permease to facilitate toxic peptidoglycan monomer release. *J. Bacteriol.* 198, 3029–3040. doi: 10.1128/JB.00437-16
- Chan, J. M., and Dillard, J. P. (2017). Attention seeker: production, modification, and release of inflammatory peptidoglycan fragments in *Neisseria* species. *J. Bacteriol.* 199:e00354-17. doi: 10.1128/JB.00354-17
- Chan, Y. A., Hackett, K. T., and Dillard, J. P. (2012). The lytic transglycosylases of *Neisseria gonorrhoeae*. *Microb. Drug Resist.* 18, 271–279. doi: 10.1089/mdr.2012.0001
- Clavel, T., Germon, P., Vianney, A., Portalier, R., and Lazzaroni, J. C. (1998). TolB protein of *Escherichia coli* K-12 interacts with the outer membrane peptidoglycan-associated proteins Pal, Lpp and OmpA. *Mol. Microbiol.* 29, 359–367. doi: 10.1046/j.1365-2958.1998.00945.x
- Cloud, K. A., and Dillard, J. P. (2002). A lytic transglycosylase of *Neisseria gonorrhoeae* is involved in peptidoglycan-derived cytotoxin production. *Infect. Immun.* 70, 2752–2757. doi: 10.1128/IAI.70.6.2752-2757.2002
- Cloud, K. A., and Dillard, J. P. (2004). Mutation of a single lytic transglycosylase causes aberrant septation and inhibits cell separation of *Neisseria gonorrhoeae*. *J. Bacteriol.* 186, 7811–7814. doi: 10.1128/JB.186.22.7811-7814.2004
- Cloud-Hansen, K. A., Hackett, K. T., Garcia, D. L., and Dillard, J. P. (2008). *Neisseria gonorrhoeae* uses two lytic transglycosylases to produce cytotoxic peptidoglycan monomers. *J. Bacteriol.* 190, 5989–5994. doi: 10.1128/JB.00506-08
- Criss, A. K., Katz, B. Z., and Seifert, H. S. (2009). Resistance of *Neisseria gonorrhoeae* to non-oxidative killing by adherent human polymorphonuclear leukocytes. *Cell. Microbiol.* 11, 1074–1087. doi: 10.1111/j.1462-5822.2009.01308.x
- Dagil, Y. A., Arbatsky, N. P., Alkhazova, B. I., L'Vov, V. L., Mazurov, D. V., and Pashenkov, M. V. (2016). The dual NOD1/NOD2 agonism of muropeptides containing a meso-diaminopimelic acid residue. *PLoS One* 11:e0160784. doi: 10.1371/journal.pone.0160784
- Demchick, P., and Koch, A. L. (1996). The permeability of the wall fabric of *Escherichia coli* and *Bacillus subtilis*. *J. Bacteriol.* 178, 768–773. doi: 10.1128/jb.178.3.768-773.1996
- Dik, D. A., Marous, D. R., Fisher, J. F., and Mobashery, S. (2017). Lytic transglycosylases: concinnity in concision of the bacterial cell wall. *Crit. Rev. Biochem. Mol. Biol.* 52, 503–542. doi: 10.1080/10409238.2017.1337705
- Dillard, J. P., and Hackett, K. T. (2005). Mutations affecting peptidoglycan acetylation in *Neisseria gonorrhoeae* and *Neisseria meningitidis*. *Infect. Immun.* 73, 5697–5705. doi: 10.1128/iai.73.9.5697-5705.2005
- Dillard, J. P., and Seifert, H. S. (2001). A variable genetic island specific for *Neisseria gonorrhoeae* is involved in providing DNA for natural transformation and is found more often in disseminated infection isolates. *Mol. Microbiol.* 41, 263–277. doi: 10.1046/j.1365-2958.2001.02520.x
- Dougherty, T. J. (1985). Analysis of *Neisseria gonorrhoeae* peptidoglycan by reverse-phase, high-pressure liquid chromatography. *J. Bacteriol.* 163, 69–74.
- Ducey, T. F., Carson, M. B., Orvis, J., Stintzi, A. P., and Dyer, D. W. (2005). Identification of the iron-responsive genes of *Neisseria gonorrhoeae* by microarray analysis in defined medium. *J. Bacteriol.* 187, 4865–4874. doi: 10.1128/JB.187.14.4865-4874.2005
- Dupont, C., and Clarke, A. J. (1991). Dependence of lysozyme-catalysed solubilization of *Proteus mirabilis* peptidoglycan on the extent of O-acetylation. *Eur. J. Biochem.* 195, 763–769. doi: 10.1111/j.1432-1033.1991.tb15764.x
- Ehlert, K., Holtje, J. V., and Templin, M. F. (1995). Cloning and expression of a murein hydrolase lipoprotein from *Escherichia coli*. *Mol. Microbiol.* 16, 761–768. doi: 10.1111/j.1365-2958.1995.tb02437.x
- Fleming, T. J., Wallsmith, D. E., and Rosenthal, R. S. (1986). Arthropathic properties of gonococcal peptidoglycan fragments: implications for the pathogenesis of disseminated gonococcal disease. *Infect. Immun.* 52, 600–608.
- Garcia, D. L., and Dillard, J. P. (2006). AmiC functions as an N-acetylmuramyl-L-alanine amidase necessary for cell separation and can promote autolysis in *Neisseria gonorrhoeae*. *J. Bacteriol.* 188, 7211–7221. doi: 10.1128/JB.00724-06
- Garcia, D. L., and Dillard, J. P. (2008). Mutations in ampG or ampD affect peptidoglycan fragment release from *Neisseria gonorrhoeae*. *J. Bacteriol.* 190, 3799–3807. doi: 10.1128/JB.01194-07
- Garcia-Bustos, J. F., and Dougherty, T. J. (1987). Alterations in peptidoglycan of *Neisseria gonorrhoeae* induced by sub-MICs of beta-lactam antibiotics. *Antimicrob. Agents Chemother.* 31, 178–182. doi: 10.1128/AAC.31.2.178
- Gaudet, R. G., Sintsova, A., Buckwalter, C. M., Leung, N., Cochrane, A., Li, J., et al. (2015). INNATE IMMUNITY. Cytosolic detection of the bacterial metabolite HBP activates TIFA-dependent innate immunity. *Science* 348, 1251–1255. doi: 10.1126/science.aaa4921
- Girardin, S. E., Boneca, I. G., Carneiro, L. A., Antignac, A., Jehanno, M., Viala, J., et al. (2003a). Nod1 detects a unique muropeptide from gram-negative bacterial peptidoglycan. *Science* 300, 1584–1587. doi: 10.1126/science.1084677
- Girardin, S. E., Boneca, I. G., Viala, J., Chamailard, M., Labigne, A., Thomas, G., et al. (2003b). Nod2 is a general sensor of peptidoglycan through muramyl dipeptide (MDP) detection. *J. Biol. Chem.* 278, 8869–8872. doi: 10.1074/jbc.C200651200
- Glauner, B., Holtje, J. V., and Schwarz, U. (1988). The composition of the murein of *Escherichia coli*. *J. Biol. Chem.* 263, 10088–10095.
- Goldman, W. E., Klapper, D. G., and Baseman, J. B. (1982). Detection, isolation, and analysis of a released *Bordetella pertussis* product toxic to cultured tracheal cells. *Infect. Immun.* 36, 782–794.
- Goodell, E. W., and Schwarz, U. (1985). Release of cell wall peptides into culture medium by exponentially growing *Escherichia coli*. *J. Bacteriol.* 162, 391–397.
- Guo, X. P., and Sun, Y. C. (2017). New insights into the non-orthodox two component Rcs phosphorelay system. *Front. Microbiol.* 8:2014. doi: 10.3389/fmicb.2017.02014
- Ha, R., Frirdich, E., Sychantha, D., Biboy, J., Taveirne, M. E., Johnson, J. G., et al. (2016). Accumulation of peptidoglycan O-acetylation leads to altered cell wall

- biochemistry and negatively impacts pathogenesis factors of *Campylobacter jejuni*. *J. Biol. Chem.* 291, 22686–22702. doi: 10.1074/jbc.M116.746404
- Hamilton, H. L., and Dillard, J. P. (2006). Natural transformation of *Neisseria gonorrhoeae*: from DNA donation to homologous recombination. *Mol. Microbiol.* 59, 376–385. doi: 10.1111/j.1365-2958.2005.04964.x
- Hebeler, B. H., and Young, F. E. (1975). Autolysis of *Neisseria gonorrhoeae*. *J. Bacteriol.* 122, 385–392.
- Heiss, L. N., Moser, S. A., Unanue, E. R., and Goldman, W. E. (1993). Interleukin-1 is linked to the respiratory epithelial cytopathology of pertussis. *Infect. Immun.* 61, 3123–3128.
- Hill, S. A., and Judd, R. C. (1989). Identification and characterization of peptidoglycan-associated proteins in *Neisseria gonorrhoeae*. *Infect. Immun.* 57, 3612–3618.
- Jacobs, C., Huang, L. J., Bartowsky, E., Normark, S., and Park, J. T. (1994). Bacterial cell wall recycling provides cytosolic muropeptides as effectors for beta-lactamase induction. *EMBO J.* 13, 4684–4694. doi: 10.1002/j.1460-2075.1994.tb06792.x
- Johnson, J. W., Fisher, J. F., and Mobashery, S. (2013). Bacterial cell-wall recycling. *Ann. N. Y. Acad. Sci.* 1277, 54–75. doi: 10.1111/j.1749-6632.2012.06813.x
- Kattner, C., Toussi, D. N., Zaucha, J., Wetzler, L. M., Ruppel, N., Zachariae, U., et al. (2014). Crystallographic analysis of *Neisseria meningitidis* PorB extracellular loops potentially implicated in TLR2 recognition. *J. Struct. Biol.* 185, 440–447. doi: 10.1016/j.jsb.2013.12.006
- Nilans, K. J., Hackett, K. T., Anderson, J. E., Weng, C., Dillard, J. P., and Duncan, J. A. (2017). *Neisseria gonorrhoeae* lytic transglycosylases LtgA and LtgD reduce host innate immune signaling through TLR2 and NOD2. *ACS Infect. Dis.* 3, 624–633. doi: 10.1021/acsinfecdis.6b00088
- Kohler, P. L., Chan, Y. A., Hackett, K. T., Turner, N., Hamilton, H. L., Cloud-Hansen, K. A., et al. (2013). Mating pair formation homologue TraG is a variable membrane protein essential for contact-independent type IV secretion of chromosomal DNA by *Neisseria gonorrhoeae*. *J. Bacteriol.* 195, 1666–1679. doi: 10.1128/JB.02098-12
- Kolappan, S., Coureuil, M., Yu, X., Nassif, X., Egelman, E. H., and Craig, L. (2016). Structure of the *Neisseria meningitidis* type IV pilus. *Nat. Commun.* 7:13015. doi: 10.1038/ncomms13015
- Koropatnick, T. A., Engle, J. T., Apicella, M. A., Stabb, E. V., Goldman, W. E., and McFall-Ngai, M. J. (2004). Microbial factor-mediated development in a host-bacterial mutualism. *Science* 306, 1186–1188. doi: 10.1126/science.1102218
- Kovacs-Simon, A., Titball, R. W., and Michell, S. L. (2011). Lipoproteins of bacterial pathogens. *Infect. Immun.* 79, 548–561. doi: 10.1128/IAI.00682-10
- Lenz, J. D., Hackett, K. T., and Dillard, J. P. (2017). A single dual-function enzyme controls the production of inflammatory NOD agonist peptidoglycan fragments by *Neisseria gonorrhoeae*. *mBio* 8:e01464-17. doi: 10.1128/mBio.01464-17
- Lenz, J. D., Stohl, E. A., Robertson, R. M., Hackett, K. T., Fisher, K., Xiong, K., et al. (2016). Amidase activity of AmiC controls cell separation and stem peptide release and is enhanced by NlpD in *Neisseria gonorrhoeae*. *J. Biol. Chem.* 291, 10916–10933. doi: 10.1074/jbc.M116.715573
- Leuzzi, R., Nesta, B., Monaci, E., Cartocci, E., Serino, L., Soriani, M., et al. (2013). *Neisseria gonorrhoeae* PIII has a role on NG1873 outer membrane localization and is involved in bacterial adhesion to human cervical and urethral epithelial cells. *BMC Microbiol.* 13:251. doi: 10.1186/1471-2180-13-251
- Lewenza, S., Mhlanga, M. A., and Pugsley, A. P. (2008). Novel inner membrane retention signals in *Pseudomonas aeruginosa* lipoproteins. *J. Bacteriol.* 190, 6119–6125. doi: 10.1128/JB.00603-08
- Lommatzsch, J., Templin, M. F., Kraft, A. R., Vollmer, W., and Holtje, J. V. (1997). Outer membrane localization of murein hydrolases: MltA, a third lipoprotein lytic transglycosylase in *Escherichia coli*. *J. Bacteriol.* 179, 5465–5470. doi: 10.1128/jb.179.17.5465-5470.1997
- Magalhaes, J. G., Philpott, D. J., Nahori, M. A., Jehanno, M., Fritz, J., Le Bourhis, L., et al. (2005). Murine Nod1 but not its human orthologue mediates innate immune detection of tracheal cytotoxin. *EMBO Rep.* 6, 1201–1207. doi: 10.1038/sj.embor.7400552
- Maharjan, S., Saleem, M., Feavers, I. M., Wheeler, J. X., Care, R., and Derrick, J. P. (2016). Dissection of the function of the RmpM periplasmic protein from *Neisseria meningitidis*. *Microbiology* 162, 364–375. doi: 10.1099/mic.0.000227
- Maier, B., Potter, L., So, M., Long, C. D., Seifert, H. S., and Sheetz, M. P. (2002). Single pilus motor forces exceed 100 pN. *Proc. Natl. Acad. Sci. U.S.A.* 99, 16012–16017. doi: 10.1073/pnas.242523299
- Mavroggiorgos, N., Mekasha, S., Yang, Y., Kelliher, M. A., and Ingalls, R. R. (2014). Activation of NOD receptors by *Neisseria gonorrhoeae* modulates the innate immune response. *Innate Immun.* 20, 377–389. doi: 10.1177/1753425913493453
- Melly, M. A., McGee, Z. A., and Rosenthal, R. S. (1984). Ability of monomeric peptidoglycan fragments from *Neisseria gonorrhoeae* to damage human fallopian-tube mucosa. *J. Infect. Dis.* 149, 378–386. doi: 10.1093/infdis/149.3.378
- Miller, S. I., and Salama, N. R. (2018). The gram-negative bacterial periplasm: size matters. *PLoS Biol.* 16:e2004935. doi: 10.1371/journal.pbio.2004935
- Moynihan, P. J., and Clarke, A. J. (2011). O-Acetylated peptidoglycan: controlling the activity of bacterial autolysins and lytic enzymes of innate immune systems. *Int. J. Biochem. Cell Biol.* 43, 1655–1659. doi: 10.1016/j.biocel.2011.08.007
- Nigro, G., Fazio, L. L., Martino, M. C., Rossi, G., Tattoli, I., Liparoti, V., et al. (2008). Muramylpeptide shedding modulates cell sensing of *Shigella flexneri*. *Cell. Microbiol.* 10, 682–695. doi: 10.1111/j.1462-5822.2007.01075.x
- Obergfell, K. P., Schaub, R. E., Priniski, L. L., Dillard, J. P., and Seifert, H. S. (2018). The low-molecular-mass, penicillin-binding proteins DacB and DacC combine to modify peptidoglycan cross-linking and allow stable Type IV pilus expression in *Neisseria gonorrhoeae*. *Mol. Microbiol.* 109, 135–149. doi: 10.1111/mmi.13955
- Pachulec, E., Siewering, K., Bender, T., Heller, E. M., Salgado-Pabon, W., Schmoller, S. K., et al. (2014). Functional analysis of the gonococcal genetic island of *Neisseria gonorrhoeae*. *PLoS One* 9:e109613. doi: 10.1371/journal.pone.0109613
- Pachulec, E., and van der Does, C. (2010). Conjugative plasmids of *Neisseria gonorrhoeae*. *PLoS One* 5:e9962. doi: 10.1371/journal.pone.0009962
- Packiam, M., Yedery, R. D., Begum, A. A., Carlson, R. W., Ganguly, J., Sempowski, G. D., et al. (2014). Phosphoethanolamine decoration of *Neisseria gonorrhoeae* lipid A plays a dual immunostimulatory and protective role during experimental genital tract infection. *Infect. Immun.* 82, 2170–2179. doi: 10.1128/IAI.01504-14
- Paradis-Bleau, C., Markovski, M., Uehara, T., Lupoli, T. J., Walker, S., Kahne, D. E., et al. (2010). Lipoprotein cofactors located in the outer membrane activate bacterial cell wall polymerases. *Cell* 143, 1110–1120. doi: 10.1016/j.cell.2010.11.037
- Park, J. T., and Uehara, T. (2008). How bacteria consume their own exoskeletons (turnover and recycling of cell wall peptidoglycan). *Microbiol. Mol. Biol. Rev.* 72, 211–227. doi: 10.1128/MMBR.00027-07
- Perez Medina, K. M., and Dillard, J. P. (2018). Antibiotic targets in gonococcal cell wall metabolism. *Antibiotics* 7:E64. doi: 10.3390/antibiotics7030064
- Priyadarshini, R., Popham, D. L., and Young, K. D. (2006). Daughter cell separation by penicillin-binding proteins and peptidoglycan amidases in *Escherichia coli*. *J. Bacteriol.* 188, 5345–5355. doi: 10.1128/JB.00476-06
- Ragland, S. A., Schaub, R. E., Hackett, K. T., Dillard, J. P., and Criss, A. K. (2017). Two lytic transglycosylases in *Neisseria gonorrhoeae* impart resistance to killing by lysozyme and human neutrophils. *Cell. Microbiol.* 19:e12662. doi: 10.1111/cmi.12662
- Rosenthal, R. S. (1979). Release of soluble peptidoglycan from growing gonococci: hexaminidase and amidase activities. *Infect. Immun.* 24, 869–878.
- Rosenthal, R. S., Blundell, J. K., and Perkins, H. R. (1982). Strain-related differences in lysozyme sensitivity and extent of O-acetylation of gonococcal peptidoglycan. *Infect. Immun.* 37, 826–829.
- Rosenthal, R. S., Nogami, W., Cookson, B. T., Goldman, W. E., and Folkner, W. J. (1987). Major fragment of soluble peptidoglycan released from growing *Bordetella pertussis* is tracheal cytotoxin. *Infect. Immun.* 55, 2117–2120.
- Rosenthal, R. S., Wright, R. M., and Sinha, R. K. (1980). Extent of peptide cross-linking in the peptidoglycan of *Neisseria gonorrhoeae*. *Infect. Immun.* 28, 867–875.
- Salgado-Pabon, W., Jain, S., Turner, N., van der Does, C., and Dillard, J. P. (2007). A novel relaxase homologue is involved in chromosomal DNA processing for type IV secretion in *Neisseria gonorrhoeae*. *Mol. Microbiol.* 66, 930–947. doi: 10.1111/j.1365-2958.2007.05966.x
- Samsudin, F., Boags, A., Piggot, T. J., and Khalid, S. (2017). Braun's lipoprotein facilitates OmpA interaction with the *Escherichia coli* cell wall. *Biophys. J.* 113, 1496–1504. doi: 10.1016/j.bpj.2017.08.011
- Sanders, A. N., and Pavelka, M. S. (2013). Phenotypic analysis of *Escherichia coli* mutants lacking L,D-transpeptidases. *Microbiology* 159(Pt 9), 1842–1852. doi: 10.1099/mic.0.069211-0

- Sauvage, E., Kerff, F., Terrak, M., Ayala, J. A., and Charlier, P. (2008). The penicillin-binding proteins: structure and role in peptidoglycan biosynthesis. *FEMS Microbiol. Rev.* 32, 234–258. doi: 10.1111/j.1574-6976.2008.00105.x
- Schaub, R. E., Chan, Y. A., Lee, M., Heseck, D., Mobashery, S., and Dillard, J. P. (2016). Lytic transglycosylases LtgA and LtgD perform distinct roles in remodeling, recycling and releasing peptidoglycan in *Neisseria gonorrhoeae*. *Mol. Microbiol.* 102, 865–881. doi: 10.1111/mmi.13496
- Schaub, R. E., Perez-Medina, K. M., Hackett, K. T., and Garcia, D. L. (2019). *Neisseria gonorrhoeae* PBP3 and PBP4 facilitate NOD1 agonist peptidoglycan fragment release and survival in stationary phase. *Infect. Immun.* doi: 10.1128/IAI.00833-18 [Epub ahead of print].
- Seydel, A., Gounon, P., and Pugsley, A. P. (1999). Testing the '+2 rule' for lipoprotein sorting in the *Escherichia coli* cell envelope with a new genetic selection. *Mol. Microbiol.* 34, 810–821. doi: 10.1046/j.1365-2958.1999.01647.x
- Sinha, R. K., and Rosenthal, R. S. (1980). Release of soluble peptidoglycan from growing gonococci: demonstration of anhydro-muramyl-containing fragments. *Infect. Immun.* 29, 914–925.
- Stefanova, M. E., Tomberg, J., Olesky, M., Holtje, J. V., Gutheil, W. G., and Nicholas, R. A. (2003). *Neisseria gonorrhoeae* penicillin-binding protein 3 exhibits exceptionally high carboxypeptidase and beta-lactam binding activities. *Biochemistry* 42, 14614–14625. doi: 10.1021/bi0350607
- Stohl, E. A., Chan, Y. A., Hackett, K. T., Kohler, P. L., Dillard, J. P., and Seifert, H. S. (2012). *Neisseria gonorrhoeae* virulence factor NG1686 is a bifunctional M23B family metalloproteinase that influences resistance to hydrogen peroxide and colony morphology. *J. Biol. Chem.* 287, 11222–11233. doi: 10.1074/jbc.M111.338830
- Stohl, E. A., Criss, A. K., and Seifert, H. S. (2005). The transcriptome response of *Neisseria gonorrhoeae* to hydrogen peroxide reveals genes with previously uncharacterized roles in oxidative damage protection. *Mol. Microbiol.* 58, 520–532. doi: 10.1111/j.1365-2958.2005.04839.x
- Stohl, E. A., Dale, E. M., Criss, A. K., and Seifert, H. S. (2013). *Neisseria gonorrhoeae* metalloproteinase NGO1686 is required for full piliation, and piliation is required for resistance to H₂O₂- and neutrophil-mediated killing. *mBio* 4:e00399-13. doi: 10.1128/mBio.00399-13
- Templin, M. F., Ursinus, A., and Holtje, J. V. (1999). A defect in cell wall recycling triggers autolysis during the stationary growth phase of *Escherichia coli*. *EMBO J.* 18, 4108–4117. doi: 10.1093/emboj/18.15.4108
- Tomberg, J., Fedarovich, A., Vincent, L. R., Jerse, A. E., Unemo, M., Davies, C., et al. (2017). Alanine 501 mutations in penicillin-binding protein 2 from *Neisseria gonorrhoeae*: structure, mechanism, and effects on cephalosporin resistance and biological fitness. *Biochemistry* 56, 1140–1150. doi: 10.1021/acs.biochem.6b01030
- Tomberg, J., Unemo, M., Ohnishi, M., Davies, C., and Nicholas, R. A. (2013). Identification of amino acids conferring high-level resistance to expanded-spectrum cephalosporins in the penA gene from *Neisseria gonorrhoeae* strain H041. *Antimicrob. Agents Chemother.* 57, 3029–3036. doi: 10.1128/AAC.00093-13
- Typas, A., Banzhaf, M., van den Berg van Saparoea, B., Verheul, J., Biboy, J., Nichols, R. J., et al. (2010). Regulation of peptidoglycan synthesis by outer-membrane proteins. *Cell* 143, 1097–1109. doi: 10.1016/j.cell.2010.11.038
- Uehara, T., Parzych, K. R., Dinh, T., and Bernhardt, T. G. (2010). Daughter cell separation is controlled by cytokinetic ring-activated cell wall hydrolysis. *EMBO J.* 29, 1412–1422. doi: 10.1038/emboj.2010.36
- Veyrier, F. J., Biais, N., Morales, P., Belkacem, N., Guilhen, C., Ranjeva, S., et al. (2015). Common cell shape evolution of two nasopharyngeal pathogens. *PLoS Genet.* 11:e1005338. doi: 10.1371/journal.pgen.1005338
- Veyrier, F. J., Williams, A. H., Mesnage, S., Schmitt, C., Taha, M. K., and Boneca, I. G. (2013). De-O-acetylation of peptidoglycan regulates glycan chain extension and affects *in vivo* survival of *Neisseria meningitidis*. *Mol. Microbiol.* 87, 1100–1112. doi: 10.1111/mmi.12153
- Viala, J., Chaput, C., Boneca, I. G., Cardona, A., Girardin, S. E., Moran, A. P., et al. (2004). Nod1 responds to peptidoglycan delivered by the *Helicobacter pylori* cag pathogenicity island. *Nat. Immunol.* 5, 1166–1174. doi: 10.1038/ni1131
- Wang, G., Lo, L. F., Forsberg, L. S., and Maier, R. J. (2012). *Helicobacter pylori* peptidoglycan modifications confer lysozyme resistance and contribute to survival in the host. *mBio* 3:e00409-12. doi: 10.1128/mBio.00409-12
- Weadge, J. T., Pfeffer, J. M., and Clarke, A. J. (2005). Identification of a new family of enzymes with potential O-acetylpeptidoglycan esterase activity in both Gram-positive and Gram-negative bacteria. *BMC Microbiol.* 5:49. doi: 10.1186/1471-2180-5-49
- Welter-Stahl, L., Ojcius, D. M., Viala, J., Girardin, S., Liu, W., Delarbre, C., et al. (2006). Stimulation of the cytosolic receptor for peptidoglycan, Nod1, by infection with *Chlamydia trachomatis* or *Chlamydia muridarum*. *Cell. Microbiol.* 8, 1047–1057. doi: 10.1111/j.1462-5822.2006.00686.x
- Wolf-Watz, H., Elmros, T., Normark, S., and Bloom, G. D. (1975). Cell envelope of *Neisseria gonorrhoeae*: outer membrane and peptidoglycan composition of penicillin-sensitive and -resistant strains. *Infect. Immun.* 11, 1332–1341.
- Woodhams, K. L. (2013). *Characterization of the Gonococcal Genetic Island and Peptidoglycan Fragment Release in Neisseria meningitidis*. Doctor of Philosophy, University of Wisconsin-Madison, Madison, WI.
- Woodhams, K. L., Benet, Z. L., Blonsky, S. E., Hackett, K. T., and Dillard, J. P. (2012). Prevalence and detailed mapping of the gonococcal genetic island in *Neisseria meningitidis*. *J. Bacteriol.* 194, 2275–2285. doi: 10.1128/JB.00094-12
- Woodhams, K. L., Chan, J. M., Lenz, J. D., Hackett, K. T., and Dillard, J. P. (2013). Peptidoglycan fragment release from *Neisseria meningitidis*. *Infect. Immun.* 81, 3490–3498. doi: 10.1128/IAI.00279-13
- Wu, Z., Xu, L., Tu, Y., Chen, R., Yu, Y., Li, J., et al. (2011). The relationship between the symptoms of female gonococcal infections and serum progesterone level and the genotypes of *Neisseria gonorrhoeae* multi-antigen sequence type (NG-MAST) in Wuhan, China. *Eur. J. Clin. Microbiol. Infect. Dis.* 30, 113–116. doi: 10.1007/s10096-010-1040-x
- Yamada, H., Yamagata, H., and Mizushima, S. (1984). The major outer membrane lipoprotein and new lipoproteins share a common signal peptidase that exists in the cytoplasmic membrane of *Escherichia coli*. *FEBS Lett.* 166, 179–182. doi: 10.1016/0014-5793(84)80068-X
- Zapun, A., Vernet, T., and Pinho, M. G. (2008). The different shapes of cocci. *FEMS Microbiol. Rev.* 32, 345–360. doi: 10.1111/j.1574-6976.2007.00098.x
- Zeth, K., Kozjak-Pavlovic, V., Faulstich, M., Fraunholz, M., Hurwitz, R., Kepp, O., et al. (2013). Structure and function of the PorB porin from disseminating *Neisseria gonorrhoeae*. *Biochem. J.* 449, 631–642. doi: 10.1042/BJ20121025
- Zielke, R. A., Wierzbicki, I. H., Weber, J. V., Gafken, P. R., and Sikora, A. E. (2014). Quantitative proteomics of the *Neisseria gonorrhoeae* cell envelope and membrane vesicles for the discovery of potential therapeutic targets. *Mol. Cell. Proteomics* 13, 1299–1317. doi: 10.1074/mcp.M113.029538
- Zou, Y., Li, Y., and Dillon, J. R. (2017). The distinctive cell division interactome of *Neisseria gonorrhoeae*. *BMC Microbiol.* 17:232. doi: 10.1186/s12866-017-1140-1

Conflict of Interest Statement: The authors declare that the research was conducted in the absence of any commercial or financial relationships that could be construed as a potential conflict of interest.

Copyright © 2019 Schaub and Dillard. This is an open-access article distributed under the terms of the Creative Commons Attribution License (CC BY). The use, distribution or reproduction in other forums is permitted, provided the original author(s) and the copyright owner(s) are credited and that the original publication in this journal is cited, in accordance with accepted academic practice. No use, distribution or reproduction is permitted which does not comply with these terms.



Mechanistic Pathways for Peptidoglycan O-Acetylation and De-O-Acetylation

David Sychantha[†], Ashley S. Brott, Carys S. Jones and Anthony J. Clarke*

Department of Molecular and Cellular Biology, University of Guelph, Guelph, ON, Canada

OPEN ACCESS

Edited by:

Stephane Mesnage,
University of Sheffield,
United Kingdom

Reviewed by:

Allison H. Williams,
Institut Pasteur, France
Abdellah Benachour,
University of Caen Normandy, France

*Correspondence:

Anthony J. Clarke
aclarke@uoguelph.ca

[†]Present address:

David Sychantha,
Department of Biochemistry
and Biomedical Sciences, Michael G.
DeGroote Institute for Infectious
Disease Research, McMaster
University, Hamilton, ON, Canada

Specialty section:

This article was submitted to
Microbial Physiology and Metabolism,
a section of the journal
Frontiers in Microbiology

Received: 05 July 2018

Accepted: 11 September 2018

Published: 01 October 2018

Citation:

Sychantha D, Brott AS, Jones CS
and Clarke AJ (2018) Mechanistic
Pathways for Peptidoglycan
O-Acetylation and De-O-Acetylation.
Front. Microbiol. 9:2332.
doi: 10.3389/fmicb.2018.02332

The post-synthetic O-acetylation of the essential component of bacterial cell walls, peptidoglycan (PG), is performed by many pathogenic bacteria to help them evade the lytic action of innate immunity responses. Occurring at the C-6 hydroxyl of *N*-acetylmuramoyl residues, this modification to the glycan backbone of PG sterically blocks the activity of lysozymes. As such, the enzyme responsible for this modification in Gram-positive bacteria is recognized as a virulence factor. With Gram-negative bacteria, the O-acetylation of PG provides a means of control of their autolysins at the substrate level. In this review, we discuss the pathways for PG O-acetylation and de-O-acetylation and the structure and function relationship of the O-acetyltransferases and O-acetylesterases that catalyze these reactions. The current understanding of their mechanisms of action is presented and the prospects of targeting these systems for the development of novel therapeutics are explored.

Keywords: peptidoglycan, O-acetylation, O-acetyltransferase, O-acetylesterase, SGNH hydrolase, catalytic mechanism, X-ray structure

INTRODUCTION

Antimicrobial resistance (AMR) among bacterial pathogens continues to pose a serious threat to human health despite extensive research and altered clinical practices. In 2015, the World Health Assembly of the United Nations (UN) endorsed a global action plan to tackle AMR (World Health Organization, 2015), and the UN General Assembly met in 2016 to commit to it. This represented only the fourth time in the history of the UN that a health topic was discussed at the General Assembly, underscoring the importance of the issue. Indeed, an extensive review on AMR recently conducted for the UK government (The Review on Antimicrobial Resistance chaired by Jim O'Neill, 2014) suggests that, despite the huge resources that have already expended to date, a continued heavy investment into pharmaceutical research is needed to defend against the threat of drug-resistant “superbugs,” such as methicillin-resistant *Staphylococcus aureus* (MRSA), vancomycin-resistant *Enterococcus* (VRE), and drug-resistant *Streptococcus pneumoniae* (DRSP). As the Gram-positive pathogens MRSA, VRE, and DRSP continue to burden public health, AMR strains of the Gram-negative pathogen *Neisseria gonorrhoeae* are now emerging (Allen et al., 2014; Martin et al., 2015) to the extent that, in the summer of 2017, the WHO began warning of the spreading of drug-resistant gonorrhoea where some strains may be untreatable by all known antibiotics (World Health Organization, 2017). With the declining impact of traditional antibiotics, and few prospects in the development pipeline, alternative strategies are being considered (Brown and Wright, 2016). One of these concerns the development of antivirulence agents as antibiotics which would increase the susceptibility of pathogens to the host immune response while minimizing deleterious effects on commensal bacteria.

As a key component of bacterial cell walls, peptidoglycan (PG; also known as murein) counters the turgor pressure of the cytoplasm to maintain cell viability. This essential feature, together with its uniqueness to bacteria, presents an “Achilles heel” that has been exploited both naturally and clinically. Thus, in addition to antibiotics that target PG metabolic events, such as the β -lactams and glycopeptides (e.g., vancomycin), PG is the initial target of the innate immune system. Specifically, lysozymes are produced (Ragland and Criss, 2017) to hydrolyze glycosidic linkages between the repeating amino sugar units that form the glycan backbone of PG (**Figure 1**). The initial PG fragments released serve to activate further immune responses (Shimada et al., 2010; Sorbara and Philpott, 2011) while the continued lytic action results in cell rupture and death. This lysozyme response is effective against both Gram-positive and Gram-negative bacteria despite the fact that the PG sacculus of the latter organisms is “protected” by an outer membrane; other factors of the innate immune system, such as lactoferrin (Ellison and Giehl, 1991) and defensins (Hancock and Scott, 2000), disrupt the outer membrane to facilitate exposure of PG to lysozyme. However, many pathogenic bacteria defend against this innate immunity by chemically modifying their PG through O-acetylation. As such, the enzymes involved in the O-acetylation of PG may represent a new opportunity for antibiotic discovery.

This review presents the current understanding of the structure and function relationship of the enzymes that catalyze the O-acetylation and de-O-acetylation of PG. This information thus presents a foundation for the identification of inhibitors that may prove to be leads for one or more novel classes of antibacterials.

PEPTIDOGLYCAN STRUCTURE AND BIOSYNTHESIS

General Structure of Peptidoglycan

The general structure of PG is composed of conserved repeating units of GlcNAc and MurNAc residues joined by β -(1,4)-glycosidic linkages (**Figure 1A**). These chains vary in length, depending on species, and adjacent strands are covalently cross-linked through stem peptides that are associated with the MurNAc residues. Over 50 unique chemotypes of PG are known (Schleifer and Kandler, 1972), which are defined by the composition of the stem peptides and the nature of their crosslinking (**Figure 1B**). Despite this, nascent PG precursors always contain MurNAc with a core pentapeptide stem where the first four stem peptide residues canonically alternate between D- and L-isomers. The first amino acid is attached to the C-3 lactyl moiety of MurNAc and is always D-Ala. At the second position, L-Glu is most often found. However, some bacteria have the ability to amidate this residue (iso-L-Gln); this amidation is catalyzed by an amidotransferase on the synthesized PG precursor (Figueiredo et al., 2012; Münch et al., 2012). The residue at the third position is the most variable, but it is commonly occupied by either L-Lys or *meso*-diaminopimelic acid (*m*DAP), followed by two D-Ala residues at the fourth and fifth positions. The type of crosslink between stem peptides also

varies and may occur either directly between the third and fourth positions of the two peptides or through a peptide bridge, such as the penta-Gly and Ser-Ala branches commonly seen in *S. aureus* and *S. pneumoniae*, respectively.

Biosynthesis of Peptidoglycan

The biosynthesis of PG can be divided into two major events, the preparation of precursor units within the cytoplasm (**Figure 2A**) and their subsequent polymerization into the existing extracytoplasmic sacculus (**Figure 2B**; reviewed in Egan et al., 2015). The nexus of these activities is the translocation of the lipid-linked PG precursor known as Lipid II.

Lipid II biosynthesis begins with the conversion of the primary metabolite fructose-6-phosphate to uridine diphosphate (UDP)-GlcNAc in three enzymatic steps. The committed PG metabolite, UDP-MurNAc, is then made through the sequential action of MurA and MurB (Marquardt et al., 1992; Benson et al., 1993; Brown et al., 1995). This is followed by the addition of the stem pentapeptide to the C-3 lactyl group of UDP-MurNAc through an enzymatic cascade involving MurC (Liger et al., 1995), MurD (Pratviel-Sosa et al., 1991), MurE (Michaud et al., 1990), and MurF (Michaud et al., 1990). The product UDP-MurNAc-5P is the substrate for MraY, which ligates the muropeptide portion to the C-55 isoprenoid lipid carrier, undecaprenyl phosphate (UndP; bactoprenol) with the release of UMP (Ikeda et al., 1991). The product Lipid I (UndPP-MurNAc-5P), localized on the cytoplasmic face of the cytoplasmic membrane, is ligated to the GlcNAc of a second UDP-GlcNAc with the release of UDP through the action of the glycosyltransferase MurG generating Lipid II (Ikeda et al., 1992).

The question of how Lipid II is translocated across the membrane was a matter of great debate. The controversy involved two opposing hypotheses, with each suggesting that either MurJ (Ruiz, 2008) or FtsW (Mohammadi et al., 2011) is the Lipid II translocase (“flippase”). Both proteins perform non-redundant and essential roles. However, a preliminary report from the Bernhardt and Walker labs (Taguchi et al., 2018) identifies FtsW as a PG polymerase that becomes activated once bound to its cognate penicillin-binding protein (PBP). The PBPs are the enzymes involved in the late steps of PG biosynthesis as they polymerize Lipid II on the extracytoplasmic face of the cytoplasmic membrane to produce the nascent glycan chains necessary for (out)growth of the sacculus. Although this is an area of ongoing research, the long-standing model has been that this assembly process is dependent on both monofunctional glycosyltransferases and the PBPs, specifically those that polymerize glycan chains and then catalyze the cross-linking of neighboring strands to produce the mature sacculus (Goffin and Ghuyssen, 1998).

Bacteria produce multiple PBPs, each playing unique roles in PG biosynthesis. In rod shaped cells, some PBPs are recruited to the site of cell division, while others function to elongate the cell. These PBPs are part of multi-protein complexes known as the divisosome and elongasome, respectively (Höltje, 1998; Naninga, 1991). These discrete complexes are organized by

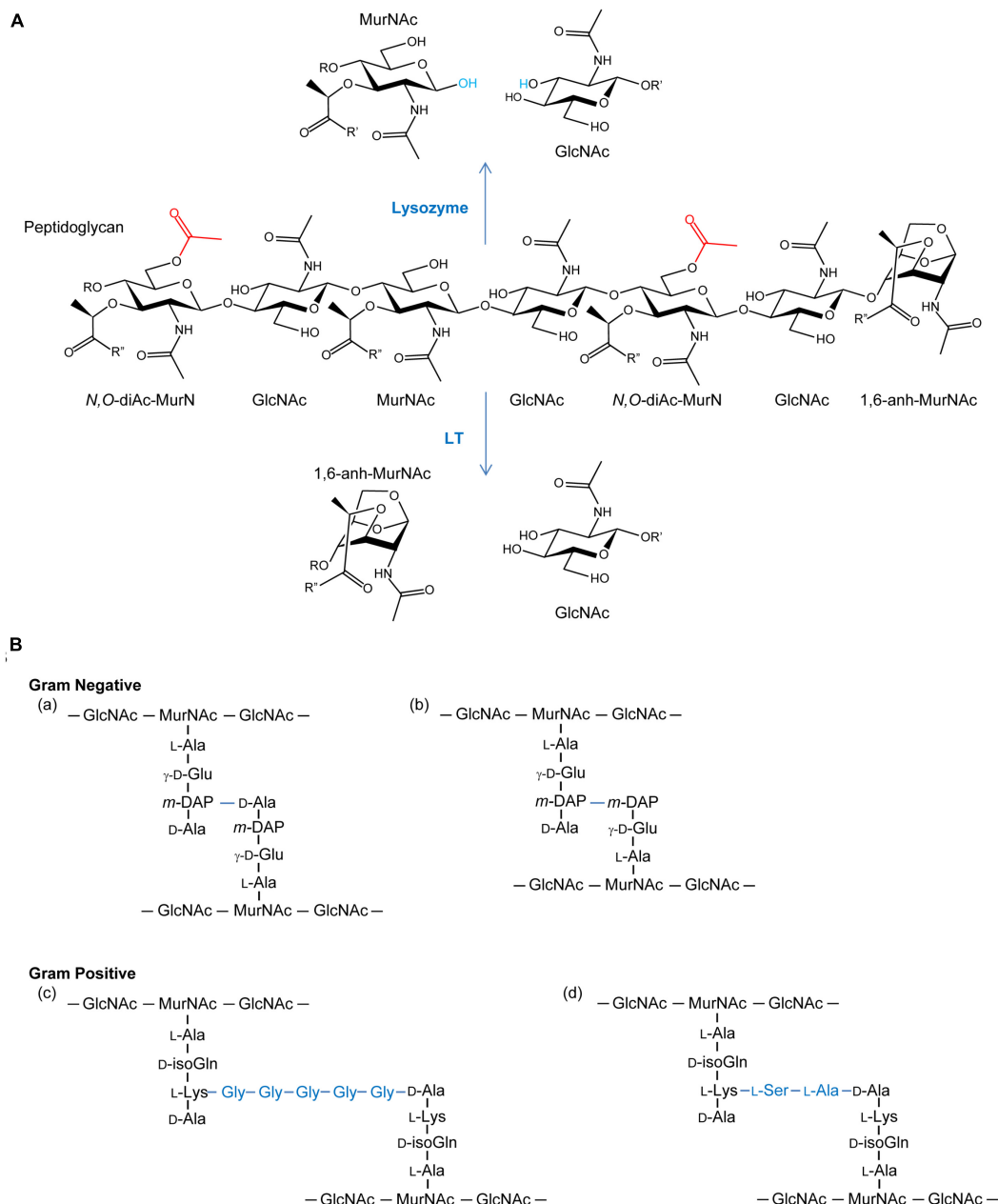
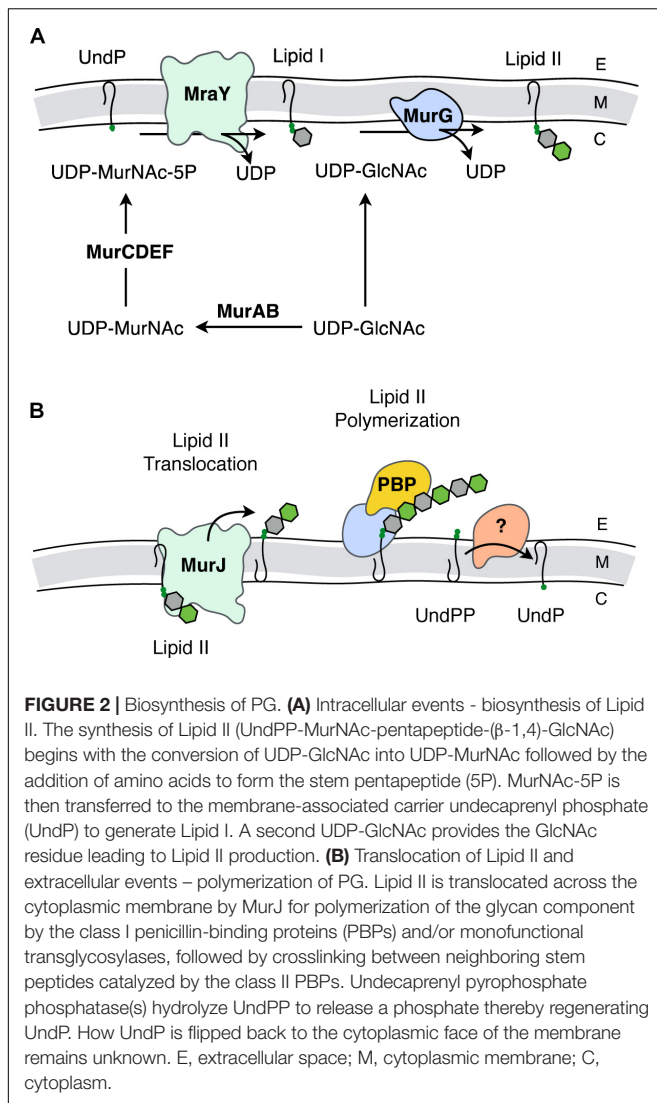


FIGURE 1 | (A) Peptidoglycan as a substrate for lysozymes and lytic transglycosylases. Both lysozymes and lytic transglycosylases (LT) cleave PG between MurNAc and GlcNAc residues but their reaction products are different. As hydrolases, lysozymes add water (blue) across the original β -1,4 glycosidic linkage, whereas LTs generate 1,6-anhydroMurNAc (1,6-anh-MurNAc) and GlcNAc products. The O-acetylation of the C-6 OH groups of MurNAc residues (depicted in red) generating *N,O*-diacetyl-muramoyl products inhibits activity of both lytic enzymes. R, R', and R'' denote GlcNAc, MurNAc, and stem peptides, respectively. **(B)** Examples of stem peptides and modes of crosslinking. The stem peptides associated with Gram-negative PG typically involve γ -D-glutamic acid (γ -D-Glu) and *meso*-diaminopimelic acid (*m*-DAP) at the second and third positions, respectively (where the peptide bond between the two involves the γ -carboxyl group of the Glu), from the lactyl moiety of MurNAc. Crosslinking (blue lines) occurs predominately between the *m*-DAP of a PG monomeric unit and the penultimate D-Ala residue of neighboring unit (a), but linkages between two *m*-DAP residues (b) also occur. A greater variation in stem peptide composition is found in the PG from Gram-positive bacteria, but typically isoglutamine (isoGln) and L-Lys occur at positions two and three, respectively. As with Gram-negative bacteria, crosslinking can be direct, but bridging peptides (blue) are often present, such as the pentaglycyl (c) and Ser-Ala (d) peptides associated with the PG in *S. aureus* and *S. pneumoniae*, respectively.

the filamentous actin-like cytoskeletal proteins MreB and FtsZ, respectively (Eraso and Margolin, 2011; Fleurie et al., 2014). The biosynthetic complexes also include autolysins, enzymes that

lyse PG to provide new sites for sacculus expansion and cell division, as well as for the insertion of transport and secretion systems, pili, and flagella through the PG sacculus.



Autolysins

The enzymes that lyse PG are glycosidases, amidases, or endopeptidases (recently reviewed in Vollmer et al., 2008). The major glycosidases produced by Gram-positive bacteria for PG metabolism are typically the β -N-acetylglucosaminidases. These enzymes hydrolyze the β -1,4 linkage specifically between GlcNAc and MurNAc residues. The only confirmed β -N-acetylglucosaminidase reported in Gram-negative bacteria is FlgJ of *Salmonella enterica* where it is responsible for the insertion of flagella (Herlihey et al., 2014). Lysis of the β -1,4-glycosidic linkage between MurNAc and GlcNAc residues is mediated by two distinct enzyme classes, the muramidases (lysozymes) and the lytic transglycosylases (LTs) (Figure 1A). Despite the identical substrate specificity however, bacteria only produce the LTs for PG metabolism, and they represent the major glycosidase produced for this purpose by Gram-negative bacteria. Muramidases, on the other hand, are predominantly produced by eukaryotes as defensive bacteriolytic agents as components of their innate immunity systems

(Irwin et al., 2011; Ragland and Criss, 2017). The fundamental difference between these two glycosidases is their mechanism of action and consequent reaction products. Whereas the muramidases are hydrolases that release PG fragments with reducing and non-reducing termini of MurNAc and GlcNAc residues, respectively, the LTs are lyases that generate products terminating with 1,6-anhydroMurNAc and GlcNAc residues (Höltje et al., 1975; Figure 1A). LTs appear to be ubiquitous in Gram-negative bacteria, and they are utilized in a wide array of physiological processes (reviewed in Scheurwater et al., 2008). LTs are also present in Gram-positive bacteria, though they are not known to be significant contributors to the autolytic profiles in most species. However, they have been identified to participate significantly in the PG lytic events required for endospore germination (Gutelius et al., 2014).

Discovery and Relevance of PG O-Acetylation

PG is O-acetylated at the C-6 hydroxyl group of MurNAc (Figure 1A), a modification that sterically inhibits the productive binding of lysozyme (Clarke et al., 2002; Pushkaran et al., 2015), while also precluding the action of LTs. First discovered in species of *Streptococcus* and *Micrococcus* 60 years ago (Abrams, 1958; Brumfitt et al., 1958), this PG modification is now known to occur primarily in pathogenic species of both Gram-positive and Gram-negative bacteria (Table 1). For example, only pathogenic species of the staphylococci, which includes *S. aureus*, O-acetylate their PG and each is highly resistant to human lysozyme (Bera et al., 2006). By contrast, the non-pathogenic staphylococci do not produce O-acetylated PG and they are thus sensitive to lysozyme. Notable pathogens that do not O-acetylate their PG involve some of the Enterobacteriaceae and Pseudomonads, including *Escherichia coli* and *Pseudomonas aeruginosa* (Clarke, 1993; Clarke et al., 2010), and *Bacillus anthracis* (Sychantha et al., 2018).

As a non-stoichiometric modification, the extent of PG O-acetylation varies with species, strain, and the age of a culture. Ranging between 20 and 70% (relative to MurNAc concentration) (Clarke and Dupont, 1991; Clarke, 1993), increases in PG O-acetylation by 10-40% can occur when cells enter stationary phase (Pfeffer et al., 2006). It should be noted that *Lactobacillus plantarum* also O-acetylates its PG-associated GlcNAc residues. This modification serves to control its major autolysin, an N-acetylglucosaminidase, but it does not influence lysozyme sensitivity (Bernard et al., 2011).

PATHOBIOLOGY OF O-ACETYLATED PG

The resistance of PG to lysozyme digestion conferred by O-acetylation has long been known to have serious implications for human health. Early studies showed that large molecular weight fragments of PG persist in the circulatory systems of hosts to induce a variety of pathobiological effects, including complement activation, pyrogenicity, and arthritogenicity

TABLE 1 | Bacterial species (known and hypothetical) that produce O-acetylated PG.

Gram-positive (OatA)		Gram-negative (PatA/PatB and Ape) ¹	
<i>Staphylococcus aureus</i>	<i>Paenibacillus aquistagni</i>	<i>Neisseria gonorrhoeae</i>	<i>Photobacterium luminescens</i>
<i>Staphylococcus capitis</i>	<i>Paenibacillus dendritiformis</i>	<i>Neisseria animalis</i>	<i>Photobacterium luminescens</i>
<i>Staphylococcus carnosus</i>	<i>Paenibacillus larvae</i>	<i>Neisseria canis</i>	<i>Photobacterium temperata</i>
<i>Staphylococcus epidermidis</i>	<i>Paenibacillus macquariensis</i>	<i>Neisseria cinerea</i>	<i>Xenorhabdus bovienii</i>
<i>Staphylococcus haemolyticus</i>	<i>Paenibacillus polymyxa</i>	<i>Neisseria flavescens</i>	<i>Xenorhabdus nematophila</i>
<i>Staphylococcus hominis</i>	<i>Paenibacillus</i> sp.	<i>Neisseria lactamica</i>	<i>Xenorhabdus poinarii</i>
<i>Staphylococcus lugdunensis</i>	<i>Paenibacillus uliginis</i>	<i>Neisseria macacae</i>	<i>Moraxella bovis</i>
<i>Staphylococcus pasteurii</i>	<i>Lactobacillus acidophilus</i>	<i>Neisseria meningitidis</i>	<i>Moraxella canis</i>
<i>Staphylococcus saprophyticus</i>	<i>Lactobacillus amylophilus</i>	<i>Neisseria mucosa</i>	<i>Moraxella caprae</i>
<i>Staphylococcus</i> sp.	<i>Lactobacillus apis</i>	<i>Neisseria perflava</i>	<i>Moraxella catarrhalis</i>
<i>Staphylococcus warneri</i>	<i>Lactobacillus bombicola</i>	<i>Neisseria polysaccharea</i>	<i>Moraxella cuniculi</i>
<i>Macrocococcus caseolyticus</i>	<i>Lactobacillus brevis</i>	<i>Neisseria shayegani</i>	<i>Moraxella equi</i>
<i>Listeria grayi</i>	<i>Lactobacillus bucheri</i>	<i>Neisseria sicca</i>	<i>Moraxella lacunata</i>
<i>Listeria monocytogenes</i>	<i>Lactobacillus casei</i>	<i>Neisseria subflava</i>	<i>Moraxella nonliquefaciens</i>
<i>Listeria seeligeri</i>	<i>Lactobacillus crispatus</i>	<i>Chromobacterium violaceum</i>	<i>Moraxella oblonga</i>
<i>Listeria welshimeri</i>	<i>Lactobacillus delbrueckii</i>	<i>Eikenella corrodens</i>	<i>Moraxella pluranimalium</i>
<i>Bacillus</i> sp.	<i>Lactobacillus jensenii</i>	<i>Kingella kingae</i>	<i>Campylobacter avium</i>
<i>Bacillus amyloliquefaciens</i>	<i>Lactobacillus jensenii</i>	<i>Kingella oralis</i>	<i>Campylobacter coli</i>
<i>Bacillus cereus</i>	<i>Lactobacillus gasseri</i>	<i>Citrobacter youngae</i>	<i>Campylobacter cuniculorum</i>
<i>Bacillus endophyticus</i>	<i>Lactobacillus helveticus</i>	<i>Cronobacter sakazakii</i>	<i>Campylobacter gracilis</i>
<i>Bacillus filamentosus</i>	<i>Lactobacillus johnsonii</i>	<i>Dickeya dadantii</i>	<i>Campylobacter helveticus</i>
<i>Bacillus licheniformis</i>	<i>Lactococcus lactis</i>	<i>Dickeya zeae</i>	<i>Campylobacter jejuni</i>
<i>Bacillus megaterium</i>	<i>Lactobacillus lindneri</i>	<i>Morganella morganii</i>	<i>Campylobacter upsaliensis</i>
<i>Bacillus mycoide</i>	<i>Lactobacillus mucosae</i>	<i>Proteus hauseri</i>	<i>Helicobacter bilis</i>
<i>Bacillus pseudomycoloides</i>	<i>Lactobacillus paracsei</i>	<i>Proteus mirabilis</i>	<i>Helicobacter cinaedi</i>
<i>Bacillus pumilus</i>	<i>Lactobacillus reuteri</i>	<i>Proteus penneri</i>	<i>Helicobacter fennelliae</i>
<i>Bacillus subtilis</i>	<i>Lactobacillus rhamnosus</i>	<i>Proteus vulgaris</i>	<i>Helicobacter hepaticus</i>
<i>Bacillus thuringiensis</i>	<i>Lactobacillus ruminis</i>	<i>Coszenzaea myxofaciens</i>	<i>Helicobacter jaachi</i>
<i>Bacillus velezensis</i>	<i>Lactobacillus sakei</i>	<i>Providencia alcalifaciens</i>	<i>Helicobacter japonicus</i>
<i>Bacillus weihenstephanensis</i>	<i>Lactobacillus salivarius</i>	<i>Providencia urhodogranariae</i>	<i>Helicobacter marmotae</i>
<i>Brevibacillus</i> sp.	<i>Lactobacillus ultunensis</i>	<i>Providencia heimbachae</i>	<i>Helicobacter mustelae</i>
<i>Eggerthella lenta</i>	<i>Enterococcus casseliflavus</i>	<i>Providencia rettgeri</i>	<i>Helicobacter muridarum</i>
<i>Lysinibacillus fusiformis</i>	<i>Enterococcus faecium</i>	<i>Providencia rustigianii</i>	<i>Helicobacter magdeburgensis</i>
<i>Lysinibacillus sphaericus</i>	<i>Enterococcus faecalis</i>	<i>Providencia sneebia</i>	<i>Helicobacter pylori</i>
<i>Lysinibacillus</i> sp.	<i>Streptococcus anginosus</i>	<i>Providencia stuartii</i>	<i>Helicobacter</i> sp.
<i>Gemella haemolysans</i>	<i>Streptococcus gordonii</i>		<i>Helicobacter trogonum</i>
<i>Exiguobacterium</i> sp.	<i>Streptococcus intermedius</i>		
<i>Exiguobacterium sibiricum</i>	<i>Streptococcus mitis</i>		
<i>Alicyclobacillus montanus</i>	<i>Streptococcus oralis</i>		
<i>Alicyclobacillus vulcanalis</i>	<i>Streptococcus parasanguinis</i>		
<i>Viridibacillus</i> sp.	<i>Streptococcus pneumoniae</i>		
<i>Serinibacter salmonis</i>	<i>Streptococcus pseudopneumoniae</i>		
<i>Jatrophihabitans</i> sp.	<i>Streptococcus pyogenes</i>		
<i>Clostridium amylophilum</i>	<i>Streptococcus salivarius</i>		
<i>Clostridium botulinum</i>	<i>Streptococcus suis</i>		
	<i>Streptococcus thermophilus</i>		

¹Whereas hypothetical homologs of PatA and/or PatB appear to be encoded in the genomes of other Gram-negative bacteria, listed are only those encoded in OAP clusters which include the coding gene for Ape.

(reviewed in Seidl and Schleifer, 1985). The direct relationship between these effects and PG O-acetylation was clearly demonstrated in a series of animal model studies conducted in the 1980s with *S. aureus* and *N. gonorrhoeae* (reviewed in Clarke et al., 2010). More recent developments at the molecular

level demonstrate the critical role that PG O-acetylation plays in the pathogenesis of *S. aureus*-mediated septic arthritis (Baranwal et al., 2017). Also, it has been shown that O-acetylated *S. aureus* PG inhibits production of the important cytokine IL-1 β , while concomitantly rendering the bacterium resistant

to lysozyme killing in macrophages (Shimada et al., 2010). Furthermore, this modification to PG limits helper T-cell priming thereby permitting reinfection by this pathogen (Sanchez et al., 2017). Similar studies demonstrating escape from the immune response and survival within macrophages due to the O-acetylation of PG have been made with *Streptococcus iniae* (Allen and Neely, 2012), *Listeria monocytogenes* (Aubry et al., 2011), *Helicobacter pylori* (Wang et al., 2012), and *Neisseria meningitidis* (Veyrier et al., 2013). The potential of PG O-acetylation as a viable antivirulence target is underscored by the direct correlation that has been observed between decreased pathogenicity and increased susceptibility of PG to host lysozymes resulting from decreased O-acetylation levels with *S. aureus* (Bera et al., 2005, 2006), *S. pneumoniae* (Davis et al., 2008), *S. iniae* (Allen and Neely, 2012), *Streptococcus suis* (Wichgers Schreur et al., 2012), *Enterococcus faecalis* (Hébert et al., 2007; Le Jeune et al., 2010), *L. monocytogenes* (Aubry et al., 2011; Burke et al., 2014), *H. pylori* (Wang et al., 2012), and *N. meningitidis* (Veyrier et al., 2013). With each of these studies, the enzyme catalyzing PG O-acetylation and/or its regulator was identified as the virulence factor responsible for the decreased pathogenicity observed. In addition to providing increased resistance to lysozyme, the action of the O-acetyltransferase in *S. pneumoniae* has been shown to attenuate resistance to β -lactam antibiotics (Crisóstomo et al., 2006).

PATHWAYS FOR PG O-ACETYLATION

Until recently, little was known about the process of PG O-acetylation. Earlier microbiological and biochemical experiments identified it is a maturation event; O-acetylated Lipid II was not found in any organism known to produce O-acetyl-PG (Clarke and Dupont, 1991). With *N. gonorrhoeae*, the percentage of O-acetylation of newly synthesized PG was observed to rapidly increase following incorporation of Lipid II into the sacculus, consistent with the notion that PG O-acetylation is a post-synthesis modification (Dougherty, 1983). Subsequent pulse-chase experiments involving *N. gonorrhoeae* (Lear and Perkins, 1983, 1986, 1987), *P. mirabilis* (Gmeiner and Kroll, 1981; Gmeiner and Sarnow, 1987), and *S. aureus* (Snowden et al., 1989) revealed a close temporal relationship between the cross-linking of newly incorporated PG strands and O-acetylation. In each case, an initial burst of PG cross-linking was immediately followed by O-acetylation. The extent of the two events then appeared to gradually rise concomitantly to their final maximal levels over the remainder of the cell cycle. The correlation between transpeptidation and O-acetylation was further demonstrated using sub minimum inhibitory concentrations (MIC) of penicillin G. With all three species, O-acetylation values sharply declined following administration of the penicillin (Martin and Gmeiner, 1979; Blundell and Perkins, 1981; Burghaus et al., 1983; Dougherty, 1985a; Sidow et al., 1990). A correlation of the PBP profiles of penicillin-resistant and susceptible strains of *N. gonorrhoeae* with their respective levels of PG O-acetylation suggested that PBP2 may have

a role in mediating the two processes (Dougherty, 1983, 1985b).

Identification of the enzymes involved in PG O-acetylation in the Gram-negative bacteria remained unknown for two decades until the availability of bacterial genomes in 2005, when Weadge and Clarke (2005) identified the existence of an AlgI paralog from *P. aeruginosa* within the chromosome of *N. gonorrhoeae*; AlgI is a member of the membrane-bound O-acyltransferase (MBOAT) family that functions as part of a multi-component system to acetylate the exopolysaccharide alginate (Franklin and Ohman, 2002). The AlgI paralog was found within a three-gene operon (named OAP for O-acetyl-PG) (Figure 3A) and knowing that *N. gonorrhoeae* does not produce alginate, the gene product was proposed to function as a PG O-acetyltransferase (Weadge and Clarke, 2005). Subsequent deletion mutants of the gene encoding this AlgI homolog in *N. gonorrhoeae*, initially named *pacA*, confirmed that it was important for the production of O-acetyl-PG (Dillard and Hackett, 2005). Immediately downstream of *pacA* is a gene encoding a protein of the SGNH/GDSL hydrolase family of esterases (Figure 3A). It was recognized to be genetically linked to *pacA*, and hence, it was initially named O-acetylpeptidoglycan esterase (*ape2*) (Weadge and Clarke, 2005). However, despite its amino acid sequence similarity with the SGNH family of esterases, Ape2 was later demonstrated to function as a PG O-acetyltransferase both *in vivo* and *in vitro* (Moynihan and Clarke, 2010; Veyrier et al., 2013; Ha et al., 2016), and consequently renamed as PatB; PacA was renamed PatA in keeping with the convention for naming acetyltransferases. Downstream of *patB*, a third gene, named *ape1*, was also identified (Figure 3A). The protein encoded by *ape1* also belongs to the SGNH/GDSL hydrolase family, and its activity was confirmed to be that of an authentic O-acetyl-PG esterase (Weadge and Clarke, 2006).

As a post-synthetic modification, PG O-acetylation occurs in the periplasm of Gram-negative cells (or on the outer surface of the cytoplasmic membrane of Gram-positive bacteria) (reviewed in Clarke and Dupont, 1991). Given the genetic organization of the encoding genes coupled with the demonstrated activities (Dillard and Hackett, 2005; Moynihan and Clarke, 2010), PatA and PatB have been proposed to function in concert as a two-component system (Moynihan and Clarke, 2010; Figure 3B). PatA, an integral membrane protein, is thought to function as a membrane transporter, translocating acetyl groups to the periplasm from a cytoplasmic source, presumably acetyl-CoA. Localized to the periplasm (Moynihan and Clarke, 2010), PatB would then transfer the acetyl groups to the C-6 hydroxyl groups of MurNAc residues in PG. Whether the acetyl group is transferred between these two proteins directly, or through an acetyl carrier molecule is not known.

Almost concurrently with the discovery of the genes for PG O-acetylation in *N. gonorrhoeae*, Bera et al. (2005) identified O-acetyltransferase A (OatA) as the enzyme responsible for PG O-acetylation in Gram-positive bacteria. Since then, homologs of OatA from several other Gram-positive bacteria have been characterized, including those from clinical isolates of *S. pneumoniae* (Crisóstomo et al., 2006), *E. faecalis*

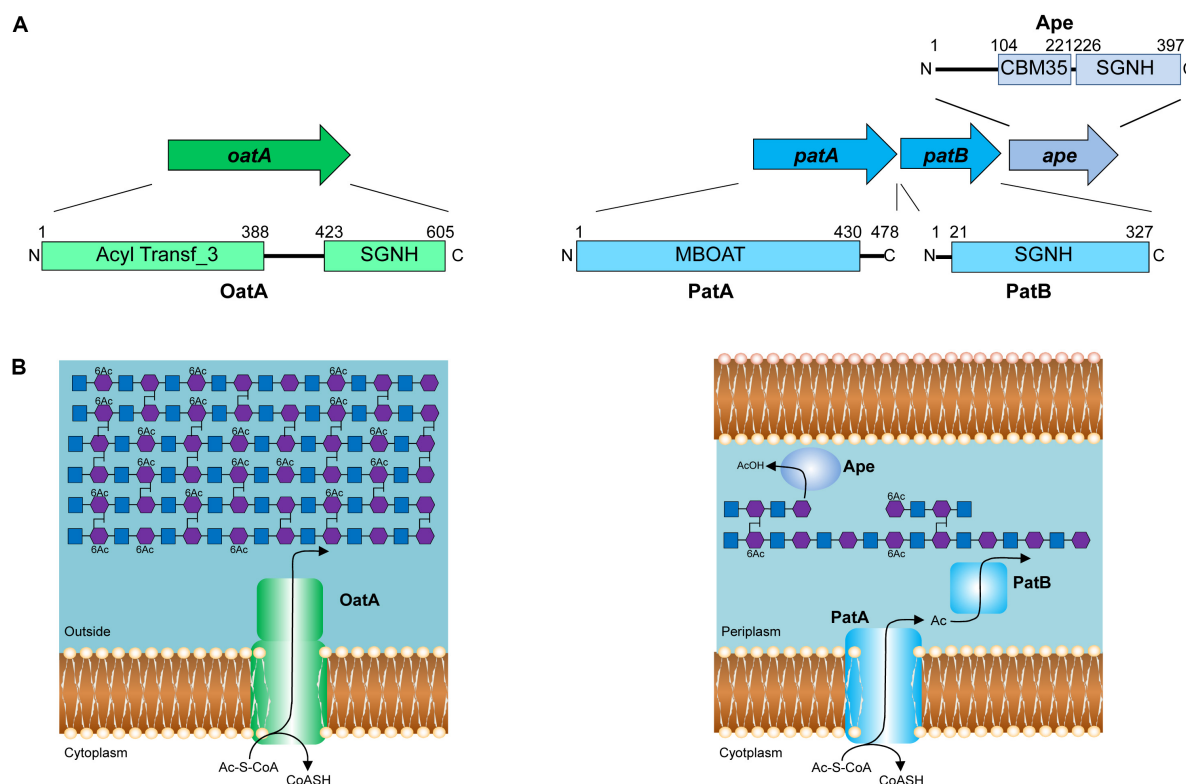


FIGURE 3 | Pathways for the O-acetylation of PG. **(A)** Genetic organization and domain structure of the enzymes involved in PG O-acetylation (OatA, PatA/B) and de-O-acetylation (Ape). **(B)** Proposed models for the O-acetylation of PG in Gram-positive and Gram-negative bacteria. The membrane-spanning N-terminal domain of OatA is thought to translocate acetyl groups across the cytoplasmic membrane from the cytoplasm (presumably provided by acetyl-CoA) for their transfer to PG by the C-terminal O-acetyltransferase domain. With Gram-negative bacteria, these two distinct activities are catalyzed by separate proteins, PatA and PatB, respectively. Again, acetyl-CoA is the presumed source of acetyl groups. Ape is produced by these bacteria and localized to the periplasm for removal of the O-acetylation as required for continued PG metabolism.

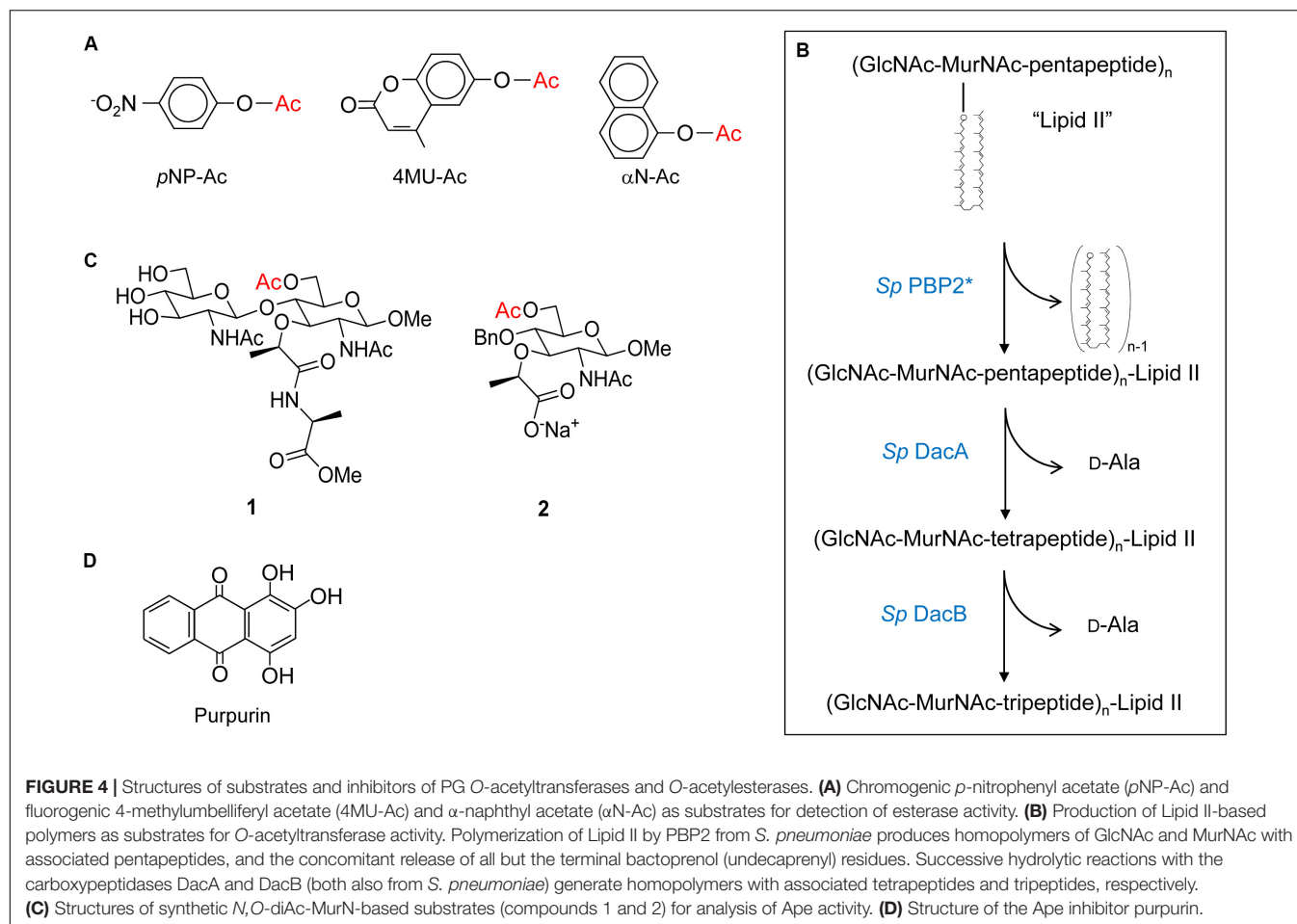
(Hébert et al., 2007), *L. plantarum* (Weadge and Clarke, 2005; Bernard et al., 2011), and *L. monocytogenes* (Aubry et al., 2011).

OatA is predicted to be bi-modular, being comprised of an N-terminal integral membrane domain (OatA_N) and a C-terminal extracytoplasmic domain (OatA_C) (Figure 3B). Interestingly, OatA_N belongs to the Acyltransferase 3 (AT3) family of proteins and not the MBOATs. This AT3 domain is linked to OatA_C which, like PatB, is a member of the SGNH/GDSL hydrolase family (Bernard et al., 2011, 2012; Sychantha et al., 2017). Thus, despite the difference in protein family membership of the membrane-spanning OatA_N, the overall domain architecture of OatA resembles the two-component PG O-acetylation system of Gram-negative bacteria. Like PatA, OatA_N is proposed to translocate acetyl groups across the cytoplasmic membrane for the surface-exposed OatA_C to function like PatB as the O-acetyltransferase (Figure 3B). Unlike the Gram-negative system, however, OatA is not known to be coupled with an Ape-like O-acetyl-PG esterase. This may be a reflection of the fact that the major autolysins of Gram-positive bacteria are not LTs, which require a free C-6 hydroxyl group on MurNAc residues for activity, but instead are mainly peptidases and glucosaminidases that are not affected by the modification.

STRUCTURE AND FUNCTION RELATIONSHIP OF PG O-ACETYLTRANSFERASES

Activity and Specificity of O-Acetyltransferases

Despite their discovery over a decade ago, it was not until recently that the biochemical details of PG O-acetyltransferases were delineated. The complexities of determining the specificity and kinetic parameters of these membrane-associated enzymes were compounded by the lack of available PG-based substrates; attempts to isolate useful quantities of homogeneous mucopeptide fractions from natural PG is futile. This changed when it was discovered that these enzymes recognized surrogate compounds as donor and acceptor substrates. Thus, a convenient assay utilizing chromogenic or fluorometric acetyl donors (Figure 4A) and GlcNAc-based acceptor substrates was developed (Moynihan and Clarke, 2013), which has been used to kinetically analyze both PatB (Moynihan and Clarke, 2013, 2014a) and OatA (Sychantha et al., 2017; Sychantha and Clarke, 2018). Both enzymes were found to be very weak esterases compared to authentic PG O-acetyltransferase



Ape. Nonetheless, this activity was exploited to determine the biochemical properties of the enzymes, in addition to the steady-state (Sychantha et al., 2017; Moynihan and Clarke, 2014a,b) and, in the case of *S. pneumoniae* OatAC, pre-steady kinetic parameters (Sychantha and Clarke, 2018). These studies revealed the dependence of the hydrolytic reaction on pH with the pK_a of an essential ionizable group between 6.25–6.4 and 6.9–7.3 for NgPatB (Moynihan and Clarke, 2014a) and SpOatAC (Sychantha and Clarke, 2018), respectively, consistent with the participation of a His residue. Neither enzyme is inhibited by metal chelators indicating that they are not metallo-enzymes. However, catalysis of hydrolysis by both is inhibited by the mechanism-based inhibitor methanesulfonyl fluoride indicating the involvement of a nucleophilic Ser residue.

Both PatB and OatA are able to utilize chitooligosaccharides as acceptor substrates. Increases in catalytic efficiency are seen with increasing length of oligosaccharide suggesting a binding cleft comprised of subsites (Moynihan and Clarke, 2014a; Sychantha et al., 2017). However, these increases are relatively small suggesting that the subsites binding MurNAc residues also accommodate elements of their associated stem peptides, which of course are not present in the chitooligosaccharides. This postulate of stem peptide involvement in substrate binding and recognition, at least

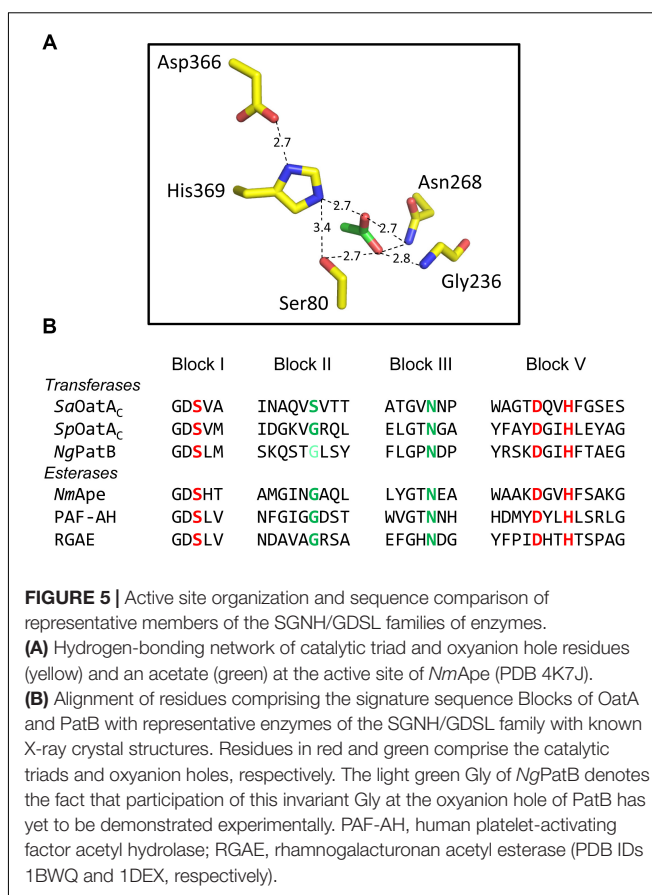
for OatAC, was borne out in a study employing a PG-based substrate produced through the polymerization of the PG biosynthetic precursor Lipid II (Sychantha et al., 2017). The PBP-catalyzed transglycosylation of Lipid II provided a pool of homopolymers of GlcNAc-MurNAc-pentapeptide with degrees of polymerization between 2 and 12 (Figure 4B). Subsequent treatment of these pools with the carboxypeptidases DacA and then DacB provided homopolymers with tetrapeptide and tripeptide stems, respectively. Using the three distinct pools of PG homopolymers, SaOatAC was shown to have high specificity for only those with pentapeptide stems. SpOatAC, on the other hand, is incapable of using the pentapeptide-based oligomers as substrate. Instead, it has specificity for those with tetrapeptide stems (Sychantha et al., 2017). Having such distinct specificities has implications regarding the timing of the O-acetylation process in these two Gram-positive human pathogens. As PG crosslinking and any subsequent carboxypeptidase activity of the PBPs generates tetrapeptide stems, the specificity of SaOatAC for mureglycans with pentapeptide stems implies O-acetylation would have to follow immediately after the transglycosylation of the Lipid II precursor into the existing PG sacculus. Furthermore, such a close temporal association of these respective activities implies that SaOatA would need to be physically associated with the transglycosylase(s) involved in *S. aureus* PG biosynthesis.

The need for this protein-protein association is supported by the observation that *SaOatA_C* only weakly binds to PG (Kell, 2016).

Steady-state kinetic analyses of the *O*-acetyltransferase activities of *NgPatB* and *SpOatA_C* using chromogenic acetyl donors and chitooligosaccharide acceptors revealed that both enzymes follow a ping-pong bi-bi mechanism of action (Moynihan and Clarke, 2014b; Sychantha and Clarke, 2018). In this two-step process, the enzymes first bind the acetyl donor molecule and transfer the acetyl moiety to a catalytic residue forming a covalent adduct while releasing the first product. With the chromogenic substrates, the chromogen would be this first product. Its release is followed by the binding of the acceptor substrate to the acetylated enzyme. The acetyl group is then transferred to the hydroxyl group of the acceptor sugar and the enzyme returns to its resting state with the release of the *O*-acetylated product. When functioning as an esterase, water simply replaces the sugar as the acceptor “substrate.” However, a follow-up pre-steady-state kinetic analysis of this esterase activity revealed that water does not serve as a very efficient acceptor for the hydrolytic event. Using *SpOatA_C* with *p*-nitrophenyl acetate as substrate, hydrolysis of the reaction intermediate was shown to be the rate-limiting step. The half-life of this intermediate was estimated to be over 70 s (Sychantha and Clarke, 2018), indicating an extremely slow process, and accounting for the overall poor hydrolytic activity of these enzymes. Indeed, acetyl-intermediates of both *NgPatB* (Moynihan and Clarke, 2014b) and *SpOatA_C* have been trapped (Sychantha and Clarke, 2018) and with both, the acetyl group was observed to be covalently linked to a Ser residue.

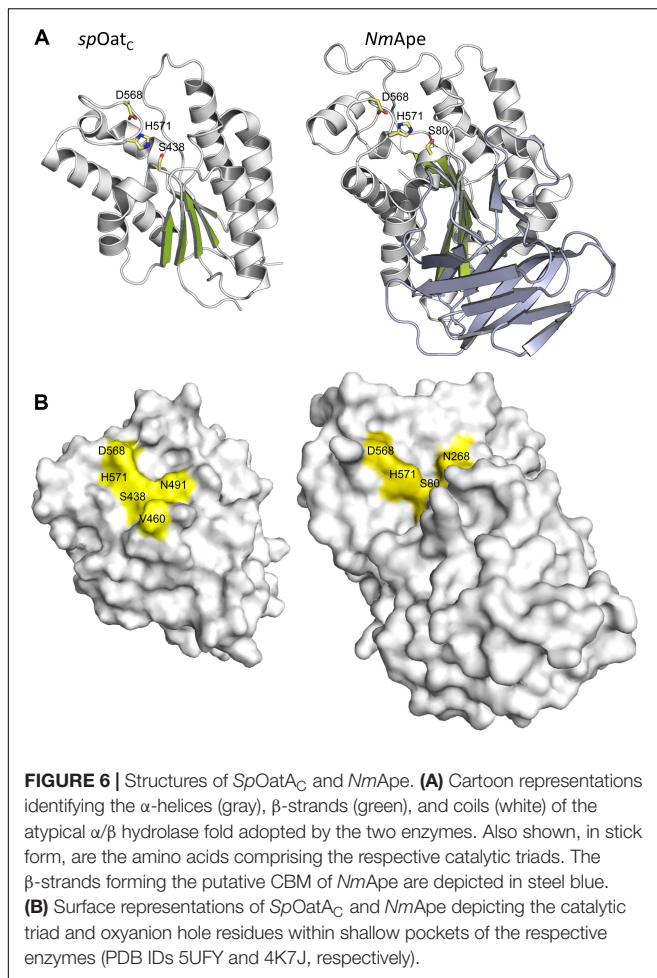
Structure and Mechanism of Action of PG *O*-Acetyltransferases

The SGNH family of the GDSL superfamily of esterases/lipases is named for the participation of Ser, Gly, Asn, and His residues in their mechanism of action. The Ser and His comprise a catalytic triad, while all four form the “oxyanion hole,” a region at the catalytic center of the enzymes that stabilizes the putative oxyanion transition states leading to and from the acyl-enzyme intermediate (Mølgaard et al., 2000; Figure 5A). The Gly and Asn are found within consensus motifs named Block II and Block III, respectively, while the catalytic Ser and His (and Asp) comprise Blocks I and V, respectively (Figure 5B). The Block II residues form a type-II β -turn to direct the backbone NH of the invariant Gly toward the active site so that it can serve together with the backbone NH of the Ser and the side-chain amide of the Asn to stabilize the oxyanion of the putative tetrahedral intermediate. Invariant Ser, His, and Asp residues are present in the respective alignments of PatB and OatA_C homologs, and the single replacements of these residues in the enzymes from *N. gonorrhoeae* and both *S. aureus* and *S. pneumoniae*, respectively, abrogates catalytic activity (Moynihan and Clarke, 2014a,b; Sychantha and Clarke, 2018). Also, it is these Ser residues that were found to form adducts to the acetyl groups of the acetyl-intermediates of both *NgPatB* and *SpOatA* mentioned above. Invariant Asn residues are also present in both the PatB and OatA_C homologs and consistent with their expected



role in stabilizing oxyanion transition states, their replacements also leads to loss of *O*-acetyltransferase activity (Moynihan and Clarke, 2014b; Sychantha and Clarke, 2018). Whereas an invariant Gly is observed Block II of all PatB homologs, this Gly is not invariant in OatA_C and it is replaced by a Ser in many homologs, including all of those produced by the streptococci (Sychantha and Clarke, 2018; Figure 5). However, it should be noted that experimental evidence for the participation of the invariant Gly residue in Block II of PatB has yet to be obtained. As such, the importance of this residue in the transferases compared to the esterases remains to be established.

The only X-ray crystal structure of a PG *O*-acetyltransferase reported is that of *SpOatA_C* (Sychantha et al., 2017). As predicted earlier for *L. plantarum* OatA (Bernard et al., 2011) and *NgPatB* (Bernard et al., 2012; Moynihan and Clarke, 2014b), the enzyme adopts an atypical α/β hydrolase fold (Figure 6A) which most closely resembles the structure of human platelet-activating factor acetylhydrolase (Ho et al., 1999) (PDB ID: 1BWQ) and *E. coli* thioesterase I/protease I/lysophospholipase L1 (Lo et al., 2003) (PDB ID: 1IVN), two other members of the SGNH/GDSL hydrolase superfamily. A core parallel β -sheet of five strands is sandwiched between seven α -helices which form a shallow active site pocket (Figure 6B). At its center, the triad of Ser-His-Asp residues is aligned appropriately to serve catalytically, and the invariant Asn is positioned to help stabilize a transition state.



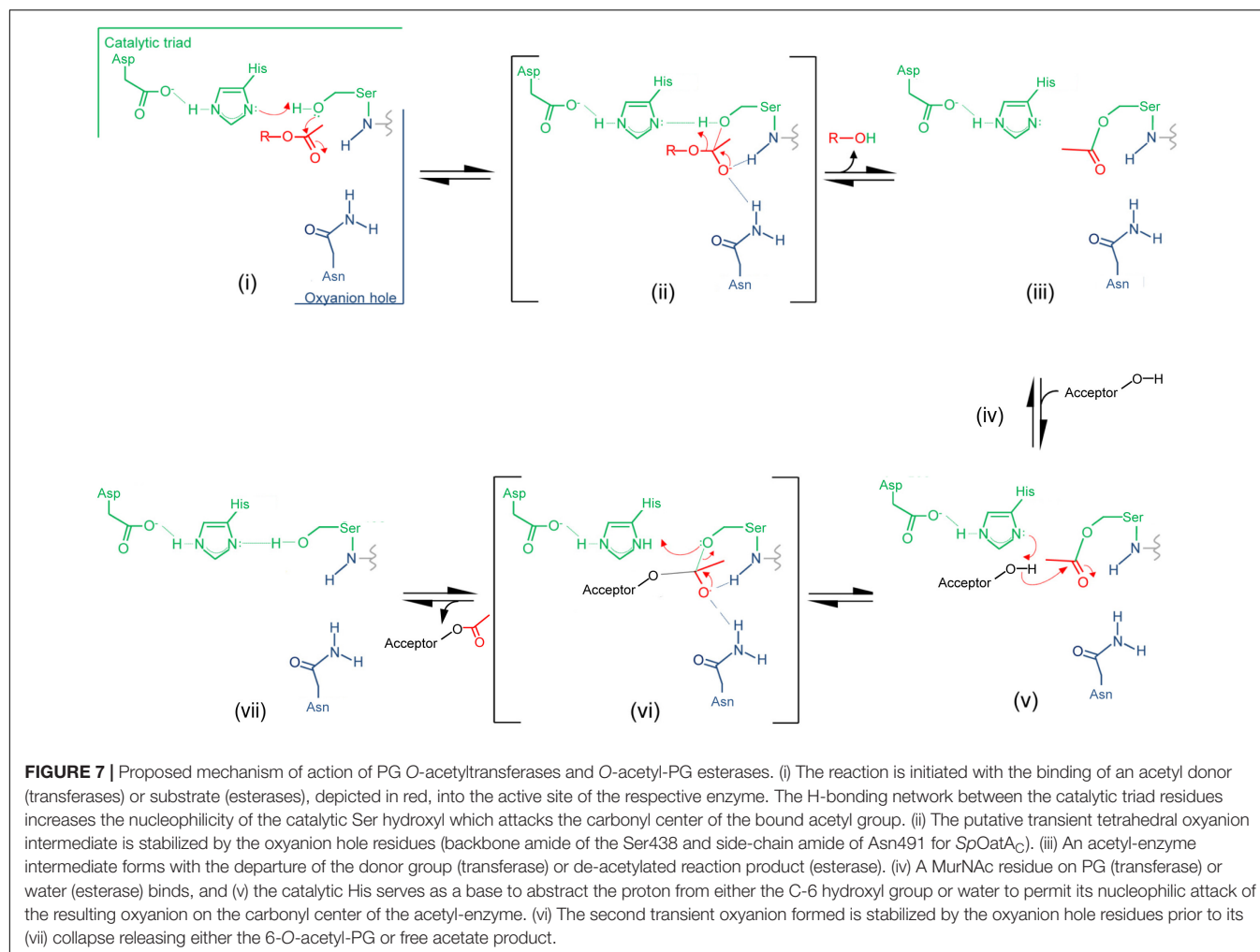
Insight provided by the structural studies, together with the understanding of their kinetic behavior and dependence on pH, supports a double-displacement, ping-pong bi-bi reaction as the mechanism of action of the *O*-acetyltransferases, analogous to that of the well-characterized serine esterases. Thus, the alignment and H-bonding network of the catalytic triad (Figure 6B) would render the hydroxyl group of the catalytic Ser nucleophilic (Figure 7). The deprotonated O δ of this Ser could attack the carbonyl carbon of the acetyl donor molecule leading to a putative tetrahedral oxyanion transition state, which would be stabilized by the oxyanion hole residues. This oxyanion would rapidly collapse to the covalent acetyl-enzyme intermediate concomitant with His-catalyzed protonation and subsequent release of the donor product. Then, instead of a water molecule associated with esterase activity, a glycan strand PG would bind into the active site cleft and the deprotonated catalytic His would now function as a base to abstract the C-6 hydroxyl proton of an appropriately positioned MurNAc residue rendering it nucleophilic. Attack of this C-6 alkoxide on the carbonyl center of the acetyl-Ser forms a second tetrahedral oxyanion transition state, which is again stabilized by the oxyanion hole residues. Collapse of this transition state leads to the release of the *O*-acetylated PG.

As noted above, the PG *O*-acetyltransferases have the capacity to function as esterases *in vitro*, at least when provided with activated esters as substrate. However, *in vivo* hydrolytic activity would have to be minimized, if not precluded, so as to limit a futile cycle of acetate uptake and loss involving a valuable cytoplasmic metabolite, presumably acetyl-CoA. With its highly exposed active site on its surface (Figure 6B), *SpOatA_C* does not appear to provide a water-limiting environment to help mitigate the hydrolytic event. However, it is possible that such an environment is formed by the juxtaposition of this catalytic domain with its associated N-terminal integral membrane domain and, additionally, with both the cytoplasmic membrane and the insoluble PG sacculus. The opportunity to observe the covalent adduct of the mechanism-based inhibitor methanesulfonyl fluoride with the catalytic Ser in the crystal structure of the inactive enzyme provides some further insight into the mechanism of action of OatA, specifically as to how the hydrolytic reaction is indeed minimized. This adduct represents a transition-state analog that mimics the attack of a water molecule on the acetyl-enzyme intermediate during the hydrolytic reaction of esterases (Myers and Jun, 1954). The orientation of the adduct suggests that the approach to the carbonyl C of the bound acetyl group by an acceptor ligand (e.g., water or a carbohydrate) would have to be from a hydrophobic region located at the back of the active site. Thus, the trajectory of a hydrolytic water passing across this hydrophobic region is an unfavorable condition that might explain the very slow half-life of the intermediate observed in the pre-steady-state kinetic experiments described above. A Val or Ile residue exists at position 490 in all aligned OatA homologs. These invariant Val/Ile residues are located at position 5 in the Block II consensus motif and they are not present in other SGNH/GDSL esterase members (Figure 4). Interestingly, site-specific replacement of Val490 in *SpOatA_C* with Ala and Gly, the residues present at this same position in the esterases, rhamnogalacturonan acetyl esterase, and platelet-activating factor acetyl hydrolase, respectively, resulted in increased esterase activity and a concomitant 5- and 10-fold decrease in transferase activity, respectively. These observations suggest that, in addition to minimizing the approach of water to an acetyl-OatA intermediate, this hydrophobic region at the active center may assist the binding and positioning of a carbohydrate acceptor, recognizing the existence of their hydrophobic regions. A co-crystal structure of the enzyme bound by a ligand would help resolve this issue, but unfortunately none have been reported to date.

PG DE-O-ACETYLATION

PG *O*-Acetylesterases

As discussed above, the *O*-acetylation of PG controls endogenous autolytic activity associated with PG metabolism (Dougherty, 1983; Strating and Clarke, 2001; Pfeffer et al., 2006; Emirian et al., 2009; Laaberki et al., 2011; Moynihan and Clarke, 2011; Rae et al., 2011; Bonnet et al., 2017), particularly in Gram-negative bacteria, including that required for cell septation/division (Dougherty, 1983; Emirian et al., 2009; Laaberki et al., 2011).



In Gram-negative bacteria, the LTs represent the major autolysins involved with PG metabolism and cell septation (Scheurwater et al., 2008). As their catalytic mechanism produces a 1,6-anhydromuramoyl reaction product, clearly the presence of a C-6 O-acetyl group would preclude this activity and thereby provide a means of autolytic control at the substrate level. Hence, Gram-negative cells producing O-acetylated PG encode an O-acetyl-PG esterase (Ape) which removes the blocking acetyl group (**Figure 3B**), thereby permitting continued PG metabolism (Weadge and Clarke, 2006).

Like PatB, Ape also belongs to the SGNH/GDSL superfamily of serine esterases, and homologs align with the acetyl-xylan esterases of carbohydrate esterase 3 (CE3) enzymes of the CAZy database (Carbohydrate-Active enZYmes Database, 1998). All members of the CE3 family have invariant Ser, His, and Asp residues that were postulated to form a catalytic triad, but no mechanistic investigations had been conducted on any of these enzymes prior to the discovery of Ape. A chemical modification and site-directed engineering study on *N. gonorrhoeae* Ape confirmed the essential role of Ser80, His369, and Asp366 in the catalytic mechanism of this enzyme (Weadge and Clarke, 2007), supporting its preliminary

identification as a GDS(L/H) serine esterase (Weadge and Clarke, 2006). In a follow-up study, the roles of eight other invariant or highly conserved residues were probed by a kinetic and substrate-binding characterization of enzyme variants possessing site-specific replacements (Pfeffer et al., 2013). Based on these data combined with a structural prediction of the enzyme, Gly236 and Asn268 were proposed to comprise the oxyanion hole that would stabilize transition states formed during the enzyme's reaction mechanism while Gly78, Asp79, His81, Asn235, Thr267, and Val368 were proposed to position the catalytic residues appropriately and/or participate in substrate binding. The identification of Gly236 and Asn268 as oxyanion hole residues confirmed the classification of Ape as an SGNH esterase and that its mechanism of action follows that of other classical Ser esterases (Pfeffer et al., 2013; **Figure 6**).

As a reflection of the complexities of working with PG as an *in vitro* substrate, and like the studies described above on PatB and OatA, preliminary kinetic information for Ape were obtained using non-carbohydrate-based, synthetic substrate analogs. But a more meaningful analysis of the binding and kinetic properties of the enzyme requires substrates more closely related to PG. With this in mind, two such specific soluble

substrates for Ape involving a MurNAc core were designed and synthesized (Hadi et al., 2011). The water-soluble mono- and disaccharide substrate analogs 1 and 2 (**Figure 4C**) were synthesized and then characterized kinetically. Both compounds 1 and 2 serve as substrates for Ape, but the k_{cat}/K_M values obtained were approximately 10-fold less than that for highly activated *p*-nitrophenyl acetate. Nonetheless, these data for the hydrolysis of an unactivated acetate ester at the C-6 of a MurNAc in the mono- and disaccharide-based substrates suggest that binding to polymeric PG is not a strict requirement for efficient catalysis. Moreover, the minimal difference in efficiency between the two substrates indicates that the presence of the methyl ester-protected L-Ala attached to the lactyl moiety of MurNAc is not an essential element for substrate recognition. Substitution of the β -1,4-linked GlcNAc residue with an *O*-benzyl ether without significant kinetic consequence also suggests that minimal contacts occur between the enzyme and this amino sugar. However, it is likely that an entropic driving force from movement of the benzyl group from bulk solvent into a relatively hydrophobic binding pocket compensates for any loss of enthalpic interactions with the GlcNAc residue covalently linked to a Ser residue.

Structure and Mechanism of Action of PG O-Acetylsterases

The crystal structure of the highly homologous Ape from *N. meningitidis* (96% identity between *N. gonorrhoeae* and *N. meningitidis* Ape) was solved and revealed some interesting and unexpected features (Williams et al., 2014). The overall fold of the enzyme involves two domains, the catalytic domain comprising residues 45–99 and 227–393, and an intervening β -sandwich domain formed by residues 104–221 (**Figure 6A**). As predicted earlier (Pfeffer et al., 2013), the catalytic domain adopts the canonical α/β -hydrolase fold of the SGNH hydrolase superfamily complete with the catalytic Ser-His-Asp residues aligned proximal to the oxyanion Asn and Gly residues (**Figure 5A**). However, in contrast to other known Ser esterase-like mechanisms, binding of substrate induces a 90° rotation of the Ser side chain to its catalytically competent position. Also, the oxyanion hole Gly residue appears to provide a gate that may close the active site in the absence of substrate. Hence, it appears that Ape, and possibly the other CE3 family enzymes, functions using an unusual substrate-induced catalytic triad.

The substrate-binding groove is open while a tight pocket accommodates the acetyl moiety (**Figure 6B**). These features, together with the rotational flexibility of the catalytic Ser, may account for the relative substrate promiscuity demonstrated by Ape (Weadge and Clarke, 2006, Clarke, 2007). The absence of any other observed contacts with added ligands in the different crystal structures reported is consistent with the kinetic data obtained with the MurNAc-based substrate analogs mentioned above. However, the smaller N-terminal domain formed by residues 104–221 is proposed to represent a carbohydrate-binding module similar to those of the CBM35 family members of the CAZY

database (Montanier et al., 2009). The family 35 CBMs are typically associated with bacterial hydrolases with specificity for plant cell wall polysaccharides. Interestingly however, rather than recognizing the substrates of the cognate catalytic domains, as typical of most CBMs, these CBMs are thought to help anchor the hydrolases to the bacterial cell wall through their capacity to bind uronic acid sugars (Montanier et al., 2009). As enzymes secreted to the periplasm, it is possible that the CBM35-like domain of Ape serves to retain it on PG for its localized activity as required for PG metabolism. How such temporal and functional specificity is conferred remains unknown, but it is also equally possible that Ape associates with the protein complexes (elongasomes and divisosomes) proposed to be responsible for cell elongation and division (Höltje, 1998; Naninga, 1991). Such associations would ensure removal of blocking *O*-acetyl groups as required for LT activity and PG growth/remodeling.

Discovery of Ape Inhibitors

With the production and employment of both PatA/B and Ape, it would appear that the Gram-negative bacteria balance the level of PG O-acetylation to control continued PG metabolism. Recognizing this important role, it was postulated that these enzymes may serve as new targets for antibiotic development (Moynihan and Clarke, 2010, 2013; Weadge and Clarke, 2006). Indeed, Ape activity is required for survival of *N. meningitidis* in animal models (Veyrier et al., 2013) and attempts to generate deletion mutants in *N. gonorrhoeae* failed (Weadge and Clarke, 2006). Also, no strain of a bacterium that normally produces *O*-acetyl-PG has been found to be devoid of the modification. For example, the chromosome of *N. gonorrhoeae* RD5 harbors a truncated *patA* gene (Dillard and Hackett, 2005), but careful analysis of the PG isolated from this strain revealed it retains between 10 and 15% *O*-acetylation (Rosenthal et al., 1982; Rosenthal et al., 1983; Swim et al., 1983). Hence, it appears that an inhibitor of either the *O*-acetyltransferase and/or *O*-acetylsterase activities would be detrimental to the pathogens that produce *O*-acetyl-PG.

To identify inhibitors that could be used to prove the principle that these enzymes would serve as novel antibiotic targets, a fluorogenic assay for *O*-acetylsterase activity was made amenable for high throughput screening. With 4-methylumbelliferyl acetate as substrate and *N. gonorrhoeae* Ape as the target, an overall Z' score of 0.62 was obtained for the assay, allowing a threshold for screening to be set at 65% residual activity. The assay was tested in a pilot screen and seven compounds were identified as true inhibitors of NgApe (Pfeffer and Clarke, 2012). Dose-response curves identified five of these compounds with respectable IC_{50} values, which ranged between 0.3 and 23 μ M. Of these, purpurin (a red/yellow dye from the madder plant) (**Figure 4D**) was selected for further analysis based on its ready availability and relative solubility. Its inhibition of Ape was determined to be competitive with a K_i value of 4.8 μ M (Pfeffer and Clarke, 2012).

FUTURE DIRECTIONS

Irrespective of the carbohydrates they modify, O-acetylation systems for modifying cell wall glycans and exopolysaccharides have been organized into two general categories: the single protein (AT3-dependent) and multi-protein (MBOAT-dependent) pathways (Moynihan and Clarke, 2011; Gille and Pauly, 2012). Of these, the respective transmembrane protein component (AT3 or MBOAT) is postulated to present an acetyl-donor substrate for an SGNH-hydrolase-like enzyme that catalyzes the glycan modification. The only other SGNH hydrolase-like enzymes involved in bacterial cell wall modifications, beyond OatA and PatB, that have been characterized biochemically are *P. aeruginosa* AlgX (Riley et al., 2013) and AlgJ (Baker et al., 2014), and *Bacillus cereus* PatB1 (Sychantha et al., 2018), enzymes responsible for the O-acetylation of alginate and secondary cell-wall polysaccharide in the respective pathogens. As with PG, the importance of cell wall O-acetylation for virulence in bacteria has also called attention to these systems as potential targets for the development of novel therapeutics. To this end, informing future discovery of O-acetyltransferase inhibitors and their development into efficacious antibiotics requires a detailed understanding of the structural and functional relationships of more of these enzymes.

A major unanswered question that remains for each of these O-acetylation systems is the nature of the biological source of acetyl group and how it is mechanistically transported to the extracytoplasmic O-acetyltransferases. Whereas the associated MBOAT or AT3 proteins have been proposed to serve this function, the precise mechanism is not known. With some AT3 family members, such as the xanthan O-acetyltransferases GumF and GumG produced by *Xanthomonas campestris* (Vorhölter et al., 2008) and the trehalose corynomycolate O-acetyltransferase TmaT from *Corynebacterium diphtheriae* (Yamaryo-Botte et al., 2015), the C-terminal SGNH hydrolase domain is absent. These enzymes modify the respective sugar moiety associated with a lipid carrier on the cytoplasmic face, and they are subsequently translocated across the membrane for further processing. Presumably, acetyl-CoA is used as source of cytoplasmic acetyl group to confer these modifications. Based on the individual activities of AT3 family proteins, it is tempting to speculate that one linked to a catalytic domain with extracytoplasmic function could produce an activated lipid-linked acetyl donor. However, a lipid species of this nature would likely be transient in order to maintain steady-state levels of O-acetylation. Hence, the constant turnover of such a molecule could be a reason why it may have been overlooked or undetected in previous lipidomic studies. Indeed, a similar phenomenon was seen recently with the O-acetyl TCMCM produced by TmaT (Yamaryo-Botte et al., 2015). Alternatively, an acetyl-lipid may not exist and instead the transmembrane domain of these proteins may function as a channel, moving acetyl groups across the membrane before presenting them to the extracytoplasmic transferases. While there is currently neither evidence nor precedent to support this, preliminary experiments performed by us with

SpOatA_C and *SaOatA_C* revealed that these proteins can use O-acetyltyrosine as a donor (unpublished data). Consistent with this observation, it was found that the predicted surface topology of the transmembrane domain of OatA from both organisms contains numerous conserved tyrosine residues throughout their predicted transmembrane helices, suggesting that a tyrosine relay could be involved. Regardless, a complete understanding of the mechanism of O-acetylation will require examination of the full length structure of OatA and/or PatA. Although X-ray crystallography could be used for these structural determinations, current advances in cryo-electron microscopy may provide an alternative and more informative approach. For example, the structure of hemoglobin (64 kDa) was recently solved at 3.2 Å resolution by cryo-EM (Danev and Baumeister, 2017; Khoshouei et al., 2017) and advances with this technology continue. As OatA is a 70-kDa protein and assumed to be monomeric, cryo-EM may represent a feasible approach for its study. Such studies, together with those discussed above, would further useful information as a foundation for drug discovery.

Finally, it remains to be established if inhibiting only PG O-acetyltransferases and/or O-acetyl-PG esterases with small molecule inhibitors will be sufficient to render bacterial pathogens exploiting these enzymes susceptible to an efficacious immune response. As the C-6 hydroxyl group of muramoyl residues in PG is also the sight for binding of cell wall polymers, such as teichoic acids and the secondary cell wall polysaccharides of Gram-positive pathogens, and lipoproteins of Gram-negative bacteria (Schleifer and Kandler, 1972), it is possible that cells may respond to the challenge of an anti-O-acetylation inhibitor by increasing production of these other modifying materials. Interestingly however, Bera et al. (2007) observed that such does not appear to occur, at least in *S. aureus*, where $\Delta tagO$ and $\Delta oatA$ mutants did not produce higher levels of PG O-acetylation or teichoic acids, respectively [TagO is essential for teichoic acid production (Weidenmaier et al., 2004)]. Nonetheless, the double knockout mutant was the most susceptible strain of the three strains to lysis by lysozyme. As it is not clear what other compensatory action these mutants may have made, such as alterations to crosslinking (Atilano et al., 2010), only the discovery of inhibitors and their use in *in vivo* experiments might prove the principle of the drugability of PG O-acetylation systems in this and other important human pathogens.

AUTHOR CONTRIBUTIONS

DS, AB, CJ, and AC prepared various sections of the manuscript and reviewed the final draft.

FUNDING

Funding to AC for studies on PG O-acetylation have been provided by the Canadian Institutes for Health Research (current Project Grant PJT 156353) and the Canadian Glycomics Network, a National Centre of Excellence.

REFERENCES

- Abrams, A. (1958). O-Acetyl groups in the cell wall of *Streptococcus faecalis*. *J. Biol. Chem.* 230, 949–959.
- Allen, J. P., and Neely, M. N. (2012). CpsY influences *Streptococcus iniae* cell wall adaptations important for neutrophil intracellular survival. *Infect. Immun.* 80, 1707–1715. doi: 10.1128/IAI.00027-12
- Allen, V. G., Seah, C., Martin, I., and Melano, R. G. (2014). Azithromycin resistance is coevolving with reduced susceptibility to cephalosporins in *Neisseria gonorrhoeae* in Ontario, Canada. *Antimicrob. Agents Chemother.* 58, 2528–2534. doi: 10.1128/AAC.02608-13
- Atilano, M. L., Pereira, P. M., Yates, J., Reed, P., Veiga, H., Pinho, M. G., et al. (2010). Teichoic acids are temporal and spatial regulators of peptidoglycan cross-linking in *Staphylococcus aureus*. *Proc. Natl. Acad. Sci. U.S.A.* 107, 18991–18996. doi: 10.1073/pnas.1004304107
- Aubry, C., Goulard, C., Nahori, M. A., Cayet, N., Decalf, J., Sachse, M., et al. (2011). OatA, a peptidoglycan O-acetyltransferase involved in *Listeria monocytogenes* immune escape, is critical for virulence. *J. Infect. Dis.* 204, 731–740. doi: 10.1093/infdis/jir396
- Baker, P., Ricer, T., Moynihan, P. J., Kitova, E. N., Walvoort, M. T. C., Little, D. J., et al. (2014). *P. aeruginosa* SGNH hydrolase-like proteins AlgJ and AlgX have similar topology but separate and distinct roles in alginate acetylation. *PLoS Pathog.* 10:e1004334. doi: 10.1371/journal.ppat.1004334
- Baranwal, G., Mohammad, M., Jarneborn, A., Reddy, B. R., Golla, A., Chakravarty, S., et al. (2017). Impact of cell wall peptidoglycan O-acetylation on the pathogenesis of *Staphylococcus aureus* in septic arthritis. *Int. J. Med. Microbiol.* 307, 388–397. doi: 10.1016/j.ijmm.2017.08.002
- Benson, T. E., Marquardt, J. L., Marquardt, A. C., Etzkorn, F. A., and Walsh, C. T. (1993). Overexpression, purification, and mechanistic study of UDP-N-acetylenolpyruvyl-glucosamine reductase. *Biochemistry* 32, 2024–2030. doi: 10.1021/bi00059a019
- Bera, A., Biswas, R., Herbert, S., and Götz, F. (2006). The presence of peptidoglycan O-acetyltransferase in various staphylococcal species correlates with lysozyme resistance and pathogenicity. *Infect. Immun.* 74, 4598–4604. doi: 10.1128/IAI.00301-06
- Bera, A., Biswas, R., Herbert, S., Kulauzovic, E., Weidenmaier, C., Peschel, A., et al. (2007). Influence of wall teichoic acid on lysozyme resistance in *Staphylococcus aureus*. *J. Bacteriol.* 189, 280–283. doi: 10.1128/JB.01221-06
- Bera, A., Herbert, S., Jakob, A., Vollmer, W., and Götz, F. (2005). Why are pathogenic staphylococci so lysozyme resistant? The peptidoglycan O-acetyltransferase OatA is the major determinant for lysozyme resistance of *Staphylococcus aureus*. *Mol. Microbiol.* 55, 778–787. doi: 10.1111/j.1365-2958.2004.04446.x
- Bernard, E., Rolain, T., Courtin, P., Guillot, A., Langella, P., Hols, P., et al. (2011). Characterization of O-acetylation of N-acetylglucosamine: a novel structural variation of bacterial peptidoglycan. *J. Biol. Chem.* 286, 23950–23958. doi: 10.1074/jbc.M111.241414
- Bernard, E., Rolain, T., David, B., André, G., Dupres, V., Dufrène, Y. F., et al. (2012). Dual role for the O-acetyltransferase OatA in peptidoglycan modification and control of cell septation in *Lactobacillus plantarum*. *PLoS One* 7:e47893. doi: 10.1371/journal.pone.0047893
- Blundell, J. K., and Perkins, H. R. (1981). Effects of beta-lactam antibiotics on peptidoglycan synthesis in growing *Neisseria gonorrhoeae*, including changes in the degree of O-acetylation. *J. Bacteriol.* 147, 633–641.
- Bonnet, J., Durmort, C., Jacq, M., Mortier-Barrière, I., Campo, N., VanNieuwenhze, M. S., et al. (2017). Peptidoglycan O-acetylation is functionally related to cell wall biosynthesis and cell division in *Streptococcus pneumoniae*. *Mol. Microbiol.* 106, 832–846. doi: 10.1111/mmi.13849
- Brown, E. D., Vivas, E. I., Walsh, C. T., and Kolter, R. (1995). MurA (MurZ), the enzyme that catalyzes the first committed step in peptidoglycan biosynthesis, is essential in *Escherichia coli*. *J. Bacteriol.* 177, 4194–4197. doi: 10.1128/jb.177.14.4194-4197.1995
- Brown, E. D., and Wright, G. D. (2016). Antibacterial drug discovery in the resistance era. *Nature* 529, 336–343. doi: 10.1038/nature17042
- Brumfitt, W., Wardlaw, A. C., and Park, J. T. (1958). Development of lysozyme-resistance in *Micrococcus lysodeikticus* and its association with an increased O-acetyl content of the cell wall. *Nature* 181, 1783–1784. doi: 10.1038/1811783a0
- Burghaus, P., Johannsen, L., Naumann, D., Labischinski, H., Bradaczek, H., and Giesbrecht, P. (1983). “The influence of different antibiotics on the degree of O-acetylation of staphylococcal cell walls,” in *The Target of Penicillin. The Murein Sacculus of Bacterial Cell Walls Architecture and Growth*, eds R. Hakenbeck, J.-V. Höltje, and H. Labischinski (New York, NY: Walter de Gruyter and Co), 317–322.
- Burke, T. P., Loukitcheva, A., Zemansky, J., Wheeler, R., Boneca, I. G., and Portnoy, D. A. (2014). *Listeria monocytogenes* is resistant to lysozyme through the regulation, not the acquisition, of cell wall-modifying enzymes. *J. Bacteriol.* 196, 3756–3767. doi: 10.1128/JB.02053-14
- Carbohydrate-Active enZymes Database (1998). *The CAZy Database Describes the Families of Structurally-Related Catalytic and Carbohydrate-Binding Modules (or Functional Domains) of Enzymes that Degrade, Modify, or Create Glycosidic Bonds*. Available at: www.CAZY.org
- Clarke, A. J. (1993). The extent of peptidoglycan O-acetylation among the Proteae. *J. Bacteriol.* 175, 4550–4553. doi: 10.1128/jb.175.14.4550-4553.1993
- Clarke, A. J., and Dupont, C. (1991). O-Acetylated peptidoglycan: its occurrence, pathobiological significance and biosynthesis. *Can. J. Microbiol.* 38, 85–91. doi: 10.1139/m92-014
- Clarke, A. J., Strating, H., and Blackburn, N. T. (2002). “Pathways for the O-acetylation of bacterial cell wall polysaccharides,” in *Glycomicrobiology*, ed. R. J. Doyle (New York, NY: Plenum Publishing Co Ltd), 187–223.
- Clarke, C. A., Scheurwater, E. M., and Clarke, A. J. (2010). The vertebrate lysozyme inhibitor Ivy functions to inhibit the activity of lytic transglycosylase. *J. Biol. Chem.* 285, 14843–14847. doi: 10.1074/jbc.C110.120931
- Crisóstomo, M. L., Vollmer, W., Kharat, A. S., Inhülsen, S., Gehre, F., Buckenmaier, S., et al. (2006). Attenuation of penicillin resistance in a peptidoglycan O-acetyl transferase mutant of *Streptococcus pneumoniae*. *Mol. Microbiol.* 61, 1497–1509. doi: 10.1111/j.1365-2958.2006.05340.x
- Danev, R., and Baumeister, W. (2017). Expanding the boundaries of cryo-EM with phase plates. *Curr. Opin. Struct. Biol.* 46, 87–94. doi: 10.1016/j.sbi.2017.06.006
- Davis, K. M., Akinbi, H. T., Standish, A. J., and Weiser, J. N. (2008). Resistance to mucosal lysozyme compensates for the fitness deficit of peptidoglycan modifications by *Streptococcus pneumoniae*. *PLoS Pathog.* 4:e1000241. doi: 10.1371/journal.ppat.1000241
- Dillard, J. P., and Hackett, K. T. (2005). Mutations affecting peptidoglycan acetylation in *Neisseria gonorrhoeae* and *Neisseria meningitidis*. *Infect. Immun.* 73, 5697–5705. doi: 10.1128/IAI.73.9.5697-5705.2005
- Dougherty, T. J. (1983). Peptidoglycan biosynthesis in *Neisseria gonorrhoeae* strains sensitive and intrinsically resistant to beta-lactam antibiotics. *J. Bacteriol.* 153, 429–435.
- Dougherty, T. J. (1985a). Analysis of *Neisseria gonorrhoeae* peptidoglycan by reverse-phase, high-pressure liquid chromatography. *J. Bacteriol.* 163, 69–74.
- Dougherty, T. J. (1985b). Involvement of a change in penicillin target and peptidoglycan structure in low-level resistance to beta-lactam antibiotics in *Neisseria gonorrhoeae*. *Antimicrob. Agents Chemother.* 28, 90–95.
- Egan, A. J., Biboy, J., van't Veer, I., Breukink, E., and Vollmer, W. (2015). Activities and regulation of peptidoglycan synthases. *Philos. Trans. R. Soc. Lond. B Biol. Sci.* 370:20150031. doi: 10.1098/rstb.2015.0031
- Ellison, R. T. III, and Giehl, T. J. (1991). Killing of Gram-negative bacteria by lactoferrin and lysozyme. *J. Clin. Invest.* 88, 1080–1091. doi: 10.1172/JCI115407
- Emirian, A., Fromentin, S., Eckert, C., Chau, F., Dubost, L., Delepierre, M., et al. (2009). Impact of peptidoglycan O-acetylation on autolytic activities of the *Enterococcus faecalis* N-acetylglucosaminidase AtlA and N-acetylmuramidase AtlB. *FEBS Lett.* 583, 3033–3038. doi: 10.1016/j.febslet.2009.08.010
- Eraso, J. M., and Margolin, W. (2011). Bacterial cell wall: thinking globally, acting locally. *Curr. Biol.* 21, R628–R630. doi: 10.1016/j.cub.2011.06.056
- Figueiredo, T. A., Sobral, R. G., Ludovice, A. M., Almeida, J. M., Bui, N. K., Vollmer, W., et al. (2012). Identification of genetic determinants and enzymes

- involved with the amidation of glutamic acid residues in the peptidoglycan of *Staphylococcus aureus*. *PLoS Pathog.* 8:e1002508. doi: 10.1371/journal.ppat.1002508
- Fleurie, A., Lesterlin, C., Manuse, S., Zhao, C., Cluzel, C., Laverigne, J.-P., et al. (2014). MapZ marks the division sites and positions FtsZ rings in *Streptococcus pneumoniae*. *Nature* 516, 259–262. doi: 10.1038/nature13966
- Franklin, M. J., and Ohman, D. E. (2002). Mutant analysis and cellular localization of the AlgI, AlgJ, and AlgF proteins required for O-acetylation of alginate in *Pseudomonas aeruginosa*. *J. Bacteriol.* 184, 3000–3007. doi: 10.1128/JB.184.11.3000-3007.2002
- Gille, S., and Pauly, M. (2012). O-Acetylation of plant cell wall polysaccharides. *Front. Plant Sci.* 3:12. doi: 10.3389/fpls.2012.00012
- Gmeiner, J., and Kroll, H. P. (1981). Murein biosynthesis and O-acetylation of N-acetylmuramic acid during the cell-division cycle of *Proteus mirabilis*. *Eur. J. Biochem.* 117, 171–177. doi: 10.1111/j.1432-1033.1981.tb06317.x
- Gmeiner, J., and Sarnow, E. (1987). Murein biosynthesis in synchronized cells of *Proteus mirabilis*. Quantitative analysis of O-acetylated murein subunits and of chain terminators incorporated into the sacculus during the cell cycle. *Eur. J. Biochem.* 163, 389–395. doi: 10.1111/j.1432-1033.1987.tb08117.x
- Goffin, C., and Ghuysen, J.-M. (1998). Multimodular penicillin-binding proteins: an enigmatic family of orthologs and paralogs. *Microbiol. Mol. Biol. Rev.* 62, 1079–1093.
- Gutelius, D., Hokeness, K., Logan, S. M., and Reid, C. W. (2014). Functional analysis of SleC from *Clostridium difficile*: an essential lytic transglycosylase involved in spore germination. *Microbiology* 160, 209–216. doi: 10.1099/mic.0.072454-0
- Ha, R., Frirdich, E., Sychantha, D., Biboy, J., Taveirne, M. E., Johnson, J. G., et al. (2016). Accumulation of peptidoglycan O-acetylation leads to altered cell wall biochemistry and negatively impacts pathogenesis factors of *Campylobacter jejuni*. *J. Biol. Chem.* 291, 22686–22702. doi: 10.1074/jbc.M116.746404
- Hadi, T., Pfeffer, J. M., Clarke, A. J., and Tanner, M. E. (2011). Water-soluble substrates of the peptidoglycan-modifying enzyme O-acetylpeptidoglycan esterase (Ape1) from *Neisseria gonorrhoeae*. *J. Org. Chem.* 76, 1118–1125. doi: 10.1021/jo102329c
- Hancock, R. E. W., and Scott, M. G. (2000). The role of antimicrobial peptides in animal defenses. *Proc. Natl. Acad. Sci. U.S.A.* 97, 8856–8861. doi: 10.1073/pnas.97.16.8856
- Hébert, L., Courtin, P., Torelli, R., Sanguinetti, M., Chapot-Chartier, M. P., Auffray, Y., et al. (2007). *Enterococcus faecalis* constitutes an unusual bacterial model in lysozyme resistance. *Infect. Immun.* 75, 5390–5398. doi: 10.1128/IAI.00571-07
- Herlihey, F. A., Moynihan, P. J., and Clarke, A. J. (2014). The essential protein for bacterial flagella formation FlgJ functions as a β -N-acetylglucosaminidase. *J. Biol. Chem.* 289, 31029–31042. doi: 10.1074/jbc.M114.603944
- Ho, Y. S., Sheffield, P. J., Masuyama, J., Arai, H., Li, J., Aoki, J., et al. (1999). Probing the substrate specificity of the intracellular brain platelet-activating factor acetylhydrolase. *Protein Eng.* 12, 693–700. doi: 10.1093/protein/12.8.693
- Höltje, J.-V. (1998). Growth of the stress-bearing and shape-maintaining murein sacculus of *Escherichia coli*. *Microbiol. Mol. Biol. Rev.* 62, 181–203.
- Höltje, J.-V., Mirelman, D., Sharon, N., and Schwarz, U. (1975). Novel type of murein transglycosylase in *Escherichia coli*. *J. Bacteriol.* 124, 1067–1076.
- Ikeda, M., Wachi, M., Jung, G., Ishino, F., and Matsushashi, M. (1991). The *Escherichia coli* MraY gene encoding UDP-N-acetylmuramoyl-pentapeptide-undecaprenyl-phosphate phospho-N-acetylmuramoyl-pentapeptide transferase. *J. Bacteriol.* 173, 1021–1026. doi: 10.1128/jb.173.3.1021-1026.1991
- Ikeda, M., Wachi, M., and Matsushashi, M. (1992). The MurG gene of the *Escherichia coli* chromosome encoding UDP-N-acetylglucosamine undecaprenyl pyrophosphoryl-N-acetylmuramoyl-pentapeptide N-acetylglucosaminyl transferase. *J. Gen. Appl. Microbiol.* 38, 53–62. doi: 10.2323/jgam.38.53
- Irwin, D. M., Biegel, J. M., and Stewart, C.-B. (2011). Evolution of the mammalian lysozyme gene family. *BMC Evol. Biol.* 11:166. doi: 10.1186/1471-2148-11-166
- Kell, L. (2016). *Research Technician at Ryerson University*. MSc. thesis, University of Guelph, Guelph, ON.
- Khoshouei, M., Radjainia, M., Baumeister, W., and Danev, R. (2017). Cryo-EM structure of haemoglobin at 3.2 Å determined with the volta phase plate. *Nat. Commun.* 8:16099. doi: 10.1038/ncomms16099
- Laaberki, M.-H., Pfeffer, J., Clarke, A. J., and Dworkin, J. (2011). O-Acetylation of peptidoglycan is required for proper cell separation and S-layer anchoring in *Bacillus anthracis*. *J. Biol. Chem.* 286, 5278–5288. doi: 10.1074/jbc.M110.183236
- Le Jeune, A., Torelli, R., Sanguinetti, M., Giard, J.-C., Hartke, A., Auffray, Y., et al. (2010). The extracytoplasmic function sigma factor SigV plays a key role in the original model of lysozyme resistance and virulence of *Enterococcus faecalis*. *PLoS One* 5:e9658. doi: 10.1371/journal.pone.0009658
- Lear, A. L., and Perkins, H. R. (1983). Degrees of O-acetylation and cross-linking of the peptidoglycan of *Neisseria gonorrhoeae* during growth. *J. Gen. Microbiol.* 129, 885–888.
- Lear, A. L., and Perkins, H. R. (1986). O-Acetylation of peptidoglycan in *Neisseria gonorrhoeae*. Investigation of lipid-linked intermediates and glycan chains newly incorporated into the cell wall. *J. Gen. Microbiol.* 132, 2413–2420.
- Lear, A. L., and Perkins, H. R. (1987). Progress of O-acetylation and cross-linking of peptidoglycan in *Neisseria gonorrhoeae* grown in the presence of penicillin. *J. Gen. Microbiol.* 133, 743–750.
- Liger, D., Masson, A., Blanot, D., van Heijenoort, J., and Parquet, C. (1995). Over-production, purification and properties of the uridine-diphosphate-N-acetylmuramate:alanine ligase from *Escherichia coli*. *Eur. J. Biochem.* 230, 80–87. doi: 10.1111/j.1432-1033.1995.0080i.x
- Lo, Y. C., Lin, S. C., Shaw, J. F., and Liaw, Y. C. (2003). Crystal structure of *Escherichia coli* thioesterase I/protease I/lysophospholipase L1: consensus sequence blocks constitute the catalytic center of SGNH-hydrolases through a conserved hydrogen bond network. *J. Mol. Biol.* 330, 539–551. doi: 10.1016/S0022-2836(03)00637-5
- Marquardt, J. L., Siegle, D. A., Kolter, R., and Walsh, C. T. (1992). Cloning and sequencing of *Escherichia coli* murZ and purification of its product, a UDP-N-acetylglucosamine enolpyruvyl transferase. *J. Bacteriol.* 174, 5748–5752. doi: 10.1128/jb.174.17.5748-5752.1992
- Martin, H. H., and Gmeiner, J. (1979). Modification of peptidoglycan structure by penicillin action in cell walls of *Proteus mirabilis*. *Eur. J. Biochem.* 95, 487–495. doi: 10.1111/j.1432-1033.1979.tb12988.x
- Martin, I., Sawatzky, P., Liu, G., and Mulvey, M. R. (2015). Antimicrobial resistance to *Neisseria gonorrhoeae* in Canada: 2009–2013. *Can. Commun. Dis. Rep.* 41, 35–41. doi: 10.14745/ccdr.v41i02a04
- Michaud, C., Mengin-Lecreulx, D., van Heijenoort, J., and Blanot, D. (1990). Over-production, purification and properties of the uridine-diphosphate-N-acetylmuramoyl-L-alanyl-D-glutamate: meso-2,6-diaminopimelate ligase from *Escherichia coli*. *Eur. J. Biochem.* 194, 853–861. doi: 10.1111/j.1432-1033.1990.tb19479.x
- Mohammadi, T., van Dam, V., Sijbrandi, R., Vernet, T., Zapun, A., Bouhss, A., et al. (2011). Identification of FtsW as a transporter of lipid-linked cell wall precursors across the membrane. *EMBO J.* 30, 1425–1432. doi: 10.1038/emboj.2011.61
- Mølgaard, A., Kauppinen, S., and Larsen, S. (2000). Rhamnogalacturonan acetyltransferase elucidates the structure and function of a new family of hydrolases. *Structure* 8, 373–383. doi: 10.1016/S0969-2126(00)00118-0
- Montanier, C., van Bueren, A. L., Dumon, C., Flint, J. E., Correia, M. A., Prates, J. A., et al. (2009). Evidence that family 35 carbohydrate binding modules display conserved specificity but divergent function. *Proc. Natl. Acad. Sci. U.S.A.* 106, 3065–3070. doi: 10.1073/pnas.0808972106
- Moynihan, P. J., and Clarke, A. J. (2010). O-Acetylation of peptidoglycan in Gram-negative bacteria: identification and characterization of PG O-acetyltransferase in *Neisseria gonorrhoeae*. *J. Biol. Chem.* 285, 13264–13273. doi: 10.1074/jbc.M110.107086
- Moynihan, P. J., and Clarke, A. J. (2011). O-Acetylated peptidoglycan: controlling the activity of bacterial autolysins and lytic enzymes of innate immune systems. *Int. J. Biochem. Cell Biol.* 43, 1655–1659. doi: 10.1016/j.biocel.2011.08.007
- Moynihan, P. J., and Clarke, A. J. (2013). Assay for peptidoglycan O-acetyltransferase: a potential new antibacterial target. *Anal. Biochem.* 439, 73–79. doi: 10.1016/j.ab.2013.04.022
- Moynihan, P. J., and Clarke, A. J. (2014a). Substrate specificity and kinetic characterization of Peptidoglycan O-Acetyltransferase B from *Neisseria gonorrhoeae*. *J. Biol. Chem.* 289, 16748–16760. doi: 10.1074/jbc.M114.567388

- Moynihan, P. J., and Clarke, A. J. (2014b). The mechanism of peptidoglycan O-acetyltransferase involves an Asp-His-Ser catalytic triad. *Biochemistry* 53, 6243–6251. doi: 10.1021/bi501002d
- Münch, D., Roemer, T., Lee, S. H., Engeser, M., Sahl, H. G., and Schneider, T. (2012). Identification and *in vitro* analysis of the GatD/MurT enzyme-complex catalyzing Lipid II amidation in *Staphylococcus aureus*. *PLoS Pathog.* 8:e1002509. doi: 10.1371/journal.ppat.1002509
- Myers, D. K., and Jun, A. K. (1954). Inhibition of esterases by the fluorides of organic acids. *Nature* 173, 33–34. doi: 10.1038/173033a0
- Naninge, N. (1991). Cell division and peptidoglycan assembly in *Escherichia coli*. *Mol. Microbiol.* 5, 791–795. doi: 10.1111/j.1365-2958.1991.tb00751.x
- Pfeffer, J. M., and Clarke, A. J. (2012). Identification of first-known inhibitors of O-acetyl-peptidoglycan esterase: a potential new antibacterial target. *Chembiochem* 13, 722–731. doi: 10.1002/cbic.201100744
- Pfeffer, J. M., Strating, H., Weadge, J. T., and Clarke, A. J. (2006). Peptidoglycan O-acetylation and autolysin profile of *Enterococcus faecalis* in the viable but nonculturable state. *J. Bacteriol.* 188, 902–908. doi: 10.1128/JB.188.3.902-908.2006
- Pfeffer, J. M., Weadge, J. T., and Clarke, A. J. (2013). Mechanism of action of *Neisseria gonorrhoeae* O-acetylpeptidoglycan esterase, an SGNH serine esterase. *J. Biol. Chem.* 288, 2605–2612. doi: 10.1074/jbc.M112.436352
- Pratviel-Sosa, F., Mengin-Lecreux, D., and van Heijenoort, J. (1991). Overproduction, purification and properties of the uridine diphosphate N-acetylmuramoyl-l-alanine: d-glutamate ligase from *Escherichia coli*. *Eur. J. Biochem.* 202, 1169–1176. doi: 10.1111/j.1432-1033.1991.tb16486.x
- Pushkaran, A. C., Nataraj, N., Nair, N., Götz, F., Biswas, R., and Mohan, C. G. (2015). Understanding the structure-function relationship of lysozyme resistance in *Staphylococcus aureus* by peptidoglycan O-acetylation using molecular docking, dynamics, and lysis assay. *J. Chem. Inf. Model.* 55, 760–770. doi: 10.1021/ci500734k
- Rae, C. S., Geissler, A., Adamson, P. C., and Portnoy, D. A. (2011). Mutations of the peptidoglycan N-deacetylase and O-acetylase result in enhanced lysozyme sensitivity, bacteriolysis, and hyperinduction of innate immune pathways. *Infect. Immun.* 79, 3596–3606. doi: 10.1128/IAI.00077-11
- Ragland, S. A., and Criss, A. K. (2017). From bacterial killing to immune modulation: recent insights into the functions of lysozyme. *PLoS Pathog.* 13:e1006512. doi: 10.1371/journal.ppat.1006512
- Riley, L. M., Weadge, J. T., Baker, P., Robinson, H., Codee, J. D. C., Tipton, P. A., et al. (2013). Structural and functional characterization of *Pseudomonas aeruginosa* AlgX: role of AlgX in alginate acetylation. *J. Biol. Chem.* 288, 22299–22314. doi: 10.1074/jbc.M113.484931
- Rosenthal, R. S., Blundell, J. K., and Perkins, H. R. (1982). Strain-related differences in lysozyme sensitivity and extent of O-acetylation of gonococcal peptidoglycan. *Infect. Immun.* 37, 826–829.
- Rosenthal, R. S., Folkening, W. J., Miller, D. R., and Swim, S. C. (1983). Resistance of O-acetylated gonococcal peptidoglycan to human peptidoglycan-degrading enzymes. *Infect. Immun.* 40, 903–911.
- Ruiz, N. (2008). Bioinformatics identification of MurJ (MviN) as the peptidoglycan lipid II flippase in *Escherichia coli*. *Proc. Natl. Acad. Sci. U.S.A.* 105, 15553–15557. doi: 10.1073/pnas.0808352105
- Sanchez, M., Kolar, S. L., Müller, S., Reyes, C. N., Wolf, A. J., Ogawa, C., et al. (2017). O-Acetylation of peptidoglycan limits helper T cell priming and permits *Staphylococcus aureus* reinfection. *Cell Host Microbe* 22, 543–551. doi: 10.1016/j.chom.2017.08.008
- Scheurwater, E. M., Reid, C. W., and Clarke, A. J. (2008). Lytic transglycosylases: bacterial space-making autolysins. *Int. J. Biochem. Cell Biol.* 40, 586–591. doi: 10.1016/j.biocel.2007.03.018
- Schleifer, K. H., and Kandler, O. (1972). Peptidoglycan types of bacterial cell walls and their taxonomic implications. *Bacteriol. Rev.* 36, 407–477.
- Seidl, P. H., and Schleifer, K. H. (eds). (1985). *Biological Properties of Peptidoglycan*. New York, NY: Walter de Gruyter.
- Shimada, T., Park, B. G., Wolf, A. J., Brikom, C., Goodridge, H. S., Becker, C. A., et al. (2010). *Staphylococcus aureus* evades lysozyme-based peptidoglycan digestion that links phagocytosis, inflammasome activation, and IL-1 β secretion. *Cell Host Microbe* 7, 38–49. doi: 10.1016/j.chom.2009.12.008
- Sidow, T., Johannsen, L., and Labischinski, H. (1990). Penicillin-induced changes in the cell wall composition of *Staphylococcus aureus* before the onset of bacteriolysis. *Arch. Microbiol.* 154, 73–81. doi: 10.1007/BF00249181
- Snowden, M., Perkins, H., Wyke, A., Hayes, M., and Ward, J. (1989). Cross-linking and O-acetylation of newly synthesized peptidoglycan in *Staphylococcus aureus* H. *Microbiology* 135, 3015–3022. doi: 10.1099/00221287-135-11-3015
- Sorbara, M. T., and Philpott, D. J. (2011). Peptidoglycan: a critical activator of the mammalian immune system during infection and homeostasis. *Immunol. Rev.* 243, 40–60. doi: 10.1111/j.1600-065X.2011.01047.x
- Strating, H., and Clarke, A. J. (2001). Differentiation of bacterial autolysins by zymogram analysis. *Anal. Biochem.* 290, 388–393. doi: 10.1006/abio.2001.5007
- Swim, S. C., Gfell, M. A., Wilde, C. E. III, and Rosenthal, R. S. (1983). Strain distribution in extents of lysozyme resistance and O-acetylation of gonococcal peptidoglycan determined by high-performance liquid chromatography. *Infect. Immun.* 42, 446–452.
- Sychantha, D., and Clarke, A. J. (2018). Peptidoglycan modification by the catalytic domain of *Streptococcus pneumoniae* OatA follows a ping-pong bi-bi mechanism of action. *Biochemistry* 57, 2394–2401. doi: 10.1021/acs.biochem.8b00301
- Sychantha, D., Jones, C., Little, D. J., Moynihan, P. J., Robinson, H., Galley, N. F., et al. (2017). Structure and molecular basis of catalysis of the peptidoglycan O-acetyltransferase A (OatA) catalytic domain. *PLoS Pathog.* 13:e1006667. doi: 10.1371/journal.ppat.1006667
- Sychantha, D., Little, D. J., Chapman, R. N., Boons, G. J., Robinson, H., Howell, P. L., et al. (2018). PatB1 is an O-acetyltransferase that decorates secondary cell wall polysaccharides. *Nat. Chem. Biol.* 14, 79–85. doi: 10.1038/nchembio.2509
- Taguchi, A., Welsh, M. A., Marmont, L. S., Lee, W., Kahne, D., Bernhardt, T. G., et al. (2018). FtsW is a Peptidoglycan Polymerase That is Activated by its Cognate Penicillin-Binding Protein. *bioRxiv* [Preprint]. doi: 10.1101/358663
- The Review on Antimicrobial Resistance chaired by Jim O'Neill (2014). *Antimicrobial Resistance: Tackling a Crisis for the Health and Wealth of Nations*. Available at: http://www.jpiaamr.eu/wp-content/uploads/2014/12/AMR-Review-Paper-Tackling-a-crisis-for-the-health-and-wealth-of-nations_1-2.pdf
- Veyrier, F. J., Williams, A. H., Mesnage, S., Schmitt, C., Taha, M. K., and Boneca, I. G. (2013). De-O-acetylation of peptidoglycan regulates glycan chain extension and affects *in vivo* survival of *Neisseria meningitidis*. *Mol. Microbiol.* 87, 1100–1112. doi: 10.1111/mmi.12153
- Vollmer, W., Joris, B., Charlier, P., and Foster, S. (2008). Bacterial peptidoglycan (murein) hydrolases. *FEMS Microbiol. Rev.* 32, 259–286. doi: 10.1111/j.1574-6976.2007.00099.x
- Vorhölter, F.-J., Schneiker, S., Goesmann, A., Krause, L., Bekel, T., Kaiser, O., et al. (2008). The genome of *Xanthomonas campestris* pv. *campestris* B100 and its use for the reconstruction of metabolic pathways involved in xanthan biosynthesis. *J. Biotechnol.* 134, 33–45. doi: 10.1016/j.jbiotec.2007.12.013
- Wang, G., Lo, L. F., Forsberg, L. S., and Maier, R. J. (2012). *Helicobacter pylori* peptidoglycan modifications confer lysozyme resistance and contribute to survival in the host. *mBio* 3:e00409-12. doi: 10.1128/mBio.00409-12
- Weadge, J. T., and Clarke, A. J. (2005). Identification of a new family of enzymes with potential O-acetylpeptidoglycan esterase activity in both Gram-positive and Gram-negative bacteria. *BMC Microbiol.* 5:49. doi: 10.1186/1471-2180-5-49
- Weadge, J. T., and Clarke, A. J. (2006). Identification and characterization of O-acetylpeptidoglycan esterase, a novel enzyme discovered in *N. gonorrhoeae*. *Biochemistry* 45, 839–851. doi: 10.1021/bi051679s
- Weadge, J. T., and Clarke, A. J. (2007). *N. gonorrhoeae* O-acetylpeptidoglycan esterase, a serine esterase with a Ser-His-Asp catalytic triad. *Biochemistry* 46, 4932–4941. doi: 10.1021/bi700254m
- Weidenmaier, C., Kokai-Kun, J. F., Kristian, S. A., Chanturiya, T., Kalbacher, H., Gross, M., et al. (2004). Role of teichoic acids in *Staphylococcus aureus* nasal

- colonization, a major risk factor in nosocomial infections. *Nat. Med.* 10, 243–245. doi: 10.1038/nm991
- Wichgers Schreur, P. J., van Weeghel, C., Rebel, J. M., Smits, M. A., van Putten, J. P., and Smith, H. E. (2012). Lysozyme resistance in *Streptococcus suis* is highly variable and multifactorial. *PLoS One* 7:e36281. doi: 10.1371/journal.pone.0036281
- Williams, A. H., Veyrier, F. J., Bonis, M., Michaud, Y., Raynal, B., Taha, M. K., et al. (2014). Visualization of a substrate-induced productive conformation of the catalytic triad of the *Neisseria meningitidis* peptidoglycan O-acetyltransferase reveals mechanistic conservation in SGNH esterase family members. *Acta Crystallogr. D Biol. Crystallogr.* 70, 2631–2639. doi: 10.1107/S1399004714016770
- World Health Organization (2015). *Global Action Plan on Antimicrobial Resistance*. Available at: <http://www.who.int/antimicrobial-resistance/publications/global-action-plan/en/>
- World Health Organization (2017). *Antibiotic-Resistant Gonorrhoea on the Rise, New Drugs Needed*. Geneva: World Health Organization.
- Yamaryo-Botte, Y., Rainczuk, A. K., Lea-Smith, D. J., Brammananth, R., van der Peet, P. L., Meikle, P., et al. (2015). Acetylation of trehalose mycolates is required for efficient MmpL-mediated membrane transport in *Corynebacterineae*. *ACS Chem. Biol.* 10, 734–746. doi: 10.1021/cb5007689

Conflict of Interest Statement: The authors declare that the research was conducted in the absence of any commercial or financial relationships that could be construed as a potential conflict of interest.

Copyright © 2018 Sychantha, Brott, Jones and Clarke. This is an open-access article distributed under the terms of the Creative Commons Attribution License (CC BY). The use, distribution or reproduction in other forums is permitted, provided the original author(s) and the copyright owner(s) are credited and that the original publication in this journal is cited, in accordance with accepted academic practice. No use, distribution or reproduction is permitted which does not comply with these terms.

Advantages of publishing in Frontiers



OPEN ACCESS

Articles are free to read
for greatest visibility
and readership



FAST PUBLICATION

Around 90 days
from submission
to decision



HIGH QUALITY PEER-REVIEW

Rigorous, collaborative,
and constructive
peer-review



TRANSPARENT PEER-REVIEW

Editors and reviewers
acknowledged by name
on published articles

Frontiers

Avenue du Tribunal-Fédéral 34
1005 Lausanne | Switzerland

Visit us: www.frontiersin.org

Contact us: info@frontiersin.org | +41 21 510 17 00



REPRODUCIBILITY OF RESEARCH

Support open data
and methods to enhance
research reproducibility



DIGITAL PUBLISHING

Articles designed
for optimal readership
across devices



FOLLOW US

@frontiersin



IMPACT METRICS

Advanced article metrics
track visibility across
digital media



EXTENSIVE PROMOTION

Marketing
and promotion
of impactful research



LOOP RESEARCH NETWORK

Our network
increases your
article's readership